Terms and Conditions of Use of Digitised Theses from Trinity College Library Dublin

Copyright statement

All material supplied by Trinity College Library is protected by copyright (under the Copyright and Related Rights Act, 2000 as amended) and other relevant Intellectual Property Rights. By accessing and using a Digitised Thesis from Trinity College Library you acknowledge that all Intellectual Property Rights in any Works supplied are the sole and exclusive property of the copyright and/or other IPR holder. Specific copyright holders may not be explicitly identified. Use of materials from other sources within a thesis should not be construed as a claim over them.

A non-exclusive, non-transferable licence is hereby granted to those using or reproducing, in whole or in part, the material for valid purposes, providing the copyright owners are acknowledged using the normal conventions. Where specific permission to use material is required, this is identified and such permission must be sought from the copyright holder or agency cited.

Liability statement

By using a Digitised Thesis, I accept that Trinity College Dublin bears no legal responsibility for the accuracy, legality or comprehensiveness of materials contained within the thesis, and that Trinity College Dublin accepts no liability for indirect, consequential, or incidental, damages or losses arising from use of the thesis for whatever reason. Information located in a thesis may be subject to specific use constraints, details of which may not be explicitly described. It is the responsibility of potential and actual users to be aware of such constraints and to abide by them. By making use of material from a digitised thesis, you accept these copyright and disclaimer provisions. Where it is brought to the attention of Trinity College Library that there may be a breach of copyright or other restraint, it is the policy to withdraw or take down access to a thesis while the issue is being resolved.

Access Agreement

By using a Digitised Thesis from Trinity College Library you are bound by the following Terms & Conditions. Please read them carefully.

I have read and I understand the following statement: All material supplied via a Digitised Thesis from Trinity College Library is protected by copyright and other intellectual property rights, and duplication or sale of all or part of any of a thesis is not permitted, except that material may be duplicated by you for your research use or for educational purposes in electronic or print form providing the copyright owners are acknowledged using the normal conventions. You must obtain permission for any other use. Electronic or print copies may not be offered, whether for sale or otherwise to anyone. This copy has been supplied on the understanding that it is copyright material and that no quotation from the thesis may be published without proper acknowledgement.

Design and synthesis of 4-[1,3-diaryl-1H-pyrazole-4-yl]-2,6-dimethyl-1,4-dihydropyridine compounds and evaluation as anti-proliferative and multi-drug resistance reversal agents

Wei Shi, B.Sc.(Hons), M.Sc

A thesis presented to the University of Dublin for the degree of Doctor of Philosophy in Pharmaceutical Chemistry

Based on research carried out under the supervision of

Prof. Mary J. Meegan B.Sc., Ph.D. (N.U.I.), M.R.S.C., C.Chem

at the School of Pharmacy and Pharmaceutical Sciences

Trinity College Dublin

2011

I declare that this thesis has not been submitted as an exercise for a degree at this or any other university and it is entirely my own work.

I agree to deposit this thesis in the University's open access institutional repository or allow the library to do so on my behalf, subject to Irish Copyright Legislation and Trinity College Library conditions of use and acknowledgement.

Wei Shi

Abstract

1,4-Dihydropyridines are well known for their use as calcium channel blockers and are extensively used in treatment of hypertension. Dihydropyridine derivatives such as nifedipine have been shown to have the potential to overcome Pgp-mediated multidrug resistance thus can function as both L-type calcium channel blockers and multi-drug resistance (MDR) reversal agents. In this thesis, the design and synthesis of a number of novel structure modifications of initially identified lead 4-(1,3-diaryl-1H-pyrazole-4-yl)-1,4-dihydropyrdines and evaluation of their anti-proliferative properties on MCF-7 (ER positive) and MDA-MB-231 (ER negative) breast cancer cell lines is described.

These compounds were shown to have negligible effects on activation or inhibition of calcium transporters in MCF-7 cells. This investigation revealed that the anti-proliferative effect of this scaffold compound is independent of effects on the calcium channel in MCF-7 cell. Moreover, flow cytometric analysis and viability assay suggest that the novel dihydropyridines were effective modulators of Pgp mediated paclitaxel resistance and induced G1 phase cell accumulation and cell death both at μM range level. Initial synthesis work focused on the modified aryl rings at N-1 and C-3 of the pyrazole structure including a comprehensive panel of substituted heterocyclic rings, together with the optimised study of N-substitution on the DHP. Synthesis of corresponding products lacking the DHP methyl substituents *via* novel synthetic route has also been carried out. A number of these scaffold derivatives were screened against a comprehensive NCI60 cell line panel and showed broad spectrum antiproliferative activity against various tumour cell lines and presented activity comparable to or exceeding that of tamoxifen.

Raloxifene is a selective estrogen receptor modulator (SERM) with a triarylthiophen structure and can used as estrogen antagonist in breast cancer treatment. As a result of SAR investigation it was found that the biochemical activity of the synthesised type II scaffold derivatives containing pyrazole heterocylic analogues could be modulated by the substitutents attached at the C-4 position.

The stability of the novel synthesised type I derivatives was determined by HPLC at difference pH values and in human blood plasma. The initial SAR has been established and the structural features optimised for further development.

Acknowledgements

"No road is too long for him who advances slowly and does not hurry, and no attainment is beyond his reach who equips himself with patience to achieve it."

------ Jean de La Bruyere

I would primarily like to thank my supervisor Prof. Mary J. Meegan for giving me the great opportunity to perform her areas of research, and to study within her group which make me proud of myself. I also appreciate her for her expert guidance, advice, encouragement, day to day assistance and the abundant provision of equipments and materials to finish the large amount of consumptive study, without which this thesis must have taken a very different shape. Her enthusiasm for research and wondrous diligence sets an excellent example on how to be a successful scientist.

I would like to thank Dr. Daniela Zisterer, School of Biochemistry and Immunology, for all the help in the biochemistry study and to let me use her instruments. A special thanks to Dr. Lisa Greene for her patient guidance and Dr Seema Nathwani for the help when it was needed.

I would also like to thank Dr Michelle Chow and Prof. Chris Shaw, Queens University Belfast, for their practical advice and generous gift for using their ECIS equipment.

I want to express sincere gratitude to Dr. Cormac O'Donohoe for your assistance and support during the whole project and in the preparation of this thesis. Moreover, I am deeply grateful for his untiring understanding and for fatherly care and attention over the past few years.

My thanks go to technicians in the school of pharmacy, Ray and Rhona, thank you for many animated conversations and for help in finding some necessary items. Thanks to Dr. Manuel Reuther and Dr Martin Feeney in the Dept. of chemistry, Trinity College, for carrying out the NMR analysis and high resolution mass spec.

Huge thank you to all the past and present postgrads and postdocs in the school of pharmacy, especially Dr Miriam Carr for her patient guidance and outstanding demonstration, never forgotten her friendly encouraging during my first two year PhD study. Thanks to Dr Niall Kelly for his help in molecular modelling and the lovely graph provided.

Finally, I wish to acknowledge all of you who helped and encouraged me during this challenging PhD study period. Special grateful to my parents, I know I owe much to their love and I wish to dedicatite this thesis to them, also to my family and all the friends, for always believing in me, and for their unconditional love and support. The last thank must go to you, Candy, to be with me in every step to pursue the final goal, to cheer me up, even with all the non-stop "How's your writing going question", and always being there to help and loving.

Abbreviations

ABC	ATP-binding cassette
AF-2	Activation function 2
AI	Aromatase inhibitors
AKt	Protein Kinase B
AR	Androgen receptors
ASR	Age-standardised incidences rates
BRCA	Breast cancer type susceptibility protein
bFGF	Basic fibroblast growth factor
CA-4	Combretastatin A-4
CAFs	Cancer-associated fibroblasts
CB1	Cannabinoid receptor
CDCl3	Deuterated chloroform
CDKs	Cyclin-dependent kinases
COX	Cyclooxygenase
DBD	DNA-binding domain
DCM	Dichloromethane
DEPT	Distortionless enhancement by polarisation transfer
DHP	Dihydropyridine
DMAD	Dimthyl acetylenedicarboxylate
DMEM	Dulbeccos modified essential medium
DMSO	Dimethylsulfoxide
DNIF	Dehydronifedipine
DPPH	1,1-Diphenyl-2-picrylhydrazyl
ECIS	Electric cell-substrate impedance sensing
EGFRs	Epidermal growth factor receptors
ER	Estrogen receptor
FACS	Fluorescence-activated cell sorter
FBS	Fetal bovine serum
FDA	Food and drug administration
Glu	Glutamine
hCASMC	Human coronary artery smooth muscle cell
HDAC	Histone deacetylase
HER-2	Human epidermal growth factor receptor 2
HMQC	Heteronuclear multiple quantum coherence
HNPCC	Hereditary nonployposis colorectal cancer
HPLC	High performance liquid chromatography
HRMS	High resolution mass spectroscopy
Hsp90	Heat-shock protein 90
^{1}H NMR	Proton nuclear magnetic resonance
IC_{50}	Concentration required to produce 50% growth inhibition
IGF-2	Insulin-like growth factor 2

IR	Infra red spectroscopy
LBD	Ligand-binding domain
LDH	Lactase dehydrogenase
LC_{50}	Concentration required to kill 50% of the cells
M.P	Melting point
m/z	Mass of ion divide by its charge
MAPK	Mitogen-activated protein kinases
MDR	Multi-drug resistant
mTOR	Mammalian target of rapamycin
mTORC1	Mammalian target of rapamycin complex 1
MTT	3-(4,5-Dimethylthiazol-2-yl)-2,5-diphenyltetrazoliumbromide
NCI60	National cancer institute of 60 cell line
NDNIF	Nitroso-analogue of dehydronifedipine
NOESY	Nuclear overhauser effect spectroscopy
NR	Nuclear receptor
NSAID	Non-steroidal anti-inflammatory drug
PBS	Phosphate buffered saline
PCC	Pyridium chlorochromate
Pd/C	Palladium on charcoal
PDGFRs	Platelet-derived growth factor receptors
PG	Prostaglandins
Pgp	P-glycorprotein
PI	propidium iodide
PKC	Protein kinase C
PKD1	Polycystic kidney disease
PPh3	Triphenyl phosphine
ppm	parts per million
PR	Progesterone receptor
RNase A	Ribonuclease A
S.E	Stardard error
SAR	Structure activity relationship
SERDs	Selective estrogen receptor downregulators
SERMs	Selective estrogen receptor modulators
SRs	Steroid receptors
SWDS	Slow wave deep sleep
THP	Tetrahydropyran
TGI	Concentration required to inhibit the growth of all cells
TGF-β1	Transforming growth factor β1
THF	Tetrahydrofuran
UV	Ultra-violet
VDR	Vitamin D receptor
VEGF	Vascular endothelial growth factor
VEGFR	Vascular endothelial growth factor receptor
XRD	X-ray diffraction

Table of Contents

Table of Contents

Table of Figures

Table of Schemes

Table of Tables

Chapter 1

Introduction

1.1 Cancer overview

This thesis presents a study of the synthesis and biochemical evaluation of a series of novel pyrazoles and 1,4-dihydropyridines. These compounds are of particular interest as potential antitumor drugs for treatment breast cancer and leukaemia as they are shown to display reversal effect on the p-glycoprotein efflux pump.

In this chapter, a review of the chemotherapeutic drugs used in breast cancer treatment is presented together with a summary of the antiproliferative effects of pyrazoles and 1,4-DHPs containing compounds.

Originating from the Latin word for crab whose limbs were historically thought to resemble the swollen blood vessels around the area of a tumour, cancer is a term used to describe a class of illnesses characterized by their malignant behaviour where abnormal cells divide without control, invade other tissues and/or spread to other parts of the body via the circulation of lymph or blood – three pernicious properties that differentiate cancer from benign tumours. Most cancer have the form of a tumour with the exception of blood cancer, medically termed leukaemia where normal blood function is prohibited by the uncontrolled accumulation of abnormal blood cells.[1, 2]

Affecting people at all ages, cancers represent the second largest mortality diseases in the world, following heart disease and leading cardiovascular disease. In 2007, 7.6 million people died from cancer, accounting for 13% of all human deaths worldwide. In Ireland, with over 20,000 new cases, and over 7,500 deaths each year that account for almost 25% of the annual death toll, cancer has become a major cause of death and disease in this country.[3] The main causes of cancer death in Ireland remain almost steady each year with those from skin, breast in woman, prostate in men, lung and colon and rectal ranking highest. **Table1.1** shows the case numbers of all the common cancers in Ireland and the age-standardised incidences rates (ASR) resulting from these cancers in the period 1994-2007, in both men and women.[4]

All cancers						
Gender	**Year**	**Number of case**	**Crude rate**	**European ASR**	**World ASR**	**Cumulative Risk(0-74)**
Female	1994	9792	543.22	545.88	392.73	35.20%
	1995	9597	529.37	528.25	379.56	33.98%
	1996	10192	558.2	553.13	400.12	35.43%
	1997	10483	568.19	561.04	404.98	35.79%
	1998	10381	556.74	543.22	393.21	34.86%
	1999	10574	561.47	547.23	396.47	35.14%
	2000	11232	589.17	571.4	414.98	36.17%
	2001	11667	603.25	583.61	425.71	36.69%
	2002	12198	618.86	600.02	440.55	37.90%
	2003	12936	646.25	620.25	454.94	38.64%
	2004	13449	661.73	630.08	463.02	39.01%
	2005	13356	646.81	614.73	451.65	38.49%
	2006	13896	655.88	623.39	457	38.84%
	2007	14561	671.7	643.92	475.75	40.12%
Male	1994	9496	532.49	626.27	419.32	38.75%
	1995	9436	527.62	614.83	413.15	38.08%
	1996	9721	539.99	627.37	421.89	38.61%
	1997	9927	545.62	629.09	420.45	38.38%
	1998	9876	537.06	615.52	415.31	38.41%
	1999	10084	542.56	622.95	417.44	38.18%
	2000	10678	567.07	648.18	435.84	39.72%
	2001	10905	569.99	648.39	437.39	40.13%
	2002	11484	590.08	667.85	449.17	40.64%
	2003	11776	595.53	669.22	451.16	40.97%
	2004	12646	628.75	700.28	474.43	43.02%
	2005	12658	618.73	684.65	462.43	42.34%
	2006	13229	623.66	693.11	468.76	42.57%
	2007	13369	615.77	688.44	467.87	43.13%

Table 1.1 National cancer registry: Number of incidences of cancer in Ireland and age-standardised rate from all cancers, 1994-2007.[4]

1.1.1 Cancer causing factors

As the functional basic unit of human body, in normal circumstance, cells develop and multiply in a controlled manner, generating more copies to maintain the configuration and function of the body. When cells become sufficiently old or damaged, they undergo a programmed death process called apoptosis and are replaced by fresh new cells.

However, sometimes this orderly process can go out of control wherein the genetic material (DNA) of a cell becomes damaged or altered, disrupting apoptosis and therefore resulting in uncontrolled and often rapid cell proliferation, and at the end of the chain, the formation of a tumour. Some type of tumours may turn malignant, which are referred as cancer. (**Figure1.1**)[5]

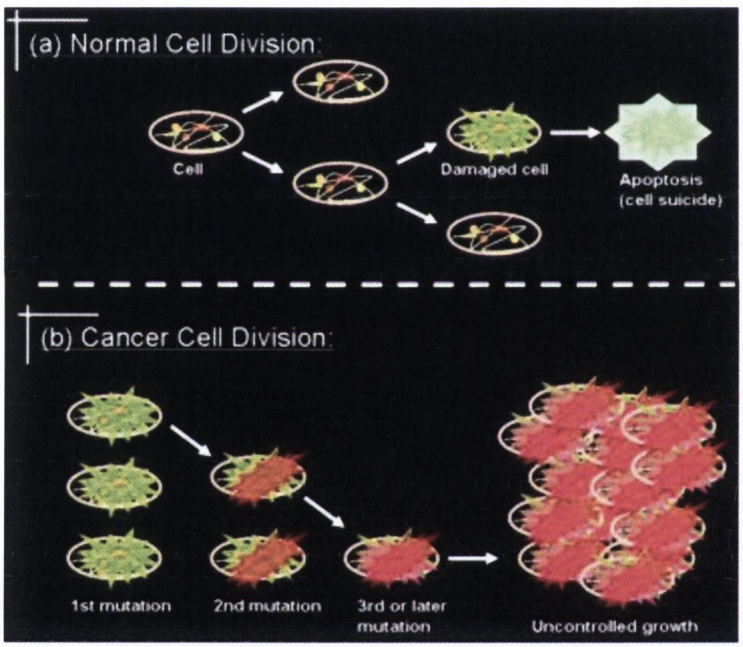

Figure 1.1 (a) Normal cell division , (b) Cancer cell division

After a half century of rapid advances, the precise reasons as to why a particular individual develops cancer rather than another are still unknown, but research related to differences in genetics (5-10%) and exposure to various environmental factors (90-95%) has generated rich and complex body of knowledge. An analysis conducted by Anand P. et al.[6] in 2008 has revealed that tobacco (25-30%), diet and obesity (30-35%), infections (15-20%), radiation, stress, lack of physical activity and environmental pollutants are the most common environmental factors causing abnormalities in the genetic material of cells, and leading to cancer death.[7] Decades

of research has demonstrated the link between the following factors and carcinogenesis.

- Chemicals

As mentioned above, cancer pathogenesis can be related to DNA mutations that bear on cell growth and metastasis. Chemicals that stimulate DNA mutations are recognized as mutagens, and mutagens that induce cancers are noted as carcinogens. Specific substances have been associated with particular forms of cancer. For instance, tobacco smoke and alcohol intake are substantial hazard agents for a lot of types of cancer.[8] Certain natural mineral fibres like asbestos can directly damage DNA because of their size and result in carcinogenic mutations. Large numbers of mutagens are also carcinogens, but several carcinogens are not mutagens. Alcohol is an exceptional chemical carcinogen that is not a mutagen.[9] Such chemicals may enhance cancers by accelerating cell division which leaves less time for repair processes where enzymes correct damaged DNA during DNA replication, increasing the chance of a mutation.

- Ionizing radiation

Ionising radiation, sourced from X-rays, cosmic rays, solar radiations and indirectly from radon gas, damages the DNA, disrupting the correct genetic sequence.[10] It is estimated that current CT investigations will result in 2% of future cancers.[11] Additionally, ultraviolet radiation from sunlight can induce mutations by causing certain segments of DNA to remain linked together. It has been recognized that prolonged exposure to ultraviolet radiation from the sun can lead to melanoma and other skin malignancies.

- Infection

Infections by certain viruses and bacteria have been discovered related to DNA mutations. Process of canceration by these biological mutagens may involve a number of different complex mechanisms. Examples of viruses that cause cancer include the human T-cell lymphyocytic virus implicated in lymphoma, the human papilloma virus implicated in cervical cancer and the hepatitis B virus implicated in

liver cancer.[12] A representative of known bacterial mutagens is *Helicobacter pylori* implicated in stomach cancer.

- Heredity

It is easily understood that genetic mutations in carriers, as part of the gene, can be passed down to the next generation, making the newborn statistically more likely to develop cancer later in life. Representatively, certain hereditary mutations in the genes BRCA1 and BRCA2 are correlated with a promoted risk of breast cancer and ovarian cancer; However interestingly, in a number of recognised syndromes where there is an inherited predisposition to cancer, the genetic defect is often found preventing tumour formation, such as Multiple Endocrine Neoplasia Syndrome type 1, 2A and 2B; Li-Fraumeni Syndrome in which various tumours such as osteosarcoma, breast cancer, soft tissue sarcoma, brain tumours develop due to mutations of p53; Turcot syndrome, characterised by polyps in the colon in addition to brain tumours; Familial Adenomatous Polyposis, involving an inherited mutation of the APC gene that leads to early development of colon cancer; Hereditary nonpolyposis colorectal cancer (HNPCC, also known as Lynach syndrome); and Down's Syndrome, with which patients are likely to have carcinoma developed such as leukaemia and testicular cancer due to an extra chromosome 21.[13]

- Other causes

Research has shown that certain hormone based menopause hormone therapy could cause serious side effects, such as increase the risk of breast cancer, stroke, or blood clots.[14] Others factors, such as overweight, a poor diet in fruits and vegetables, or lack of physical activity may give rise to the risk of developing cancers in breast, colon, uterus and prostate.

1.1.2 Classification

Cancer is not referred as a single disease but a variety of diseases. There are more than 200 distinct types of cancer, and subtypes of tumour can be found within specific organs. Generally cancers are classified by the type of cell that is initially affected, therefore, the tissue presumed to be the origin of the tumor. Examples of general categories include:[15]

- **Carcinoma:** Malignant tumours derived from epithelial cells. This group comprises the majority of cancers, including the common classes of breast, lung and colon cancer.
- **Sarcoma:** Malignancies derived from connective tissue, or mesenchymal cells.
- **Leukemia and lymphoma:** Malignant tumours derived from hematopoietic cells
- **Germ cell tumour:** Tumours derived from totipotent stem cells. In adults, these tumours are most often found in the testicle and ovary, and in fetuses, babies, and young children, on the body midline, particularly at the tip of the tailbone
- **Blastic tumour or blastoma:** Tumours caused by malignancies in blast cells and resembling an immature or embryonic tissue. These tumours most often occur in children.

1.1.3 Cancer at molecular level

Suggested by a number of lines of research evidence, carcinogenesis in humans involves a series of steps that reflect genetic mutations by which progressive transformation of normal cells are driven into highly malignant derivants. However, the immense catalogue of the genetic constitution of cancer cells is a manifestation of six substantial alterations in cell physiology that conjointly result in malignancy: self-direction in growth signalling, escape of programmed cell death (apoptosis), unlimited divisional potential, prolonged angiogenesis, and tissue invasion and metastasis.[16]

The many series of molecules examined in various studies during the past decade reveal the pathogenesis of cancer. These molecules contain various structures implicated in anticancer activity. In order to understand how these molecules exert their anticancer effects, it is required to understand the cell cycle occurring in healthy cells, as well as the factors that produce disregulation of this cycle.

1.1.3.1 The cell cycle

Cell proliferation plays a major role in many pathological and physiological processes, including growth, repair, immune response and tumour formation. Within a normal cell, the cell replicates all of its genetic material and then undergoes mitosis

to produce two distinct daughter cells. The cell cycle (Figure1.2)[17] refers to the series of events that takes place inside a cell thus leading to cell segmentation and cell replication.

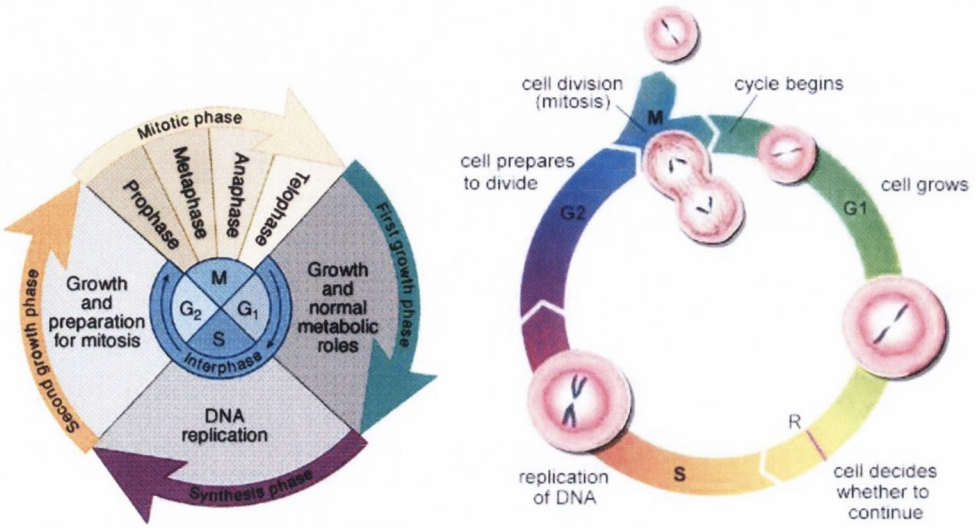

Figure 1.2 Physiological cell cycle

The rounded succession of events from one cell division to the next usually comprises the phase when this genetic material is being copied (S phase), the phase when the cell actually splits into two daughter cells (M phase), the two interposing gap phases (G_1 and G_2), and a resting state named quiescence (G_0).

- G_1 Phase – The cell develops dimensionally and checks the conditions of its internal systems. If everything is operating normally and any impairment in the DNA has been repaired, the cell is committed to the proliferation cycle. If the conditions do not meet the requirement for the transition, the cell exits its cycle and may initiate apoptosis.[18] In Figure 1.2, R marks the restriction point of a cell cycle.
- S phase – The DNA is synthesized during this phase. At the end of the S phase, every chromosome has duplicated and has a sister chromatid.[19, 20]
- G_2 phase – This stage prepares the cell for division before entering mitosis. During G2 phase, microtubules are generated and proteins are synthesized. If any of these activities fail to occur, the cell will be prevented from undergoing mitosis.
- Mitosis phase – The nuclear material and proteins equally divide, producing two new identical daughter cells which then enter the G_1 phase of their own

cell cycle. Mitosis is a highly regulated and complicated process, involving many phases, such as Prophase, Metaphase, Anaphase and Telophase. If any slight error occurs in any of these processes, it may result in cancer or cell death by apoptosis.[21]

- G_0 phase (Resting phase) — G_0 phase is a time period in the cell cycle when cells remain in a dormant stage, during which cell cycle machineries are dismantled and cyclin and cyclin-dependent enzymes disappear. This often occurs to prevent cell destruction by apoptosis.

1.1.3.2 Hallmark capabilities of cancer

If the cell cycle can be described as an cancer defence mechanism hardwired into cells and tissues, the following eight capabilities of cancer hallmark most if not all cancers during their development,through various mechanistic strategies.[16]

✓ Self Sufficiency in Growth Signals

Cells require growth signals to switch from a quiescent state to a proliferating state. Cancer cells have the ability to become autonomous of the growth signals in the cell cycle. The most obvious mechanism available to the cancer cell is to develop a method of producing its own growth factors independently of the cell cycle. Cancer cells can also over-express growth factor receptors (e.g. Her2 in breast cancer) which lead to the cell becoming more sensitive to normal levels of growth factor. The third method available to the cell is to alter its cell machinery to become more sensitive to signals from growth factor receptors.

✓ Ignoring Anti-growth Signals

In the physiological cell cycle there also exists a number of anti-growth signals that are used by the cell to switch from a proliferating state to a quiescent state. These signals lead the cell to enter the G_0 phase of the cell cycle or else to start on the path to cell death. Cancer cells develop the ability to disrupt these signals.(**Figure 1.3**)[16]

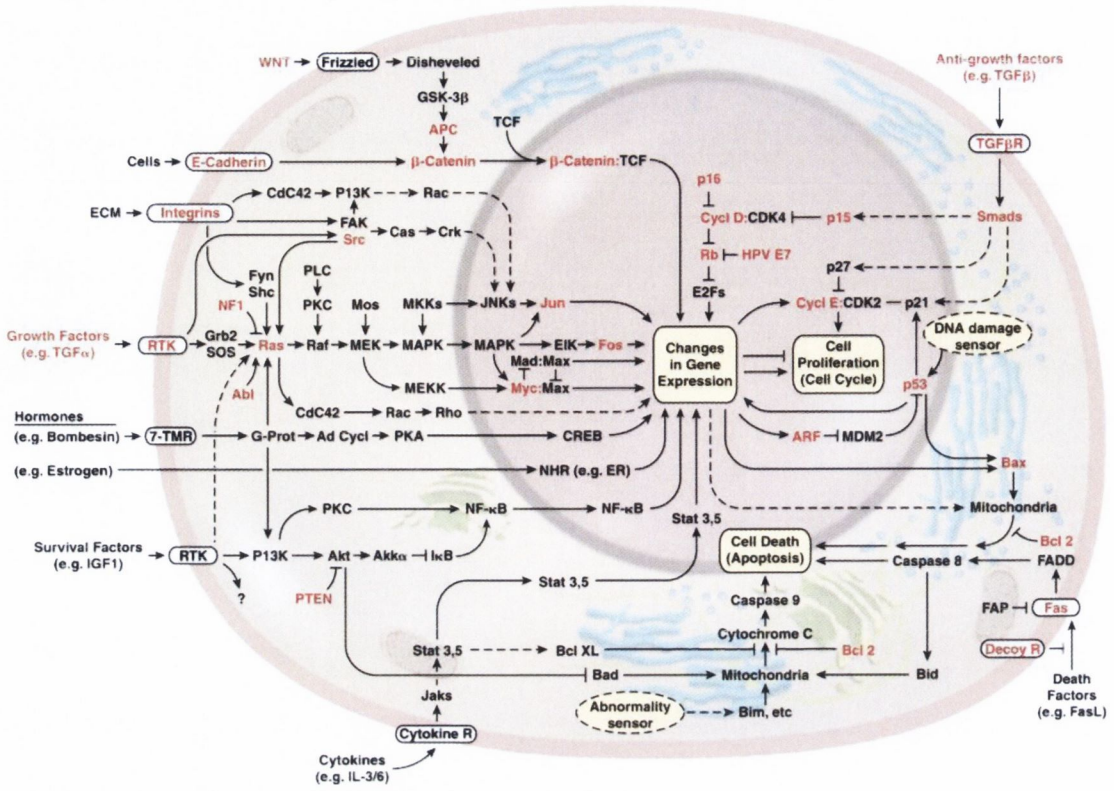

Figure 1.3 The Emergent Integrated Circuit of the Cell

✓ Bypassing Apoptosis

Apoptosis is a major barrier to a cell turning cancerous. The cell has safeguards to sense that the normal cell cycle has gone awry. This leads to the triggering of apoptosis which is the programmed death of the cell. Cancer cells can bypass this pathway by either turning off the apoptotic signals (such as mutating p53), or by overwhelming the apoptotic signals with anti-apoptotic signals (switching on IGF-2 genes)

✓ Replication

Even with achieving the first three hallmarks of cell replication, a cancer cell cannot go on replicating forever. Telomeres are strands of DNA located at the end of chromosomes that function as a kind of internal clock, becoming shorter with each replication of the cell. As the telomeres shorten, the cells genome becomes unstable and eventually apoptosis is triggered. Cancer cells are able to maintain telomeres usually by using telomerase to replace the short strands of DNA at the end of chromosomes. This allows the cell to maintain a stable genome and avoid apoptosis through countless replications.

✓ Angiogenesis

In order for a cancer tumour to grow beyond a few millimetres in diameter, it needs to develop its own vasculature. Such vasculature is required to disperse the nutrients and oxygen needed for further growth throughout the tumour. Angiogenesis is required to develop such vasculature. This angiogenesis is controlled by both initiating and inhibiting signals. The cancer cell learns to tip the balance in favour of the initiating signals such as vascular endothelial growth factor (VEGF).

✓ Metastasis

The final hallmark of cancer is the ability of the primary tumour to migrate to distant parts of the body and to initiate secondary tumours. This represents the most lethal aspect of cancer. Through the process of angiogenesis the tumour has access to the circulatory system. For metastasis to occur the tumour cells must have the ability to break off from the primary tumour, migrate through the stroma, enter and survive in the bloodstream while they migrate to a secondary site, penetrate the blood vessel walls at the secondary site, migrate into surrounding tissue, and proliferate until a critical mass is reached that allows it to generate its own vasculature and hence a secondary tumour. Although the example given above describes metastasis through the circulatory system, the tumour can also spread through the lymphatic system or through body cavities.

✓ Genome instability

Genomic instability has been revealed by the recent studies of human cancers as another original hallmark of cancer. It occurs in hereditary cancer, which are characterized by instability in either the microsatellite or chromosomes, as a result of the mutations in DNA repair genes. In sporadic cancers, genomic instability is not shown due to alterations in DNA repair genes or mitotic checkpoint genes during the early stages of cancer development.[22]

✓ Contribution of surrounding stroma

One act of genetic mutations that turn normal cells into tumours is to affect the tightly controlled systems for growth control, making the surrounding

microenvironment more suitable for the initiation and growth of tumours, by employing the cancer- associated fibroblasts (CAFs), endothelial cells, pericytes, leukocytes, and extracellular matrix. The dynamic signalling circuitry in the stroma contributes to the whole process of cancer development, and eventually leads to a fatal disease. Tumour cell interaction with the surrounding stroma in the context of the original hallmarks of cancer is a continuous focus in cancer research.[23]

1.2 Estrogen receptor

1.2.1 Breast cancer

The breast consists of lobes and ducts. Each breast contains 15 to 20 separate lobes, each comprising several secretory lobules. Lobules end in dozens of tiny bulbous mammary glands that secrete milk during lactation. The lobes, lobules, and mammary glands are linked by thin tubes named ducts.(**Figure 1.4**)[24]

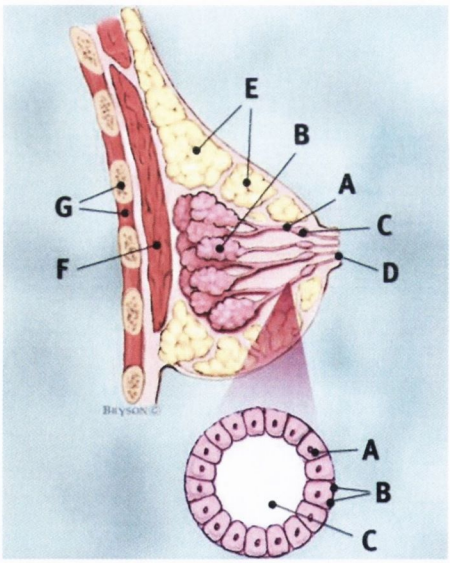

Figure 1.4 Breast profile and Enlargement

Breast profile: **A** Ducts **B** Lobules **C** Dilated section of duct to hold milk **D** Nipple **E** Fat **F** Pectoralis major muscle **G** Chest wall/rib cage.

Enlargement: **A** Normal duct cells **B** Basement membrane **C** Lumen (centre of duct)

Breast tissue also has blood vessels and lymphatic vessels. The lymphatic vessels carry lymph, and lead to lymph nodes, which are small bean-shaped organs being found throughout the body. They filter lymph fluid by removing antigens, helping to fight infection and disease. Clusters of lymph nodes near the breast are found in the axilla, above the collarbone, and in the chest.

Breast cancer is a disease where malignant cancer cells form in the mammary glands. It is the number two leading malignancy female disease, causing 519,000 deaths worldwide in 2004 (7% of cancer deaths, almost 1% of all death).[25] Although breast cancer occurs over 100 fold more commonly in women than in men, it is still the most common type of non-skin cancer and accounting for 10.4% of all cancer incidence among female.[25] Genetic alterations, as a result of the aging process and the special lifestyle in general, are always a reason for development of breast cancer, causing about 90% of the disease. Multiple factors, such as gender, age, lack of childbearing or breastfeeding, higher hormone levels, race, economic status and obesity, have been implicated primary in causing breast cancer. A recent review made by World Cancer Research Fund, taking into account hundreds of separate studies, announced that more that 30% of breast cancer cases could be prevented through reducing alcohol intake, avoiding tobacco use, increasing physical activity levels and maintaining a healthy body weight.[26]

Most commonly, breast cancer begin in the cells of the lobules or the ducts. Over time, malignant cells can infiltrate nearby healthy tissue, and enter the circulatory system by invading blood vessels and/or lymphatic vessels, and relocate at other parts of the body. Breast cancers are classified by the expression status of three important receptors - estrogen receptor (ER), human epidermal growth factor receptor-2 (HER2) and progesterone receptor (PR). ER-positive breast cancer rely on estrogen for the cancer cells to growth, and usually has a better prognosis; HER2/neu breast cancer is much more aggressive than ER cancer; and PR cancers. Those without these receptors are called basal-like, or triple negative breast cancers.[27]

1.2.2 Estrogen receptor

Estrogen receptors are a group of ligand-activated transcriptional regulators that are activated by the steroid hormone 17β-estradiol. Two distinct forms of the estrogen receptors - ERα and ERβ, have been identified, each encoded by a separate gene ESR1 and ESR2, respectively.[28](**Figure 1.5 and 1.6**) DNA transcriptional activation is the main function of estrogen receptors. They regulate the expression of target genes, carry out and modulate the effects of estrogen in various organs and systems in human body.[29]

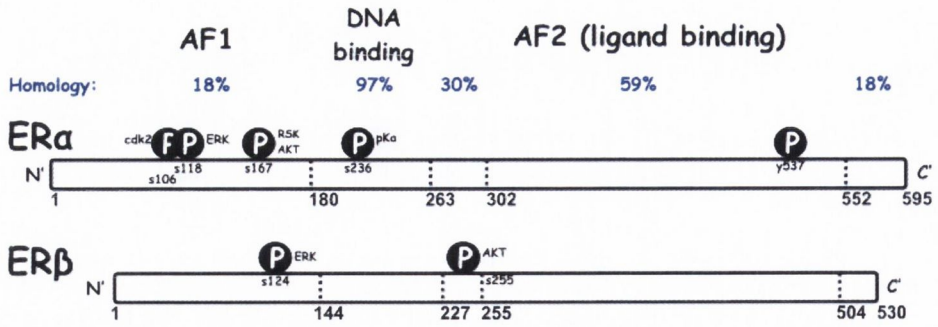

Figure 1.5 The domain structures of ERα and ERβincluding some of phosphorylation sites[30]

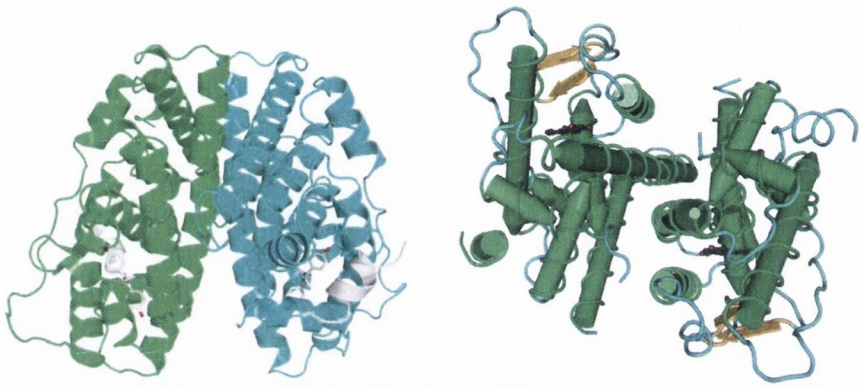

(a) **(b)**

Figure 1.6 (a) A dimer of the ligand-binding region of ERα, (b) A dimer of the ligand-binding region of ERβ[31]

ERs are a group of related molecules that belong to the nuclear receptor (NR) superfamily, which is a family of over 100 known structurally related ligand-inducible transcription factors, including steroid receptors (SRs), vitamin D receptor (VDR), and estrogen receptors, ect. The structure of ERs contains function specific domains (**Figure 1.7**). The regulatory N-terminal A/B domain is responsible for transactivation of gene transcription without estrogen as the bound ligand, providing a weak but more selective activation compared with that by the E domain. The C domain, also known as the DNA-binding domain (DBD), binds to estrogen response elements in DNA. The D domain is a hinge region that is believed to connect DBD with the LBD. The E domain contains the ligand binding cavity as well as binding sites for coactivator and corepressor proteins, called the Ligand-binding domain (LBD). Gene transcription can be activated by the activation function 2 (AF-2) within the LBD in the presence of estrogen. The C-terminal F domain function is not

entirely clear and is variable in sequence and length between various nuclear receptors (NRs).[32]

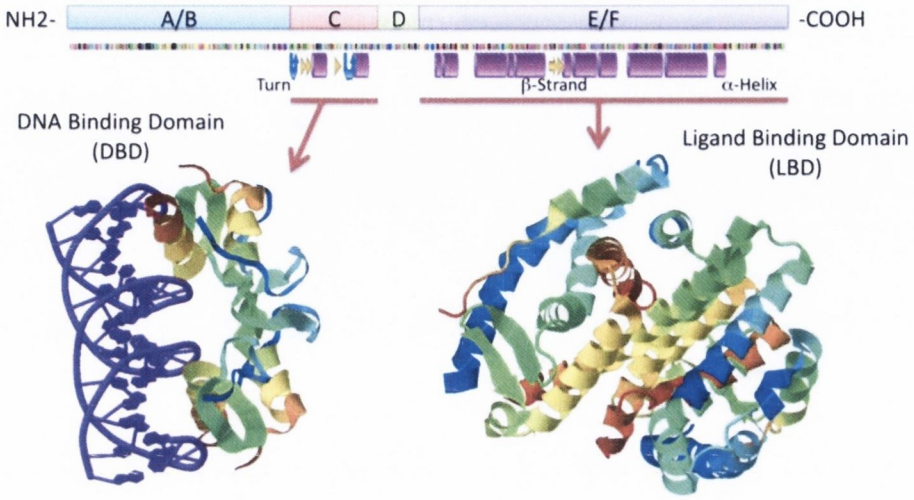

Figure 1.7 Domain structure of nuclear receptors (NRs)

Breast cancer is caused by DNA damage (mutations) in genes that control cell proliferation. However, breast cancer cells do not always have receptors for estrogen. Usually breast cancer is divided into estrogen receptor (ER) positive and estrogen receptor (ER) negative. Estrogen receptor (ER) positive breast cancer refer to that possess estrogen receptors, in contrast, those that do not have estrogen receptor are said to be estrogen receptor negative. Two-thirds of all breast cancers are ER positive breast cancer, which is much less aggressive than ER negative breast cancer.

1.3 Breast Cancer therapy

Most patients who have been diagnosed with cancer will undergo some types of treatment for the disease, such as surgery, chemotherapy, and radiotherapy, or a combination of two or three of modes of therapy. Since the first dose of cytotoxic chemotherapy was given about 60 years ago, hundreds of thousands of chemical agents have been tested for their activity in inhibiting cancer cells. Unfortunately, few of these drugs reached the stage of clinical trials, yet fewer still were found safe and effective enough to be tested in humans. However, only a very small number of those agents that have been tested in humans were demonstrated helpful in cancer patients. (**Figure 1.8** and **Table 1.3**) illustrate the breast cancer-specific molecular targets and corresponding therapeutic compounds below.

For anticancer drug treatment to be effective, several features must be present. The agent must reach the cancer cell, sufficiently toxic amounts of drug or its active metabolite must enter the cells and remain there for a long enough period time, the cancer cells must be sensitive to the effects of the drug, and all this must occur before resistance emerges.[33,34] The development of resistance to chemotherapeutic drugs is one of the major obstacles to the cure of many malignant tumours,[35,36] which is discussed below. On the other hand, chemotherapy can not ensure to cure all types of cancer so far. It involves poisoning the rapidly growing cancer cells, but also destroys rapidly growing healthy cells in the bone marrow, gastro-intestinal tract etc, hence bring side effects such as organ damage in liver, heart, kidneys, lung.

1.3.1 Overview of breast cancer chemotherapy regimens

1.3.1.1 Combination Chemotherapies for breast cancer

The current treatment of breast cancer includes single drug therapy and combination therapies. Single drugs currently used for breast cancer chemotherapy are listed in **Section 1.3.1.2**, and the existing combination therapies for breast cancer are listed in (**Table 1.2**) below.

Combination chemotherapy	Composition	Reference
'AC' chemotherapy	Doxorubicin and Cyclophosphamide	[37]
'AVM' chemotherapy	Doxorubicin, Vinblastine and Mitomycin	[38]
'CAF' chemotherapy	Cyclophosphamide, Doxorubicin and 5-Fluorouracil	[39]
'CFP' chemotherapy	Cyclophosphamide, 5-Fluorouracil, and Prednisone	[40]
'CMF' chemotherapy	Cyclophosphamide, Methotrexate, 5-Fluorouracil	[41]
'CMFP'chemotherapy	Cyclophosphamide, Methotrexate, 5-Fluorouracil, and Prednisone	[42]
'Copper regimen'	5-Fluorouracil, Methotrexate, Vincristine, Cyclophosphamide, Prednisone	[43]
'FAC' chemotherapy	5-Fluorouracil, Doxorubicin, Cyclophosphamide	[44]

'MV' chemotherapy	Mitomycin and Vinblastine	[45]
'Six-Drug Regimen'	5-Fluorouracil, Methotrexate, Vincristine, Cyclophosphamide, Prednisone, and Prednisolone	[46]
'VATH' Chemotherapy	Vinblastine, Doxorubicin, Thiotepa, and Fluoxymesterone	[47]

Table 1.2 Combination chemotherapies of breast cancer

1.3.1.2 Current treatment of breast cancer agents

As mentioned above, therapeutic methods for cancer encompass surgery, radiotherapy and chemotherapy, the latter using medicinal chemistry in a combined strategy to eliminate or at least halt the maligancy. The medicinal chemistry of anti-cancer drugs incorporates several mechanisms and presented in (**Table 1.3**) below:

Therapeutic class	Examples	Mechanism of action
Antimetabolites	Inhibiting hormone action	Interfere with the formation or utilisation of natural mechanisms to inhibit essential metabolic routes
	Regulation of steroidal hormone synthesis	
	Glucocorticoids and inhibitors of their biosynthesis	
Drug acting via radical species	Anthracylines and their analogues	Create iron-mediated free oxygen radicals that damage the DNA and cell membranes[48]
	Mitoxantrone and related quinines	
	Actinomycin	
	Enediyne antibiotics	
DNA alkylating agents	Aziridines	Interfere with DNA replication by reacting with DNA base pairs
	Nitosureas	
	Triazenes	
	Methylhydrazines	
Alkylating and non-alkylating compounds interacting with the DNA minor groove	Mitomycins	As a potent DNA crosslinker, a single crosslink per genome shown to be effective in killing bacteria
	Tetrahydroisoquinolone alkaloids	
DNA intercalators and topoisomeras inhibitor	Monofunctional and biofunctional intercalating agents	Interfere with DNA replication by engaging the site between the DNA double helix
Drug targeting tubulin and microtubulin (To control cell division)	docetaxel	Drugs that inhibit microtubule polymerisation at high concentration
	Paclitaxel, epothilone	Microtuble-stabilising agents:

		compounds binding at the taxane site
	Vincristine, Laulimalide	Antivascular effects of microtubule-targeted agents[49]
	Substituted thienopyrimidinone	Mitotic Kinesin inhibitors
Drugs that inhibit signalling pathway for tumour cell growth and proliferation (Targets a cancer specific pathway in the cell)	Broystatin	Drugs target protein kinases
	ST1571	Inhibitors of tyrosine kinases
	ZD1839	Inhibitors of EGFRs (HER1)
	Trastuzumab	Inhibitors of other receptors of the EGFR family:HER2
	Bevacizumab	Inhibitors of TKs with pro-angiogenic activity: VEFGR and related kinases
	Perifosine	Inhibitors of Serine-threonine kinases
	R115777	Inhibitors of the RAS-RAF-MEK signalling pathway and farnesyl transferase
	17-AAG	Inhibitors of heat shock proteins (HSP90)
Other approaches to targeted therapy	Bortezomib, Disulfiram	Proteasome inhibitors
	Thalidomide	Antiangiogenic agents unrelated to kinase signalling[50]
Drugs that modulate resistance to antitumour agents	Sav1866, MsbA	ATP-Binding cassette efflux pumps in anticancer drug resistance, drugs which target ABC efflux pumps such as P-glycoprotein[51-53]

Table 1.3 Summary of medicinal chemistry of anti-cancer agents

1.3.1.2.1 Classes of chemotherapy agents for breast cancer

The group includes those conventional cytostatic drugs such as anthracyclines, taxanes, alkylating drugs, antimetabolites, vinca alkaloids. Alkylating agents are a class of drugs that works directly on DNA to prevent the cancer cell from reproducing and works in all phases of the cell cycle. Some examples of alkylating agents include busulfan [1], cisplatin[2], carboplatin[3], and temozolomide[4]. Antimetabolites are a group that interfere with DNA and RNA growth. These agents work during the S phase and are commonly used to treat leukaemia, tumours of the breast, ovary and the gastrointestinal tract as well as other cancers. Examples include

5-Fluorouracil[5], capecitabine[6], and 6-mercaptopurine[7]. paclitaxel[8] and vinca alkaloids are mitotic inhibitors and natural products. They can stop mitosis or inhibit enzymes from making proteins needed for reproduction of the cell. These work during the M phase of the cell cycle. The clinical response of those drugs above can be achieved in more than 80-90% cases. However, they also have some distinct features such as severe adverse effects, limited duration of response, overlapping spectrum of drug resistance, limited ability to predict response and non-response to a given cytostatic compound.[54]

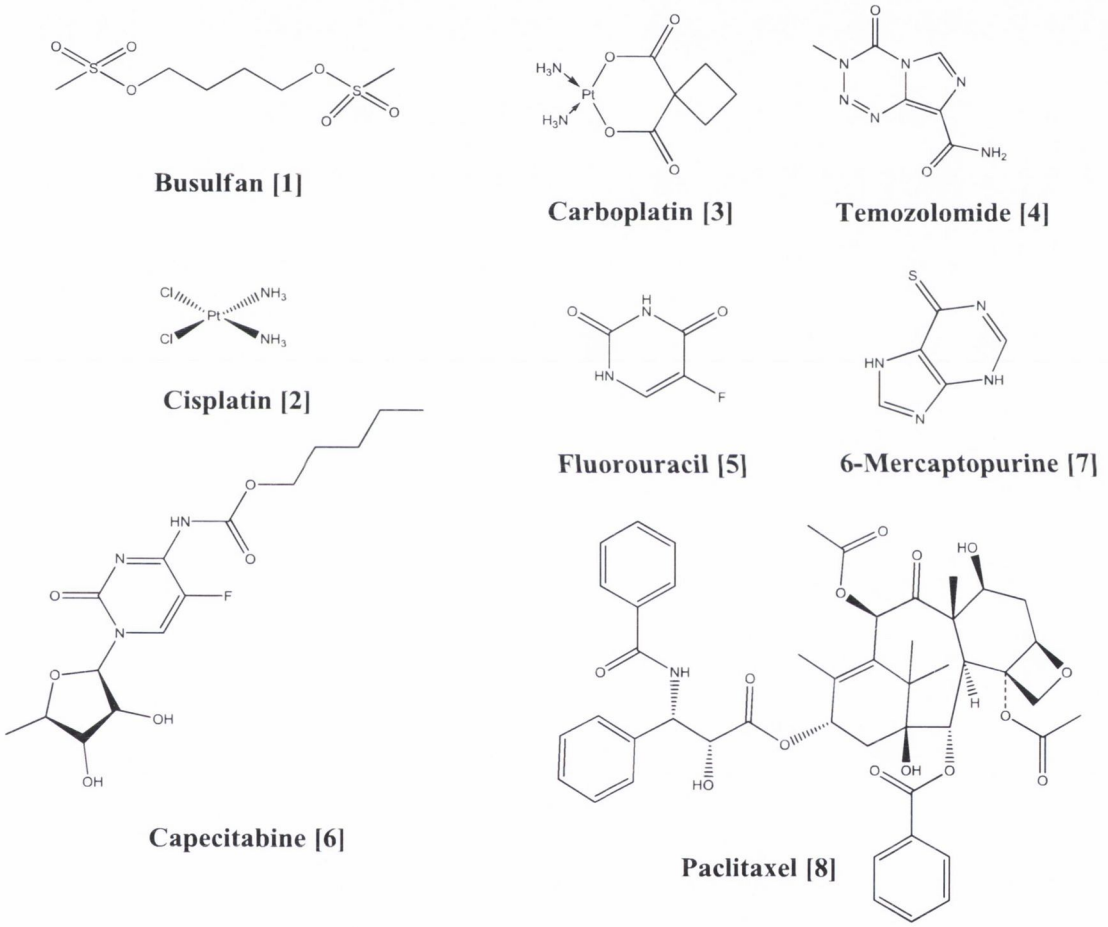

Figure 1.8 Examples of chemotherapy agents

1.3.1.2.2 Genuine targets (molecules essential for breast cancer development and maintenance)

The principle genuine targets available for breast cancer proliferation are estrogen/progesterone receptor proteins drugs, such as selective estrogen receptor modulator (SERMs) and selective estrogen receptor downregulators (SERDs), inhibit hormone action, in particular steroid hormones which may be the main determinants

in the development and growth of several types of tumours. Hormonal manipulation had tended to be one of the mainstays of cancer chemotherapy. Examples would be the compounds acting on estrogen (ER) or androgen receptors (AR) involved in the treatment of breast and prostatic cancers, among others, while corticosteroids are used in myelomas and lymphomas because of their role in the function of lymphoid tissues. Examples of such drugs will be discussed in the following sections.

- ✓ Selective estrogen receptor modulators (SERMs)

Tamoxifen

Tamoxifen (**Figure 1.9, [9]**), (Z)-2-[4-(1,2-diphenyl-1-butenyl)phenoxy]-N,N-dimethylethanamine, was the first SERM approved for the treatments of breast cancer, and was also the most widely used hormonal therapy for all stages of breast cancer since 1977. In the same year, it was approved by the Food and Drug Administration for the treatment of advanced breast cancer, and has recently been approved for the prevention of women with breast cancer in high-risk. It binds to the estrogen receptor and induces a conformational change, however, it also has an estrogenic effect in endometrial tissue and may bring a secondary cancer.[55]

Tamoxifen is the first nonsteroid antiestrogen proven effective against breast cancer. It is now known a synthetic triphenylethylene agent and has varying estrogen agonist and antagonist properties.[56] It binds to the estrogen receptor and thus induces a conformational change. In breast cancer, tamoxifen acts as an antagonist primarily. However, it also has an estrogenic effect in endometrial tissue and may cause a secondary cancer. Tamoxifen is beneficial in approximately 60% of patients with ER positive tumours in clinic.[57] Subsequently, most women respond to tamoxifen therapy will eventually become resistance to the drug, therefore, alternative SERMs are constantly being investigated.

Toremifene

Toremifene (**Figure 1.9, [10]**), is a nonsteroidal antiestrogen that blocks the effects of estrogen in the breast tissue, stopping or slowing the growth of cancer cells. Toremifene has been used in postmenopausal women to treat metastatic breast cancer since it was licenced as the first antiestrogen which helps to oppose the action of estrogen in the body.[55, 58] Despite this positive result, toremifene is almost completely cross-resistance with tamoxifen, with similar estrogen agonist effects on the uterus

and its efficacy on bone is less than tamoxifen so that it does not offer a significant advantage.[55]

Raloxifene

Although tamoxifen is the most extensively used hormonal treatment for all stages of hormone responsive breast cancer and has been approved for the prevention of breast cancer in high-risk women, its use is limited by unwanted side-effects.[59, 60] A major adverse effect of tamoxifen is uterine cancer. To date, the new agents are needed for use after tamoxifen. Our research group has published results on novel flexible antiestrogen. These compounds show antiproliferative potency against MCF-7 cells with lower associated cytotoxicity than tamoxifen, meanwhile maintaining good receptor binding affinity and were well tolerated by the ER.[61, 62]

Raloxifene (**Figure 1.9, [11]**), a 2,3-disubstitued benzothiophene containing compound, is a second generation of Selective Estrogen Receptor Modulators (SERMs) that is a potent antiestrogen in the uterus and breast and has estrogenic actions on bone. It binds to the ER with higher affinity than tamoxifen or 4-hydroxytamoxifen. Raloxifene was used for the treatment of osteoporosis in postmenopausal women in 1997. The docked structure of raloxifene in the ERα is shown in Figure 1.10.[63] On September 14, 2007, raloxifene was approved by U.S. FDA for reducing the risk of malignant breast cancer in postmenopausal women with osteoporosis and in postmenopausal women in high-risk of breast cancer.[64]

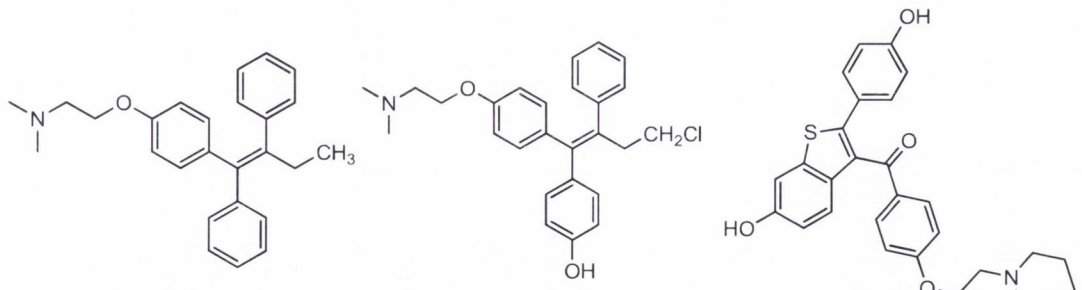

[9] **[10]** **[11]**

Figure 1.9 Tamoxifen [9], Toremifene [10] and Raloxifene [11]

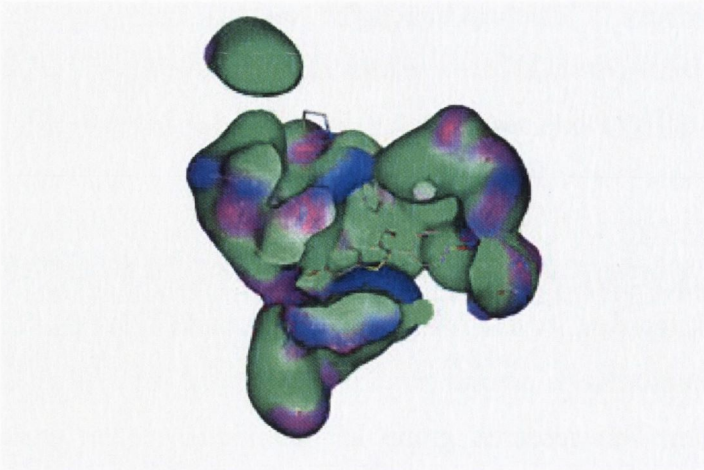

Figure 1.10 Docked structure of Raloxifene in ligand binding site of Estrogen Recepor alpha[65]

✓ Selective estrogen receptor downregulators (SERDs)

Faslodex (Fulvestrant)

Faslodex (**Figure 1.12, [12]**), also known as Fulvestrant or ICI 182,780, is the first agent in the new class of estrogen receptor down-regulator (SERD) to be evaluated in clinical trials.[66] Being an estrogen receptor antagonist with no agonist effects, Faslodex works by down-regulating, as well as degrading the estrogen receptor.[67] *In vivo* studies of Faslodex have shown that this agent exerts a longer suppression of tumour growth than tamoxifen and has antitumor activity in tamoxifen resistant tumours, a finding that is consistant with its mechanism of action.[66] It is prescribed in clinics to help postmenopausal patients who are diagnosed of hormone receptor positive metastatic breast cancer and have developed disease following anti-estrogen therapy.[68]

✓ Aromatase inhibitors

Aromatase inhibitors (AI) are a class of drugs applied in the treatment of breast cancer and ovarian cancer in postmenopausal women. Aromatase is an enzyme that produces estrogen by converting testosterone to estradiol, or androstenedione to estrone (**Figure 1.11**). Owing to their blockade of the synthesis of estrogen, aromatase inhibitors can reduce the estrogen level and slow down the growth of tumours which require estrogen to progress.[69]

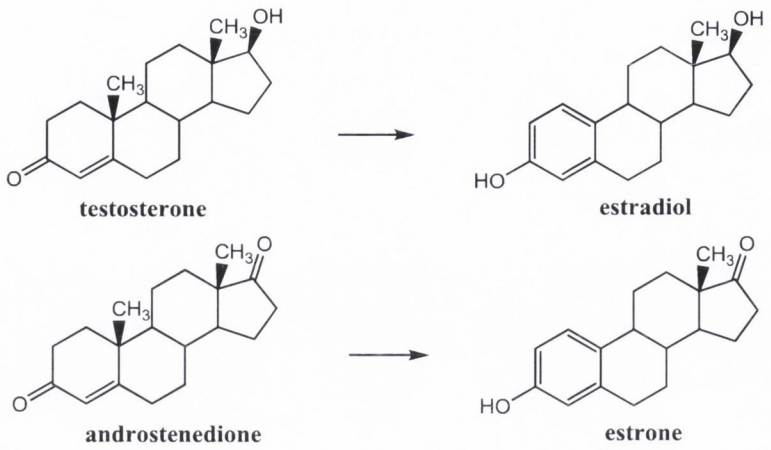

Figure 1.11 Aromatase synthesis route for estrogen

Aromatase inhibitors are divided into two types: non-steroidal inhibitors such as anastrozole, letrozole, which inhibit the enzyme in a reversible mode; and irreversible steroidal inhibitors, which generate a stable irreversible bond with the aromatase enzyme complex, like exemestane.

Anastrozole

Anastrozole (**Figure 1.12 [13]**) is a breast cancer chemotherapy agent used after tumorectomy and for metastases in pre and post-menopausal women. Anastrozole exerts its effective by competitively inhibiting the action aromatase, an enzyme which catalyse androgens into estrogen by aromatization. Since accumulation of estrogens in the body could make breast cancer more malicious through hyperplasia and differentiation in the cancer cells at estrogen receptor sites, decrease of the production of estrogen in peripheral tissues may prevent the progress of breast tumour development in postmenopausal women.[70]

Letrozole

Letrozole (**Figure 1.12, [14]**), is another example of the non-steroidal aromatase inhibitor used in breast cancer chemotherapy. It was approved by the FDA in 1997 for the treatment of primary or metastatic breast tumours which are either known to express hormone receptors or lack of information on their receptor status, in postmenopausal women.[71] Letrozole reduces the body's estrogen level by inhibiting the catalysis of armoatase via competitive and reversible binding to the heme of its cytochrome p450 unit which play an important role in estrogen synthesis. Letrozole acts specifically on the production of estrogen without any effect of decrease the

corticosteroids level. As the main source of estrogen is from the peripheral tissue in postmenopausal women and from ovaries in pre-menopausal women, letrozole is effective only in the former but not the latter.[70]

Exemestane

Exemestane (**Figure 1.12 [15]**), is a steroidal aromatase inhibitor used in the adjuvant treatment of estrogen receptor positive breast cancer in postmenopausal women. It has a similar structure to the substrate of aromatase, and irreversibly and permanently binds to the active site of the enzyme, thus preventing androgens from being converted into estrogen in the peripheral tissues.[70] Additionally, exemestane is superior over tamoxifen by being active in tamoxifen-resistant tumors. However, it is efficient only in postmenopausal women.

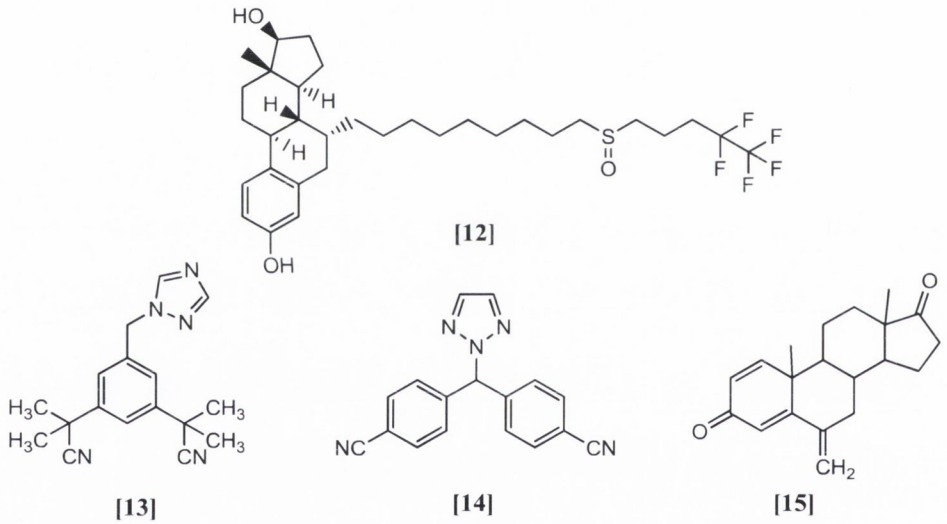

Figure 1.12 Structure of the pure antioestrogens fulvestrant [12] and the aromatase inhibitors anastrozole[13], letrozole[14], exemestane[15]

✓ HER2 (ERBB2) Antibodies

Trastuzumab

Trastuzumab (**Figure 1.13**), is the first molecular-targeted cancer therapy agent approved by FDA for the treatment of invasive breast cancer in 1998.[71] It is a humanised monoclonal antibody that suppresses tumour growth through interfering with the Human Epidermal growth factor Receptor 2 (HER2 or ErbB-2).

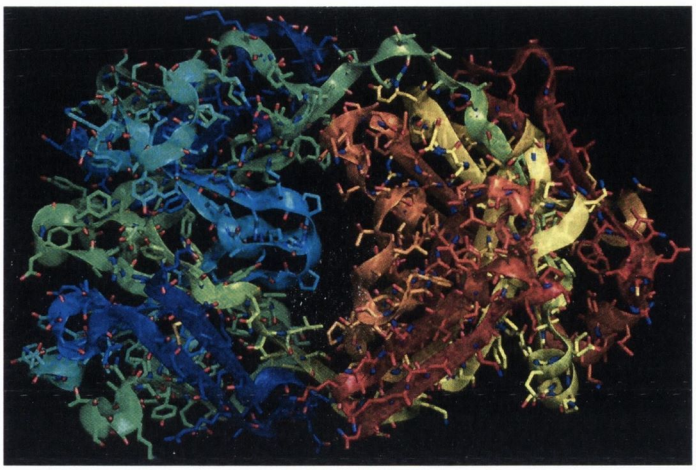

Figure1.13 3D model of the Trastuzumab structure

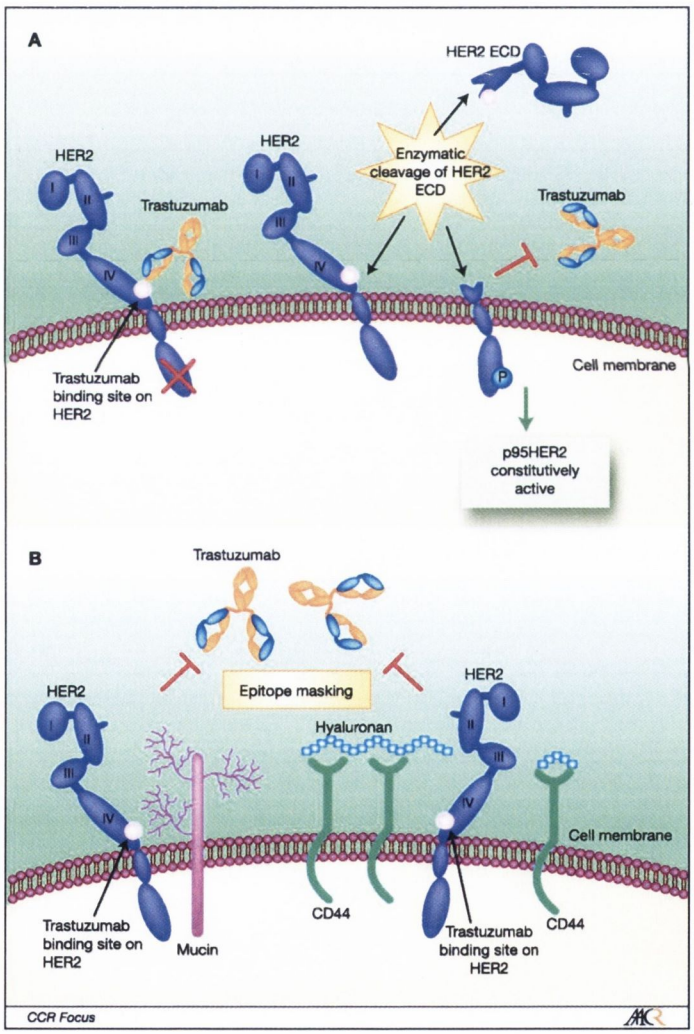

Figure 1.14 General mechanisms of resistance to trastuzumab[72]

HER2 is a member of the HER family which is a group of transmembrane tyrosine kinase receptors that mediate cell growth, survival and other cellular responses.[73] In breast cancer, HER2 is over-expressed and causes uncontrolled cell proliferation.[74]

When trastuzumab is introduced, its two antigen-specific sites selectively bind to the juxtamembrane portion of the extracellular domain of HER2, preventing the activation of its intracellular tyrosine kinase, and as a consequence, results in disruption of cancer cell growth signalling mediated by HER2.[75, 76] Besides, several other possible modes of signalling decreasing activity of trastuzumab have been suggested through studies in animal models, these include prevention of HER2 receptor dimerization, increased endocytotic destruction of the receptor, inhibition of shedding of the extracellular domain, and immune activation (**Figure 1.14**).[77]

Pertuzumab(2C4)

Pertuzumab is a monoclonal antibody and is the first of its class of agents known as a "HER dimerization inhibitor". It impedes HER2 from dimerization with other HER receptors by binding to it, which is suggested to slow down the tumour growth.[78] More efficient increase of inhibition of heterodimerization by pertuzumab has been demonstrated, and is believed to be due to its property of binding further from the cell membrane.[79, 80]

- ✓ HER2 (ERBB2) Small molecule inhibitors

CP-724,714

Small molecule HER2 inhibitors, such as CP-724,714 (**Figure 1.15, [16]**), is an alternative strategy to HER2 antibodies in chemotherapy for patients with HER2-positive breast cancer who do not respond to HER2 antibody therapy.[76, 81] Recent research has shown that CP-724,714 potently inhibited HER2 from autophosphorylation in intact cells, while a serious of biological and biochemical studies revealed that it can induce block of G1 phase of the mitotic cycle in HER2 over-expressing human breast cancers without adverse effects.[76, 82] This agent is currently undergoing phase I clinical trials.

TAK-165

TAK-165 (**Figure 1.15, [17]**), is a relatively new potent HER2 tyrosine kinase with low molecule weight.[83] In previous studies, TAK-165 was confirmed to have effect on bladder cancer, prostate cancer and renal cell carcinoma both *in vitro* and *in vivo*. More recently, TAK-165 has been reported to inhibit HER2 phosphorylation and its down-stream Akt and MAPK in HER2 expressing breast cancer cell (BT474) *in vitro*.

Compared with trastuzumab, TAK-165 has been shown to more significantly inhibit the progression of tumours.[84]

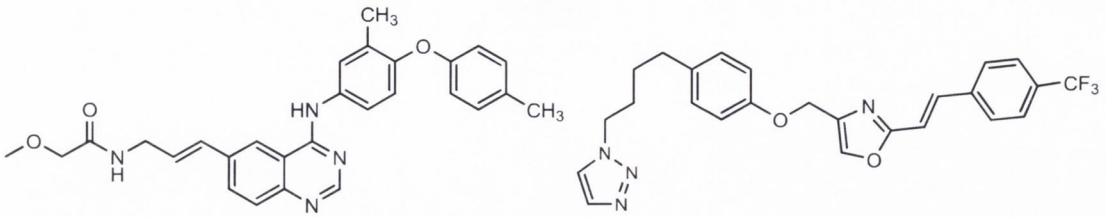

[16] [17]

Figure 1.15 Structure of CP-724,714[16] and TAK-165[17]

✓ HER1 (EGFR)

ZD1839 (Iressa)

ZD1839, also known as Iressa, (**Figure 1.16 [18]**), is the first selective inhibitor that binds to the tyrosine kinase domain of the epidermal growth factor receptor EGFR.[85] It is over-expressed in certain types of human carcinomas such as breast and lung cancers. More specifically, ZD1839 binds to the adenosine triphosphate (ATP) binding site of the tyrosine kinase domain of EGFR, inhibiting the receptor from activating the anti-apoptotic pathways, thereby eliminating tumour growth through the recovered apoptosis.[86] ZD1839 has been used in clinic for non-small cell lung cancer since 2003, and is currently going through the Phase II clinical trials.

OSI-774 (Tarceva)

OSI-774 or Tarceva (**Figure 1.16, [19]**) is a reversible and highly specific inhibitor of EGFR tyrosine kinase. It reversibly binds to the ATP binding site of the receptor. By inhibiting the ATP, the conformational change in intracellular structure is caused and the signalling is stopped which results in apoptosis and suppression of proliferation in tumor cells.[87] Tarceva has been used in the treatment for various cancer forms, including non-small cell lung cancer, locally advanced pancreatic cancer and metastatic breast cancer.[86]

EKB-569

EKB-569 (**Figure 1.16, [20]**) is another potent, selective and irreversible inhibitor of EGFR with low molecular weight. Being developed as an anticancer agent, EKB-569 is now under evaluation in phase II clinical trials for breast cancer.[88]

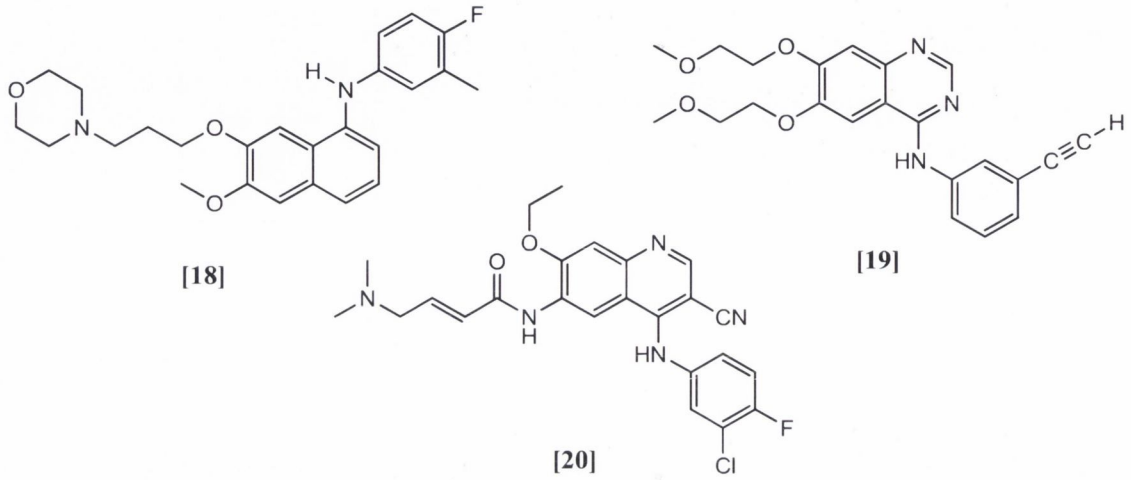

Figure 1.16 Structure of ZD1839 [18], OSI-774 [19] and EKB-569 [20]

✓ HER2 and HER1

GW572016

GW572016 (**Figure 1.17, [21]**), also named as Lapatinib, was developed by GSK as an anti-cancer agent for the treatment of solid tumours, such as breast and lung cancer.[89, 90] It was approved by FDA in 1997 for combination therapy with Capecitabine for advanced metastatic breast cancer. It is a dual inhibitor of EGFR and HER2 tyrosine kinase, binding to the intracellular phosphorylation domain to prevent receptor autophosphorylation upon ligand binding and subsequent activation of the receptor tyrosine kinase signal transduction.[91]

✓ HER Kinases

CI-1033(canertinib)

CI-1033 (**Figure 1.17, [22]**) is an irreversible ErbB inhibitor targeting multiple ErbB receptors and extends inhibition of ErbB-mediated signalling.[92] Most tyrosine kinase inhibitors compete with the ATP binding site to inhibit phosphorylation. *In vitro* studies of human cancer cell lines showed that CI-1033 have prompt, potent, sustained and highly selective inhibition of ErbB tyrosine kinase activity without

inhibiting tyrosine kinase activity of other types of receptors.[93, 94] Phase II clinical trials were carried out.[95]

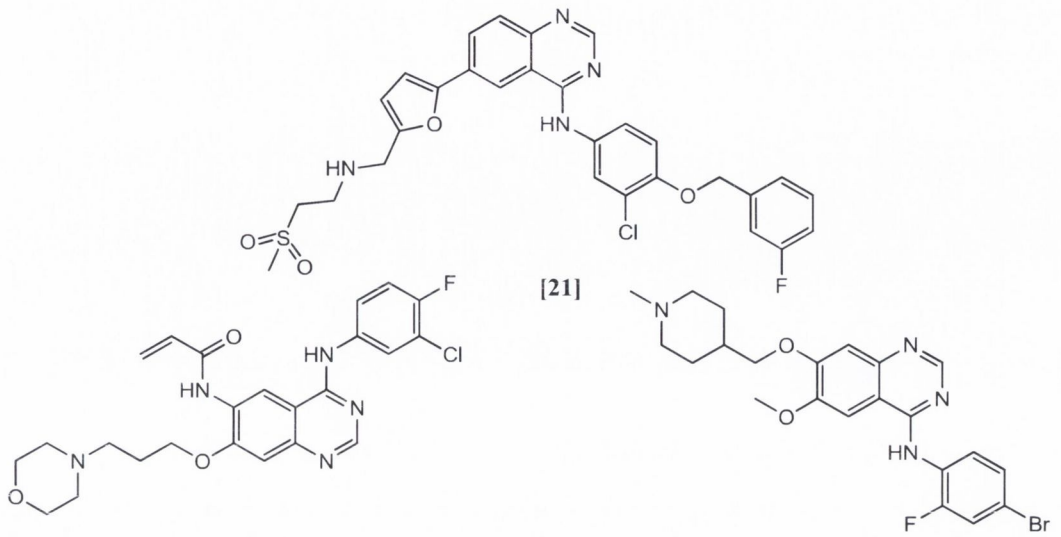

[21]

[22]

[23]

Figure 1.17 Structure of GW572016 [21], CI-1033 [22] and ZD6474 [23]

✓ VEGF

Bevacizumab

As a humanized monoclonal antibody and the first angiogenesis inhibitor used in clinic, bevacizumab (trade name Avastin) was used for treatment of cancer and eye disease when it was approved by FDA a few years ago. It blocks vascular endothelial growth factor A (VEGF), which is a chemical signal stimulating the growth of new blood vessels, especially in cancer, and other disease.[96] Tumour growth is therefore stopped due to prohibited formation of new blood vessels. Clinical studies of Bevacizumab are undergoing in non-metastatic breast cancer, ovarian cancer, and other carcinomas. However, it was suggested to be removed from use by FDA in December 2010,[97] since this drug has not been shown to be safe and effective in breast cancer patients.

✓ VEGFR2

ZD6474

ZD6474 (**Figure 1.17, [23]**) or Vandetanib, is a tyrosine kinase inhibitor currently underway of clinical trials in phase II as a potential targeted treatment for non-small cell lung cancer and breast cancer.[98] ZD6474 is an antagonist of the vascular

endothelial growth factor receptor (VEGFR) and the epidermal growth factor receptor (EGFR) inhibiting the RET-tyrosine kinase activity which is an important growth driver, eventually leading to the halting of tumour growth.[99]

✓ Farnesyl transferase

R115777 (Zarnestra)

R115777, or Zarnestra (**Figure 1.18, [24]**), is a selective inhibitor of farnesyltransferase, which adds a 15-carbon farnesyl lipid to the carboxy-terminal cysteine of a number of cell-signalling proteins.[100] However, clinical trials on this farnesyl transferase inhibitor have failed to show any benefit for treatment in breast cancer while high toxicity adverse effects being observed.[101]

SCH66336 (Sarasar)

SCH66336, also named as Sarasar (**Figure 1.18, [25]**), is a faresyl-OH-transferase inhibitor that prevents the enzyme from transferring a farnesyl group from farnesyl pyrophosphate to the pre-Ras protein. Since without the farnesyl group, Ras proteins can not attach to cell membrane to transfer signals from membrane receptors.[102, 103] However, clinical studies showed that Sarasar was found to have major side effect such as fatigue, diarrhea and nausea.[104]

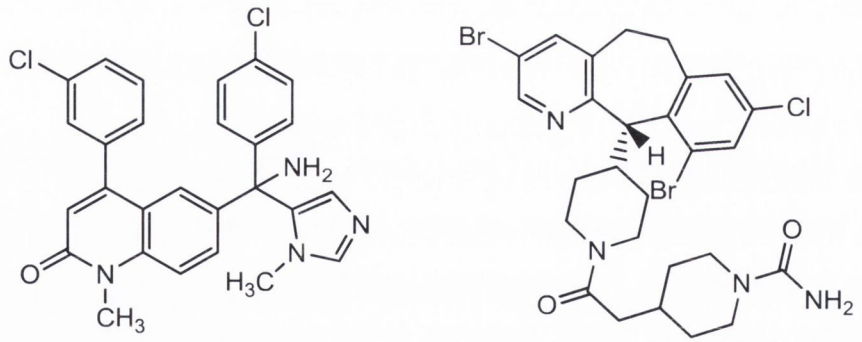

[24] **[25]**

Figure 1.18 Chemical structure of R115777[24], SCH66336[25]

✓ CDK kinases

Cyclin-dependent kinases (CDKs) are a family of protein kinases which play an essential role in regulating the cell cycle. They also play a part in regulating transcription, mRNA processing, and the differentiation of nerve cells.[105] Regulation of cell cycle by CDKs is controlled by a serious of positive and negative upstream

mechanisms as indicated in **Figure 1.19**. A CDK inhibitor interacts with a cyclin-CDK complex to block its kinase activity, normally during G1, or in response to signals from damaged DNA or from the environment.[106]

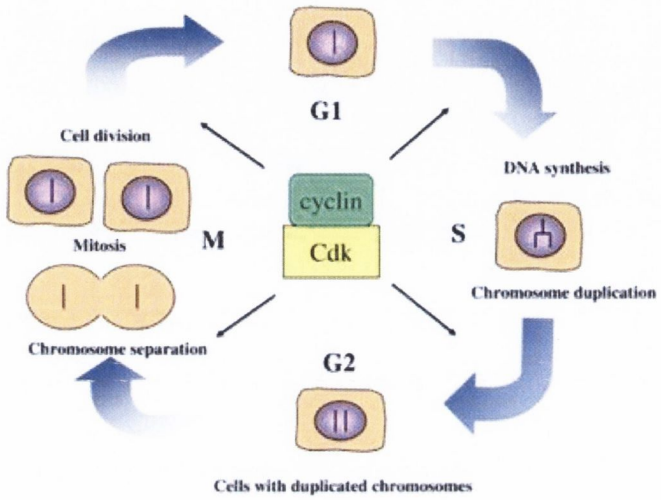

Figure 1.19 CDKs are the regulators in eukaryotic cells

Flavopiridol

Flavopiridol, also known as Alvocidib, (**Figure 1.20, [26]**) was the first CDK inhibitor to be tested for clinical use since it was indentified as an anti-cancer agent in 1992. It is a semisynthetic flavonoid derived from rohitukine (**Figure 1.20, [27]**), an alkaloid isolated from a plant in India. It competes for the ATP site of the CDKs.[107] Flavopiridol was indicated in initial studies to have clear effects on cell cycle progression, induce differentiation and apoptosis, modulates transcription, and has antiangiogenic properties.[108] Phase II clinical trials on Flavopiridol for treatment of breast cancer are underway.[109]

UCN-01

The small molecule UCN-01 (**Figure1.20, [28]**), is a cyclin-dependent kinase (CDK) modulator demonstrated to have antiproliferative activity against several cancer models. It was also investigated with respect to isozyme-specific PKC inhibition, and exhibited anti-tumour activity *in vitro* and *in vivo*.[110] The exact mechanism of how UCN-01 promotes cell cycle arrest is still unclear, although it may inhibit several serine-threonine kinases.[111] Currently it being tested in Phase I clinical trials for breast cancer.[112]

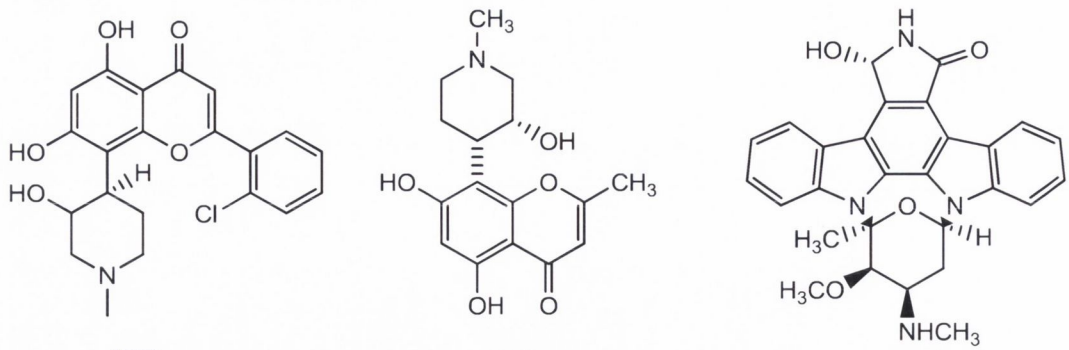

[26] [27] [28]

Figure 1.20 Structure of Flavoporodol[26], Rohitukine[27] and UCN-01[28]

✓ mTOR kinase

CCI-779 (Temsirolimus)

The mammalian target of rapamycin (mTOR) is a serine/threonine protein kinase that regulates cell growth, cell motility, cell proliferation, cell survival, DNA transcription and protein synthesis.[113, 114] Being the catalytic subunit of two molecular complexes, mTORC1 and mTORC2,[114] mTOR collects and interprets the input from upstream pathways, such as insulin (shown in **Figure 1.21**), growth factors and mitogens. In tumour cells, mTOR is activated by various mechanisms including growth factor surface receptor tyrosine kinases, oncogenes, and loss of tumour suppressor genes, which play a key role in malignant cell transformation and progression.[115] Regulation of mTOR pathwayis disordered in certain human cancers.

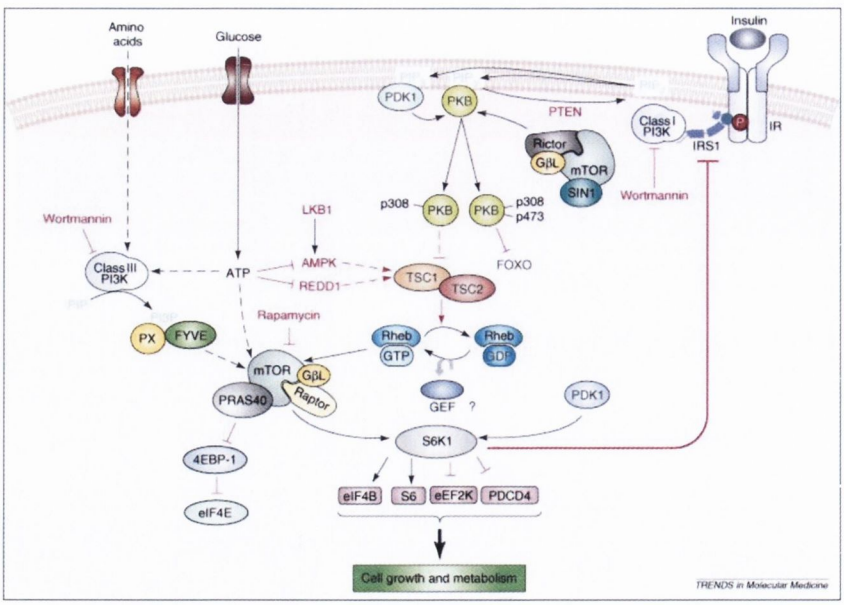

Figure 1.21 mTOR signalling pathway[116]

CCI-779 (Temsirolimus)

Temsirolimus (CCI-779) (**Figure1.22 [29]**) is an intravenous drug for the treatment of miscellaneous cancer. It specifically inhibits mTOR and interferes with the production of proteins that regulate tumour cell growth, survival and proliferation, leading to cell cycle arrest in the G1 phase. Additionally, temsirolimus inhibits the development of tumour blood vessels by down-regulating the synthesis of VEGF.[117] However temsirolimus carry many toxic side effects based on currently clinical trials in phase II for breast cancer.[118]

RAD001 (Everolimus)

As a member of derivatives of sirolimus which work similarly as mTOR inhibitors, RAD001, also named Everolimus, (**Figure 1.22 [30]**) is currently used to prevent rejection of organ transplants. It has been investigated with other mTOR inhibitors for use in treatment of a number of cancers. In a similar fashion to other mTOR inhibitors, RAD001 is only active on the mTORC1 protein and not on the mTORC2 protein. It inhibits the mTORC1 negative feedback loop while not interacting with the mTORC2 positive feedback to AKT, leading to a hyper-activation of the kinase AKT, which in turn extends survival in some cell types.[119] Phase III clinical trials of RAD001 were underway in breast cancer and lymphoma in October 2010.[120]

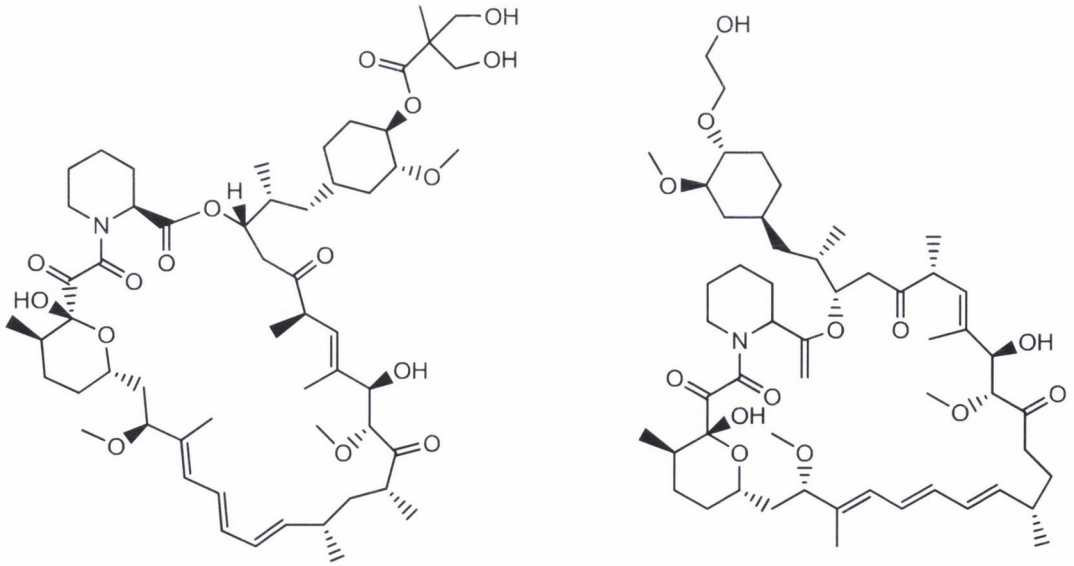

[29] [30]

Figure 1.22 Structure of CCI-779[29], EAD001[30]

Many other targets have been identified as novel agents for treatment of breast cancer. These include the potent modulator of protein kinase C (PKC) broystatin (**Figuer**

1.23, [31]),[121] Bay 43-9006 (**Figure 1.23, [32]**), a novel signal transduction inhibitor that targets RAF pathway in tumour cells,[122] CI-1040 (**Figure 1.23,[33]**), a potent, selective and non-competitive inhibitor of MEK1 and its activation,[123] Perifosine (**Figure 1.24,[34]**), an Akt inhibitor in human cancer,[124] 17-allylamino-17-demtehoxygeldanamycin (17-AAG) (**Figure 1.23, [35]**), a potent heat-shock protein 90 (Hsp90) inhibitor that can degrade polyglutamine-expanded mutant androgen receptor (AR),[125] Marimastat (BB-2516) (**Figure 1.23, [36]**), the first matrix metalloproteinase inhibitor to have entered clinical trials,[126] ST1571 (**Figure 1.23, [37]**), a tyrosine kinase inhibitor initially developed as a BCR/ABL inhibitor, selectively inhibiting platelet-derived growth factor receptors (PDGFRs) and c-kit,[127] and suberoylailide hydroxamic acid (SAHA) (Figure 1.23, [38]), a potent inhibitor of histone deacetylases (HDACs) that causes growth arrest, differentiation and apoptosis of tumour cells[128].

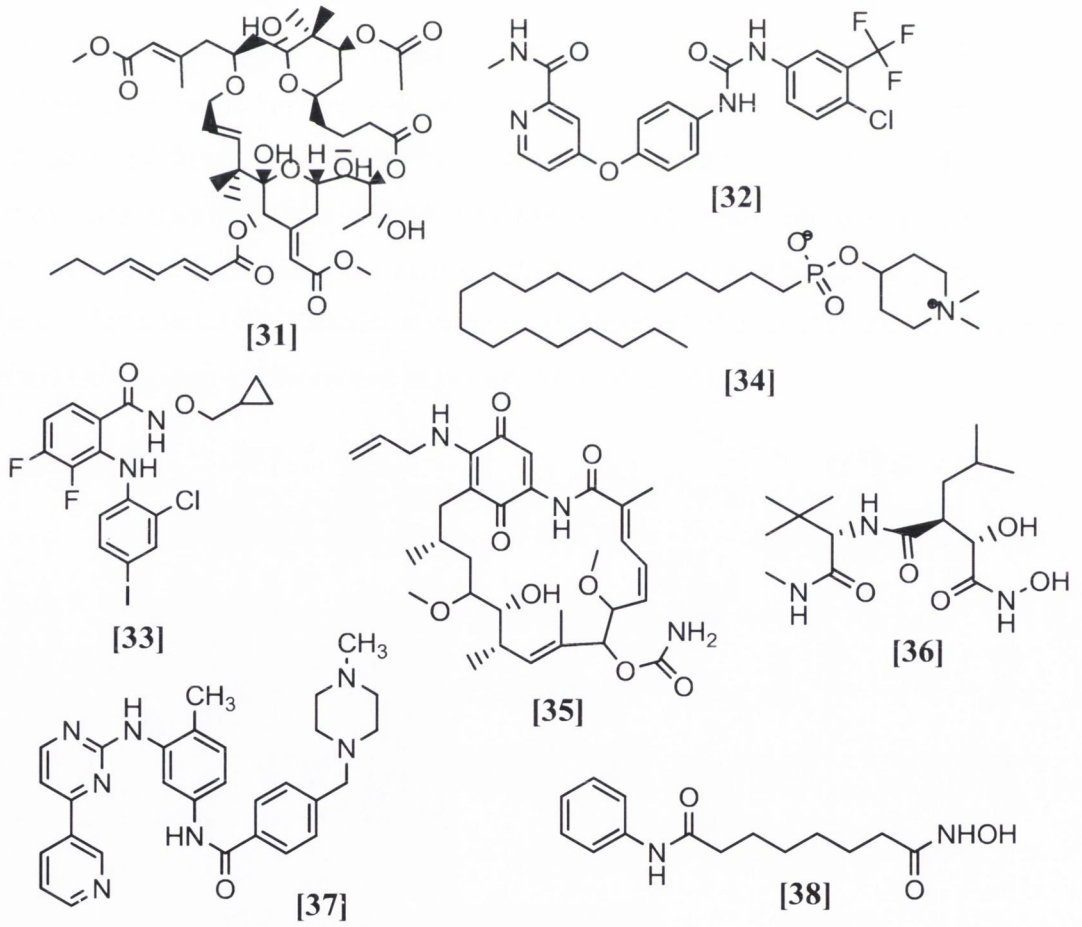

Figure1.23 Structure of some chemotherapy agents for breast cancer

1.4 Pyrazoles as bioactive compounds

In this thesis a comprehensive series of novel heterocyclic compounds containing the 1,4-dihydropyridine and pyrazole scaffold structures which display interesting antiproliferative properties are investigated. These structures were developed as part of an *in silico* high throughput screening programme in our research group.[129] As an introduction to these heterocycles, the pharmacological activity associated with 1,4-dihydropyridines and pyrazole containing compounds is reviewed in the following section, with particular emphases on the associated cytotoxic properties.

1.4.1 Structure

Pyrazoles are heterocyclic compounds characterized by a five-membered aromatic ring structure consisting of three carbon atoms and two nitrogen atoms in contiguous positions. Similar to its structural isomer imidazole, pyrazole contains a pyrrole-like and a pyridine-like N-atom positioned in the 1- and 2-positions. (**Figure 1.24**) Structurally related compounds are pyrazolidine and pyrazoline.

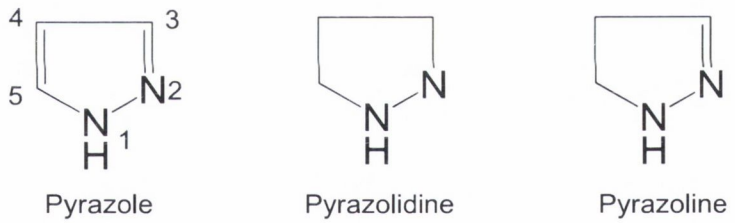

Figure1.24 Chemical structure of Pyrazole related compounds

Pyrazole as a scaffold is a feature of a number of bioactive compounds, such as celecoxib (Figure 1.24,[40]), fomepizole (Figure 1.28, [49]), AM251 (Figure 1.27 [47]).[130] However, they were rarely found in nature until 1-pyrazolyl-alanine was firstly isolated from seeds of watermelons in 1959.[131] Normally pyrazoles are produced synthetically through various ways. Pyrazole can be synthesized from acetylene and diazomethane in a classical method developed by Pechmann, H. in 1898.[132] Several synthetic routes are discussed below.

1.4.2 Methods for synthesis

There are a number of synthetic routes which are very helpful for the formation of the heterocycle ring. The most popular synthetic methods are the Knorr pyrrole reaction, Vilsmeier-Haack reaction.[133] These methods are summarized below:

1.4.2.1General synthetic route for pyrazole-containing fused rings

Heller, S.T. et al[134] has described the use of 1,3-diketones that were synthesized *in situ* from ketones and acid chloride and then converted into pyrazoles by the addition of hydrazine. (**Scheme 1.1**) This method gives a fast and general synthetic route for pyrazole-containing fused rings.

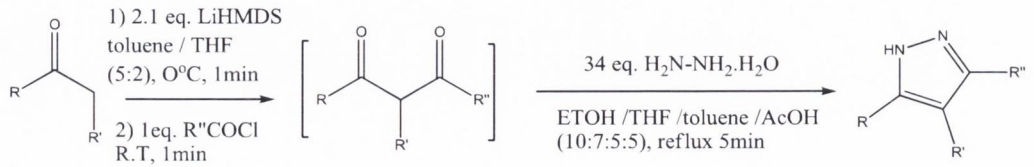

Scheme 1.1 General synthesis route for pyrazole-containing fused rings

1.4.2.2 Highly regioselective synthesis of 1-Aryl-3,4,5-Substituted Pyrazoles

The synthesis of 1-aryl-3,4,5-substituted pyrazoles based on the condensation of 1,3-diketones with arylhydrazines is illustrated in **scheme 1.2**. This highly regioselective synthesis proceeds at room temperature in N,N-dimethylacetamide and obtains pyrazoles in good yields.[135]

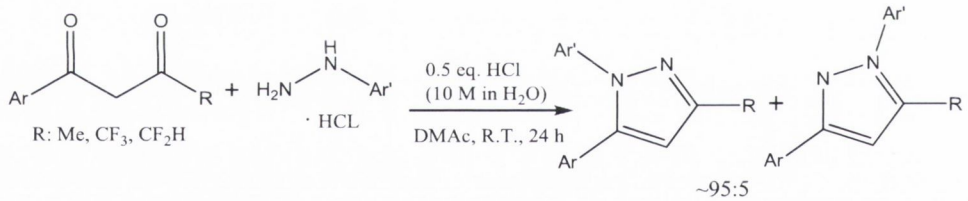

Scheme 1.2 Highly regioselective synthesis of 1-aryl-3,4,5-substituted Pyrazoles

1.4.2.3 Construction of pyrazole with palladium catalyzed four component coupling

Pyrazoles serves as biologically active molecules with wide application. Ahmed, M.S.S. et al[136] synthesized five-membered heteroaromatics such as pyrazole via one-pot, four component coupling of terminal alkynes, hydrazine, and aryl iodide at room temperature and an ambient pressure of carbon monoxide in the presence of a palladium catalyst. (**Scheme 1.3**) Hydrazine and hydroxylamine were used as components not only for ring formation but also for activating agents for the carbonylation coupling reaction.

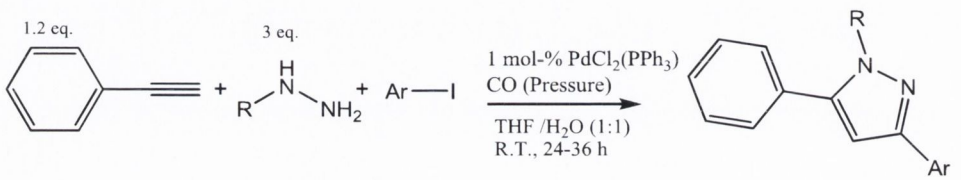

Scheme 1.3 Construction of pyrazole with palladium catalyzed four component coupling

1.4.2.4 One-Pot synthesis of N-Arylpyrazoles from Aryhalides

It has been showed by Gerstenberger, B.S. et al[137] that N-arylpyrazoles are an important structural class in pharmaceuticals and agrochemicals. These authors reported a quick and simple one-pot synthesis of N-arylpyrazoles and diversely functionalized pyrazoles from arylnucleophiles, di-*tert*-butylazodicarboxlate, and 1,3-dicarbonyl or equivalent compounds as presented in (**Scheme 1.4**).

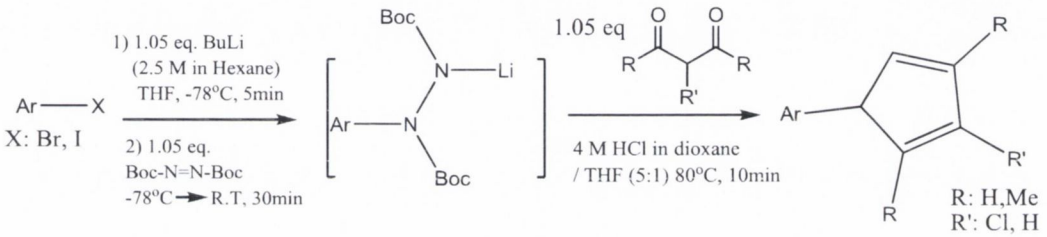

Scheme 1.4 One-Pot synthesis of N-arylpyrazoles from aryhalides

1.4.2.5 Base-meduated reaction of hydrazone and nitroolefins

Substituted pyrazoles are a particularly important class of bioactive compounds in the pharmaceutical industry. Specially interesting in agents are 1,3,5-tri and 1,3,4,5-tetrasubstituted pyrazoles, which are contained in the core structures of currently used drugs such as Celecoxib. Two general protocols are developed for the regioselective synthesis of 1,3,5-tri and 1,3,4,5-tetrasubstituted pyrazoles by the reaction of electron-deficient N-arylhydrazones with nitroolefins are outlined by Deng, X.H. et al[138] Research on the stereochemistry of the key pyrazolidine intermediate indicate a stepwise cycloaddition mechanism.

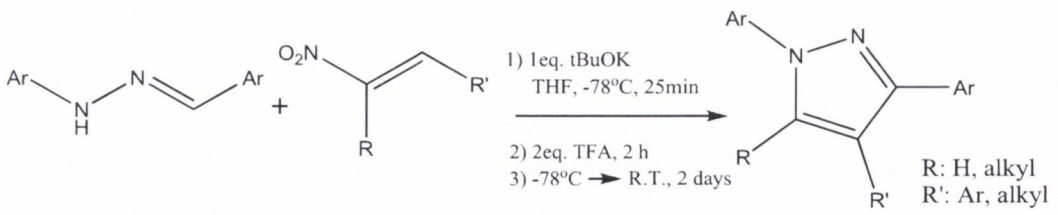

Scheme 1.5 Base-meduated reaction of hydrazone and nitroolefins

1.4.2.6 N-monosubstituted hydrazone with nitroolefins for pyrazole synthesis

In a further extension of this work, a novel regioselective synthesis of substituted pyrazoles from N-monosubstituted hydrazones and nitroolefins is described by Deng et al. [139] (**Scheme 1.6**) This reaction is performed in a one-pot manner and achieved

good yields which is suitable for library synthesis in drug discovery efforts. Therefore, a key nitropyrazolidine [39] intermediate was characterized and the mechanism for the heterocycle synthesis was provided. (**Scheme 1.7**)

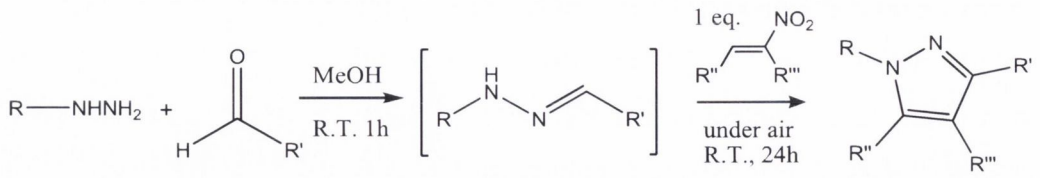

Scheme 1.6 N-monosubstituted hydrazone with nitroolefins for pyrazole synthesis

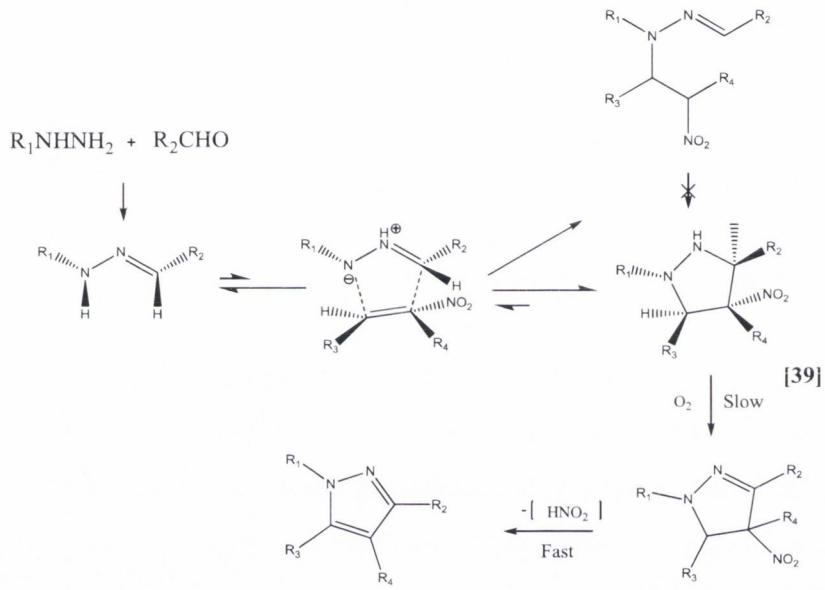

Scheme 1.7 Mechanism of pyrazole synthesis

1.4.2.7 Cu-catalyzed C-N coupling/Hydroamidation

Nitrogen-containing heterocycles compounds occur as biologically active natural products which have some clinical uses.[140] The strategies for the synthesis of heterocycles which are based on metal-catalyzed reactions have been developed by Martin et al.[141] They demonstrated a general, highly flexible and efficient Cu-catalyzed domino C-N coupling/hydroamidation reaction for the preparation of pyrazoles and pyrroles. (**Scheme 1.8**) The proposed mechanism has shown the metal to play a dual role in facilitating amidation and hydroamidation reaction.

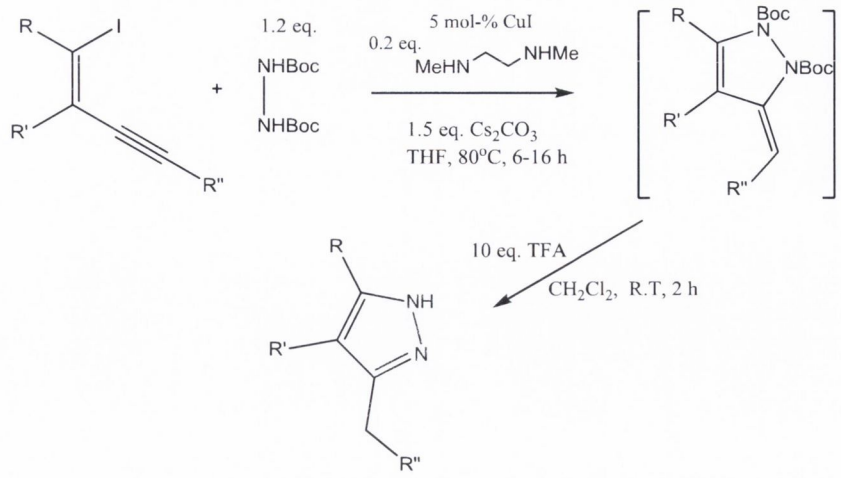

Scheme 1.8 Synthesis of heterocycles through a domino copper-catalyzed amidation/hydroamidation sequence

1.4.2.8 Selective route to substituted 1-Acyl-4-iodo-1H-pyrazole

To date, pyrazole and derivatives have exhibited the wide variety of biological activities such as analgestic, anti-inflammatory, hypoglycaemic, antihypertensive, and antimicrobial activity in pharmaceutical applications.[142-145] Waldo et al.[146] reported that a number of substituted 1-acyl-5-hydroxy-4,5-dihydro-1H-pyrazoles have been synthesized as intermediate from the corresponding 2-alkyn-1-ones. In most cases, preparation of the 1-acyl-4-iodo-1H-pyrazoles proceeded in good yield by undergoing dehydration and iodination in the presence of ICI and Li_2CO_3 under mild reaction conditions. (**Scheme 1.9**)

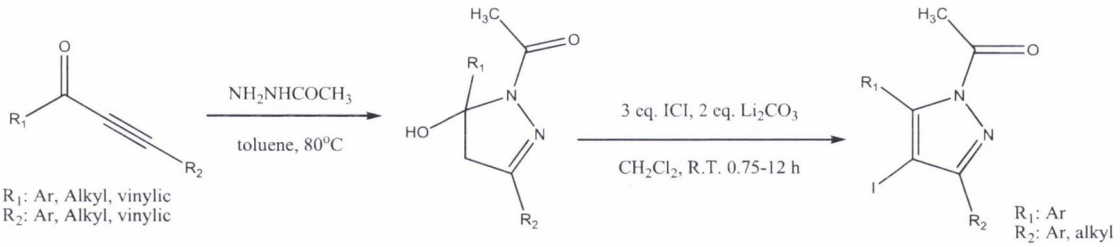

Scheme 1.9 Selective route to substituted 1-Acyl-4-iodo-1H-pyrazole

1.4.2.9 Regiospecific synthesis of pyrazole-5-carbonylates from enaminodiketones

Rosa et al[147] demonstrated a variety of enaminodiketones used as precursors for the construction of new heterocycle derivatives. Therefore, a regioselective method for the synthesis of 4-substituted 1H-pyrazole-5-carboxylates which were prepared from the cyclocondensation reaction of unsymmetrical enaminodiketones with *tert*-butylhydrazine or carbonoxymethylhydrazine has been developed. However, the

obtained compounds were a mixture of two or three regioisomers A, B or C, which can be purified by chromatography. (**Scheme 1.10**)

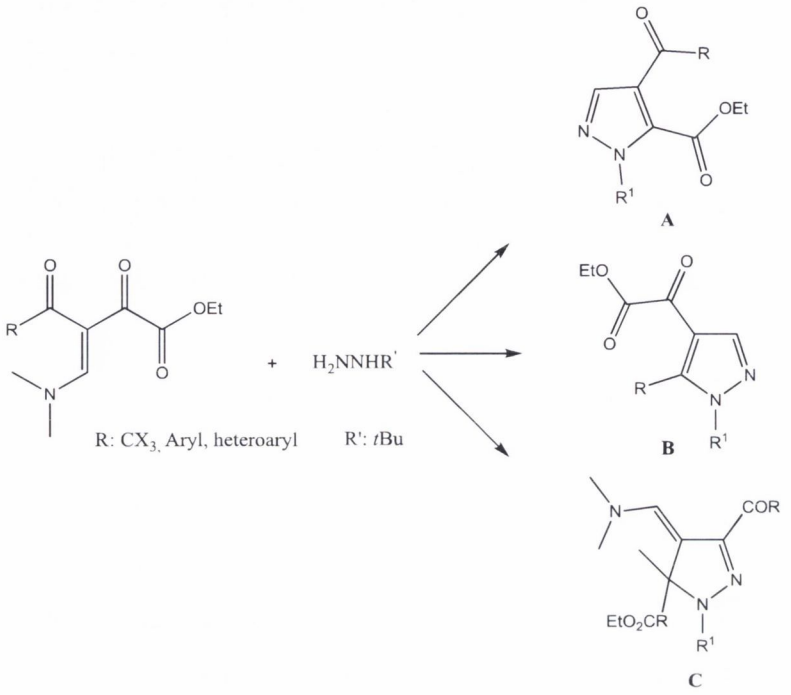

Scheme 1.10 Regiospecific synthesis of pyrazole-5-carbonylates from enaminodiketones

1.4.2.10 Synthesis of di- and trisubsituted pyrazoles via [3+2] cycloaddition reaction

Recently, Hari et al.[148, 149] reported that pyrazole can be synthesized by [3+2] cycloaddition reaction with ethyl propiolate or dimethyl acetylenedicarboxylate(DMAD). In this case, they described how TMSC(MgBr)N_2 would react with simple aldehydes and ketones to achieve the corresponding 2-diazo-2-trimethylsilyl ethanols. Afterwards a variety of diazoalcohols reacted with DMAD to give the trisubstituted pyrazole in good yield in two steps.(S cheme 1.10)

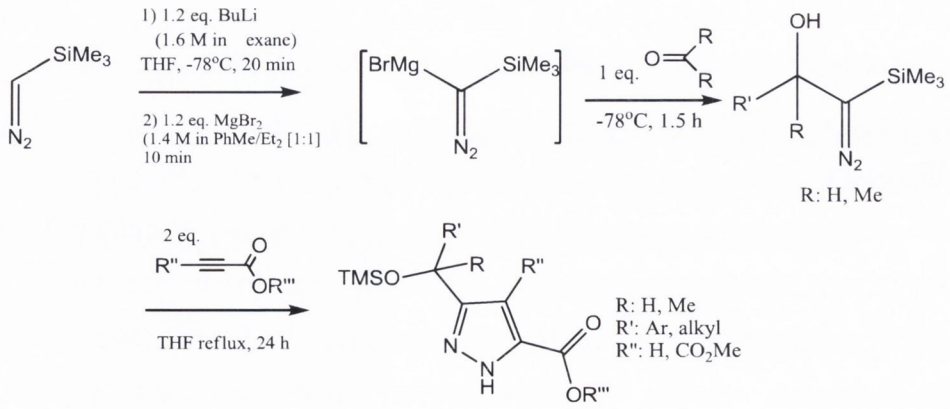

Scheme 1.11Synthesis of di- and trisubsituted pyrazoles via [3+2] cycloaddition reaction

1.4.2.11Oxidative aromatization of 1,3,5-Trisubstituted pyrazolines for corresponding pyrazoles

1,3,5-trisubstituted pyrazolines can be easily prepared from phenylhydrazine and chalcone derivatives. Nakamichi et al.[150] examined the reaction of dihydro compounds such as pyrazolines and dihydropyridines with oxidizing reagents, catalytic amount of Pd/C in acetic acid to produce pyrazole and pyridine derivatives. (**Scheme 1.12**)

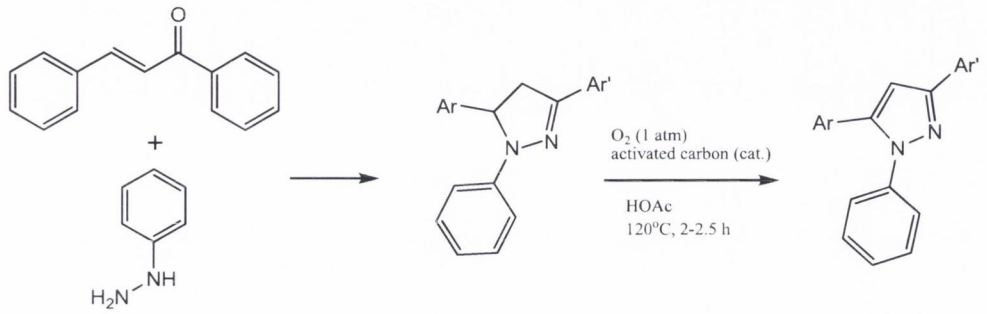

Scheme 1.12 Oxidative aromatization of 1,3,5-Trisubstituted pyrazolines for corresponding pyrazoles

1.4.2.12 Heterocycle formation from 1,3-dinitroalkanes via Nef reaction

Aliphatic nitro compounds are useful intermediates in organic synthesis, 1,3-dinitroalkanes has been reported by Escribano et al.[151] as synthetic equivalents for 1,3-dicarbonyl compounds through Nef reaction under usual conditions(NaOH, conc.H_2SO_4). Subsequently, they can be converted into azole heterocycles (**Scheme 1.13**). The pyrazole-forming reaction mechanism probably is processed by the nucleophilic attack of hydrazine on the electron-deficient C-1 of the nitronic acid, and then followed by dehydration and elimination of the elements of hyponitrous acid (HNO). Eventually the pyrazole is obtained by intramolecular attack of the amino group of the resulting hydrazone on C-3 and elimination of H_2O and HNO again. (**Scheme 1.14**)

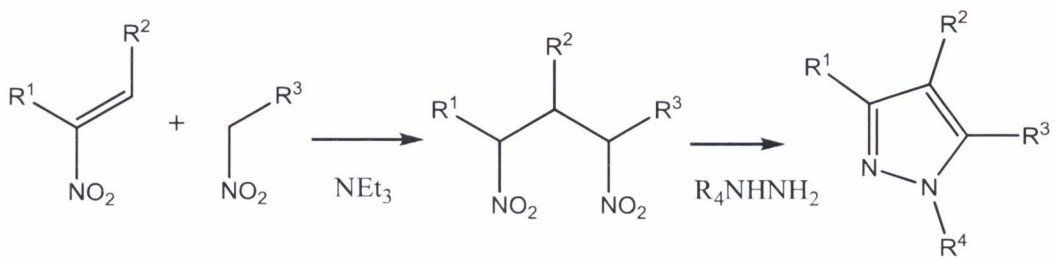

Scheme1.13 Heterocycle formation from 1,3-dinitroalkanes via Nef reaction

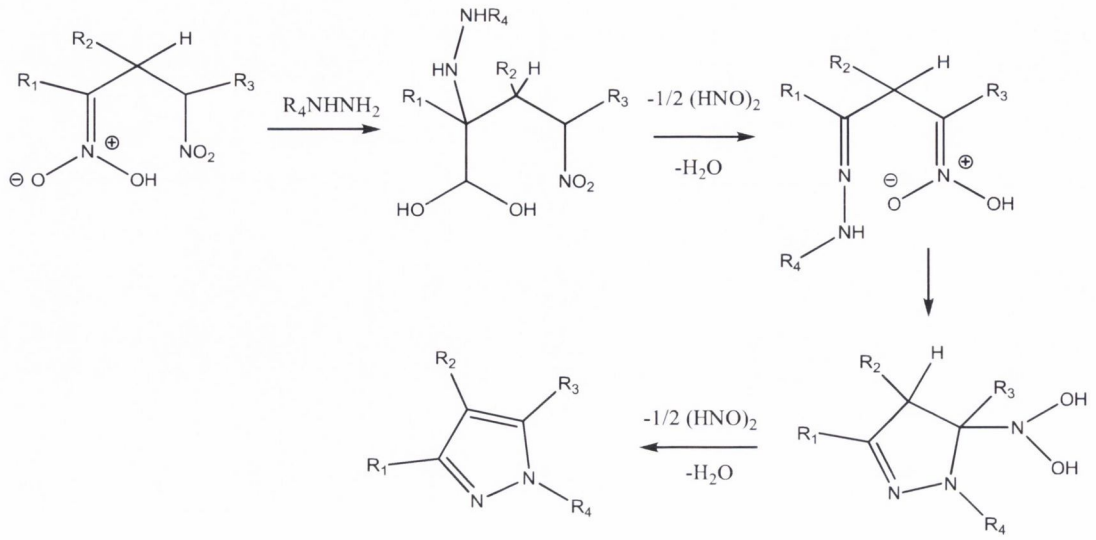

Scheme 1.14 Mechanism of pyrazole-forming reaction

1.4.3 Pyrazoles as biologically active compounds

Compounds containing the structure of the pyrazole ring have been shown to possess a large variety of biochemical and pharmacological properties. Examples of pyrazole derivatives are given below.

1.4.3.1 Non-steroidal anti-inflammatory drug (NSAID)

Celecoxib

Celecoxib (**Figure 1.25, [40]**) is a diaryl-substituted pyrazole, chemically described as 4-[5-(4-methylphenyl)-3-(trifluoromethyl)-1H-pyrazol-1-yl] benzenesulfonamide. It is a non-steroidal anti-inflammatory drug (NSAID) clinically used in relief of pain and inflammation in osteoarthritis, rheumatoid arthritis and ankylosing spondylitis. Application of celecoxib for the treatment of acute pain, painful menstruation and menstrual symptoms was also reported.[151] Moreover patients with familial adenomatous polyposis benefit from celecoxib for its reduction of numbers occurring in colon and rectum. Because of its over 7 times more selectivity for COX-2 inhibition over COX-1, celecoxib was originally intended to relieve pain while in theory minimizing the gastrointestinal adverse drug reactions usually caused by conventional NASIDs which inhibit both COX-1 and COX-2.[152] Related drugs include Deracoxib **[41]** and Tepoxalin **[42]**.

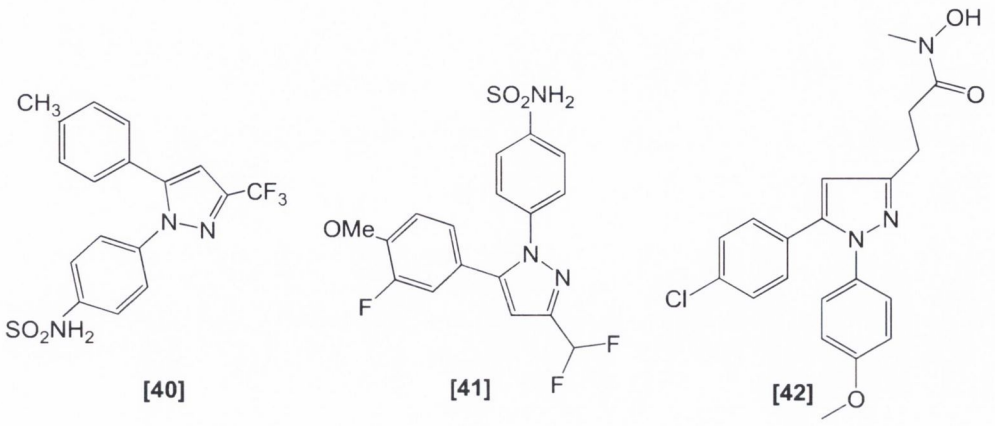

Figure1.25 Structure of Celecoxib[40], Deracoxib[41],Tepoxalin[42]

1.4.3.2 GABA receptor antagonist

Indiplon

Indiplon (**Figure 1.26, [44]**) is a nonbenzodiazepine primarily binding to the α_1 subunits of the $GABA_A$ receptors in the brain and upon that, like most other nonenzodiazepine sedatives, enhancing the action of the inhibitory neurotransmitter GABA. It is being developed as a hypnotic sedative in 2 formulations - an immediate release product for the treatment of insomnia and a modified release version for sleep maintenance.[153] Another related GABA targeting compound is Fipronil (**Figure 1.26, [43]**).

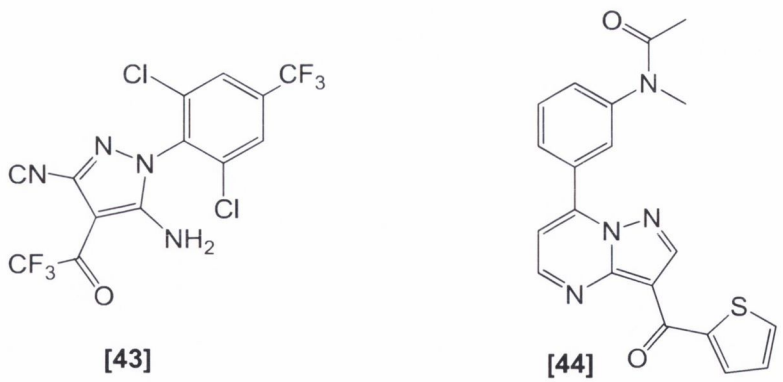

Figure 1.26 Structure of Fipronil[43], Indiplon[44]

Ocinaplon

Ocinaplon (**Figure 1.27, [45]**) is an anxiolytic drug in the class of drugs of pyrazolopyrimidine. Pharmacologically similar to the benzodiazepine family of drugs, it is distinguish by its relatively little sedative or amnestic effect but mainly anxiolytic properties where ocinaplon modulates $GABA_A$ receptors, although it is

more subtype-selective than most benzodiazepines.[154] Zaleplon (**Figure 1.27, [46]**) is a nonbenzodiapine hypnotic/sedative from the pyrazolopyrimidine family mainly used for insomnia and controlling of anxiety. Like ocinaplon, zaleplon has a similar pharmacological profile to benzodiazepines in the increase in slow wave deep sleep (SWDS) with rapid onset of hypnotic action and acts as a full agonist for the benzodiazepine α_1 receptor which is located on the $GABA_A$ ionophore receptor complex in the brain.[155]

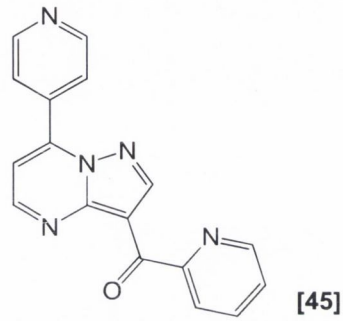

[45]

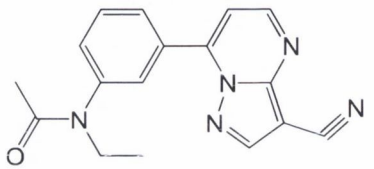

[46]

Figure 1.27 Structure of Ocinaplon[45], Zaleplon [46]

1.4.3.3 Cannabinoid receptor antagonist

AM251

AM251 (**Figure 1.28, [47]**) is a brain cannabinoid receptor (CB1) antagonist, in which a *p*-iodo group, in replacement of the *p*-chloro group, is present as the phenyl substituent at C-5 of the pyrazole ring. Structurally close to rimonabant, AM251 is also in common with this lead compound in the role of being biarylpyrazole cannabinoid receptor antagonists, whereas it exhibits about two-fold more selective for the CB1 receptor when compared to rimonabant (**Figure 1.28, [48]**) in binding affinity.[156]

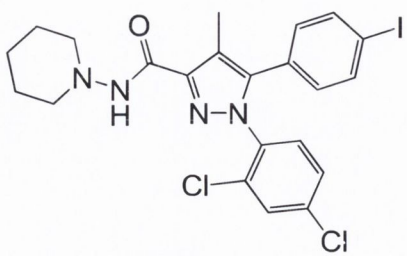

[47]

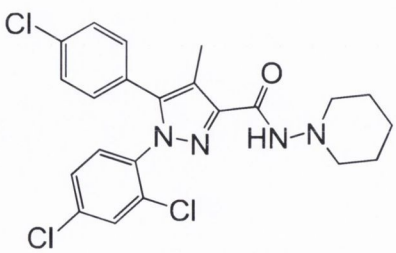

[48]

Figure 1.28 Structure of AM251[47], Rimonabant[48]

1.4.3.4 Fomepizole

Fomepizole (**Figure 1.29, [49]**) or 4-methylpyrazole competitively inhibits the catalysis of alcohol dehydrogenase, a member of oxidoreductases, the initial steps in the metabolism of ethylene glycol and methanol to their toxic metabolites,[157] therefore could be applied as an antidote alone or in combination with hemodialysis in confirmed or suspected methanol or ethylene glycol poisoning.[158] Tebufenpyrad (**Figure 1.29, [50]**) is a pyrazole acaricide in the form of a white crystalline solid commonly used in aqueous solution in commercial greenhouses as an insecticide. Practically innocuous to birds, it is nevertheless found to be very toxic to fish.[159]

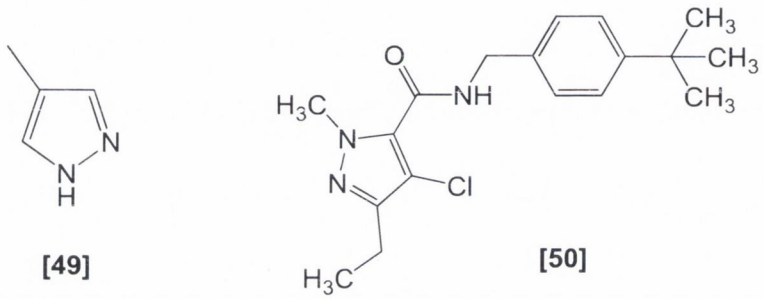

[49] [50]

Figure 1.29 Structure of Fomepizole[49], Tebufenpyrad[50]

1.4.4 Antiproliferative activity of pyrazoles

The uses of biologically active pyrazoles range from insecticides to non-steroidal anti-inflammatory drugs (NSAIDs). Traditional NSAIDs such as aspirin, indomethacin and ibuprofen have been shown to inhibit the prostaglandins (PG) synthesis and thereby reduce tumor growth, metastasis and angiogenesis.[160] Prostaglandins were found to be proangiogenic by themselves and to up-regulate the expression of vascular endothelial growth factor (VEGF) gene transcription in many cancer types. Meanwhile, the pyrazole derivative like celecoxib (**Figure 1.25, [40]**) have been found to exhibit potential antimigratory activity, inhibit neovascularization, decrease VEGF production and increase apoptosis of tumor cells. These actions are mediated through PEG_2 synthesis inhibition.

Celecoxib (**Figure 1.25, [40]**) had been approved for the treatment of familial adenomatous polyposis and ongoing clinical trials are assessing its potential therapeutic role in both prevention and treatment of a diverse range of human cancers. So, a number of pyrazole analogues with a 1,3,4-substitution pattern such as celecoxib were evaluated for their anti-tumour and anti-angiogenic properties.[161]

Furthermore, pyrimidinyl pyrazoles were reported to have antiproliferative and inhibitory activities on tubulin polymerization. Two major binding sites on tubulin have been identified and are named the colchicine and vincristine sites for tubulin polymerization inhibitors. The binding site of pyrimidinyl pyrazole derivatives was found located at the colchicine site. The pattern of tubulin polymerization inhibitory effect was different from that of colchicine. These discoveries may suggest that pyrimidinyl pyrazole derivatives could become novel leading compounds for the development of multi-drug resistant (MDR)-overcoming antitumour agents targeting tubulin.[162]

1.5 1,4-Dihydropyridines

1,4-Dihydropyridine (DHP), such as nifedipine and amlodipine have been found to possess the ability of down-regulation of cross-membrane calcium ion Ca^{2+} flux by blocking calcium channels.[163] As an intracellular messenger for regulation of cellular activity, Ca^{2+} is importantly involved in early G1, and at the G1/S and G2/M transitions of mammalian cell cycle, and therefore blockade of calcium channel has a significant impact in many cellular processes including proliferation, metabolism and gene transcription.[164]

P-glycoprotein is one of the trans-membrane efflux pumps that transport chemotherapeutic drugs, such as vinca alkaloids, anthracycline derivatives and podophyllotoxins, out of the cells, resulting in the intracellular drug concentrations being too low to reach therapeutic effects.[165] However, P-glycoprotein-mediated multidrug resistance (MDR) reversal effects have been demonstratedby 1,4-dihydropyridines such as nifedipine, in tumour cells, with some specific derivatives overcoming drug resistance to doxorubicin and paxclitaxel in multidrug resistant human cancer cell lines.[166, 167]

In this section the up-to-date developments in the design and synthesis of the MDR active DHPs are reviewed, along with extensive insight into the significant SAR studies. Antiproliferative activity of these MDR modulator molecules indicates significant potential for their clinical application as MDR modulating drugs, especially in breast cancer where the expression of MDR phenotype is critical in the development of insensitivity to chemotherapeutic drugs.[168]

1.5.1 Chemistry and general biological activity of 1,4-dihydropyridines (1,4-DHPs)

Dihydropyridine chemistry was initially developed by Arthur Rudolf *Hantzsch* et al. and the generally known synthesis now bears his name[169]. The initial investigation of model dihydropyridines, generally N-substituted dihydronicotinamides started in the 1930's as a result of the discovery that NADH, a hydrogen transferring coenzyme was a reduced nicotinamide derivative, whose fine structure was not recognized until the late 1950's. The reduced nicotinamide adenine dinucleotide or the oxidised pyridinium form of NADH was known as NAD. It was believed at an early stage that NADH was a 1,2-dihydronicotinamide derivative (**Figure 1.30, [51]**), giving rise to a confusion which was lately resolved by the unambiguous discovery that NADH was in fact the 1,4-dihydropyridine[170]. The NAD/NADH interconversion is shown in **Figure 1.31**.

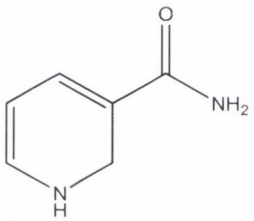

Figure 1.30 [51] 1,2-dihydronicotinamide

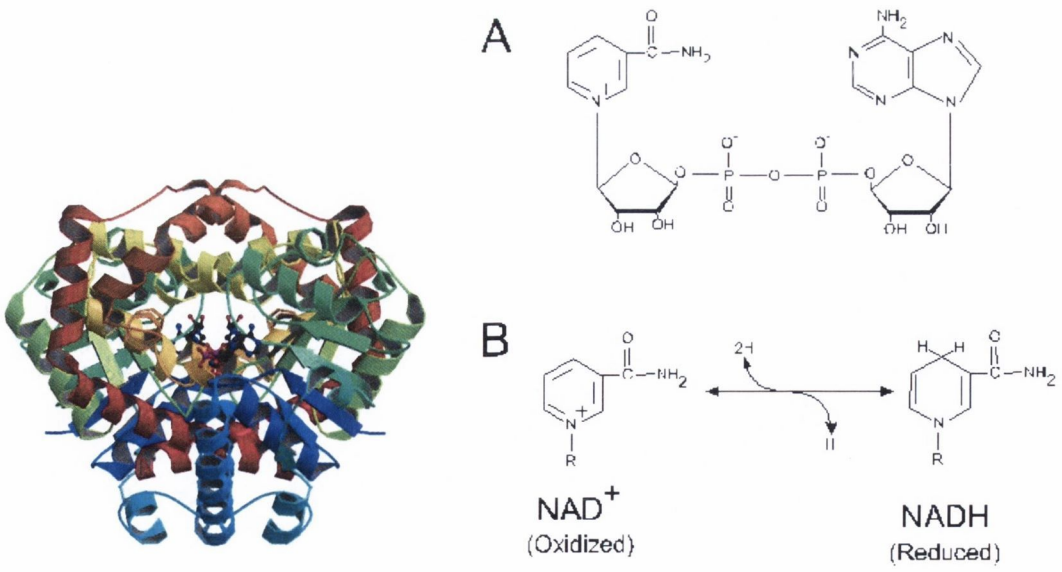

Figure 1.31 Structure of the Rabbit L-Gulonate 3-Dehydrogenase (NADH Form) and the NAD/NADH interconversion

In theory there could be five dihydropyridine isomers, as illustrated in **Figure 1.32**, but most of the better known dihydropyridines have either the 1,2-dihydropyridine or the 1,4-dihydropyridine structure.[171]

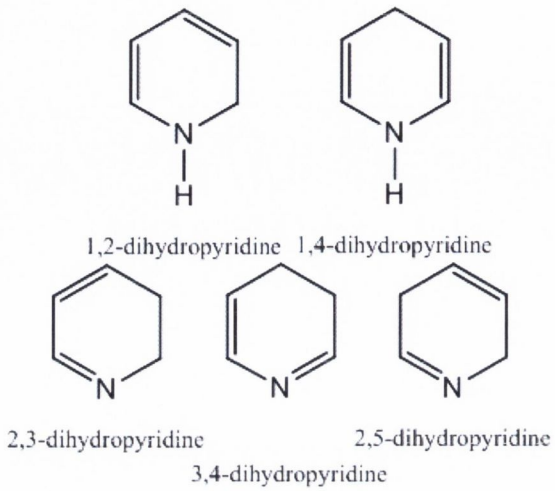

Figure 1.32 Structure of dihydropyridine isomers

The 1,2-dihydropyridine, or the 1,4-dihydropyridine structure are thought to be more common than the other three isomeric forms. This is probably because of the involvement of the nitrogen lone pair in the π electron system, as well as the existence of the higher number of sp^2-hybridised centres. The structure and X-Ray crystallographic structure of the well known Ca^{2+} channel antagonist nefidipine determined in the present work (**Figure 1.33, [52]**) are given below.

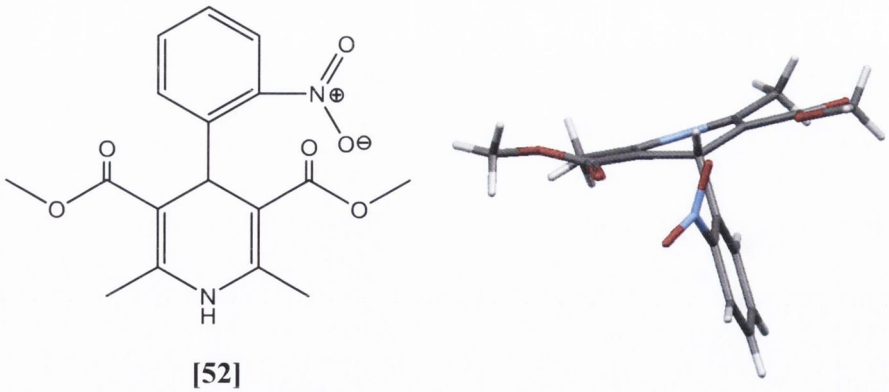

[52]

Figure 1.33 Structure and X-ray structure of Nifedipine (TCD)

Indeed other key geometrical and chemical aspects of this molecule have been revealed in association to its pharmacological activity. These are:

- The ortho-nitro group provides steric bulk, helping to maintain the required perpendicular property of the phenyl and DHP rings.

- The oxidised pyridine form is not pharmacologically active
- The conformations of the C3 and C6 esters of nifedipine are interesting whereby the C3 carbonyl is synplanar to the C2-C3 bond and the C6 ester carbonyl is antiplanar to the C5-C6 bond.

Known as Ca^{2+} channel blockers, 1,4-DHPs in fact exert their effect through receptor sites in the L type potential-dependent channels, acting as either antagonists or agonists, by opening or blocking the channel. Nifedipine (**Figure 1.33, [52]**) has been followed by the second generation of 1,4-DHPs, such as Amlodipine (**Figure 1.34, [53]**), Isradipine (**Figure 1.34, [54]**), Nicaripine (**Figure 1.34, [55]**), Nimodipine (**Figure 1.34, [56]**), Nisoldipine (**Figure1.34, [57]**), Felodipine (**Figure 1.34, [58]**)[172] which are illustrated in **Table 1.4** and Figure **1.34**.

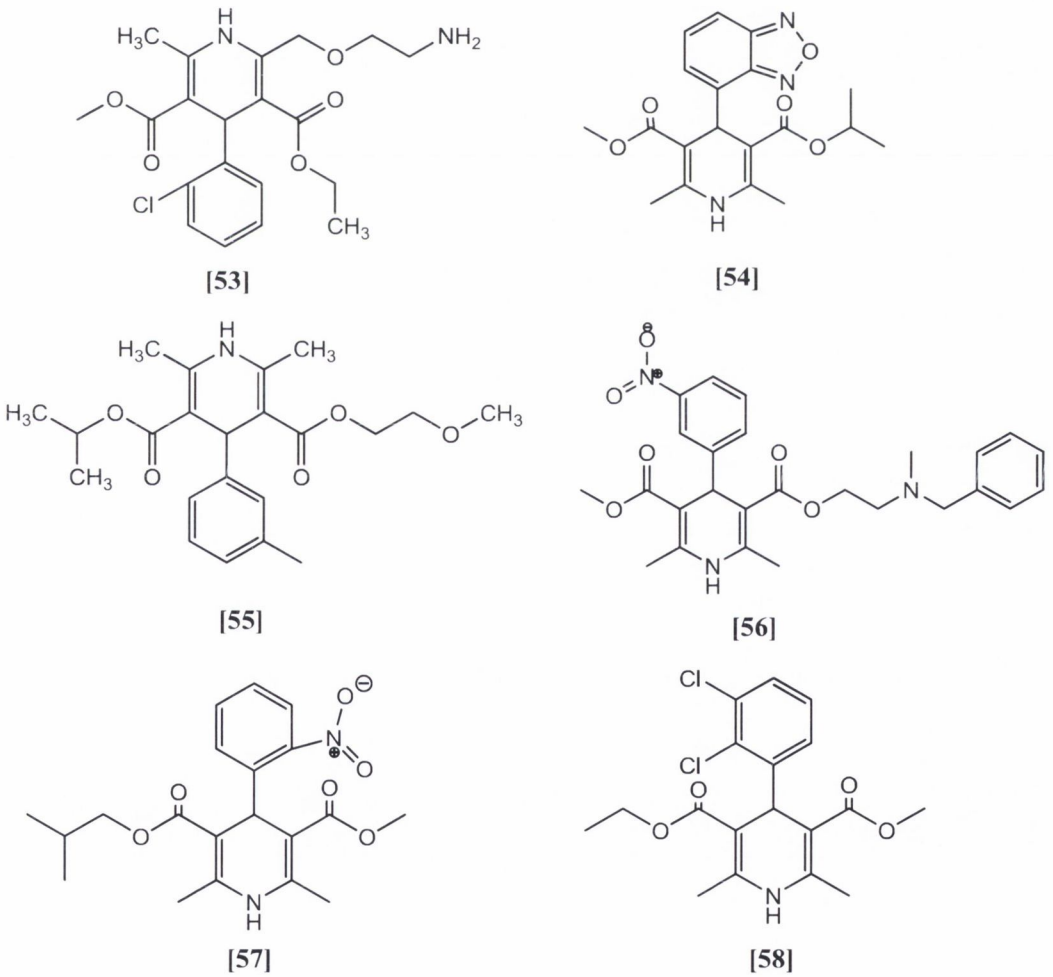

Figure 1.34 Chemical structure of 1,4-dihydropyridine class compounds

1,4-DHP Calcium Channel Blockers	Protein binding %	Description of activity	Structure
Amlodipine	93-97	Anti-hypertensive and treatment of angina[173]	[53]
Isradipine	>99	Usually prescribed for treatment of high blood pressure to prevent stroke and heart attack.Also reported used for treating Parkinson's disease[174]	[54]
Nicaripine	>95	Used to treat vascular disorders such as chronic stable angina, hypertension, and raynaud's phenomenon[175]	[55]
Nimodipine	>95	Previously indication for the treatment of high blood pressure, current use is a complication of subarachnoid hemorrhage[176]	[56]
Nisoldipine	>99	Treatment for high blood pressure, also treat patients with angina and congestive heart failure[177]	[57]
Nifedipine	92-98	Main uses are as an anti-anginal and antihypertensive,another commonly uses is the small subset of pulmonary hepertension	[52]
Felodipine	>99	Control hypertension drug, however studies indicated in combination with grapefruit may cause toxic effects.[178]	[58]

Table 1.4 Second generation of 1,4-DHPs drugs

Owing to their Ca^{2+} channel blockade activity, 1,4-DHPs primarily work as vasodilators, whereas other cardiovascular drugs such as verapamil and diltiazem, have both vasodilator and cardiodpressant properties. Ca^{2+} is one of the most versatile and universal signalling agents in the human body. Ca^{2+} acts as intracellular messenger relaying information within cells to regulate their activity. Ca^{2+} triggers life at fertilisation and controls the development and differentiation of cells into specialised types. It mediates in the subsequent activity of these cells and finally is invariably involved in cell death.[179] Every cell expresses a unique complement of components from a Ca^{2+} signalling toolkit that enables it to generate intracellular Ca^{2+} signals of a particular amplitude, time and course of intracellulat action.[180]

It is generally recognised that[181]

- ✓ Changes in Ca^{2+} levels are versatile and dynamic signalling events that control diverse cellular events over a wide range of timescales

- ✓ Tumour cells are characterised by their acquisition of different physiological traits that allow them to proliferate independently of growth signals and learn how to avoid apoptosis signals
- ✓ The Ca^{2+} signalling toolkit which comprise the proteins in regulating Ca^{2+} signalling is often remodelled in tumours to sustain proliferation
- ✓ Ca^{2+} signalling proteins and organelles are emerging as additional cellular targets of oncogenes and tumour suppressors
- ✓ Ca^{2+} signalling pathways remodelled in cancer provide novel opportunities for therapeutic action.

The calcium ion Ca^{2+} is a versatile and universal signalling agent acting as an intracellular messenger for regulation of cellular activity. Increase in free cytosolic Ca^{2+} influence the signalling mechanism which controls many cellular processes including proliferation, metabolism and gene transcription. Ca^{2+} plays a role throughout the mammalian cell cycle and is especially important early in G1, at the G1/S and G2/M transitions.[182]

1.5.2 Antiproliferative and multidrug resistance reversing activity of 1,4-dihydihydropyridines

1,4-Dihydropyridine is an important scaffold with a wide pharmacological activity spectrumemcompassing antiatherosclerosis, antidiabetes, antitumor, antimutagenic, antioxidant activities, as well as their roles in vasodilation, bronchodilation, hepatoprotection and geroprotection.[183] Primarily developed as cardiovascular agents, DHPs have been shown in recent investigations to possess the potential of antiproliferative activity and MDR reversing effect in chemotherapy, a finding that directed research to the studies of improvement of the MDR reversing effect and notable reduction of the calcium channel blocking activity of these compounds.

Multidrug resistance (MDR) is one of the major problems in the chemotherapy of cancer. It is believed that exportation of cytotoxic agents mediated by p-plycoprotein (p-gp or MDR1) importantly contributes to multidrug resistance. Following the early introduction of the calcium antagonist verapamil as a MDR inhibiting agent in 1981 which down-regulates the outward transport of vincristine and adriamycin from tumour cells, a variety of compounds have been developed to overcome MDR, including dihydropyridines and isoquinoline, and 1,4-dihydropyridine derivatives such as Nifedipine and Nicardipine (**Figure 1.35, [59]**).

An example is amlodipine (**Figure 1.35, [60]**), a long acting calcium channel blocker which reduces peripheral vascular resistance and blood pressure by directly dilating the vascular smooth muscle and is used for attenuation of hypertension and angina. In the last decade, amlodipine was discovered to inhibit cell proliferation by suppressing the expression of growth factors such as platelet-derived growth factor (PDGF), transforming growth factor β_1(TGF-β_1), and basic fibroblast growth factor (bFGF) which are required in the initiation and progression of mitosis.[184, 185] Ziesche et al. reported in 2004 that amlodipine exerts its antiproliferative effect by activating the p21 Waf1/Cip1 gene within section 21 of the short arm of chromosome 6.[186] Later Ito's research group[187] demonstrated that amlodipine down-regulates the proliferation of human coronary artery smooth muscle cell (hCASMC) via a PKD1- related pathway, which the research proposed might be potential targets in the therapy of coronary artery disease.[187]

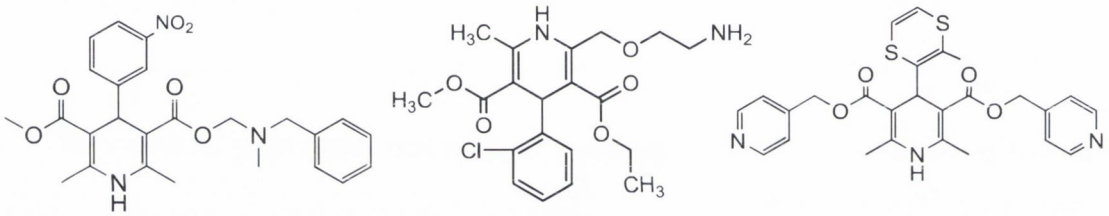

[59] [60] [61]

Figure 1.35 Structure of Nicardipine[59], Amlodipine[60], NIK-250[61]

Another example of a 1,4-dihydropyridine is Lacidipine (**Figure 1.36, [62]**), a member of the fourth generation dihydropyridines.[188] Compared to other 1,4-DHPs, lacidipine has a high membrane partition coefficient, and also exhibits a longer life, which were suggested underlay an optimal pharmacokinetic basis for the application of lacidipine in the treatment of hypertension, and an important potential indication as an antiproliferative agent in the treatment of atherosclerosis.[189] To date, the fourth generation of the highly lipophilic dihydropyridines have been subjected to comprehensive studies which have revealed their properties of reduction in adverse effects and a broad therapeutic spectrum.[190] Particularly, when administrated in combination with daunomycin, lacidipine exhibited a great MDR reversal activity than verapamil in erythroleukemia cell line.[191]

However, due to their vasodilator activity, the early dihydropyridines have caused some side effects, giving rise to the third generation agents, such as NIK-250 (**Figure**

1.35, [61]). This compound was reported to successfully reverse MDR *in vivo* as well as *in vitro* via suppression of the p-plycoprotein function.

In past decade, some new 1,4-DHP derivatives(**Figure 1.36,[63]**) containing alkyl esters have been found to potentially overcome the resistance to doxorubicin and vincristine in multidrug resistance human cancer cell lines, owing to the alkyl chains which were believed to be one of the effective substituents to promote the MDR reversing activity.[192, 193]

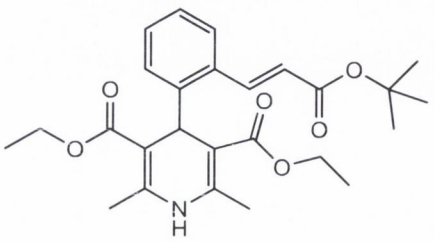

[62]

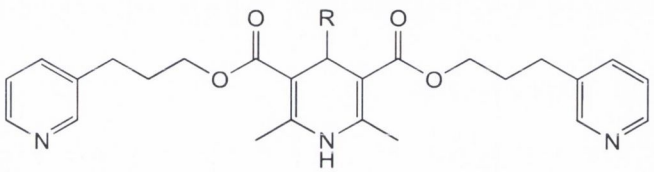

[63]

Figure 1.36 Overcome MDR agents Lacidipine[62], and 1,4-DHP derivatives[63]

Many more novel 1,4-dihydropyridine compounds have been identified with MDR reversal properties for cytotoxic drugs, and minimum effects on calcium channel activity. The cytotoxicity and MDR reversal effects of a series of 3,5-dibenzoyl-1,4-dihydropyridines (**Figure 1.37, [64]**) has been reported where cell death was attributed to as non-apoptotic pathway.[194] G1 cell cycle arrest by amlodipine has been suggested in human epidermoid carcinoma A431 cells,[195] while a 1,4-dihydropyridine derivative AV-153 (**Figure 1.37, [65]**)has been reported to be effective in reducing DNA strand breaks, and stimulates apoptosis in human peripheral blood lymphocytes following gentoxic stress.[196] 1,4-Dihydropyridines were recently also shown to modulate the activity of NAD dependent sirtuin deacetylases.[197]

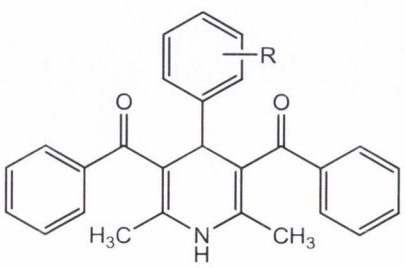

[64]

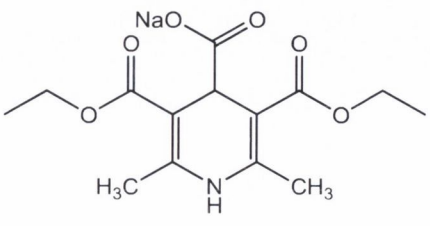

[65]

Figure 1.37 Structure of 3,5-dibenzoyl-1,4-dihydropyridine derivatives[64] and AV-153[65]

1.6 Objectives of the thesis

The general objective of this research is to investigate the design, synthesis, structure-activity relationships and pharmacokinetics of a comprehensive range of 4-(1,3-diaryl-1H-pyrazol-4-yl)-1,4-dihydropyridine products, related in structure to compound **(Figure 1.38, [66])**. This compound was identified from an *in silico* screening programme for ER ligands. These molecules will incorporate the structural features required for antiproliferative activity, while allowing design of compounds with minimal Ca^{2+} channel effects. This approach will permit the development of a novel cytotoxic drug which may also act as multi-drug resistance reversal agent. The cytotoxic mechanism of action of this compound will be determined as it is currently unclear.

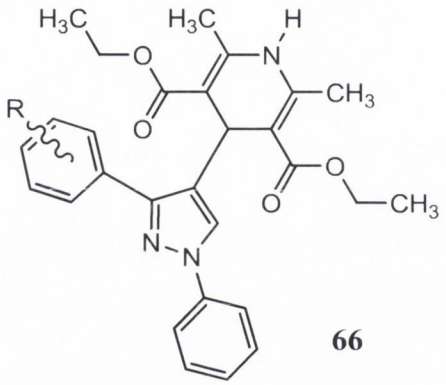

66

Figure 1.38 Structure of derivatives of substituted pyrazole-1,4-dihydropyridine

The specific objectives of research project are:

- ✓ Design and synthesis of a library of structurally focused library of compounds based on the recently discovered 4-(1,3-diaryl-1H-pyrazol-4-yl)-1,4-dihydropyridine product structure (**Figure 1.38**).The aryl rings at N-1 and C-3 of the pyrazole structure will be modified to include a comprehensive panel of heterocyclic rings and substutuents, together with an investigation of N-substitution on the DHP ring.[63,203] Related 4-(1,3-diaryl-1H-pyrazol-4-yl)-1,4-dihydropyridine products without the DHP-methyl substituents will also be synthesized, together with similar piperazine-type compounds .
- ✓ Biochemical evaluation of the synthesized compounds for cytotoxic effects against human breast cancer cell lines to select the most promising lead structure for further development

- ✓ Determination of the potential of the compounds to activate or inhibit calcium transporters and produce a change in the nature of cytosolic calcium increase in MCF-7 breast cancer cells stimulated with an agonist (ATP)
- ✓ Cell cycle studies to determine the precise target of these compounds, and their mechanism of antiproliferative action in tumour cells. The effects of compounds on the cell cycle of HL-60 acute myeloid leukaemia cells will be determined by flow cytometry to identify the optimised compounds for induction of apoptosis.
- ✓ Investigation of the ability of the novel DHP derivatives to reverse the resistance of paclitaxel and related drugs in HL-60-MDR cells over-expressing PgP.
- ✓ Determination of antioxidant effects of 4-(1,3-diaryl-1H-pyrazol-4-yl)-1,4-dihydropyridine products
- ✓ SAR studies on the most active compounds to identify the structural features for optimum activity, solubility, bioavailability and stability
- ✓ The ability of the compounds to reverse multi-drug resistance will be correlated with the overall cytotoxicity of the drugs towards the selected tumor cell lines, and the optimised compounds will be selected for further development.

Chapter 2

Synthesis of 4-(1,3-diphenyl-1H-pyrazole-4-yl)-1,4-dihydropyridines as MDR reversal agents

2.1 Introduction

More than a century ago, the synthesis of the dialkyl 1,4-dihydro-2,6-dimethylpyridine-3,5-dicarboxylates (1,4-DHP) was described by Hantzsch.[198] This scaffold structure has been a core component of many vital drugs which are extensively used in treatment of angina and hypertension. Dihydropyridines can also function as both L-type calcium channel blockers and multi-drug resistance (MDR) reversal agents in recent years. The dihydropyridines derivatives have been shown to have the potential to overcome P-glycoprotein-mediated multidrug resistance in cultured cancer cells, with some specific derivatives overcoming drug resistance to doxorubicin and vincristine in multidrug resistant human cancer cell lines.[198, 199] P-glycoprotein is an important efflux pump and causes resistance to various cytostatics classes of compounds such as vinca alkaloids, anthracycline derivatives or podophyllotoxins.[200]

1,4-Dihydropyridines such as nifedipine have been reported to show multidrug resistance reversal effects. However, they act pharmacologically as calcium antagonists like verapamil and so are not thought to be suitable for therapy in MDR cancer.[201] Abadi *et al* have also demonstrated 1,3,4-trisubstituted pyrazole derivatives as being non-cytotoxic but of apparent antiangiogenic profile, mainly through inhibiting the motility of endothelial cells rather than its proliferation.[202] Therefore, using molecular modelling our research group have identified a novel 1,4-dihydropyridines contained an aryl substituted pyrazole ring at the C-4 position, which suggested potential anti-proliferative activity in human cancer cells including those displaying multi-drug resistance.[203]

The scaffolds investigated in this study were mainly divided into two types, scaffold I and scaffold II. Both scaffold I and II are further subdivided into four and two categories, respectively. The classified categories are dependent on the various substituents and their position on the 1,4-dihydropyridine ring. In Scaffold IA, IB and IC, the 1,4-DHP ring has been substituented by ethyl ester, methyl ester and phenylmethanone groups at the C-3 and C-5 positions. While the fourth subdivision Scaffold ID obtained does not contain the two methyl groups directly attached to the 1,4-DHP ring, but possesses different substituents at the N-1 position. On the other hand, novel 1,3,4-trisubstituted pyrazole derivatives, Scaffold II, possess apparent

antitumor and antiangiogenic profile, reported by Abadi et al.[202] Therefore two different scaffold II categories have been developed in our studies, and are discussed in chapter 3. **Figure 2.1** shows 4-hydroxytamoxifen, the related 1,3,5-trisubstituted pyrazole **67** and the different types of scaffolds discussed in the present work.

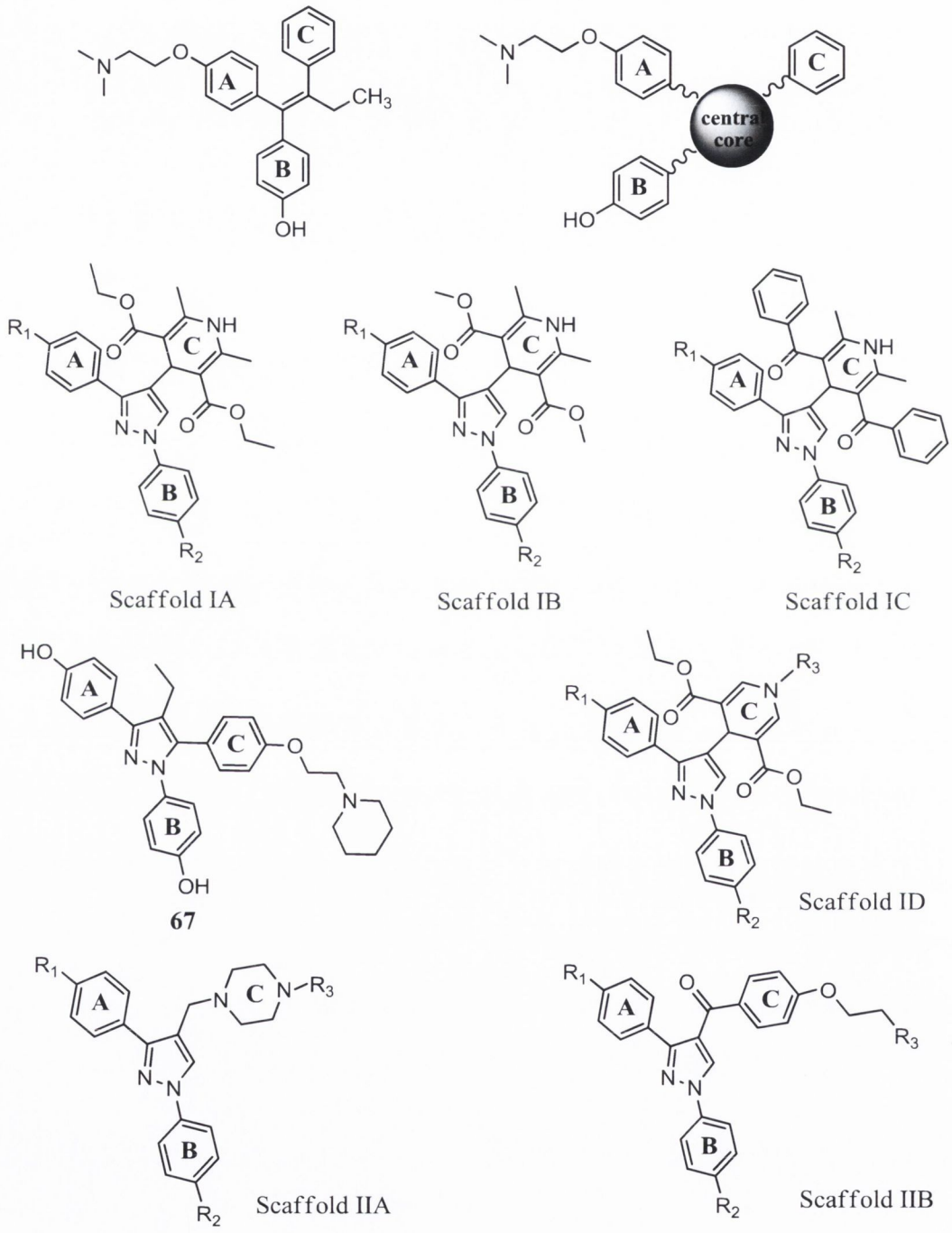

Figure 2.1 Structure of scaffold I and II type agents for potential antiproliferative activity

2.2 Synthetic route to 1,4-dihydropyridines analogues

The general outline for the synthesis of 1,4-dihydropyridine to be investigated as MDR agents is displayed in **scheme2.1**. The first step in the synthesis of the 1,4-dihydropyridines is the preparation of a selection of appropriately substituted phenylhydrazones.

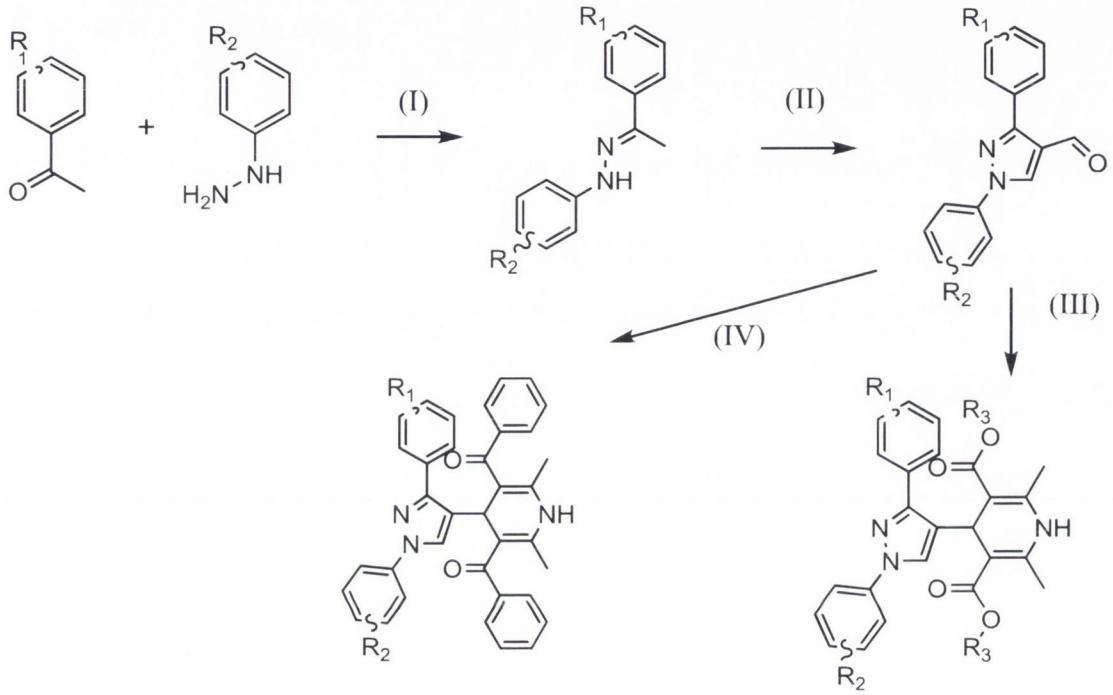

Scheme 2.1 General reaction scheme for synthesis of 1,4-dihydropyridine analogues

Scheme reagents: (I) $Mg(ClO_4)_2$, 1,2-dichloroethane 25 °C 2 h. (II) phosphorous oxychloride, Dimethylformamide, reflux 5 h. (III) Ethyl acetoacetate/ Methyl acetoacetate, 33% NH_4OH, ethanol, reflux 16 h. (IV) Benzoylacetone, 33% NH_4OH, Methanol, reflux 36 h.

2.2.1 Synthesis of phenylhydrazone

A series of phenylhydrazones (**68-85**) were formed by the condensation of the appropriately substituted acetophenone with phenylhydrazine or 4-methoxy phenylhydrazine at room temperature in ethanol. The reaction generally proceeds in high yields and is shown in **Scheme 2.2**. Initially nucleophilic attack occurs on the carbonyl carbon by a pathway similar to that for the addition of H_2O to a carbonyl π bond. The higher nucleophilicity of the amine makes it unnecessary to employ either acid or base catalysis to start the reaction. The single pair of electrons on the nitrogen attacks the carbonyl carbon to form a carbinolamine intermediate. Rapid deprotonation at the nitrogen and reprotonation at the oxygen lead to a neutral species.

Protonation on the oxygen results in the loss of a water molecule and the formation of the C=N bond. With simple aliphatic substituents on carbonyl or hydrazine components, these compounds are unstable and decompose or polymerise, however when there is an aryl group substituent on either the carbon or the nitrogen the compounds are stable.[204] The preparation of the Schiff base, also known as a phenylhydrazone can be progressively more difficult if an aldehyde instead of a ketone used as starting material, longer reaction time and removel of water is usually required.

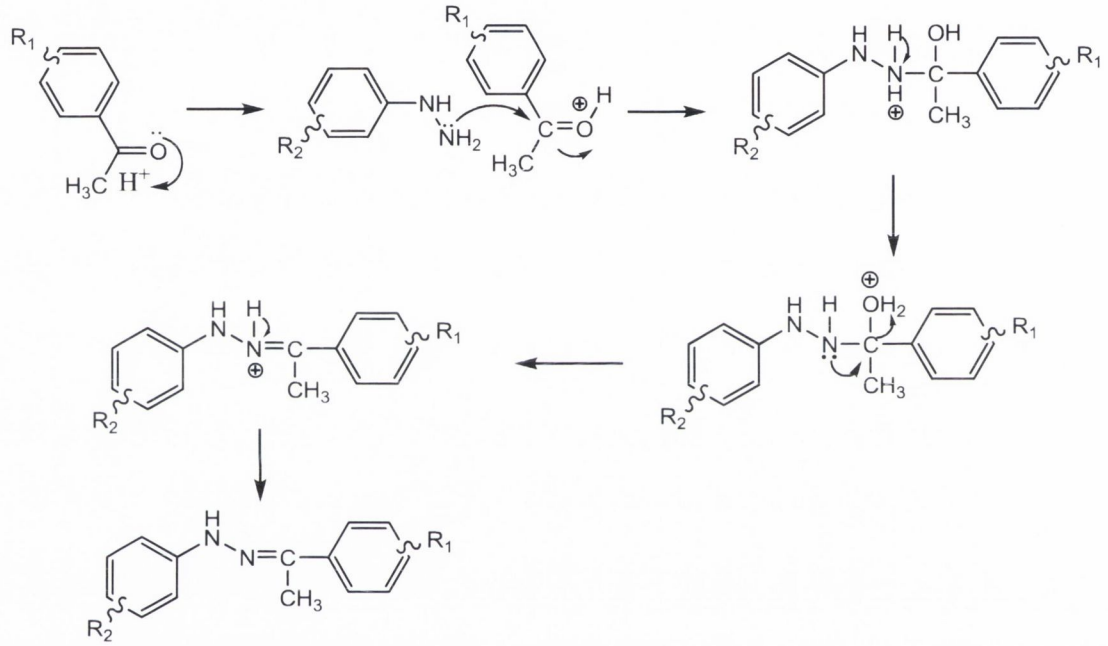

Scheme 2.2 Phenylhydrazone (Schiff base) formation

The preparation of the phenylhydrazones (**68-85**) was carried out as indicated in the experimental general procedure. After formation they were isolated from the reaction by reduction of the reaction volume followed by cooling to room temperature, meanwhile the impurities were removed by recrystallisation from ethanol. They are solid powder products in high yields and initially indicated by ^{1}H NMR and infrared spectroscopy. It is possible for Schiff bases to be formed as the E or Z isomers; however in the majority of cases the E isomer is exclusively formed as the aromatic substituents both are the large group.

Data for the IR spectra, melting point and yields for the phenylhydrazones (**68-85**) is presented in **Table 2.1**. All of the phenylydrazones display a characteristic absorption in the IR spectrum at approximately υ1600-1640 cm^{-1} indicated the presence of a C=N bond.

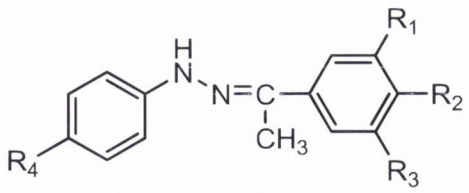

Compound	Structure				MP (^{0}C)	IR (υ_{max} cm^{-1}) C=N	Yield (%)
	R_1	R_2	R_3	R_4			
68 [311]	H	OBz	H	H	146	1600.7	54.7
69 [312]	H	Br	H	H	116	1600.4	52.3
70 [313]	H	NH_2	H	H	132	1598.5	31.9
71 [314]	H	H	H	H	140	1611.6	40.3
72 [315]	H	OH	H	H	110	1595.1	67.6
73 [316]	H	OMe	H	H	138	1657.1	30.2
74	H	Br	H	OMe	158	1587.4	76.8
75	F	OMe	H	H	138	1619.6	97.3
76 [317]	OMe	OMe	OMe	H	96	1599.9	90.2
77 [318]	H	I	H	H	104	1600.3	74.6
78	H	OH	OMe	H	240	1603.1	36.6
79 [319]	OMe	OMe	H	H	120	1602.6	94.3
80	Br	OMe	Br	H	163	1603.3	58.8
81 [320]	H	NO_2	H	H	134	1602.8	42.6
82	NO_2	OMe	H	H	152	1595.2	87.0
83	Cl	OMe	H	H	110	1599.8	80.8
84	H	OMe	H	OMe	98	1607.3	90.5
85	H	OMe	H	2,4-NO_2	108	1615.3	85.7

Table 2.1 Melting points, IR and Yield for phenylhydrazones 68-85

.

A typical ^{1}H NMR spectrum for the phenylhydrazone (**85**) was obtained from 2,4-dinitro phenylhydrazine (**86**) and 4-methoxyacetophenone (**87**) is presented in **Figure 2.2**. The IR spectrum revealed the C=N stretch at υ1615.30 cm^{-1}. The ^{1}H-NMR spectrum shows two singlets at δ 2.47 and δ 3.91 that correspond to the methyl and methoxy groups. The H_2 and H_6 protons are equivalent and appear as a multiplet at δ 7.01 as H_2 and H_6 are coupled to H_3 and H_5 which integrated for 2 protons. A singlet at δ 7.29 corresponds to the NH-N from the imine. The signals at δ 8.14, δ 8.37 and δ 9.19 integrated 1 proton each are represented for the H_6', H_5' and H_3', respectively.

The carbon atoms for the methyl and methoxy groups appear at δ 13.56 and δ 55.46 in the ^{13}C NMR spectrum.

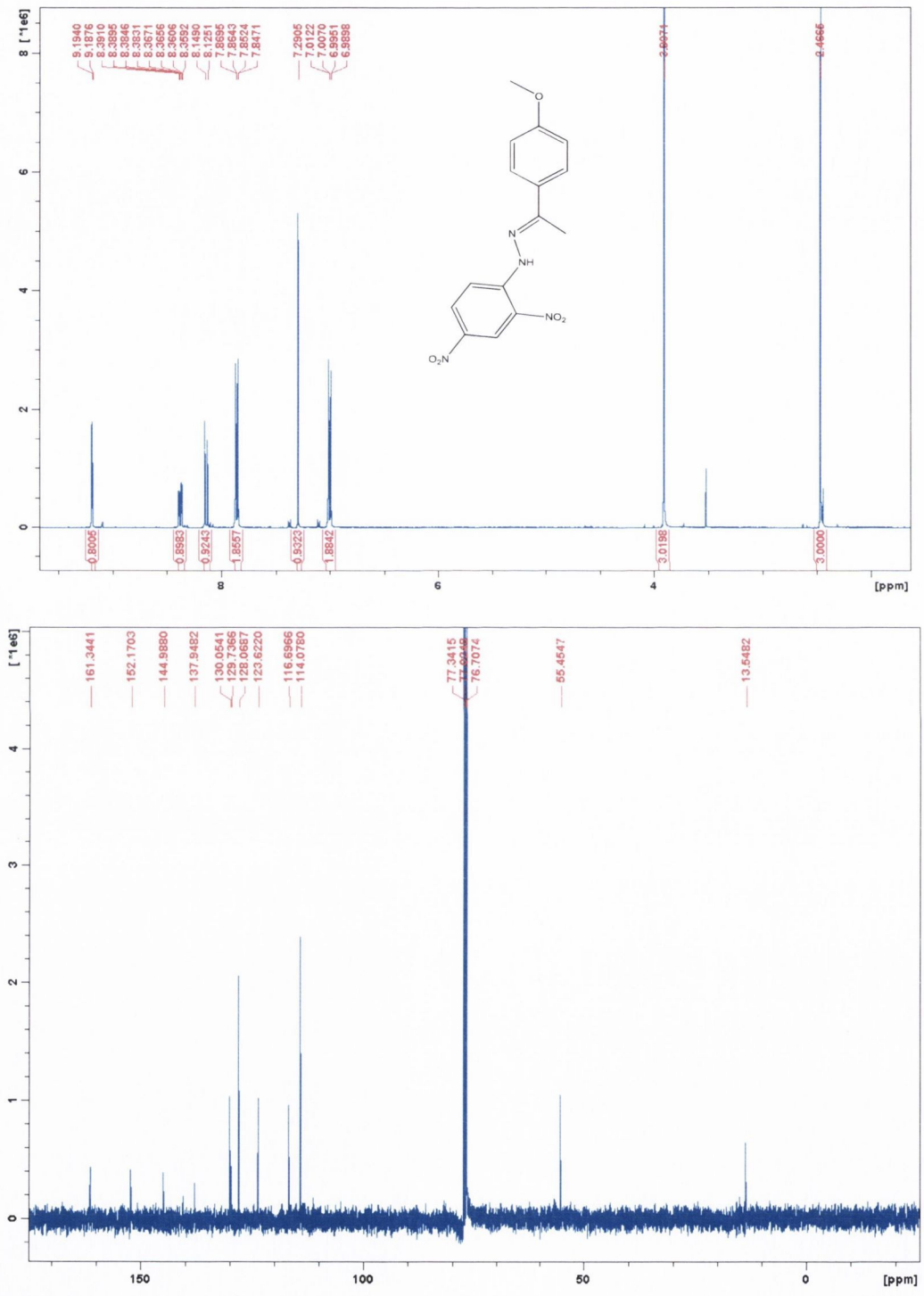

Figure 2.2 ^{1}H NMR and ^{13}C NMR spectrum for compound 85

2.2.2 Pyrazole formation by the Vilsmeier-Haack reaction

To form the required 1,4-dihydropyridines derivatives, the second step of the reaction is the synthesis of the pyrazole carbaldehydes by Vilsmeier-Haack reaction. The reaction is easily and frequently used in this study to afford the pyrazole products and facilitates the subsequent modification of the pyrazole at C-4.

2.2.2.1 Introduction of the Vilsmeier-Haack reaction

The Vilsmeier-Haack reaction was initially reported for the formylation of carbonyl compounds and aromatic substrates.[205] It provides a widely used tool for the construction of many heterocyclic compounds such as indoles, quinolines, pyridines and pyrazole derivatives.[206] The Vilsmeier-Haack reagent refers to the adduct which has important applications in the formylation of electron rich aromatic compounds. Normally the reagent is prepared *in situ* from acid chlorides, such as phosphoryl chloride or phosgene with N,N-disubstituted formamide, DMF or N-methylformanilide **88**.

2.2.2.2 The mechanism of Vilsmeier-Haack reaction

To date, the Vilsmeier-Haack reagent has been isolated and the structure and constitution has been determined. The Vilsmeier-Haack reaction has also been considered as a stepwise reaction. The initial step of the reaction is the formation of the adduct **89** via the attack of the carbonyl oxygen of the amide, leading to the isolation of chloromethylene iminium salt **90** subsequently. (**Scheme 2.3**) The conventional Vilsmeier-Haack reaction involves the reaction of the electron rich aromatic or heterocyclic compounds with the iminium salts obtained from formamides and acid chlorides. The following step is an iminoalkylation which is essentially an electrophilic substitution where the iminium salt of the intermediate **89** and **90** act as the electrophile. The reaction leads to the formation of an aldehyde on alkaline hydrolysis. The reaction of 1,3-diphenyl-1H-pyrazole **91** with the reagent prepared *in situ* from $POCl_3$ and DMF is illustrated in **Scheme2.3**.[207] The iminium salt **92** formed as a result of the iminoalkylation on hydrolysis provides the 1,3-diphenyl-1H-pyrazole-4-carbaldehyde.

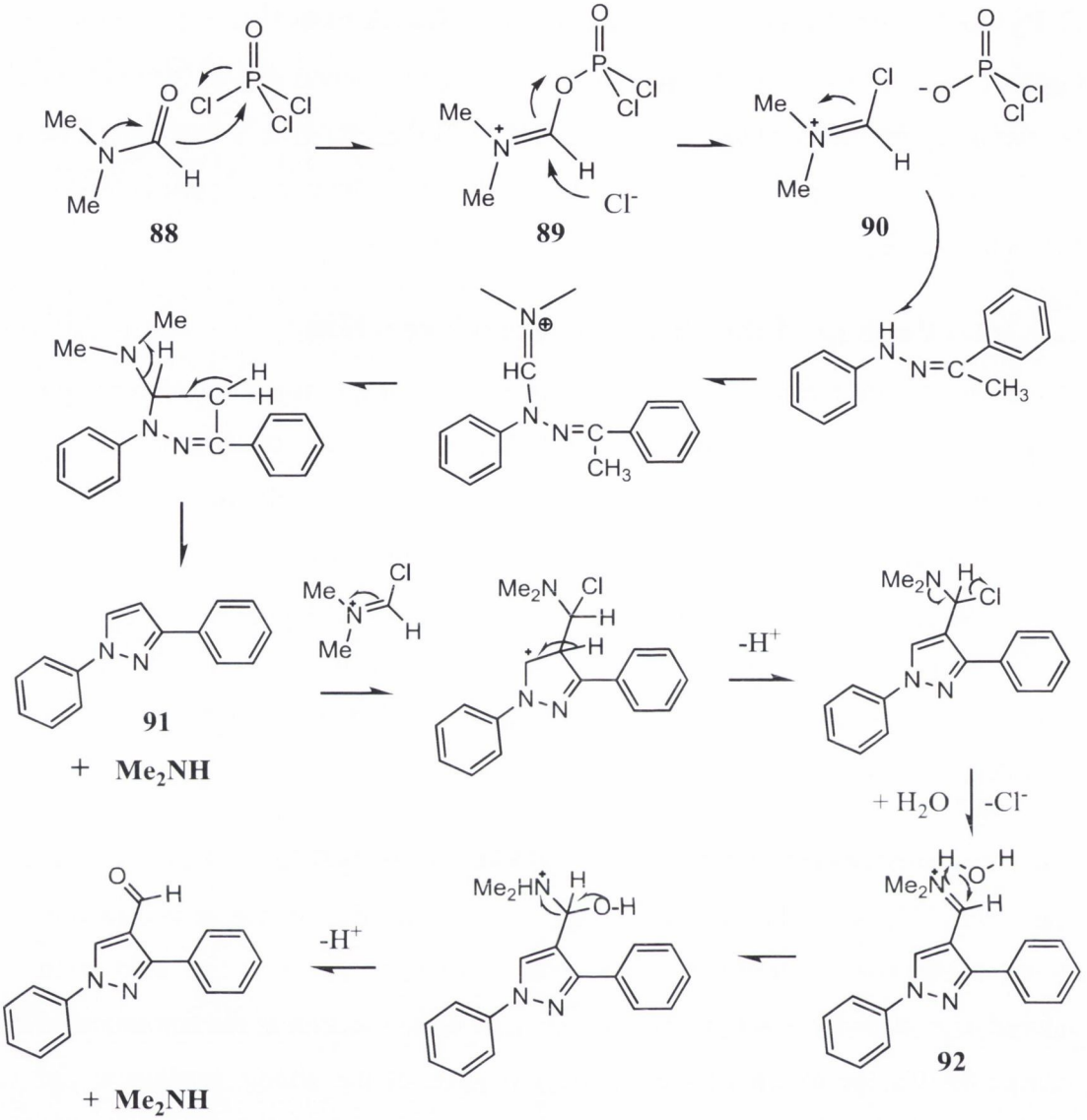

Scheme 2.3 Mechanism of the Vilsmeier-Haack reaction

2.2.2.3 Overview of Vilsmeier-Haack reaction

The Vilsmeier-Haack reaction is an important method for the synthesis of various aromatic aldehydes and α,β-unsaturated aldehydes. Furthermore, the reactions of carbonyl compounds or derivatives, such as aldehyde, ketone, dithioacetal, amide, lactam and carboxylic acid with Vilsmeier reagent are perhaps the most versatile and therefore widely used.[208] The reagent is also employed in a variety of cyclization and cycloaromatization reactions.

2.2.2.3.1 Reactions of aromatic compounds

The preparation of corresponding formylated products (**97-100**) by Vilsmeier –Haack reaction from aromatic compounds (**93-96**) substituted with electron donating substituents is widely reported. Heteroaromatic compounds also undergo

formylations at the electron rich positions when reacted with Vilsmeier-Haack reagents as reviewed by Loader, C.E. et. al. [209] Therefore, the reaction of thiophene **(101)**, furan, pyrrole(**102**), selenophene and benzo derivatives (**103-104**) of these heterocycles which participated in the Vilsmeier-Haack reaction and were formylated at the 2 or 5 position (**105-108**) is reported. Selected examples which illustrate the formylation reactions of electron rich aromatic and heteroaromatic substrates are given in **Scheme 2.4** and **Scheme 2.5**.

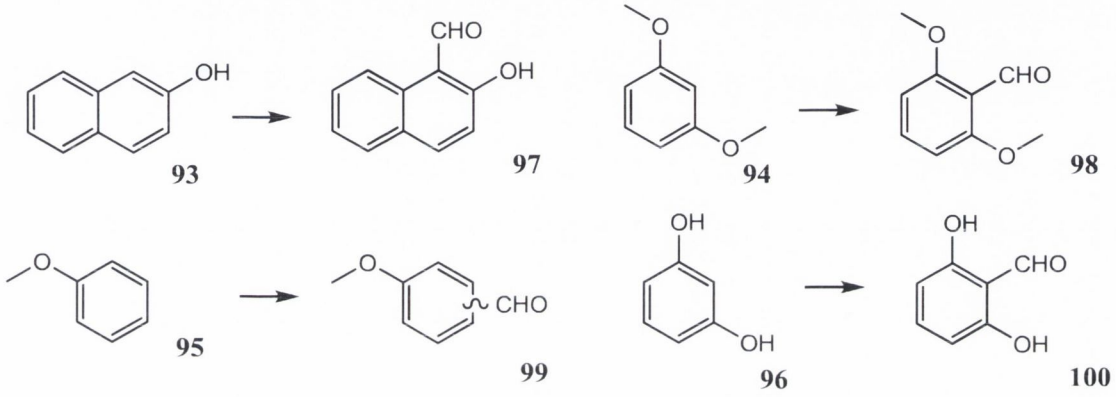

Scheme 2.4 Selected examples illustrate the formation reaction of aromatic substrates

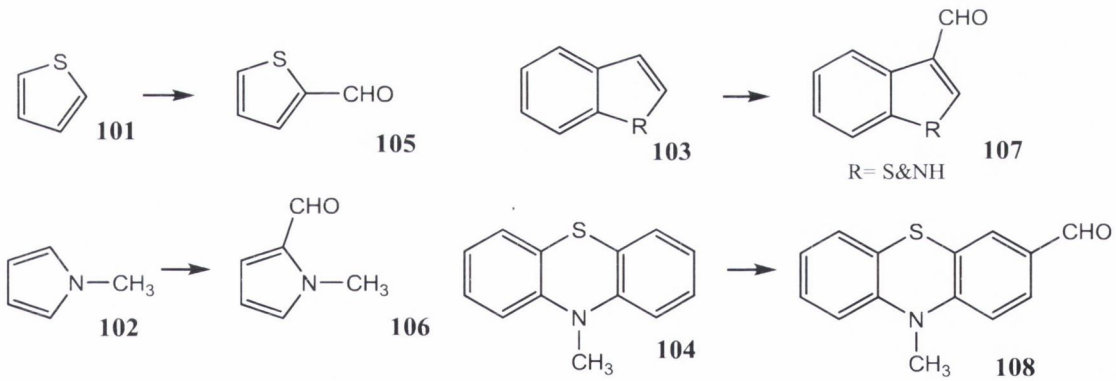

Scheme 2.5 Formation reaction of heteroaromatic compounds with Vilsmeier-Haack reagents

2.2.2.3.2 Reactions of carbonyl compounds

The Vilsmeier-Haack reagent prepared from N,N-disubstituted formamides and phosphorous oxychloride or oxalyl chloride lead to the formation of iminium salts, which provide the respective formylated products via alkaline hydrolysis, reported by Pellet et al.[210] **Scheme 2.6** shows the Vilsmeier-Haack reaction of enolizable ketones **109** lead to the formation of chlorovinyl iminium salts **110**. Subsequently the β-chloro substituted enealdehydes **111** was obtained by base hydrolysis. The Vilsmeier reagent, under mild conditions, is able to convert an enolizable carbonyl compound to

the corresponding chlorovinyl functionality, without undergoing subsequent imino-alkylation. The reaction of enolizable ketones (**112-115**) which has been converted to the respective β-chloroacroleins (**116-119**) were first reported by Arnold and Zemlicka.[211,212] Therefore, the application in synthesis of these useful multifunctional intermediates starting from carbonyl compounds is highly versatile.

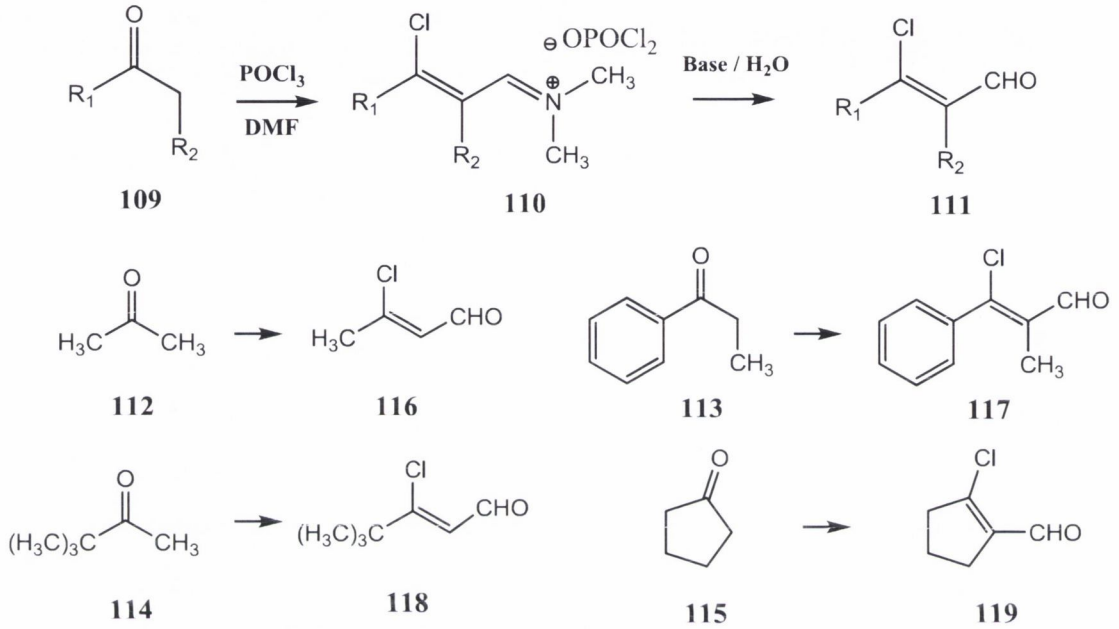

Scheme 2.6 Enolizable ketones converted to β-chloroacroleins with Vilsmeier reagent

2.2.2.3.3 Reactions of Alkenes

The Vilsmeier reactions of simple alkenes with alkyl substituents are more complex due to subsequent imino alkylation and migration of carbon-carbon double bonds, discussed by Jutz et al. in 1967.[213] **Scheme 2.7** shows the reaction of isobutene **120** and 2-phenyl propene **121** preceded with multiple iminioalkylation by the iminium salt **122** and preceded with isolation of the 2,7-naphthyridine **123** and pyridine derivatives **124** respectively. Meanwhile, Vilsmeier-Haack formylations of alkenes conjugated with aromatic systems are simple and straightforward. The reaction of substituted styrenes **125** with the Vilsmeier reagent leads to the formation of cinnamaldehyde derivatives **126** on hydrolysis of the intermediate iminium salts (**Scheme 2.7**). In this case, the Vilsmeier reagent is used to eliminate the hydroxyl group and the subsequent iminolakylation leads to the formation of the styryl methyleneiminium salts.

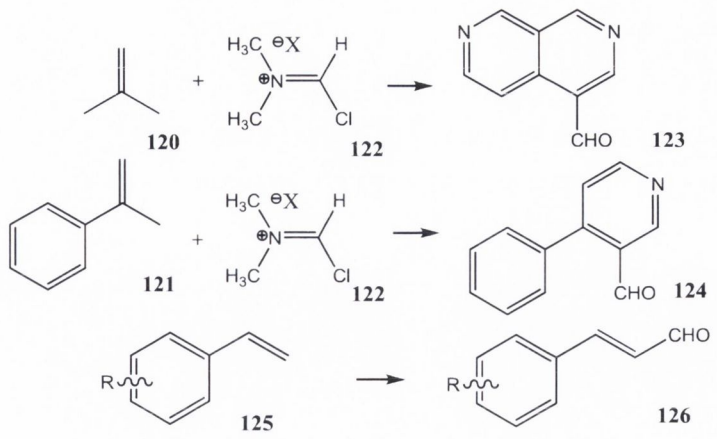

Scheme 2.7 Vilsmeier Haack formylation reaction of alkene derivatives

2.2.2.3.4 Cyclization and cycloaromatization reactions

Raju and Krishna Rao[214] have reported cycloaromatization of benzene tricarboxylaldehydes or dicarboxylaldehydes derivatives from 2,4-dienoic acids. For instance the reaction of 2.4-hexadienoic acid **127** gave a mixture of 2,4,6-chloro benzene tricarboxaldehyde **128** and 1,3,5-benzene tricarboxaldehyde **129**. (**Scheme 2.8**) The formation of heterocycles under Vilsmeier-Haack reaction condition is due to intramolecular attack of heteronucleophiles on the iminium salts. Thus phenyl hydrazones **130** and semicarbazones **131** could be converted to pyrazoles derivatives **132** and **133** when treated with the Vilsmeier-Haack reagent. (**Scheme 2.8**)

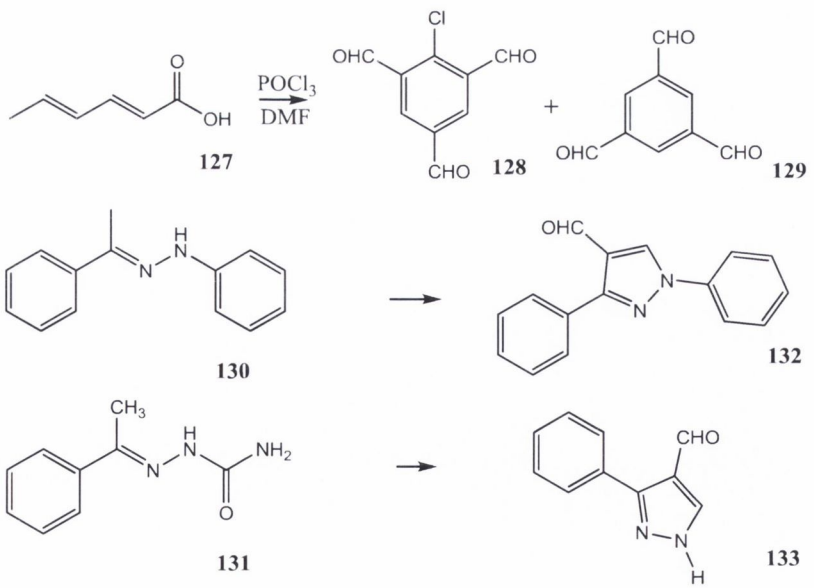

Scheme 2.8 Cyclization and cycloaromatization by Vilsmeier Haack reaction

2.2.2.3.5 Miscellaneous reactions

The malonaldehyde derivatives of substituted benzoxazoles **136** or naphthoxzole **137** can be prepared from α-hydroxy acetophenones **134** and 2-acetyl-1-naphthol **135** by

the Vilsmeier reaction of oximes. The reactions proceeds via a Beckmann rearrangement followed by cyclization and double iminomethylation result in isolation of various heterocycles such as pyrimidines **138**, pyrazoles **139** and oxazoles **140**. The conversion of malonaldehydes **136** to the corresponding cyanoacetaldehyde **141** and further transformations to the aminopyrazoles **142** have also been reported. (**Scheme 2.9**) [215]

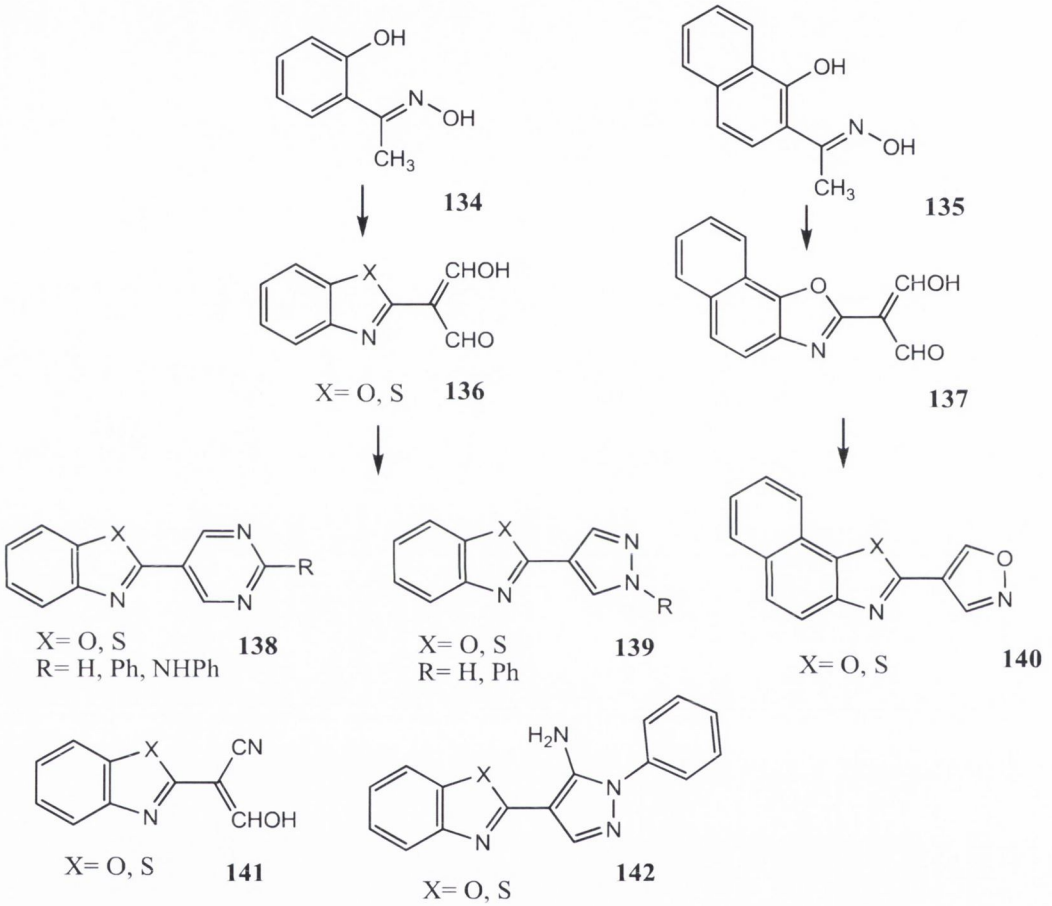

Scheme 2.9 Miscellaneous Vilsmeier Haack reactions

2.2.2.4 General synthesis of pyrazole

In the present work, compounds **143-158** were prepared by reaction of phenylhydrazones (**68-85**) with phosphorous oxychloride ($POCl_3$) in the presence of dimethylformamide (DMF) **Table 2.2**. The selection of substitutents was based on the requirement for potential estrogen receptor bonding substituents on the N-1 and C-3 phenyl ring. The pure products were obtained in good yields, generally no less than 70%, and recrystallized from ethanol. All the pyrazole carbaldehyde products were identified by Infra red (IR) spectroscopy and nuclear magnetic resonance spectroscopy (NMR). The characteristic carbonyl bond generally appears between υ

1665 cm^{-1} and υ 1690 cm^{-1} in IR spectra. **Table 2.2** gives melting point, IR data and isolated yields for the various substituted pyrazole carbaldehydes synthesised.

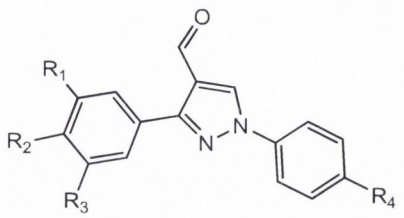

Compound	Structure				MP (^{0}C)	IR (υ_{max} cm^{-1}) C=O	Yield (%)
	R_1	R_2	R_3	R_4			
143	H	OBz	H	H	148-150	1669.3	69.2
144 [321]	H	Br	H	H	138	1670.4	87.5
145	H	NH_2	H	H	176-180	1675.2	90.8
146 [322]	H	H	H	H	142	1675.5	91.3
147 [323]	H	OH	H	H	216-220	1685.3	73.37
148 [324]	H	OMe	H	H	138-140	1672.0	70.01
149	H	Br	H	OMe	156-158	1667.5	19.71
150	F	OMe	H	H	250	1674.5	90.1
151 [325]	OMe	OMe	OMe	H	220	1688.5	58.60
152	H	I	H	H	154	1671.6	90
153	OMe	OMe	H	H	130	1669.2	60.85
154	Br	OMe	Br	H	250	1663.1	81.90
155 [326]	H	NO_2	H	H	162-164	1685.1	90.2
156 [327]	NO_2	OMe	H	H	162	1687.6	97.5
157	Cl	OMe	H	H	136	1668.2	89.3
158	H	OMe	H	2,4-NO_2	102	1686.8	49.71

Table 2.2 Melting points, IR and Yield for pyrazole (143-158)

Compound **153** was identified initially from IR spectroscopy with the C=O absorption observed at υ 1669.2 cm^{-1}. In **Figure 2.3**, the ^{1}H NMR spectrum displayed a singlet at δ 10.08 which represents the aldehyde CH. The next singlet appears at δ 8.55 corresponding to the proton at the C-5 position of pyrazole ring. The aromatic protons integrate for 8 protons and all appear in the region from δ 7.00-7.83. The two methoxy groups have similar chemical shift which appear as two singlets at δ 3.98 and δ 4.00. In the DEPT 90 carbon spectrum (**Figure 2.3**) the carbonyl carbon is identified at δ 185.13. The signals at δ 139.02, δ 149.15, δ 150.11, δ 154.50 were found in the ^{13}C NMR spectrum while missing in the DEPT 90 therefore corresponds

to the quaternary aromatic carbon C(1'), C(4), C(3), and C-3 of pyrazole ring, respectively. The two CH_3 signals are identified at δ56.01, δ 56.06 in the ^{13}C NMR spectrum and correspond to the two methoxy groups.

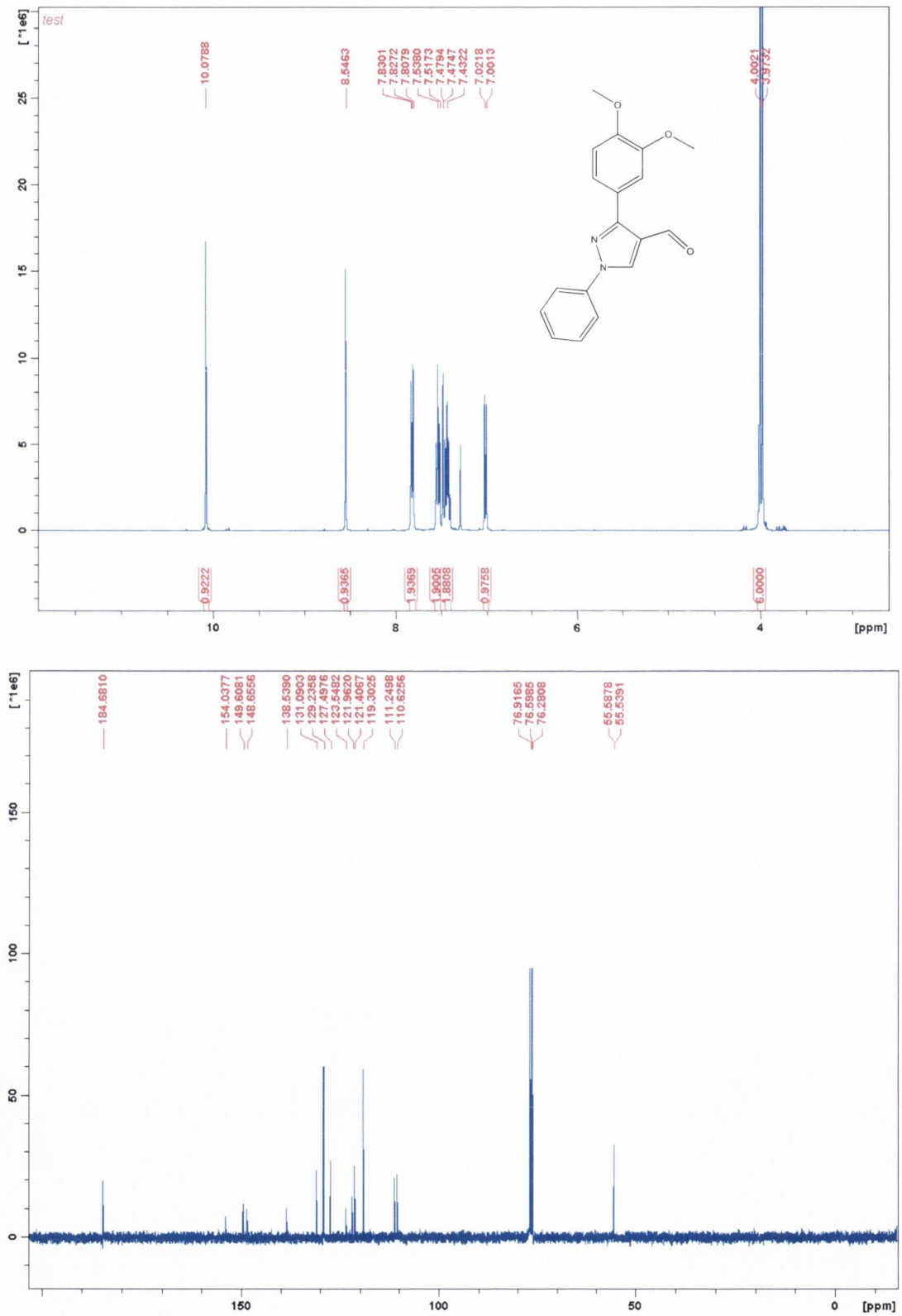

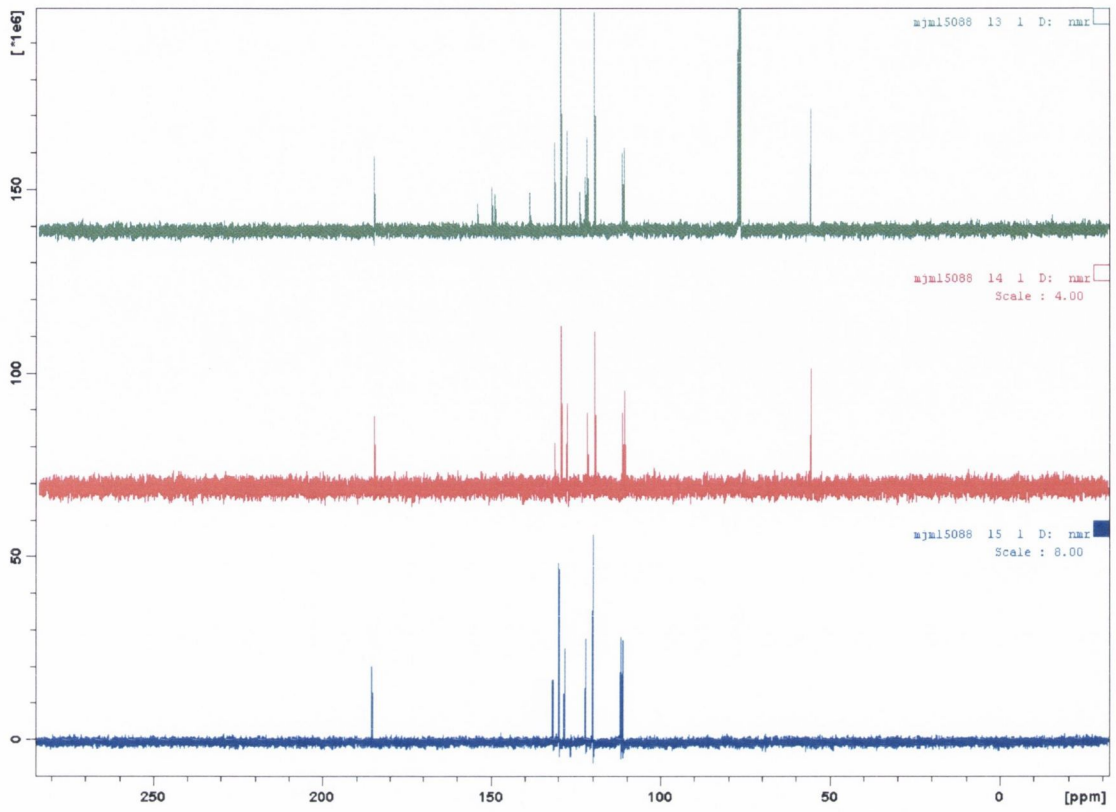

Figure 2.3 ^{1}H ,^{13}C and DEPT NMR spectra for compound 153

2.2.3 General methods for 1,4-dihydropyridine synthesis

As outlined in chapter 1, the 1,4-dihydropyridines are well-known calcium channel blockers with antihypertensive properties and play an important role in a broad range of other pharmacological activity. There are many synthetic routes available for the formation of the 1,4-dihydropyridine ring.[216-220] The choice of route is based on the structural features desired in the final product. An obvious retrosynthesis is presented in **Scheme 2.10** where the 1,4-dihydropyridine derivatives can be formed by condensation of an aldehyde with two equivalents of a β-ketoester in the present of ammonia. This common method for the preparation of dihydropyridine is the Hantzsch reaction, the reason to choose it is because it is adaptable for use with structurally diverse β-ketoester (**159**), the readily available precursors (pyrazole carbaldehyde) (**160**) and its ease of use.

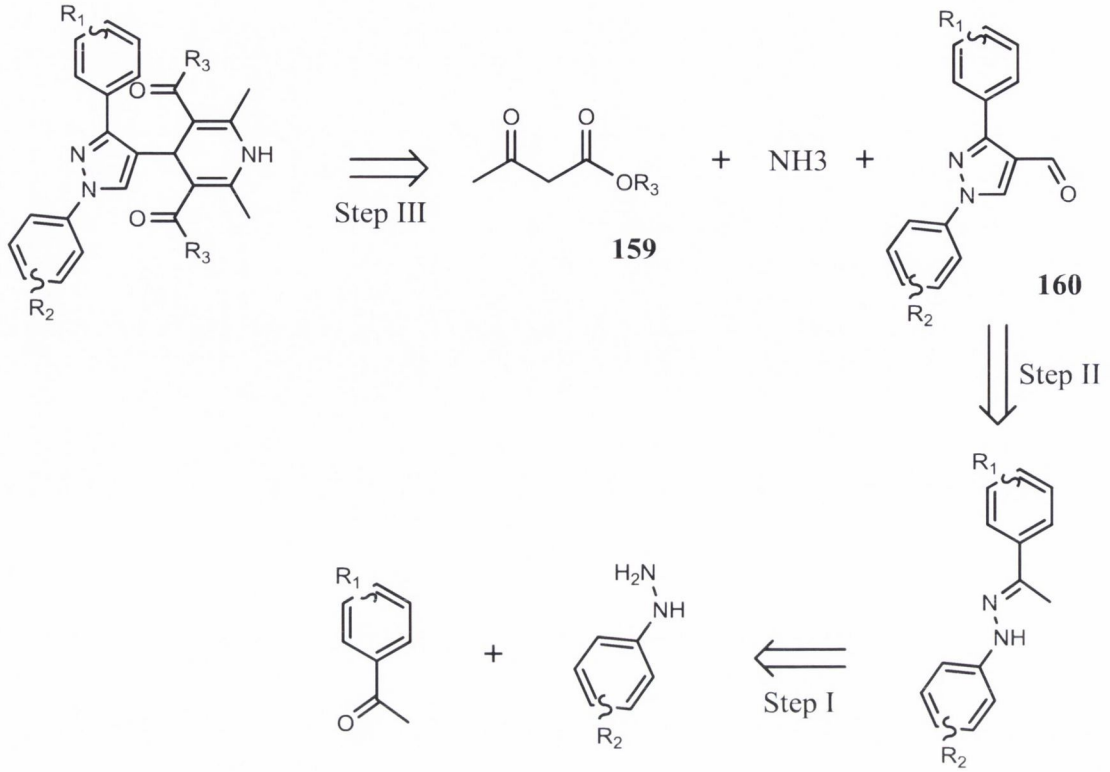

Scheme 2.10 Retrosynthesis of 1,4-dihydropyridine analogues

The reaction can be visualized as proceeding through a Knoevenagel condensation product as a key intermediate, the second key intermediate is an ester enamine, which is produced by condensation of the second equivalent of the β-ketoester with ammonia. Further condensation between these two fragments gives the dihydropyridine derivative as illustrated in **Scheme 2.11**.[221,222]

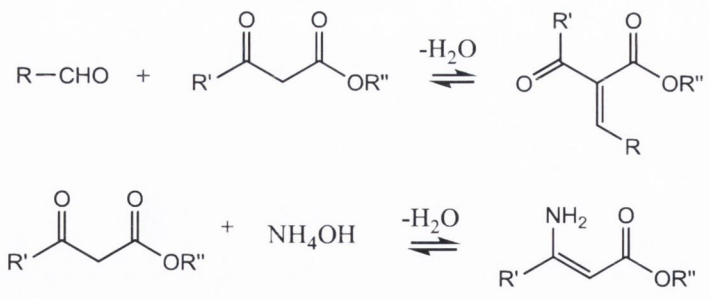

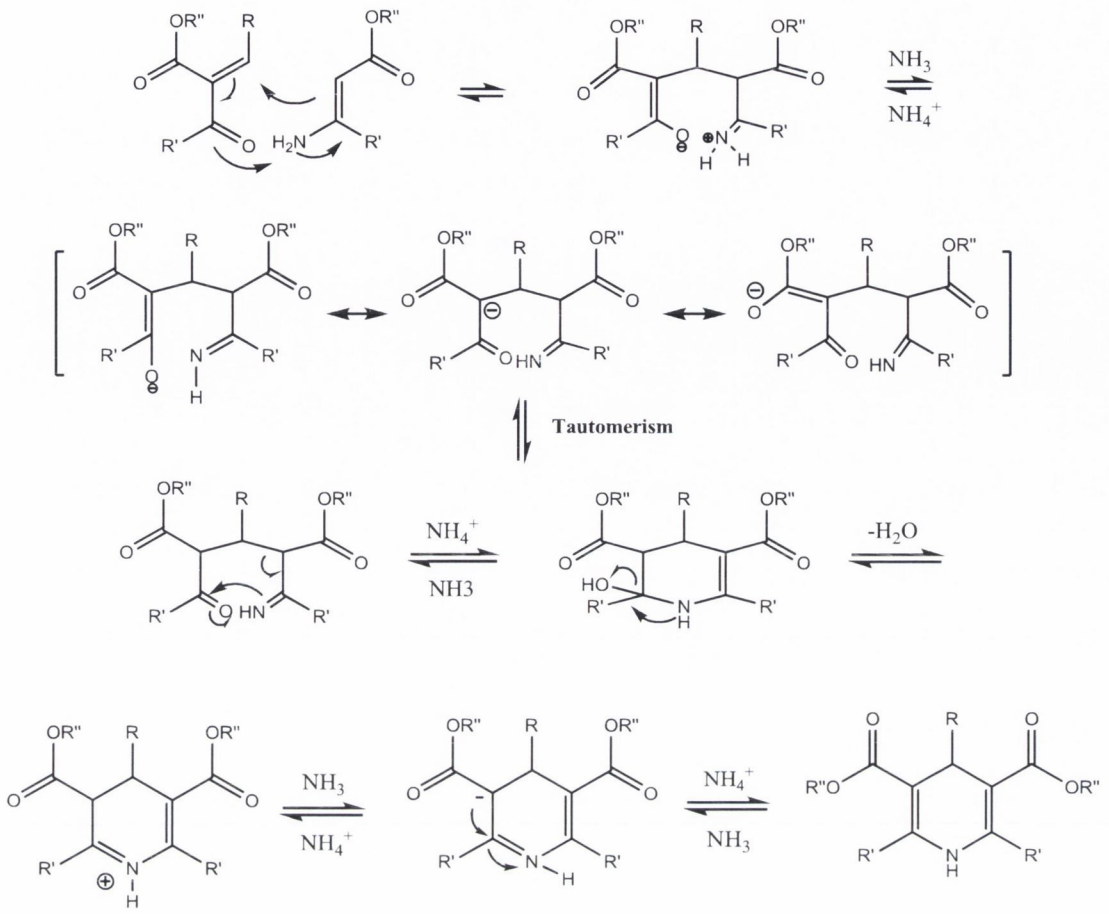

Scheme 2.11 Mechanism for Hantzsch reaction to form 1,4-dihydropyridines derivatives

2.2.3.1 Efficient synthesis of 5,6-unsubstituted 1,4-dihydropyridines

A user-friendly, mild protocol that allowed the transformation of the 6-alkoxy-2-methyl-1,4,5,6-tetrahydropyridines into the corresponding 1,4-dihydropyridines was reported by Maiti el al. more recently.[223] This new method provides a very efficient synthesis of relevant 1,4-dihydropyridines from readily available, inexpensive acyclic starting materials and results in excellent yields. (**Scheme 2.12)**

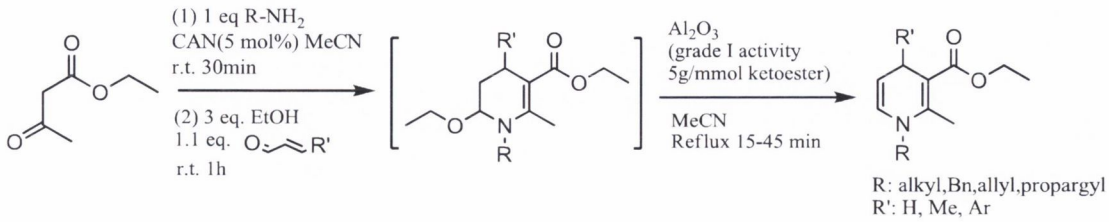

Scheme 2.12 Synthesis of 5,6-unsubstituted 1,4-dihydropyridines

2.2.3.2 A simple and convenient route to 1,4-dihydropyridines

Various modification of the original procedure by Hantzsch have been explored to improve the yields and the reaction conditions since it considered as classical

synthetic route 100 years ago. Sambri, et. al. demonstrated a new method for the synthesis of various 1,2,3,4-tetrasubstituted 1,4-dihydropyridines from enamino or carbonylic derivatives promoted by $Mg(ClO_4)_2$.[224] Metal perchlorates act as Lewis acid catalysts for the reaction and led to moderate yields. (**Scheme 2.13**)

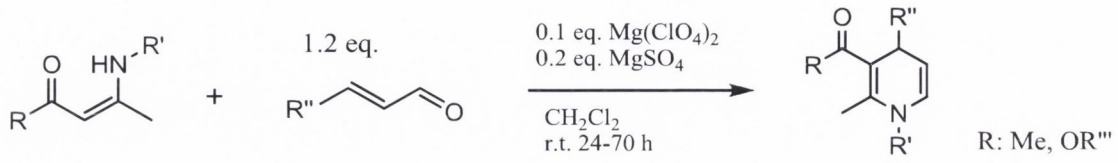

Scheme 2.13 Convenient route to synthesis 1,4-dihydropyridines

2.2.3.3 One-pot synthesis of polyhydroquinoline derivatives via Hantzsch reaction

Over the past few years, much effort has gone into developing the one-pot condensation reaction to form 1,4-dihydropyridines, which obviously has many disadvantages such as long reaction time, harsh reaction conditions, the use of a large quantity of volatile organic solvents and normally gives low yields. Wang et. al. presented a four-component Hantzsch reaction which can effectively be performed with promotion by $Yb(OTf)_3$, which provided a simple and efficient method for the preparation of polyhydroquinoline derivatives.[225] (**Scheme 2.14**)

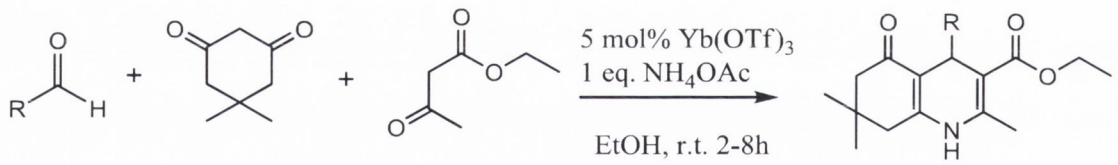

Scheme 2.14 One-pot synthesis of polyhydroquinoline derivatives

2.3 General synthesis of 1,4-dihydropyridines

In the present work, the final step in the synthesis of the target MDR reversal agent 1,4-DHP derivatives is to introduce the substituted 1,4-dihydropyridine to the C-4 position of the pyrazole ring. In 1882 Hantzsch reported the first synthesis of 1,4-DHP. The classical method for the synthesis of 1,4-dihydropyridines is a one-pot condensation of an aldehyde with β-ketoester (methyl acetoacetate & ethyl acetoacetate), and aqueous ammonia refluxing in ethanol. (**Scheme 2.15**) That multicomponent reaction usually affords the products in good yields and this experimental method remains the most widely used protocol to access to 1,4-DHP differently substituted in position C-1.

2.3.1 Diethyl-4-(1,3-diphenyl-1H-pyrazol-4-yl)-2,6-dimethyl-1,4-dihydropyridine-3,5-dicarboxylate (scaffold I A)

Tweenty one 4-(1,3-diaryl-1H-pyrazole-4-yl)-2,6-dimethyl-1,4-dihydropyridine-3,5-dicarboxylic acid diethyl esters compounds (**161-181**) were prepared by the Hantzsch reaction of the 1,3-diaryl-1H-pyrazole-4-carbaldehydes with ethyl acetoacetate or methyl acetoacetate in aqueous ammonia.[222,226] (**Scheme 2.15**) This reaction has been previously used for the synthesis of many 1,4-dihydropyridines with heterocyclic substitutes such as flavones or thiazole at C-4. Up to date, the substitution of the aryl ring at C-3 in compounds (**161-181**) included halogens, nitro, amino, alkyl, phenyl, methoxy and hydroxyl groups while additional pyrazole C-3 substitutes included the 2-naphthyl, 2-thienyl and 3-pyridyl and biphenyl ring system (**Table2.3**). The 2,6-dimethyl-1,4-dihydropyridine-3,5-dicarboxylic acid diethyl ester **182** was also synthesized as a control for the subsequent biochemical experiments and was obtained from benzaldehyde, ammonia and ethyl acetoacetate in a similar procedure. The 1,4-dihydropyridine products were identified from ^{1}H NMR and ^{13}C NMR spectroscopy.

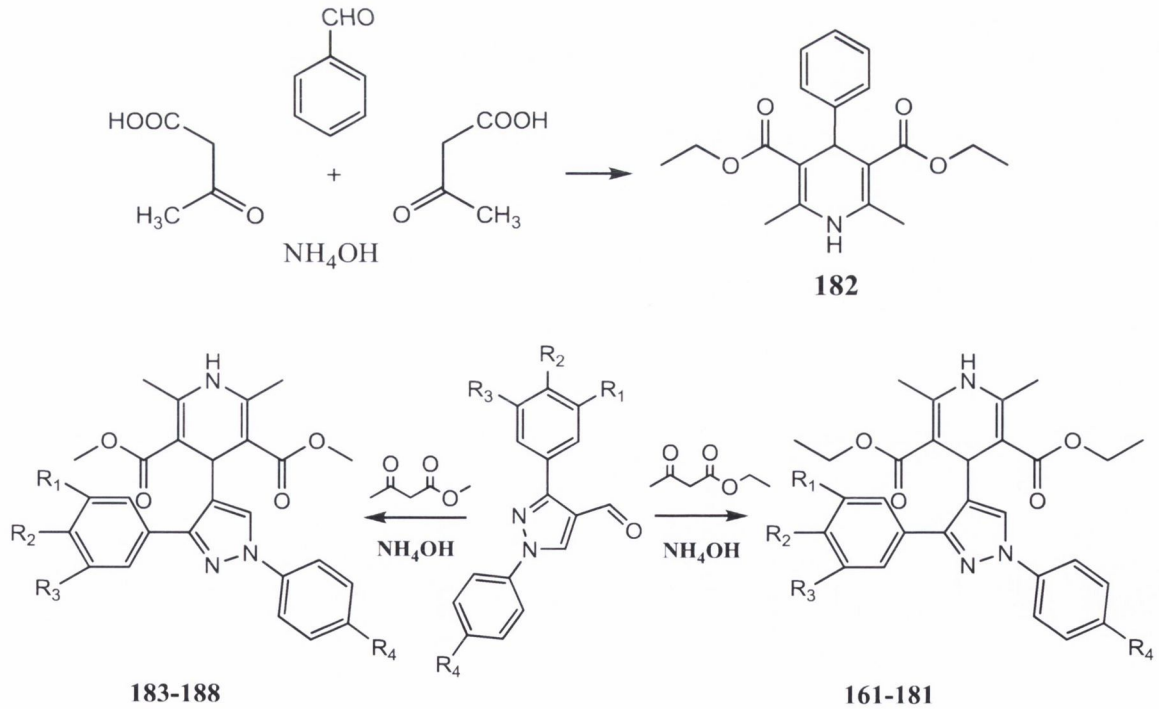

Scheme 2.15 Synthesis of 1,4-dihydropyridines derivatives by Hantzsh reaction

Compound	Structure				MP (^{0}C)	IR (υ_{max} cm^{-1}) C=N, C=O & C-O-ester	Yield (%)
	R_1	R_2	R_3	R_4			
161	H	OBz	H	H	196	1600.3 1690.2 1209.1	7.7
162	H	Br	H	H	160	1599.4 1677.7 1210.6	7.9
163	H	NH_2	H	H	124	1599.7 1677.7 1212.2	9.3
164	H	H	H	H	196	1599.7 1693.2 1211.0	7.8
165	H	OH	H	H	270	1601.1 1208.1	18.7
166	H	OMe	H	H	140	1600.1 1693.9 1212.6	15.3
167	H	Br	H	OMe	192	1642.5 1207.8	48
168	F	OMe	H	H	152	1599.9 1693.5 1210.6	3.1
169	OMe	OMe	OMe	H	183	1600.4 1690.4 1205.1	8.9
170	H	CH_3	H	H	143	1603.2 1682.0 1217.2	38.6
171	H	I	H	H	172	1598.7 1676.1 1213.3	17
172	OMe	OMe	H	H	186	1599.9 1693.5 1211.5	48.6
173	Br	OMe	Br	H	168	1599.7 1649.8	13.8

						1214.3	
174	H	NO_2	H	H	172	1596.6 1667.3 1210.5	25.5
175	NO_2	OMe	H	H	152	1623.0 1687.7 1211.2	52.5
176	H	F	H	H	134	1599 1693 1213	25.4
177	Cl	OMe	H	H	172	1599.5 1652.9 1210.4	33.9
178	biphenyl			H	144	1594 1688 1114	43.6
179	naphthalene			H	165	1579 1682 1116	50.3
180	thienyl			H	178	1600.5 1679.4 1204.2	16.3
181	pyridine			H	121	1599 1679 1116	22.3

Table 2.3 Melting points, IR and Yield for type I A 1,4-dihydropyrdines (161-181)

Compound **167** was identified from ^{1}H NMR spectroscopy (**Figure 2.4**). H-4 was clearly identified as a singlet at δ 5.27, while the two methyl groups are observed as a singlet at δ 2.27, the two ethyl ester methyl groups appear as a triplet at δ 1.09 (6H, J=7.12Hz). The singlet at δ 3.84 integrated for three protons represent the methoxy group of the aryl ring at N-1 position. The aromatic protons all appear in the region from δ 6.94–δ 7.81, while C-5 proton appear as a singlet at δ 7.65 in this region. The two diastereotopic methylene groups are observed as two distinct multiplet signals centred at δ 3.80 and δ 4.05, possibly due to the non-planar nature of the 1,4-dihydropyridine ring. In the HMBC experiment, long range correlations were observed between the following protons and carbons: pyrazole H-5 with pyrazole carbons 3,4 and dihydropyridine C-4; dihydropyridine H-4 with 1,4-dihydropyridine

C-2, pyrazole carbons C-3, C-4, C-5 and carbonyl ester carbons; dihydropyridine C-3 with dihydropyridine H-4, the dihydropyridine methyl protons at C-2 and pyrazole H-5. Observation of an NOE at N-phenyl H-2 and dihydropyridine H-4 on irradiation of pyrazole H-5 together with an NOE at pyrazole H-5, and at C-phenyl H-2 on irradiation of dihydropyridine H-4 confirmed the structural assignment.

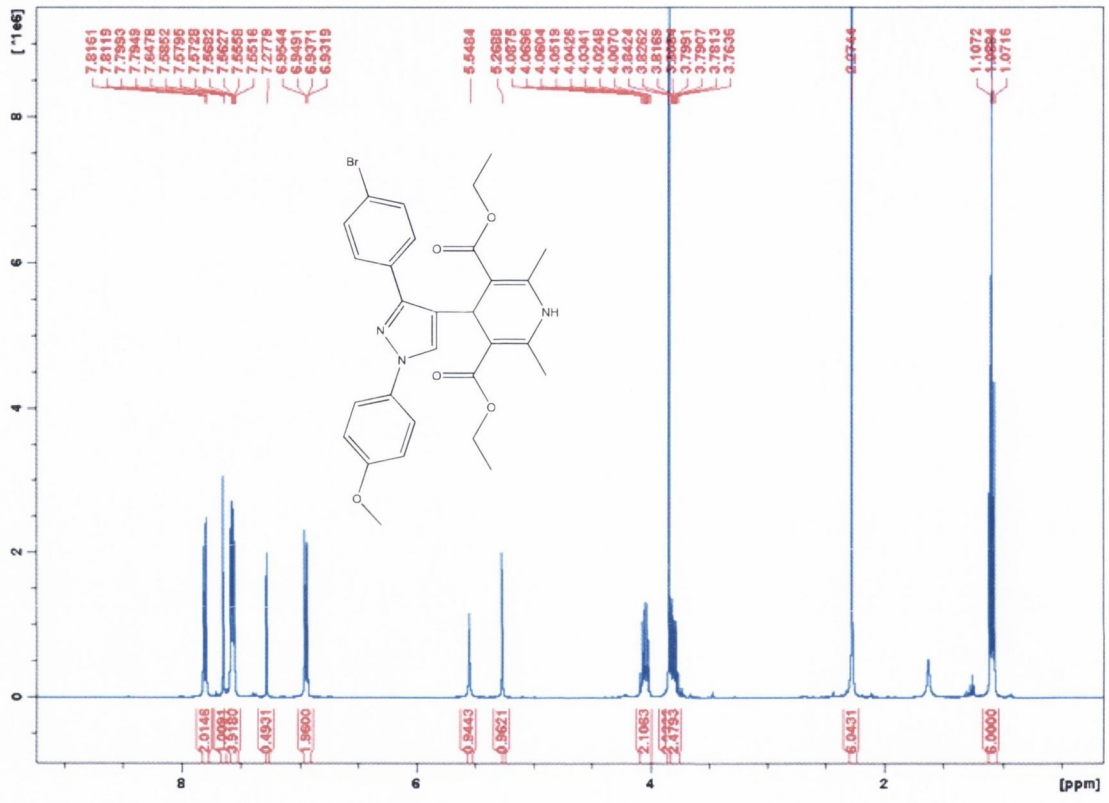

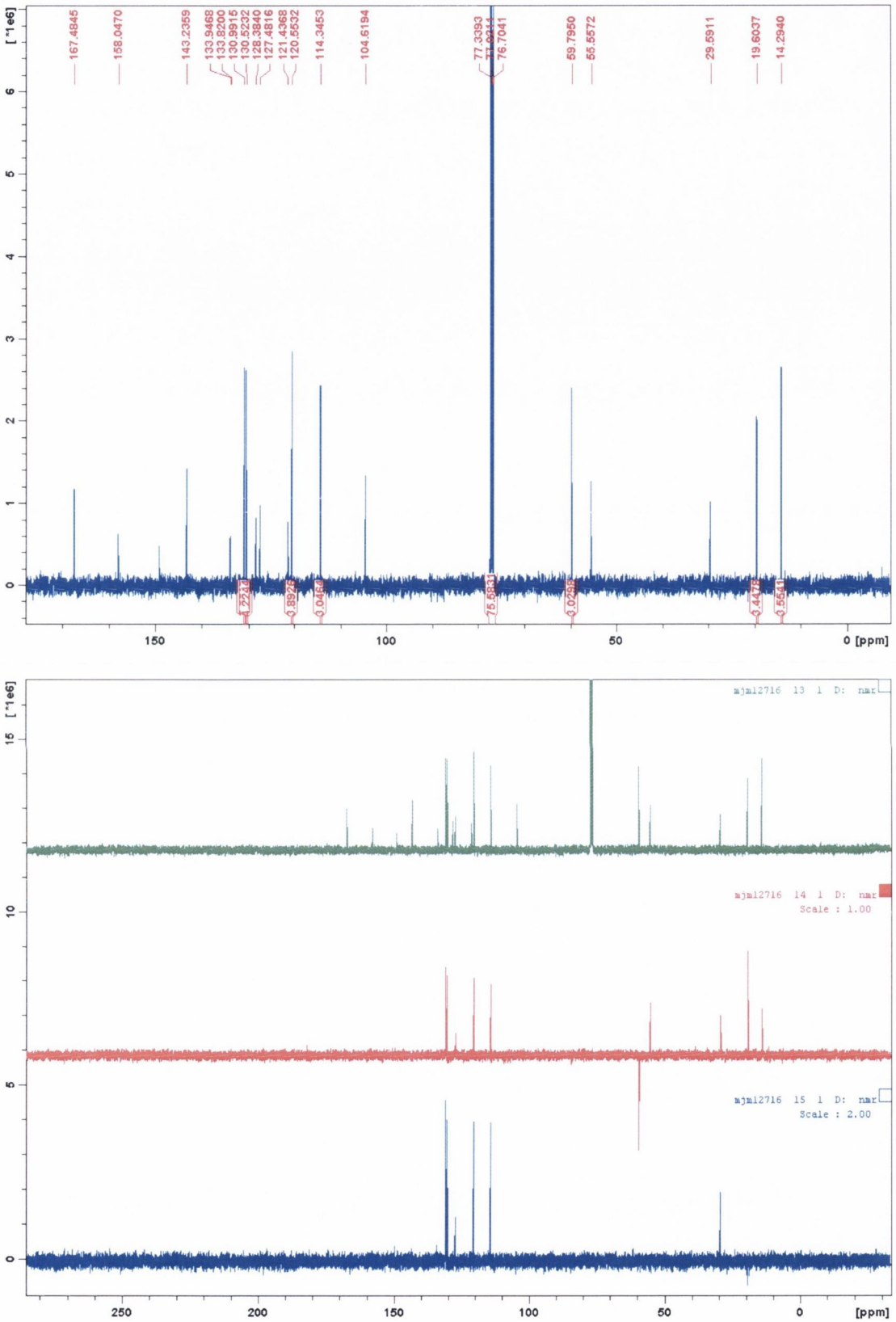

Figure 2.4 ^{1}H ,^{13}C and DEPT NMR spectrum for compound 167

2.3.2 Sythesis of dimethyl-4-(1,3-diphenyl-1H-pyrazol-4-yl)-2,6-dimethyl-1,4-dihydropyridine-3,5-dicarboxylates (scaffold I B)

Compounds (**183-188**) containing the benzyloxy, halogen, amino, phenyl, hydroxyl and methoxy functionality were successfully synthesised from their respective pyrazole carbaldehydes (**143-148**). The reaction of appropriate methyl acetoacetate instead of ethyl acetoacetae was applied with the same condition as in the previous reaction to favour the production of the scaffold I B 1,4-dihydropyridines (**Scheme 2.15**). **Table 2.4** presents the isolated yield (by column chromatography on silica gel) and spectroscopic data obtained for products (**183-188**).

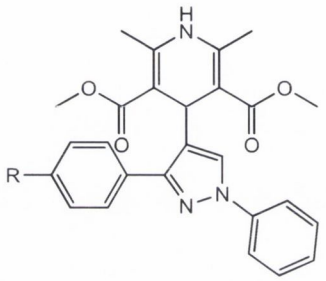

Compound	Structure R	MP (^{0}C)	IR (υ_{max} cm^{-1}) C=N, C=O &C-O-ester	Yield (%)
183	OBz	184	1578.5 1698.8 1215.3	23.6
184	Br	206	1601.0 1674.3 1216.2	16.8
185	NH_2	156	1599.4 1685.2 1215.4	3.4
186	H	166	1599.7 1674.5 1216.3	4.6
187	OH	270	1530.3 1682.5 1216.5	15.3
188	OMe	100	1578.6 1696.0 1208.4	15.7

Table 2.4 Melting points, IR and Yield for type I B 1,4-dihydropyridines (183-188)

Compound **187** was identified initially from IR spectroscopy with the C=O and OH absorption at υ1682.59 cm^{-1} and υ3338.56 cm^{-1}. The ^{1}H NMR spectrum of **187** (**Figure 2.5**) displayed two singlets at δ 2.31 and δ 3.33 both integrate for six protons each and represent the methyl groups. The other singlet appears at δ 5.30

corresponding to the proton at the C-4 1,4-dihydropyridine ring. The aromatic protons all appear in the region from δ 6.97-7.83. Where a double doublets at δ 6.97 (J=2.36 Hz and 4.48 Hz) represent the protons at the H-3 and H-5 in the ring A. Two multiplets appear at δ 7.24 and δ 7.43 integrate for one and two protons respectively, which corresponding to ring B protons at H-4' and H-3', H-5' position. The second and third double of doublets observed at δ 7.77 and δ 7.81 with coupling constant of 3.92Hz, 4.68Hz and 2.36Hz, 4.48Hz. Therefore those signals identified as protons at the H-2', H-6' and H-2, H-6 in aromatic ring B and ring A, respectively. In addition, compared to type IA 1,4-DHPs, it was observed in the 600MHz ^{1}H NMR spectrum of some of type IA compounds e.g. compound **161**, additional broad quartet signals appearing at δ 4.11 (J=7.1Hz) and 4.20 (J=7.1Hz) which are thought to arise from the presence of a minor rotamer. These signals were approximately in a 1:7 ratio with the primary multiplet signals from the $-CH_2$ components if the ethoxy side chains of the 1,4-dihydropyridine section of the molecule which are observed centred at δ 3.77 and δ 4.03 respectively for compound **161**. Obviously, these characteristic methylene group signals were disappeared in the ^{1}H NMR spectra of scaffold I B compounds.

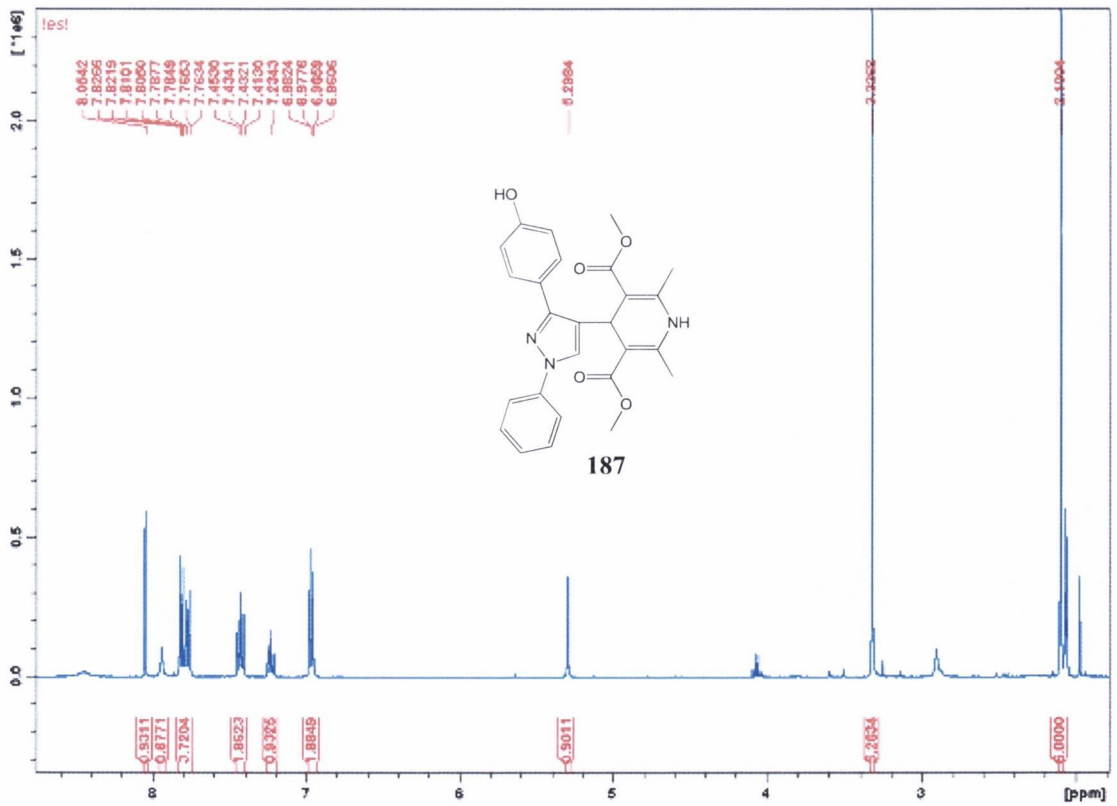

187

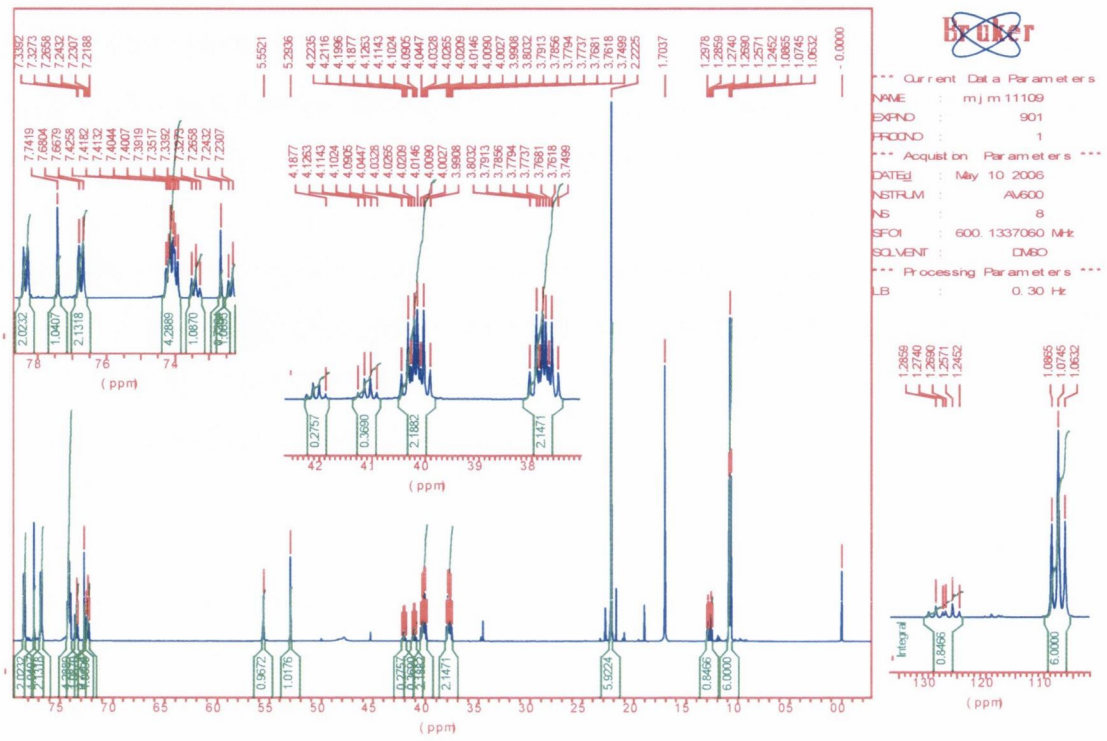

Figure 2.5 ^{1}H NMR spectrum of representive Scaffold IB and scaffold IA 1,4-DHP compounds 187 & 161

2.3.3 3,5-Dibenzoyl-2,6-dimethyl-1,4-dihydro-4-phenylpyridine derivatives (scaffold I C)

Reported by Kawase et al. 3,5-dibenzoyl-2,6-dimethyl-1,4-dihydro-4-phenylpyridine derivatives (BzDHPs) (**189**) were prepared by variation of the Hantzch reaction. (**Scheme 2.16**) This series of BzDHP derivatives possesses the MDR-reversal activity which was dependent on the nature of substituents and their positions on the 4-phenyl ring of BzDHPs.[227] Therefore, six novel potential MDR-modulators were synthesised by refluxing the mixture of excess aqueous ammonia, substituted pyrazole carbaldehyde and 2 equivalents of benzoylacetone in methanol, which gave scaffold I C 1,4-DHPs (BzDHPs) (**190-194**) in low yields.(**Table 2.5**)

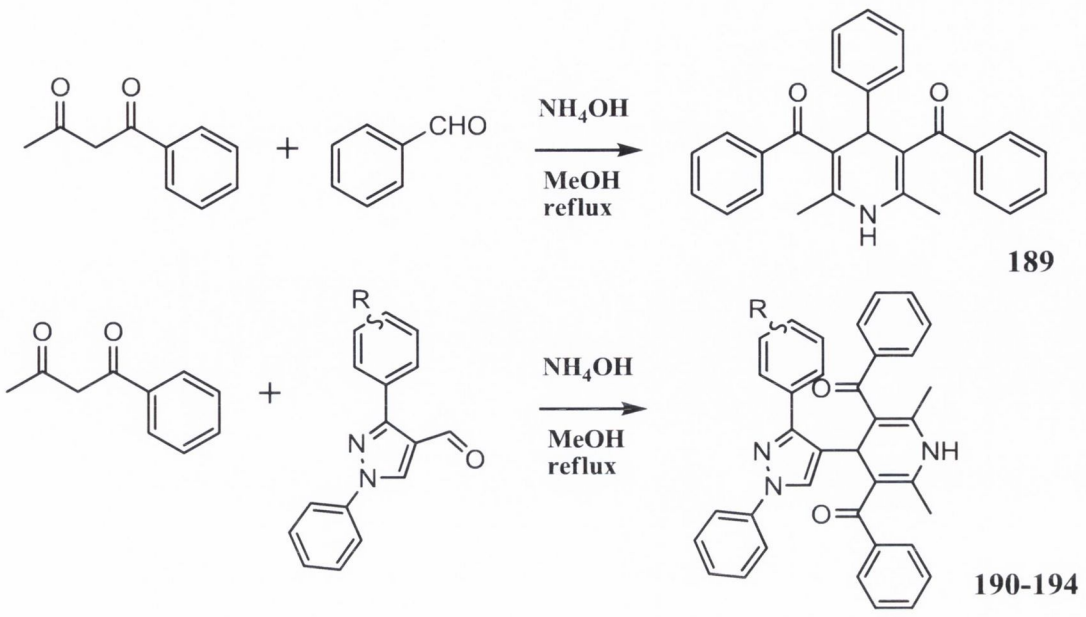

Scheme 2.16 BzDHPs derivatives synthesised by Hantzch reaction

Compound	Structure R	MP (°C)	IR (υ_{max} cm^{-1}) C=N, C=O	Yield (%)
190	NH_2	140	1597.89 1677.63	1.1
191	Br	180	1602.28 1655.40	8.8
192	H	116	1596.47 1656.40	15.8
193	OBz	116	1598.90 1653.30	7.5
194	OMe	220	1596.97 1655.79	11.5

Table 2.5 Melting points, IR and Yield for type IC 1,4-dihydropyridines (190-194)

The ^{1}H NMR spectrum of **192** (**Figure 2.6**), shows two singlets at δ 2.00 and δ 5.34 respectively, which correspond to the methyl groups and the proton at C-4 of the dihydropyridine ring. The region from δ 6.98-7.65 indicated the aromatic protons and integrated for 21 protons derived from four different phenyl rings and pyrazole ring. The ^{13}C NMR spectrum of **192** also shows the signals at δ 18.33 and δ 33.77 which assigned to the methyl group and C-4 (CH) carbons, respectively. The carbonyl signal appears at δ 197.25. These assignments were confirmed in the DEPT spectrum.

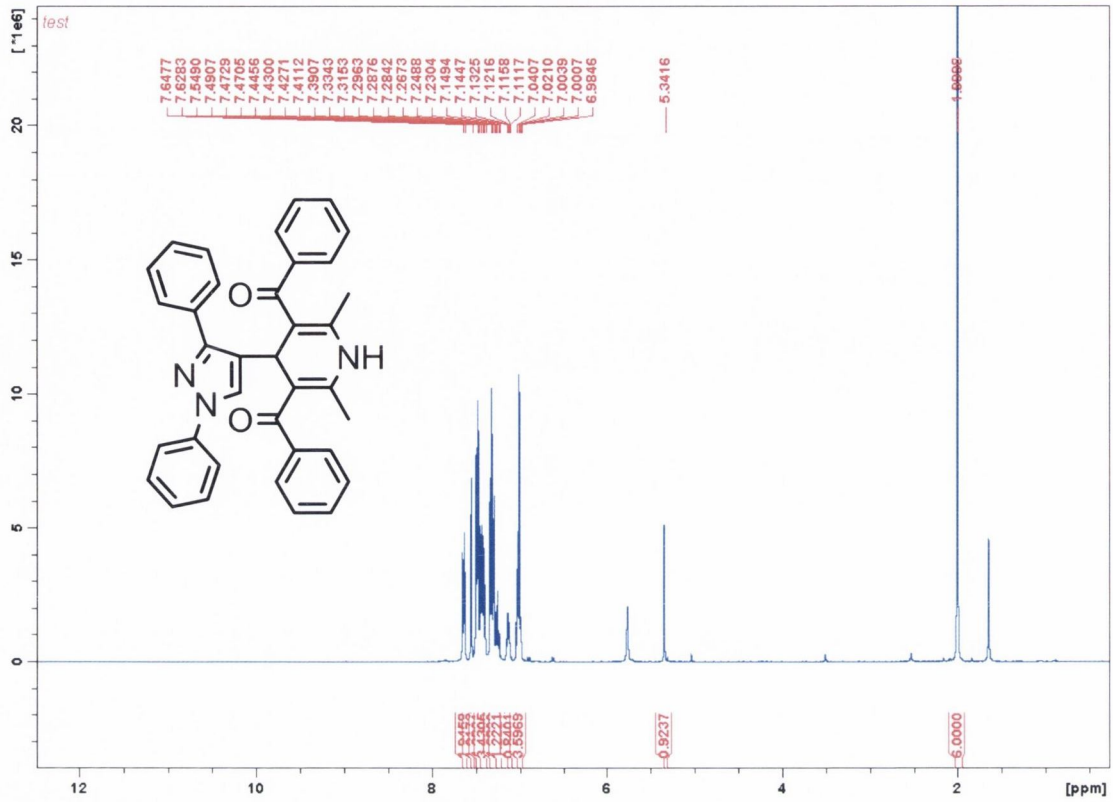
test
7.6477
7.6283
7.5490
7.4907
7.4729
7.4705
7.4456
7.4300
7.4271
7.4112
7.3907
7.3343
7.3153
7.2963
7.2876
7.2842
7.2673
7.2488
7.2304
7.1494
7.1447
7.1325
7.1216
7.1158
7.1117
7.0407
7.0210
7.0039
7.0007
6.9846
5.3416
1.9998
0.9237
6.0000
[*1e6]
[ppm]

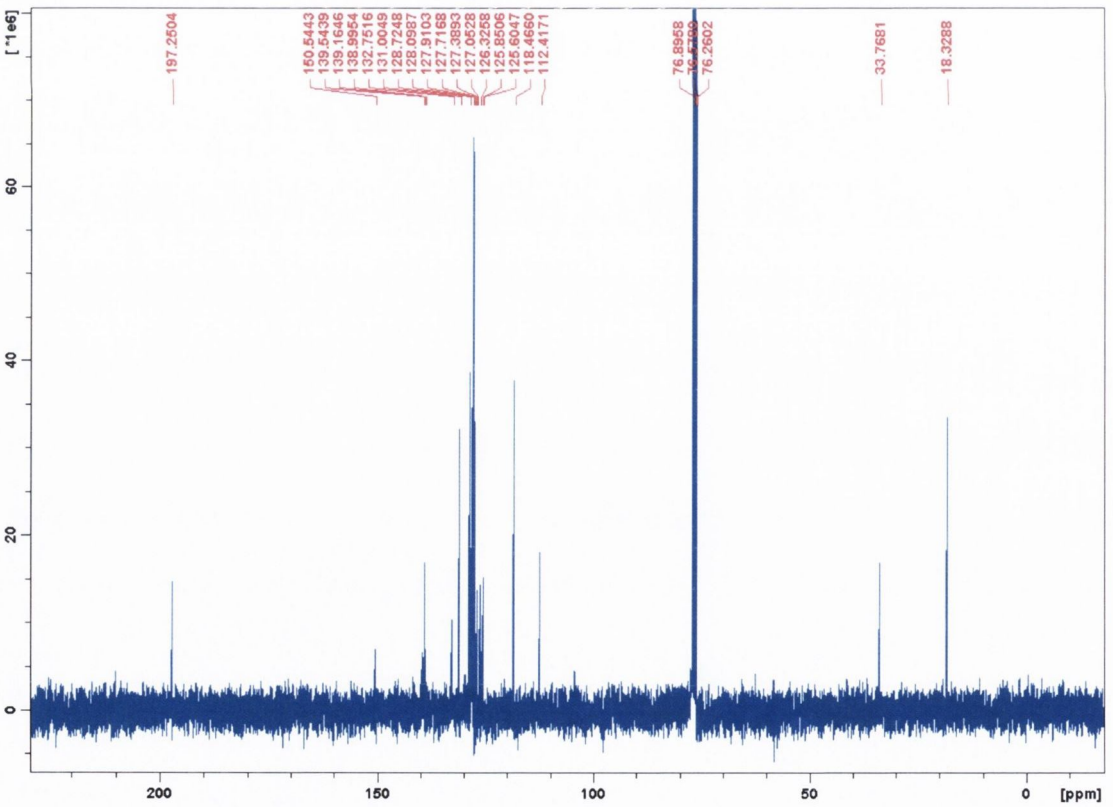
197.2504
150.5443
139.5439
139.1646
138.9954
132.7516
131.0049
128.7248
128.0987
127.9103
127.7168
127.3893
127.0528
126.3258
125.8506
125.6047
118.4660
112.4171
76.8958
76.2602
33.7681
18.3288
[*1e6]
[ppm]

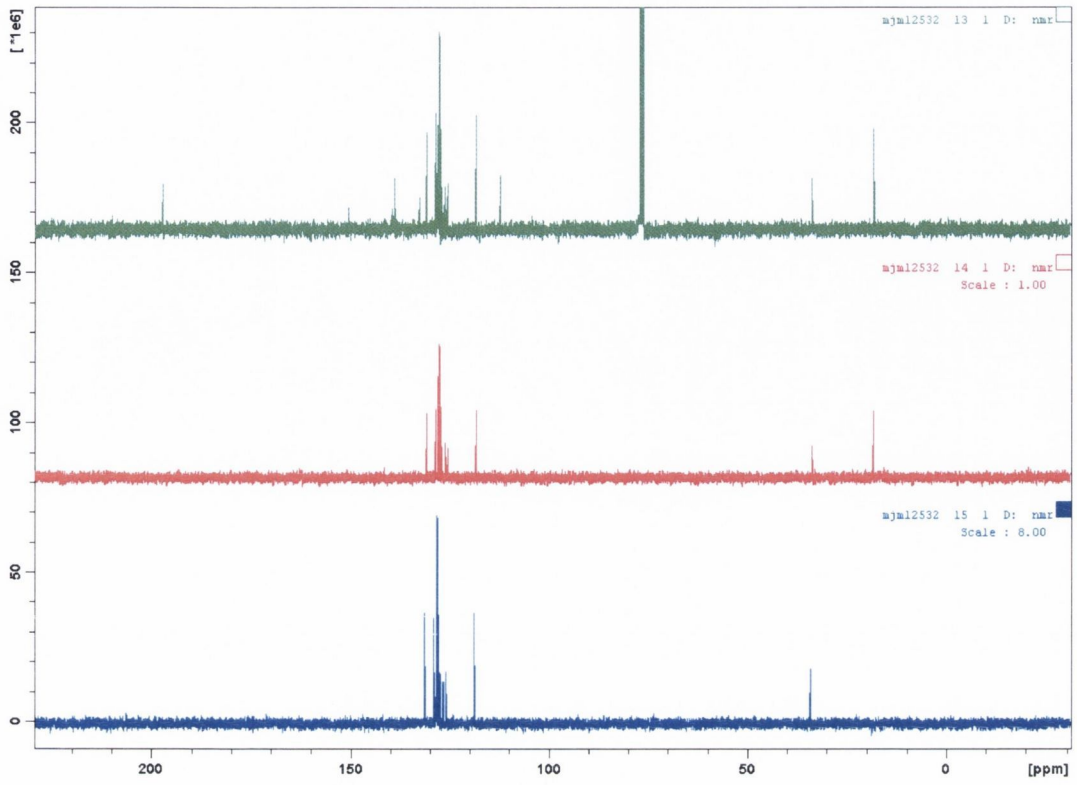

Figure 2.6 ^{1}H ,^{13}C and DEPT NMR spectra for compound 192

2.3.4 Determination of crystal structures by XRD

To determine the stereochemistry and potential for further molecule modelling studies, a number of the 1,4-dihydropyridines products synthesised in **section 2.5** were examined by XRD analysis.

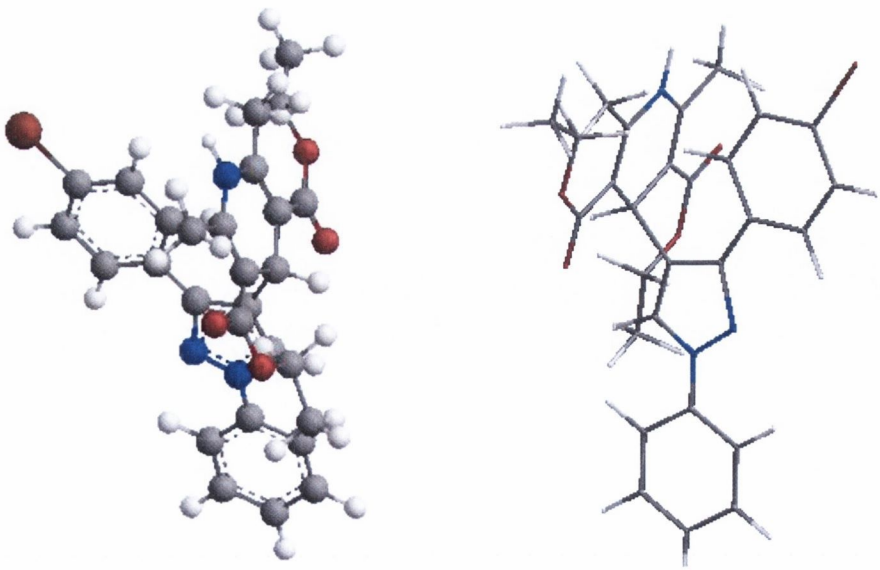

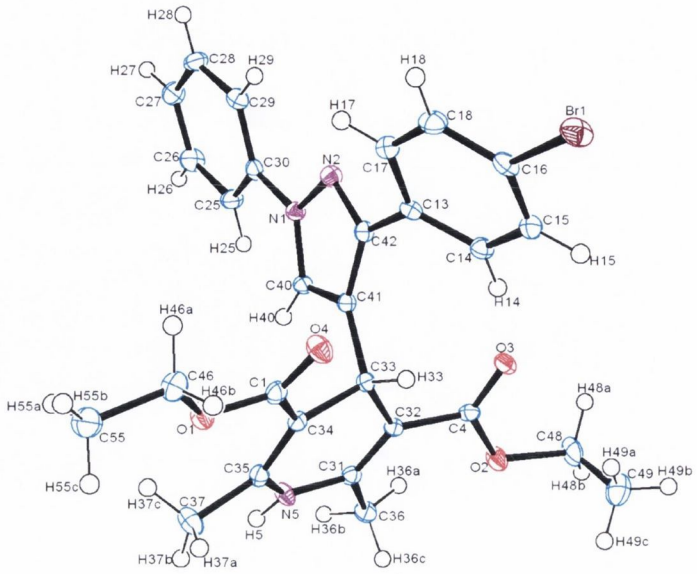

Figure 2.7 Ortep representation of the crystal structure of compound 162 with 50% thermal ellipsoids

In order to obtain the high quality crystals for XRD, it is necessary to consider what are the best method and the solvent. After few attempts by different solvents including methanol, DCM and hexane, it was found ethanol is good to produce the crystal when the diluted (approx. 5 mg of compound in 1 mL of solvent) solution by very slow evaporation. The typical procedure involved the preparation of a solution which placed it in a capped small test tube, with pinhole on the top to allow the slow evaporation of solvent. The whole procedure should occur in the dark over a period of 1~2 months. Subsequently, only few compounds synthesised above yielded crystals for structure determination by XRD.

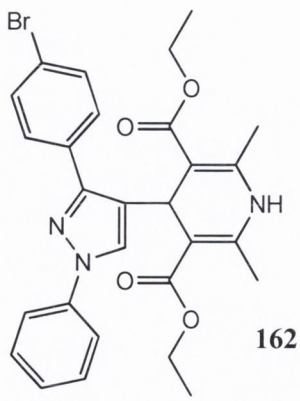

162

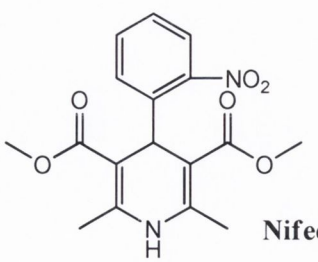

Nifedipine

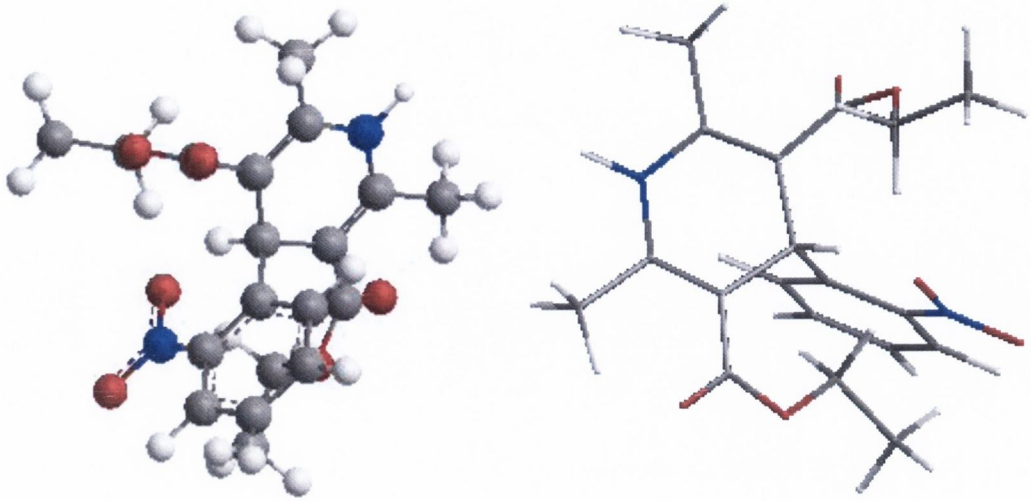

The data for crystals **162** and nifedipine were collected on a Rigaku Saturn 724 CCD Diffractometer. A suitable crystal from each compound was selected and mounted on a glass fiber tip and placed on the goniometer head in a 123K N2 gas stream. The data sets were collected using Crystalclear-SM 1.4.0 software and in each case, 1680 diffraction images, of 0.5° per image, were recorded. Data integrations, reductions and corrections for absorption and polarization effects were all performed using Crystalclear-SM 1.4.0 software. Space group determination, structure solution and refinement were obtained using Crystalstructure ver. 3.8 and Bruker Shelxtl Ver. 6.14 software. The ORTEP structure for compound **162** and nifedipine are presented in **Figure 2.7** and **Figure 2.8** with the 50% ellipsoids shown, in which carbon atoms are displayed in white, oxygen atoms in red, nitrogen atoms in blue and bromine atom in brown.

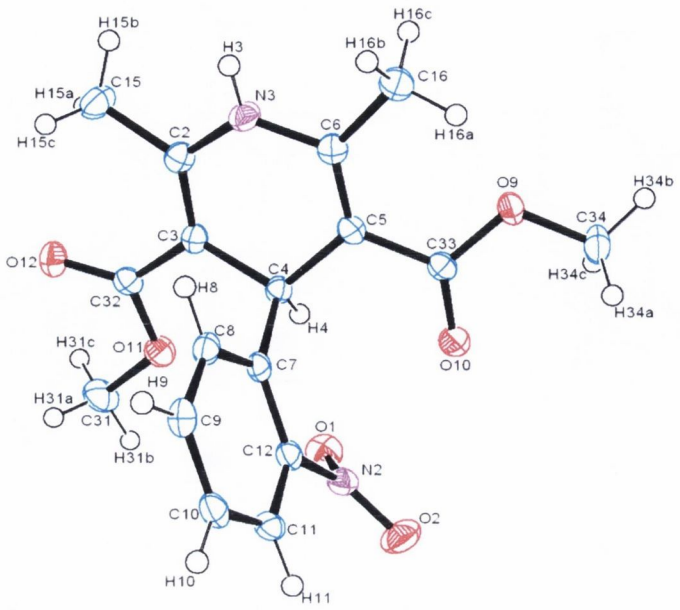

Figure 2.8 Ortep representation of the crystal structure of nifedipine with 50% thermal ellipsoids

2.3.5 Synthesis of 1,4-dihydropyridines by microwave irradiation

Although the application of microwave heating to modify chemical reactions can be traced back to the 1950s, the first article on the use of microwave irradiation to carry out organic chemical transformations by the groups of Gedye was published in 1986.[228] Since then, the applications of microwave irradiation in chemistry has become a fast moving and exciting technique in the multistep synthesis and medicinal chemistry/drug discovery, and have additionally extended to related fields such as polymer synthesis, nanotechnology, material sciences and biochemical processes.[228, 229]

Microwave heating is the technology of applying microwave irradiation to chemical reactions. As high frequency electric fields, microwaves will normally heat any material such as polar molecules in a solvent or conducting ions in a solid. The microwaves interact directly with the molecules that are present in the reaction time, led to an instantaneous localized superheating of anything that will react to either dipole rotation or to ionic conduction, which are the two fundamental mechanisms for transferring energy from microwave to the substance being heated.[230]

Certainly, solvents also play a very important role in conventional organic synthesis as well as microwave chemistry. Polarity is very important in terms of microwaves

which directly interact with the molecules that are present in the reaction mixture. The more polar a reaction mixture is, the great its ability to couple with the microwave energy. Solvents are generally classified as three categories, low, medium and high absorbance level which is determined by their dielectric parameters. Although non-polar and low b.p. solvents (i.e. hexane, dichloromethane) are generally not used in microwave synthesis as they do not couple efficiently to microwave irradiation, its capability can be applied in microwave synthesis sometimes for which the reaction mixture are temperature sensitive. While not interacting with the irradiation, the non-polar solvent will decrease the thermal heat being produced from the polar reagent and ensure a constant reaction condition in microwave synthesis.

Microwave-assisted organic synthesis has shown some advantages compared to traditional heating, such as dramatically reduced reaction time, typically from days or hours to minutes or even seconds, increased product yields and reduction in unwanted side reactions to enhance product purity. The short reaction time provided by microwave synthesis is ideal for rapid reaction and optimization of reaction conditions of pharmaceutical development.[231] Many reaction parameters can therefore be evaluated. With fully optimised procedure, the corresponding products are produced in few hours, which is the time to take to run a single conventional reaction. Therefore, heating chemical reaction by microwave energy has been an incredibly popular topic in the scientific community.

2.3.5.1 Hantzsch reaction using microwave technology

The single-mode microwave reactor was used for the first time to accelerate the organic synthesis in 2000.[232] In comparison with reactions performed in domestic ovens, this device was designed to produce ultra-fast, highly reproducible and verified methods organic synthesis by a software-based chemistry workflow platform. In a microwave reactor, there are four major instrument parameters that produce microwave instrumentation dedicated to organic synthesis; these are temperature, pressure, power control and reaction time which are monitored by software operation and sophisticated safety control in real time.

The first report on synthesis of 1,4-dihydropyridines under microwave irradiation was published by Alajarin et al. in 1992. Since then, microwave irradiation has been

successfully used to promote multicomponent Hantsch type reactions yielding 4-arylsubstituted-1,4-dihydropyridines.[233] Many literature reports indicate that construction of 1,4-DHPs in a microwave has been performed in different conditions, either in solution or dry media, to develop the incredibly short reaction time, higher yield and somehow unexpected results from the reaction. Since microwave chemistry has been investigated in our group for few years and the isolated yields for the DHPs initially synthesized above were low, the Hantzsch reaction for synthesis of compound **164** was carried out using a single-mode microwave system (Biotage intiator, **Figure 2.9**)

Figure 2.9 Biotage microwave heating system

To some extent, the reaction conditions that would usually be used (i.e. concentration of reaction, solvent, reagent, temperature etc.) should be varied with significant improvement. So the temperature, reaction time and concentration have been chosen as factors which might affect the yield. To optimise the best combination conditions for this 1,4-DHP microwave assisted synthesis, methods of orthogonal design (OD) using the properties of the fractional factorial design were investigated. In statistics, fractional factorial designs are experimental designs which involve a carefully chosen fraction of the experimental runs of a full factorial design.[234] With these studies, a three factor, three levels experiment (reaction temperature (120 °C, 130 °C, 140 °C), reaction time (10 min, 20 min, 30 min) and concentration of reactants (ammonia, ethyl acetoacetate and pyrazole carbaldehyde (0.1 mmol, 0.15 mmol, 0.2 mmol)) was designed with the capability of sampling a small, but representative set of level combinations, to help us promote the most effective reaction condition under microwave irradiation with short time-consuming. Details of specific reaction and the

variable conditions were investigated and resultant yields obtained are presented in **Table 2.6**.

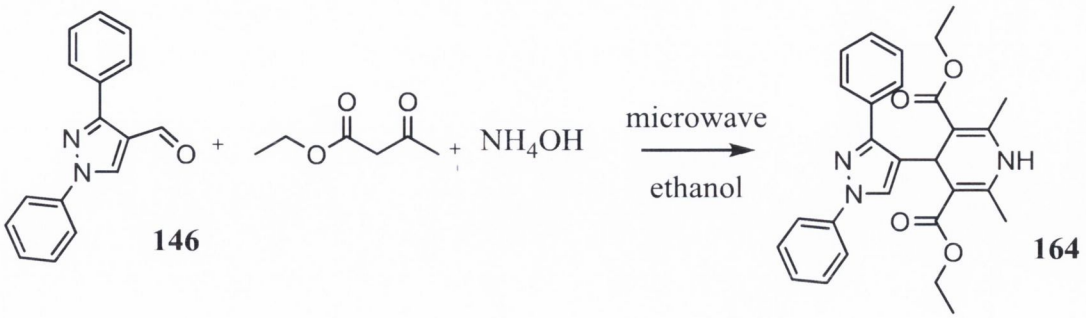

146 **164**

Scheme 2.17 Microwave synthetic route for scaffold I A analogues

Using the conditions shown above, it was concluded that a significant reduction in the reaction time was possible under microwave conditions. (18 hours to 30 minutes) The yellow highlighted results are an average of the isolated yields based on various levels from different factors, which indicated using the following combination of conditions (temperature 140 ^{o}C, time: 30 min and reactant concentration 0.1 mmol/L) could be best combination for 1,4-DHP synthesis. For instance, the synthesis of compound **164** was achieved with significant improvement in isolated yield from 7.9% to 30%.

No	A 1	B 2	C 3		Test No	Combinations of levels	Factor			Result
							Temp ^{0}C	Time min	Concentration mmol/L	yield %
1	1	1	1		1	$A_1B_1C_1$	120	10	0.1	24.43
2	1	2	2		2	$A_1B_2C_2$	120	20	0.15	7.27
3	1	3	3		3	$A_1B_3C_3$	120	30	0.2	4.14
4	2	1	2		4	$A_2B_1C_2$	130	10	0.15	10.16
5	2	2	3		5	$A_2B_2C_3$	130	20	0.2	29.68
6	2	3	1		6	$A_2B_3C_1$	130	30	0.1	23.96
7	3	1	3		7	$A_3B_1C_3$	140	10	0.2	15.69
8	3	2	1		8	$A_3B_2C_1$	140	20	0.1	20.86
9	3	3	2		9	$A_3B_3C_2$	140	30	0.15	29.96
I							35.84%	50.28%	69.25%	
II							63.8%	57.81%	47.35%	
III							66.51%	58.06%	49.51%	
K_1							11.95%	16.76%	23.08%	
K_2							21.27%	19.27%	15.78%	
K_3							22.17%	19.35%	16.5%	

Table 2.6 Orthogonal design (OD) determination of the best condition for microwave irradiation synthesis

*Results in I, II, III cells presented the sum of isolated yield in a specific factor level, (i.e 35.84% equal a total of yields from test No 1&2&3) and K_1,K_2, K_3 are the average of isolated yield related to the reaction factor (Temp, Time, concentration)

2.4 DHP prodrugs synthesis

In the present work, novel derivatives of the DHP compounds was synthesised by introduction of non-steroidal anti-inflammatory drugs (NSAIDs) and other established chemotherapy agent to the hydroxy (**165**) or amino (**163**) scaffold I A compounds. The study of such a coupling reaction may be useful for improvement of the combination chemotherapy treatment and production of more lipophobic compounds comparing to their corresponding parent compounds in the future development of these prodrugs.

2.4.1 Coupling with alkylating chemotherapy agent

The combination of an antitumor drug with either radiotherapy and/or additional chemotherapy agents is generally necessary in cancer treatment.[235] A method to increase the ER antagonist activity for the 1,4-DHP analogues by coupling of the hydroxy (**165**) and amino (**163**) to the conventional alkylating chemotherapy agent chlorambucil has been developed for this study. Consequently, using EDCI as coupling reagent, an ester or amide linkage gives **195** and **196** when chlorambucil was coupled to **165** or **163** respectively. (**Scheme 2.18**)

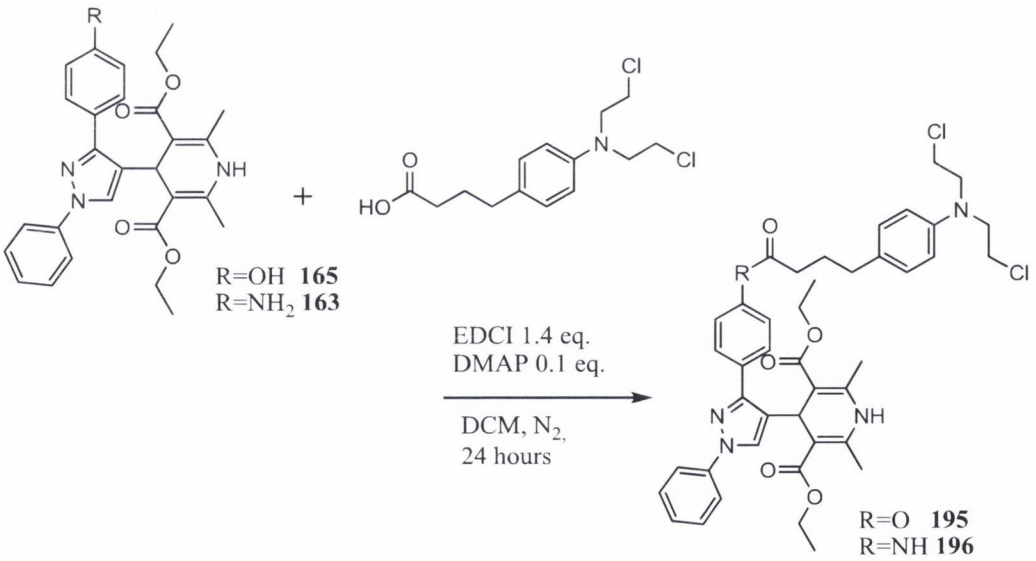

Scheme 2.18 Coupling of 165&163 with chlormabucil to form 195&196

The reaction was carried out in dry DCM using EDCI&DMAP. **In scheme 2.19**, carbodiimide EDCI activates the carboxylic acid in a similar way to DCC. While used as a catalyst, DMAP act as a stronger nucleophile than the alcohol in the reaction which can produce an amide type intermediate to react towards the alcohol.

The reaction also occurs in this manner for compound **163** which containing the amino group. The yield and spectroscopic data of ester and amide conjugations are displayed in **Table 2.7**.

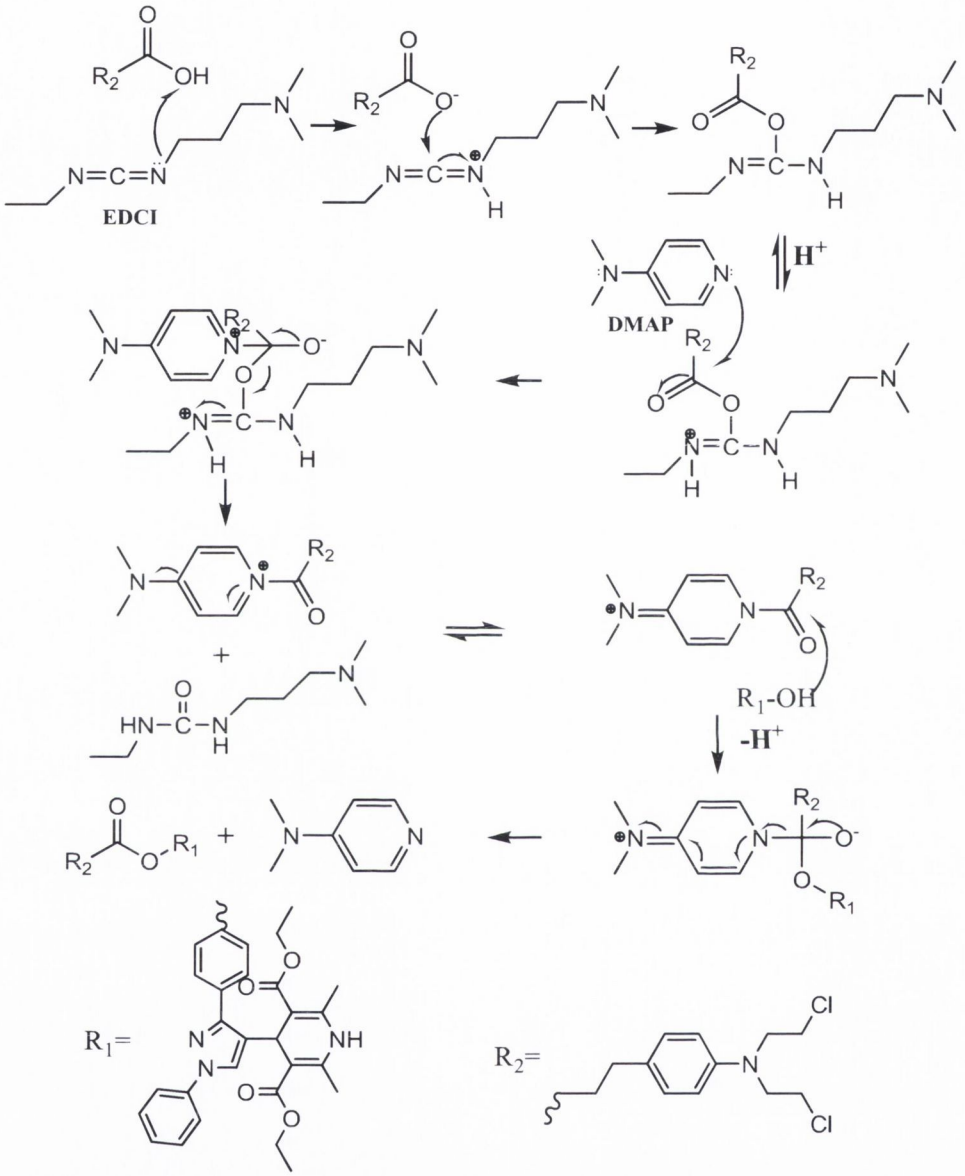

Scheme 2.19 Mechanism for the coupling of chlorambucil to DHP ester by using EDCI/DMAP

Compound	MP (^{O}C)	IR (υ_{max} cm^{-1}) C=O, N-H	Yield (%)
195	152	1615 3335	85.9
196	186	1598 3312	29.6

Table 2.7 yield, melting point and infrared data for 195 & 196

2.4.2 Coupling reactions for phenol products

Non-steroidal anti-inflammatory drugs (NSAIDs) are usually used for the symptomatic treatment of inflammation in acute and chronic conditions, particularly for different types of arthritis. These drugs also have analgesic and antipyretic effect when they block the COX enzymes, inhibit thrombocyte aggregation and decrease prostaglandins throughout the body, reviewed by Yadav et al.[236] However, NSAIDs shows many undesired side effects, most important are gastrointestinal irritation and ulceration, on long term use. Several strategies have been designed to overcome this drawback from parent drug, which involves development of prodrugs by ester or amide conjugates with the free carboxylic group of NASIDs.[237]

In this section, two pharmacologically active agents are coupled together so that potential mutual prodrugs may result in increased antiproliferation properties over the parent compound, and improve the solubility of our new scaffold 1,4-DHP during the prolonged administration. In this section, a simple procedure to couple several various categories of the NSAIDs, such as sulindac **197** (arylalkanoic acid), aspirin **201** (salicylate acid), ibuprofen **199**, ketoprofen **200** (arylpropionic acids), and indomethacin **198**, with phenolic of 1,4-DHPs to obtain corresponding ester derivatives was carried out. A similar reaction can be applied to the anti-tumor drug Combretastatin A-4 derivatives **203** and acetic acid **202**, which also contain the free carboxylic group in the molecule for the coupling reaction.

The synthesis of ester 1,4-DHP analogues (**204-210**) from appropriate NASIDs and CA-4 is presented in **scheme 2.20**. EDCI was used as the carboxylic acid activating agent and the typical procedure included dropwise addition of a solution of the NASIDs to a refluxing solution of phenol 1,4-DHP (**165**) in dry DCM. The melting point, yields and infrared data for these products are displayed in **Table 2.8**. The compounds **204-210** represent a novel type of 1,4-DHP analogue containing NASIDs and CA-4 and should afford biochemical properties different from the 1,4-DHPs previously reported. Ongoing modelling and biochemical studies have shown that some of these products have potent antiproliferative activity which is discussed in chapter 4.

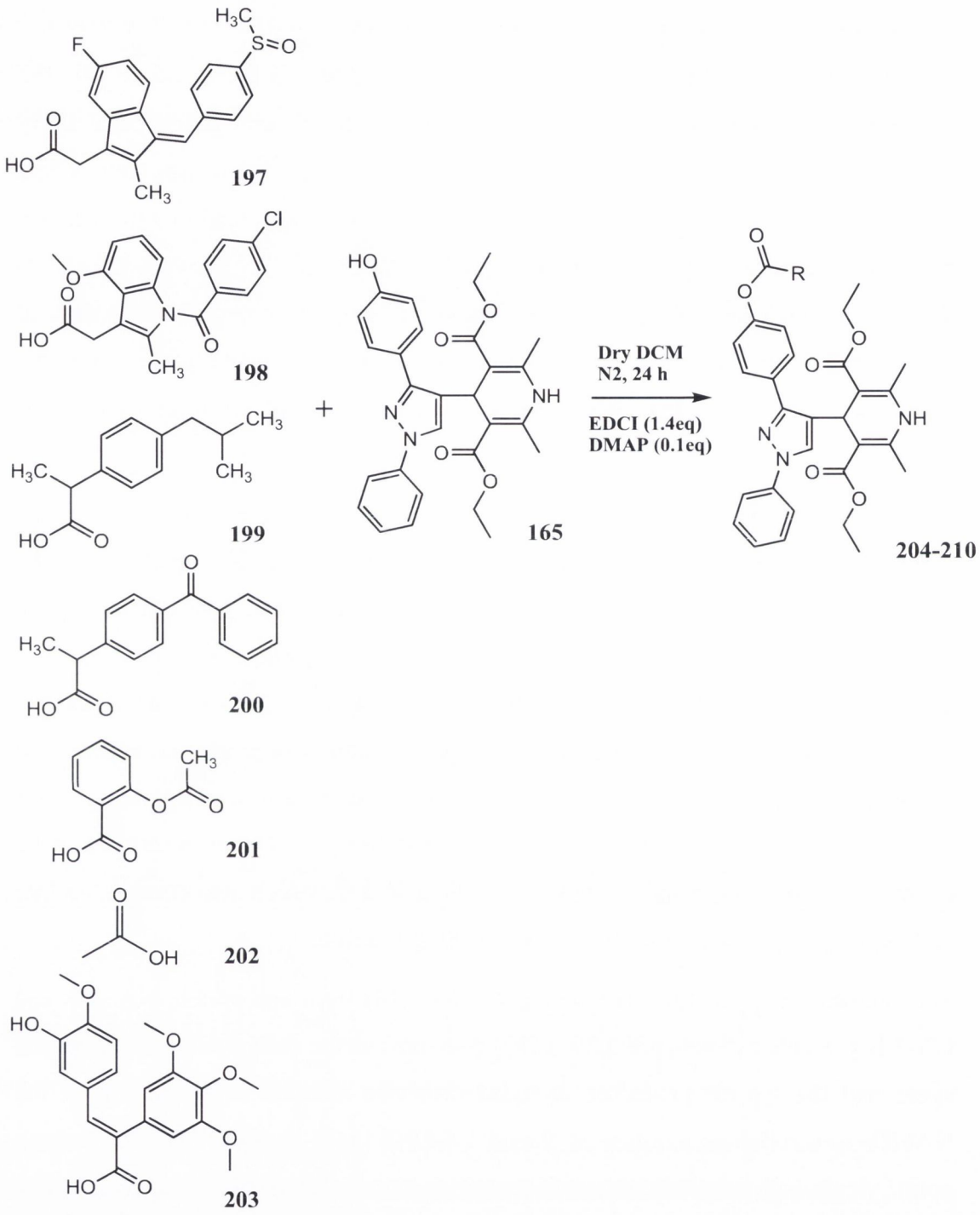

Scheme 2.20 Addition of NASIDs or acetic acid to phenol 1,4-DHP analogues

Compound	Structure R	MP (^{O}C)	IR (υ_{max} cm^{-1}) C=N, C=O &C-O-ester	Yield (%)
204	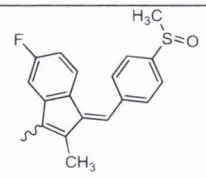	**182**	**1600.7 1688.9 1209.1**	**32.6**
205	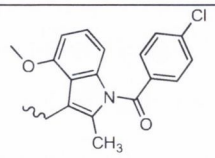	**168**	**1599.9 1699.6 1213.5**	**14.2**
206	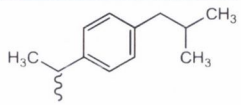	**192**	**1600.9 1694.0 1211.7**	**46.0**
207	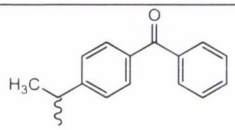	**178**	**1599.2 1693.3 1211.4**	**30.26**
208	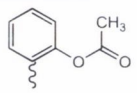	**186**	**1604.4 1689.1 1208.0**	**21.4**
209		**Oil**	**1615.3 1690.6 1209.7**	**53.2**
210	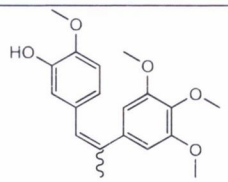	**180**	**1612.3 1683.3 1210.3**	**16.2**

Table 2.8 Mp, yield and spectroscopic data for conjugation analogues 204-210

The structural assignment of **208** was characterized by IR and NMR spectroscopy. In **Figure 2.10**, it is clearly evident that the proton of the two ethyl ester methyl groups are observed as a triplet centred around δ 1.23, integrated for 6 protons with coupling constant of 7.12 Hz. The HSQC spectrum (**Figure 2.11**) indicates that these protons are attached to carbon signal at δ 14.46 as is expected for the CH_3 group. The two methyl groups appear as a singlet at δ 2.12 which integrated for 6 protons. The singlet signal associated with the carbon signal at δ 21.01 which integrated for 3 protons indicated that it is assigned to a methyl group attached to the carbonyl. The multiplet signals in the region δ 3.99 to δ 4.14 integrated for 4 protons represent the two diastereotopic methylene groups. H''-4 was clearly identified as a singlet at δ 5.20 which is also attached to carbon signal at δ 30.24. (**Figure 2.10&2.11**). The

aromatic protons appear as a series of multiplet in the region δ 7.18 to δ 8.28 integrating for a total 14 protons, and these signals are associated to the series of carbons in the region δ 118.77 to δ 134.91 shown in the HSQC spectrum. Except for the singlet signal integrating for the single proton corresponding to a CH group at δ 122.43 which is assigned to the CH group linked to the N-1 position in the pyrazole ring, the assignments of the rest of aromatic proton signals were ambiguous. In the NOE and HSQC spectrum, the two double doublet signals were observed at δ 7.18 and δ 7.62 integrating for 4 protons with coupling constant of J=4.26, J=2.34. These two signals represent to H_2, H_6 and H_3, H_5 interact with aromatic carbons at δ 121.11 and δ 132.36. The two mutliplet signals in the region δ 7.22-7.24 and δ 7.70-7.74 respectively integrating for a total of 5 protons are shown to be assigned to H_4', H_2', H_6'(corresponding to C_4', C_2', and C_6' carbon appear at δ 124.01 and δ 118.77) and H_3''', H_4'''(corresponding to C_3''' and C_4''' at δ 126.06, δ 134.91). The multiplet signal at δ 7.43-7.47 was assigned to the H_3', H_5' and H_5''' with corresponding carbon appear at δ 126.32, 126.41 and δ 129.32. The multiplet signal at δ 8.27-8.30 can be assigned to the H_6''' related to the carbon appear at δ 133.12. While the weak singlet signal at δ 5.71 has no corresponding carbon signal in the HSQC spectrum so that was assigned to the amine group.

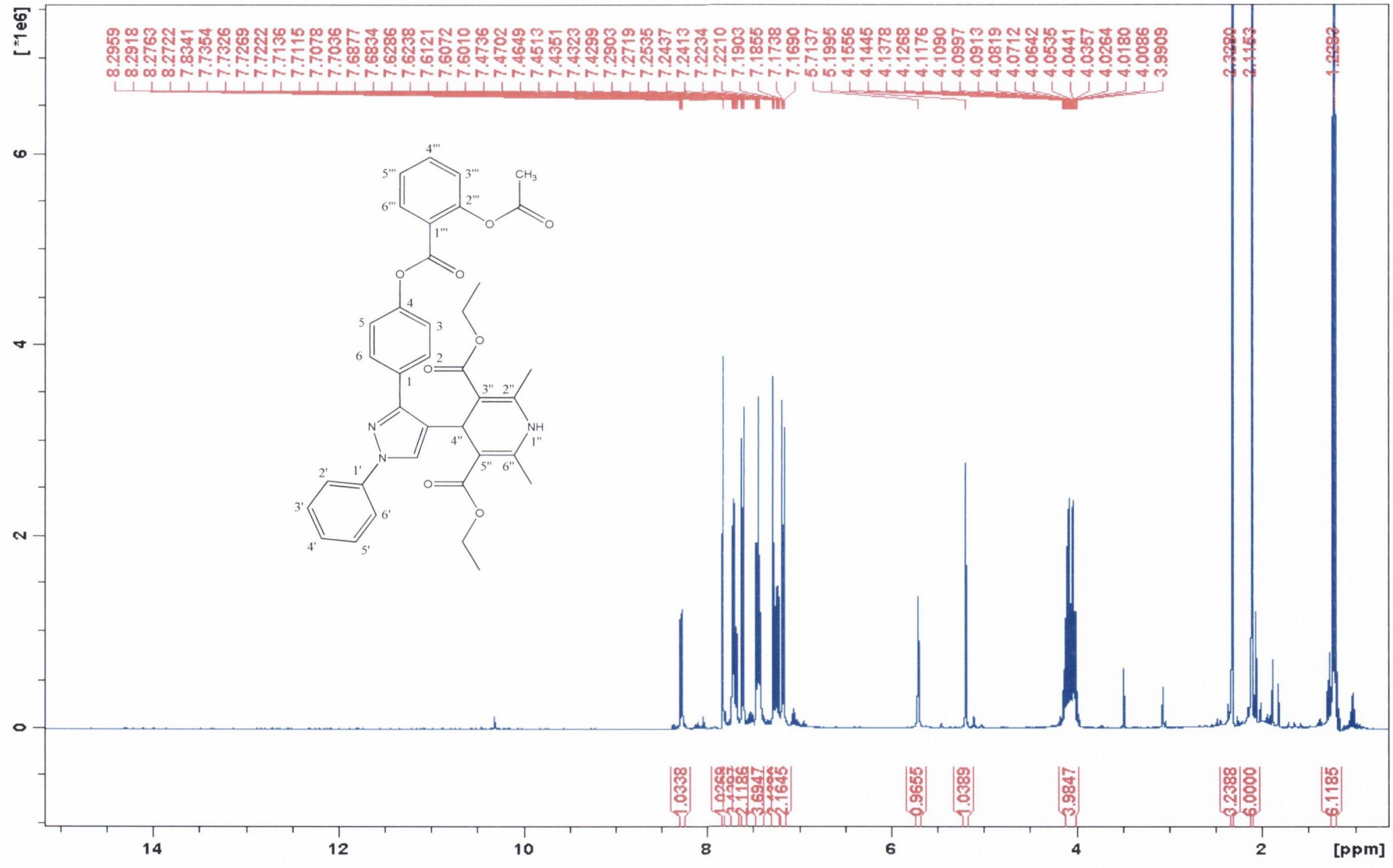
[*1e6]
8.2959
8.2918
8.2763
8.2722
7.8341
7.7354
7.7326
7.7269
7.7222
7.7136
7.7115
7.7078
7.7036
7.6877
7.6834
7.6286
7.6238
7.6121
7.6072
7.6010
7.4736
7.4702
7.4649
7.4513
7.4351
7.4323
7.4299
7.2903
7.2719
7.2535
7.2437
7.2413
7.2234
7.2210
7.1903
7.1855
7.1738
7.1690
5.7137
5.1995
4.1556
4.1445
4.1378
4.1268
4.1176
4.1090
4.0997
4.0913
4.0819
4.0712
4.0642
4.0535
4.0441
4.0357
4.0264
4.0180
4.0086
3.9909
2.3280
2.1153
1.2282
1.0338
0.9655
1.0389
3.9847
3.2388
6.0000
6.1185
[ppm]

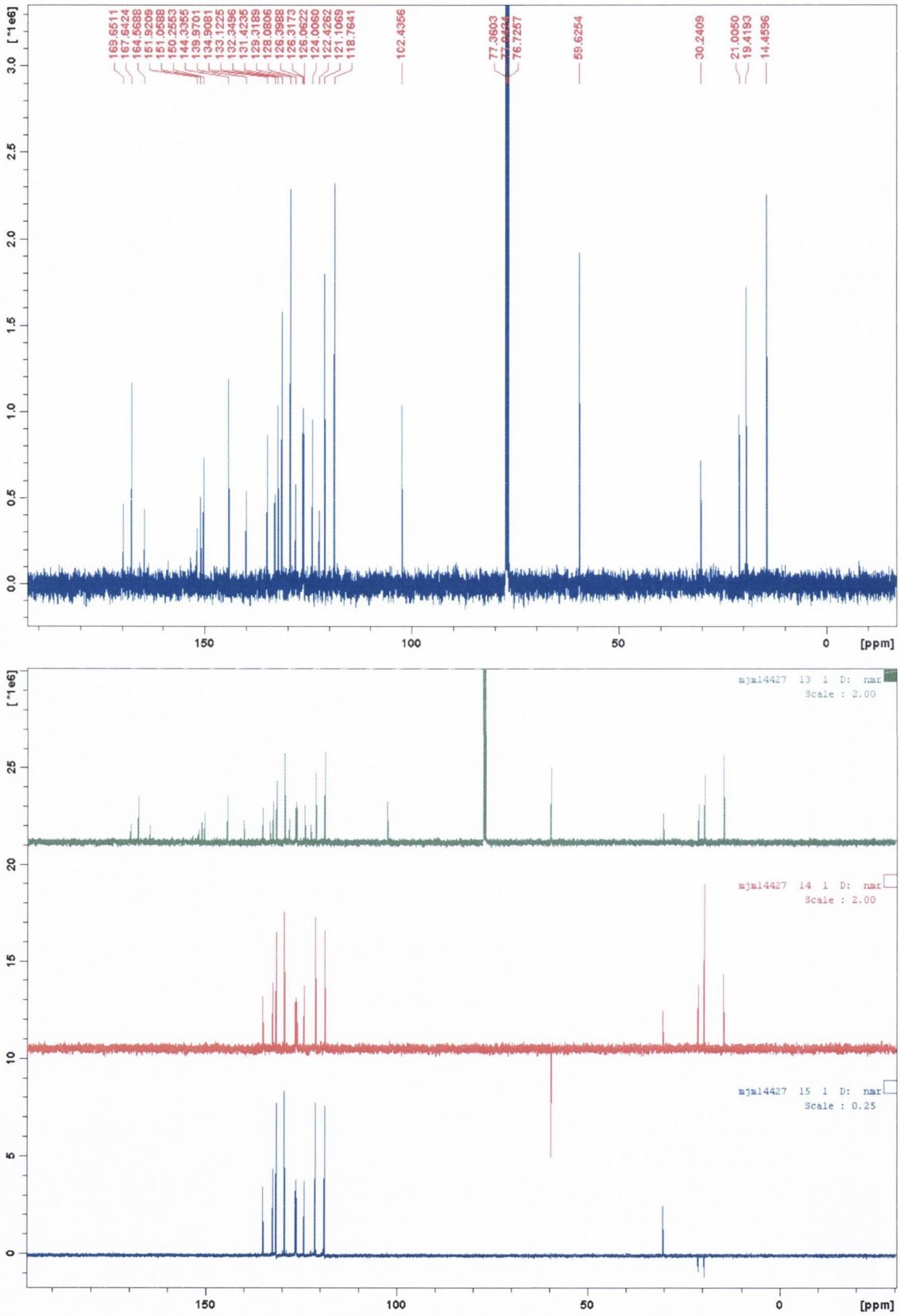

Figure 2.10 ^{1}H NMR, ^{13}C NMR and DEPT spectrum of compound 208

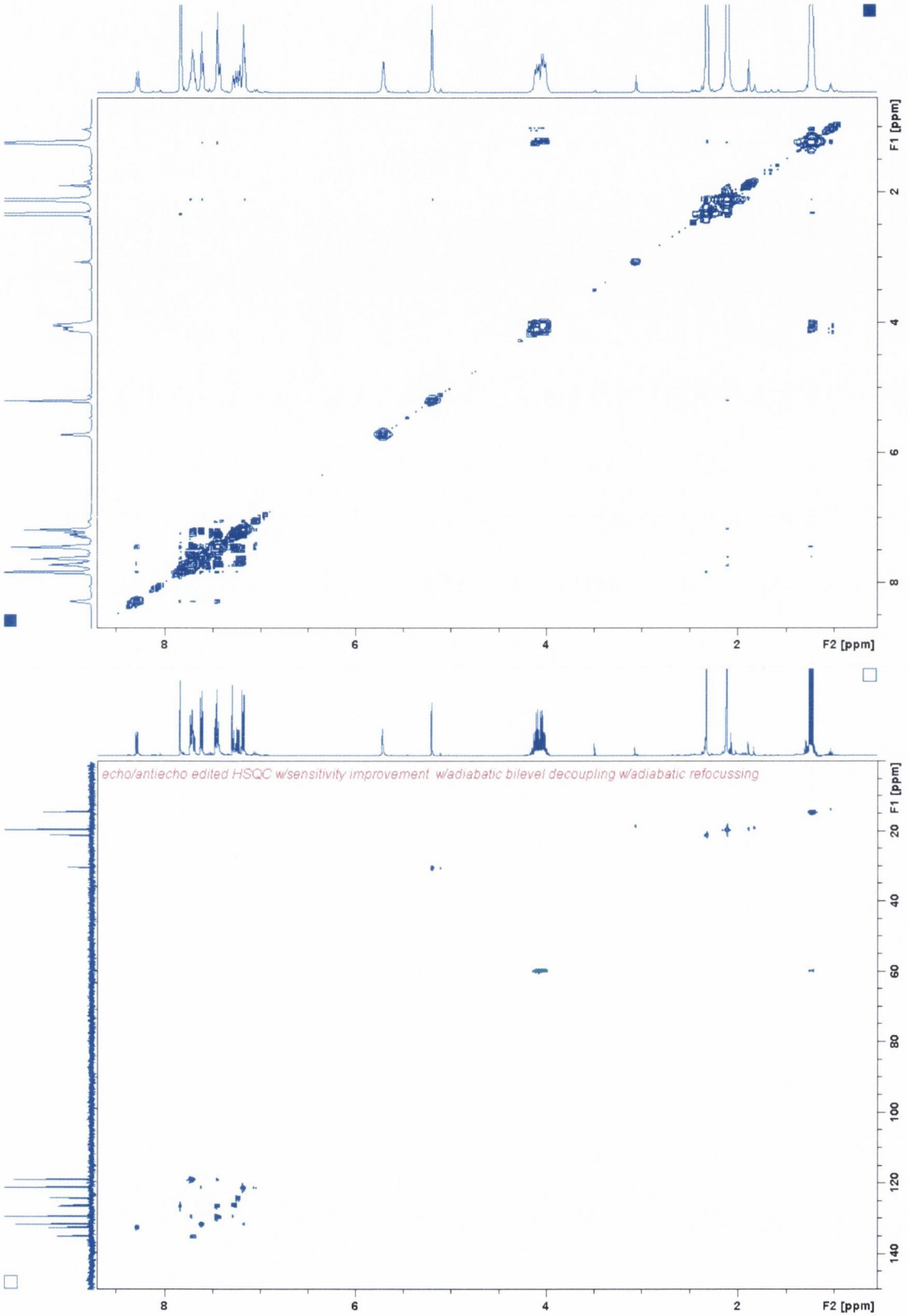

Figure 2.11 NOESY and HSQC spectrum of compound 208

2.5 Introduction of basic ether to the phenolic scaffold I A compound

Following SAR studies of the products synthesised above for their antiproliferative activity in MCF-7 cells, it has been shown that addition of the nucleophilic basic ether, such as 2-chloroethylpiperidine, 2-chlorothylmorpholine and 2-chloroethylpyrrolidine, etc., to the phenolic 4-(1,3-diphenyl-1H-pyrazole-4-yl)-1,4-dihydropyridine scaffold may have positive effects for antiproliferative activity. **Scheme 2.21** illustrates the reaction of a series of basic alkyl halides were introduced onto the compound **165**, where anhydrous potassium carbonates is used as the base. Subsequently, the nucleophilic substitution reaction on proceeds on removal of the phenolic proton, oxygen attacks the electrophilic carbon of the alkyl chloride. The biochemical studies discussed in chapter 4 identified the piperidine ring as being the most potent for antiproliferative activity and thus this ring was chosen as the optimum basic side chain for further modification.

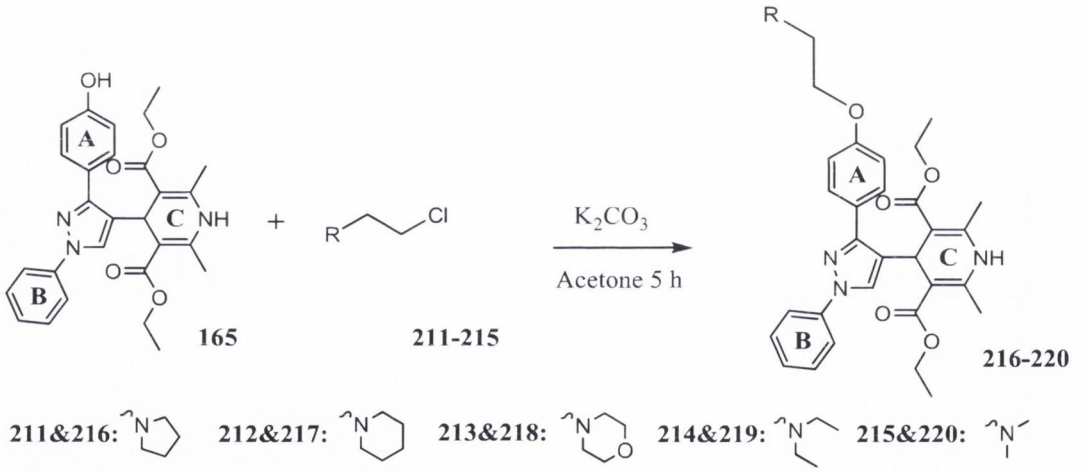

Scheme 2.21 Addition of basic side chain to phenol 1,4-DHPs

Initially 4-(1,3-diphenyl-1H-pyrazole-4-yl)-1,4-dihydropyridine **165** substituted with a variety of basic side chains were synthesised(**216-220**). **Table 2.9** presents the yields, spectroscopy data and melting points for these products. Compound **165** reacted with 2-chloroethylmorpholine **213** to yield diethyl 2,6-dimethyl-4-(3-(4-(2-morpholinoethoxy)phenyl)-1-phenyl-1H-pyrazol-4-yl)-1,4-dihydropyridine-3,5-dicarboxylate**218**, while with 2-chloro-dimethylethanamine**215** afforded diethyl 4-(3-(4-(2-(dimethylamino)ethoxy)phenyl)-1-phenyl-1H-pyrazol-4-yl)-2,6-dimethyl-1,4-dihydropyridine-3,5-dicarboxylate **220** in a similar reaction.

Compound	Structure R	MP (^{O}C)	IR (υ_{max} cm^{-1}) C=N C=O&C-O-ester	Yield (%)
216		**178**	**1600.2 1692.2 1211.3**	**23.6**
217		**182**	**1600.3 1693.7 1211.3**	**9.3**
218	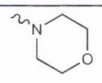	**170**	**1621.0 1691.2**	**28.6**
219		**168**	**1600.2 1692.8 1211.3**	**30.8**
220		**192**	**1600.1 1693.6 1211.5**	**16.2**

Table 2.9 Mp, yield and spectroscopic data for 165 conjugate with basic side chain products

The ^{1}H NMR spectrum of both products (**Figure 2.12**) revealed the distinctive 1,4-dihydropyridine signals appearing as multiplets in the region δ3.98-4.03, δ4.14-4.20 (**220**) and δ 3.73-3.81, δ 3.99-4.03 (**218**) integrating for 4 protons each and corresponding to the two diastereotopic methylene groups. While the basic dimethyl side chain (**220**) and morpholine side chain (**218**) were identified by the signals as two sets of multiplets in the region δ 1.23-1.31and δ 3.73-3.81 respectively, which integrate for a total of 12 protons. These signals overlap with other 6 protons signals from the methyl groups corresponding to N-(**CH$_3$**)$_2$ (H_9, H_{10}) and those signals integrated for 6 protons are also overlapping with signals from methylene group assigned to **CH$_2$**-N-**CH$_2$** (H_9, H_{12}). The aromatic protons of both compounds were observed in the region δ 6.94-7.81 (**218**) and δ 7.20-8.09 (**220**) respectively and integrate for 10 protons each.The ^{13}C NMR and DEPT spectra of **218** (**Figure 2.13**) were in agreement with the expected basic side chain products, in which the carbonyl carbon can clearly be seen at δ 167.24. The **CH$_2$**-O-**CH$_2$** (H_{10}, H_{11}) signal centred at δ 2.58 as a multiplet integrating for 4 protons are associated with carbon signals from C_{10}, C_{11} at δ 65.33. The 135° DEPT spectrum indicated that C_7, C_8 as negative signals at δ 57.17 and δ 66.39, which are assigned as two mutliplets centred at δ 4.13 and δ 2.81 in the ^{1}H NMR spectrum.

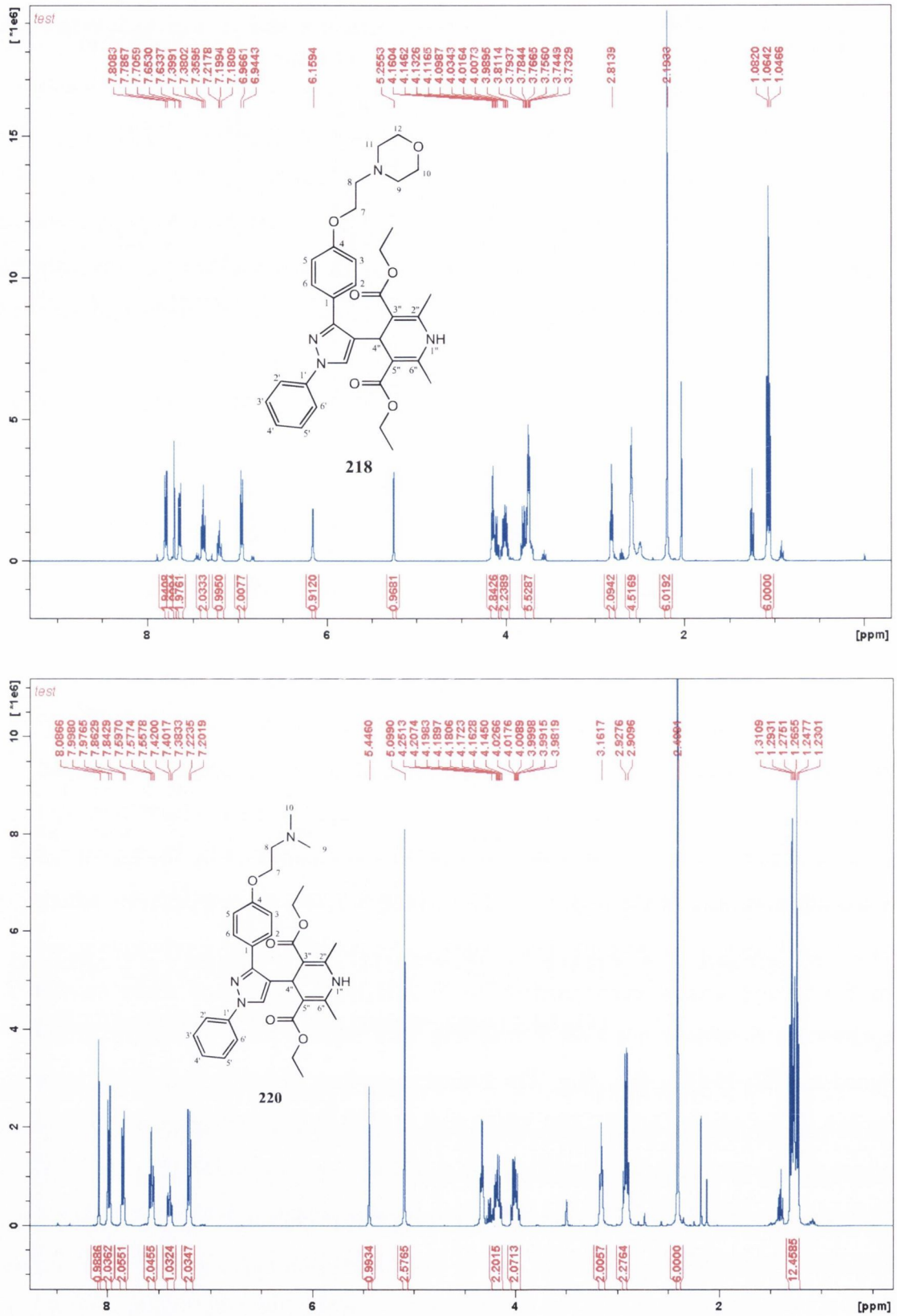

Figure 2.12 ^{1}H NMR spectra of compounds 218&220

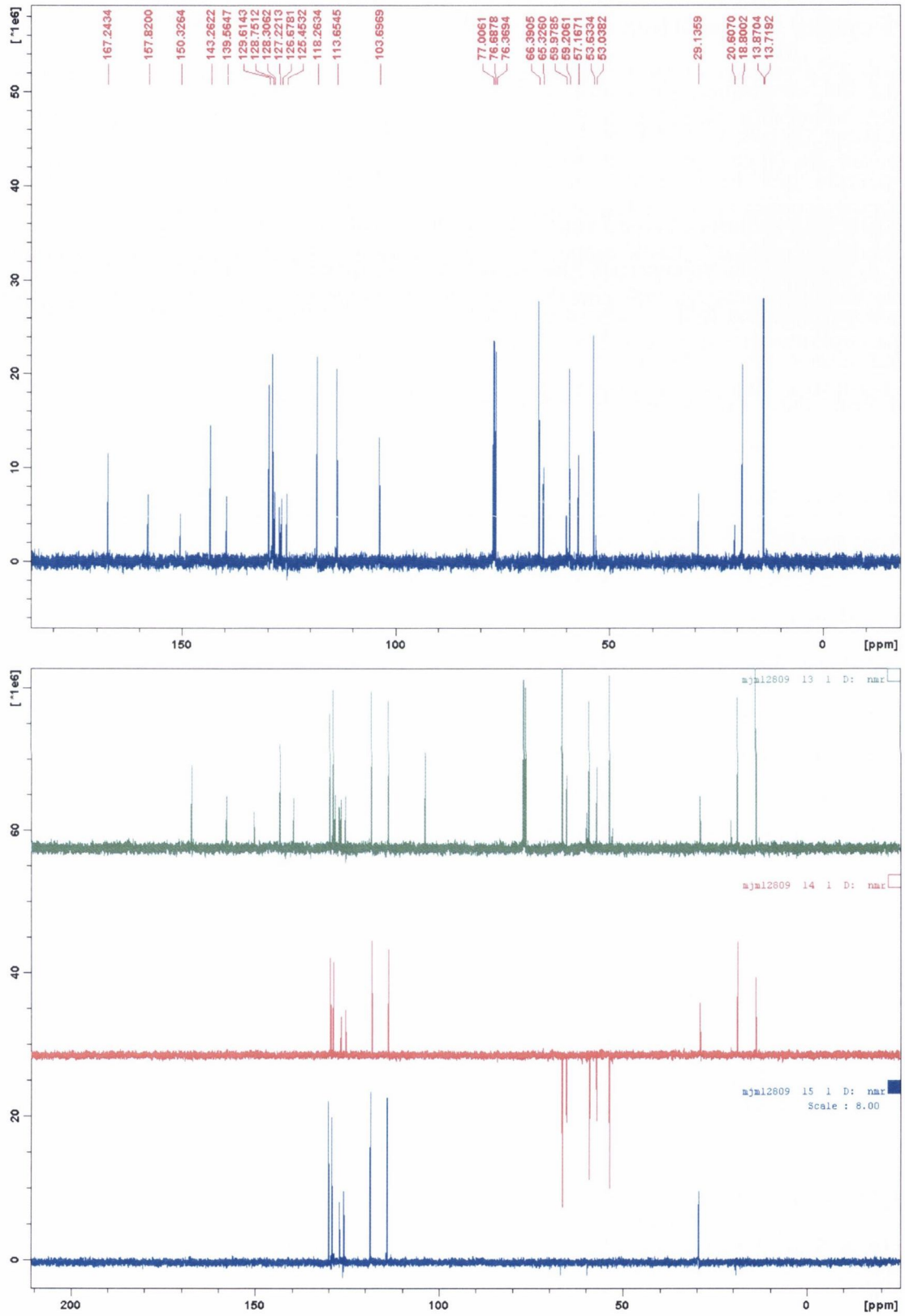

Figure 2.13 ^{13}C NMR and DEPT spectra of compound 218

2.6 Further optimisation

All of the compounds discussed in this chapter were designed for biochemical evaluation (detailed in Chapter 4). To optimise the structure of synthesised compounds and to improve the biochemical activity, more investigations on modification synthesis of type I scaffold will be carried out. The investigation in the type I compounds represented the novel 4-(1,3-diphenyl-1H-pyrazole-4-yl)-1,4-dihydropyridine scaffold, which vary in the aromatic substituents in the rings A and B and also contains the basic side chain component of the ring A substituent. Therefore, they can be considered to be similar to heterocyclic analogues of tamoxifen. As outlined below, we were interested in developing a new series of type I analogues containing the *p*-biphenyl substituent in Ring A, which could alternatively increase lipophilicity and possibly improve bioavailability.

2.6.1 Modification of Suzuki reaction

To optimise the structure activity relationship of type I scaffold, a classic and effective synthetic route to modify the Ring A to biaryls was carried out. The Suzuki cross-coupling reactions of arylboronic acid derivatives with aryl halides in the presence of $Pd(PPh_3)_4$ and base to form biaryls is powerful method for the synthesis of conjugated biaryls, styrenes and olefins which was first reported in 1981 by Suzuki et al.[238] The catalytic cycle shown in **Scheme 2.22** illustrates the mechanism for the Suzuki reaction. The mechanism can be divided into three key steps: (1) oxidative addition, (2) transmetalation, and (3) reductive elimination.[239]

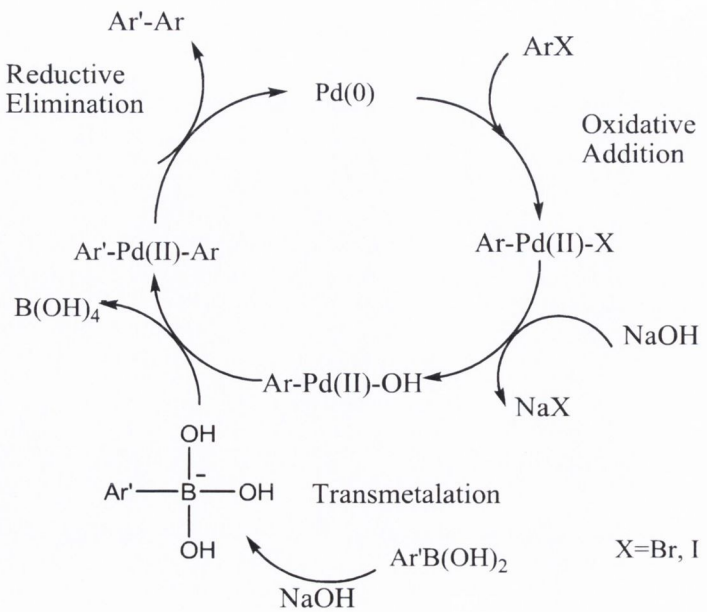

Scheme 2.22 Mechanism of Suzuki cross-coupling reaction

According to the proposed mechanism of Suzuki reaction shown in **scheme 2.22**, this cross-coupling reaction is catalyzed by Pd(0) species. After oxidative addition of aryl halide, the same substrate in the reaction, Pd(0) is converted in to a Pd(II) species as an active intermediate.[240241] Although phosphine based palladium as catalyst works successfully for most Suzuki cross coupling, in some cases, various catalyzed Pd/ligand systems can be employed in organic solvents for this reaction, such as $Pd(OAc)_2$, $[(\eta^3\text{-}C_3H_5)\text{-}PdCl]_2$ and $Pd/P(t\text{-}Bu)_2Me$.[241]The Suzuki-Miyaura reaction can also be employed in several types of coupling reaction such as alkyl-alkyl or alkyl-aryl cross-coupling as displayed below.(**Scheme 2.23**)

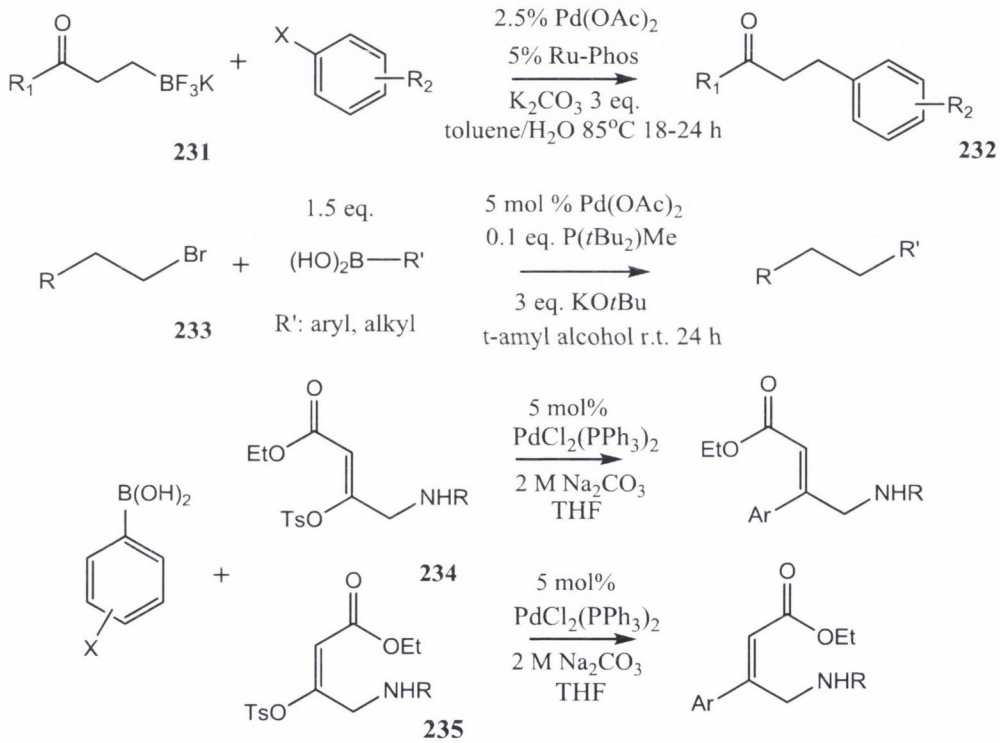

Scheme 2.23 Suzuki coupling reaction of aryl/alkyl halides with appropriate boronic acids

A variety of ketone, ester and amide-containing potassium trifluoroboratohomoenolates **231** act as the effective coupling partners in the Suzuki-Miyaura reaction, which are readily prepared from the unsaturated carbonyl compounds.[242]These new coupling reagents react with electrophiles aryl bromides/chlorides to give conjugation products **232**. The novel method for Suzuki cross-coupling reaction has developed by Kirchhoff et al.[243] A diverse set of inactivated alkyl electrophile **233** that are catalyzed by palladium or nickel with

boronic acids to afford the alkyl-alkyl product. Baxter et al. reported that aromatic trisubstituted α,β-unsaturated esters can readily prepared by the effective Suzuki-Miyaura coupling reaction. Both geometric enol tosylate **234**, **235** derivative reacted with electronically diverse aryl boronic acids to obtain a wide variety of expected ester product.[244]

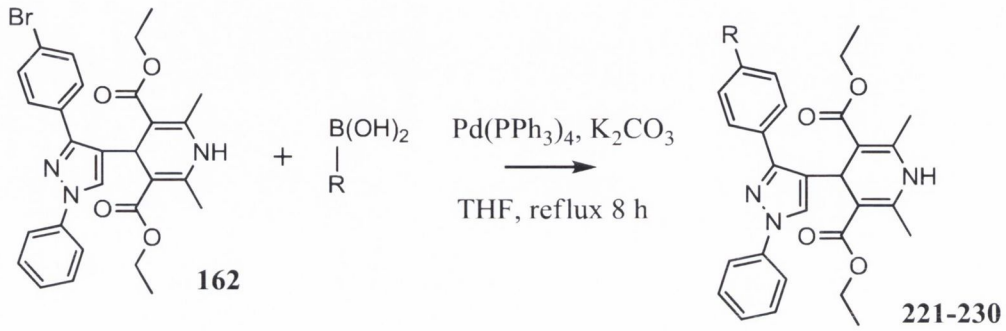

Scheme 2.24 Arylation of the Ring A by Suzuki reaction

In the present work, for newly synthesised type I analogues, Suzuki arylation of the bromide compound **162** with the appropriate boronic acids was achieved to afford the products (**221-230**) as outlined in **Scheme 2.24**. The spectroscopic data, melting point, and isolated yields were given in **Table 2.10**.

Compound	Structure R	MP (^{O}C)	IR (υ_{max} cm^{-1}) C=N, C=O &C-O-ester	Yield (%)
221	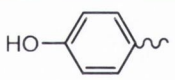	**182**	**1598.9 1679.0 1212.7**	**67.6**
222	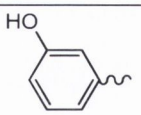	**178**	**1595.8 1677.4 1215.6**	**6.6**
223	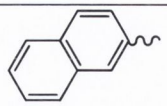	**184**	**1599.0 1651.5 1210.1**	**51.4**
224	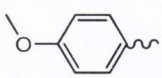	**176**	**1599.8 1693.6 1211.6**	**21.6**
225	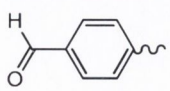	**180**	**1601.0 1693.7 1209.9**	**16.8**
226	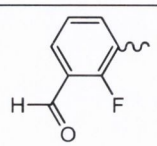	**196**	**1599.8 1694.0 1212.1**	**30.9**

227	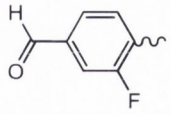	**184**	**1600.6 1693.7 1210.5**	**16.2**
228	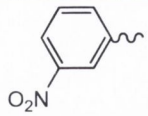	**194**	**1599.9 1692.3 1211.8**	**32.4**
229	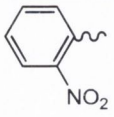	**164**	**1600.1 1681.9 1212.6**	**12.8**
230	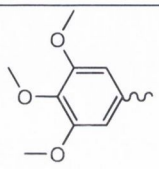	**172**	**1599.8 1693.6 1211.6**	**45.2**

Table 2.10 Mp, yield and spectroscopic data for arylation products 221-230

Diethyl 4-(3-(4-bromophenyl)-1-phenyl-1H-pyrazol-4-yl)-2,6-dimethyl-1,4-dihydropyridine-3,5-dicarboxylate **162** was reacted with 4-hydroxyphenylboronic acid in combination of $Pd(PPh_3)_4$ and aqueous Na_2CO_3 in THF to afford the desired substituented diphenyl product **221**. In the IR spectrum, the broad carbonyl absorption band at υ1679.06 cm^{-1} and the absorption band corresponding to the hydroxyl group appeared at υ 3302.3 cm^{-1}. From ^1H NMR and ^{13}C NMR spectrum (**Figure 2.14**) it was apparent that the signals arising from the protons of additional phenyl ring were located in the aromatic proton area δ 6.59-7.86, which integrated for 14 protons including the proton of CH in pyrazole ring. In comparison with the parent compound **162**, conjugated product **221** depicted the similar assignment to **162**. The methyl groups and methylene groups integrating for 6 protons and 4 protons as singlet and two multiplets centred at δ 2.20 and δ 3.87, δ 4.08 respectively.

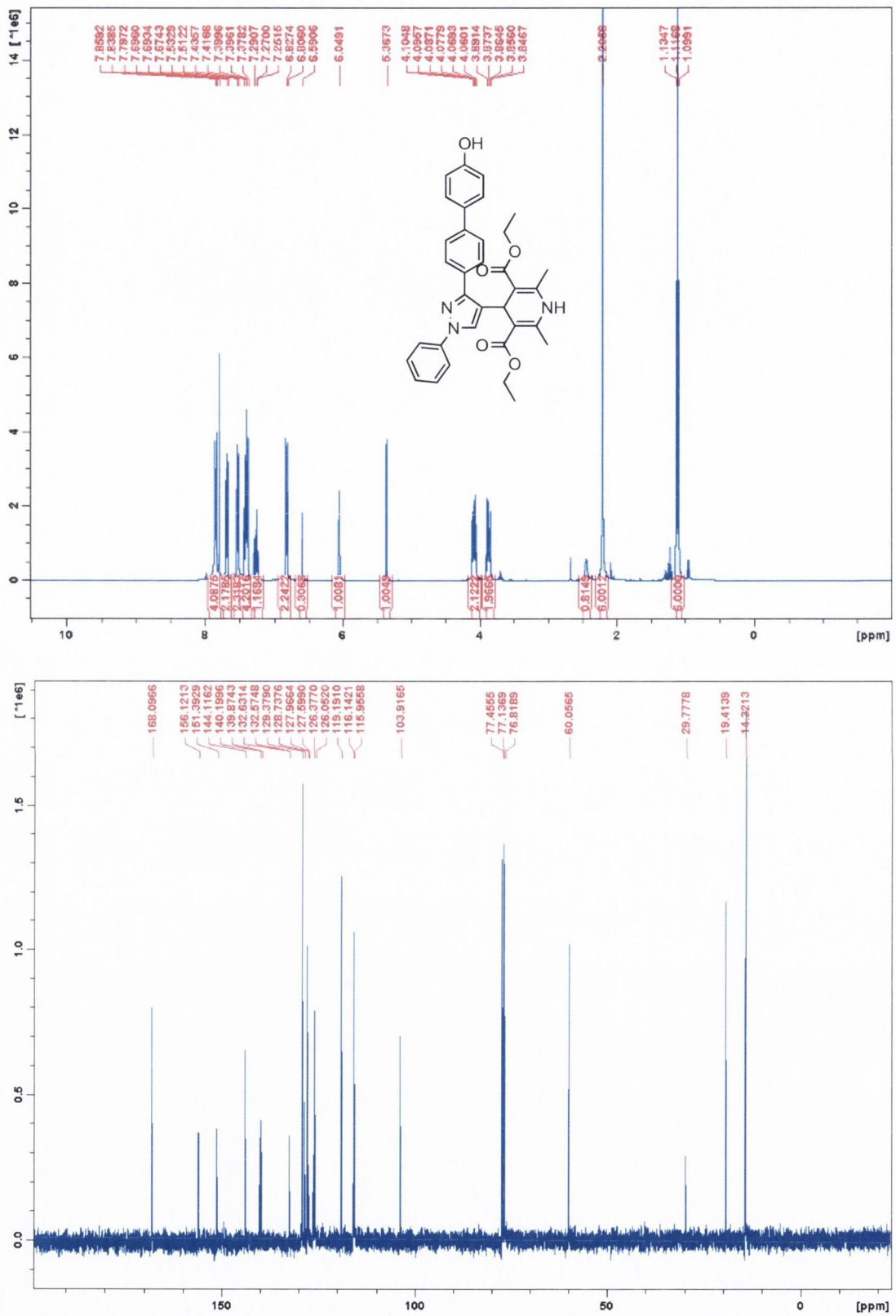

Figure 2.14 ^{1}H NMR and ^{13}C NMR of Suzuki product 221

2.6.2 Carboxylic acid modification of scaffold I A derivatives

Following the antiproliferative study on the previously synthesised scaffold I A compounds, the substituents on the Ring A were confirmed as the substitution pattern required for biochemical activity. (see chapter 4) Additional structure modification on Ring A was then carried out by esterification of phenolic analogues and the subsquent hydrolysis of these ester products.

Diethyl 4-(3-(4-(2-ethoxy-2-oxoethoxy)phenyl)-1-phenyl-1H-pyrazol-4-yl)-2,6-dimethyl-1,4-dihydropyridine-3,5-dicarboxylate **238** and diethyl 4-(3-(4-(4-ethoxy-4-oxobutoxy)phenyl)-1-phenyl-1H-pyrazol-4-yl)-2,6-dimethyl-1,4-dihydropyridine-3,5-dicarboxylate **239** were readily prepared by nucleophilic reaction from substrate compound **165** with ethyl bromoacetate **236** and ethyl-4-bromobutanoate **237** respectively in the mild condition.(**Scheme 2.25**)

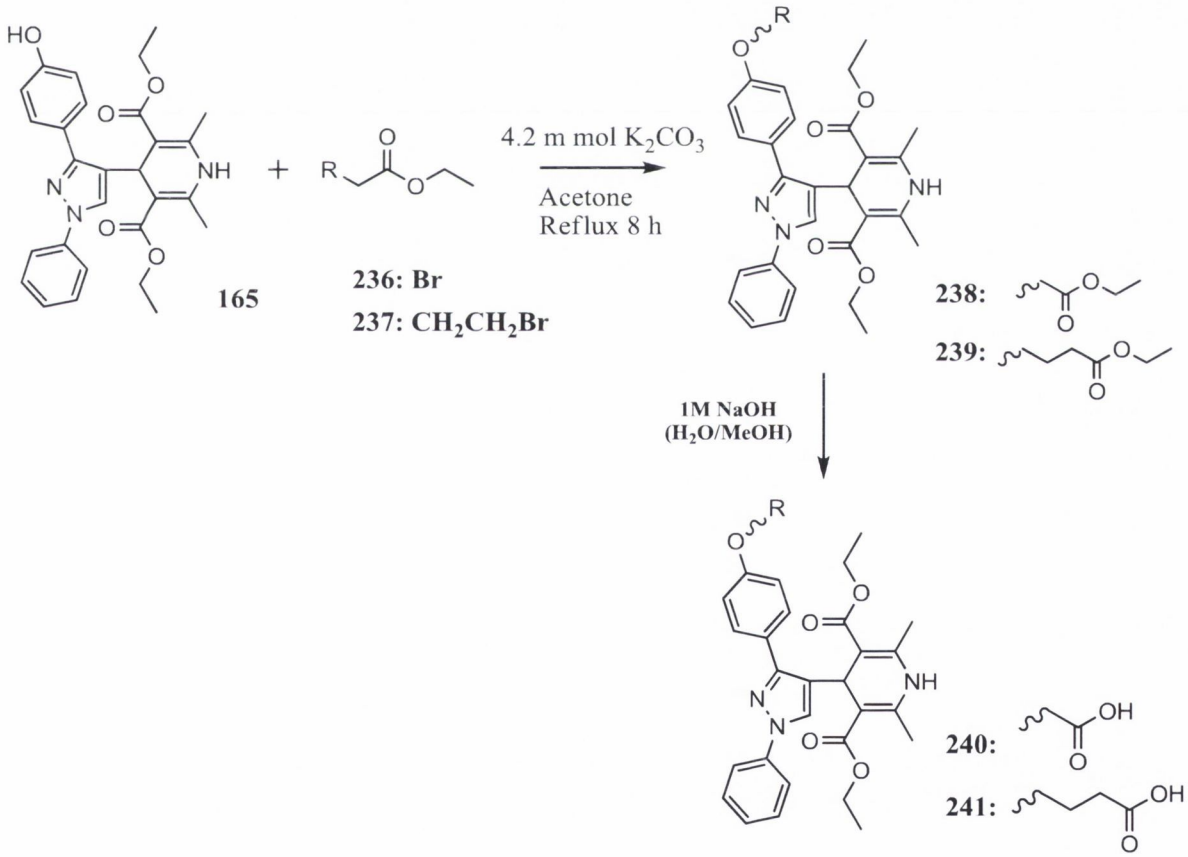

Scheme 2.25 Formation of carboxylic acid derivatives

Compound	MP (^{O}C)	IR (υ_{max} cm^{-1}) C=N, C=O&C-O-ester	Yield (%)
238	196	1600.01 1693.34 1210.20	32.5
239	202	1611.44 1670.23 1210.79	18.7
240	188	1600.08 1682.27 1214.21	22.8
241	194	1613.11 1695.30 1212.73	32.2

Table 2.11 Yield and spectroscopic data for compounds 238-241

It is seen from **Table 2.11**, the phenolic derivatives **238&239** and their relevant hydrolysis products **240&241** were obtained in the moderate yields. The compounds **239** and **241** were all identified using IR spectroscopy and NMR spectroscopy.(**Figure 2.15**) For compound **239**, the two ethyl ester methyl groups were identified as a triplet at δ1.08, while H_{12} CH_3 signal integrating for 3 protons centred at δ 1.26 as a triplet with coupling constant of 7.0Hz. CH_2 signals arising from H_8, H_9 appear as multiplets at δ 2.12 and δ 2.52 respectively. The characteristic methylene groups attached to dihydropyridine ring was assigned as two multiplets centred around δ 3.80 and δ 4.14. The other two methylene groups H_7 and H_{11} were observed as a multiplet in the region δ 4.00-4.06, integrating for four protons. The CH signal H_4'' appear as a singlet at δ 5.25. All aromatic proton signals are located in the region δ 6.92-7.77 and integrate for a total of 10 protons, in agreement with assignment from ^{13}C NMR. Among them, two separate multiplet signals in the region δ 6.92-6.94 and δ 7.75-7.77 were assigned to the aromatic protons H_2, H_6 and H_3, H_5, respectively. The CH signal from pyrazole ring was also identified as a singlet at δ 7.71.

Both of products **239** and **241** showed similar carbon spectra in ^{13}C NMR. By comparison with **239**, the DEPT spectrum of **241** shows the absence of one CH_2

signal at δ 60.08 (**Figure 2.16**), which was expected to be lost after the hydrolysis reaction.

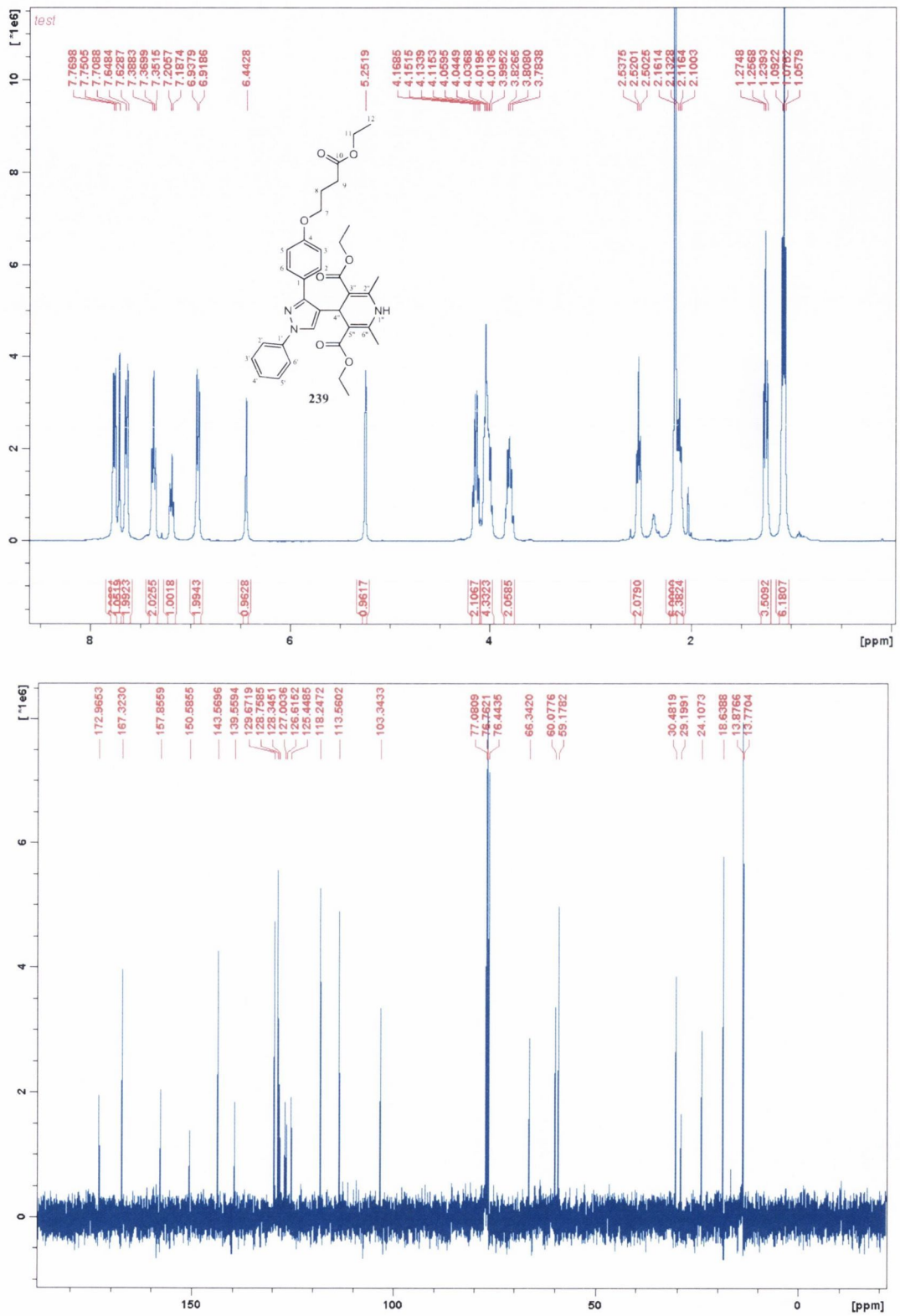

Figure 2.15 ^{1}H NMR and ^{13}C NMR of phenolic derivatives 239

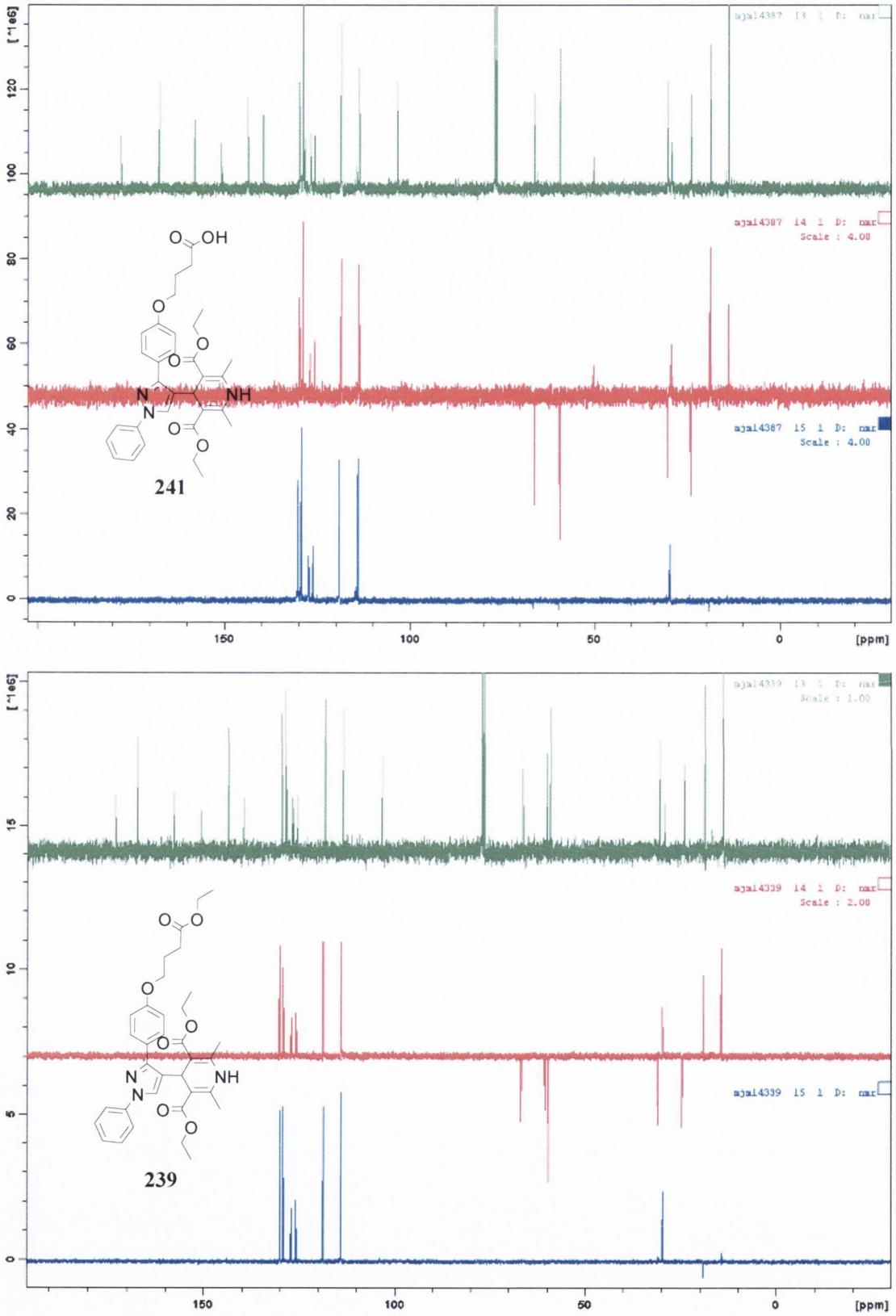

Figure 2.16 DEPT 90 and DEPT 135 spectroscopy for compound 239&241

2.7 Alternative synthesis route to 1,4-dihydropyridine derivatives

Many approaches to the synthesis of heterocyclic 1,4-dihydropyridine derivatives with various substitutions have been reported in the past decade.[245] The DHP molecule is recognised for the calcium channel antagonist activity and this heterocyclic ring is also a common feature for various biological activities such as antitumor, anti-inflammatory activity, antihypertensive, antitubercular and antithrombotic activity.[246] It not only binds to L-type channel, also shown action by binding to N-type channel, which exhibit more pharmacological activities such as vasodilation, stress protective and anticonvulsant.[247]

To pursue our studies on these multifunctional molecules, a novel synthetic route to explore the 1,4-dihydropyridines scaffold for the design of new compounds with potential biochemical activity prodrug was developed. A panel of 1,4-dihydropyridine-based derivatives has reported by Mai et al. as sirtuin modulator in 2009. [248] NAD^+-dependent sirtuin deacetylases was revealed as therapeutic targets for treatment of cancer, metabolic, cardiovascular and neurodegenerative diseases. In the present work, the preparation of 3,5-dicarbethoxy-4-phenyl-1,4-dihydropyridines **242-246** was carried out in a one-pot reaction using three component, (benzaldehyde, ethyl propiolate and aliphatic/aromatic amine), employing a modification of literature procedure. The reaction mixture was heated at 80°C in glacial acetic acid and subsequently underwent alkaline hydrolysis in ethanol to afford the corresponding 3,5-dicarboxy derivative **247**.(**Scheme 2.26**) Isolated yields, melting points and IR data for compounds **242-247** are presented in **Table 2.12**.

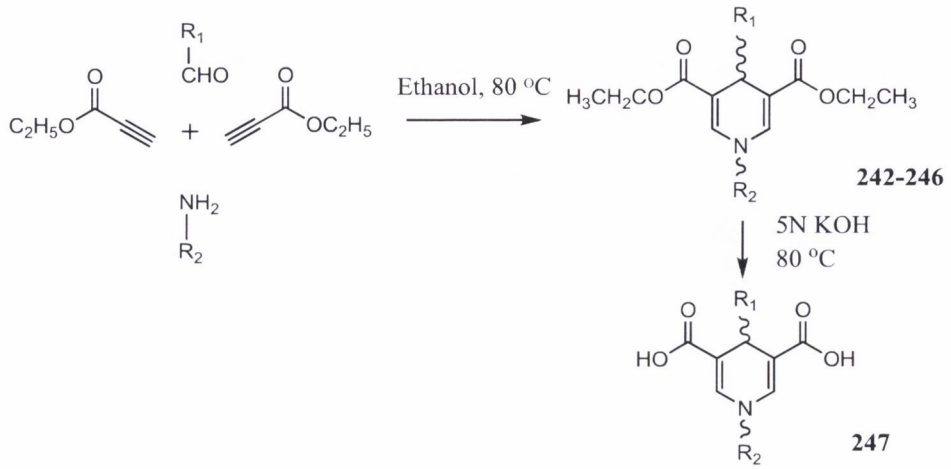

Scheme 2.26 Novel synthetic route to obtain 1,4-dihydropyridine derivatives

Compound	Structure		MP (^{O}C)	IR (υ_{max} cm^{-1}) C=O	Yield (%)
	R_1	R_2			
242		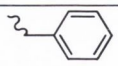	136	1693.8	71.0
243	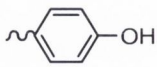	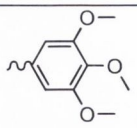	172	1715.9	28.3
244	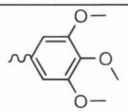	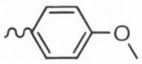	128	1682.2	24.7
245	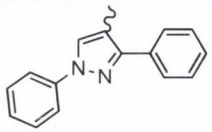	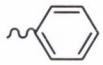	162	1672.9	1.5
246	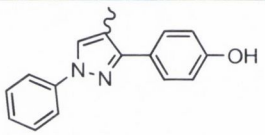		168	1684.7	30.4
247		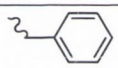	192	1686.4	83.2

Table 2.12 Mp, yield and IR data for compounds 242-247

The preparation of diethyl 1-(4-methoxyphenyl)-4-(3,4,5-trimethoxyphenyl)-1,4-dihydropyridine-3,5-dicarboxylate **244**, **scheme 2.24** is by a simple one-pot reaction from 3,4,5-trimethoxybenzaldehyde, ethyl propiolate, and 4-methoxyaniline. The ^{1}H-NMR spectrum (**Figure 2.17**) shows the characteristic two ethyl ester methyl groups and methylene group signals centred at δ 1.25 and δ 4.16 as triplets with coupling constant of J=7.12 Hz and multiplets, integrating for three protons and four protons respectively. The presence of all other relevant signals from the two substitutented aryl rings is indicated by the existence of four singlets and two multiplets. The four methoxy groups signals were observed as three singlets, whereas overlapping with each other around δ 3.83, 3.84, 3.86 and corresponding to the carbon methoxy signals at δ 55.20, δ 55.53 and δ 60.33. The proton of H_4 integrates for 1 proton at δ 4.94 and corresponds to carbon signal C_4 at δ 37.06. H_2, H_6 and H_2', H_6' appear as singlets at δ 6.63 and δ 7.58, both integrating for two protons. The latter two multiplets signals integrating for two protons each and centre δ 6.98 and δ 7.22 with coupling constant of 4.44 Hz, which were identified as H_2'', H_6'' and H_3'', H_5''. HRMS confirms the

proposed compound demonstrating a $[M+Na]^+$ ion at 520.1955 which corresponds to the mass of **244** (calculated for $C_{27}H_{31}NO_8Na$, 520.1947).

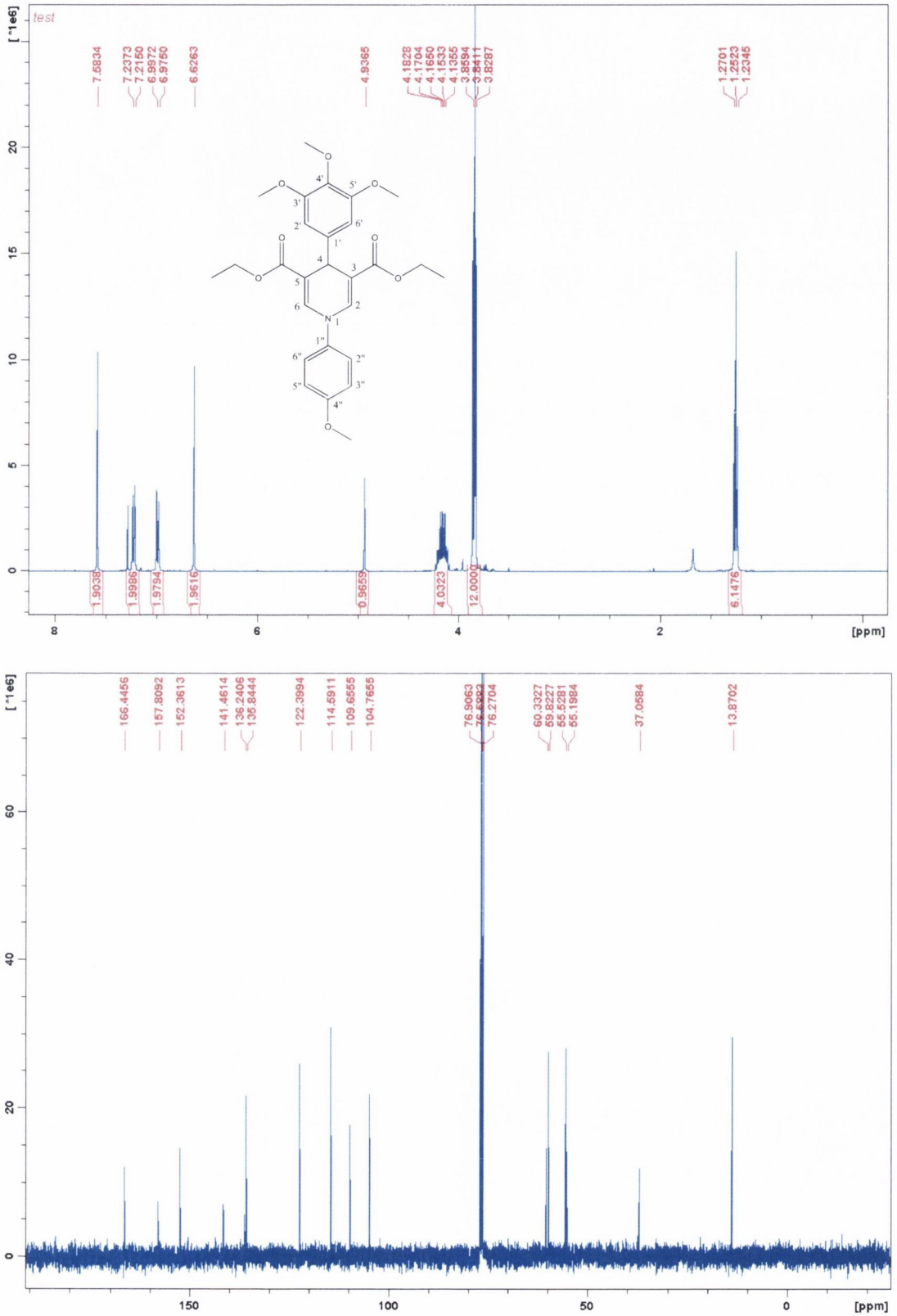

Figure 2.17 ^{1}H and ^{13}C NMR spectrum of compound 244

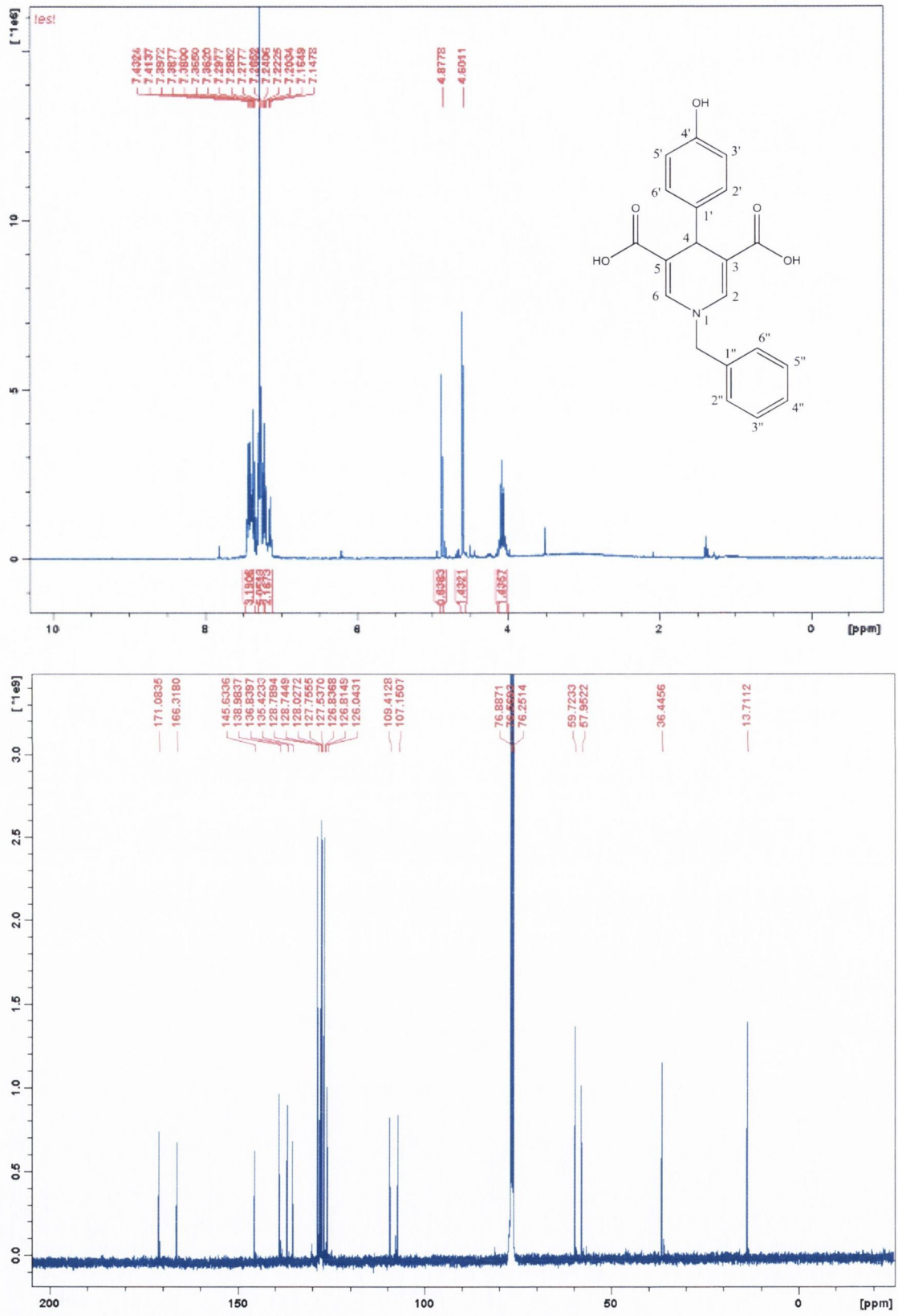

Figure 2.18 ^{1}H and ^{13}C NMR spectrum of compound 247

The hydrolysis product 1-benzyl-4-(4-hydroxyphenyl)-1,4-dihydropyridine-3,5-dicarboxylic acid **247** was prepared by alkaline hydrolysis of **242**. The characteristic ethyl ester ^{1}H NMR signals disappeared. Apart from the CH_2 and H-4 signals which

appear at δ 4.60 and δ 4.88 corresponding to ^{13}C NMR signals at δ 57.95 and δ 36.44, all other relevant proton signals are observed in the region δ 7.15-7.43 integrating for a total of 11 protons.

2.8 Summary

The purpose of this study was to design and synthesise antiproliferative compounds, based on the lead 4-(1,3-diaryl-1H-pyrazol-4-yl)-1,4-dihydropyridine scaffold structure compound. The initial design of the target compounds was focused on the modification of a number of key structural features, specifically the nature of the aryl ring substituent at C-3 of the pyrazole. Various functionalities were introduced, on the basis of previous SAR studies on 4-aryl-1,4-dihydropyridines as calcium channel blockers and P-glycoprotein modulators. The single crystal X-ray structure of compound **162** was determined, and in contrast to the single crystal X-ray structure of nifedipine, it was found to adopt the *syn* rather than *anti*periplanar conformation for the ester substituents on the 1,4-dihydropyridine ring. In this series of scaffold I A compounds, the aryl-substituted pyrazole ring replaces the more usual aryl ring at the C- position of the 1,4-dihydropyridine ring system and the presence of this bulky substituent is required for the antiproliferative activity of these compounds and may also contribute to the required lack of calcium effects.

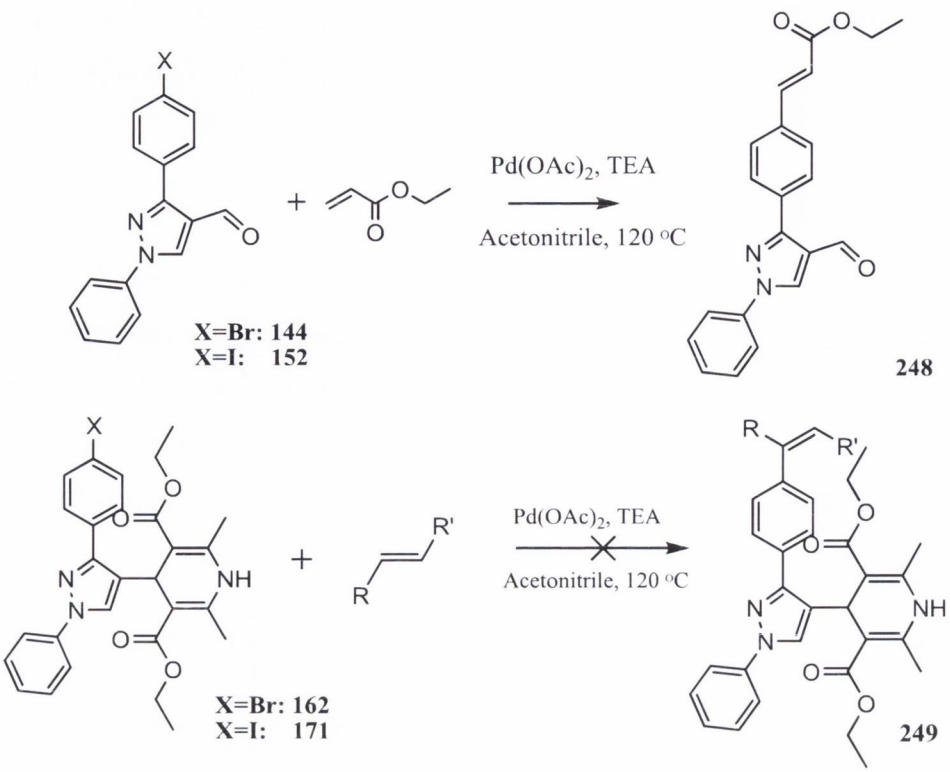

Scheme 2.27 Utilisation of Heck reaction to replace halide group with olefin derivatives unsuccessfully

In this chapter, the appropriate basic side chain ethers were incorporated into the molecule structure to investigate if affinity for the ER could be improved and if this had a positive effect on antiproliferative activity. The cross-coupling Suzuki-Miyaura reaction was proved as an effective method, in our studies, for arylation of 3-(4-bromophenyl)-1-phenyl-*1H*-pyrazole-4-carbaldehyde with various boronic acids to produce a library of substituted biaryl pyrazole introduced at the C-1 position of DHP ring. Attempted introduction of an acrylate ester onto the bromo or iodo substituted pyrazolyl 1,4-dihydropyridine ring (**162&171**) to afford **249** was not successful. However, this reaction was successfully demonstrated for the ethyl-3-(4-(4-formyl-1-phenyl-1H-pyrazol-3-yl)phenyl)acrylate **248** which was isolated in moderate yield *via* Heck reaction.(**Scheme 2.27**)

Chapter 3

Synthesis of 1,3,4-trisubstituted pyrazole (Scaffold II) derivatives as antiproliferative agents

3.1 Introduction

The investigation of scaffold II type raloxifene **11** analogues is discussed in this chapter. This library of compounds was subdivided into two different types dependent on whether the phenolic aryl ring or piperazine ring is located at the C-4 position of the pyrazole ring.

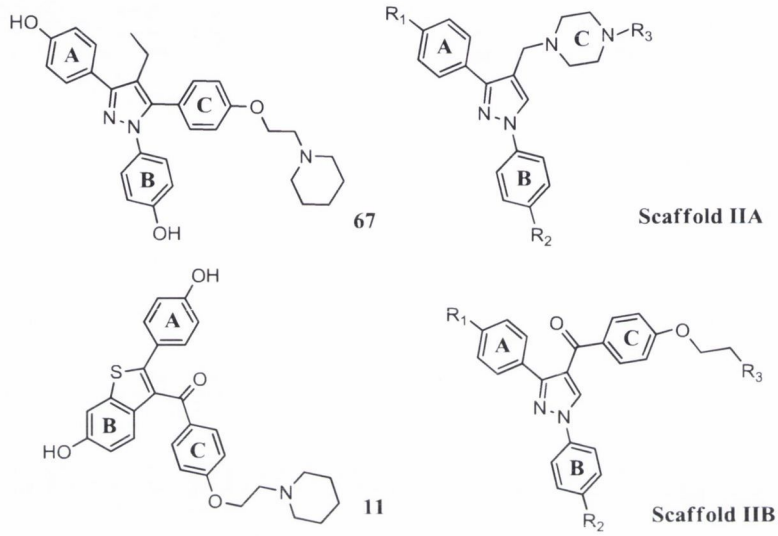

Figure 3.1 Structure of different trisubstituted pyrazole (scaffold II) derivatives

In chapter 1 the pyrazole core structure has been reviewed, which plays an important role in many different classes of bioactive compounds. Katznellenbogen's group has designed and carried out research on the pyrazole ring as a scaffold for SERMs. It was discovered that the C-5 piperidinyl-ethoxy-substituted pyrazole **67** possess good affinity for ERα.[249] Raloxifene **11** is another SERM, which shows potent binding ability to the ER active site based on the position of the piperidine side chain and the phenolic aryl ring around the core thiophene ring.[250] Therefore a series of similar compounds (scaffold II B) modified at the C-4 position of the pyrazole ring was synthesised in an attempt to increase biological activity. The synthetic route is depicted in **scheme 3.1**. A variety of methods available for the synthesis of the pyrazole ring was outlined in **section 1.4.2**. In the initial synthesis, it was necessary to include a diverse range of substituents on the aromatic ring A which was linked to the C-3 position of the pyrazole. There are also a number of synthetic routes to prepare the free phenolic group which subsequently can be conjugated with various basic side chains. The structural features desired in the final product determined which route was used and the results are detailed in **section 3.3**.

3.2 Reductive amination reaction

The subtype scaffold II A analogues designed for antiproliferactive activity contain a piperizine ring directly linked to the pyrazole core structure at the C-4 position. The reductive amination reaction, also known as Borch reaction, is the most common and important method in the synthesis of different kinds of amines.[251] It is very critical to choose the reducing agent for successful reaction, since the reducing reagent may reduce imines (or iminium ions) selectively over aldehydes under the reaction conditions.[252] The two most commonly used direct reductive amination synthetic routes differ in the nature of the reducing agent. The first method is catalytic hydrogenation with palladium, platinum or nickel catalysts. The second method uses hydride reducing agents such as sodium cyanoborohydride ($NaBH_3CN$) or sodium borohydride ($NaBH_4$) for the reduction step.[253]

3.2.1 Mechanism of reductive amination (Borch) reaction

The reductive amination of the carbonyl compound or reductive alkylation of the amine are most efficient and important approach to synthesis of primary, secondary, or tertiary amines from the reaction of aldehydes or ketones with ammonia, primary amines, or secondary amines in the presence of reducing agents.[254] The reaction mechanism depicted in **scheme 3.2** demonstrated that the initial step of the reaction is to form the intermediate hydroxylamine which can be converted to an imine by dehydration. In the acidic to neutral condition, the imine is protonated to form an iminium ion, which can produce the alkylated amine product subsequently.[255]

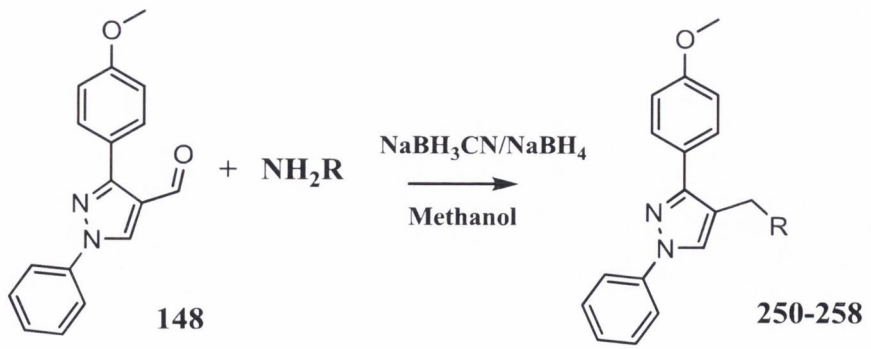

Scheme 3.1 Reductive amination to obtain the Scaffold II B analogues

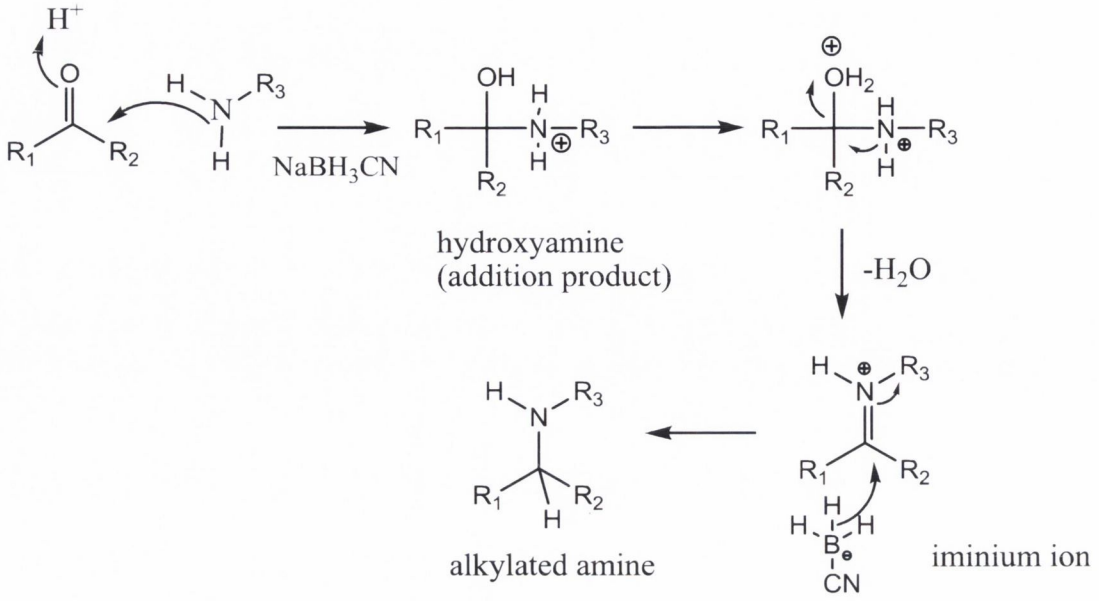

Scheme 3.2 Mechanism of action for reduction amination of pyrazole

3.2.2 Reductive amination with piperazine derivatives

To investigate the effect on the biochemical activity of modification on ring C of the 1,3,4-trisubstituted pyrazole derivatives to increase the antiproliferative property, scaffold II A products were synthesised as illustrated in **Scheme 3.1** using the reductive amination (Borch) reaction of 3-(4-methoxyphenyl)-1-phenyl-*1H*-pyrazole-4-carbaldehyde **148** and the appropriate substituted piperazine. All of the reductive amination products **250-257** were synthesised and presented in **Table 3.1** with their infra red data, melting point, and isolated yields. For comparison, **258** was obtained by sodium borohydride $NaBH_4$ reduction of the pyrazole carbaldehyde **148**.

Most products (**250-257**) contain the piperazine ring at the C-4 position of 3-(4-methoxyphenyl)-1-phenyl-*1H*-pyrazole-4-carbaldehyde, thus the heterocyclic ring can be identified by ^{1}H NMR spectra. **Figure 3.2** illustrates the ^{1}H NMR spectrum for compound **254**, The four methylene group linked to the amine appear as two triplets centred at δ 2.72 (J=4.84 Hz) and δ 3.26(J=4.72 Hz), respectively. A singlet signal at δ 3.89 corresponding to the methoxy group was observed, while the other methylene group signal was observed at δ 3.61 as a singlet in the ^{1}H NMR spectrum. In agreement with the ^{13}C NMR spectrum, the carbon signals at δ 48.8, δ 52.09, and δ 52.39 displayed negative signals in the DEPT 135 sepctrum where the 5 CH_2 group containing the 2 overlapped carbon signals were observed. All the aromatic protons and CH at C-5 of the pyrazole ring were located in the region δ 6.90-7.99, integrating for a total of 15 protons.

Compound	Structure	MP (^{O}C)	IR (υ_{max} cm^{-1}) C=N	Yield (%)
	R			
250		156	1600.0	23.2
251	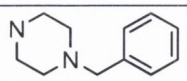	138	1598.9	43.2
252	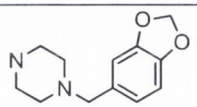	124	1600.4	11.5
253	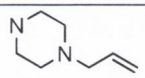	Oil	1600.1	36.2
254	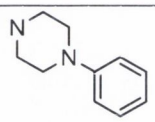	148	1599.1	38.7
255		126	1599.8	13.6
256		162	1599.6	12.4
257		124	1600.1	8.72
258	OH	168	1599.8	69.8

Table 3.1 IR, melting points and yields for reductive products 250-258

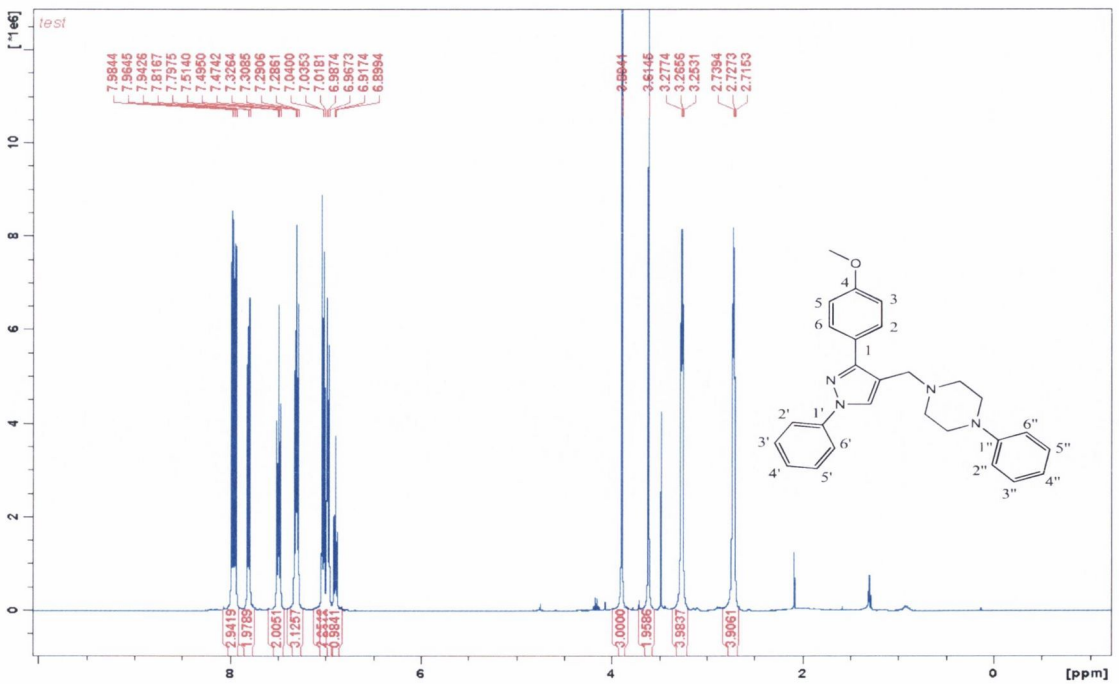

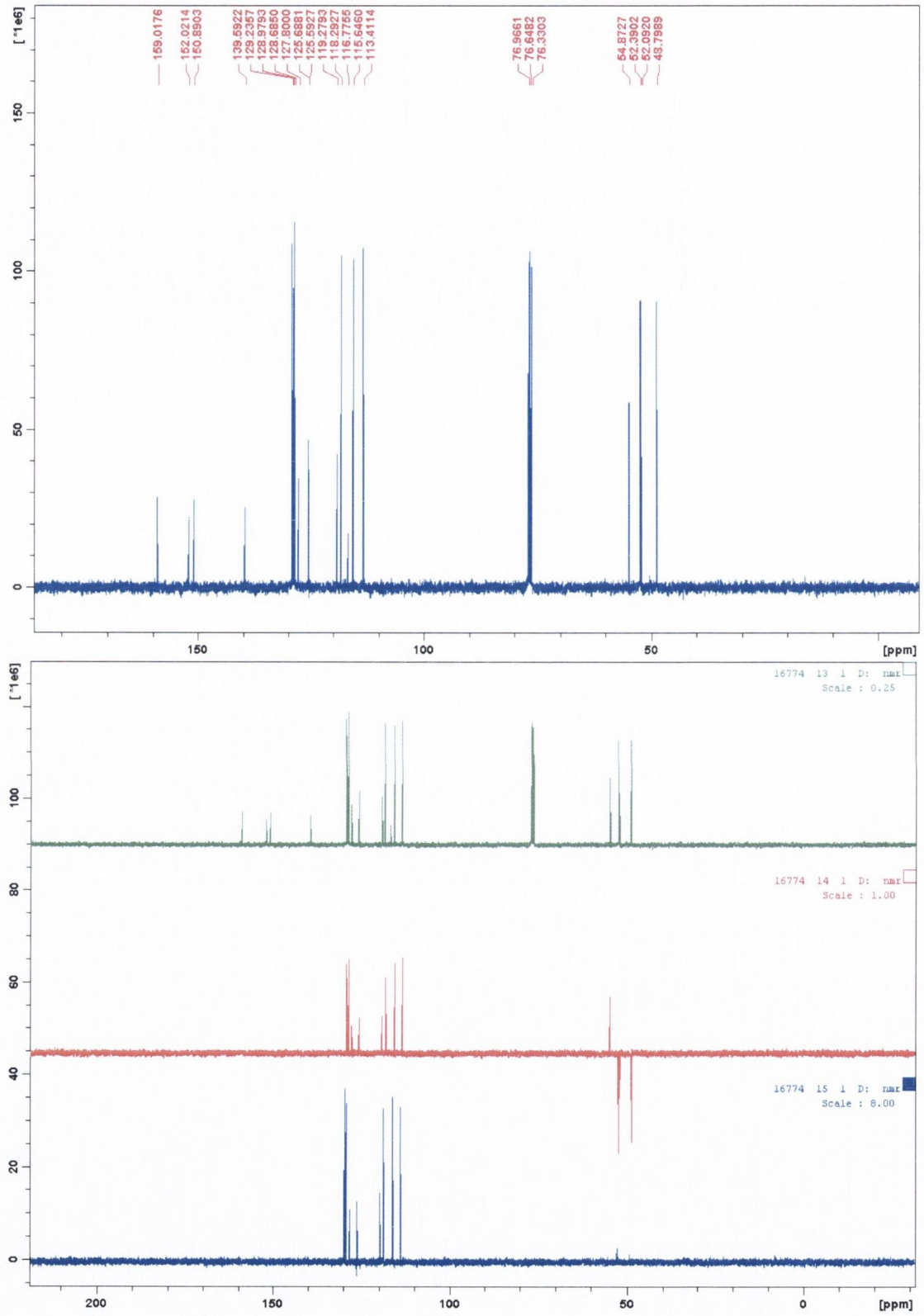

Figure 3.2 ^{1}H NMR, ^{13}C NMR and DEPT spectra for compound 254

3.3 Synthetic route to novel scaffold II B

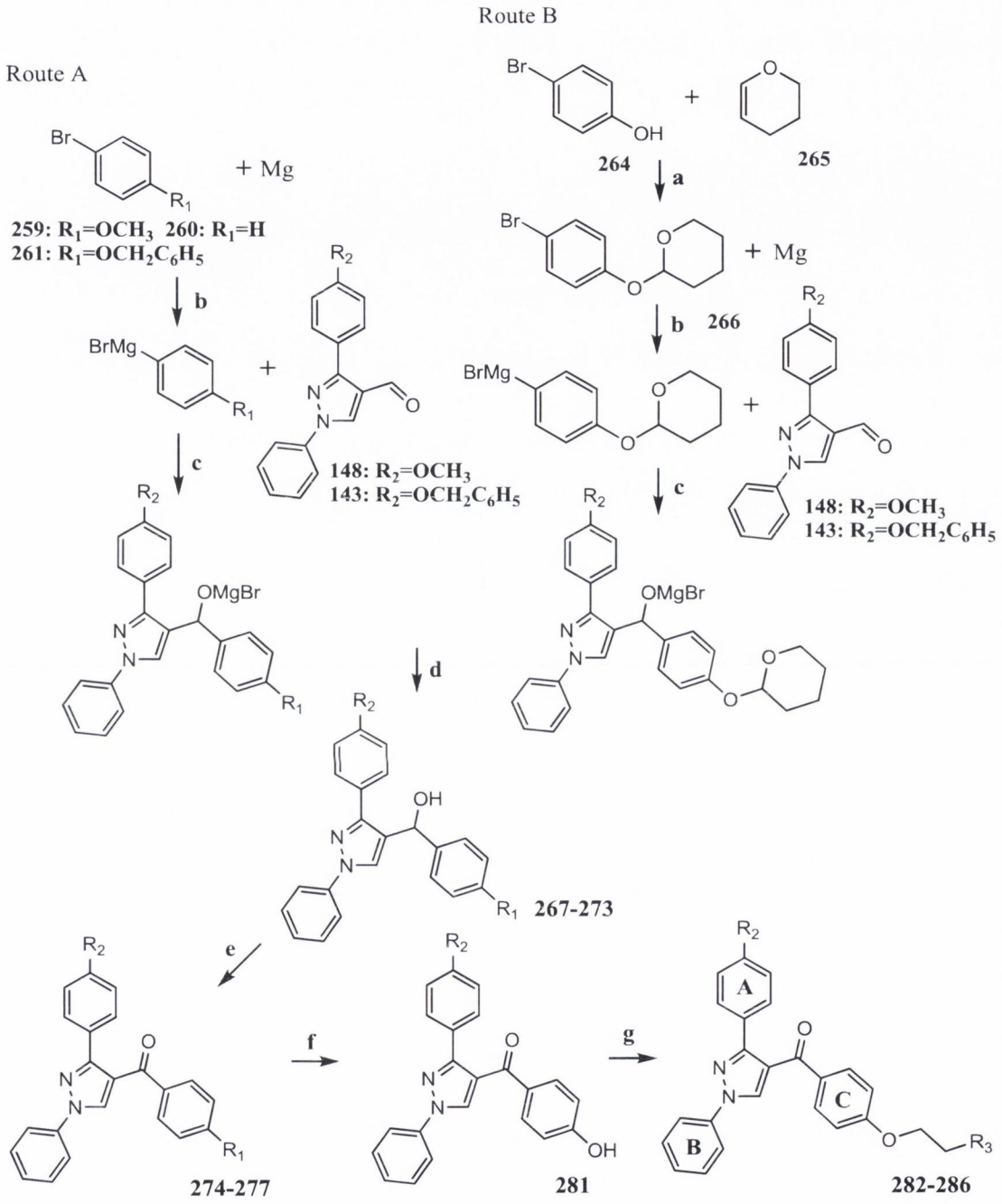

Scheme 3.3 Synthetic route for scaffold II B analogues

Scheme reagents: (a) 2N HCl, r.t. 3 h (b) THF, reflux 15 min (c) THF, reflux 20min
(d) 10% H_2SO_4 (e) PCC, DCM, 2 h (f) CBr_4, Methanol, reflux 0.5-3 h
(g) Acetone, basic side chain halides **211-215**, reflux 5 h

As initial biochemical investigation indicated compound **250** (scaffold II A) to have good activity in both MCF-7 and HL-60 cancer cell lines (see chapter 4), it was decided to study the effect on activity of an additional piperazine ring at the C-4 position of the pyrazole system. An alternative plan was to introduce more complex

aryl contains substituents at the C-4 position. The synthetic route chosen for the preparation is illustrated in **Scheme 3.3**. A variety of Grignard reagents were thus reacted with **148** to give the secondary alcohol, and then to form the scaffold II B analogues by subsequent reaction with basic side chain halides. These products can be classified as pyrazole analogues of raloxifene.

3.3.1 Grignard reaction

A study of the synthesis 1,3,4-trisubstituted pyrazole derivatives with optimisation of substituents attached to the phenyl ring at the C-4 position of the pyrazole ring was carried out using the Grignard reaction. Formation of the Grignard reagent, an organometallic species is achieved by reaction of alkyl, benzyl, or aromatic halide with magnesium in an anhydrous solvent (ie. diethyl ether or THF).[256] The characteristic reaction with carbonyl compound is an efficient synthetic route to form new carbon-carbon bond.

3.3.1.1 Mechanism of Grignard reaction

The general reaction mechanism for the Grignard reaction is depicted in **Scheme 3.4**. The reaction has been divided into two steps, the first part of the reaction is the formation of the Grignard reagent R-Mg-X. The secondary or tertiary alcohol then can be synthesised when the Grignard reagent is reacted with an aldehyde or ketone.[257] As can be seen in **Scheme 3.4**, the Grignard reagent is a carbanion and acts as a nucleophile which adds to the carbonyl carbon to form an alkoxide, which is then protonated to afford the alcohol product in acidic condition.[258]

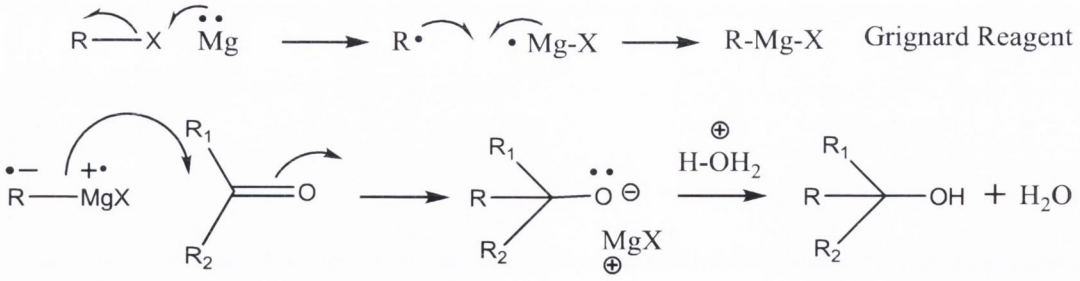

Scheme 3.4 Mechanism for the Grignard reaction

3.3.1.2 Introduction of additional phenyl ring to pyrazole derivatives

To obtain the scaffold II B analogues, preparation of intermediate secondary alcohol derivatives is necessary in the synthetic route as discussed previously. The reaction of a variety of substituted bromobenzenes (**259-261**,**264**) and magnesium ribbon in

mild conditions could afford the Grignard reagent, which was then reacted with the aldehyde at C-4 position of pyrazole derivatives for preparation of the desired products **267-273**. (**Scheme 3.5**) The biochemical result in the antiproliferative assay shown in chapter 4 for the 1,3,4-trisubstituted type pyrazole were encouraging and it was believed that could be important for ER antagonist activity if the substituted phenyl ring of the optimised scaffold II B can be conjugate with the anti-estrogen type basic side chain. Two synthetic routes are available to reach the final products which possess one or two basic side chains in the molecular structure. Initial attempts to form the free hydroxyl group at ring A or ring C by demethylation reaction was tried without success, (Detailed in **Section 3.3.4**). Meanwhile removal of benzyloxy group from **270** to afford phenolic product was achieved in very low yield. Therefore, an alternative route was utilized which resulted in initial isolation of phenolic product **273** from reaction of the protected *p*-tetrahydropyranyloxy bromobenzene **266** and 3-(4-methoxyphenyl)-1-phenyl-1H-pyrazole-4-carbaldehyde **148**.

Thus, the secondary alcohol 3-(4-methoxyphenyl)-1-phenyl-*1H*-pyrazol-4-yl)(4-(tetrahydro-2H-pyran-2-yloxy)phenyl)methanol **273** was readily prepared when bromophenol **264** was reacted with 3,4-dihydro-*2H*-pyran **265** in acetic acid to afford the protected phenol **266**, which was immediately employed in the Grignard reaction with pyrazole carbaldehyde **262**. The yield, melting point and spectroscopic data for secondary alcohols **267-273** is presented in **Table 3.2**.

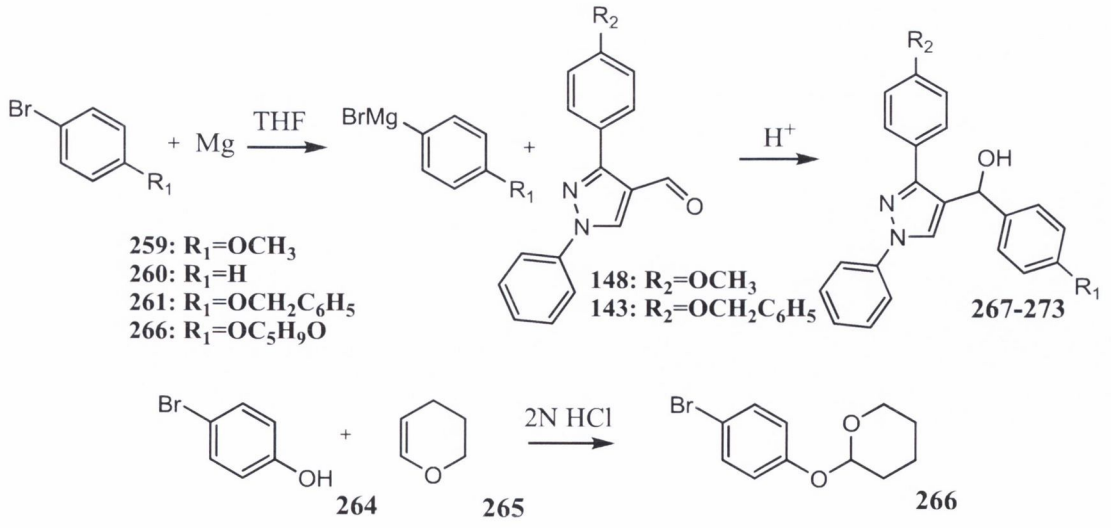

Scheme 3.5 Synthesis of secondary alcohols *via* Grignard reaction

Compound	Structure		MP (^{O}C)	IR (υ_{max} cm^{-1}) C=N O-H	Yield (%)
	R_1	R_2			
267	H	OCH_3	126	1601.0 3306.4	28.4
268	OCH_3	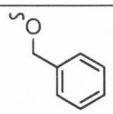	162	1601.3 3360.2	23.3
269	H	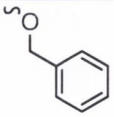	146	1595.0 3366.3	42.6
270	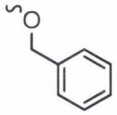	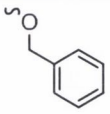	182	1597.8 3273.4	21.2
271	OCH_3	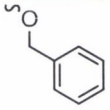	168	1611.1 3337.1	49.6
272	OCH_3	OCH_3	182	1599.8 3400.0	51.1
273	OCH_3	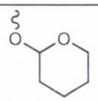	186	1600.4 3420.1	17.2

Table 3.2 IR data, melting points and yields for intermediate of scaffold II B 267-273

In the IR spectrum of **273**, the secondary imine and hydroxyl group absorption appear at 1600.45 cm^{-1} and 3420.18 cm^{-1} respectively. The ^{1}H and ^{13}C NMR spectra for **273** are presented in **Figure 3.3**. The methoxy group appears as a singlet at δ 3.83 integrating for 3 protons. The CH proton attached at C-5 position of the pyrazole appears as a singlet at δ 5.42 integrating for 1 proton. The 13 protons in the aromatic area appear from δ 6.79 to δ 7.86. The protons at C_7'', C_8'', C_9'', C_{10}'' and C_{11}'' are non-equivalent and coupled with each other integrating for a total of 9 protons. They appear as broad mutliplets centered on δ 5.66, δ 2.07, δ 1.88, δ 1.69 and δ 3.96, respectively. The presence of CH_2 groups carbon corresponding to C_9'', C_{10}'', C_8'' and C_{11}'' were confirmed by the DEPT 135 which give 4 negative signal at δ 18.45, δ 24.76, δ 29.96 and δ 61.73 respectively. HRMS also confirms the proposed product revealing M^{+}+1 ion at 457.2125 which related to the mass of **273** (457.2127, $C_{28}H_{29}N_2O_4$)

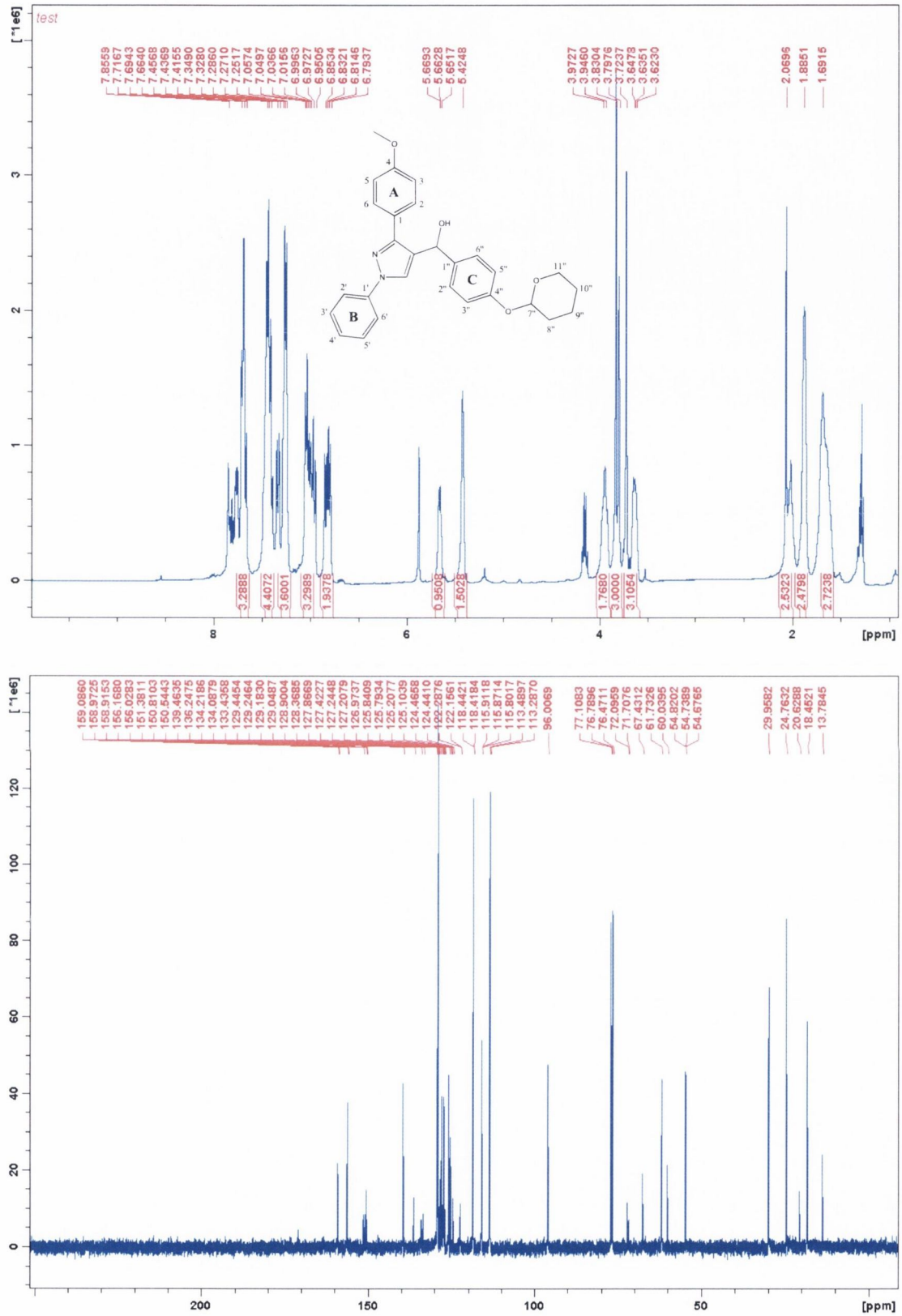
test
[*1e6]
7.8559
7.7167
7.6943
7.6640
7.4568
7.4369
7.4155
7.3490
7.3280
7.2860
7.2710
7.2517
7.0574
7.0497
7.0366
7.0156
6.9963
6.9727
6.9505
6.8534
6.8321
6.8146
6.7937
5.6693
5.6628
5.6517
5.4248
3.9727
3.9460
3.8304
3.7976
3.7237
3.6478
3.6351
3.6230
2.0696
1.8851
1.6915
A
B
C
OH
3.2888
4.4072
3.6001
3.2989
1.9378
0.9508
1.5028
1.7680
3.0000
3.1054
2.5323
2.4798
2.7238
[ppm]
[*1e6]
159.0860
158.9725
158.9153
156.1680
156.0283
151.3811
150.8103
150.5443
139.4635
136.2475
134.2186
134.0879
133.4358
129.4454
129.2464
129.1830
129.0487
128.9004
128.3685
127.8669
127.4227
127.2448
127.2079
126.9737
125.8409
125.7934
125.2077
125.1039
124.4658
124.4410
122.2876
122.1661
118.4421
118.4184
115.9118
115.8714
115.8017
113.4897
113.2870
96.0069
77.1083
76.7896
76.4711
72.0959
71.7076
67.4312
61.7326
60.0396
54.8202
54.7389
54.6766
29.9582
24.7632
20.6288
18.4521
13.7845
[ppm]

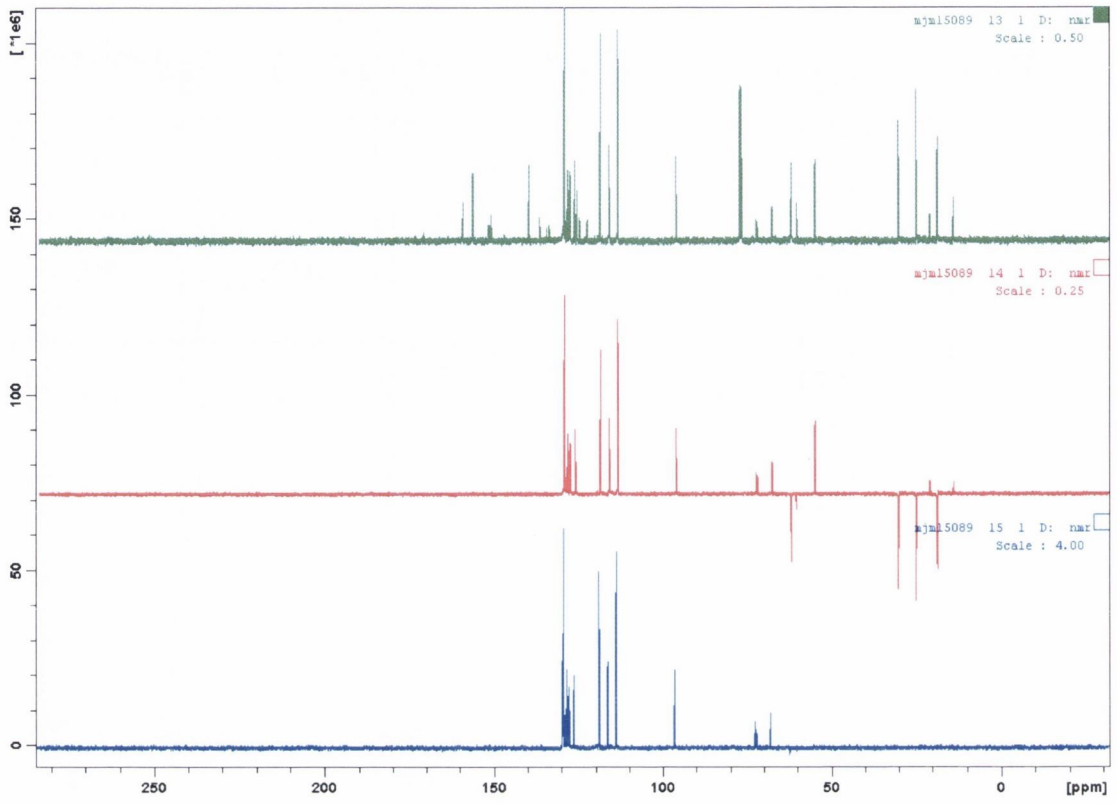

Figure 3.3 ^{1}H NMR, ^{13}C NMR and DEPT spectra for compound 273

3.3.2 Oxidation of secondary alcohol

To synthesise the required scaffold II B type compound containing the basic side chain linked to phenyl ring and to investigate the effect on antiproliferative activity when the a carbonyl group is introduced to C-4 position of pyrazole, the secondary alcohols (**267, 268, 271, 273**) were oxidised to the corresponding ketones **274-277**. Several reagents are available for this oxidation reaction, such as PCC, PDC and chromium(VI) reagent. PCC, an air-stable solid reported by Corey et al is a popular oxidizing reagent.[259] It was employed in this reaction to achieve the ketone derivative products by treatment of the appropriate secondary alcohol in DCM. Pyridium chlorochromate (PCC) is useful tool for the oxidation of primary alcohols to aldehydes and secondary alcohols to ketones.[260] The reaction solution becomes briefly homogeneous on addition of PCC to the reaction. However, isolation of product from the PCC residue was difficult, and the residue is then removed by filtration.

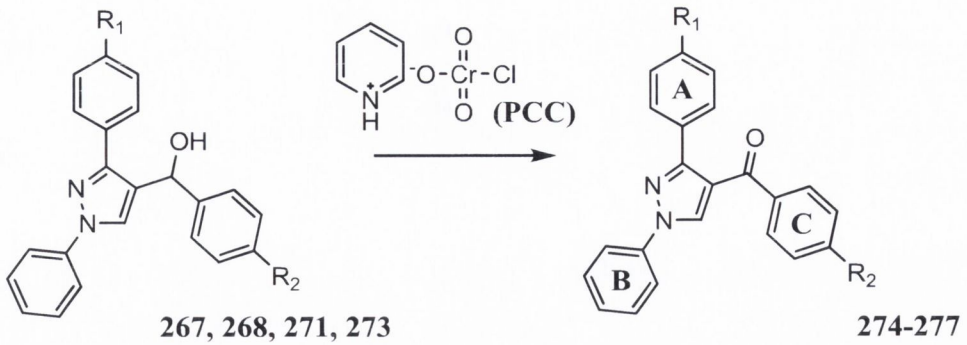

267, 268, 271, 273 **274-277**

Scheme 3.6 Oxidation of secondary alcohol

Compound	Structure		MP (^{O}C)	IR (υ_{max} cm^{-1}) C=N, C=O	Yield (%)
	R_1	R_2			
274	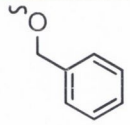	H	176	1599.7 1693.3	34.2
275	OCH_3	H	174	1597.3 1695.3	18.8
276	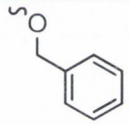	OCH_3	170	1598.1 1696.2	26.3
277	OCH_3	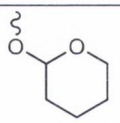	162	1599.8 1693.3	54.1

Table 3.3 IR data, melting points and yields for oxidation of secondary alcohols 266-269

As can be clearly seen from the IR spectrum for **275**, the carbonyl and secondary imine signals appear at 1695.3 cm^{-1} and 1597.3 cm^{-1} corresponding to the newly formed ketone and C=N group of the pyrazole ring. High resolution mass spectrometry identified the product with corresponding M^{+}+1 ion at 355.1451 and related to the mass of **275** (355.1447, $C_{23}H_{19}N_2O_2$).

3.3.3 Hydrolysis of (3-(4-methoxyphenyl)-1-phenyl-1H-pyrazol-4-yl)(4-(tetrahydro-2H-pyran-2-yloxy)phenyl)methanone

It was essential to protect the precursor of the scaffold II B analogues containing a hydroxy functionality in this step before taking part in the planned conjugation reaction with basic side chain alkyl halides. For that reason, reaction of carbaldehyde compound with core structure pyrazole ring and *p*-tetrahydropyranyl bromobenzene by Grignard reaction gives the secondary alcohol intermediate **273**.[261] Subsequently,

compound **277** containing the protecting group tetrahydropyranyl ether was prepared by oxidation of **273**.

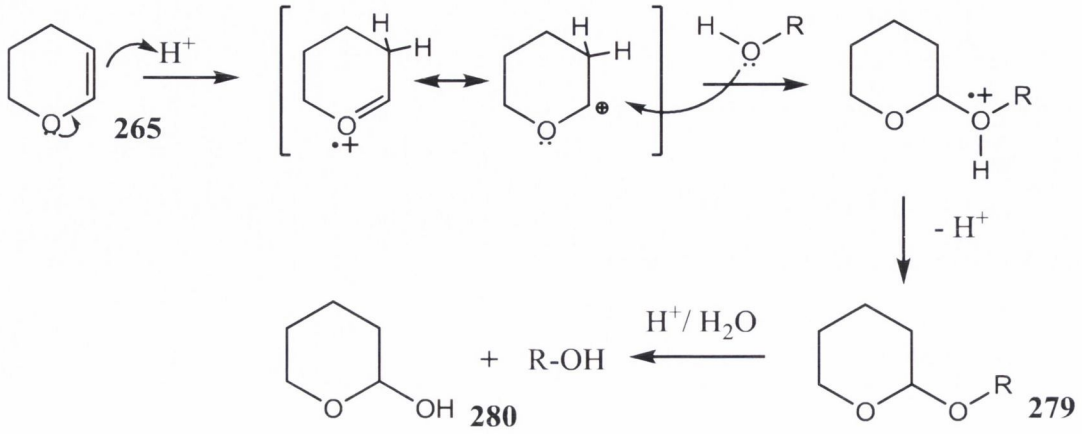

Scheme 3.7 Deprotection of tetrahydropyranyl ether for free hydroxyl group

The tetrahydropyranyl ether is an important protecting group for the protection of alcohols and phenols, providing stability in the strong basic reaction conditions, hydrides, alkylation reagent, acylating reagents and organometallics in organic synthesis.[262] Reaction of the alcohol with dihydropyran **265** forms a tetrahydropyranyl ether **279**, protecting the alcohol from a variety of reactions.[263] The hydroxyl group can be restored readily by acidic hydrolysis with formation of phenol/alcohol and 5-hydroxypentanal **280**. (**Scheme 3.7**)

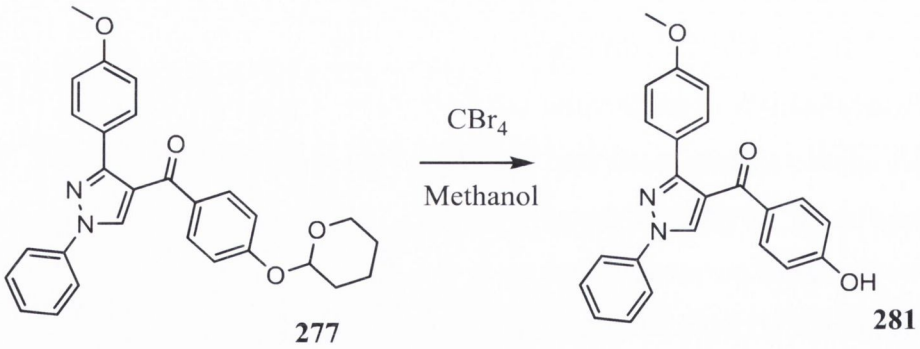

Scheme 3.8 Synthetic route to obtain free hydroxyl group

The compound **281**, an orange yellow solid, was obtained as the hydrolysis of **277** in mild reaction condition with tetrabromomethane (CBr_4) and it was achieved good yield (85.9%). (**Scheme 3.8**) From the IR spectra the hydrolysis of the ether to the hydroxyl group was apparent from the appearance of a broad absorption at approximately 3417.90 cm^{-1} and the presence of the C=N at 1599.25 cm^{-1}. On examination of the ^1H NMR spectrum (**Figure 3.4**) the loss of the tetrahydro-*2H*-pyran group was evidence by the absence of the characteristic signals in the region δ

1.69 to δ 3.96. The methoxy proton is still present with a singlet at δ 3.82 integrating for 3 protons and corresponds to carbon signal at δ 54.83 in the ^{13}C NMR spectrum. All of the aromatic proton signals are located in the region δ 6.82 to δ 7.83 integrating for a total of 13 protons. The carbon signal at δ 209.23 in the ^{13}C NMR spectrum clearly confirmes the carbonyl group in the molecule structure. The $M^{+}+1$ ion at 369.1255 can also confirm the expected compound has been formed which related to the mass of **281** ($C_{23}H_{17}N_2O_3$, 369.1239) by HRMS.

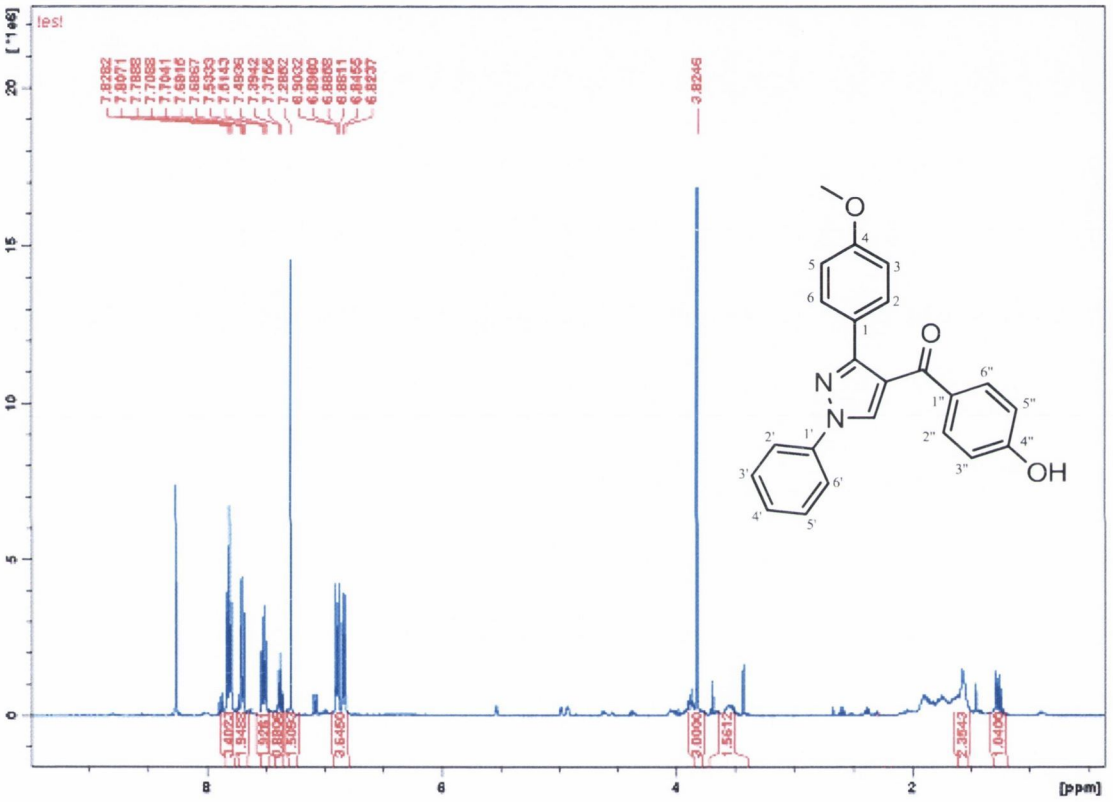

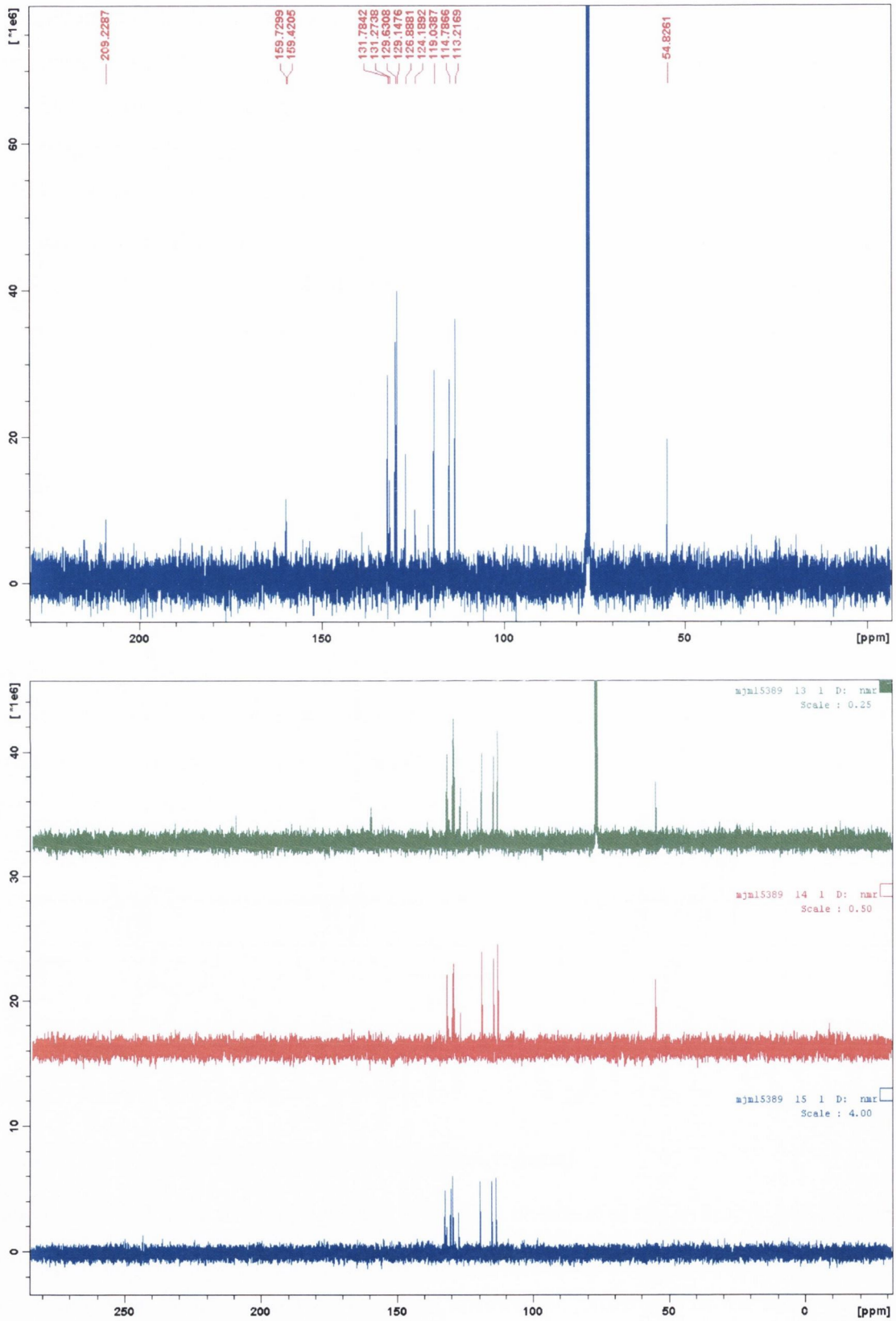

Figure 3.4 ^{1}H NMR, ^{13}C NMR and DEPT spectra for compound 281

3.3.4 Synthesis of scaffold II B product containing phenolic ring at C-4 and C-3 positions

The introduction of various basic side chain substituents to ER ligand scaffolds such as tamoxifen led to the significant improvement in antiproliferative activity as it facilitates binding to the ER successfully. Thus it was desirable to investigate formation of the corresponding pyrazole analogues containing basic side chains to evaluate their biological activity. In **scheme 3.9**, addition of various basic side chain alkyl halides onto the free hydroxyl group of compound **281** produced a first library of scaffold II B type derivatives (**282-286**). The melting point, isolated yield and spectroscopic data is presented in **Table 3.4**.

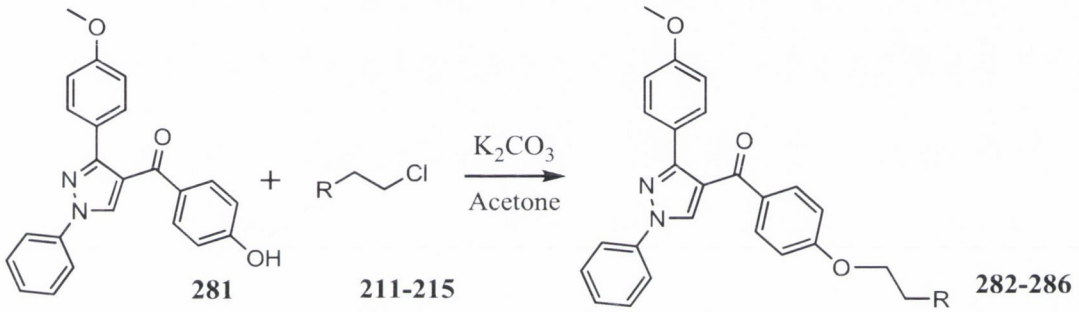

Scheme 3.9 Addition of basic ether for scaffold II B derivatives 282-286

Investigation of further optimisation for this molecular structure was carried out. We were interested in biochemical evaluation of a novel pyrazole product containing two substituted phenolic rings such as **288**. However, initial attempts to isolate **287** directly from **282** and **286** by demethylation were not successful. (**Scheme 3.10**) Several different reagent such as boron tribromide (BBr_3) and ethanethiol were employed in order to remove the methyl ether group without success.[264] Therefore, an alternative method of synthesis of **288** was developed from **276** which contains a benzyl protected phenol group at the C-3 position of pyrazole ring. This protected compound was then treated with hydrogen and the palladium/carbon catalyst deprotected to the free phenol at the C-3 position **287**. The reaction resulted in very poor yield and thus an alternative protecting group, (e.g. silyl ether protecting group) is necessary for future work.

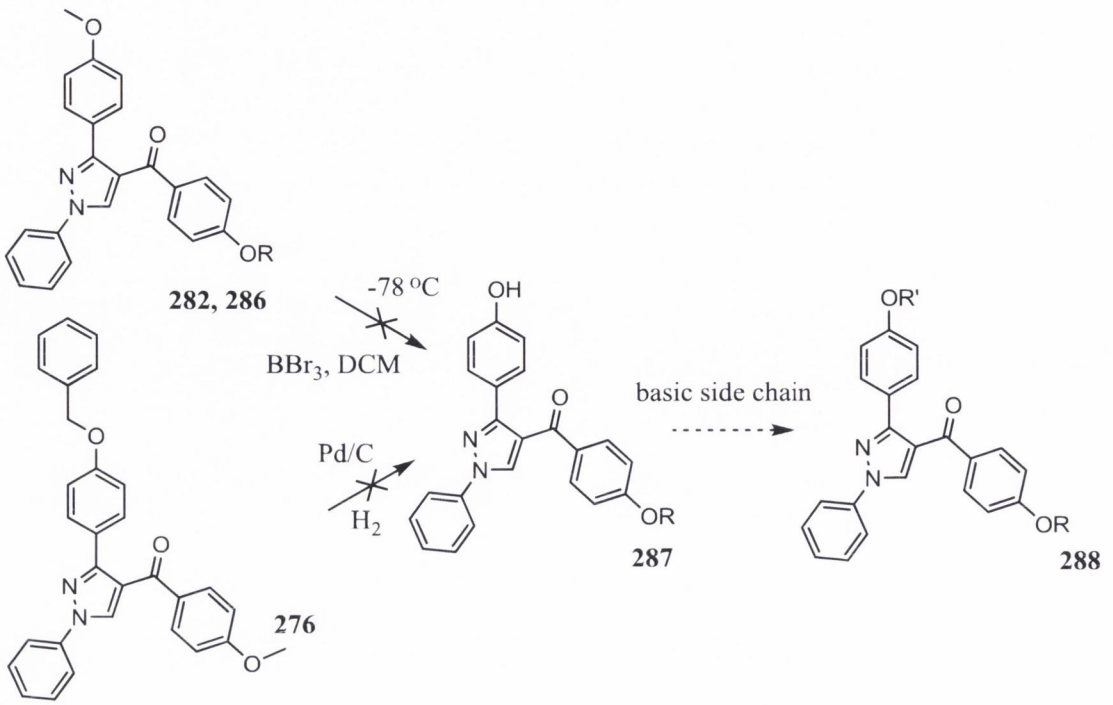

Scheme 3.10 Synthetic route for phenolic derivatives at C-3 position of pyrazole

Compound	Structure R	MP (^{O}C)	IR (υ_{max} cm^{-1}) C=N, C=O	Yield (%)
282	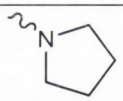	178	1599.2, 1712.3	12.4
283	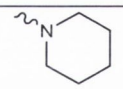	184	1600.4, 1700.9	23.2
284	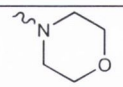	190	1600.7, 1711.4	32.1
285	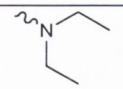	168	1601.2, 1711.6	9.2
286	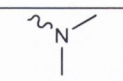	192	1600.2, 1712.5	13.4

Table 3.4 Melting point, yield and spectroscopic data for basic ether products 282-286

From the examination of ^{1}H NMR spectrum of expected Type II B product **286** (**Figure 3.5**), the singlet signal at δ2.36 is assigned the methyl group of the H_9'', H_{10}'' integrating for 6 protons, while the methoxy group appears as a singlet at δ 3.83 integrating 3 protons. The H_8'' and H_7'' split with each other with the same coupling constant J=5.52 Hz and therefore appear as two triplets signal centred on δ 2.76 and δ 4.13 ppm respectively, and both integrating for 2 protons. A total of 13 aromatic protons can be clearly seen as series of multiplets in the aromatic region from δ 6.88

to δ 7.88. One singlet signal appears at δ 8.26 which was assigned to CH proton of pyrazole which integrated for a single proton. The successful synthesis of **286** was also identified by HRMS shows $[M+H]^+$ ion at 442.2141 ($C_{27}H_{28}N_3O_3$).

The DEPT 135 spectra of products **283** with **286** were compared, the negative carbon signals at δ 21.43, δ 22.19 and δ 36.14 corresponding to CH_2 group of piperidine ring observed for **283** but not present for compound **286**. (**Figure 3.6**) The remaining two negative signals at δ 57.66 and δ 65.77 were assigned to C_8'' and C_7'' respectively. The carbonyl carbon appears at δ 188.52 and methoxy carbon shows at δ 54.82 in ^{13}C NMR spectrum of **278**; likewise the assignment of **275**, which confirmed these compounds have a similar molecular structure.

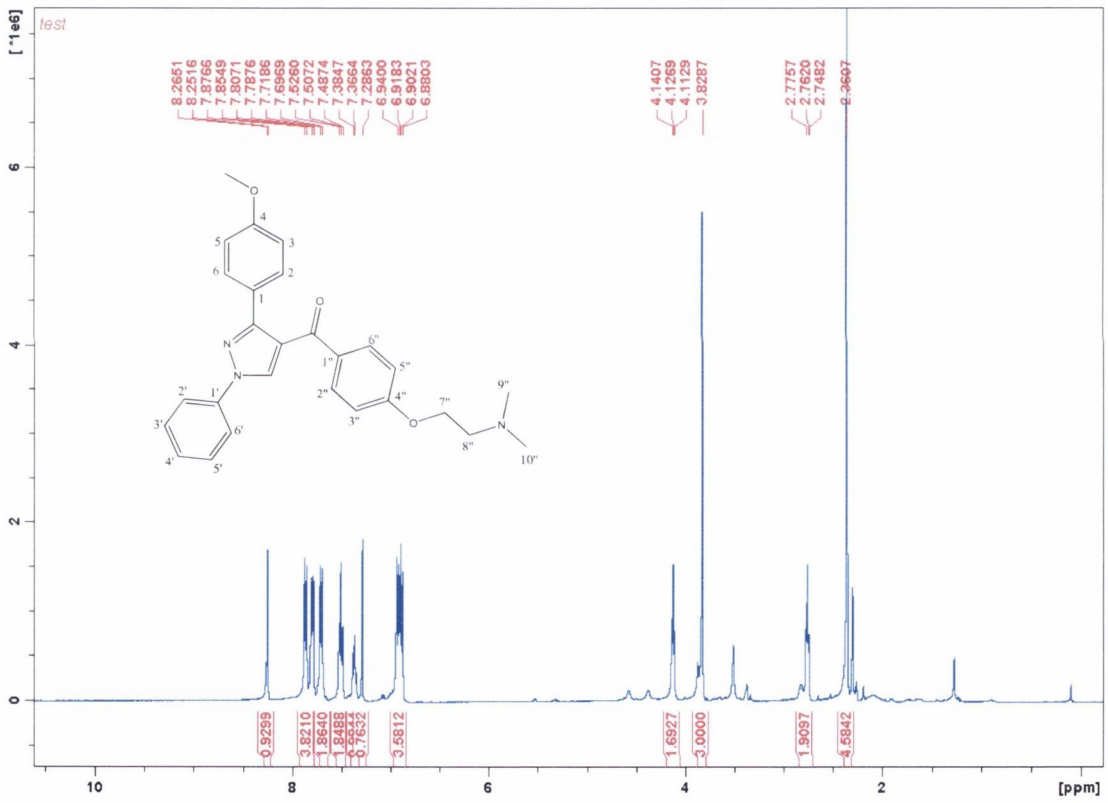

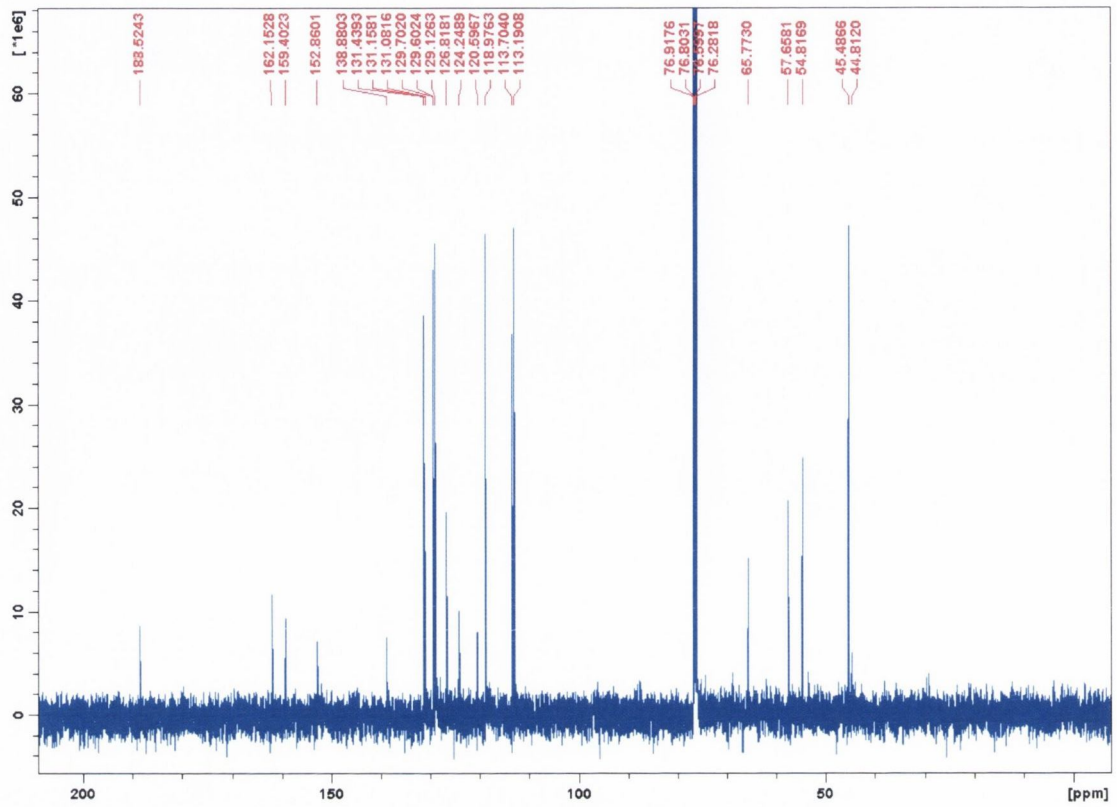

Figure 3.5 ^{1}H and ^{13}C NMR spectrum for compound 286

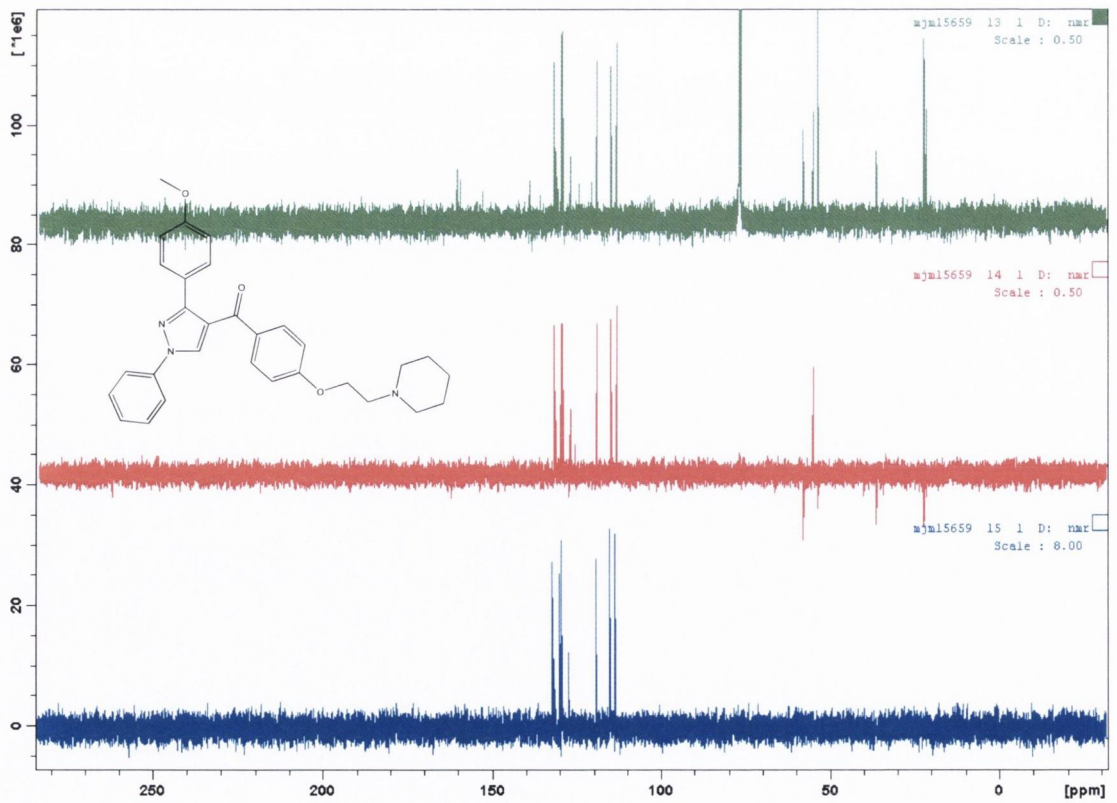

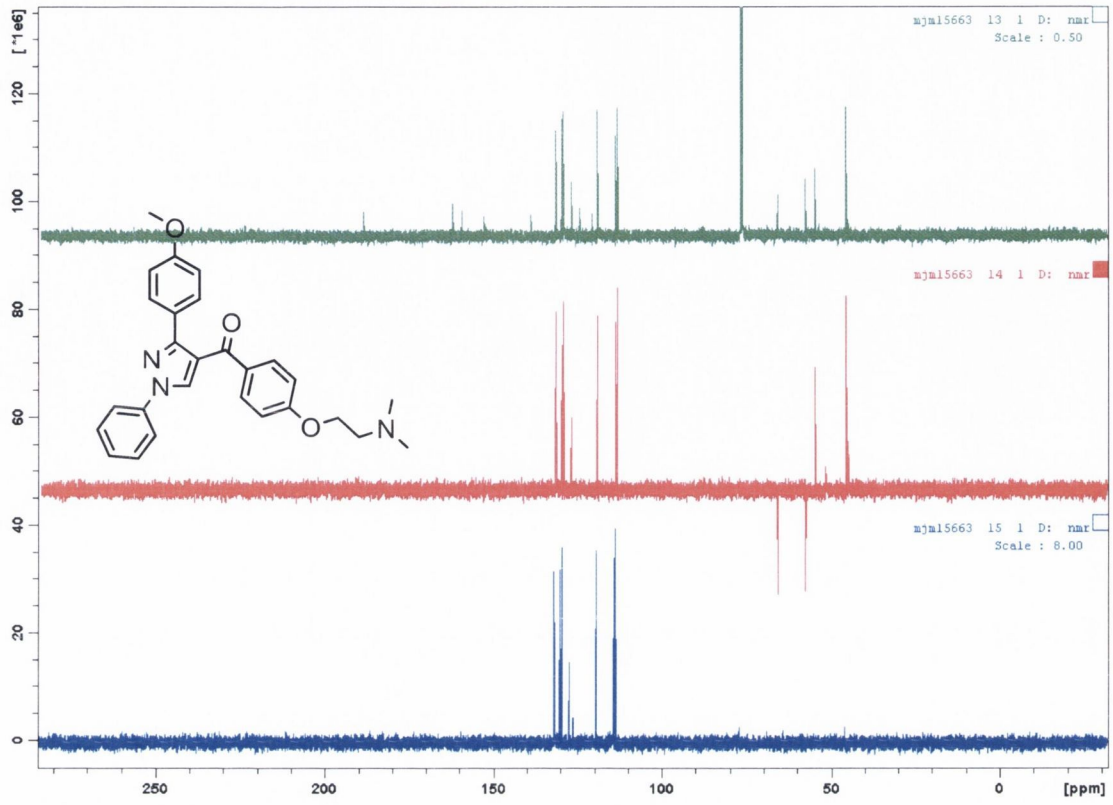

Figure 3.6 DEPT NMR spectrum of compounds 283&286

3.4 Summary

In conclusion, two series of novel antiproliferative agents designed to containg the pyrazole ring scaffold (type II) were synthesised. These products are prepared by reaction of relevant pyrazole carbaldehyde with appropriately substituted bromobenzene or piperazine utilizing the Grignard reaction and reduction amination respectively. The optimised structure design was based on introduction of the basic side chain to C-3 or C-4 position of the pyrazole ring system. The biochemical evaluation for the novel scaffold II analogues is presented in chapter 4.

Chapter 4

Biochemical analysis, stability investigation and molecular modelling study of novel antiproliferative pyrazole & dihydropyridine compounds

4.1 Introduction

According to the 2008 World Cancer Report, cancer will soon replace heart disease as the leading cause of deaths worldwide by 2010. This devastating disease will make both poor and rich countries experience the impact of higher cancer incidence and death rates more sharply than the past 30 years of the 20th century. It is estimated that this will double again by 2020 and nearly triple between 2020 and 2030. Reports forecast that 2.4 million people will be diagnosed with some form of cancer in 2010 and 7.6 million people will die. By 2030, 27million people will be diagnosed with a cancer, resulting in 17 million deaths annually. These statistics show the disease burden is immense, and it is considerable challenges for our current health care systems to find novel and power treatment for this malignant diseases[265].

Breast cancer is the second leading cuase of cancer death in women and the most common cancer among women. Breast cancers are classified as estrogen receptor (ER) positive and estrogen receptor (ER) negative. 70-80% of all primary breast tumours are ER positive. MCF-7 cells are human carcinoma cells which are used extensively as a model for ER positive breast cancer *in vitro* tests. The MDA-MB-231 cell line is a model of malignant human breast cancer(ER negative). The dihydropridine and pyrazole SERM analogues discussed in Chapter 2 and 3 were initially evalated for their antiproliferation and cytotoxic effects in MCF-7 and MDA-MB-231 cells. Subsequently we examined whether these novel DHP derivatives can reverse the resistance of paclitaxel over-expressing P-GP and MDR effects evaluated in HL-60-MDR cells.

Dihydropyridines (DHPs) are investigated for antiproliferative activity as a number of clinically used. Ca^{2+}channel-blocking drugs are derivatives of various DHPs. Despite this, these DHPs are significantly potent inhibitors of p-glycoprotein (Pgp), which are the main cause of the efflux of drugs and toxins from tumour cells. Dihydropyridine derivatives have been shown to have the potential to overcome P-glycoprotein (Pgp)-mediated multidrug resistance to doxorubicin and vincristine in cultured human cancer cells. The efflux of cytotoxic drugs is recognised as an important mechanism of multidrug resistance (MDR) which is a severe limitation to the successful treatment of many cancers such as metastatic breast cancer, as the active drugs are transported out of the cells by the trans-membrane efflux pumps so

that intracellular drug levels are too low to reach effective therapeutic effects. P-glycoprotein is a 170kDa plasma membrane transporter protein which is encoded by the human MDR-1 gene.[266, 267] It was the first of the ABC drug transporters identified and characterised in drug selected tumour cell lines, P-glycoprotein acts as an ATP-dependent efflux pump which decreases the intracellular accumulation of the drug resulting in resistance to various classes of chemotherapeutic drugs such as the vinca alkaloids, vincristine and vinblastine, the anthracyclines daunorubicin and doxorubicin and the related podophyllotoxin-based chemotherapeutic agent etoposide and taxol.[268]

Many different classes of compounds have been identified as multidrug resistance modifiers such as the calcium channel antagonists, protein kinase C inhibitors, and immunosupressants such as cyclosporine and others[269, 270]. The mechanism of action of P-glycoprotein modulators has been identified as direct binding to P-glycoprotein, and reducing ATP activity, to inhibiting protein kinase C(PKC) phosphorylation of P-glycoprotein. 1,4-Dihydropyridines such as nifedipine, nicardipine and amlodipine have been extensively investigated for their MDR effects, (See chapter 1). However, because of their pharmacological properties as calcium channel antagonists (active on L-type calcium channels), they are not suitable for therapy in MDR cancer.

Many novel 4-aryl-1,4-dihydropyridine compounds have been investigated with MDR reversal properties for cytotoxic drugs, and minimum effects on calcium channel activity. The cytotoxicity and MDR reversal effects of a series of 3,5-dibenzoyl-1,4-dihydropyridines has been reported where cell death was attributed to as non-apoptotic pathway.[265, 271] G1 cell cycle arrest by amlodipine has been suggested in human epidermoid carcinoma A431 cells,[272] while a 1,4-dihydropyridine derivative AV-153 has been reported to be effective in reducing DNA strand breaks, and stimulates apoptosis in human peripheral blood lymphocytes following gentoxic stress.[273] 1,4-Dihydropyridines were recently shown to modulate the activity of NAD dependent sirtuin deacetylases.[274] In our efforts to identify novel scaffold structures with intrinsic cancer cell growth inhibitory effects, we have identified a 4-(1,3-diaryl-1H-pyrazol-4-yl)-1,4-dihydropyridine scaffold structure using *in silico* screening techniques for estrogen receptor antagonists, indicating potential anti-proliferative activity for this pharmacophore in human estrogen

receptor positive MCF-7 breast cancer cells. The hepatoprotective properties of a series of related 4-pyrazolyl-1,4-dihydropyridines had been previously reported[275].

We now report the synthesis of a series of novel 4-(1,3-diaryl-1H-pyrazol-4-yl)-1,4-dihydropyridines and the initial evaluation of their anti-proliferative properties on MCF-7 and MDA breast cancer cell lines and also in a comprehensive NCI 60 cell line screen. The compounds were also examined for their potential to activate or inhibit calcium transporters and produce a change in the nature of cytosolic calcium increase in MCF-7 breast cancer cells stimulated with an agonist (ATP). The NCI 60 screen also highlighted significant potential in leukemia cells, amongst others. The effects of compounds on the cell cycle of HL-60 acute myeloid leukemia cells were determined by flow cytometry. Finally, we examined whether these novel DHP derivatives can reverse the resistance of paclitaxel in HL-60-MDR cells over-expressing Pgp.

4.2 Materials and suppliers

4.2.1 Materials

The full name and addresses of the suppliers are given at the end of the list.

Materials	Supplier
Activated charcoal	Sigma
Alamar blue	Biosource
DMSO	Sigma
Dulbecco's Modified Eagle's Medium	Gibco
Eagle's Minimum Essential Medium	Sigma/Gibco
Calf serum	Gibco
Foetal bovine serum	Sigma
L-glutamine	Gibco
4-Hydrotamoxifen	Sigma
Hl-60 cells	E.C.A.C.C.
Hl-60 parental Cells	E.C.A.C.C.
MCF-7 Cells	E.C.A.C.C.
MDA-MB-231	E.C.A.C.C.
MTT	Sigma
LDH assay kit	Promega

Non-essential amino acids	Sigma
Penicillin/streptomycin	Sigma
Phosphate Buffer Saline(PBS)	Oxoid Ltd.
Paclitaxel	Sigma
Prism GraphPad 4.0	Graphpad software, Inc.
RPMI 1640 Medium	Biosciences
Trypsin-EDTA	Sigma
Tamoxifen OHT	Sigma
Tubulin polymerization kit	Tebu-bio Ltd.

All sterile tissue culture flasks, pipettes, pipette tips, plates and tubes were from Greiner Bio-One Ltd. And all compounds from this thesis used in these tests are described in chapter 2 and 3.

4.2.2 Postal and e-mail addresses of suppliers/distributors

Biosciences: 3 Charlemont Terrace, Crofton Road, Dub Laoghaire, Co. Dublin, Ireland. orders@bioscicencs.ie

E.C.A.C.C: Health protection Agency, Salisbury Sp4 0JG, U.K.eiorders@europe.sial.com

GraphPad Software, Inc: 2236 Avenida de la Playa, California 92037, U.S.A.

sales@graphpad.com

Greiner Bio-One Ltd.: Brunel Way, Stroudwater Bussiness Park, Stonehouse, Gloucestershire GL10 3SX, U.K. orders@cruinn.ie

Invitrogen Ltd.: 3 Fountain Drive, inchinnan Bussiness park, Paisley PA4 9RF, U.K. orders@biosciences.ie

Oxoid Ireland Ltd.: Blackthorn Road, Sandyford Industrial, Estate, Foxrock, Dublin 18, Ireland.orders@fanninhealthcare.com

Promega U.K.: Delta House, Southampton Science Park, Southampton SO16 7NS, U.K. info@medical-supply.ie

Sigma-Aldrich Ltd.: Airton Road, Tallaght, Dublin24, Ireland.eiorders@europe.sial.com

Tebu-bio Ltd.: Unit 7, Flag Business Exchange, Vicarage Farm Road, Peterborough, Cambs DE1 5TX.

4.3 Cell culture

4.3.1 Cell lines

The MCF-7 cells(**Figure4.1**) are human breast cancer cell line, isolated from a 69-year-old Caucasian woman in 1970. MCF-7 is the acronym of Michigan Cancer Foundation-7.[276] The MCF-7 human breast tissue adenocarcinoma cell line was used to screen all of the compounds. Both our group and various other groups used the MCF-7 cell line extensively as model for estrogen receptor positive breast cancer.

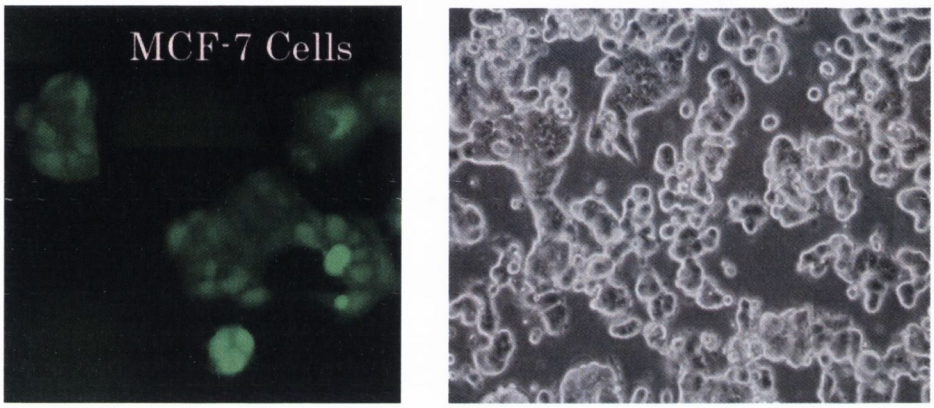

Figure 4.1 MCf-7 human breast cancer cells reproduced from ATCC(American type culture collection) website

The MDA-MB 231 Cells (**Figure4.2**) are human breast cancer cell line, cloned from a 51-year-old Caucasian woman.

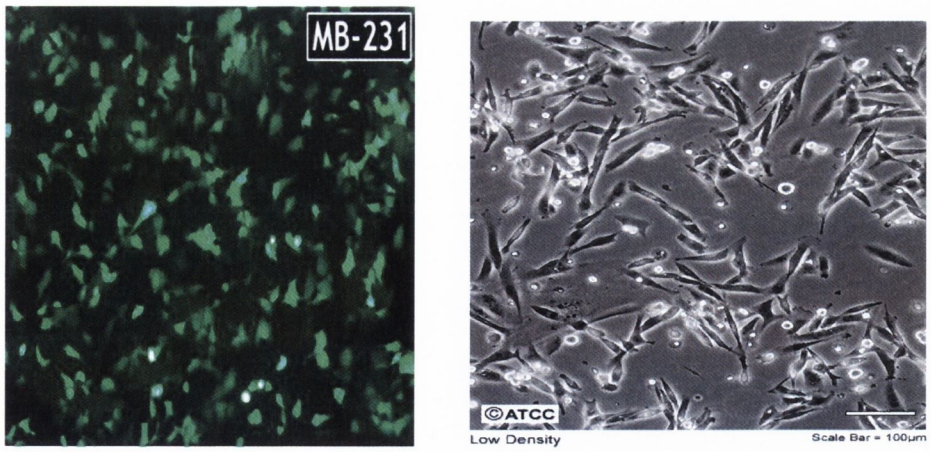

Figure 4.2 MDA-MB 231 human breast cancer cells reproduced from ATCC website.

The HL-60 cell line was originally obtained by leukopheresis from a 36-year-old Caucasian female with promyelocytic leukaemia. About 10% of these peripheral blood lymphocytes can spontaneously differentiate.[277]

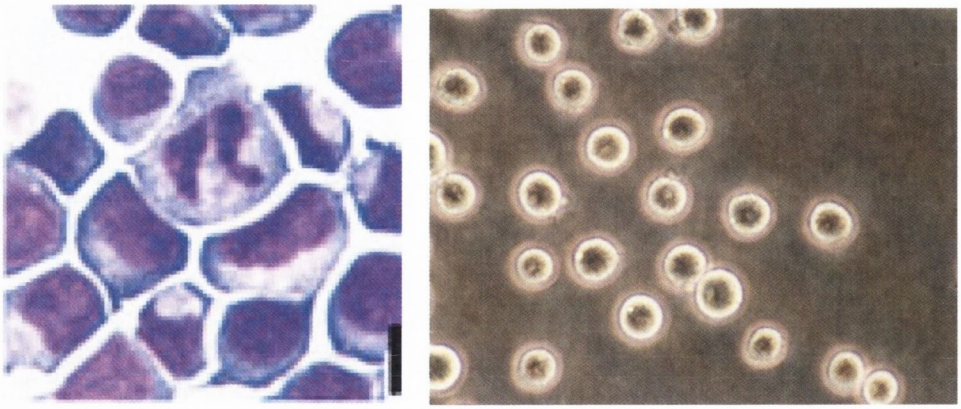

Figure 4.3 HL-60 human promyelocytic leukaemia cells[278]

4.3.2 Growth and maintenance of cell lines

The MCF-7 and MDA-MB 231 cell lines were grown as a monolayer culture at 37 ^{o}C, under a humidified atmosphere of 5% CO_2/95% O_2. The cells were maintained in Eagles Minimum Essential Medium(EMEM) supplemented with 10%(v/v) Foetal Bovine Serum(FBS), 2 mM L-glutamine, 100 μg/mL penicillin/streptomycin and 1%(v/v) non-essential amino acids (complete medium), and in Dulbecco's Modified Eagle's Medium(DMEM) supplemented with 10%(v/v) Foetal Bovine Serum(FBS), 2 mM L-glutamine and 100 μg/mL penicillin/streptomycin (complete medium), respectively. HL-60 Cells were growth in RPMI 1640 (Glutamax) medium supplemented with 20%(v/v) FBS and 50 μg/mL pencillin/streptomycin. Stock cultures were grown in T75cm^2 flasks in 20 mL of complete medium and were passaged at least twice weekly depending on their levels of confluency. When required for sub-culturing, growth medium was heated to 37 ^{o}C, removal of the cells from the surface of the flask was achieved by incubation with 3 ml of trypsin(10X) for 3-5 minutes depending on the adherency of the cells. Prior to the use of trypsin, the cells were washed by 10 mL of serum free EMEM/DMEM to prevent denaturation of the trypsin occurring. The 10 mL of complete medium was added and the cells were transferred to a sterile 20 mL tube and centrifuged at 1250xg for 5 min after trypsinisation. The supernatant was discarded and the pellet was resuspended in 3 mL of complete medium. Cells were then counted using a haemocytometer and seeded at the optimised density of $2x10^5$ cells/mL for HL-60 cells and $1.5x10^6$ cells/75 cm^2 for MCF-7 and MDA-MB 231 cells.

4.3.3 Use of a haemocytometer

A haemocytometer is a modified microscope slide containing an accurately sub-divided grid that enables the counting of cells in suspension. Each grid (of which there are two) consists of nine primary or large squares, each measuring an area of 1 mm^2. Each of these primary squares contains 25 medium squares, each measuring an area of 0.04 mm^2. When a particular seeding density of cells was required, a clean cover slip was placed on the haemocytometer; 10μL of the cell suspension as then pipetted into the groove at the end of the plane. The cell suspension was then drawn across the grid by capillary action. The number of cells within the four outer primary squares was counted; those cells that touched the lower or right hand side of the grid were not counted. As each medium square is 0.04 mm^3, the total volume per primary square is $1x10^{-4}$ mL. This indicated that the total cell concentration in the original suspension (cells/mL) is the average cell count per primary square multiplied by 10^4. At least two primary squares were counted and average was calculated. The concentration of original cells suspension was obtained by calculation.

4.3.4 Cell storage and cryopreservation

All cells were first sub-cultured as previously described (Section 4.3.2), the supernatant was discarded and the pellet was dissolved in 1mL of freezing medium (10%(v/v) DMSO, 30% FBs in RPMI medium) and transferred to sterile labelled cryotubes. In an effort to minimise damage caused during cryopreservation, cryotubes were incubated on ice for 15 minutes and subsequently placed in a freezer at -80 ^{o}C overnight. Samples could then be stored in liquid nitrogen at -180 ^{o}C indefinitely. When an aliquot of cells was required, the cells were quickly removed from the liquid nitrogen and thawed at 37 ^{o}C for 2 min. Just before the samples had fully thawed, their contents were gently pipetted into a sterile 20 mL tube to prevent damage to the cells that can be very fragile after cryopreservation. The cells were then centrifuged at 500xg for 5 min. The supernatant was discarded and the pellet was resuspended in 1 mL of medium. This solution was then added to a small flask containing a further 6 mL of medium. Following 48 hours, cells were confluent enough to be passaged as previously described (Section 4.3.2). All cells had been sub-cultured at least once and analysed by flow cytometry to ensure background levels of apoptotic cells were sufficiently low before any assay were carried out.

4.4 Preparation of stock solution

Most of compounds in this thesis were solubility free in ethanol, so 10 mM stock solution were made up in 100%(v/v) ethanol(for in *vitro* experiments) and maintained at -20 ^{o}C. Working stock solutions were then made up in ethanol by serial dilutions of the primary stock solution.

Paclitaxel was initially made up as a 10 mM stock solution in 100%(v/v) DMSO and subsequently aliquoted out into 10 μL samples to prevent repeated freeze-thawed, aliquots were kept for up to 6 months at -20 ^{o}C. Immediately before any experiments, paclitaxel was diluted to 100 μL in RPMI medium, the required volume of which was added to cells.

4.5 Methods for biochemical analysis

4.5.1 Antiproliferation studies

The antiproliferative effects of the designed compounds were evaluated using the method firstly described by Mosmann.[279] The MTT [3-(4,5-dimethylthiazol-2-yl)-2,5-diphenyltetrazolium bromide] assay was first performed to assess the antiproliferative effect of compounds nearly 30 years ago. The assay is based on the cleavage of MTT by mitochondrial dehydrogenase enzymes present within the MCF-7 cells. The cleavage of MTT results in the formation of formazan crystals and makes an obvious colour change from the pale yellow MTT to the purple/blue formazan which can be read at 595 nm on a plate reader. The proliferating cells will take up the MTT and cleave it to formazan which are impermeable to cell membranes, thus resulting in their accumulation within surviving cells. The number of proliferating cells in the well is directly proportional to the level of the formazan product created. In contrast to the cytotoxic assay, the antiproliferative assay requires the use of the cells present in the wells.

MCF-7 and MDA-MB-231 cells were pelleted and counted as previously described in **Section 4.3.2** and **4.3.3**. Complete medium was added to give a density of $2.5x10^4$ cells/mL. The cells were placed in 96-well plates at 200 μl per well. The outside wells were not used, therefore two compounds could be tested per plate over seven concentrations and with a control, vehicle and blank for each compound. The cells were left at 37 ^{o}C under a humidified atmosphere of 95% O_2, 5% CO_2 for 24 h. A

stock solution of 10 mM of the selected compounds was made up in ethanol and serial dilutions were carried out to obtain solutions of 5 mM, 1 mM, 0.5 mM, 0.1 mM, 10 μM, 1μM and 100 nM and stored at -20 °C until further required. The cells were treated with a 2 μL of vehicle (1% (v/v) ethanol) or a range of concentrations of the synthesised compounds 2μL, therefore resulting in a final concentration ranging from 50 μM to 1 nM of the selected compound in the well. The treated plates were placed again in the incubator for 72 h. Following the incubation period, 20 μl of lysis solution was added to the 'blank' wells and left for 1 h to insure 100% cytotoxicity prior to the MTT was added into. Meanwhile, 50 μL was then transferred from each well to a new 96-well non-sterile plate for further use in the LDH assay.

Subsequently, the cell medium was removed from the plate and the plate was gently washed with phosphate buffered saline (PBS) solution to remove any remaining medium and inverted to remove all PBS solution. The plates were dried and 50 μL of MTT solution (1 mg/mL) was added to each well. Then the added MTT solution was taking good care to ensure that was not exposed to light as it can cause inadvertent cleavage of the MTT. The cells were incubated in the dark for 2-3 h at 37 °C when the cells will take up and cleave the MTT (**Figure 4.4**). Dark blue crystals were formed and completely dissolved in 200 μL of dimethyl sulfoxife (DMSO). The absorbance was monitored at a wavelength of 595 nm in a Dynatech MR5000 plate reader and cell viability presented as a percent of control. In the antiproliferative assay, the control wells provide values for 0% while the vehicle wells provide values for 100% proliferation. IC_{50} values were calculated by the program Graphpad Prism 4.0 for each compound.

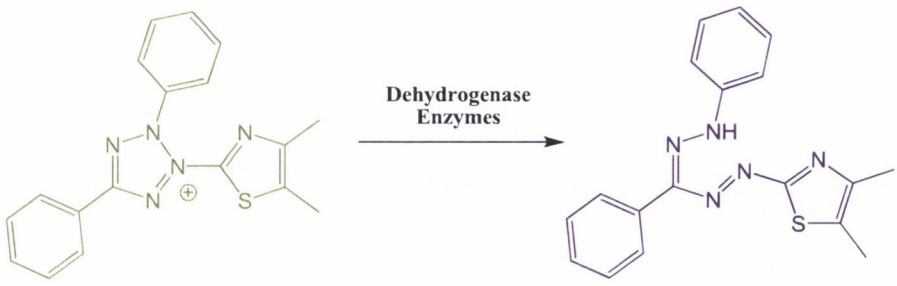

Figure 4.4 Ezymatic cleavage of MTT by dehydrogenase enzymes in the mitochondria of metabolically active cells

4.5.2 Lactate dehydrogenase (LDH) assay

The cytotoxic evaluation was determined using the Cyto Tox 96 Non-radioactive cytotoxicity assay which is commercial kit available from Promega. The assay quantitatively measures lactate dehydrogenase (LDH) a stable cytosolic enzyme that is released upon cell lysis. The release of LDH in culture supernatant is measured in coupled enzymatic assay which leads to the convension of a tetrazolium salt (INT) into a red formazan product (**Figure 4.5**). The assay involves an initial step of treating the control well with a suitable lysis solution such as 10% Triton in PBS to induce complete cell lysis which give a value represent 100% cell death. The wells that were treated with only vehicle represent 0% cytoxicity.

MCF-7 and MDA-MB-231 cells were seeded in 96-well plates and incubated for 24 hours and then treated with synthesized compounds as described in section 4.3.2. After 72 h, 20 µl of lysis solution (10x) was added to the 'blank' wells. The plates were left in the incubator at 37 °C for minimum of 1 hour to ensure 100% cell death. 40 µL of cell medium was removed from each well and transferred into a fresh 96-well plate for LDH assay. 40 µL of the prepared substrate mix from the LDH assay kit was added into each well and the plate was then covered with tinfoil to prevent from light and placed at room temperature for 30 min. Afterward, 40 µL of stop solution was added to each well before recorded the absorbance at a wavelength of 490 nm using a Dynatech MR5000 plate reader. The cleavage of the tetrazolium salt is noticeable from the appearance of red coloured crystals in the well. The percentage of cell death was calculated at 10 µM.

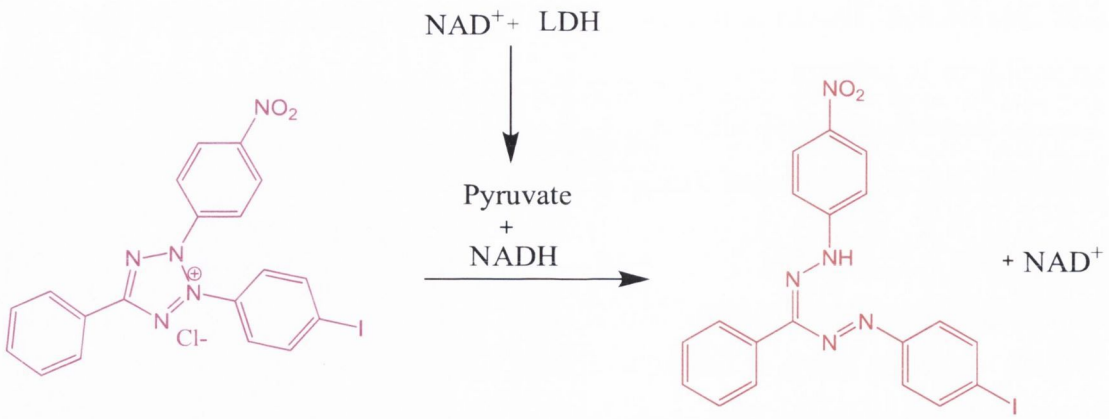

Figure 4.5 Enzymatic conversion of tetrazolium salt to formazan for the detection of LDH released from dead cells

4.5.3 Alamar blue viability assay

Alamar blue is a proven cell viability indicator that uses the natural reducing power of living cells to convert resazurin to the fluorescent molecule, resorufin. The non-fluorescent indicator dye named resazurin as the active ingredient of alamar blue will convert to bright red and fluorescent resorufin via the reduction reactions of metabolically active cells (**Figure 4.6**). The amount of fluorescence produced is proportional to the number of living cells.

HL-60 cells were seeded at the relevant density in 200 µL medium in a 96-well plate. Cells were treated and incubated as required. Alamar blue (20 µL) was then added to each well and incubated at 37 °C in the dark for between 3 or 4 hours (depending on the cell type). Plates were then recorded on a fluorescence plate reader (SpectraMax Gemini, Molecular Devices) with excitement and emission wavelengths of 544 nm and 590 nm respectively. Experiments were performed in triplicate. A sample containing only reagent and medium (without any cells) was used as a blank. Vehicle samples were set as 100% viability from which any decrease in viability was calculated.

Figure 4.6 Alamar blue mechanism as an indicator

4.5.4 Flow cytometry

The HL-60 cells were seeded at the relevant density in 5 mL of medium ($18x10^5$ cells/mL, 900,000 cells per flask). After 24 hours, the range of concentrations of selected compound (10 nM-10 µM 1% v/v) and corresponding vehicle (50 µL of ethanol, 1% v/v) were treated. The cells were removed from the bottom of flask and the medium was transferred to a 20 mL tube after the required treatment time 24, 48 or 72 hours. They were centrifuged at 650xg for 10 min. The supernatant was removed and the cells were resuspended in 100 µL ice-cold phosphate buffer saline (PBS). Subsequently 2 mL of ice-cold 70% (v/v) ethanol was slowly added to the tube to fix the samples as it was gently vortexed. The cells were kept at -20 °C until required (At least one hour, can be left overnight). After the fixation 5 µL of PBS

was added to the samples. The cells were harvested by centrifugation at 650xg for 10 min. The ethanol was carefully removed and the pellet resuspended in 400 µL of PBS and transferred to FACS microtubes. A 25 µL aliquot of RNase A (1 mg/mL) and 75 µL of propidium iodide (PI) 1 mg/mL, a DNA binding fluorescent dye, was added to each tube. The sample were wrapped in aluminium foil and incubated for at least 30 min at 37 °C.

The samples were read at 488 nm using FACscalibur flow cytometer from Becton Dickinson. The FACS data for 10,000 cells was analysed using the Macintosh-based application Cell quest and the data was stored as frequency histograms.

4.5.5 ECIS

Electric Cell-substrate Impedance Sensing (ESIC) is a non-invasive method to electronically monitor the behaviour of cells grown in relevant tissue culture in real time, including migration, proliferation, signal transduction, attachment and spreading, barrier function and metastasis potential.[280]

A

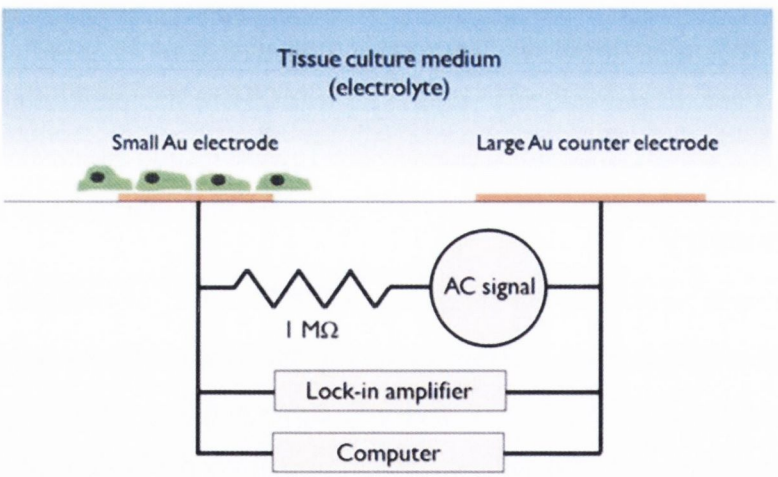

B

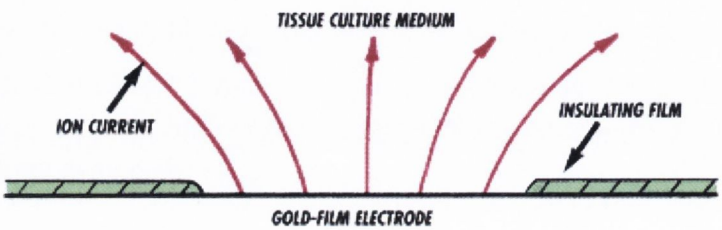

C

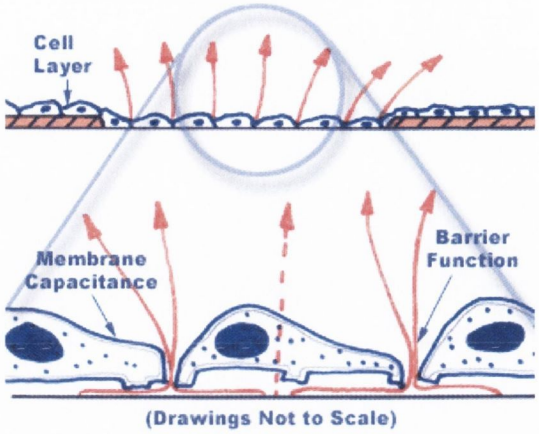

Figure 4.7 (A) A schematic diagrams of the ECIS measurement system Current flows without cells (B) and with cells (C) on the surface of the electrode

Figure 4.7 shows the working principle of an ECIS system.[281] Technically, cells are grown on the surface of small gold-film electrodes that are microfabricated on the bottom of a tissue culture dish. Due to the insulating properties of their membranes, while attaching and spreading on the electrodes, cells act as dielectric particles causing the current to pass around the cells and subsequently increasing the measured impedance until a confluent or continuous layer of cells is formed. When monitoring cell proliferation, culture arrays are inoculated with a low cell density providing room for the dividing cell population. As the cell number increases, the amount of electrode area covered with the spread cells grows accordingly, causing the electrode impedance to rise. These impedance changes can be related to the relative cell proliferation rates or, more accurately, the rate at which the substrate becomes occupied with spread cells.[282]

In the present study, the estrogen receptor positive human breast cancer cell line MCF-7 was used for determination of the antiproliferative activity of a variety of the synthesized compounds described in this chapter. The 8W10E sensing array (Applied Biophysics, Tory, NY) was chosen which consists of 8 wells, each containing 10 circular 250 μm diameter active electrodes connected in parallel on a common gold pad (**Figure. 4.8**).

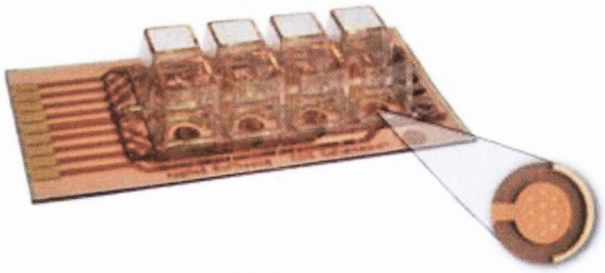

Figure 4.8 8W10E ECIS sensing array

Briefly, 8W10E arrays were first precoated with 400 µL of complete growth media and allowed to incubate for 2 hours while MCF-7 cells were being trypsinised, pelleted and counted. The 400 µL of media was then gently removed from each well and 400 µL of cell suspension was added. There were a total of $1x10^5$ MCF-7 cells per 600 µL well volume. After inoculation, arrays were returned to CO_2 incubator and incubated for approximately 20 h to allow cells to spread and attach to the substrate. Following the incubation, 2 µL of each synthetic DHP compound at 1mM concentration was added in duplicate to 400µL media, resulting in a final concentration of 5 µM in each well. The arrays were then returned to the CO_2 incubator and connected to the ECIS1600 instrument (Applied Biophysics, Tory, NY). Impedance values were collected every 1 min for a total run time of 48 h.

4.5.6 Antioxidant assay (DPPH assay)

Several methods to determine free radical scavenging have been reported. DPPH assay is most popular and was run to measure the relative antioxidant capacity of the tested compounds by 2,2-diphenyl-1-picrylhydrazyl (DPPH) (**Figure 4.9**). [283] Trolox, also named 6-hydroxy-2,5,7,8-tetramethylchroman-2-carboxylic acid (as standard) and sample were dissolved in methanol at different concentrations, and DPPH methanol solution in 2.5 mg/L prepared daily. DPPH solution 2.4 mL was added to 0.1 mL standard solution in a cuvette located in Cary 300 spectrophotometer and immediately the absorbance was read at 515 nm at different time intervals until a plateau is reached.

Antioxidant activities were monitored using DPPH. 2.4 mL of 0.2 mM solution of DPPH in methanol is added to 0.1 mL of 1.2 mM solution of sample in DMSO in a 2.5 ml spectrophotometer cell. The maximum volume of DMSO used in the experiments was less than 4% compared to methanol. Kinetic traces were obtained at

515 nm using a Cary 300 scan spectrophotometer. Observed rate constants (*Kobs*) were expressed from first-order fitting of the corresponding kinetic traces.

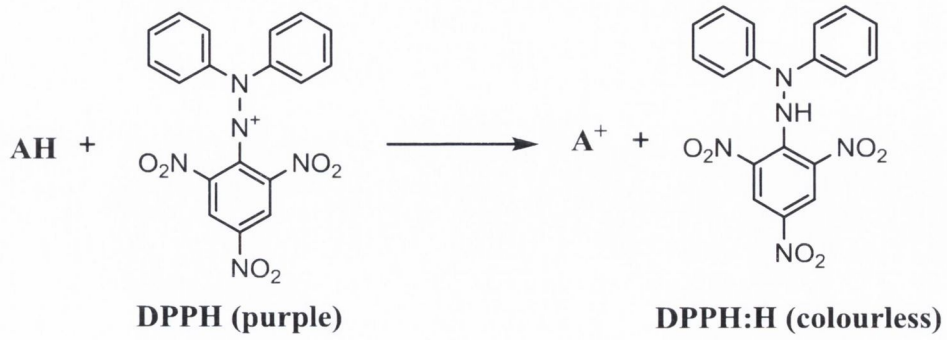

Figure 4.9 DPPH radical scavenging assay (AH: antioxidant compound)

4.6 Results and discussion

4.6.1 Biological evaluation of novel 4-(1,3-diaryl-1H-pyrazole-4-yl)-1,4-dihydropyridines

4.6.1.1 Antiproliferative and cytotoxic effects of selected dimethyl-2,6-dimethyl-4-(1-phenyl-1H-pyrazol-4-yl)-1,4-dihydropyridine-3,5-dicarboxylate compounds (Type I) in MCF-7 cell line

The antiproliferative and cytotoxic effects of type I 1,4-dihydropyridines were evaluated using MCF-7 (ER positive) breast cancer cells. Table 4.1 shows the structure of a series of compounds that were initially synthesised via Hantzsch reaction of 1,3-diaryl-1H-pyrazole-4-carbaldehydes with methyl acetoacetate. The effect on activity depending on the substitutent at C-3 of the aryl ring and at C-4 of the pyrazole ring was examined. The results for this library are presented in **Table 4.1**.

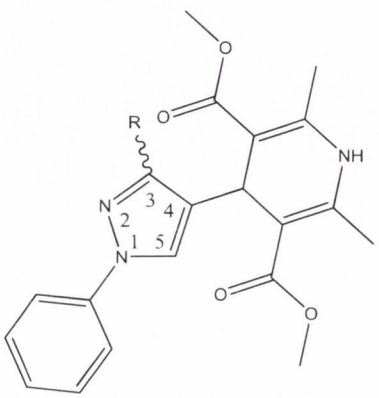

Compound No.	R	MCF-7		ClogP
		Antiproliferative activity IC_{50} (μM)	Cytotoxicity % cell death at 10μM	
186	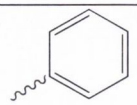	7.17(±0.034)	16.32(±5.56)	5.084
188	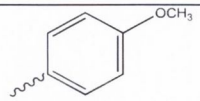	2.69(±0.397)	13.11(±1.08)	5.058
183	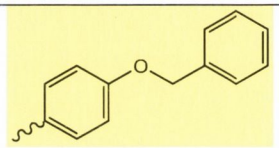	0.84(±0.89)	8.7(±1.32)	6.826
184	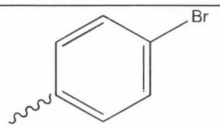	3.46(±0.28)	19.72(±4.66)	5.965
187	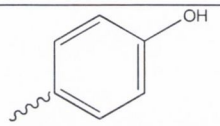	13.1(±0.57)	3.79(±2.79)	3.508
185	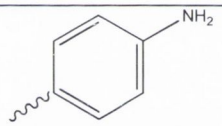	2.1(±0.65)	8.10(±1.28)	3.753
1,4-DHP	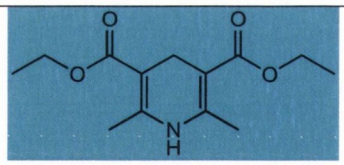	>1000	0	2.962
Tamoxifen	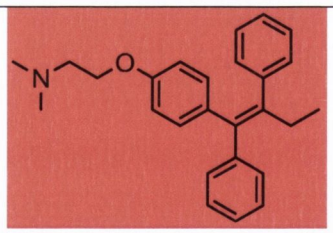	4.48±0.038	13.4	6.818

Table 4.1 Antiproliferative and cytotoxic effects of initial type I DHPsin MCF-7 cells.
IC_{50} values: the concentration required to inhibit 50% of MCF-7 cells growth. Results represent the mean±S.E for at least two independent experiments performed in triplicate

Abadi et al have reported a number of 1,3,4-trisubstituted pyrazole derivatives which are non-cytotoxic but with an apparent antiangiogenic profile, mainly through inhibiting the motility of endothelial cells rather than its proliferation.[202] In the present work, the 2,6-dimethyl-1,4-dihydropyridine-3,5-dicarboxylic acid diethyl ester was found to be inactive, with $IC_{50}>10^{-1}$M(Highlighted in blue), indicating a requirement for the heterocyclic pyrazole substituent at C-4 of the 1,4-

dihydropyridine ring for antiproliferative activity of these compounds as displayed in **Table 4.1**. For this reason a novel class of compounds was designed and synthesised to study the effect on antiproliferative activity of substitution patterns in the aryl ring at C-3 including phenyl, halogens, amino, methoxy and hydroxyl groups.

The IC_{50} values of the initial library of compounds biochemically evaluated are reported above and compared to that of tamoxifen (IC_{50} = 4.48 μM, highlighted in red). Most of the compounds have values similar or less than the values obtained for tamoxifen. More impressively, compound **183** (highlighted in yellow) represented an IC_{50} vaules of 840 nM which presents a 6 fold increase in potency and still retaining reasonable cell cytotoxicity at 10 μM of 8.7%. Compound **183** contains the benzyloxy group at the *para*position on the phenyl ring at the C-3 position of the pyrazole ring. **Figure 4.10** show a representative antiproliferative and cytotoxicity dose response curves for compound **183**.

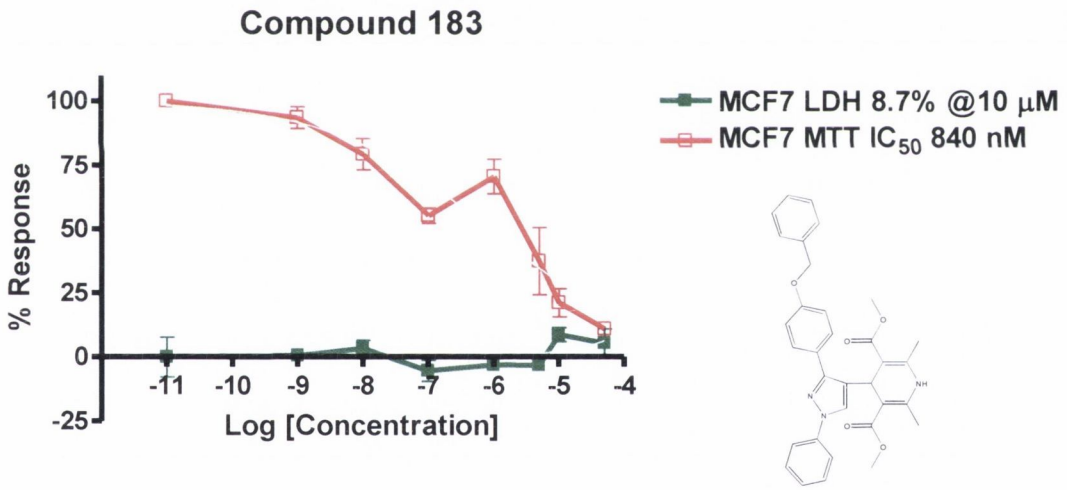

Figure 4.10 Compound 183 inhibited proliferation and induced cytotoxicity of MCF-7 cells.

MCF-7 cells were seeded at a density of 2.5x104 cells/mL in 96-well plates and allowed adhere to the surface of the 75 cm2 culture flask wells for 24 h.The cells were treated with compound 1 nM-50 μM (final concentration) and incubated for 72 h. Determination of cell proliferation was carried out using MTT assay described in section 4.5.1 and the cytotoxicity was evaluated using the LDH assay as described in section 4.5.2

4.6.1.2 Antiproliferative and cytotoxic effects of diethyl 2,6-dimethyl-4-(1-phenyl-1H-pyrazol-4-yl)-1,4-dihydropyridine-3,5-dicarboxylates (Type II) in MCF-7 cell line

Twenty 4-(1,3-diaryl-1H-pyrazole-4-yl)-2,6-dimethyl-1,4-dihydropyridine-3,5-dicarboxylic acid diethyl esters were prepared by Hantzsch reaction of the 1,3-diaryl-1H-pyrazole-4-carbaldehydes with ethyl acetoacetate in aqueous ammonia as discussed in chapter 2. The different effects on cell viability related to the substitution of the aryl ring at C 3 in compounds **161-181** including alkyl, phenyl, amino, nitro, halogens, methoxy and hydroxyl groups while additional pyrazole C-3 substituents included the 2-naphthyl, 2-thienyl and 3-pyridyl and biphenyl ring systems were also assessed. The results obtained are illustrated in Table **4.2**.

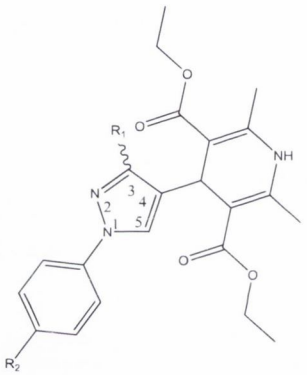

Compound No.	R_1	R_2	MCF-7		ClogP
			Antiproliferative activity IC_{50} (μM)	Cytotoxicity % cell death at 10μM	
164	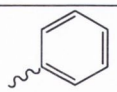	**H**	**5.2(±1.74)**	**10.6(±4.17)**	**6.142**
166	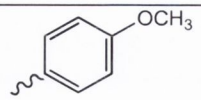	**H**	**8.0(±1.08)**	**5.0(±3.63)**	**6.116**
161	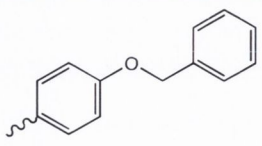	**H**	**3.9(±0.67)**	**7.8(±3.08)**	**7.884**
162	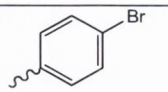	**H**	**6.8(±2.74)**	**6.22(±4.50)**	**7.023**
165	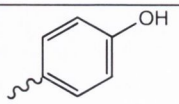	**H**	**7.9(±4.72)**	**7.7(±1.88)**	**5.568**

163	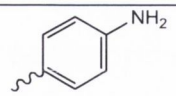	**H**	**6.4(±5.52)**	**12.5(±8.69)**	**5.003**
167	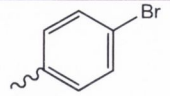	**OCH_3**	**2.95(±0.052)**	**9.21(±1.75)**	**7.186**
168	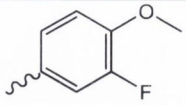	**H**	**47.26**	**1.28**	**6.166**
177	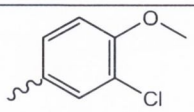	**H**	**1.01**	**14.23**	**6.706**
169	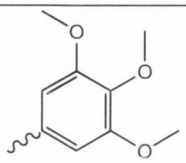	**H**	**10.8(±4.23)**	**8.9(±1.70)**	**5.822**
172	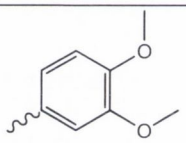	**H**	**8.9(±0.25)**	**7.5(±8.56)**	**5.450**
174	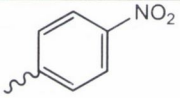	**H**	**6.3(±1.64)**	**6.8(±4.55)**	**5.924**
171	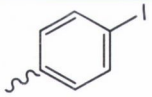	**H**	**6.2(±0.31)**	**1.55(±0.55)**	**7.283**
175	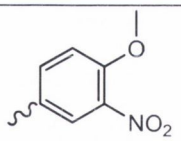	**H**	**6.7(±3.98)**	**6.9(±3.02)**	**5.852**
166	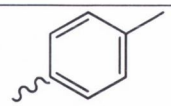	**H**	**5.0(±3.04)**	**5.9(±1.72)**	**6.641**
181	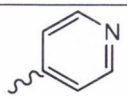	**H**	**5.9(±1.17)**	**13.3(±0.6)**	**4.744**
178	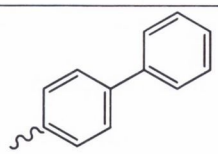	**H**	**2.6(±5.39)**	**9.2(±3.62)**	**8.030**
179	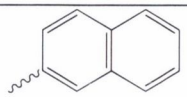	**H**	**4.7(±1.34)**	**10.1(±3.05)**	**7.316**
180	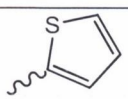	**H**	**7.5(±3.49)**	**9.2(±1.18)**	**6.257**

176	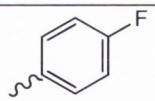	H	5.7(±0.62)	6.6(±2.97)	6.303
Tamoxifen	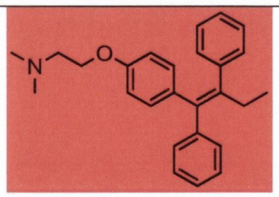		4.48±0.038	13.4	6.818
Nifedipine	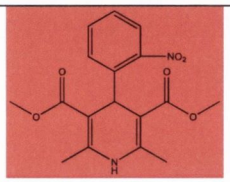		51.61	13.93	2.087

Table 4.2 Antiproliferative and cytotoxic effects of initial type II 1,4-DHPs in MCF-7 cells.

IC_{50} values: the concentration required to inhibit 50% of MCF-7 cells growth. The values represent the mean±S.E for independent experiments determined at least twice

The IC_{50} values of compounds **161-181** in (ER-positive) MCF-7 human breast cancer cell line using the MTT assay are displayed in **Table 4.2**. The IC_{50} value obtained for the calcium channel antagonist nifedipine in cell viability studies in MCF-7 cells was determinded to be 51.61 μM with a cytotoxicity of 13.93% at 10 μM and positive control drug tamoxifen gives IC_{50} value of 4.48±0.038 μM and cytotoxicity 13.4% (both highlighted in red). The results show that many of the compounds evaluated have IC_{50} values in the low to mid micromolar range, and are better or similar than the value obtained for tamoxifen in this assay. The most potent compounds in the series were the 4-benzoxyl product **161**, the 4-methoxy-3-chlorophenyl compound **177** and the biphenyl substituted compound **178** displaying good activity with IC_{50} = 3.9 μM, 1.01 μM and 2.6 μM respectively. Compound **167** contains the bromophenyl substituent at C-3 of the pyrazole and contains the methoxy group at the para position on the phenyl ring at N-1 position also displayed low micromolar activity (IC_{50} = 2.96 μM) less than tamoxifen (IC_{50} =4.48 μM) which is encouraging for the template chosen for further such analogue synthesis. The dose response curve for antiproliferative and cytotoxic effects for compound **167** is illustrated in **Figure 4.11.**

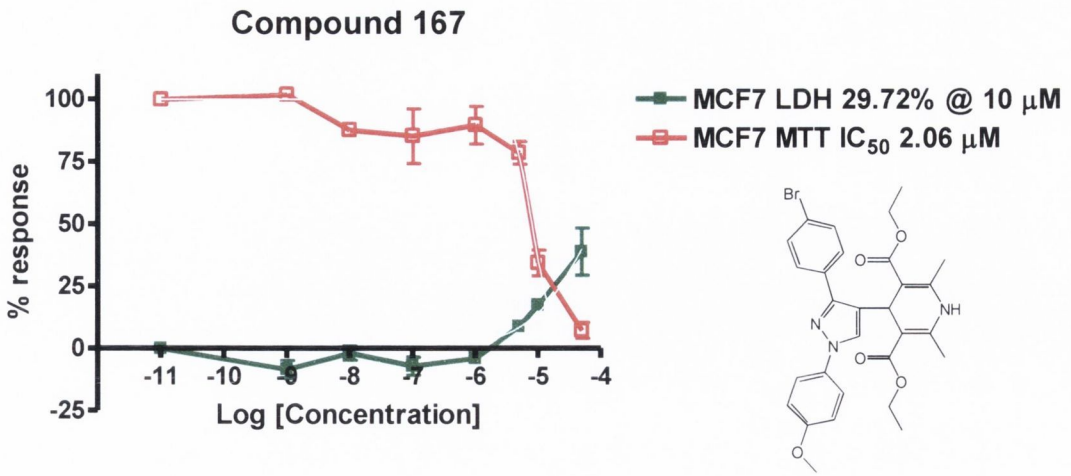

Figure 4.11 Compound 167 inhibited proliferation and induced cytotoxicity of MCF-7 cells.

MCF-7 cells were seeded at a density of $2.5x10^4$ cells/mL in 96 well plates and allowed adhere to the surface of the 75 cm^2 culture flask wells for 24 h. The cells were treated with compound 1 nM-50 μM (final concentration) and incubated for 72 h. Determination of cell proliferation was carried out using MTT assay described in section 4.5.1 and the cytotoxicity was evaluated using the LDH assay as described in section 4.5.2.

4.6.1.3 Antiproliferative and cytotoxic effects of 3,5-dibenzoyl-1,4-dihydropyridines (Type III) in MCF-7 cell line

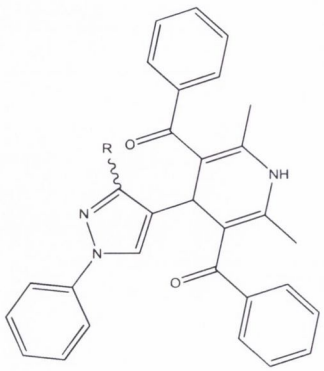

Compound No.	R	MCF-7		ClogP
		Antiproliferative activity IC_{50} (μM)	Cytotoxicity % cell death at 10μM	
192	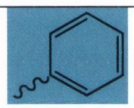	2.92(±1.10)	12.55(±1.35)	7.767
194	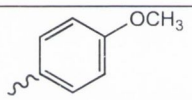	18.74(±2.06)	4.93(±0.95)	7.741
193	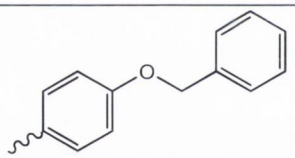	53.84(±3.68)	11.65(±1.25)	9.509
191	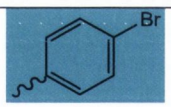	9.04(±4.05)	15.70(±6.7)	8.648
190	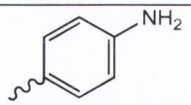	17.98(±7.24)	1.62(±1.32)	6.436
Tamoxifen	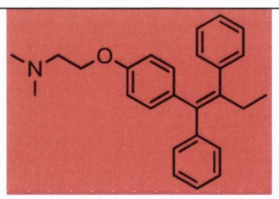	4.48±0.038	13.4	6.818

Table 4.3 Antiproliferative and cytotoxic effects of Type III 1,4-DHP derivatives in MCF-7 cells.

IC_{50} : the concentration required to inhibit 50% of MCF-7 growth. The results represent the mean± S.E for three experiments performed in triplicate.

Multidrug resistance (MDR) of cancer cells has often been correlated with the overexpression of P-glycoprotein (Pgp). Therefore, it is essential to develop molecules that can inhibit Pgp activity. For this reason, the dihydropyridines (DHPs)

as the possible resistance modifiers have been studied extensively for possible MDR reversal activity effects. In this section, five of Type III compounds (**190-194**) were prepared by the Hantzch reaction and showed significant variation in their cytotoxic activity against MCF-7 cell line and MDA-MB-231 cell line (discussed in further **section 4.6.6**). As shown in **Table 4.3**, the benzoyl DHP derivatives were first formed and displayed low to mid micromolar activity. Compound **192**(IC_{50}=2.92 μM) and compound **191**(IC_{50} = 9.04 μM) showed the most potent cytotoxic activity of this series of compounds against MCF-7 cells while still maintaining reasonable cell death at 10 μM of 12.55% and 15.7%, respectively.(**Figure 4.12**)

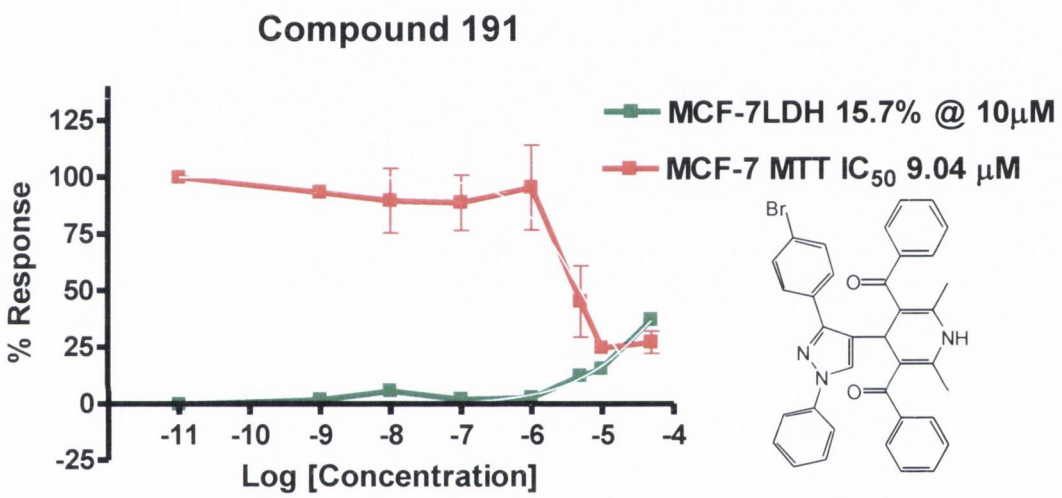

Figure 4.12 Compound 191 inhibited proliferation and induced cytotoxicity of MCF-7 cells.

MCF-7 cells were seeded at a density of $2.5x10^4$ cells/mL in 96 well plates and allowed adhere to the surface of the 75 cm^2 culture flask wells for 24 h. The cells were treated with compound 1 nM-50 μM (final concentration) and incubated for 72 h. Determination of cell proliferation was carried out using MTT assay described in section 4.5.1 and the cytotoxicity was evaluated using the LDH assay as described in section 4.5.2.

4.6.2 Antiproliferative and cytotoxic effects of ester and amide containing analogues diethyl 2,6-dimethyl-4-(1-phenyl-1H-pyrazol-4-yl)-1,4-dihydropyridine-3,5-dicarboxylate (Type IV) in MCF-7 cell line

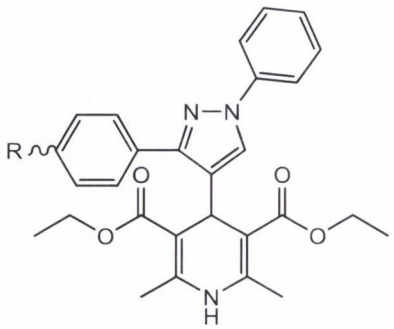

Compound No.	R	MCF-7		ClogP
		Antiproliferative activity IC_{50} (μM)	Cytotoxicity % cell death at 10μM	
195	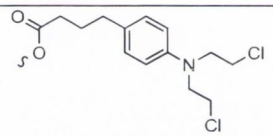	1024.5(±7.5)	7.86(±1.02)	9.667
196	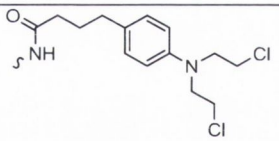	4.098(±2.18)	14.74(±3.00)	8.914
216	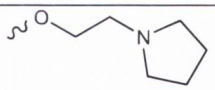	>1000	1.08(±0.21)	6.890
217	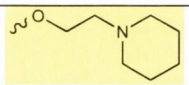	4.69(±0.37)	24.89(±1.13)	7.450
218	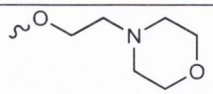	>1000	7.41(±2.84)	6.236
219	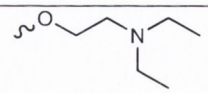	3.38(±2.04)	11.86(±5.54)	7.273
220	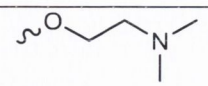	4.75(±3.08)	5.51(±2.05)	6.215
210	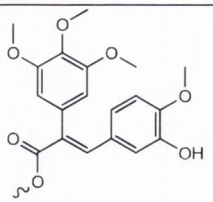	4.72(±4.31)	18.52(±1.24)	8.743

240	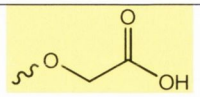	**0.40(±0.22)**	**80.5(±0.47)**	**5.405**
CA-4	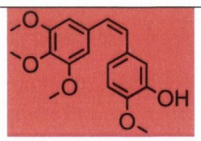	**0.0031**	**5.5**	**3.316**

Table 4.4 Antiproliferative and cytotoxicity effect of NASID and basic side chain analogues

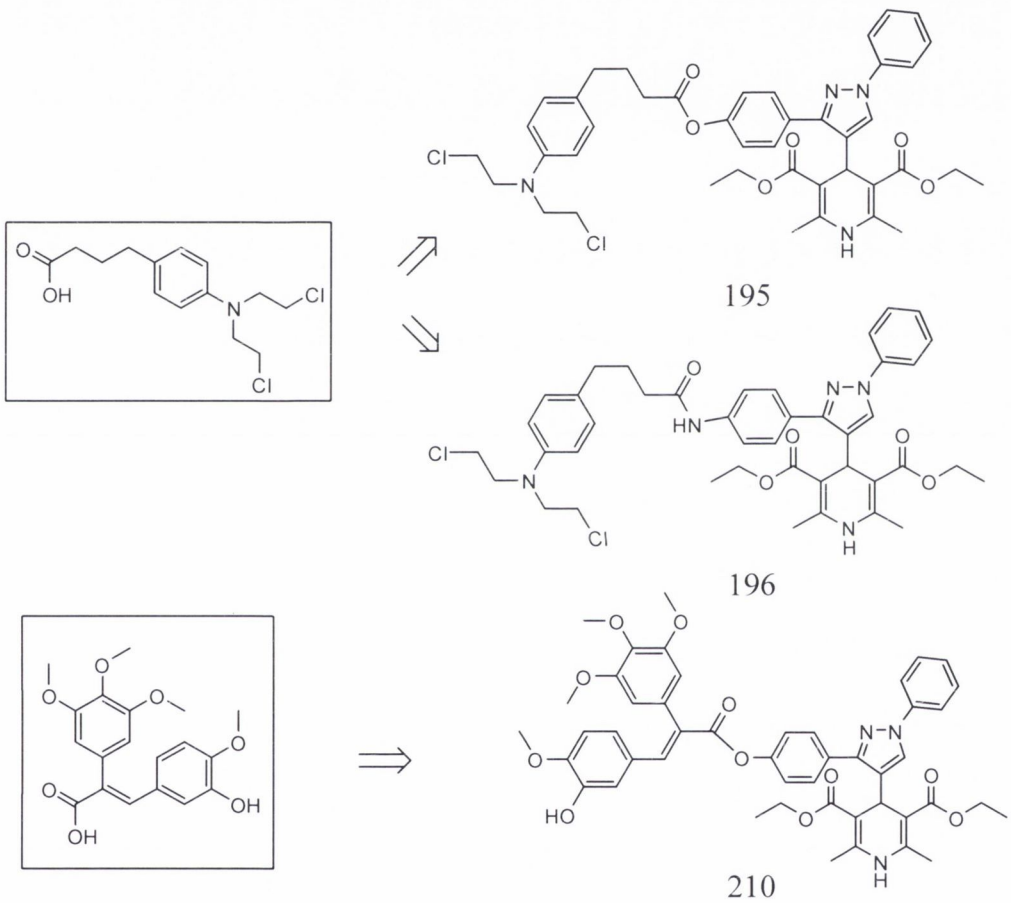

The synthesis of a number of analogues containing non-steroidal anti-inflammatory drugs (NSAID) or basic side chain ethers on the C-3 phenyl ring was carried out *via* ester or amide type coupling reactions summarised in the chapter 2 (**Figure 4.13**). **Table 4.4** presents the antiproliferative effects of these analogues in MCF-7 cell line. The results showed that the many of compounds (**196, 217, 219, 220& 210**) have low mircomolar IC_{50} values (3.38 – 4.75 μM) in MCF-7 cells and no significant cytotoxicity. The cytotoxic effects of most analogues displayed above are lower than that of tamoxifen (approx. 13.4%) with the exception of compound **217** and **240** (highlighted in yellow) with percentage death of 80.5% and 24.9% in MCF-7 cell line. The high level cytotoxicity might be the cause of dramatically good proliferative

effect in MCF-7. In agreement with this reason compound **240** resulted in IC_{50} values in the namomolar region for antiproliferative effects for the first time.

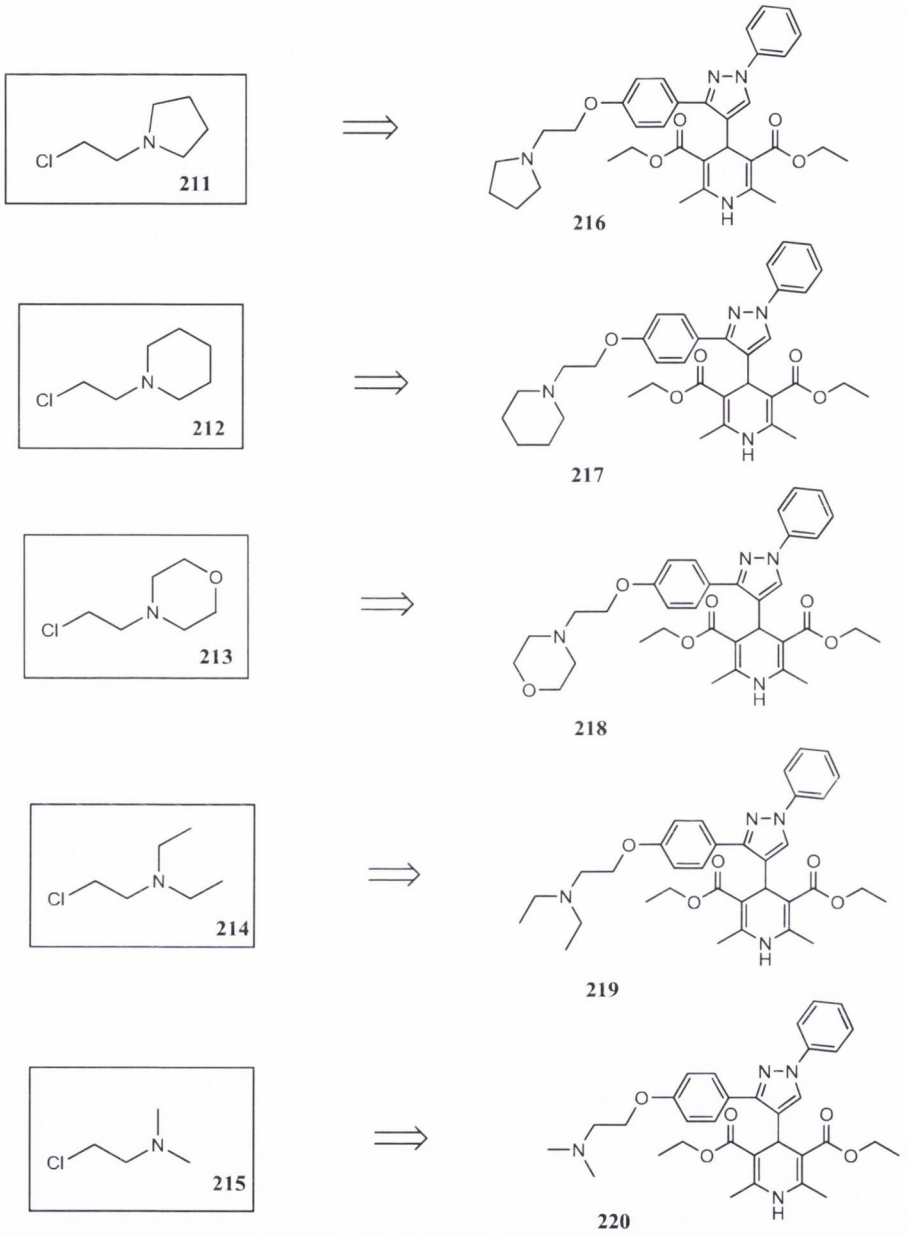

Figure 4.13 Illustration of various non-steroidal anti-inflammatory drugs (NASID) or stilbenoid prodrug and their corresponding coupling to 1,4-DHPs *via* ester and amide linkage.

For most ester compounds, a similar IC_{50} value to the parent compound hydroxyl DHP **165** was observed of approx. 4 μM, however there were significant increases in cell death to 7.4-24.9% from 7.7% for compound **165**. On its own the IC_{50} value for chlorambucil in the MCF-7 cell line has been reported as being 97 μM[284]. In contrast to the ester compound **195** (IC_{50}>1 mM), the amide compound **196** is more potent in

MCF-7 (IC_{50} = 4.1 μM). It is difficult to rationalise this result as the ester compound **195** may be likely to be hydrolysed during the experiment.

The activity of the hydroxy 1,4-DHP coupled with CA-4 (e.g. compound **210)** is in general agreement with the previous results with low micromolar activity (IC_{50} = 4.7 μM). The result for the MTT and LDH assay for **210** are presented in **Figure 4.14**. Compound **210** is significantly less active than CA-4 with an increase in cell death at 10 μM of 18.5% compared to 5.5% for CA-4 (Highlighted in red). It still can be regard as a promising lead compound to establish a more detailed SAR and further evaluation for coupled ester products.

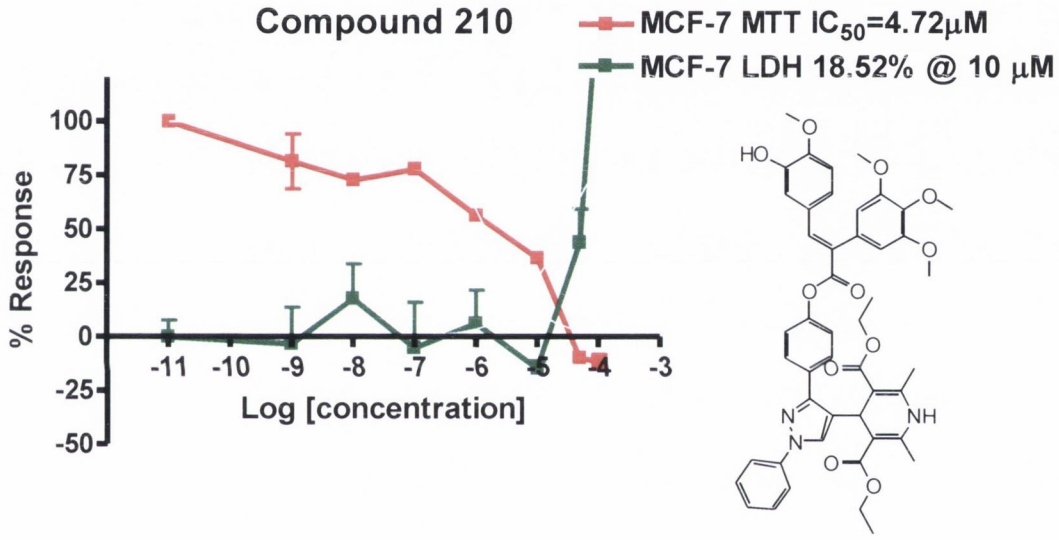

Figure 4.14 Compound 210 inhibited proliferation and induced cytotoxicity of MCF-7 cells.

MCF-7 cells were seeded at a density of 2.5x104 cells/mL in 96 well plates and allowed adhere to the surface of the 75 cm^2 culture flask wells for 24 h. The cells were treated with compound 1 nM-50 μM (final concentration) and incubated for 72 h. Determination of cell proliferation was carried out using MTT assay described in section 4.5.1 and the cytotoxicity was evaluated using the LDH assay as described in section 4.5.2.

4.6.3 Antiproliferative and cytotoxic effects of synthesised compounds via Suzuki reaction (Type V) in MCF-7 cell line

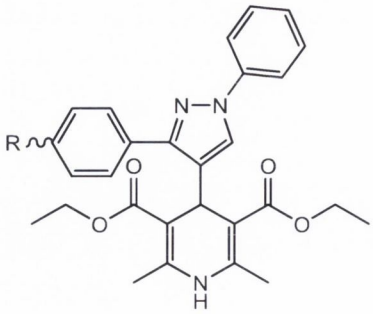

Compound No.	R	MCF-7		ClogP
		Antiproliferative activity IC_{50} (μM)	Cytotoxicity % cell death at 10μM	
221	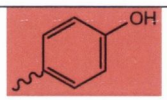	**1.28(±0.0065)**	**27.65(±4.02)**	**7.363**
222	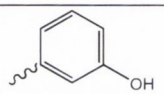	2.56(±1.45)	8.74(±3.38)	7.363
229	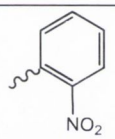	149.16(±8.44)	36.12(±1.00)	7.773
223	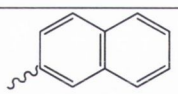	24.74(±9.24)	22.89(±8.04)	9.204
225	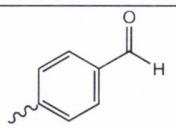	5.54(±2.61)	19.91(±3.00)	6.454
224	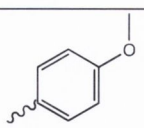	4.51(±2.02)	20.82(±0.54)	7.949
228	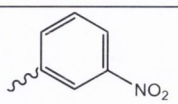	10.68(±6.04)	27.51(±3.92)	7.773
227	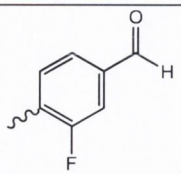	9.83(±1.14)	22.52(±8.43)	6.597
226	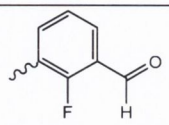	8.78(±3.30)	23.18(±1.26)	6.597

230	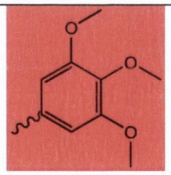	**1.21(±0.48)**	**29.51(±7.94)**	**7.330**
165	**OH**	**7.9(±4.72)**	**7.7(±16.88)**	**5.568**

Table 4.5 Antiproliferative effects of boronic acid coupled DHPs in MCF-7 cells. IC_{50} values: the concentration required to inhibit 50% of cell growth. The results are representative of an experiment performed at least twice. Compound highlighted in red shows better activity relative to parent compound (highlighted in yellow)

Further SAR studies and examine the effect on antiproliferative activity with a variety of structural modifications such as introduction of additional aryl ring to the phenyl ring at C-3 position of pyrazole were carried out. These changes were made at the *para* position of C-3 phenyl ring and afforded products with a wide variety of nitro, halogens, methoxy and hydroxyl groups being introduced on the substituted phenyl ring. The position of substituents was also examined at *para*, *ortho* and *meta* positions to establish a more clear SAR for the products. These structural variations and the assessed biological activity in MCF-7 cells are indicated in **Table 4.5**.

The results shown in **Table 4.5** demonstrated the most potent compounds in MCF-7 cell line are compounds **221** and **230** with IC_{50} values of 1.28 μM and 1.21 μM respectively. However, the presence of the substituent at the *para* position appears to be optimum with a slight decrease in activity if it is placed in the *meta* position. The *para* position substituted hydroxy compound **221** has a lower IC_{50} value 1.28 μM compared to the *meta* position substituted hydroxyl compound **222** IC_{50} value 2.56 μM. Moreover, a significant decrease in activity was noted if the substituent is in the *ortho* position. e.g.compound **228** (*meta* substituted, IC_{50} = 10.68 μM) compared to compound **229** (*ortho* substituted, IC_{50} = 149.16 μM). Interestingly disubstituted compound yielded less antiproliferative activity in MCF-7 cells, for instance the formyl substituted DHP (compound **225**) (IC_{50} = 5.54 μM) showed nearly 2 fold increase in activity compared to fluoro and formyl disubsituted compound **227** and compound **226** with IC_{50} value of 9.83 μM and 8.78 μM, respectively. The trisubstituted compound **230** demonstrated good activity (IC_{50} = 1.21 μM) and is similarly substituented to CA-4, (**Figure 4.15&4.16**) the reason could be due to it also showing high level cytotoxic effects with 29.51% cell death at 10 μM.

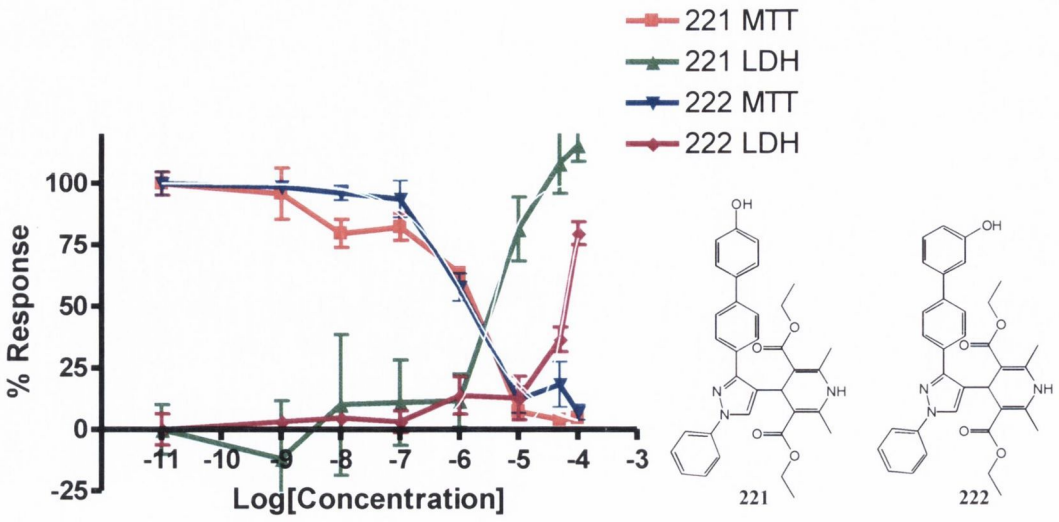

Figure 4.15 Antiproliferation and cytotoxicity effect of compound 221, 222 in MCF-7 cells

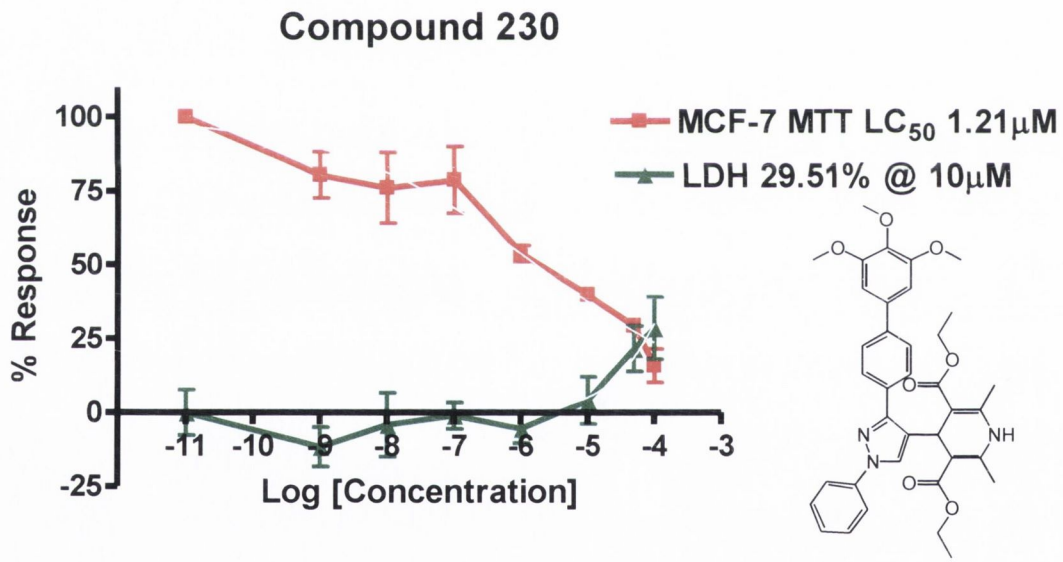

Figure 4.16 Antiproliferation and cytotoxicity effect of compound 230 in MCF-7 cells

4.6.4 Antiproliferative and cytotoxic effects of pyrazole ketone derivatives (Type VI) in MCF-7 cell line

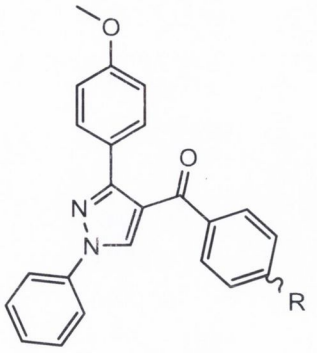

Compound No.	R	MCF-7		ClogP
		Antiproliferative activity IC_{50} (μM)	Cytotoxicity % cell death at 10μM	
284	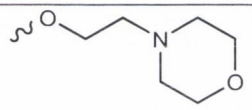	22.05(±1.89)	8.63(±3.81)	5.723
286	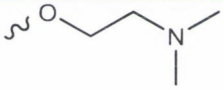	11.64(±1.46)	18.81(±3.32)	5.703

Table 4.6 Antiproliferative effects of ketone derivatives in MCF-7 cells

IC_{50} values: the concentration required to inhibit 50% of cell growth. The results are representative of an experiment performed at least twice. Data are present as the mean±S.E from at least three independent experiments

The results obtained for the pyrazole ketone derivatives are demonstrated in **Table 4.6**. **276&278** (IC_{50} =22.05 μM and IC_{50} =11.64 μM) and give moderately active compounds in MCF-7 cells with antiproliferative values in the same micromolar range as those basic side chain substituted DHPs derivatives Type IV. The higher cLogP value of compounds displayed above compared to parent pyrazole compound **148** might be a reason for the relative lack of antiproliferative activity. The cLogP value of the compound, indicating the logarithm of its partition coefficient between n-octanol and water log ($C_{octanol}$ / C_{water}), is a well established measure of the compound's hydrophilicity.[285] Molecules with higher clogP value are more hydrophobic, and with a low clogP are hydrophilic. Hydrophilicity influences solubility, transport and absorption processes in pharmacokinetic phase.[286]

4.6.5 Antiproliferative and cytotoxic effects of C-4 heterocyclic modification (Type VII) in MCF-7 cell line

Compound No.		MCF-7		ClogP
		Antiproliferative activity IC_{50} (μM)	Cytotoxicity % cell death at 10μM	
250	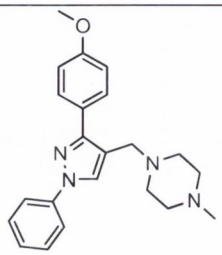	0.10(±0.032)	4.90(±2.54)	4.157

Table 4.7Antiproliferative effects of heterocycle modified analogues in MCF-7 cells

IC_{50} values: the concentration required to inhibit 50% of cell growth. The results are representative of an experiment performed at least twice. Data are present as the mean±S.E from at least three independent experiments

Table 4.7 showed the results of antiproliferative effects of heterocycle derivative obtained by reductive amination of pyrazole carbaldehyde. Compound **250** contains the piperazine ring and shows the submicromolar IC_{50} value both in MCF-7 cells and HL-60 cells (discussed in **Section 4.7**) with IC_{50} of 100 nM (**Figure 4.17**) and 24.2 nM, respectively. While it also mainaining the incredible low cell death at 10 μM of 4.9%. It could be a lead compound to warrant further evaluation.

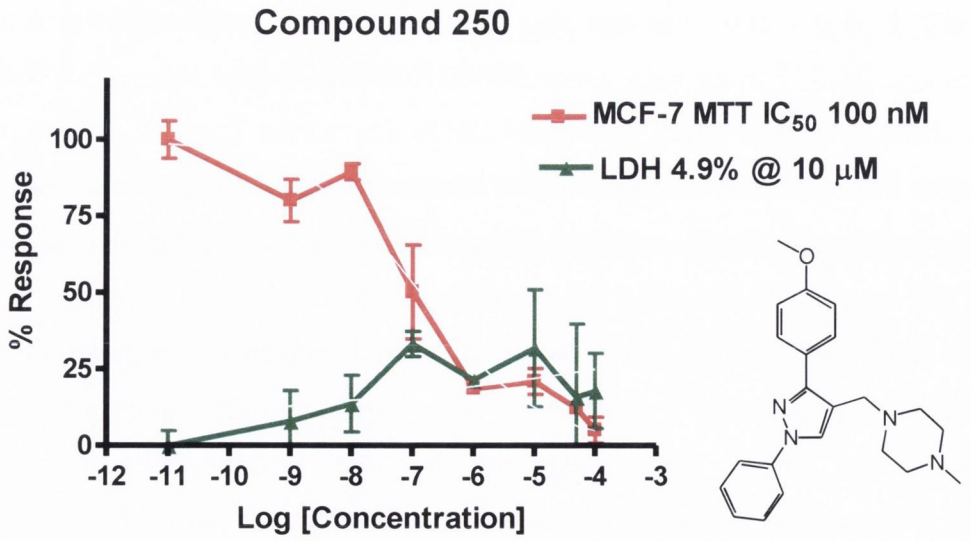

Figure 4.17 Antiproliferation and cytotoxicity effect of compound 250 in MCF-7 cells

4.6.6 Antiproliferative and cytotoxic effects of Type I 1,4-DHPs & Type IV side chain coupled analogues in MDA-MB-231 cell line

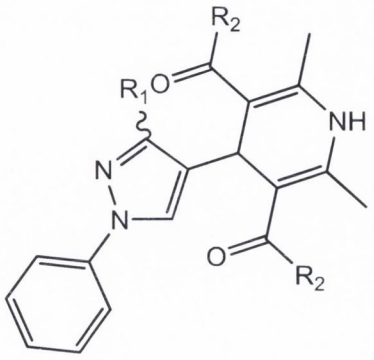

Compound No.	R_1	R_2	MDA-MB-231	
			Antiproliferative activity IC_{50} (μM)	Cytotoxicity % cell death at 10μM
164	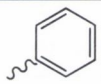	OCH_2CH_3	13.5	6.2(±0.32)
165	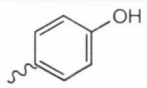	OCH_2CH_3	42.0	3.71(±2.80)
175	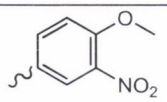	OCH_2CH_3	118.0	21.04(±10.5)
174	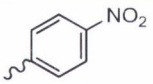	OCH_2CH_3	21.0	7.3(±2.40)
171	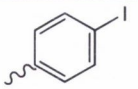	OCH_2CH_3	11.3	9.87(±5.0)
192	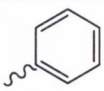	C_6H_5	1907	2.80
Tamoxifen	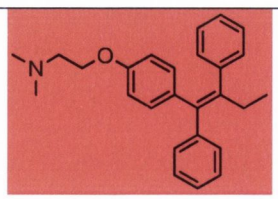		~20	[α]nd

Table 4.8 Antiproliferation and cytotoxicity effects of activity of analogues in MBA-MB-231 cells. [α]nd= not determined

The most active compounds in the MCF-7 antiproliferative and cytotoxic studies from Type IV were subsequently investigated against MDA-MB-231 human breast cancer cells. (**Table 4.8**) The results illustrated that most of compounds show moderate micromolar activity with IC_{50} value in the range (11.3-21.0 μM) similar to tamoxifen, which demonstrated much less antiproliferative effects in ER negative cell lines (approx. 20 μM) than in MCF-7 cells. Compounds **175** and **192** displayed a large decrease in activity in MDA-MB-231 cells of 10-fold and 100-fold, respectively.

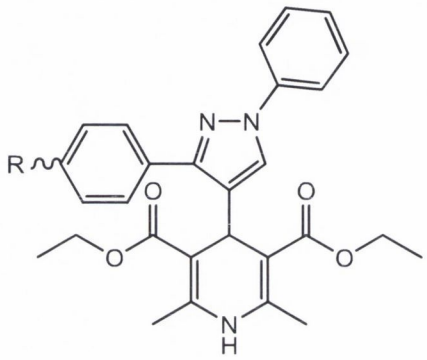

Compound No.	R	MDA-MB-231	
		Antiproliferative activity IC_{50} (μM)	Cytotoxicity % cell death at 10μM
195	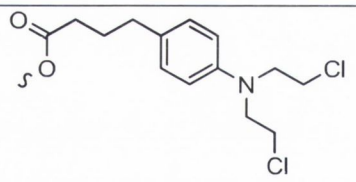	**>1000**	**3.03**
217	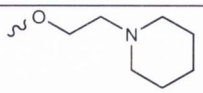	**4.79**	**27.75**
219	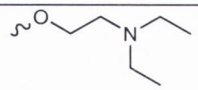	**4.95**	**3.47**
220	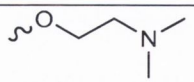	**3.68(±0.64)**	**11.78(±9.34)**

Table 4.9 Antiproliferation and cytotoxicity effects of most potent analogues in MDA-MB-231 cells.

A selection of the ester and ether products (Type IV) was also evaluated in MDA-MB-231 cells. (**Table 4.9**) Of the four compounds tested, compound **217**, **219&220** proved to have good activity both in MCF-7 cells and MDA-MB-231 cells with low IC_{50} value and reasonable cell death at 10μM. Impressively, compound **195** with chlormabucil side ester substituent was inactive in both cell lines. The results for these compounds testing in MDA cell line suggest that an alternative mechanism of

antiproliferative may be in place. It is essential to carry out further investigation to determine the action of these compounds.

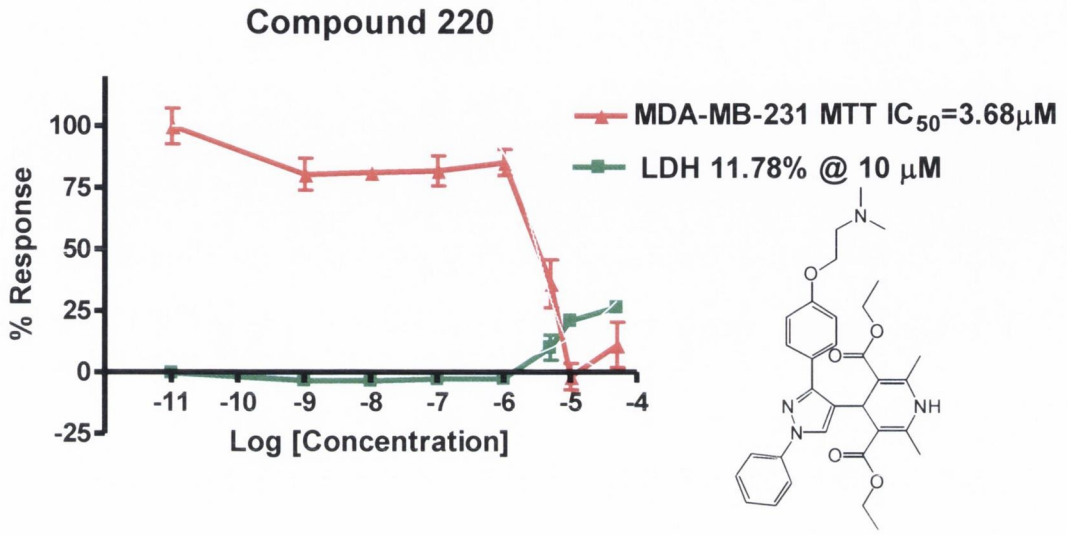

Figure 4.18 Antiproliferation and cytotoxicity effect of compound 214 in MDA-MB-231 cells

MDA-MB-231 cells were seeded at a density of $2.5x10^4$ cells/mL in 96 well plates and allowed adhere to the surface of the 75 cm^2 culture flask wells for 24 h. The cells were treated with compound 1 nM-50 μM (final concentration) and incubated for 72 h. Determination of cell proliferation was carried out using MTT assay described in section 4.5.1 and the cytotoxicity was evaluated using the LDH assay as described in section 4.5.2.

4.6.7 Preliminary screening of selected synthesized compounds in MCF-7 cell line

Thirty-nine of the prepared compounds were initially screened for potential antiproliferative activity at concentration 5 μM in ethanol in MCF-7 cell line.(**Table 4.10**) Test compounds are added to 25,000 cells/mL of MCF-7 cell line at a single concentration ($5x10^{-6}$ M) and the culture incubated for 72 hours. Results for each test agent are displayed as the percent of growth of the treated MCF-7 cells when compared to the untreated control cells. By comparison with the positive control tamoxifen, (IC_{50}= 4.48 μM in human MCF-7 cells), any compound that killed the approximately 80% or more of the cells are considered active and subsequently evaluated for IC_{50} value in the ER expressing MCF-7 human breast cancer cell line or ER-negative MDA-MB-231 human breast cancer cell line over 7-log dose range. The library of compounds evaluated in this preliminary screening is illustrated in **Table 4.10**.

As shown in **Table 4.10** below, tamoxifen (5 μM) induced 83.62% cell death in MCF-7 cells. Fifteen compounds were identified for subsequent evaluation at the same concentration of 5 μM. These compounds are as follows and percentage cell death shown in brackets: **222** (96.12%), **229** (91.26%), **223** (76.15%), **225** (97.69%), **224** (80.10%), **228** (70.27%), **226** (97.09%), **227** (96.72%), **230** (73.79%), **240** (93.93%), **210** (96.12%), **284** (83.13%), **286** (88.35%), **250** (82.16%). These compounds gave percentage inhibition values that were higher than or similar to tamoxifen (83.62% at 5 μM) and were thus selected for further testing. e.g. cell proliferation determination and cytotoxicity evaluation using MTT (Described in **section 4.5.1**) and LDH assays (Described in **section 4.5.2**), respectively. Results are displayed in the previous section above.

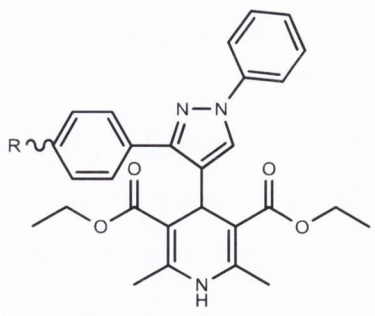

A

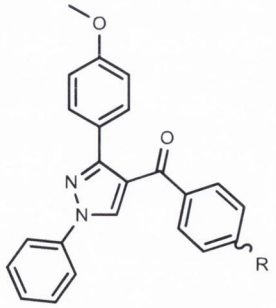

B

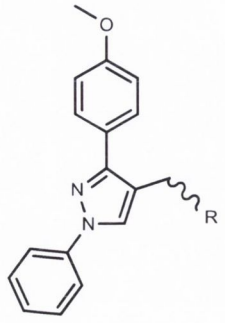

C

No	Scaffold	R	% cell death@ 5μM	No	Scaffold	R	% cell death@ 5μM
Tamoxifen		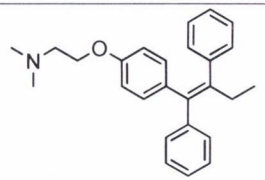	83.62	207	A	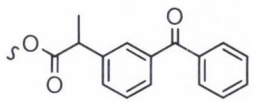	39.93
222	A	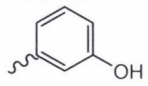	96.12	209	A	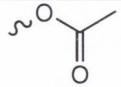	57.77
229	A	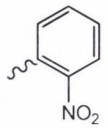	91.26	210	A	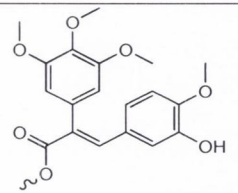	96.12
223	A	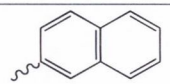	76.15	283	B	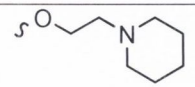	19.30
225	A	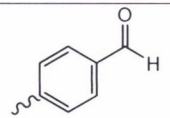	97.69	284	B	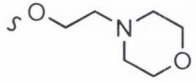	83.13
224	A	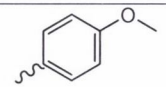	80.10	286	B	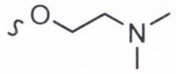	88.35
228	A	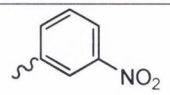	70.27	250	C	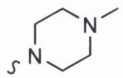	82.16

226	**A**	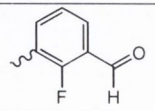	**97.09**	**251**	**C**	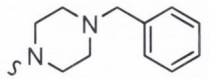	**49.94**
227	**A**	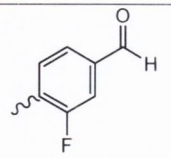	**96.72**	**255**	**C**	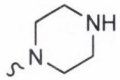	**27.55**
230	**A**	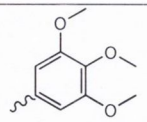	**73.78**	**253**	**C**	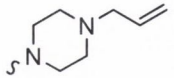	**27.55**
238	**A**	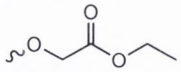	**54.49**	**254**	**C**	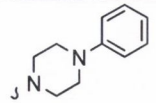	**33.37**
239	**A**	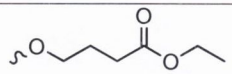	**41.87**	**258**	**C**	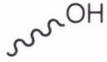	**27.79**
204	**A**	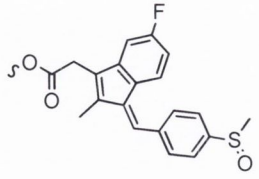	**11.04**	**242**	**Novel 1,4-DHP**	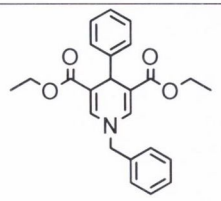	**37.38**
241	**A**	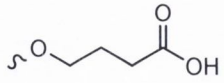	**7.71**	**246**	**Novel 1,4-DHP**	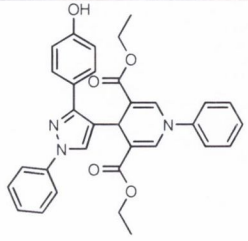	**63.23**

240	**A**	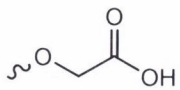	**93.93**	**245**	**Novel 1,4-DHP**	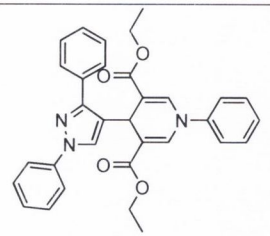	**65.05**
205	**A**	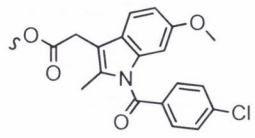	**20.63**	**244**	**Novel 1,4-DHP**	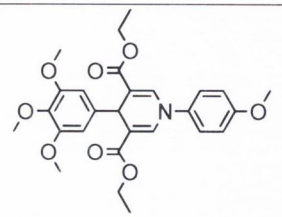	**7.16**
208	**A**	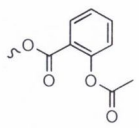	**30.83**	**243**	**Novel 1,4-DHP**	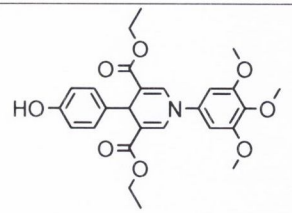	**47.94**
206	**A**	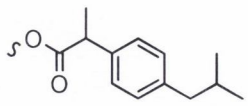	**43.45**	**247**	**Novel 1,4-DHP**	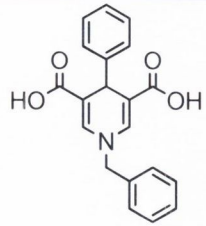	**21.60**

Table 4.10 Preliminary screening of selected synthesized compounds in MCF-7 cell line

4.7 Alamar Blue viability assay in HL-60 cell line

4.7.1 Effects of compounds 170 and 176 on the cell cycle of HL-60 cells

The effects of selected compounds **170** and **176** on the cell cycle were determined by flow cytometric analysis propidium iodide (PI) stained cells. The flow cytometry assay described in previous **Section 4.5.4**. The PI fluorescence was measured on a linear scale using a FACSCalibur flow cytometer (Becton Dickinson, San Jose, CA, USA). The fluorescent dye, PI intercalates with the DNA and hence, the amount of fluorescence measured per cell is proportional to the DNA content and thus indicated the stage of the cell cycle. Cells were treated with solvent control [1% ethanol (v/v)] or varying concentrations of compound [10-50μM] for 24 hour. As shown in **Figure 4.19**, at 20μM both compound induced a significant increase in the percentage of cells in the G1 phase of the cell cycle. At higher concentrations the majority of cells were in the sub-G1 DNA fraction (apoptotic population).

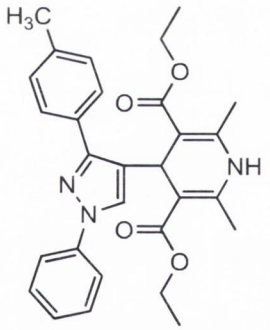

170

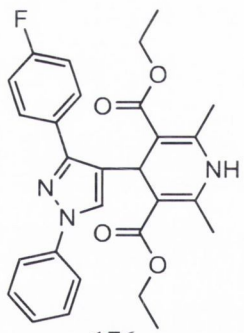

176

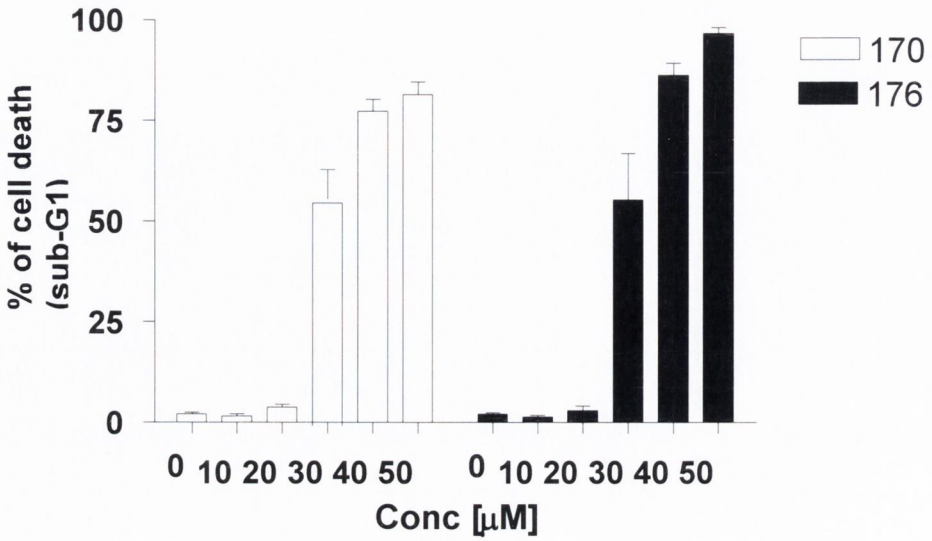

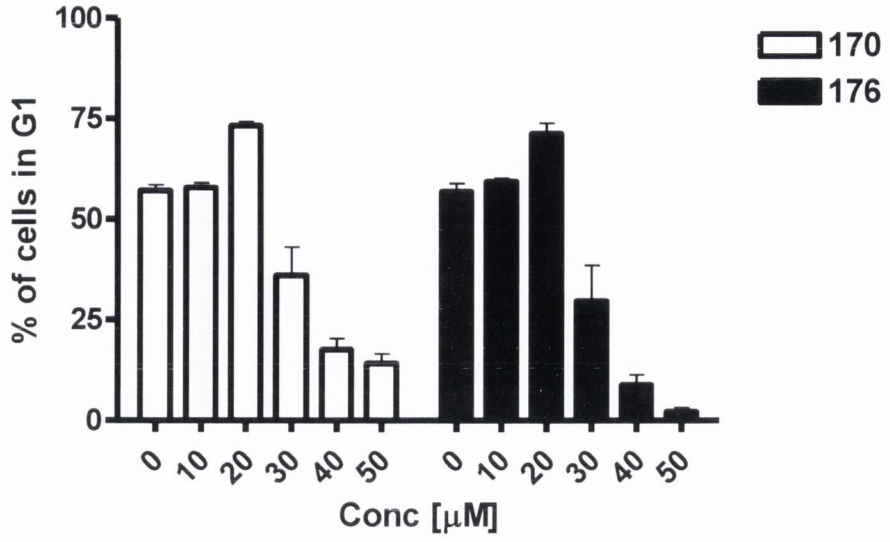

Figure 4.19 Effects of Compound 170 and 176 on the cell cycle and cell death in HL-60 cells.

HL-60 cells in the log phase of growth were exposed to solvent control [1% ethanol (v/v)] or varying concentrations of compound [10-50 μM] for 24 h. Cells were then fixed, stained with PI and analysed by flow cytometry. Cell cycle analysis was performed on histograms of gated counts per DNA area (FL2-A). The number of cells with <2N (pre-G1), 2N (G0G1), 4N (G2M) DNA content was determined using the Cell Quest software. A, percentage of apoptotic cells are indicated as determined by quantification of the pre-G1 peak. B, percentage of cells in G1 phase of the cell cycle is indicated. Values represent the mean ± SEM for at least three separate experiments. The absence of error bars indicates that the errors were smaller than the size of the symbol. *, $P < 0.05$; **, $P < 0.001$ as determined by one way Anova followed by the by the Bonferroni multiple comparison test, comparing all columns.

4.7.2 Effect of compounds 170 and 176 on the reversal of paclitaxel resistance in HL-60 MDR cells

The effect of 1,4-dihydropyridine compounds **170** and **176** (containing the pyrazole heterocycle at C-4 of the1,4-dihydropyridine ring) on the reversal of paclitaxel resistance in HL-60 MDR cells was next examined. Other heterocycles have been investigated at the C-4 position of 1,4-dihydropyridines for optimisation of P-glycoprotein resistance activity including imidazoles, thiazoles,[287] pyrazolo[1,5-a]pyridines.[288] Tasaka et al suggest that the introduction of alkyl groups at the 4-position of 1,4-dihydropyridines was effective for both overcoming multidrug resistance and reducing the calcium antagonistic activity.[289, 290]

Paclitaxel, verapamil, nifedipine and compounds **170** and **176** were initially evaluated for antiproliferative effects in HL-60 parental and HL-60-MDR leukaemia cells,

(**Figure 4.20**). IC_{50} values and calculated resistance factors are detailed in **Table 4.11**. The resistance factor (RF) was calculated by dividing the IC_{50} of the resistant cell line/IC_{50} of the parental cell line. HL-60-MDR cells are >2,000 fold more resistant to paclitaxel as compared with parental HL-60 cells. As single agents the novel DHP display no resistance. Moreover, pre-treatment of HL-60 MDR cells with a non-toxic concentration of DHPs **170** and **176** [10 μM] reduced the IC_{50} for paclitaxel to a clinically achievable concentration [<1 μM] in HL-60- MDR cells. The MDR-reversal properties of compounds **170** and **176** were comparable with the well characterised MDR reversal Ca^{2+} antagonist, verapamil and superior to the DHP, nifedipine. We next sought to determine whether the observed augmentation of paclitaxel induced cell death by representative DHPs, compounds **170** and **176** were synergistic. The Calcusyn program was used perform a median dose analysis of the compound **170** and paclitaxel combination. As shown in **Figure 4.21**, both compounds **170** and **176** in combination with 1 or 10 μM paclitaxel was considered to be synergistic.

Cell line	Compound	IC50 [μM]	RF
HL-60 parental	**Verapamil**	**>10**	
	Nifedipine	**>10**	
	Paclitaxel	**0.011**	
	170	**15.78**	
	176	**10.0**	
HL-60-MDR	**Verapamil**	**>10**	**>1**
(PGP)	**Nifedipine**	**>10**	**>1**
	Paclitaxel	**>10**	**892**
	170	**16.33**	**1.03**
	176	**24.3**	**2.4**

Table 4.11 Evaluation of DHPs and verapamil in HL-60 MDR cells.

Cells were exposed to multiple concentrations of the indicated compound for 72 h. Cell viability was assessed using the Alamar blue assay and respective IC50 values were calculated. The resistance factor (RF) was calculated by dividing the IC50 of the resistant cell line/IC50 of the parental cell line.

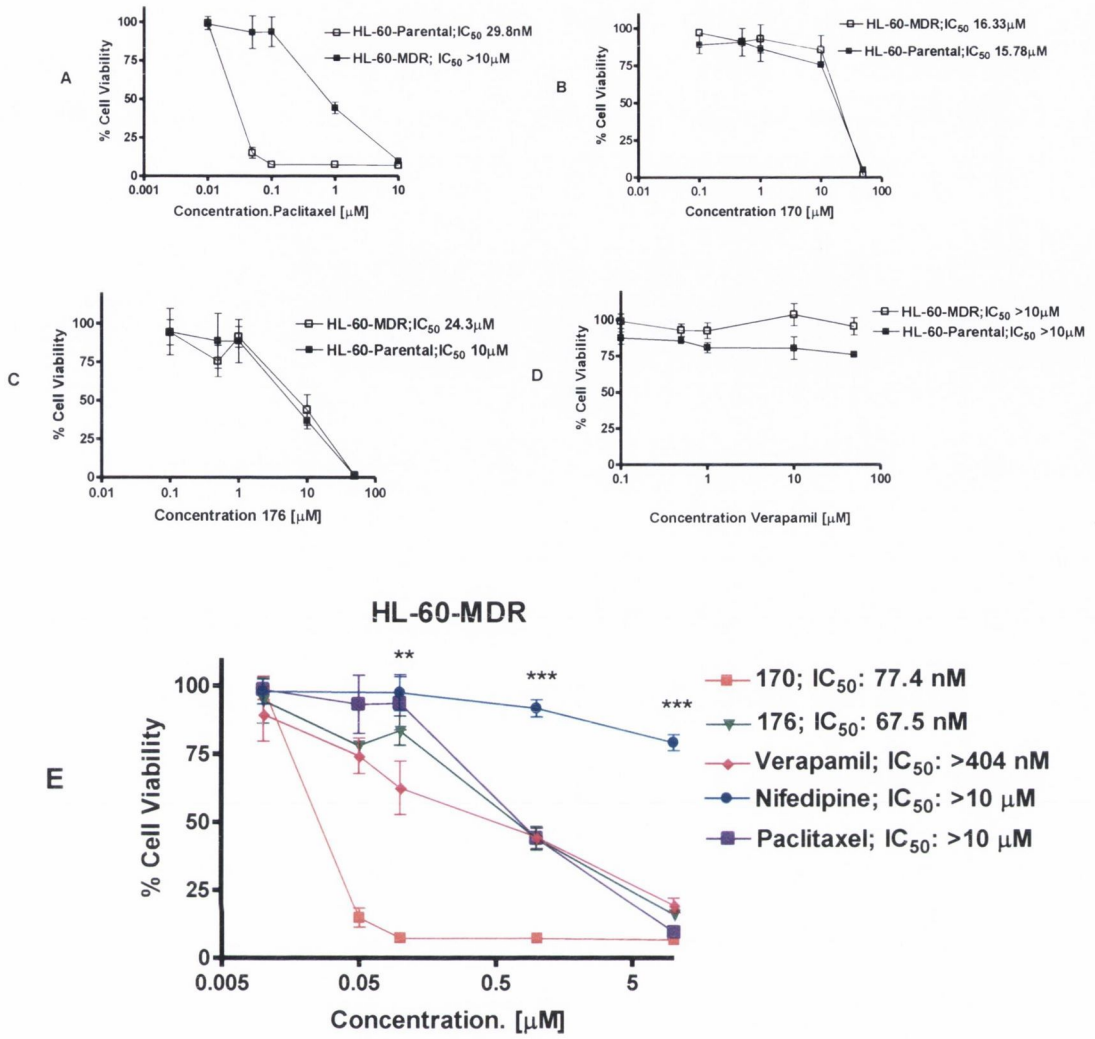

Figure 4.20 Effect of compound 170 and 176, nifedipine and a well known MDR modulator, verapamil on re-sensitising HL60-MDR cells to paclitaxel.

A: HL60-parental and HL60-MDR cells were treated with paciltaxel [0.1-10μM] or B, C, D: compound 170, 176 and nefidipine [0.1-50μM] for 72 hours. E: HL60-MDR cells were treated with a dose of paclitaxel alone or pre-treated with the indicated DHPs or the DHPs modulator verapamil at 10μM for 1 hour prior to the addition of paclitaxel. Cell viability was assessed by the AlamarBlue assay. Results represent the mean±SEM for three independent experiments, carried out in triplicate. **; $P < 0.01$, denotes a significant difference between cells treated with paclitaxel alone and cells pre-treated with Verapamil prior to paclitaxel for the dose indicated. ***; $P < 0.001$, denotes a significant difference between cells treated with paclitaxel alone to those pre-treated with verapamil and compounds 170 and 176 prior to paclitaxel at doses indicated. Results are based on a two-way *ANOVA* test followed by the *Bonferroni* multiple comparisons test, comparing all columns.

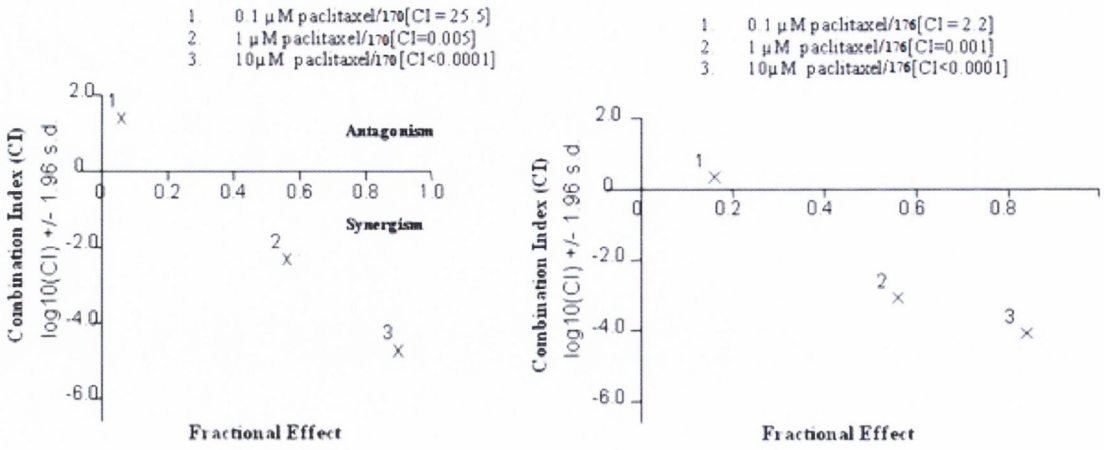

Figure 4.21 DHP compounds 170 and 176 synergistically enhanced paclitaxel induced cell death HL-60 MDR cells overexpressing P-glycoprotein

HL60-MDR cells were treated with a dose of paclitaxel alone [0.1-10 μM] or pre-treated with 10 μM of compound 170 for 1 h prior to the addition of paclitaxel. Cell viability was assessed by the AlamarBlue assay. Results were then analysed using the software program CalcuSyn. Combination index (CI) values for varying concentrations of Paclitaxel and 10 μM compound 170 were generated. A CI value <1 indicates synergism while CI value >1 represents antagonism.

4.7.3 Effect of DHPs on the reversal of paclitaxel resistance in HL-60 MDR cells

Selected compounds from the various structural synthesised type (I-VII) were next examined. HL60 parental and resistant cells were treated for 72 h with a range of concentrations of the indicated drugs. (**Table 4.12**) Cell viability was then assessed by AlamarBlue assay and IC_{50} values determined using Prism GraphPad 4.0. Results are representative of two independent experiments, each carried out in triplicate.

Cell line	Compound	IC_{50} [μM]	RF
HL-60 parental	**Paclitaxel**	**0.011**	
	221	**1.04**	
	229	**3.02**	
	223	**69.67**	
	224	**>10**	
	227	**>10**	
	230	**8.73**	
	203	**3.94**	
	284	**>10**	
	242	**>10**	
	246	**8.27**	
	244	**>10**	
	250	**0.131**	
	251	**7.50**	
	254	**>10**	
HL-60-MDR (PGP)	**Verapamil**	**>10**	**>1**
	Paclitaxel	**>10**	**892**
	221	**2.64**	**2.54**
	229	**3.97**	**1.31**
	223	**1971**	**28.29**
	224	**6.34**	**<1**
	227	**>10**	**>1**
	230	**9.8**	**1.12**
	210	**4.82**	**1.22**
	284	**>10**	**>1**
	242	**>10**	**>1**
	246	**>10**	**>1**
	244	**>10**	**>1**
	250	**0.057**	**<1**
	251	**10.2**	**>1**
	254	**>10**	**>1**

Table 4.12 Evaluation of DHPs and other heterocyclicanalogues in HL-60 MDR cells

Results represent the mean±S.E.M for at least two independent experiments performed in triplicate.

HL60, HL60-MDR1 cells were treated for 72 h with a range of concentrations of paclitaxel, verapamil, nefidipine and selected synthesised compounds and cell proliferation measured by AlamarBlue assay (**Table 4.12**). In HL60 parental strain, the IC_{50} value for paclitaxel was as low as 11 nM, but in HL60-MDR1 cells even concentration as high as 10 μM failed to reduce cell proliferation, indicating a resistance factor of 892 between the parental and the p-glycoprotein-expressing HL60-MDR1 cells. Results showed that pre-treatment of HL-60 MDR cells with a

non-toxic concentration [10 nM-10 μM] of selected compounds (**221**, **224**, **227**, **230**, **284**, **244**, **251**, **254**, **250**) reduced the IC_{50} for paclitaxel to a clinically achievable concentration [<1 μM] in HL-60- MDR cells.(**Figure 4.22**, **4.23**). The most exciting results was that compound **250** showed potent effects with nanomolar range IC_{50} values in both MCF-7 and HL-60 cell lines, and also displayed excellent reversal activity of paclitaxel resistance in HL-60 MDR cells, which could decrease the IC_{50} value for paclitaxel to 36.82 nM in HL-60-MDR cells with only 10 nM concentration of drug used. (**Figure 4.24)**

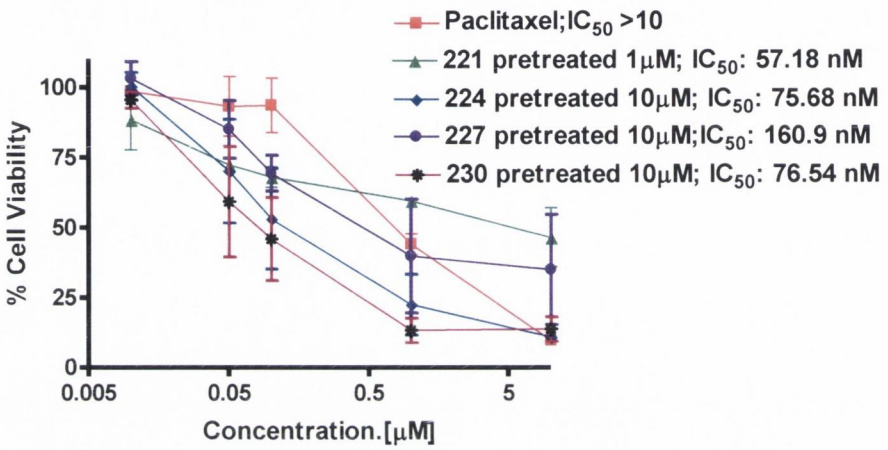

Figure 4.22 Effect of DHPs analogues on re-sensitising HL60-MDR cells to paclitaxel

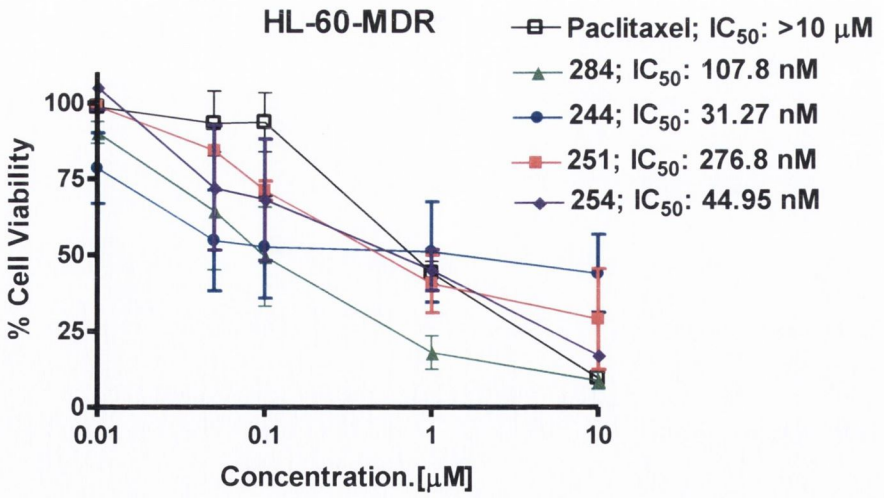

Figure 4.23 Effect of selected heterocyclic modification derivatives and novel DHPs on re-sensitising HL60-MDR cells to paclitaxel prior to treat with 10μM

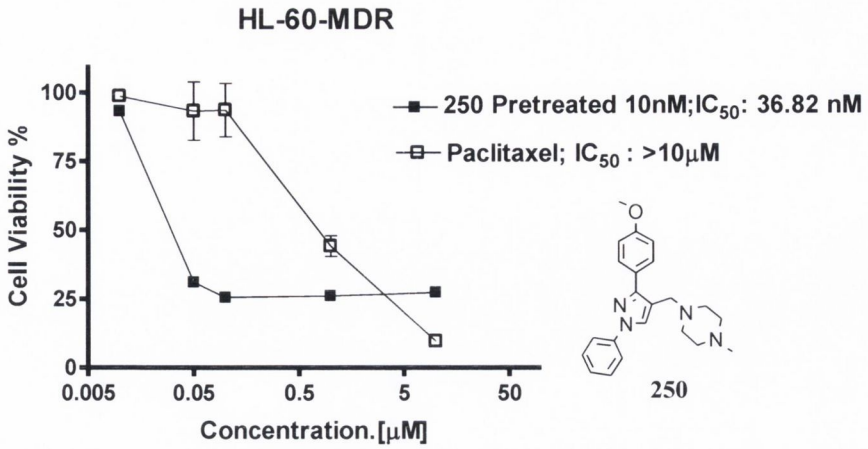

Figure 4.24 Effect of reductive amination product 250 on re-sensitising HL60-MDR cells to paclitaxel prior to treat with 10nM

A frequent problem in cancer chemotherapy is the development of multi-drug resistance (MDR) which renders tumours unresponsive to a diverse array of compounds. There are many mechanisms by which a cell can be acquire MDR, however, one of the most predominant causes is due to over-expression of numbers of the ATP-binding cassette (ABC) transporter family. As described in beginning of this chapter, multi-drug resistance protein-1 (MDR-1), also known as P-glycoprotein or ABCB1, is one of three main ABC transporters specifically associated with MDR.[291]

The potent effects of selected DHP and related pyrazole compounds synthesised in this thesis have been demonstrated in HL60-MDR cells for their MDR reversal activity. These results showed that pre-treatment over a range of concentration [10 nM-10 μM] of a number of selected compounds can reduce the IC_{50} of paclitaxel to nanomolar range in HL60-MDR cells. It is indicated that these analogues are potential lead compounds for the further synthesis and evaluation studiesas MDR reversal agents to overcome drug resistance in tumour cells with P-glycoprotein over-expression.

4.8 Screening and antiproliferative activity of novel DHPs by Electric Cell-substrate Impedance Sensing

The antiproliferation activity of 12 novel DHPsand related compounds (**176**, **192**, **218**, **241**, **254**, **282**, **226**, **220**, **221**, **224**, **227**, **207**) were examined at the concentration of 5μM were evaluated using ECIS method (**Section 4.5.5**), by comparison of the

growth rate of MCF-7 cells in the presence of these compounds with that of tamoxifen (IC_{50} = 4.48 μM). Growth rate was represented by the linear slope of each corresponding impedance data curve (**Figure. 4.25**).

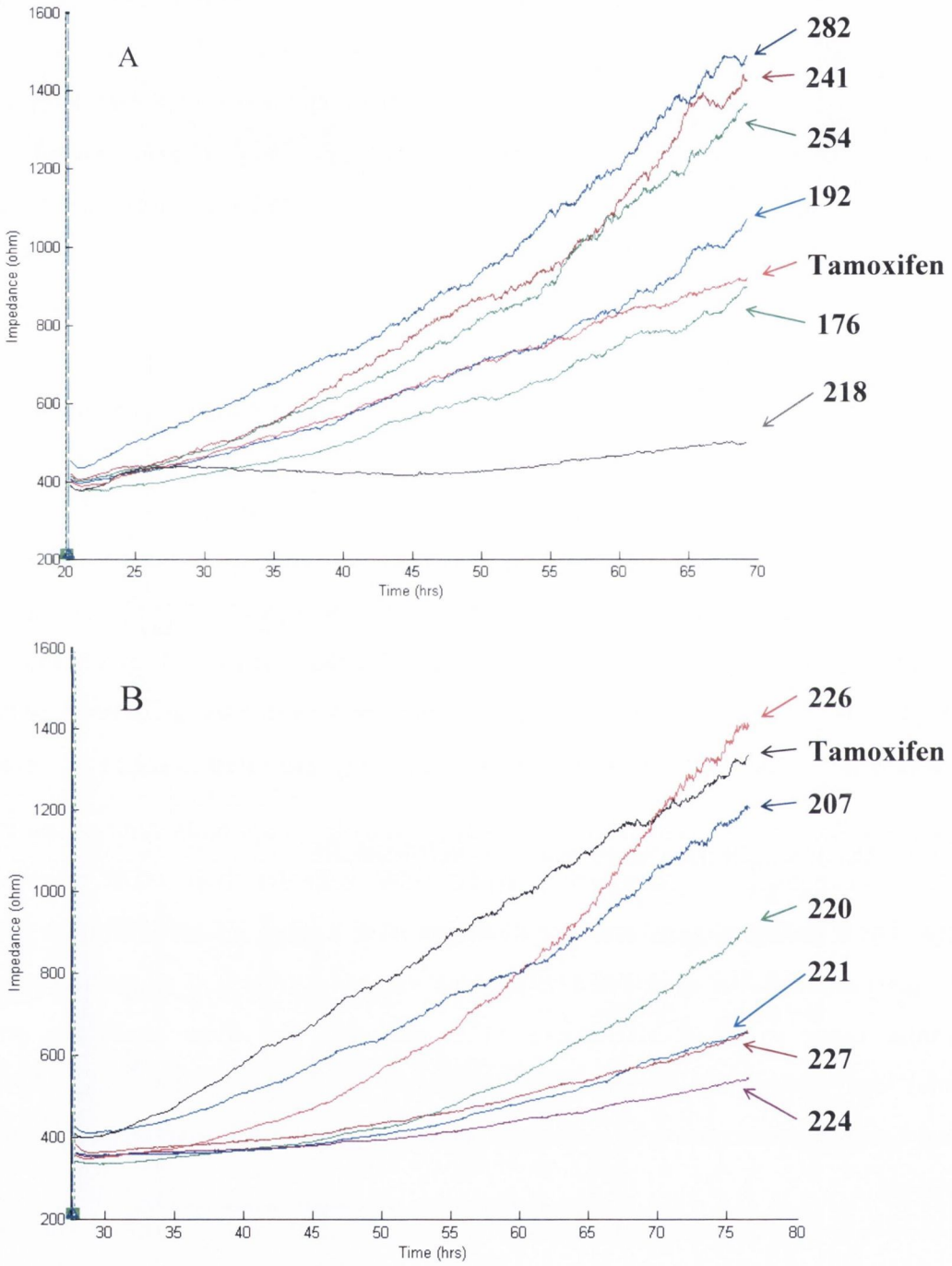

Figure 4.25 ECIS real-time impedance response to MCF-7 cells during culturing at 5uM of A: compounds 282, 241, 254, 192, 176, 218 and B: compound 226, 207, 220, 221, 227, 224.

Impedance curves from every two duplicate wells are grouped. The impedance value shows the effect of proliferation. Greater impedance correlates with greater coverage of the electrodes.

The initial data can be evaluated in the following way. The raw data have been normalized by subtracting the value of impedance at 2.5 hours after the start of the experiment. The normalized data from each well is exported to Excel, subsequently the time that the impedance reach 250 ohms and when it first reaches 1000 ohms plotted together. This gives the absolute growth rate and normalised growth rate, respectively (**Table 4.13**) The graphs shown in (**Figure 4.26**) demonstrated the calculated linear slope of each curve (Absolute rate) and this slope divided by the slope of vehicle ethanol (Normalised rate) to compare directly.

Compound	Well No.	Abs. Rate	Norm. Rate
Tamoxifen	A1	23.29	0.80
	B1	17.12	0.59
226	A2	38.25	1.32
	A5	27.54	0.95
220	A3	18.92	0.65
	A6	27.95	0.96
221	A4	20.05	0.69
	A8	12.87	0.44
224	B5	14.46	0.70
	B7	4.711	0.22
227	B2	16.00	0.77
	B6	16.72	0.80
207	B4	21.21	1.02
	B8	20.82	1.00

Table 4.13 Absolute growth rate and normalized growth rate for selected compounds in MCF-7 cells line

As the growth rates could be varied from different wells, a quick ANOVA test between the two sides of wells has been carried out. So each experiment from each side was normalized to the ethanol control on that side, which gave the following results (**Table 4.14**) and statistically they are different. Several factors affect the reproducibility between electrodes, which might include human error, initial seeding variability and electrodes already collected small amounts of minute particles that effect the impedance of the electrodes randomly.

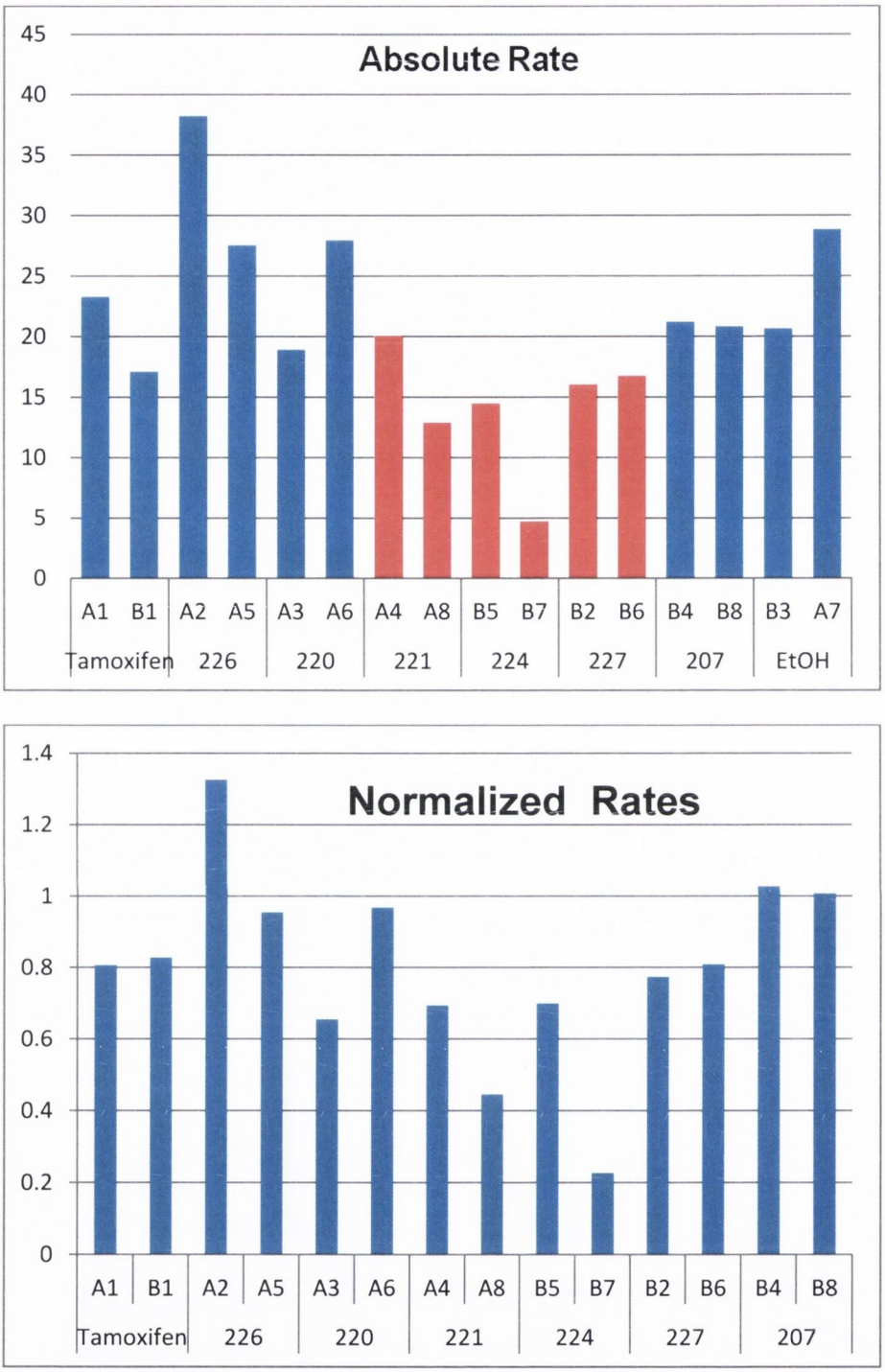

Figure 4.26 Absolute growth rate and normalized growth rate for selected compounds in MCF-7 cells line

Anova: single Factor

Groups	*Count*	*Sum*	*Average*	*Variance*	*F*	*P-value*	*F crit*
A	8	197.74	24.71	59.46	6.168	0.02627	4.6001
B	8	131.72	16.46	28.85			

Table 4.14 ANOVA test between A side and B side of test array

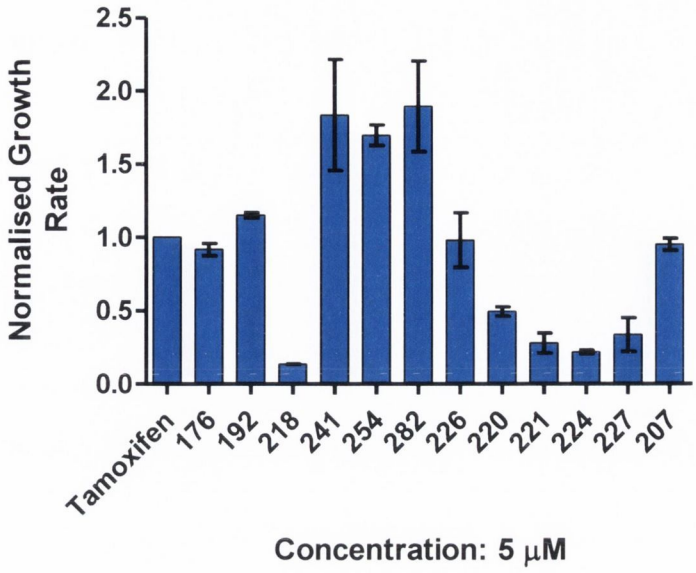

Figure 4.27 Normalised growth rates of MCF-7 cells in the presence of DHP compounds over culturing. Error bar indicates median and range of value.

The following calculation has been carried out by dividing the run time of 48 hours with the increase of impedance over this period of time. Slopes were normalised to the tamoxifen control to illustrate the efficacy of each compound (**Figure. 4.27**). Preliminary estimation can be made that at the concentration of 5 μM, **176**, **218**, **220**, **221**, **224**, **227** significantly inhibited proliferation of MCF-7 cells, resulting in a further inhibition of approximate 114%, 192%, 150%, 134%, 132% and 146% respectively when compared with tamoxifen. **226** and **207** exhibited equivalent inhibition to tamoxifen. **192**, **241**, **254** and **282** respectively were shown to be approximately 15%, 84%, 70% and 89% less potent than tamoxifen in supressing the growth of MCF-7 cells. Finally, the conculsion was drawn that ESIC can be as a novel and intuitive method to monitor the cell growth during the whole culturing period and give even more details to verify the antiproliferative activity which was obtained from the other assay. It was found clearly that most potent compounds are **218, 221, 227** etc, which in good agreement with previous results obtained in our in-house MTT assay. IC_{50} value of these compounds in MCF-7 cell lines are 1.28 μM, 4.51 μM and 1.21 μM respectively, with greater activity compared to Tamoxifen (IC_{50}=4.48 μM).

4.9 The effect of selected 4-(1,3-diaryl-1H-pyrazol-4-yl)-1,4-dihydropyridine compounds on ATP induced calcium responses in MCF-7 cells

1,4-Dihydropyridines represent the most extensively investigated structural class of multidrug resistance modulators. However, these compounds exhibit toxic cardiovascular effects at doses required for P-glycoprotein reversal, due to their calcium channel blocking activities. Previous investigations have shown that the calcium channel blocking effects of 1,4-dihydropyridines is independent of their P-glycoprotein inhibitory activity. Ca^{2+} plays a role throughout the mammalian cell cycle and is especially important early in G1, at the G1/S and G2/M transitions and the role of altered Ca^{2+} signalling in the development of breast cancer is unclear.[292] Changes in Ca^{2+} expression levels have been detected as a cell passes through G1, G_2/M and mitosis.[293]

The compounds **170, 163, 178, 179** and **176** were first examined for their potential to produce a direct change in cytosolic free calcium in MCF-7 breast cancer cells, (**Figure 4.28**). At 10 μM concentration of the compounds did not produce a rapid change in calcium compared with the positive control 10 μM ATP.

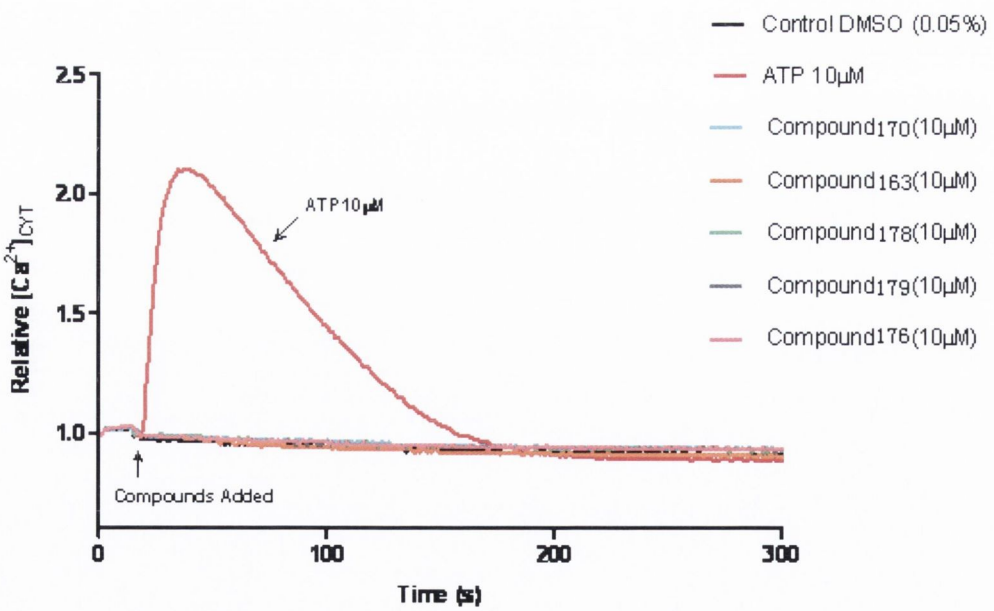

Figure 4.28 Relative $[Ca^{2+}]_{CYT}$ in MCF-7 cells in the presence of compounds 170, 163, 178, 179 and 176. At the time indicated, ATP (10 μM) or compounds (10 μM) were added. Traces display mean response over baseline (relative $[Ca^{2+}]_{CYT}$) from 4 individual wells

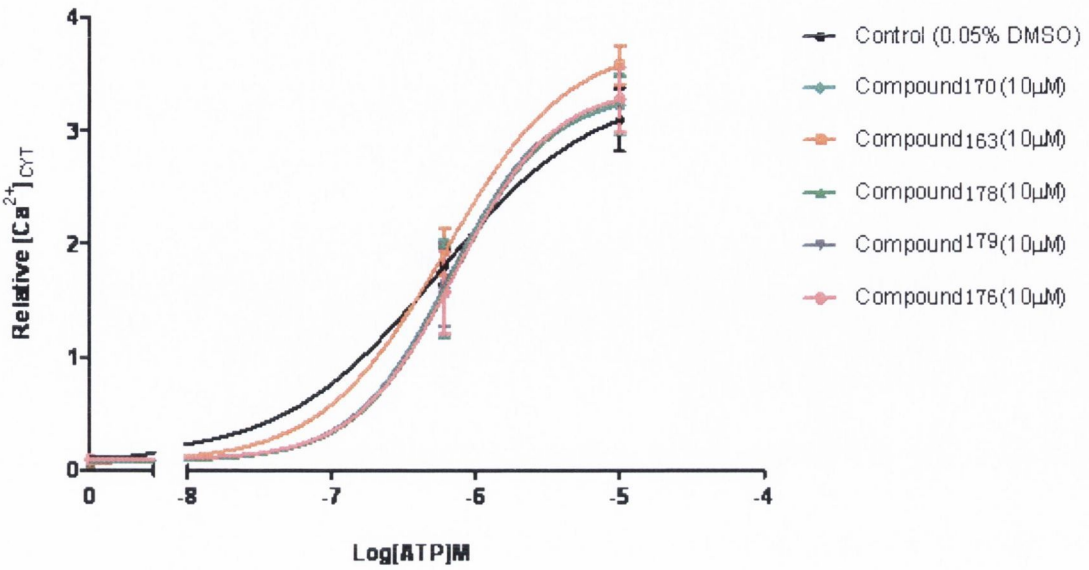

Figure 4.29 Relative $[Ca^{2+}]_{CYT}$ ATP (0.6μM, 10μM) dose response curve in MCF-7 cells pre-treated with compound 170, 163, 178, 179 and 176 for 15 min.Traces display mean response over baseline (relative $[Ca2+]_{CYT}$)±SD from 12 individual wells from 3 independent experiments

The compounds **170, 163, 178, 179** and **176** were then examined for their effect the nature of cytosolic calcium increases in MCF-7 breast cancer cells elicited by the agonist (ATP). Preincubation (15 min) with 10 μM of the compounds did not produce a change in increases in cytosolic free calcium by the purinergic G-protein coupled receptor activator ATP. No change in peak response for sub-maximal ATP was observed, (**Figure 4.29**). There was also no change in the nature (e.g. rate of recovery) of the increase at maximal and sub-maximal concentrations of ATP as shown in **Figure 4. 30**. These results indicate that the antiproliferative effects of the 4-(1,3-diaryl-1H-pyrazol-4-yl)-1,4-dihydropyridines examined are calcium independent in MCF-7 cells, as they display negligible calcium effects in MCF-7 breast cancer cells. A previous study had reported that the 1,4-dihydropyridine calcium channel antagonist amlodipine inhibited the HT-39 human breast cancer cell proliferation and lowered intracellular calcium levels.[294]

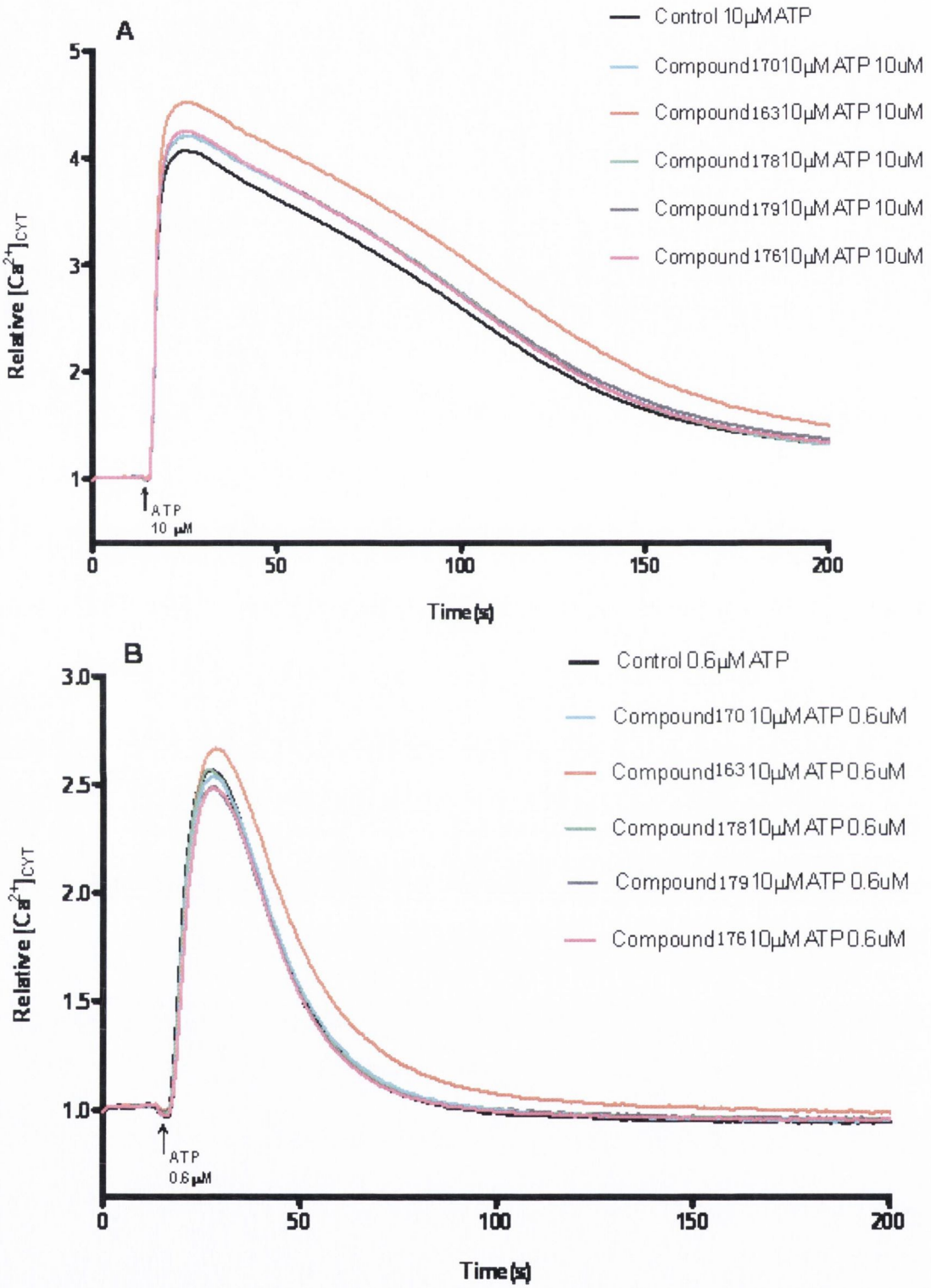

Figure 4.30 Relative $[Ca^{2+}]_{CYT}$ in MCF-7 cells pre-treated with compounds 170, 163, 178, 179 and 176 for 15 minute.

Maximal (10 μM) (A) or sub-maximal (0.6 μM) (B) ATP was added at the time indicated. Traces display mean response over baseline (relative $[Ca2+]_{CYT}$) from 12 individual wells from 3 independent experiments.

4.10 The NCI 60 cell line panel

To develop the anti-cancer drugs is a very expensive and time-consuming process. The Development Therapeutics Program (DTP) of United States (U.S.) National Cancer Institute (NCI) provides a good opportunity to optimise this process by providing *in vitro* and *in vivo* screening services. As a new anticancer drug screening program using a disease oriented panel of cultured human tumor cell lines for the initial stages of screening, the DTP anticancer drug discovery program has been run by the National Cancer Institute (NCI) since 1990. Up to 3,000 compounds are screened per year for potential anticancer activity. The panel consisted of 60 cell lines, including lung, brain, colon, ovarian, breast, prostate, kidney, melanoma, and leukaemia cancers. Synthetic compounds or natural product showing selective growth inhibition or cell killing of particular tumor cell lines can be used in pattern recognition algorithms in this unique screen. It is possible to suggest mechanism of action for the test compound and to select compounds most likely to interact with a specific molecular target by COMPARE program. This is a two-stage process screening, starting from the online submission of the compound structure along with any relevant information. The compound is then evaluated before a sample of the compound is shipped to NCI. Usually 10-15 mg of test compound is requested. The tested pure compounds are evaluated against the 60 cell lines at a single dose of 10 μM.[295] Thus only compounds which show significant growth inhibition are screened at five concentrations in the full panel of 60 cell lines for the next stage of testing.

NCI60 DTP human tumor cell line screening panel are inoculated into 96 well plates. For a typical screening experiment, 100μL suspension of cancer cells at various densities ranging from 5,000-40,000 cells/well is used to seed the plates depending on the type of cell. The plates are incubated at 37°C for 24 hours prior to addition of test samples. The experimental compound is dissolved in DMSO to 400 times the final test concentration and diluted to twice the final working concentration with complete medium. Following addition of 100 μL of a series of drug dilutions to appropriate wells give a final concentration between 100 μM and 10 nM. (Tz) represent a measurement of fixed cell population at the time of drug addition. The plate is incubated for a further 48 hours prior to the cells are fixed *in situ*, washed with water and air dried. Subsequently sulforhodamine B (SRB) solution at 0.4% (w/v) in 1% acetic acid was added to each well, and incubated for 10 minutes before

the excess SRB is removed by 1% acetic acid and then plated are dried. The bound SRB was solubilised with 10mM trizma base prior to being read on plate reader at 515 nm to find the absorbance and the control growth (C), growth in the presence of the test compound (Ti). The GI_{50} (Growth inhibition of 50%) is calculated from [(Ti-Tz)/(Z-Tz)]x100 = 50%. The drug concentration resulting in total growth inhibition (TGI) is calculated from Ti = Tz. The TGI is a parameter indicating the cytostatic effects of the compound. The LC_{50} (concentration of drug resulting in a 50% reduction in the measured protein) is calculated from [(Ti-Tz)/Tz] x 100 = -50%. Therefore the LC_{50} measure the cytotoxic effects of the compounds. Where GI_{50} can not be accurately evaluated, the result is reported as being less than/greater than the upper/lower limit for the test compound. In the case the lower limit for GI_{50} is 10 nM, which means that compounds that may be more potent than this will be reported only as being lower than 10 nM. If the average GI_{50} value of a compound has exceeded these limits an approximation of the GI_{50} is used. A compound which is significantly more potent than 10 nM is subjected to a second round of testing at a lower dose. [296]

4.10.1 Five dose screening test in NCI 60 cell line

Compounds **170**, **179**, **176**, **221**, **222**, **227**, **229** and **240** were chosen for specific analysis and further development (screening in the National Cancer Institute (NCI) 60-cell line panel, determination of reversal of resistance in HL-60 MDR cells and investigation of calcium effects in MCF-7 cells) based on the analysis of their drug-like properties from a Tier-1 profiling screen (including experimentally determined solubility and chemical stability together with predictions of permeability, metabolic stability, Pgp substrate status, blood-brain barrier partition, plasma protein binding and human intestinal absorption properties which indicated the suitability of these compounds for further development). As an example compound **176** satisfies Lipinski's 'rule of five' for drug-like properties e.g. molecular weight (490) is less than 500, the number of oxygen/nitrogen atoms is less than 10, the number of hydrogen bond donors is less than 5 and the cLogP value of 3.72 (<5), implying that this is a moderately lipophilic-hydrophobic drugs and is a suitable candidates for further investigation.

Compounds **170**, **179**, **176**, **221**, **222**, **227**, **229** and **240** were evaluated in the National Cancer Institute (NCI)/Division of Cancer Treatment and Diagnosis

(DCTD)/Developmental Therapeutics Program (DTP),[297] in which the activity of each compound was determined using approximately 60 different cancer cell lines of diverse tumor origins. These studies were performed at the NCI as part of their drug-screening program. Compounds **170**, **179**, **176**, **221**, **222**, **227**, **229** and **240** were tested for inhibition of growth (GI_{50}) and for cytotoxicity (LC_{50}) in the NCI panel of 59 cell lines and showed broad-spectrum antiproliferative activity against tumour cell lines derived from leukaemia, breast cancer, non-small cell lung cancer, colon cancer, CNS cancer, melanoma, ovarian cancer, renal cancer and prostate cancer, as described previously. 1,4-Dihydropyridines **170, 179** and **176** showed low micromolar GI_{50} values in all cell lines (The GI_{50} value is the concentration of drug required for 50% inhibition of cellular growth). In MCF-7 cells, **170, 179** and **176** were found to have a GI_{50} value of 3.48 μM, 2.55 μM and 3.51 μM respectively, comparable to the values of 5.0 μM, 4.7 μM and 5.7 μM respectively obtained in our in-house assay. The mean GI_{50} value for compounds **170, 179** and **176** across all cell lines is 3.39 μM, 3.47 μM and 3.31 μM respectively. The mean LC_{50} (a measure of cytotoxicity) for **170, 179** and **176** across the range of cell lines is 85.1 μM, 64.6 μM and 75.9 μM respectively. These results confirm the basic structural requirements of the 4-(1,3-diaryl-1H-pyrazol-4-yl)-2,6-dimethyl-1,4-dihydropyridine-3,5-dicarboxylic acid diethyl esters for optimum antiproliferative activity.(**Table 4.15**)

The type V compounds **221, 222, 227, 229** and **240** were also subjected to this analysis. In the standard agent database 240 was the top ranked with an R value of 0.765 based on GI50 mean graph. Compounds **223, 224, 225, 226, 228, 230, 238, 239, 204, 241, 161, 181, 163** have also been screened in the *in Vitro* Cell Line Screening Project by NCI. (**Appendix I**)

NCI Ref. Number	S750277			S750282		S750281	
Compound	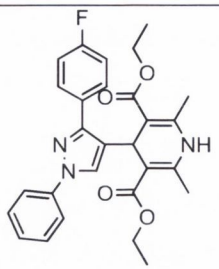			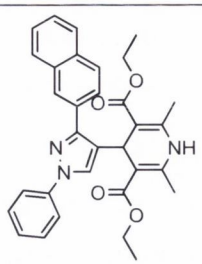		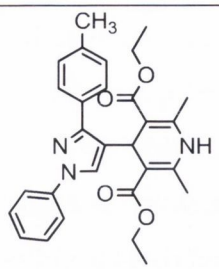	
Cell line	GI_{50} (μM) 176	GI_{50} (μM) 179	GI_{50} (μM) 170	Cell line	GI_{50} (μM) 176	GI_{50} (μM) 179	GI_{50} (μM) 170
Leukemia							
CCRF-CEM	3.55 e-06	3.75 e-06	6.70 e-06	**MOLT-4**	2.13 e-06	2.11 e-06	3.26 e-06
HL-60(TB)	2.77 e-06	2.22 e-06	2.83 e-06	**RPMI-8226**	2.51 e-06	2.14 e-06	3.66 e-06
K-562	3.77 e-06	3.26 e-06	3.44 e-06	**SR**	1.56 e-06	1.31 e-06	2.11 e-06
NSCLC							
A549/ATCC	3.79 e-06	3.46 e-06	3.09 e-06	**NCI-H23**	3.33 e-06	3.26 e-06	4.11 e-06
EKVX	2.46 e-06	2.26 e-06	2.97 e-06	**NCI-H332M**	3.93 e-06	3.96 e-06	3.84 e-06
HOP-62	3.45 e-06	4.71 e-06	4.44 e-06	**NCI-H460**	3.07 e-06	3.34 e-06	2.18 e-06
HOP-92	1.48 e-06	1.51 e-06	1.97 e-06	**NCI-H552**	7.39 e-06	1.59 e-05	3.67 e-06
NCI-H226	5.32 e-06	5.38 e-06	5.90 e-06				
Colon							
COLO 205	1.86 e-06	1.55 e-06	1.68 e-06	**HCT-15**	4.07 e-06	4.54 e-06	2.57 e-06
HCT-2998	2.45 e-06	2.14 e-06	4.68 e-06	**KM12**	1.98 e-06	2.04 e-06	2.14 e-06
HCT-116	2.18 e-06	2.57 e-06	2.56 e-06	**SW-620**	2.10 e-06	2.92 e-06	2.80 e-06
HT-29	3.91 e-06	3.49 e-06	3.44 e-06				
CNS							
SF-268	3.35 e-06	4.28 e-06	6.11 e-06	**SNB-19**	1.31 e-06	3.30 e-05	1.76 e-06
SF-295	nd	nd	3.66 e-06	**SNB-75**	1.97 e-06	2.78 e-06	1.68 e-06
SF-539	2.84 e-06	3.46 e-06	1.98 e-06	**U251**	3.21 e-06	3.22 e-06	2.82 e-06
Melanoma							

LOX IMVI	2.94 e-06	2.36e-06	1.51 e-06	**SK-MEL-28**	3.79 e-06	5.97 e-06	5.18 e-06
M14	2.42 e-06	3.28 e-06	3.74 e-06	**SK-MEL-5**	3.76 e-06	4.14 e-06	1.85 e-06
MDA-MB-435	2.85 e-06	2.83 e-06	3.79 e-06	**UACC-257**	4.37 e-06	3.35 e-06	4.26 e-06
SK-MEL-2	3.14 e-06	4.31 e-06	2.12 e-06	**UACC-62**	6.69 e-06	1.43 e-05	1.04 e-05
Ovarian cancer							
IGROV1	1.39 e-06	1.50 e-06	2.39 e-06	**OVCAR-8**	5.36 e-06	9.33e-06	4.15 e-06
OVCAR-3	1.69 e-06	2.13 e-06	2.18 e-06	**SK-OV-3**	1.26 e-05	3.27 e-06	4.67 e-06
OVCAR-4	5.19 e-06	7.37 e-06	3.46 e-06	**NCI/ADR-RES**	3.61 e-06	1.08 e-05	8.64 e-06
OVCAR-5	1.13 e-06	3.85 e-06	8.75 e-06				
Renal cancer							
786-0	3.14 e-06	3.41 e-06	2.35 e-06	**RXF 393**	2.61 e-06	2.07 e-06	2.20 e-06
A498	3.30 e-06	2.45 e-06	2.27 e-06	**SN12C**	3.38 e-06	4.17 e-06	3.63 e-06
ACHN	2.47 e-06	2.43 e-06	2.44 e-06	**TK-10**	4.83 e-06	2.92 e-06	3.86 e-06
CAKI-1	1.28 e-06	1.47 e-06	2.61 e-06	**UO-31**	2.26 e-06	2.34 e-06	2.21 e-06
Prostate cancer							
PC-3	2.19 e-06	1.58 e-06	2.32 e-06	**DU-145**	4.08 e-06	5.27 e-06	7.87 e-06
Breast cancer							
MCF-7	3.48 e-06	3.51 e-06	2.55 e-06	**BT-549**	7.35 e-06	4.53 e-06	5.53 e-06
MDA-MB-231/ATCC	3.97 e-06	3.84 e-06	3.57e-06	**T-47D**	3.06 e-06	3.42 e-06	3.48 e-06
HS 578T	1.91 e-06	2.04 e-06	3.40 e-06	**MDA-MB-468**	9.71 e-06	1.66 e-05	4.04e-06

Table 4.15 Summary of NCI 60 cell line screening results for compound 170, 176 and 179

GI_{50} and LC_{50} are the concentrations required to inhibit the growth and kill 50% of the cells in the assay respectively. TGI is the concentration required to completely inhibit the growth of all cells

4.10.2 COMPARE analysis for selected compounds

To date, hundreds of thousands of synthetic and natural products have been screened by the NIH DTP. Paull et al. developed the COMPARE algorithm,[298] which creates a characteristic fingerprint pattern for each compound by comparison of data obtained from the test compounds to others in the database. Experimental application of the COMPARE program creates a list of compounds to rank the similarity of the mean graph pattern of a specified seed compound to the patterns of all the other compounds in the NCI screening project database. Pearson correlation factor is then used to rank such compounds. Compounds with ranking scores may possess a similar mode of action to the test compound. The database of NCI compounds consists of a number of subgroups. The three main groups are synthetic and natural products with a known structure, crude natural product extracts and standard agents. The current standard agent database is comprised of around 171 entries of standard chemotherapy agents of clinical importance, while the synthetic and natural products database with >40,000 and >20,000 compounds and growing.

Matrix COMPARE analysis[298] of five dose data for 1,4-dihydropyridines **170, 179** and **176** was used to compare the differential antiproliferative activity of **170, 179** and **176** to compounds with known mechanisms of action in the NCI Standard Agent Database.[299] All three measures of activity (GI_{50}, TGI and LC_{50}) were used and the analysis showed correlations to vincristine, paclitaxel, maytansine and rhizoxin (tubulin targeting agents) and tamoxifen (ER antagonist) (**Appendix I**), however there is no evidence that the COMPARE algorithm distinguishes between different tubulin-based mechanisms of action[300].

4.11 Stability studies for dihydropyridine derivatives

Stability is a critical part of the drug development process and an essential factor of quality, safety and efficacy of a drug product. Insufficient stability of a drug product can result in changes in physical as well as chemical characteristics.[301] The chemical stability evaluation of a drug is of great important in drug development since the drug becomes less effective as it undergoes degradation, while the drug decomposition may yield toxic by products that are harmful to the patient.[302]

Since the 1,4-dihydropyridines ring is the core structure of a number of clinical products in current use, the degradation of the 1,4-DHPs ring has been extensively studied. Some 1,4-dihydropyridines are well known to be unstable,[303, 304] especially nifedipine (**52**) which degraded through photodecomposition.[305] The degradation route is shown in **Figure 4.31**. There are two chemical components identified for nifedipine decomposition, one is dehydronifedipine (DNIF) and another is the nitrosopyridine photodegradation product of nifedipine (NDNIF). (**Figure 4.31**) Shamsipur et al. have assessed that the kinetics of nifedipine degradation consisted of two separate regions. The first one was confirmed to show zero order kinetics at the beginning of the reaction and was linear with time, while the second regions indicated a first-order kinetic pathway when the reaction proceded more than 50%.[306] The stability study presented here will focus on evaluating the pH dependent hydrolysis of the dihydropyridines analogues and some related ester compounds.(**Figure 4.32**)

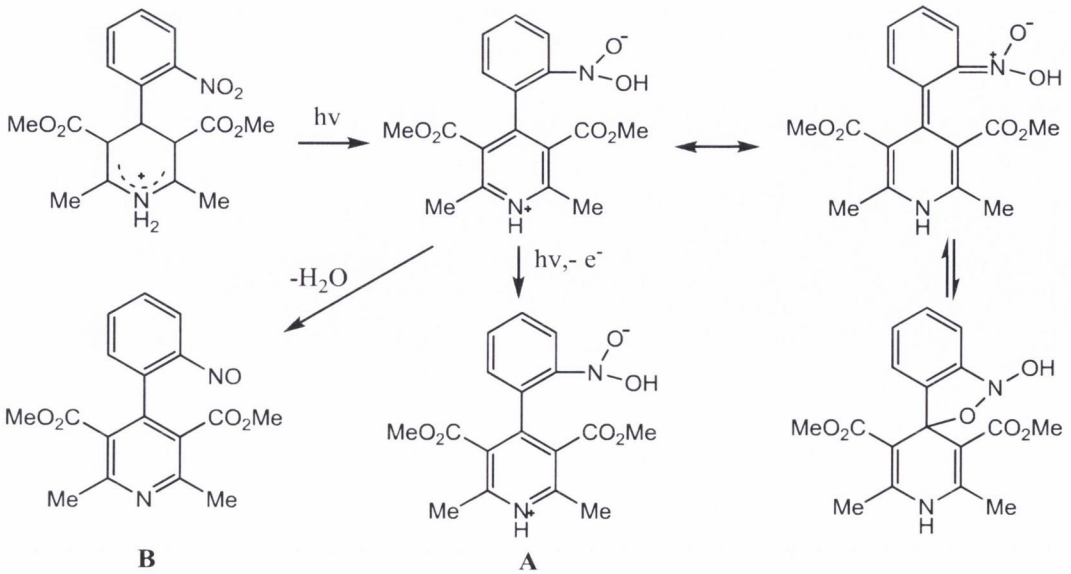

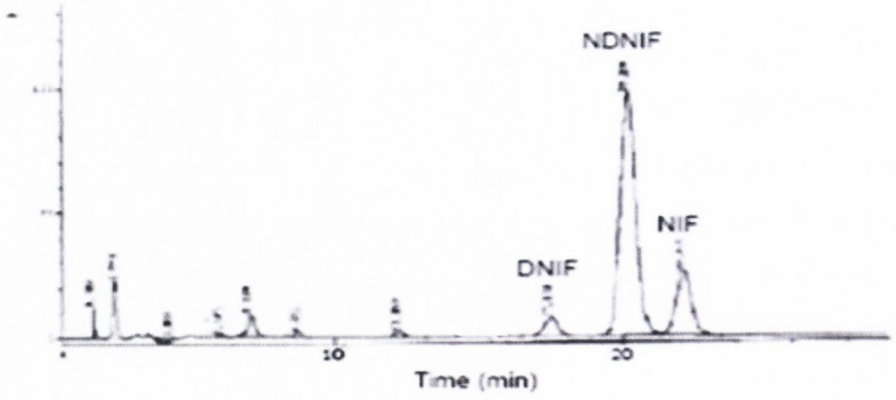

Figure 4.31 Degradation route of nifedipine [52] and chemical structure of nifedipine and degradation compounds (A) nitro- analogue of dehydronifedipine (DNIF) and (B) nitroso-analogue of dehydronifedipine (NDNIF) and chromatogram of nifedipine and its photodegradation products DNIF and NDNIF

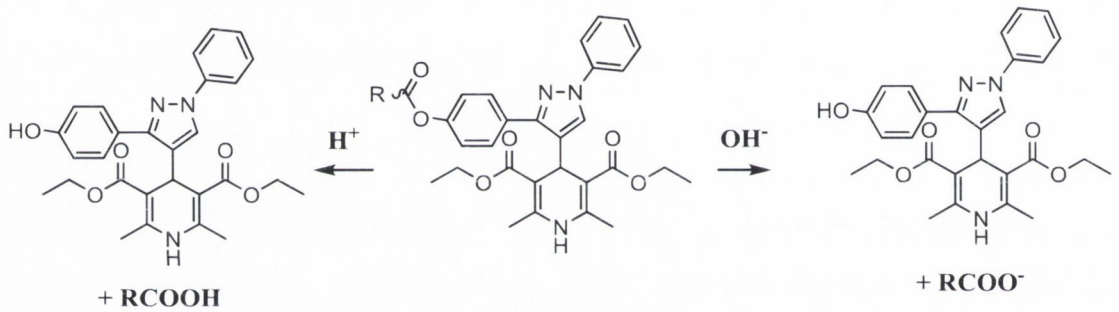

Figure 4.32 Proposed hydrolysis of 1,4-DHPs compounds containing hydroxyl or ester group under acidic/basic conditions

4.11.1 Stability studies for 1,4-DHP analogues and related products

The stability studies on 1,4-dihydropyridines were carried out by Dr Bassem Yassin and Mr Donal Conaill as part of their research in the School of Pharmacy Trinity College Dublin.[307] Two 1,4-DHPs **OH, NH_2** and nine conjugate DHP ester products **195, 196, 204, 205, 206, 207, 208, 209, 210** (**Figure 4.33**) were examined by HPLC to assess their stability over a range of pH conditions from 4.0 to 9.0 in buffered solution, together with stability study in 0.1 M HCl and NaOH solutions and also in human blood plasma.

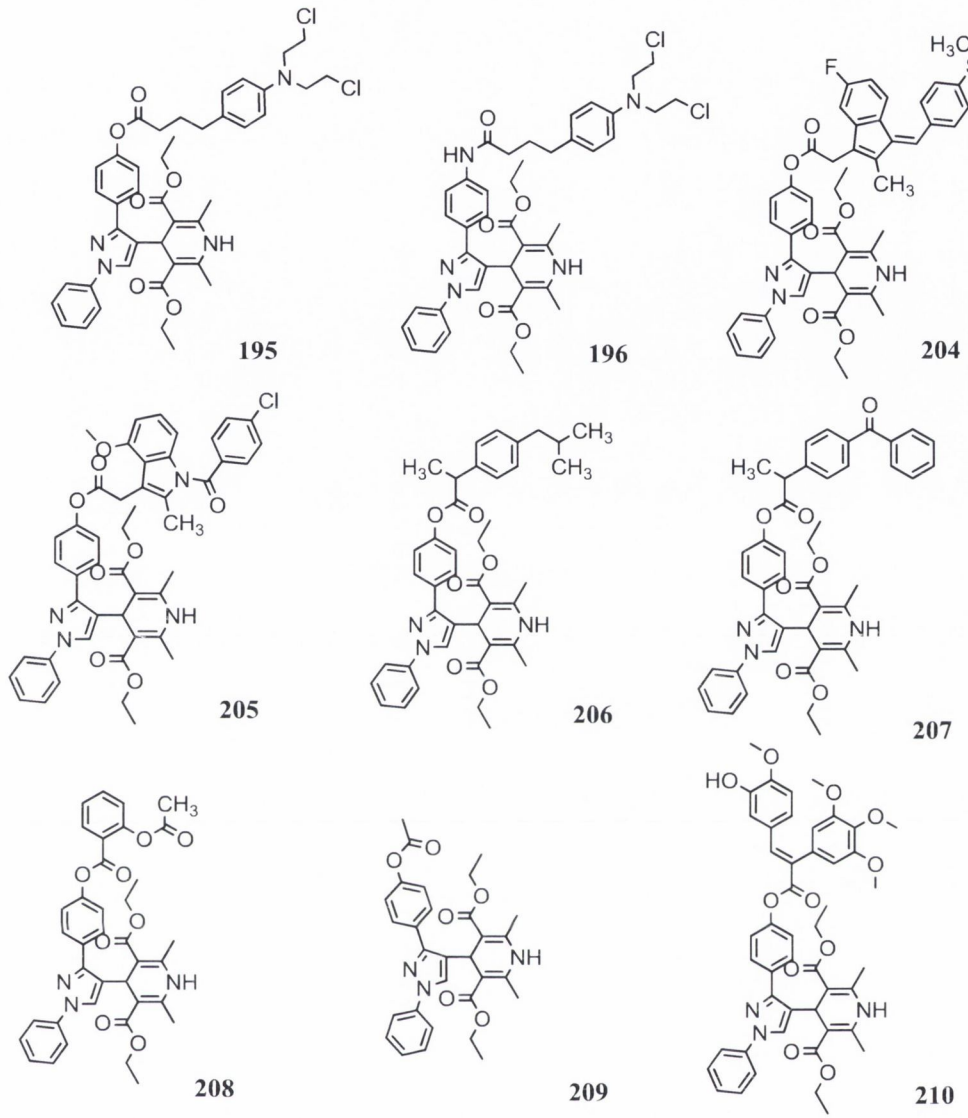

Figure 4.33 structure of compounds tested for stability

The HPLC method is described in the experimental section, with details on the preparation of the buffers and blood plasma. The separation was run on a spherisorb column along with isocratic mobile phase consisting of 80:20 acetonitrile:water. To optimise the peak shape of initial chromatogram, 0.1% v/v trifluoroacetic acid was added which resulted in symmetry peak in good agreement with the BP specifications. (Symmetry factor of the peak lies in 0.8-1.5. Appendix III BP 2008). Compounds were placed in various buffers at 37 ^{o}C then immediately injected. Subsequently these samples were left at 37 ^{o}C and then sampled at 15 min, 1 h, 4 h, 12 h and finally after 1 day.

Various decomposition pathways for type IV 1,4-DHPs are possible. The major pathway is the acid and base catalysed hydrolysis of any 1,4-DHPs containing ester or amide groups. The stability of compounds showing the percentage of compound

remaining and the degree of degradation over time can be clearly seen in the graphs displayed below (**Figure 4.34-4.39**). The results obtained showed the majority of type IV 1,4-DHP ester compounds to be completely stable over the 24 hours except ester and amide 1,4-DHP coupling with chlorambucil e.g. compound **195** and **196.** Both of these compounds appear to undergo degradation of approximately 40% in the first half hour of contact with acidic medium at pH4.0 (**Figure 4.34**). The degradation of the analytes **195** and **196** resulted in a half life of nearly 5 hours.

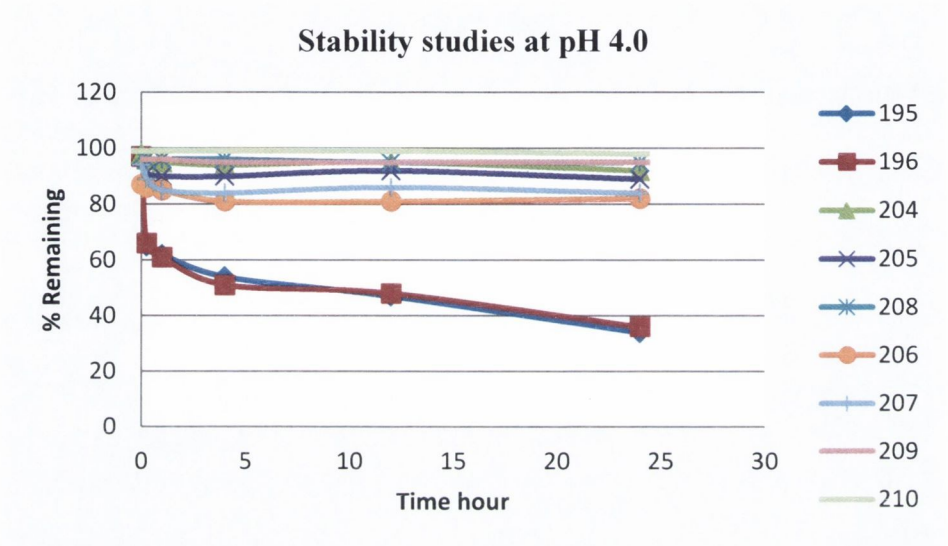

Figure 4.34 Stability studies of 1,4-DHP analogue at pH 4.0

At neutral pH 7.4 all the tested compounds were almost complete stable and resulted in more than 80% remaining throught the 24 hour period. However the two chlormabucil conjugate compounds **195** and **196** again displayed less stability with 70% and 60% present after 24 hours, respectively. This indicates that the two conjugate compounds containing chlormabucil are less stable compounds at both acidic and neutral pH. The ibuprofen analogue **206** also showed slight degradation at pH7.4.(**Figure 4.35**)

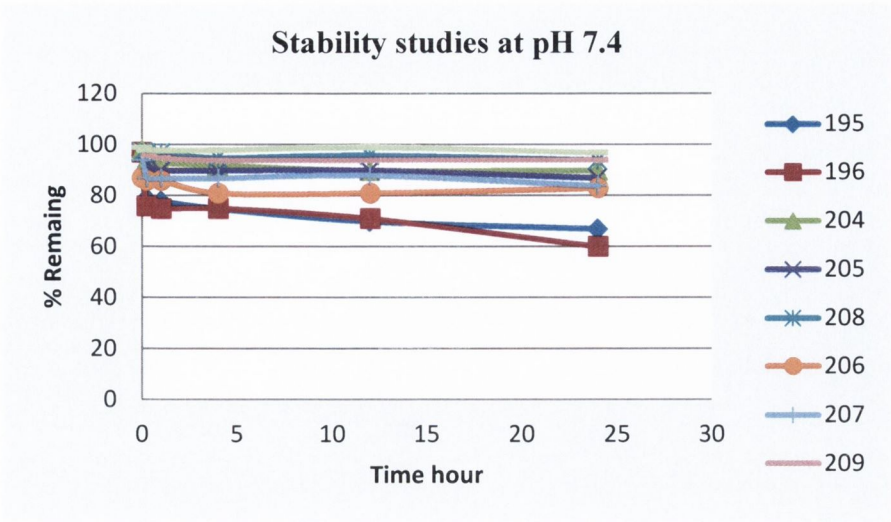

Figure 4.35 Stability studies of 1,4-DHP analogue at pH 7.4

At pH 9.0, there is an initial loss of the analyte of approximately 10-20% for each compound when placed in basic buffer, after which time no further degradation is observed up to 24 hours in the study.(**Figure 4.36**) The reason that test analogues were obviously more stable at the physiological and basic pH than acidic condition is unclear since to some extent hydrolysis in alkline pH over the long time period should be obseved.

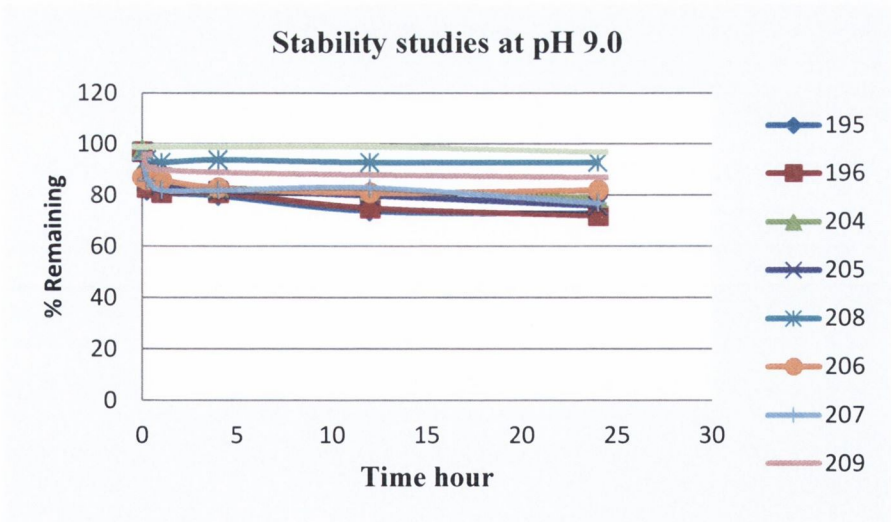

Figure 4.36 Stability studies of 1,4-DHP analogue at pH 9.0

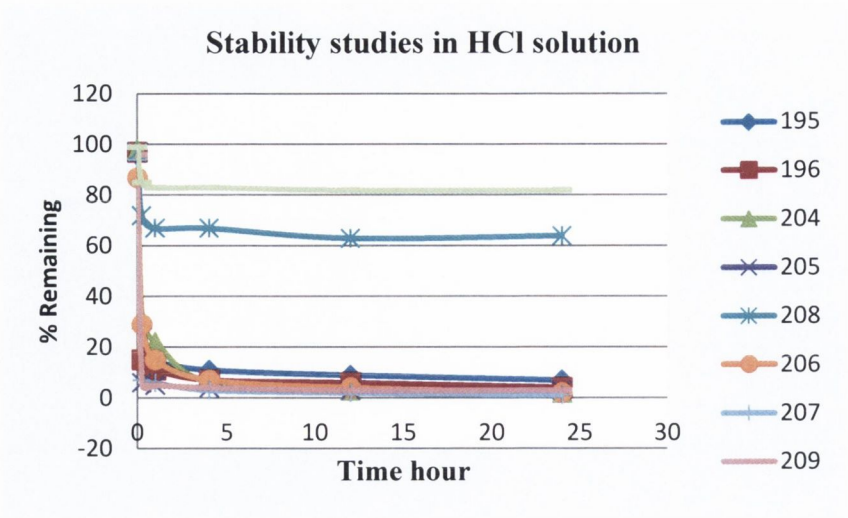

Figure 4.37 Stability studies of 1,4-DHP analogue in 0.1M HCl MeOH solution

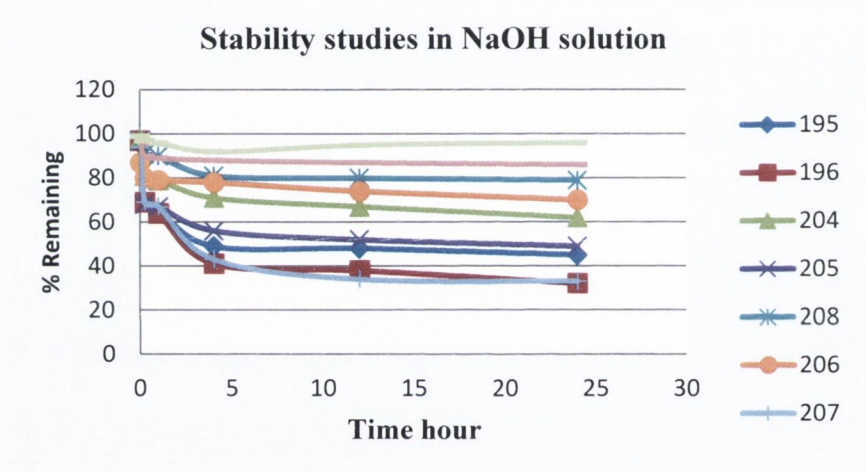

Figure 4.38 Stability studies of 1,4-DHP analogue in 0.1M NaOH MeOH solution

Stability studies on the degradation of conjugate ester 1,4-DHPs also carried out in forced degradation conditions (0.1M HCl and 0.1M NaOH methanol solution). As obviously seen from **Figure 4.37**, the majority of these analogues completely degraded within 15 minutes when placed in the acidic condition. Compounds **208**, **210** were observed to degradate at initial time, but more than 60% remained throughout the timescale of the studies. In basic condition, the selected test compounds degraded at a much slower rate than observed in acidic pH. There is an initial loss in the first 2.5 hours for most of compounds before the degradation curve reached a plateau.(**Figure 4.38**) The results demonstrated that degradation of conjugate ester compounds can occur at different pH, but the rate of degradation could be varied.

Stability studies in blood plasma(**Figure 4.39**) showed the degradation of 1,4-DHPs analogue is likely to be linear throughout the experiment resulting in a half life of approximately 24 hours. However these compounds showed slight degradation once in contact with blood plasma medium at T_0 hour. The most stable compound is CA-4 analogue **210** which is demonstrated to be present at nearly 100% throughout the 24 hours period.

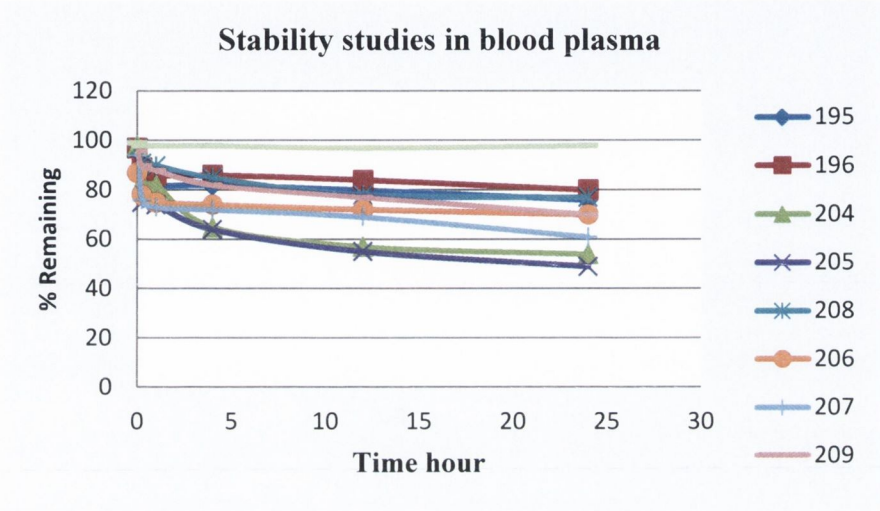

Figure 4.39 Stability studies of 1,4-DHP analogue in human blood plasma

In a separate study, the pH stability study of selected 4-(1,3-diaryl-1H-pyrazol-4-yl)-2,6-dimethyl-1,4-dihydropyridine-3,5-dicarboxylic acid diethyl esters **163** and **165** by HPLC was also carried out, which indicated the compounds are moderately stable at acidic (pH4), physiological (pH7.4) or basic conditions (pH9). (**Figure 4.41-4.43**) For examplefor compound **165**, the percentage remaining after 6 hours wasdetermined to be 98%, 97% and 75% at pH4, 7.4 and 9 respectively. The selected compounds showed an average half life more than 12 hours at all pH condition, indicating that 1,4-DHPs may be stable at the physiological pH *in vivo*. (**Table 4.16**) Plasma studies carried out determined that the percentage remaining after 18 hours for compound **165** was 85%. For nifedipine, the percentage remaining under the same conditions in plasma was determined to be 57%.

Time (min)	Compound 165 % remaining			Compound 163 % remaining		
	pH4.0	pH7.4	pH9.0	pH4.0	pH7.4	pH9.0
0	0.99	0.99	0.98	0.99	0.99	0.99
15	0.99	0.98	0.96	0.99	0.99	0.99
60	0.99	0.97	0.98	0.99	0.99	0.97
240	0.98	0.97	0.75	0.83	0.99	0.81
720	0.98	0.96	0.42	0.4	0.94	0.55
1440	0.97	0.96	0.4	0.15	0.24	0.31
$T_{1/2}$ (min)	97% remaining after 24 hour	96% remaining after 24 hour	996.9	784.9	1152.4	976.6

Table 4.16 Percentages remaining in 24 hours and calculated half life for 1,4-DHPs analogues 163 and 165

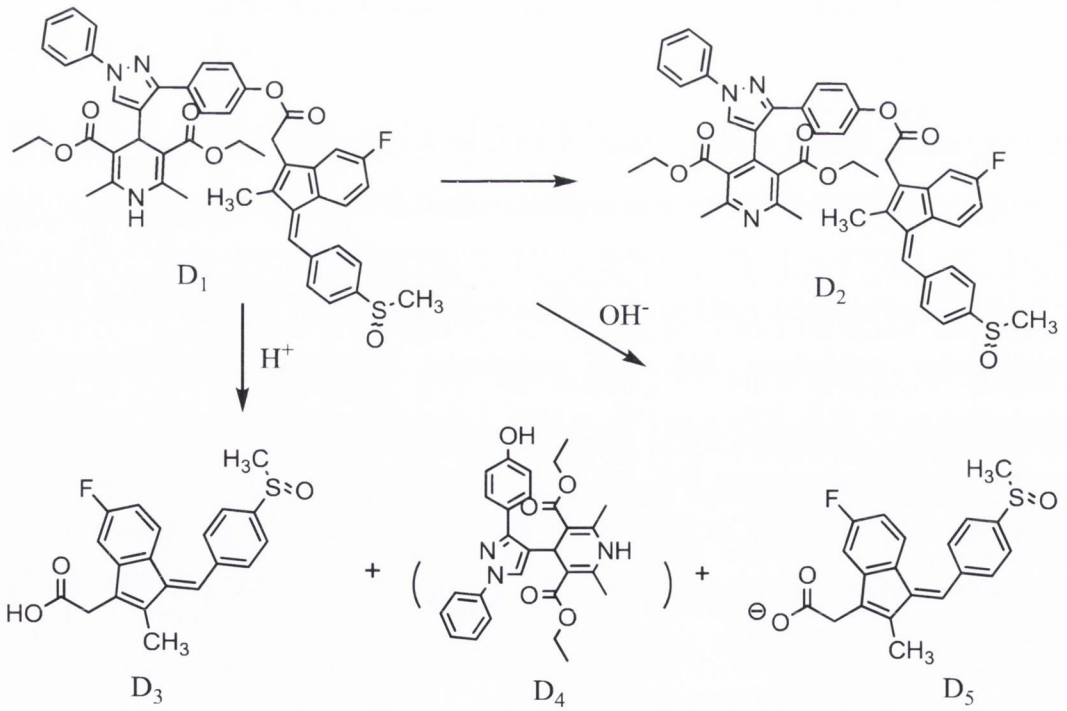

Figure 4.40 Proposed hydrolysis & degradation products of conjugated ester compound 204

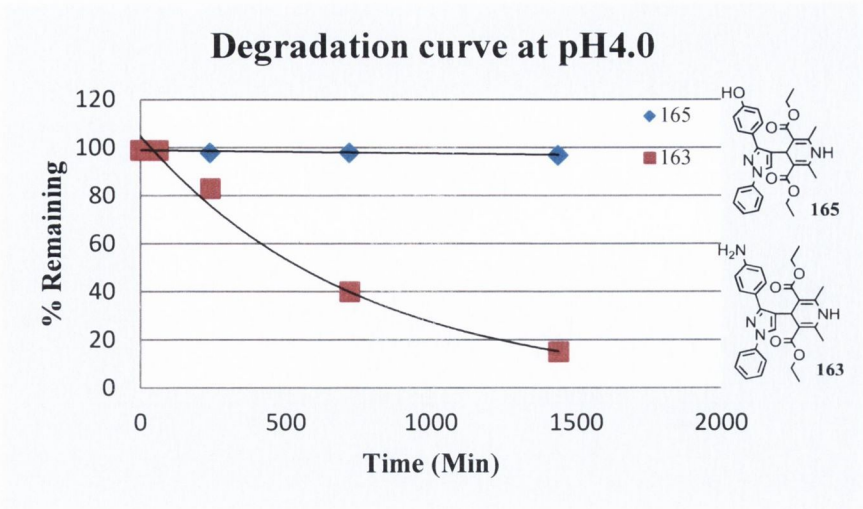

Figure 4.41 Decomposition study of compound 163, 165 at pH4.0

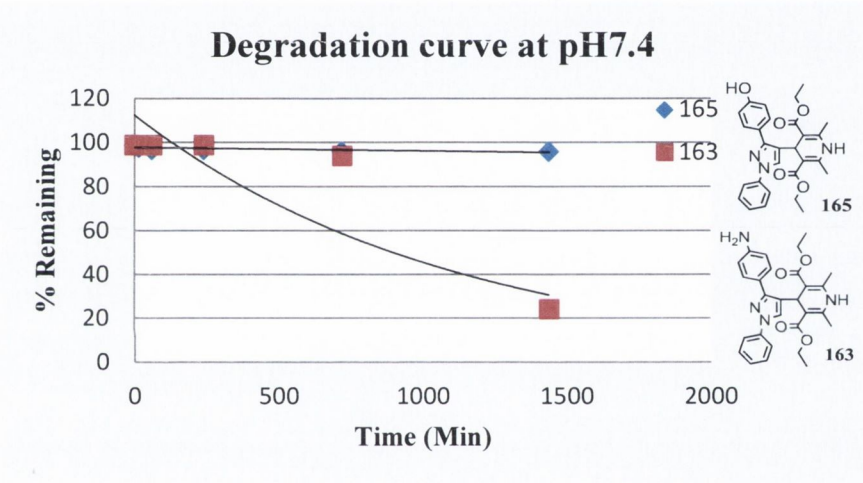

Figure 4.42 Decomposition study of compound 163, 165 at pH7.4

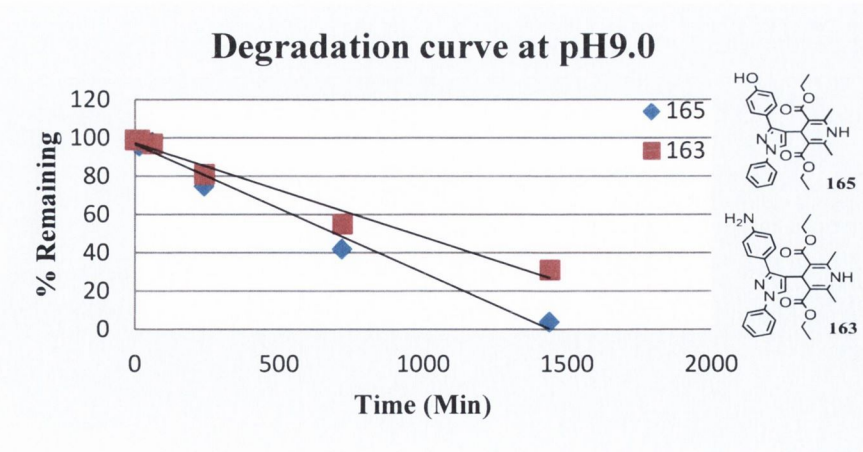

Figure 4.43 Decomposition study of compound 163, 165 at pH9.0

Figure 4.40 and **4.44** show the various products that can form when sulindac conjugate compound **204** is exposed to different pH conditions. The proposed

products are D2, D3, D4, D5, which were indentified by HPLC. In conclusion, the stability of a series of 1,4-DHP compounds and conjugated ester compounds over a range of pH conditions has been assessed. A further study of the metabolism of the conjugate esters of 1,4-DHPs *in vivo* is required, which would provide more detailed information of possible metabolites and their potential biochemical activity.

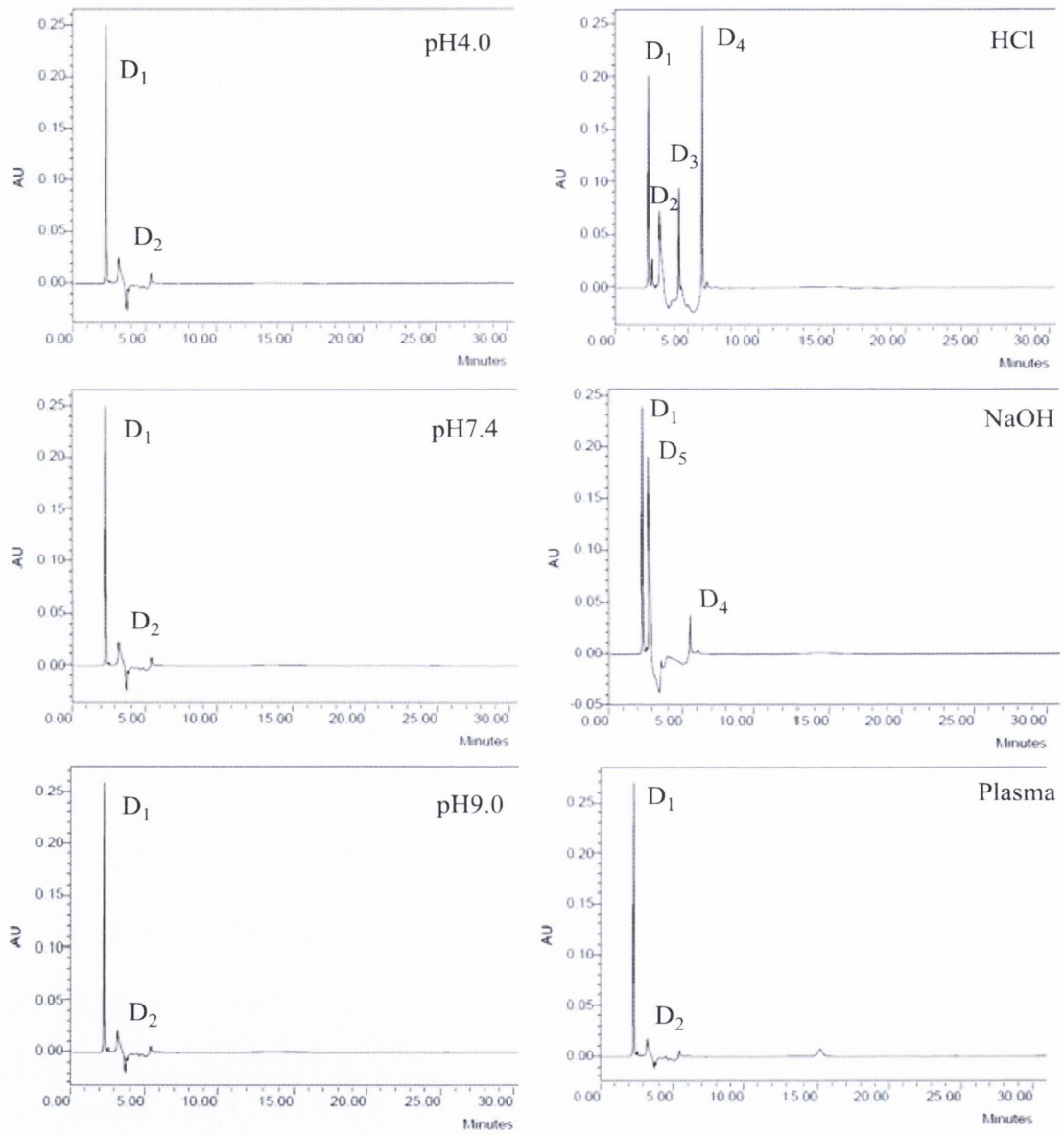

Figure 4.44 HPLC chromatogram of conjugated ester 1,4-DHP 204 and its predicted degradation and hydrolysis products in various conditions

4.12 Antioxidant activity

The antioxidant activity of selected DHP products was determined. Oxidation is one of the most important processes of the drug degradation because it may affect drug

safety, composition, activity and shelf life. Antioxidants may protect drug quality by preventing oxidative deterioration of lipid *in vivo*.[308] Determination of antioxidant activity is based on the measurement of free radical scavenging of the antioxidant compounds using DPPH radical. The effect of each antioxidant on DPPH radical was estimated according to the procedure described in **section 4.5.6**.

Absorbances at 515 nm were measured at different time intervals on a Cary 300 UV-Vis spectrophotometer until the reaction reached a plateau. The DPPH concentration in the reaction medium was calculated as follows:

$$[\mathbf{DPPH}]\mathbf{rem} = [\mathbf{DPPH}]\mathbf{T_0}/\mathbf{AT_0} \times [\mathbf{DPPH}]\mathbf{T}$$

The percentage of remaining DPPH (%$DPPH_{REM}$) was obtained as follows:

$$\%\mathbf{DPPH\ rem} = [\mathbf{DPPH}]\mathbf{T}/[\mathbf{DPPH}]\mathbf{T_0}$$

The percentage of remaining DPPH against the sample and standard concentrations was then plotted to obtain the amount of antioxidant necessary to decrease the initial DPPH concentration by 50%. The results obtained for compound **162**, **165** and nifedipine were displayed in **Table 4.17**

Conc. Trolox mg/L	A t_0	A t	DPPH rem	%DPPH rem	EC_{50}mg/L
50.000	0.079	0.009	0.285	11.392	25.508
25.000	0.080	0.036	1.119	44.750	
12.500	0.083	0.061	1.825	73.012	
6.250	0.086	0.073	2.116	84.651	
165					
Conc. mg/L	A t_0	A t	DPPH rem	%DPPH rem	EC_{50}mg/L
1170.000	0.061	0.044	1.947	77.897	3140.000
2240.000	0.061	0.032	1.435	57.398	
3510.000	0.066	0.026	1.176	47.059	
162					
Conc. mg/L	A t_0	A t	DPPH rem	%DPPH rem	EC_{50}mg/L
1320.000	0.063	0.050	1.992	79.683	4083.000
2640.000	0.054	0.035	1.401	56.032	
3960.000	0.053	0.027	1.278	51.132	
Nifedipine					
Conc. mg/L	A t_0	A t	DPPH rem	%DPPH rem	EC_{50}mg/L
1248.000	0.056	0.051	2.2768	91.071	11780.000
823.000	0.055	0.052	2.3636	94.545	
416.000	0.057	0.054	2.3684	94.737	

Table 4.17 Standard concentration needed to decrease by 50% the initial DPPH concentration (EC_{50}) for compounds 162 and 165

Nifedipine will convert photochemically into 2,6-dimethyl-4-(2-nitrosophenyl)-3,5-pyridinedicarboxylic acid dimethyl-ester (NTP) under daylight conditions. Others

studies found that nifedipine had lower antioxidant potency than NTP. A decade ago, Diaz-Araya,G. et al. reported that nitro-substituted 1,4-dihydropyridines, such as nicardipine and nisoldipine exhibited the more potent antioxidant activities than non-nitro-substituted 1,4-dihydropyridines,such as amolodipine and isradipine.[309] Therefore, the antioxidant properties of selected 1,4-dihydropyridine derivatives synthesised in this study and nifedipine were assessed using the DPPH assay.

As a stable nitrogen radical, the scavenging of the DPPH can be measured by its decay at 515 nm. This assay is normally used to quantify antioxidant capacity and is useful for comparisons within structural families.[310] As shown is **Figure 4.45**, trolox is used as a standard for the antioxidant capacity compared to two potential antioxidant agents **162** and **165**, which contain bromo and hydroxyl substituents on the phenyl ring of 1,4-dihydropyridine analogues. The steeper the slope, the lower the EC_{50} and the higher the antiradical power. The result showed that the antioxidant effects of trolox (EC_{50}=25.5 mg/L) was significantly greater than these two tested 1,4-dihydropyridipines derivatives and nifedipine, whose concentration needed to decrease by 50% the initial DPPH concentration (EC_{50}) are 4.08 g/L, 3.14 g/L and >10 g/L, respectively. It was indicated that two selected 1,4-DHPs are weak antioxidant agent, while still have greater effect than nifedipine. Thereby these analogues which are substituted 1,4-dihydropyridine compounds can be regarded as potential antiradical agents and show wide antioxidant properties.

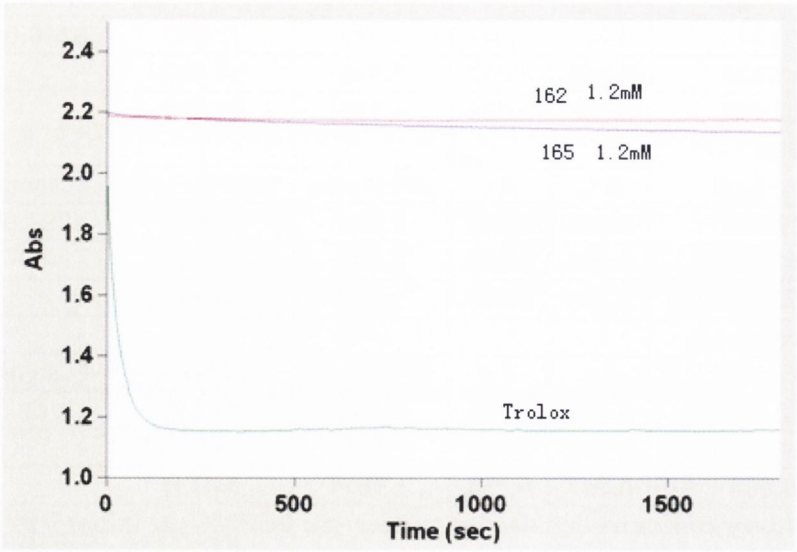

Figure 4.45 Time plot of relative absorbance (515 nm) showing decay of DPPH radical in the presence of selected 1,4-dihydropyridines derivatives

Chapter 5

General Discussion and Conclusion

This purpose of the work presented in this thesis was to design and synthesize a series of novel 1,4-dihydropyridine containing analogues of aryl-substituted pyrazoles and to determine their antiproliferative activity against the human MCF-7 breast cancer cells by MTT cell viability assay. The initial design of the target compounds was focused on the modification of lead 4-(1,3-diaryl-1H-pyrazole-4-yl)-1,4-dihydropyridine scaffold structure, specifically the nature of the aryl ring substituent at C-3 of the pyrazole ring system. (Chapter 2) Various functionalities were introduced, on the basis of previous SAR studies on 4-aryl-1,4-dihydropyridines as calcium channel blockers and p-glycoprotein modulators. In these novel compounds, the aryl-substituted pyrazole ring replaces the more usual aryl ring at the C-position of the 1,4-dihydropyridine ring and the presence of this bulky substituent of these compounds is required for the antiproliferative activity and may contribute to the complete lack of calium effects observed in MCF-7 cells.

Initial biological study of the lead 1,4-dihydropyridine analogues results in the identification of the 4-methoxy-3-chloroaryl substituted compound **177** as the most potent member of the series of scaffold IA analogues in MCF-7 cells line (IC_{50}=1.01 μM), while most these analogues possessed low mircomolar activity in this breast cancer line. For comparison, the IC_{50} value obtained for the calcium channel antagonist nifedipine in cell viability studies in MCF-7 cells was determined to be 51.61 μM and the 2,6-dimethyl-1,4-dihydropyridine-3,5-dicarboxylic acid diethyl ester was found to be inactive, with IC_{50} >100mM, which confirmed the requirement for the heterocyclic pyrazole substituent at C-4 of the 1,4-dihydropyridine ring for antiproliferative activity is necessary. The biphenyl substituted compound **178** and 4-bromophenyl-4'-methoxyphenyl compound **167** also displaying good activity with IC_{50}= 2.6 μM and 2.9μM respectively. Further modification on dihydropyridine ring to optimise the molecule structure was carried out. Two series of scaffold IB and scaffold IC derivatives with dicarboxylic acid dimethyl ester or phenylmethanone substituents on C-3 and C-5 of the dihydropyridine ring were prepared and evaluation of their antiproliferactive activity against MCF-7 cells and indicated no improvement in potency.

To establish the more detailed SAR and explore the further effect on antiproliferative activity, the lead scaffold IA 4-hydroxylphenyl compound **165** and 4-bromophenyl compound **162** were replaced with a wide variety of phenolic and coupling products,

such as basic side chain ether, NASIDs ester and substituted biphenyl. Larger substituents at this position led to moderate increase in activity compared to the parent substituted DHP compounds. For instance, piperidine side chain **217** (IC_{50}= 4.69 μM), 4-hydroxyl biphenyl **221** (IC_{50}=1.28 μM), 3,4,5-trimethoxyl biphenyl **230** (IC_{50}= 1.21 μM) and phenoxyacetic acid **240** (IC_{50}=0.40 μM). These phenolic and substituted biphenyl products have higher cLogP value of 6.22-9.67 compared to 5.57 for parent compound **165**. The increase in hydrophobicity may contribute to its lack of improvement in antitumour activity. The initial molecular structural design in this potential inhibitory antitimour agent does not result in significant improvement for antiproliferative activity against human breast cancer cells line. Future work should focues on the molecular docking study and evaluation of binding affinity to identify a more potent compound and possible molecular target of these analogues. However, investigation on effect of some scaffold IA compounds on the reversal of paclitaxel resistance in HL-60 MDR cells suggest that these analogues can be developed as potential MDR reversal agents. Pretreatment of resistance to paclitaxel HL-60 MDR cells with a non-toxic concentration (10 μM) of DHPs **170** and **176** led to >100 fold reduction in IC_{50} value for paclitaxel and increase in potency of this drug.

Moreover, a second library of a similar raloxifene scaffold compounds was designed and synthesised. These analogues prepared from reductive amination of biphenyl substituted pyrazole carbaldehyde and with extended side chains patterns in place of 1,4-dihydropyridine at the C-4 position of the pyrazole ring which resulted in increase in activity. The activity of phenolic derivatives **284** with morpholine side chain and **286** with dimethyl side chain fall in the high micromolar range. (IC_{50} value of 22.05 and 11.64). The most potent compound **250** was found in scaffold IIA analogues. It possesses the highest activity not only in MCF-7 human breast cancer cells, but in HL-60 Leukemia cells (IC_{50} =0.10 μM and 0.13 μM). Meanwhile it displayed greater reversing effect with only 10 nM concentration of drug used in HL-60 MDR cell compared with the well characterised MDR reversal Ca^{2+} antagonist verapamil. However, the other substituents amination products in this scaffold IIA do not show the similar activity. To extend this library of compounds and discover the mechanism of action may be the next step for research investigation. More investigation on the role of pyrazoles containing the basic side chain substituted at C-

3 position, or design of the possible novel scaffold II B analogues containing 2 basic side chains, which may be of interest for biochemical activity, will be carried out.

The initial stability studies revealed that most of 1,4-dihydropyridines and their related derivatives such as conjugated ester products were subject to hydrolysis at acidic (pH4.0), with $t_{1/2}$ of approximately 4-5 hours, but remained stable at neutral pH (pH7.4) and at alkaline pH (pH9.0). The major metabolites of these compounds are expected to be formed by hydrolysis and/or by oxidation of the 1,4-dihydropyridine ring. The metabolite compounds should be evaluated for their own biological activity.

In conclusion, these novel 4-(1,3-diaryl-1H-pyrazole-4-yl)-1,4-dihydropyridines and their derivatives were synthesised and evaluated for their antiproliferative activity and/or multidrug resistance reversing activity against breast cancer cells or leukemia cells. The results obtained demostrated that compounds **240** and **250** displayed potent antiproliferative activity in MCF-7 cell. The results of the study indicated that these analogues are potentially useful scaffolds for the further development of antitumour agents and are valueable lead compounds for further synthesis and evaluation studies of new dihydropyridines or pyrazoles as MDR reversal agents to overcome drug resistance in tumour cells with P-glycoprotein overexpression. Comprehensive molecular modeling study of these compounds to identify the possible binding site(s) with P-glycoprotein and tubulin will be carried out.

Chapter 6

Experimental Data

6.1 Materials & Methods

Chemicals were purchased from Sigma Aldrich and Lancaster Synthesis with a minimum assay of 98% unless otherwise stated. Solvents were either purchased dry or purified by distillation in accordance with literature methods.

^{1}H and ^{13}C NMR spectra were collected on a Brucker DPX 400 spectrometer, and analysed with Bruker WIN-NMR software. ^{1}H at 400.13 MHz and ^{13}C at 100.61MHz. Experiments were run in deuterated chloroform ($CDCl_3$) with tetramethylsilane (TMS) as the internal standard, unless other wise stated. The spectra were analysed with Bruker WIN-NMR, MestREC and Bruker TopSpin. Coupling constants were reported in Hertz (Hz). Abbreviations used in the assigning of the spectra include s = singlet, br s = broad singlet, d = doublet, t = triplet, q = quartet, qn = quintet and m = multiplet.

The crystal structure of compounds was determined by X-ray diffraction on a Bruker SMART APEX (2001) diffractometer using MoKa radiation from a fine focus sealed source and a graphite monochromator. The structure solution was found using SHELXS-97 and the structure refinement was carried out using SHELXL-97.

IR spectra were obtained on a Perkin Elmer Spectrum 100 FTIR spectrometer using either potassium bromide (KBr) disks or thin film on sodium chloride plates (NaCl).

High resolution mass spectrometry (HRMS) was carried out using a Micromass LCT electrospray mass spectrometer.

Melting points were determined on a Gallenkamp melting point apparatus using a mercury 300°C thermometer and are uncorrected.

Thin layer chromatography was carried out using Merck F-254 plates visualised with UV at 254 nm. Separation by flash chromatography was carried out using Merck Kiese gel 60 silica with a particle size of 0.040 mm to 0.063 mm. Alternatively flash chromatography using a Biotage SP1 ™ separation system was carried out using 12+M and 40+M silica cartridges and detection at 280 nm. A typical separation employed a gradient elution with hexane/ethylacetate over the course of 15 column volumes with fractions of 12 mL collected from the 12+M columns and 24 mL from the 40+M columns.

Compound purity was determined by HPLC using a Waters HPLC system fitted with a Spherisorb column (2-5 μm particle size, 4.5x250 mm) supplied by Alltech Associates Incorporated. A mobile phase of 80/20 acetonitrile/water with 0.1% (v/v) TFA added to prevent peak tailing was used throughout. The mobile phase was only prepared from HPLC grade solvents and degassed by sonication prior to use. Flow rate was maintained at 1 mL per minute with a pressure of approximately 1300 psi on a Waters 1525 binary pump equipped with an in line degasser. Where samples were run over a protracted period of time, the mobile phase was recycled back to the reservoir without any detriment to separation. Elution was detected at 280 nm with a Waters 2487 dual wavelength detector. Multiple injections were carried out using a Waters 717 autosampler. All samples were filtered via a syringe filter (Pall, 0.45 μM) prior to injection. The system was flushed with 2-propanol before shutting down for protracted periods of time.

Nomenclature was determined using Chemdraw 2004.

6.2 General procedure for preparation of phenylhydrazones

100 mmol of acetophenone (ca. 12 g) and 100 mmol of phenylhydrazine ca. 10 ml were mixed in 100 ml 1, 2-dichloroethane at room temperature (20-25°C) for two hours. Magnesium perchlorate (1.231 g) was added as a catalyst. The mixture was stirred until reaction was complete, as monitored with TLC. The completed reaction was dried with anhydrous Na_2SO_4 and extracted with methanol. The liquor was reduced by rotary evaporation. The crude product was then recrystaillised from minimum ethanol and vacuum filtered. The dried product was washed with hexane and dried again. Products were stored in a freezer as the phenylhydrazones tend to decompose at room temperature.

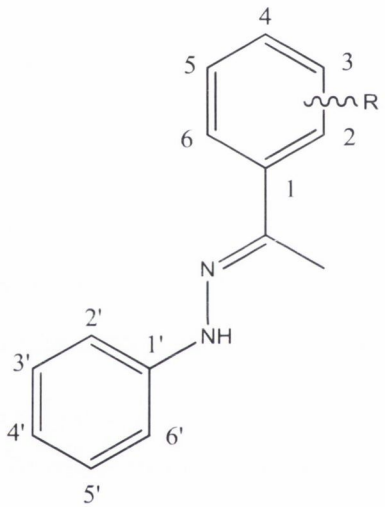

6.2.1 Synthesis of (E)-1-(1-(4-(benzyloxy)phenyl)ethylidene)-2-phenylhydrazine 68

This product was obtained from 4-benzyloxyacetophenone (22.6 g, 100 mmol), phenyl hydrazine (10.81 g, 100 mmol).

Yield: 54.76%, white solid

MP: 146 °C

^{1}H NMR 400.13MHz $CDCl_3$: δ2.17(s,3H,CH_3), δ5.10(s,2H,CH_2), δ6.84-6.88(t,1H,Ar-H(4')), δ6.98(d,2H,J=9.0 Hz,Ar-H(3,5)), δ 7.14-7.45(m,10H,Ar-H(2',3',5',6',2'',3'',4'',5'',6''),NH), δ7.76(d,2H,J=9.04 Hz,Ar-H(2,6))

^{13}C NMR 100.61MHz $CDCl_3$: δ11.80(CH_3), δ69.60(O-CH_2), δ112.82(Ar-C(2',6')), δ114.08-114.28(Ar-C(3,5)), δ119.68-128.78(Ar-C(2,6,3',4',5',2'',3'',4'',5'',6'')), δ130.17(Ar-C(1)),δ135.71(Ar-C(1'')), δ 136.35(Ar-C(1')), δ 144.84(N=C-CH3),

δ158.68(Ar-C(4)

IR (KBr): C=N absorbance at 1600.77 cm^{-1}

6.2.2 Synthesis of (E)-1-(1-(4-bromophenyl)ethylidene)-2-phenylhydrazine 69

This product was obtained from 4-bromoacetophenone (19.9 g, 100 mmol), phenyl hydrazine (10.81 g, 100 mmol).

Yield: 52.34%, yellow solid

MP: 116 °C

^{1}H NMR 400.13MHz $CDCl_3$: δ 2.24(CH_3), δ6.90-6.94(t,1H,Ar-H(4')), δ7.19-7.22(m,2H,Ar-C(3',5'), δ7.29-7.34(m,3H,Ar-H(2',6'),NH), δ7.52(dd,2H,J=8.56 Hz,Ar-H(3,5)), δ7.69(dd,2H,J=8.56 Hz,Ar-H(2,6))

^{13}C NMR 100.61MHz $CDCl_3$: δ11.21(CH_3), δ112.79(Ar-C(2',6')), δ121.51(Ar-C(4)), δ126.53-130.95(Ar-C(2,3,5,6,3',5')), δ 137.54(Ar-C(1)), δ139.44(Ar-C(1')), δ144.47(N=C-CH_3)

IR (KBr): C=N absorbance at 1600.46 cm^{-1}

6.2.3 Synthesis of (E)-4-(1-(2-phenylhydrazono)ethyl)aniline 70

This product was obtained from 4-aminoacetophenone (13.5 g, 100 mmol), phenyl hydrazine (10.81 g, 100 mmol).

Yield: 31.91%, red brown solid

MP: 132 °C

^{1}H NMR 400.13MHz $CDCl_3$: δ2.21(s,3H,CH_3), δ6.71(d,2H,J=8.52 Hz,Ar-H(3,5)), δ6.87(m,1H,Ar-H(4')), δ7.18-7.31(m,4H,A-H(2',3',5',6')), δ6.64(dd,2H,J=8.56 Hz, Ar-H(2,6))

^{13}C NMR 100.61MHz $CDCl_3$: δ11.40(CH_3), δ112.62(Ar-C(2',6')), δ114.38(Ar-C(3,5)), δ119.24-128.75(Ar-C(3',4',5')), δ 141.50(Ar-C(1')), δ145.20(N=C-CH_3), δ146.03(Ar-C(4))

IR (KBr): C=N absorbance at 1598.51 cm^{-1}

6.2.4 Synthesis of (E)-1-phenyl-2-(1-phenylethylidene)hydrazine 71

This product was obtained from acetophenone (12.0 g, 100 mmol), phenyl hydrazine (10.81 g, 100 mmol).

Yield: 40.35%, brown solid

MP: 140 °C

^{1}H NMR 400.13MHz $CDCl_3$: δ 2.28(s,3H,CH_3), δ6.92-6.96(m,1H,Ar-H(4')),

δ7.23-7.25(m,2H,Ar-H(3',5')), δ7.32-7.37(m,4H,Ar-H(3,5,1',6')), δ7.42-7.46(m,1H,Ar-H(4)), δ7.85(dd,2H,J=7.52 Hz,Ar-H(2,6))

^{13}C NMR 100.61MHz $CDCl_3$: δ11.43(CH_3), δ112.78(Ar-C(2',6')), δ119.74-128.84(Ar-C(2,3,4,5,6,3',4',5')), δ138.71(Ar-C(1)), δ140.67(Ar-C(1')), δ144.78(N=C-CH_3)

IR (KBr): C=N absorbance at 1611.65 cm^{-1}

6.2.5 Synthesis of (E)-4-(1-(2-phenylhydrazono)ethyl)phenol 72

This product was obtained from 4-hydroxyacetophenone (13.6 g, 100 mmol), phenyl hydrazine (10.81 g, 100 mmol).

Yield: 67.65%, orange solid

MP: 110 °C

^{1}H NMR 400.13MHz $CDCl_3$: δ2.25(s,3H,CH_3), δ3.61(s,OH), δ6.74-6.78(m,1H,Ar-H(4')), δ6.86(dd,2H,J=6.52 Hz,Ar-H(3,5)), δ7.23-7.24(m,2H,Ar-H(3',5')), δ7.72(d,2H,J=8.52 Hz,Ar-H(2',6')), δ8.55(d,2H,J=8.04 Hz,Ar-H(2,6))

^{13}C NMR 100.61MHz $CDCl_3$: δ11.10(CH_3), δ112.36(Ar-C(2',6')), δ114.52(Ar-C(3,5)), δ118.33-130.78(Ar-C(2,6,3',4',5'), δ140.58(Ar-C(1')), δ146.15(N=C-CH_3), δ156.93(Ar-C(4))

IR (KBr) C=N absorbance at 1595.19 cm^{-1} , OH absorbance at 3460.82 cm^{-1}

6.2.6 Synthesis of (E)-1-(1-(4-methoxyphenyl)ethylidene)-2-phenylhydrazine 73

This product was obtained from 4-methoxyacetophenone (15.0 g, 100 mmol), phenyl hydrazine (10.81 g, 100 mmol).

Yield: 30.26%, white solid

MP: 138 °C

^{1}H NMR 400.13MHz $CDCl_3$: δ2.25(s,3H,-CH_3), δ 3.87(s,3H,O-CH_3), δ6.88-6.92(m,1H,Ar-H(4')), δ6.69-6.96(m,2H,Ar-H(3,5)), δ7.20(d,2H,J=8.04 Hz,Ar-C(2',6')), δ7.29-7.33(m,2H,Ar-H(3',5')), δ 7.78(dd,2H,J=9.0 Hz,Ar-H(2,6))

^{13}C NMR 100.61MHz $CDCl_3$: δ11.51(CH_3), δ54.90(O-CH_3), δ112.69(Ar-C(2',6')), δ113.26(Ar-C(3,5)), δ119.50-131.40(Ar-C(2,6,3',4',5')), δ141.05(Ar-C(1')), δ144.96(N=C-CH_3) , δ159.20(Ar-C(4))

IR (KBr): C=N absorbance at 1657.10 cm^{-1}

6.2.7 Synthesis of (E)-1-(1-(4-bromophenyl)ethylidene)-2-(4-methoxyphenyl)hydrazine 74

This product was obtained from 4-bromoacetophenone (19.9 g, 100 mmol), 4-methoxyphenyl hydrazine (13.8 g, 100 mmol).

Yield: 76.8%, brown solid

MP: 158 °C

^{1}H NMR 400.13MHz $CDCl_3$: δ 2.61(s,3H,CH_3), δ3.83(s,3H,O-CH_3), δ7.03(dd,2H,J=8.76 Hz,Ar-H(3',5')), δ 7.50-7.54(m,2H,Ar-H(2',6')), δ7.62-7.64(m,2H,Ar-H(3,5)), δ7.83-7.86(m.2H,Ar-H(2,6))

^{13}C NMR 100.61MHz $CDCl_3$: δ 26.11(CH_3), δ 55.22(O-CH_3), δ113.42-113.87(Ar-C(2',3',5',6')), δ 120.20(Ar-C(4)), δ124.41-129.40(Ar-C(2,3,5,6), δ 135.34(Ar-C(1')), δ138.41(Ar-C(1)), δ159.06(N=C-CH_3), δ 162.18(Ar-C(Ar-C(4'))

IR (KBr): C=N absorbance at 1587.49 cm^{-1}

6.2.8 Synthesis of (E)-1-(1-(3-fluoro-4-methoxyphenyl)ethylidene)-2-phenylhydrazine 75

This product was obtained from 3-fluoro-4-methoxy acetophenone (16.8 g, 100 mmol), phenyl hydrazine (10.81 g, 100 mmol).

Yield: 97.36%, light yellow solid

MP: 138 °C

^{1}H NMR 400.13MHz $CDCl_3$: δ2.22(s,3H,CH_3), 3.94(s,3H,O-CH_3), 6.90-6.93(m,1H,Ar-H(4')), 6.95-6.99(m,2H,Ar-H(3',5')), 7.19(d,2H,J=7.52 Hz, Ar-H(2',6')), 7.30-7.34(m,1H,Ar-H(5)), 7.46(d,1H,J=8.52 Hz,Ar-H(6)), 7.66(dd,1H,J=2.04,11.04 Hz,Ar-H(2))

^{13}C NMR 100.61MHz $CDCl_3$: δ11.21(CH_3), 55.84(O-CH_3), 112.28,112.81(Ar-C(2',6')),119.76(Ar-C(2)), 120.78, 120.81, 128.84, 132.16(Ar-C(5,6,3',4',5')), 139.28(Ar-C(1)), 144.68(N=C-CH_3), 147.14(Ar-C(1')), 150.70(Ar-C(4)), 153.13(Ar-C(3))

IR (KBr): C=N absorbance at 1619.61 cm^{-1}

6.2.9 Synthesis of (E)-1-phenyl-2-(1-(3,4,5-trimethoxyphenyl)ethylidene)hydrazine 76

This product was obtained from 3,4,5-trimethoxyacetophenone (21.0 g, 100 mmol), phenyl hydrazine (10.81 g, 100 mmol).

Yield: 90.2%, white solid

MP: 96 °C

^{1}H NMR 400.13MHz $CDCl_3$: δ2.26(s,3H,CH_3), 3.90,3.96(ds,9H,O-CH_3), 6.89-6.93(m,1H,Ar-H(4')), 7.06(s,2H,Ar-H(2,6)), 7.19(d,2H,J=8.04 Hz,Ar-H(2',6')), 7.28-7.36(m,3H,Ar-H(3',5'),NH)

^{13}C NMR 100.61MHz $CDCl_3$: δ11.75(CH_3), 55.78, 58.03, 60.51(O-CH_3), 102.53(Ar-C(2,6)), 112.70(Ar-C(2',6')), 119.77(Ar-C(4')), 128.84(Ar-C(3',5')), 134.50(Ar-C(1)), 137.91(Ar-C(1')), 140.42(Ar-C(4)), 144.68(N=C-CH_3), 152.64(Ar-C(3,5))

IR (KBr): C=N absorbance at 1599.92 cm^{-1}

6.2.10 Synthesis of (E)-1-(1-(4-iodophenyl)ethylidene)-2-phenylhydrazine 77

This product was obtained from 4-iodoacetophenone (24.6g, 100 mmol), phenyl hydrazine (10.81 g, 100 mmol).

Yield: 74.66%, orange solid

MP: 104 °C

^{1}H NMR 400.13MHz $CDCl_3$: δ2.23(s,3H,CH_3), 6.91-6.95(m,1H,Ar-H(4')), 7.20(d,2H,J=7.52 Hz,Ar-H(2',6')), 7.21-7.34(m,2H,Ar-H(3',5')), 7.56(dd,2H,J=2.0,8.52 Hz,Ar-H(2,6)), 7.72(m,2H,Ar-H(3,5))

^{13}C NMR 100.61MHz $CDCl_3$: δ11.22(CH_3), 93.27(Ar-C(4)), 112.83(Ar-C(2',6')), 120.04, 126.82, 128.86(Ar-C(2,6,3',4',5')), 136.93(Ar-C(3,5)), 138.03(Ar-C(1)),139.90(Ar-C(1')), 144.40(N=C-CH_3)

IR (KBr): C=N absorbance at 1600.39 cm^{-1}

6.2.11 Synthesis of (E)-2-methoxy-4-(1-(2-phenylhydrazono)ethyl)phenol 78

This product was obtained from 3-methoxy 4-hydroxyacetophenone (16.6 g, 100 mmol), phenyl hydrazine (10.81 g, 100 mmol).

Yield: 36.60%, light yellow solid

MP: 240 °C

^{1}H NMR 400.13MHz $CDCl_3$: δ 2.26(s,3H,CH_3), 4.00(s,3H,O-CH_3), 5.82(s,OH), 6.89-6.93(m,1H,Ar-H(4')), 6.95(d,1H,J=8.56 Hz,Ar-H(2)), 7.22(d,1H,J=2.0 Hz,Ar-H(5)), 7.18-7.20(m,2H,Ar-H(2',6')), 7.29-7.34(m,2H,Ar-H(3',5')), 7.56(d,1H,J=2.0 Hz,Ar-H(6))

^{13}C NMR 100.61MHz $CDCl_3$: δ 11.73(CH_3), 55.56(O-CH_3), 107.42,112.73,113.42,118.87, 119.64(2,5,6,2',6'), 128.82(Ar-C(3',5')),

130.92(Ar-C(1)), 144.89(N=C-CH_3), 145.85(Ar-C(3)), 146.17(Ar-C(4))

IR (KBr): C=N absorbance at 1603.16 cm^{-1}

6.2.12 Synthesis of (E)-1-(1-(3,4-dimethoxyphenyl)ethylidene)-2-phenylhydrazine 79

This product was obtained from 3, 4-dimethoxyacetophenone (18.0 g, 100 mmol), phenyl hydrazine (10.81 g, 100 mmol).

Yield: 94.39%, white solid

MP: 120 °C

^{1}H NMR 400.13MHz $CDCl_3$: δ2.28(s,3H,CH_3), 3.94,3.99(ds,6H,O-CH_3), 6.88-6.92(m,2H,Ar-H(5,4')), 7.17(d,2H,J=7.52 Hz,Ar-H(2',6')), 7.25(dd,1H,J=2.0,8.56 Hz,Ar-H(6)), 7.28-7.31(m,2H,Ar-H(3',5')), 7.58(d,1H,J=1.52 Hz,Ar-H(2))

^{13}C NMR 100.61MHz $CDCl_3$: δ11.80(CH_3), 55.51(O-CH_3), 108.04, 109.48, 110.04, 112.78(Ar-C(2,5,2',6')), 118.32, 119.74, 122.88, 128.82(Ar-C(6,3',4',5')), 131.08(Ar-C(1')), 144.78(N=C-CH3), 148.51(Ar-C(3)), 149.28(Ar-C(4))

IR (KBr): C=N absorbance at 1602.64 cm^{-1}

6.2.13 Synthesis of (E)-2,6-dibromo-4-(1-(2-phenylhydrazono)ethyl)phenol 80

This product was obtained from 3,5-dibromo 4-hydroxyacetophenone (29.4 g, 100 mmol), phenyl hydrazine (10.81g, 100 mmol).

Yield: 58.82%, red solid

MP: 163 °C

^{1}H NMR 400.13MHz $CDCl_3$: δ 2.19(s,3H,CH_3), 6.92-6.95(m,1H,Ar-H(4')), 7.18(d,2H,J=8.52 Hz,Ar-H(2',6')), 7.29(s,NH), 7.31-7.35(m,2H,Ar-H(3',5')), 7.90(s,2H,Ar-H(2,6))

^{13}C NMR 100.61MHz $CDCl_3$: δ 11.23(CH_3), 109.48(Ar-C(3,5)), 112.81(Ar-C(2',6')), 120.14, 128.56, 128.89(Ar-C(2,6,3',4',5')), 133.64(Ar-C(1)), 137.58(Ar-C(1')), 144.28(N=C-CH_3), 148.49(Ar-C(4))

IR (KBr): C=N absorbance at 1603.36 cm^{-1}

6.2.14 Synthesis of (E)-1-(1-(4-nitrophenyl)ethylidene)-2-phenylhydrazine 81

This product was obtained from 4-nitroacetophenone (16.5 g, 100 mmol), phenyl hydrazine (10.81 g, 100 mmol).

Yield: 42.66%, deep red solid

MP: 134 °C

^{1}H NMR 400.13MHz $CDCl_3$: δ 2.30(s,3H,CH_3), 6.96-6.70(m,1H,Ar-H(4')), 7.25(d,2H,J=8.52 Hz,Ar-H(2',6')), 7.33-7.37(m,2H,Ar-H(3',5')), 7.95(d,2H,J=9.0 Hz,Ar-H(2,6)), 8.24(d,2H,J=9.04 Hz,Ar-H(3,5))

^{13}C NMR 100.61MHz $CDCl_3$: δ11.04(CH_3), 113.04(Ar-C(2',6')), 120.75, 123.28, 125.28, 128.98(Ar-C(2,3,5,6,3',4',5')), 137.47(Ar-C(1')), 143.77(Ar-C(1)), 144.65(N=C-CH_3), 146.38(Ar-C(4))

IR (KBr): C=N absorbance at 1602.85 cm^{-1}

6.2.15 Synthesis of (E)-1-(1-(4-methoxy-3-nitrophenyl)ethylidene)-2-phenylhydrazine 82

This product was obtained from 3-nitro 4-methoxyacetophenone (19.5 g, 100 mmol), phenyl hydrazine (10.81 g, 100 mmol).

Yield: 87.05%, orange solid

MP: 152 °C

^{1}H NMR 400.13MHz $CDCl_3$: δ 2.24(s,3H,CH_3), 4.00(s,3H,O-CH_3), 6.91-6.95(m,1H,Ar-H(4')), 7.11(d,1H,J=8.52 Hz,Ar-H(5)), 7.19(d,2H,J=7.52 Hz,Ar-H(2',6')), 7.29(s,NH), 7.30-7.34(m,2H,Ar-H(3',5')), 8.05(dd,1H,J=2.48,9.0 Hz,Ar-H(6)), 8.23(d,1H,J=2.0 Hz,Ar-H(2))

^{13}C NMR 100.61MHz $CDCl_3$: δ11.15(CH_3), 56.21(O-CH_3), 112.79, 112.93(Ar-C(5,2',6')), 120.13, 122.04, 128.89(Ar-C(2,3',4',5')), 130.45(Ar-C(6)), 131.45(Ar-C(1)), 137.96(Ar-C(1')), 139.02(Ar-C(3)), 144.29(N=C-CH_3), 152.05(Ar-C(4))

IR (KBr): C=N absorbance at 1595.24 cm^{-1}

6.2.16 Synthesis of (E)-1-(1-(3-chloro-4-methoxyphenyl)ethylidene)-2-phenylhydrazine 83

This product was obtained from 3-chloro 4-methoxyacetophenone (18.5 g, 100 mmol), phenyl hydrazine (10.81 g, 100 mmol).

Yield: 80.80%, yellow solid

MP: 110 °C

^{1}H NMR 400.13MHz $CDCl_3$: δ 2.24(s,3H,CH_3), 3.95(s,3H,O-CH_3), 6.90(d,1H,J=9.0 Hz,Ar-H(5)), 6.92-6.96(m,1H,Ar-H(4')), 7.18(d,2H,J=7.52 Hz,Ar-H(2',6')), 7.30-7.34(m,2H,Ar-H(3',5')), 7.66(dd,1H,J=2.52,9.04 Hz,Ar-H(6)), 7.87(d,1H,J=2.0 Hz,Ar-H(2))

^{13}C NMR 100.61MHz $CDCl_3$: δ 11.56(CH_3), 55.81(O-CH_3), 110.81, 111.20, 112.83(Ar-C(5,2',6')), 119.91(Ar-C(4')), 122.11(Ar C(3)), 124.59, 127.05, 127.90, 128.37, 128.85(Ar-C(2,6,3',4',5')), 130.20(Ar-C(1)), 144.58(N=C-CH_3), 154.53(Ar-C(4))

IR (KBr): C=N absorbance at 1599.83 cm^{-1}

6.2.17 Synthesis of (E)-1-(4-methoxyphenyl)-2-(1-(4-methoxyphenyl)ethylidene)hydrazine 84

This product was obtained from 4-methoxyacetophenone (15.0 g, 100 mmol), 4-methoxyphenyl hydrazine (13.8 g, 100 mmol).

Yield: 90.52%, yellow solid

MP: 98 °C

^{1}H NMR 400.13MHz $CDCl_3$: δ 2.59(s,3H,CH_3), 3.84,3.89(ds,6H,O-CH_3), 6.88(d,2H,J=9.04 Hz,Ar-H(3,5)), 6.94(d,2H,J=8.56 Hz,Ar-H(3',5')), 7.78(d,2H,J=8.52 Hz,Ar-H(2',6')), 7.97(d,2H,J=8.52 Hz,Ar-(2,6))

^{13}C NMR 100.61MHz $CDCl_3$: δ 11.98(CH_3), 54.92,55.24(O-CH_3), 113.23,113.33,114.20(Ar-C(3,5,2',3',5',6')), 126.71(Ar-C(2,6)), 128.89(Ar-C(1)), 130.17(Ar-C(1')), 159.54(Ar-C(4))

IR (KBr): C=N absorbance at 1607.30 cm^{-1}

6.2.18 Synthesis of (E)-1-(2,4-dinitrophenyl)-2-(1-(4-methoxyphenyl)ethylidene)hydrazine 85

This product was obtained from 4-methoxyacetophenone (15.0 g, 100 mmol), 2,4-dinitrophenyl)hydrazine (19.8 g, 100 mmol).

Yield: 85.76%, dark red solid

MP: 108 °C

^{1}H NMR 400.13MHz $CDCl_3$: δ 2.47(s,3H,CH_3), 3.91(s,3H,O-CH_3), 7.00(d,2H,J=9.0 Hz,Ar-H(3,5)), 7.29(s,NH), 7.86(dd,2H,J=2.28,9.04 Hz,Ar-H(2,6)), 8.14(dd,1H,J=0.76,2.76 Hz,Ar-H(6')), 8.37(d,1H,Ar-H(5')), 9.19(s,1H,Ar-H(3'))

^{13}C NMR 100.61MHz $CDCl_3$: δ13.56(CH_3), 55.46(O-CH_3), 114.08(Ar-C(3,5)), 116.70(Ar-C(6')), 123.63(Ar-C(3')), 128.07(Ar-C(2,6)), 129.74(Ar-C(1)), 130.06(Ar-C(5')), 137.95(Ar-C(2')), 140.57(Ar-C(4')), 144.99(N=C-CH_3), 152.17(Ar-C(1')), 161.35(Ar-C(4))

EIMS (HR): $C_{15}H_{15}N_4O_5$ calculated [M^++H]331.1042, observed [M^++H] 331.1058.

IR (KBr): C=N absorbance at 1615.30 cm^{-1}

6.3 General procedure for preparation of pyrazole carbaldehydes

Dimethylformamide (2.58 g, 35.3 mmol) and phosphorous oxychloride (5.4 g, 35.3 mmol) were previously cooled separately to 0 °C before being stirred at this temperature. A solution of phenylhydrazone (c. 3 g, 14.26 mmol.) in DMF (3 mL) was added drop-wise to the reaction mixture which was then warmed to room temperature and then heated at 70-80 °C for 3-5 h. After cooling to room temperature the mixture was basified with a cool saturated K_2CO_3 solution. The solution was filtered and washed with water and the product recrystallized from ethanol. The final product was filtered, washed with hexane and dried.

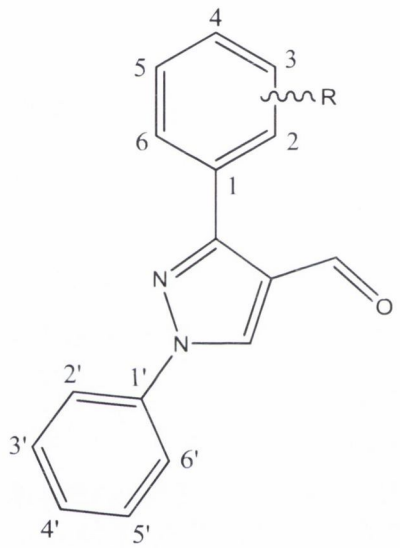

6.3.1 Synthesis of 3-(4-(benzyloxy)phenyl)-1-phenyl-*1H*-pyrazole-4-carbaldehyde 143

The product was obtained from *1*-(1-(4-(benzyloxy)phenyl)ethylidene)-2-phenylhydrazine(3.96 g, 14.26 mmol), dimethylformamide (2.58 g, 35.3 mmol) and phosphorous oxychloride (5.4 g, 35.3 mmol).

Yield: 69.2%, light brown solid

MP: 148-150 °C

^{1}H NMR (400.13MHz, $CDCl_3$): δ 5.17 (s, 2H, Ar-CH_2-O),

7.13(dd,2H,J=2.0,8.52 Hz,Ar-H(3,5)),

7.29-7.56(m,8H,Ar-H(3',4',5',2'',3'',4'',5'',6'')),

7.80-7.82(m,4H,Ar-H(2,6,2',6')), 8.55(s,1H,N-C<u>H</u>=C), 10.06(s,1H,C<u>H</u>=O)

^{13}C NMR (100.61MHz, $CDCl_3$): δ 69.64(O-<u>C</u>H_2), 114.70, 116.80,

119.31(Ar-C(3,5,2',6')), 121.84(Ar-C(1)), 123.55(N-<u>C</u>H=C), 119.31,

121.84(Ar-C(2',6')), 123.55(Ar-C(1)), 127.07, 127.51, 127.66, 128.22, 129.25, 129.86, 130.8, 131.96(Ar-C(2,6,3',4',5',2'',3'',4'',5'',6'')), 136.21(Ar-C(1'')), 138.54(Ar-C(1')), 154.47 (N=CH-), 159.30(Ar-C(4)), 184.95(C=O).

EIMS (HR): $C_{23}H_{18}N_2O_2$ calculated $[M^+ +Na]$ 377.1266,
observed $[M^+ +Na]$ 377.1277.

IR (KBr) C=O absorbance at 1669.36cm^{-1}

6.3.2 Synthesis of 3-(4-bromophenyl)-1-phenyl-*1H*-pyrazole-4-carbaldehyde 144

The product was obtained from 1-(1-(4-bromophenyl)ethylidene)-2-phenylhydrazine(3.92g, 14.26 mmol), dimethylformamide (2.58 g, 35.3 mmol) and phosphorous oxychloride(5.4 g, 35.3 mmol).

Yield: 87.5%, yellow solid

MP: 138 ^oC

^{1}H NMR 400.13MHz $CDCl_3$: δ 7.44(m,1H,Ar-H(4')), 7.54(d,2H,J=8.0 Hz,Ar-H(2',6')), 7.66(d,2H,J=8.56 Hz, Ar-H(3,5)), 7.78-7.82(m,4H,Ar-H(2,6,3',5')), 8.56(s,1H,N-CH=C), 10.06(s,1H,CH=O)

^{13}C NMR 100.61MHz $CDCl_3$: δ119.31(Ar-C(2',6'), 122.04(Ar-C(4')), 127.70,129.31, 129.84,(Ar-C(2,6,3',4',5')), 130.00(N-CH=C), 131.45, 131.57(Ar-C(3,5)), 138.44(Ar-C(1')), 148.68(N=C-C), 184.02(C=O)

IR (KBr): C=O absorbance at 1670.40.cm^{-1}

6.3.3 Synthesis of 3-(4-amino-phenyl)-1-phenyl-*1H*-pyrazole-4-carbaldehyde 145

The product was obtained from 4-[1-(phenyl-hydrazono)-ethyl]-phenylamine (3.75 g, 14.26 mmol), dimethylformamide (2.58 g, 35.3 mmol) and phosphorous oxychloride (5.4 g, 35.3 m mol).

Yield: 90.8%, dark brown solid

MP: 176-180 ^oC

^{1}H NMR (400.13MHz, $CDCl_3$): δ7.11(d,2H,J=8.56 Hz,Ar-H(3,5)), 7.39-7.43(m,1H,Ar-H(4')), 7.53(d,2H,J=8.0 Hz,(Ar-H(3',5')), 7.75(dd, 2H,J=2.0, 8.52 Hz,Ar-H(2,6)), 7.82(dd, 2H, J=2.0, 8.0 Hz Ar-H(2',6')), 8.55(N-CH=C), 10.09(CH=O).

^{13}C NMR (100.61MHz,$CDCl_3$): δ119.28(Ar-C(3,5)), 121.05,121.94(Ar-C(2',6')), 124.82(Ar-C(4')), 127.36(Ar-C(2,4)), 129.20,129.30(Ar-C(3',5')), 130.24(N-CH=C), 138.66(Ar-C(1')), 152.76(N=C), 153.10(Ar-C(4)), 185.19(C=O)

EIMS (HR): $C_{16}H_{14}N_3O$ calculated $[M+H]^+$ 264.1137, observed $[M+H]^+$ 264.1142.

IR (KBr): C=O absorbance at 1675.25cm^{-1}

6.3.4 Synthesis of 1,3-diphenyl-*1H*-pyrazole-4-carbaldehyde 146

The product was obtained from (E)-1-phenyl-2-(1-phenylethylidene)hydrazine(3.54 g, 14.26 mmol), dimethylformamide (2.58 g, 35.3 mmol) and phosphorous oxychloride (5.4 g, 35.3 mmol)

Yield: 91.3%, yellow solid

MP: 142 ^oC

^{1}H NMR 400.13MHz $CDCl_3$: δ7.32-7.35(m,1H,Ar-H(4)), 7.41-7.48(m,5H,Ar-H(3,5,3',4',5')), 7.73-7.77(m,4H,Ar-H(2,6,2',6')), 8.49(s,1H,N-C<u>H</u>=C), 10.00(s,1H,CH=O)

^{13}C NMR 100.61MHz $CDCl_3$: δ119.33(Ar-C(2',6'), 122.06(Ar-C(4')), 127.55, 128.35, 128.53, 128.87, 129.26(Ar-H(2,3,4,5,6,3',5')), 130.48(N-<u>C</u>H=C), 138.57(Ar-C(1')), 154.40(N=<u>C</u>-C), 184.83(C=O)

EIMS (HR): $C_{16}H_{13}N_2O$ calculated $[M^+ +H]$249.1028, observed $[M^+ +H]$ 249.1022.

IR (KBr): C=O absorbance at 1675.54.cm^{-1}

6.3.5 Synthesis of 3-(4-hydroxyphenyl)-1-phenyl-*1H*-pyrazole-4-carbaldehyde 147

The product was obtained from 4-(1-(2-phenylhydrazono)ethyl)phenol (3.23 g, 14.26 mmol), dimethylformamide (2.58 g, 35.3 mmol) and phosphorous oxychloride (5.4 g, 35.3 mmol).

Yield: 73.37%, brown solid

MP: 216-220 ^oC

^{1}H NMR 400.13MHz $CDCl_3$: δ6.99(d,2H,J=8.56 Hz,Ar-H(3,5)), 7.42-7.46(m,1H,Ar-H(4')), 7.57-7.61(m,2H,Ar-H(3',5')), 7.90(d,2H,J=8.52 Hz,Ar-H(2,6)), 8.02(d,2H,J=8.04 Hz,Ar-H(2',6')), 9.02(s,1H,N-C<u>H</u>=C), 10.06(s,1H,CH=O)

^{13}C NMR 100.61MHz $CDCl_3$: δ114.75(Ar-C(3,5), 118.79(Ar-C(2',6')), 122.62(Ar-C(4')), 127.04, 129.15, 129.84(Ar-C(2,6,3',5')), 133.13(N-<u>C</u>H=C), 138.80(Ar-C(1')), 152.92(N=<u>C</u>-C), 158.04(Ar-C(4)), 183.60(C=O)

EIMS (HR): $C_{16}H_{12}N_2O_2K$ calculated $[M+K]^+$ 303.0536, observed $[M+K]^+$ 303.0527.

IR (KBr): C=O absorbance at 1685.38 cm^{-1}

6.3.6 Synthesis of 3-(4-methoxyphenyl)-1-phenyl-*1H*-pyrazole-4-carbaldehyde 148

The product was obtained from 1-(1-(4-methoxyphenyl)ethylidene)-2-phenylhydrazine(3.43 g, 14.26 mmol), dimethylformamide (2.58 g, 35.3 mmol) and phosphorous oxychloride(5.4 g, 35.3 mmol).

Yield: 70.01%, white solid

MP: 138-140 °C

^{1}H NMR 400.13MHz $CDCl_3$: δ3.90(s,3H,O-CH_3), 7.05(d,2H,J=9.04 Hz,Ar-H(3,5)), 7.41(m,1H,Ar-H(4')), 7.51-7.55(m,2H,Ar-H(3',5')), 7.80-7.83(m,2H,Ar-H(2,6,2',6')), 8.55(s,1H,N-C<u>H</u>=C), 10.06(s,1H,CH=O)

^{13}C NMR 100.61MHz $CDCl_3$: δ113.75(Ar-C(3,5), 119.26(Ar-C(2',6')), 121.89(Ar-C(1)), 123.38(Ar-C(4')), 127.44, 129.23, 129.82(Ar-C(2,6,3',5')), 130.74(N-<u>C</u>H=C), 138.59(Ar-C(1')), 154.08(N=<u>C</u>-C), 160.09(Ar-C(4)), 184.77(C=O)

IR (KBr): C=O absorbance at 1672.02 cm^{-1}

6.3.7 Synthesis of 3-(4-bromophenyl)-1-(4-methoxyphenyl)-*1H*-pyrazole-4-carbaldehyde 149

The product was obtained from 1-(1-(4-bromophenyl)ethylidene)-2-(4-methoxyphenyl)hydrazine(4.55g, 14.26 mmol), dimethylformamide (2.58 g, 35.3 mmol) and phosphorous oxychloride (5.4 g, 35.3 mmol)

Yield: 19.71%, brown solid

MP: 156-158 °C

^{1}H NMR 400.13MHz $CDCl_3$: δ 3.88(s,3H,O-CH_3), 7.01-7.04(m,2H,Ar-H(3',5')), 7.63-7.65(m,2H,Ar-H(3,5)), 7.68-7.70(m,2H,Ar-H(2',6')), 7.75-7.78(m,2H,Ar-H(2,6)), 8.45(s,1H,N-C<u>H</u>=C), 10.03(s,1H,CH=O)

^{13}C NMR 100.61MHz $CDCl_3$: δ55.66(O-CH_3), 114.77(Ar-C(3',5'), 121.89(Ar-C(1)), 122.20(Ar-C(4)), 123.64(Ar-C(2,6)), 130.44(N-<u>C</u>H=C), 131.80, 131.88(Ar-C(3,5)),132.45(Ar-C(1')), 159.41(Ar-C(4')), 184.48(C=O)

IR (KBr): C=O absorbance at 1667.59 cm^{-1}

6.3.8 Synthesis of 3-(3-fluoro-4-methoxyphenyl)-1-phenyl-*1H*-pyrazole-4-carbaldehyde 150

The product was obtained from 1-(1-(3-fluoro-4-methoxyphenyl)ethylidene)-2-phenylhydrazine (3.68 g, 14.26 mmol), dimethylformamide (2.58 g, 35.3 mmol) and phosphorous oxychloride (5.4 g, 35.3 mmol).

Yield: 90.1%, yellow solid

MP: 250 °C

^{1}H NMR 400.13MHz $CDCl_3$: δ3.99(s,3H,O-CH_3), 7.08-7.13(m,1H,Ar-H(5)), 7.41-7.45(m,1H,Ar-H(4')), 7.53-7.57(m,2H,Ar-H(3',5')), 7.66-7.73(m,2H,Ar-H(2,6)), 7.81(d,2H,J=7.52 Hz,Ar-H(2',6')), 8.55(s,1H,N-C<u>H</u>=C), 10.08(s,1H,CH=O)

^{13}C NMR 100.61MHz $CDCl_3$: δ55.85(O-CH_3), 112.77(Ar-C(5)), 116.02(Ar-C(2)), 119.25(Ar-C(2',6')), 121.94(Ar-C(1)), 124.66, 127.60, 129.28(Ar-C(6,3',4',5')), 131.54(N-<u>C</u>H=C), 138.46(Ar-C(1')), 150.64(Ar-C(4)), 152.60(Ar-C(3)), 153.08(N=<u>C</u>-C), 184.12(C=O)

IR (KBr): C=O absorbance at 1674.51 cm^{-1}

6.3.9 Synthesis of 1-phenyl-3-(3,4,5-trimethoxyphenyl)-*1H*-pyrazole-4-carbaldehyde 151

The product was obtained from 1-phenyl-2-(1-(3,4,5-trimethoxyphenyl)ethylidene)hydrazine(4.28 g, 14.26 mmol), dimethylformamide (2.58 g, 35.3 mmol) and phosphorous oxychloride(5.4 g, 35.3 mmol).

Yield: 58.60%, white solid

MP: 220 °C

^{1}H NMR 400.13MHz $CDCl_3$: δ3.95,3.98(ts,9H,O-CH_3), 7.16(s,2H,Ar-H(2,6)), 7.41-7.45(m,1H,Ar-H(4')), 7.54-7.58(m,2H,Ar-H(3',5')), 7.82(d,1H,J=2.24 Hz,Ar-H(2',6')), 8.57(s,1H,N-C<u>H</u>=C), 10.10(s,1H,CH=O)

^{13}C NMR 100.61MHz $CDCl_3$: δ56.31,61.00(O-CH_3), 106.16(Ar-C(2,6)), 119.82(Ar-C(2',6')), 122.50(Ar-C(1)), 126.73(Ar-C(4)), 128.10, 129.75(Ar-C(3',4',5')), 131.88(N-<u>C</u>H=C), 138.94(Ar-C(1')), 153.47(N=<u>C</u>-C), 154.49(Ar-C(3,5)), 184.96(C=O)

EIMS (HR): $C_{19}H_{18}N_2O_4$ calculated [M^++H]339.1267, observed [M^++H] 339.1246.

IR (NaCl/KBr): C=O absorbance at 1688.51 cm^{-1}

6.3.10 Synthesis of 3-(4-iodo-phenyl)-1-phenyl-*1H*-pyrazole-4-carbaldehyde 152

The product was obtained from N-[1-(4-iodo-phenyl)-ethylidene]-N'-phenyl-hydrazine (5.35 g, 14.26 mmol), dimethylformamide (2.58 g, 35.3 mmol) and phosphorous oxychloride (5.4 g, 35.3 mmol).

Yield: 90%, light brown solid

MP: 154 °C

^{1}H NMR 400.13MHz $CDCl_3$: δ 7.41-7.45(m,1H,Ar-H(4')),

7.54(d,2H,J=8.0 Hz,Ar-H(3',5')), 7.65(d,2H,J=8.52 Hz,Ar-H(2',6')),
7.79-7.87(m,4H,Ar-H(2,3,5,6)), 8.56(N-CH=C), 10.06(CH=O).

^{13}C NMR (100.61MHz,$CDCl_3$): δ 95.14(Ar-C(4)), 119.30(Ar-C(2',6')),
122.02(Ar-C(4')), 127.69(Ar-C(1)), 129.30, 130.12, 130.40, 131.55(Ar-C(2,6,3',5')),
137.41(Ar-C(3,5)), 138.43(Ar-C(1')), 152.91(N=C), 184.05(CH=O).

EIMS (HR): $C_{16}H_{12}IN_2O$ calculated $[M+H]^+$ 374.9994, observed $[M+H]^+$ 375.0002.

IR (KBr): C=O absorbance at 1671.65cm^{-1}

6.3.11 Synthesis of 3-(3,4-dimethoxy-phenyl)-1-phenyl-*1H*-pyrazole-4-carbaldehyde 153

The product was obtained from N-[1-(3,4-dimethoxy-phenyl)-ethylidene]-N'-phenyl-hydrazine (4.40g, 14.26 mmol), dimethylformamide (2.58 g, 35.3 mmol) and phosphorous oxychloride (5.4 g, 35.3 mmol)

Yield: 60.85%, white solid

MP: 130 °C

^{1}H NMR 400.13MHz $CDCl_3$: δ3.98-4.00(ds,6H,CH_3),
7.01(d,1H,J=8.28 Hz,Ar-H(5)), 7.29(s,1H,Ar-H(2)),
7.41-7.56(m,4H,Ar-H(6,3',4',5',)), 7.81-7.83(m,2H,Ar-H(2',6')),
8.55(s,1H,N-CH=C), 10.08(s,1H,CH=O).

^{13}C NMR 100.61MHz $CDCl_3$: δ56.01,56.06(O-CH_3), 110.64(Ar-C(2)),
111.14,111.78(Ar-C(2,5,)), 119.78(Ar-C(6)), 121.88, 122.44(Ar-C(2',6')),
127.96(Ar-C(2',5')), 129.7(Ar-C(4')), 131.57(N-CH=C), 139.02(Ar-C(1')),
149.15(Ar-C(4)), 150.11(Ar-C(3)), 154.50(N=C-C), 185.13(C=O).

EIMS (HR): $C_{18}H_{17}N_2O_3$ calculated $[M+H]^+$ 309.1239, observed $[M+H]^+$ 309.1248.

IR (KBr): C=O absorbance at 1669.24.cm^{-1}

6.3.12 Synthesis of 3-(3,5-dibromo-4-hydroxyphenyl)-1-phenyl-*1H*-pyrazole-4-carbaldehyde 154

The product was obtained from 2,6-dibromo-4-(1-(2-phenylhydrazono)ethyl)phenol(5.48 g, 14.26 mmol), dimethylformamide (2.58 g, 35.3 mmol) and phosphorous oxychloride(5.4 g, 35.3 mmol).

Yield: 81.90%, brown solid

MP: 250 °C

^{1}H NMR 400.13MHz $CDCl_3$: δ4.91(s,OH), 7.40-7.44(m,1H,Ar-H(4')),
7.54-7.58(m,2H,Ar-H(3',5')), 7.89-7.92(m,2H,Ar-H(2',6')), 7.99(s,2H,Ar-H(2,6)),

8.89(s,1H,N-CH=C), 9.98(s,1H,CH=O)

^{13}C NMR 100.61MHz $CDCl_3$: δ114.74(Ar-C(3,5)), 119.27(Ar-C(2',6')), 121.72(Ar-C(1)), 127.37, 129.33(Ar-C(3',4',5')), 133.08(Ar-C(2,6)), 131.63(N-CH=C), 139.08(Ar-C(1')), 153.25(N=C-C), 162.43(Ar-C(4)), 185.05(C=O)

IR (KBr): C=O absorbance at 1663.12 cm^{-1}, OH absorbance at 3139.76 cm^{-1}

6.3.13 Synthesis of 3-(4-nitrophenyl)-1-phenyl-*1H*-pyrazole-4-carbaldehyde 155

The product was obtained from1-(1-(4-nitrophenyl)ethylidene)-2-phenylhydrazine(3.64 g, 14.26 mmol), dimethylformamide (2.58 g, 35.3 mmol) and phosphorous oxychloride(5.4 g, 35.3 mmol).

Yield: 90.2%, red solid

MP: 162-164 °C

^{1}H NMR 400.13MHz $CDCl_3$: δ7.45-7.49(m,1H,Ar-H(4')), 7.56-7.60(m,2H,Ar-H(3',5')), 7.83(d,2H,J=8.04 Hz,Ar-H(2',6')), 8.19(d,2H,J=8.56 Hz,Ar-H(2,6)), 8.37(d,2H,J=8.52 Hz,Ar-H(3,5)), 8.61(s,1H,N-CH=C), 10.11(s,1H,CH=O)

^{13}C NMR 100.61MHz $CDCl_3$: δ119.34(Ar-C(2',6')), 122.50(Ar-C(1)), 123.38(Ar-C(3,5)), 128.03, 129.26, 129.41(Ar-C(2,6,3',4',5')), 133.15(N-CH=C), 138.24(Ar-C(1')), 147.71(Ar-C(4)), 150.88(N=C-C), 183.17(C=O)

EIMS (HR): $C_{16}H_{11}N_3O_3$ calculated $[M+H]^+$ 294.0800, observed $[M+H]^+$ 294.0844.

IR (KBr): C=O absorbance at 1685.15 cm^{-1}

6.3.14 Synthesis of 3-(4-methoxy-3-nitrophenyl)-1-phenyl-*1H*-pyrazole-4-carbaldehyde 156

The product was obtained from1-(1-(4-methoxy-3-nitrophenyl)ethylidene)-2-phenylhydrazine(4.07 g, 14.26 mmol), dimethylformamide (2.58 g, 35.3 mmol) and phosphorous oxychloride (5.4 g, 35.3 mmol).

Yield: 97.5%, brown solid

MP: 162 °C

^{1}H NMR 400.13MHz $CDCl_3$: δ4.06(s,3H,O-CH_3), 7.22(d,1H,J=8.8 Hz,Ar-H(5)), 7.29(s,1H,Ar-H(2)), 7.42-7.46(m,1H,Ar-H(4')), 7.54-7.58(m,2H,Ar-H(3',5')), 7.81(d,2H,J=8.52 Hz,Ar-H(2',6')), 8.24(dd, H,J=2.24,8.76 Hz,Ar-H(6)), 8.56(s,1H,N-CH=C), 10.07(s,1H,CH=O)

^{13}C NMR 100.61MHz $CDCl_3$: δ56.73(O-CH_3), 113.49(Ar-C(5)), 119.69(Ar-C(2',6')),122.47(Ar-C(1)), 126.05, 128.25, 129.81(Ar-C(2,3',4',5')), 133.67(N-CH=C), 134.54(Ar-C(6)), 138.75(Ar-C(3)), 139.66(Ar-C(1')), 151.10(N=C-C), 153.51(Ar-C(4)), 183.68(C=O)

IR (KBr): C=O absorbance at 1687.60 cm^{-1}

6.3.15 Synthesis of 3-(3-chloro-4-methoxyphenyl)-1-phenyl-*1H*-pyrazole-4-carbaldehyde 157

The product was obtained from1-(1-(3-chloro-4-methoxyphenyl)ethylidene)-2-phenylhydrazine(3.92 g, 14.26 mmol), dimethylformamide (2.58 g, 35.3 mmol) and phosphorous oxychloride(5.4 g, 35.3 mmol).

Yield: 89.3%, yellow solid

MP: 136 °C

^{1}H NMR 400.13MHz $CDCl_3$: δ4.00(s,3H,O-CH_3), 7.07(d,1H,J=8.52 Hz,Ar-H(5)), 7.29(s,1H,Ar-H(2)), 7.41-7.45(m,1H,Ar-H(4')),7.53-7.57(m,2H,Ar-H(3',5')), 7.81(dd,2H,J=1.28,9.28 Hz,Ar-H(2',6')), 7.97(d,2H,J=2.0 Hz,Ar-H(6)), 8.55(s,1H,N-CH=C), 10.07(s,1H,CH=O)

^{13}C NMR 100.61MHz $CDCl_3$: δ56.29(O-CH_3), 111.94(Ar-C(5)), 119.74(Ar-C(2',6')), 122.40(Ar-C(1)), 124.75(Ar-C(3)), 128.06, 128.56, 129.74, 130.55(Ar-C(2,6,3',4',5')), 131.98(N-CH=C), 138.94(Ar-C(1')), 152.91(N=C-C), 155.89(Ar-C(4)), 184.55(C=O)

IR (KBr): C=O absorbance at 1668.29 cm^{-1}

6.3.16 Synthesis of 1-(2,4-dinitrophenyl)-3-(4-methoxyphenyl)-*1H*-pyrazole-4-carbaldehyde 158

The product was obtained from1-(2,4-dinitrophenyl)-2-(1-(4-methoxyphenyl)ethylidene)hydrazine(4.71g, 14.26 mmol), dimethylformamide (2.58 g, 35.3 mmol) and phosphorous oxychloride(5.4 g, 35.3 mmol).

Yield: 49.71%, dark brown solid

MP: 102 °C

^{1}H NMR 400.13MHz $CDCl_3$: δ3.90(s,3H,O-CH_3), 7.03(d,2H,J=8.76 Hz,Ar-H(3,5)), 7.72(dd,2H,J=2.24,9.0 Hz, Ar-H(2,6)), 8.45(s,1H,N-CH=C), 8.45(s,1H,Ar-H(3')), 8.60(dd,1H,J=2.52,8.8 Hz,Ar-H(5')), 8.80(d,1H,J=2.52 Hz,Ar-H(6')), 10.09(s,1H,CH=O)

^{13}C NMR 100.61MHz $CDCl_3$: δ55.43(O-CH_3), 114.08, 114.37(Ar-C(3,5)),

121.38(Ar-C(3')), 122.48(Ar-C(1)), 126.29, 127.79, 130.34, 134.65(Ar-C(2,6,5',6'), 131.23(N-CH=C), 136.52(Ar-C(1')), 143.72(Ar-C(2')), 146.56(Ar-C(4')), 155.96(N=C-C), 161.08(Ar-C(4)), 184.59(C=O)

EIMS (HR): $C_{17}H_{12}N_4O_6$ calculated $[M+Na]^+$ 391.0655,

observed $[M+Na]^+$ 391.0665.

IR (KBr): C=O absorbance at 1686.87 cm^{-1}

6.4 General procedure for synthesis of pyrazole 1,4-dihydropyridines

The pyrazole carbaldehyde product from last step (0.074 g, 0.3 mmol), ethylacetoacetate (0.195 g , 1.5 mmol) (or methylacetoacetate) and 33% NH_4OH (0.159 g, 1.5 mmol) were refluxed in 40 mL ethanol (80 °C) for approximately 16 h. The mixture was stirred until reaction was almost complete as monitored by TLC. The completed reaction was diluted and quenched with ice-water.The aqueous layer was further extracted with $CHCl_3$ (3x20 mL). The organic layers was dried with anhydrous Na_2SO_4, filtered using the funnel with cotton wool; then followed solvent reduction by rotary evaporation and recrystallisation from a minimum volume of ethanol, and washed with hexane. The product was finally purified using column chromatography (Biotage SP1 instrument) to obtain yields of 13%-46%.

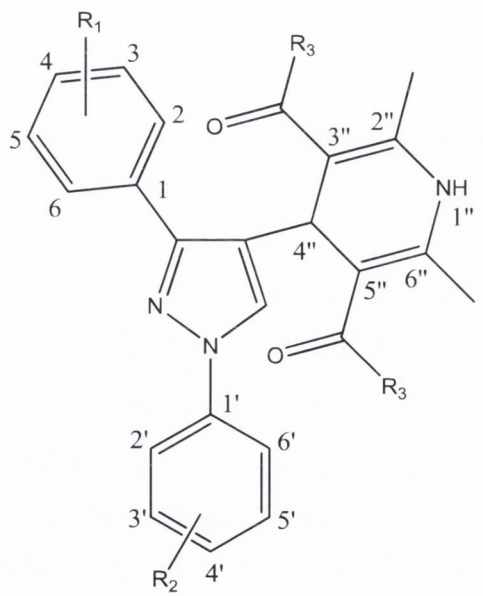

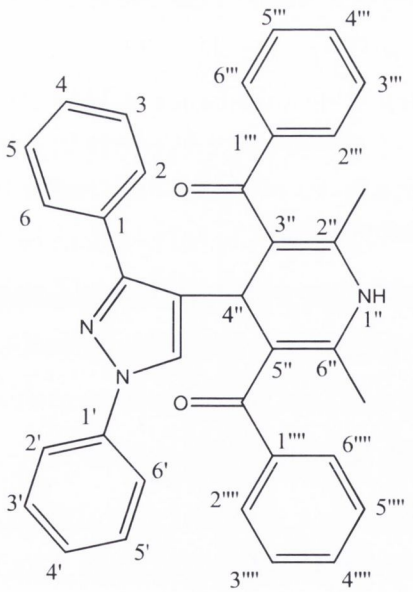

6.4.1 Synthesis of 2,6-dimethyl-4-[3-(4-phenoxy-phenyl)-1-phenyl-*1H*-pyrazol-4-yl]-1,4-dihydro-pyridine-3,5-dicarboxylic acid diethyl ester 161

This product was obtained from 3-benzyloxy-1-phenyl-1H-pyrazole-4-carbaldehyde (0.106 g, 0.3 mmol), ethylacetoacetate (0.195 g, 1.5 mmol) and 33% NH_4OH(0.159 g, 1.5 mmol).

Yield: 7.79%, white solid

MP: 196 °C

^{1}H NMR (400.13MHz, $CDCl_3$): δ1.07(t, 6H, J=7.52 Hz,CH_2-$C\underline{H}_3$), 2.15 (s, 6H, -$C\underline{H}_3$), 3.79-3.84 (m, 2H, $C\underline{H}_2$-CH_3), 3.97-4.02 (m, 2H,$C\underline{H}_2$-CH_3), 5.14 (s, 1H, C-H(4'')), 5.21(s,1H, O-$C\underline{H}_2$-Ar), 7.00(d,2H,J=9.0 Hz,Ar-H(3,5)), 7.18-7.22(m,2H,Ar-H(3''',5''')), 7.29-7.31(m,1H,Ar-H(4''')), 7.36-7.46(m,5H,Ar-H(2,6,4',2''',6''')), 7.64-7.68(m,4H,Ar-H(2',3',5',6')), 7.69(s,1H,N-CH=C)

^{13}C NMR(100.61MHz.$CDCl_3$): δ 13.88 (-$CH_2\underline{C}H_3$), 19.07 (-CH_3), 29.35 (-CH(4'')), 59.25(-$\underline{C}H_2CH_3$), 69.39(O-CH_2), 103.70(-C(3'',5'')), 114.04(Ar-C(3,5)), 118.24(Ar-C(2',6')), 125.37, 126.39, 126.96, 127.30, 127.50, 127.87, 128.16, 128.75(ArC(2,6,3',4',5',2''',3''',4''',5''',6''')), 129.83(Ar-C(1), 136.83(Ar-C(1''')), 142.75(C(2'',6'')), 150.78(N=C-), 157.63(Ar-C(4)), 167.12(C=O).

EIMS (HR): $C_{35}H_{36}N_3O_5$ calculated $[M+H]^+$ 578.2655, observed $[M+H]^+$ 578.2664.

IR (NaCl/KBr): C=N absorbance 1600.36 cm^{-1}, C=O absorbance at 1690.27 cm^{-1}, C-O-ester absorbance at 1209.18 cm^{-1}.

6.4.2 Synthesis of 4-[3-(4-bromo-phenyl)-1-phenyl-*1H*-pyrazol-4-yl]-2,6-dimethyl-1,4-dihydro-pyridine-3,5-dicarboxylic acid diethyl ester 162

This product was obtained from 3-(4-bromo-phenyl)-1-phenyl-1H-pyrazole-4-carbaldehyde (0.098 g, 0.3 mmol), ethylacetoacetate(0.195 g, 1.5 mmol) and 33% NH_4OH(0.159 g, 1.5 mmol).

Yield: 7.9%, dark yellow solid

MP: 158-160 °C

^{1}H NMR (400.13MHz $CDCl_3$): δ 1.10(t, 6H,J=7.04 Hz, CH_2-$C\underline{H}_3$), 2.29 (s, 6H, -CH_3), 3.77-3.86 (m, 2H, $C\underline{H}_2$-CH_3), 4.03-4.06(m, 2H, $C\underline{H}_2$-CH_3), 5.29 (s, 1H, C-H(4'')), 5.58(s, N-H), 7.25-7.29(m,1H,Ar-H(4')), 7.41-7.45(m,2H,Ar-H(3',5')), 7.58(d,2H,J=8.52 Hz,Ar-H(3,5)), 7.68(d,2H,J=8.52 Hz,Ar-H(2',6')), 7.76(s,1H,N-CH=C),

7.83(d,2H,J=8.52 Hz,Ar-H(2,6))

^{13}C NMR (100.61MHz, $CDCl_3$): δ 13.86 (-$CH_2\underline{C}H_3$), 19.17 (-CH_3), 29.18 (-CH(4'')), 59.37 (-$\underline{C}H_2CH_3$), 104.08 (-C(3'',5'')), 118.41(Ar-C(2',6')), 121.13(Ar-C(4)), 125.74, 126.95, 128.42, 128.83, 130.08, 130.57(Ar-C(2,3,5,6,3',4',5')), 133.37 (Ar-C(1)), 139.50(Ar-C(1')), 142.87(C(2'',6'')), 149.31(C(3'',5'')), 167.01(C=O).

EIMS (HR): $C_{28}H_{29}BrN_3O_4$ calculated $[M+H]^+$: 550.1341, observed $[M+H]^+$: 550.1328

IR (NaCl/KBr): C=N absorbance 1599.45 cm^{-1}, C=O absorbance at 1677.71 cm^{-1}, C-O-ester absorbance at 1210.65 cm^{-1}.

6.4.3 Synthesis of 4-[3-(4-amino-phenyl)-1-phenyl-*1H*-pyrazol-4-yl]-2,6-dimethyl-1,4-dihydro-pyridine-3,5-dicarboxylic acid diethyl ester 163

This product was obtained from 3-(4-amino-phenyl)-1-phenyl-*1H*-pyrazole-4-carbaldehyde (0.079 g, 0.3 mmol), ethylacetoacetate (0.195 g, 1.5 mmol) and 33% NH_4OH(0.159 g, 1.5 mmol).

Yield: 9.3%, orange solid

MP: 120-124 °C

^{1}H NMR (400.13MHz, $CDCl_3$): δ 1.08 (t,6H,J=7.04 Hz,-$CH_2C\underline{H}_3$), 2.31(s,6H,CH_3), 3.80-3.91(m,2H,$C\underline{H}_2CH_3$), 4.05-4.17(m,2H,$C\underline{H}_2CH_3$), 5.30(s,1H,-CH(4'')), 5.67(s,1H,N-H), 7.17(d,2H,J=8.52 Hz,Ar-H(3,5), 7.25(d,2H,J=10.52 Hz,Ar-H(2',6')), 7.41-7.46(m,2H,Ar-H(3',5')), 7.56(d,2H,J=8.52 Hz,Ar-H(2,6)), 7.77-7.79(m,1H,Ar-H(4'))

^{13}C NMR (100.61MHz,$CDCl_3$): δ 13.85 (-$CH_2\underline{C}H_3$), 19.08-19.25 (-CH_3), 29.42 (-CH(4'')), 59.35($\underline{C}H_2CH_3$)), 103.47,104.28 (-C(3'',5'')), 117.83(Ar-C(3,5)), 118.37, 118.40(Ar-C(2',6')), 125.60, 126.64, 128.82, 129.44, 129.78(Ar-C(2,6,3',4',5')), 142.80(Ar-C(1')), 143.14(-C(2'',6'')), 158.73(N=$\underline{C}$), 161.57(Ar-C(4)), 167.14(C=O).

EIMS (HR): $C_{28}H_{31}N_4O_4$ calculated $[M+H]^+$ 487.2345, observed $[M+H]^+$ 487.2906.

IR (NaCl/KBr): C=N absorbance 1599.75 cm^{-1}, C=O absorbance at 1677.71 cm^{-1}, C-O-ester absorbance at 1212.28 cm^{-1}.

6.4.4 Synthesis of 4-(1,3-diphenyl-*1H*-pyrazol-4-yl)-2,6-dimethyl-1,4-dihydro-pyridine-3,5-dicarboxylic acid diethyl ester 164

This product was obtained from 1,3-diphenyl-1H-pyrazole-4-carbaldehyde (0.074 g, 0.3 mmol), ethylacetoacetate(0.195 g, 1.5 mmol)and 33% NH_4OH (0.159 g, 1.5 mmol).

Yield: 7.86%, light yellow solid

MP: 196 °C

^{1}H NMR (400.13MHz $CDCl_3$): δ1.10(t, 6H, J=7.52 Hz,CH_2-$C\underline{H}_3$), 2.25 (s, 6H, -CH_3), 3.76-3.84 (m, 2H, $C\underline{H}_2$-CH_3), 4.00-4.08(m, 2H,$C\underline{H}_2$-CH_3), 5.32 (s, 1H -CH(4'')), 5.51(s, N-H), 7.23-7.27 (m, 1H, Ar-H(4')), 7.34-7.38(m, 1H, Ar-H(4)), 7.41-7.45(m,4H,Ar-H(3,5,3',5')), 7.70(d,2H,J=8.04 Hz,Ar-C(2',6')), 7.77(s,1H,N-C$\underline{H}$=C), 7.86(d,2H, J=7.04 Hz,Ar-C(2,6)).

^{13}C NMR.(100.61MHz $CDCl_3$): δ 13.87 (-$CH_2\underline{C}H_3$), 19.09 (-CH_3), 29.22 (-CH(4'')), 59.26(-$\underline{C}H_2CH_3$), 103.89(-C(3'',5'')), 118.35(Ar-C(2',6')), 126.62(Ar-C(4')), 127.00 (Ar-C(4)), 127.44(N-$\underline{C}$H=C)), 128.15 (Ar-C (3,5)), 128.51(Ar-C(2,6)), 128.77 (C-$\underline{C}$=C), 134.40(Ar-C(1)), 142.90(-C(2'',6''), 150.79(N=$\underline{C}$-), 167.11(C=O).

EIMS (HR): $C_{28}H_{30}N_3O_4$ calculated $[M+H]^+$ 472.2236, observed $[M+H]^+$ 472.2253.

IR (NaCl/KBr): C=N absorbance 1599.76 cm^{-1}, C=O absorbance at 1693.27 cm^{-1}, C-O-ester absorbance at 1211.06 cm^{-1}.

6.4.5 Synthesis of 4-[3-(4-hydroxy-phenyl)-1-phenyl-*1H*-pyrazol-4-yl]-2,6-dimethyl-1,4-dihydro-pyridine-3,5-dicarboxylic acid diethyl ester 165

This product was obtained from 3-(4-hydroxy-phenyl)-1-phenyl-*1H*-pyrazole-4-carbaldehyde (0.079 g, 0.3 mmol), ethylacetoacetate (0.195 g, 1.5 mmol) and 33% NH_4OH(0.159 g, 1.5 mmol).

Yield: 18.7%, white solid

MP: 270 °C

^{1}H NMR (400.13MHz, $CDCl_3$): δ 1.04 (t, 6H,J=7.04 Hz, CH_2-$C\underline{H}_3$), 2.30 (s, 6H, -$C\underline{H}_3$), 3.71-3.79 (m, 2H, $C\underline{H}_2$-CH_3), 3.94-4.02 (m, 2H, $C\underline{H}_2$-CH_3), 4.80(s, O-H), 5.34 (s, 1H, -CH(4'')), 6.94 (d, 2H,J=8.52 Hz, Ar-H(3,5), 7.21-7.25 (m, 1H, Ar-H(4'), 7.41-7.46(m,2H,Ar-H(3',5')), 7.78(d,2H,J=8.04 Hz,Ar-H(2',6')), 7.87(d,2H,J=8.52 Hz,Ar-H(2,6))

^{13}C NMR (100.61MHz, $CDCl_3$): δ13.36 (-$CH_2\underline{C}H_3$), 17.51(-CH_3), 58.41 (-$\underline{C}H_2CH_3$),

103.20(C(3'',5'')), 114.13(Ar-C(3,5)), 117.40(C=CH), 117.75(Ar-C(2',6')), 125.00(N-CH=C), 126.17, 126.54, 128.78, 129.34, 129.42(Ar-C(1,2,6,3',4',5')), 139.75(Ar-C(1')), 144.05(C(2'',6'')), 149.50(N=C), 156.60(Ar-C(4)), 166.72(C=O).

EIMS (HR): $C_{28}H_{30}N_3O_5$ calculated $[M+H]^+$ 488.2185, observed $[M+H]^+$ 488.2176.

IR (NaCl/KBr): C=N absorbance 1601.14 cm^{-1}, OH absorbance at 3335.13 cm^{-1}, C-O-ester absorbance at 1208.12 cm^{-1}.

6.4.6 Synthesis of 4-[3-(4-methoxy-phenyl)-1-phenyl-*1H*-pyrazol-4-yl]-2,6-dimethyl-1,4-dihydro-pyridine-3,5-dicarboxylic acid diethyl ester 166

This product was obtained from 3-(4-methoxy-phenyl)-1-phenyl-1H-pyrazole-4-carbaldehyde (0.083 g, 0.3 mmol),ethylacetoacetate (0.195 g, 1.5 mmol) and 33% NH_4OH (0.159 g, 1.5 mmol).

Yield: 15.3%, light yellow solid

MP: 136-140 ^oC

^{1}H NMR (400.13MHz $CDCl_3$): δ 1.10 (t, 6H,J=7.04 Hz, CH_2-CH_3), 2.25 (s, 6H, C-CH_3), 3.79-3.85 (m, 2H, CH_2-CH_3), 3.87(s,3H, O-CH_3), 4.01-4.09 (m, 2H, CH_2-CH_3), 5.27 (s, 1H, CH(4'')), 5.60(s, N-H), 6.98(d, 2H,J=9.04 Hz,Ar-H(3,5)), 7.22-7.26 (m,1H,Ar-H(4')), 7.40-7.44 (m, 2H, Ar-H(3',5'), 7.68(d, 2H,J=7.52 Hz,Ar-H(2',6')), 7.75(s,1H,N-CH=C), 7.79-7.82 (d,2H,J=9.04 Hz,Ar-H(2,6))

^{13}C NMR (100.61MHz $CDCl_3$): δ13.76,13.87(-CH_2CH_3), 19.09(-CH_3), 29.24 (CH (4'')), 54.94(O-CH_3), 59.28,59.98 (-CH_2CH_3), 104.01 (C(3'',5'')), 112.90(Ar-C(3,5)), 118.27 (Ar-C(2',6')), 125.40(N-CH=C), 126.56, 127.05, 128.04, 129.66(Ar-C(2,6,3',4',5')), 139.64 (Ar-C(1')), 142.83(C(2'',6'')), 150.51 (N=C), 158.73(Ar-C(4)), 167.16(C=O).

EIMS (HR): $C_{29}H_{32}N_3O_5$ calculated $[M+H]^+$ 502.2342, observed $[M+H]^+$ 502.2325

IR (NaCl/KBr): C=N absorbance 1600.12 cm^{-1}, C=O absorbance at 1693.98 cm^{-1}, C-O-ester absorbance at 1212.67 cm^{-1}.

6.4.7 Synthesis of diethyl 4-(3-(4-bromophenyl)-1-(4-methoxyphenyl)-*1H*-pyrazol-4-yl)-2,6-dimethyl-1,4-dihydropyridine-3,5-dicarboxylate 167

This product was obtained from 3-(4-bromophenyl)-1-(4-methoxyphenyl)-1H-pyrazole-4-carbaldehyde(0.107 g, 0.3 mmol), ethylacetoacetate (0.195 g,1.5 mmol) and 33% NH_4OH(0.159 g, 1.5 mmol).

Yield: 48%, light yellow solid

MP: 192 °C

^{1}H NMR (400.13MHz, $CDCl_3$): δ 1.09(t, 6H, J=7.0 Hz, CH_2-$C\underline{H}_3$), 2.27(s, 6H, -$C\underline{H}_3$), 3.76-3.83 (m, 2H, $C\underline{H}_2$-CH_3), 3.84(s,3H,O-CH_3), 4.01-4.09(m,2H,$C\underline{H}_2$-CH_3), 5.27 (s, 1H, -CH(4'')), 5.55(s,NH), 6.94(dd,2H,J=2.24,9.0 Hz,Ar-H(3',5')), 7.55-7.58(m,4H,Ar-H(3,5,2',6')), 7.65(N-C$\underline{H}$=C), 7.81(dd,2H,J=1.76,8.52 Hz,Ar-H(2,6))

^{13}C NMR 100.61MHz $CDCl_3$: δ 14.30(-$CH_2C\underline{H}_3$), 19.61(-CH_3), 29.59(-CH(4'')), 55.56(O-CH_3), 59.80(-$\underline{C}H_2CH_3$), 104.63(-C(3'',5'')), 114.35(Ar-C(2',6')), 120.56(Ar-(3',5')), 121.44(Ar-C(4)), 127.49, 128.39, 130.53, 131.00(Ar-C(2,3,5,6)), 126.63(N-$\underline{C}$H=C), 133.95(Ar-C(1')), 143.24(C(2'',6'')), 149.25(N=$\underline{C}$-C), 158.05(Ar-C(4')), 167.49(C=O).

EIMS (HR): $C_{29}H_{31}N_3O_5Br$ calculated $[M+H]^+$ 580.1447, observed $[M+H]^+$ 580.1459

IR (NaCl/KBr): C=O absorbance at 1642.51 cm^{-1}, C-O-ester absorbance at 1207.81 cm^{-1}.

6.4.8 Synthesis of diethyl 4-(3-(3-fluoro-4-methoxyphenyl)-1-phenyl-*1H*-pyrazol-4-yl)-2,6-dimethyl-1,4-dihydropyridine-3,5-dicarboxylate 168

This product was obtained from 3-(3-fluoro-4-methoxyphenyl)-1-phenyl-1H-pyrazole-4-carbaldehyde (0.089 g, 0.3 mmol), ethylacetoacetate, (0.195 g, 1.5 mmol) and 33% NH_4OH(0.159 g, 1.5 mmol).

Yield: 3.10%, dark yellow solid

MP: 152 °C

^{1}H NMR (400.13MHz, $CDCl_3$): δ 1.10 (t, 6H,J=7.24 Hz, CH_2-$C\underline{H}_3$), 2.28 (s, 6H, -$C\underline{H}_3$), 3.81-3.89 (m, 2H, $C\underline{H}_2$-CH_3), 3.95(s,3H,O-CH_3), 4.03-4.11(m, 2H,$C\underline{H}_2$-CH_3), 5.28 (s, 1H, -CH(4'')), 5.84(s, N-H), 7.03-7.07(m,1H,Ar-H(5)), 7.23-7.27(m,1H,Ar-H(4')), 7.40-7.44 (m, 2H,Ar-H(3',5')), 7.67-7.69(m,2H,Ar-H(2',6')), 7.73-7.76(m,2H,Ar-H(2,6))

^{13}C NMR 100.61MHz $CDCl_3$: δ 14.28 (-$CH_2C\underline{H}_3$), 19.49 (-CH_3), 29.65 (-CH(4'')), 56.44(O-CH_3)), 59.79(-$\underline{C}H_2CH_3$), 104.46 (-C(3'',5'')), 113.02(Ar-C(5)), 116.59(Ar-C(2)), 118.81(Ar-C(2',6')), 128.83(Ar-C(1)), 124.74, 126.10, 127.72, 129.26(Ar-C(6,3',4',5')), 143.51(C(2'',6'')), 147.16(Ar-C(1')), 149.57(N=C-), 150.82(Ar-C(4)), 153.24(Ar-C(3)), 167.57(C=O).

EIMS (HR): $C_{29}H_{30}N_3O_5NaF$ calculated $[M+Na]^+$ 542.2067,

observed $[M+Na]^+$ 542.2070

IR (NaCl/KBr): C=N absorbance 1599.96 cm^{-1}, C=O absorbance at 1693.58 cm^{-1}, C-O-ester absorbance at 1210.60 cm^{-1}.

6.4.9 Synthesis of 2,6-dimethyl-4-[1-phenyl-3-(3,4,5-trimethoxy-phenyl)-*1H*-pyrazol-4-yl]-1,4-dihydro-pyridine-3,5-dicarboxylic acid diethyl ester 169

This product was obtained from 1-phenyl-3-(3,4,5-trimethoxy-phenyl)-1H-pyrazole-4-carbaldehyde (0.102 g, 0.3 mmol), ethylacetoacetate (0.195 g, 1.5 mmol) and 33% NH_4OH(0.159 g, 1.5 mmol).

Yield: 8.97%, brown solid

MP: 183 ^oC

^{1}H NMR (400.13MHz,$CDCl_3$): δ1.12 (t, 6H,J=7.04 Hz, CH_2-$C\underline{H}_3$), 2.23 (s, 6H, C-$C\underline{H}_3$), 3.88-3.98 (m, 2H, $C\underline{H}_2$-CH_3), 3.90(s,3H,O-CH_3), 3.96(ds,6H,O-CH_3), 4.04-4.12 (m, 2H, $C\underline{H}_2CH_3$)), 5.32 (s, 1H, CH(4'')), 5.55(s, N-H), 7.11(s,2H,Ar-H(2,6), 7.24-7.28(m,1H,Ar-H(4')), 7.42-7.46(m,2H,Ar-H(3',5')), 7.71(d, 2H,J=7.52 Hz, Ar-H(2',6')), 7.78(s,1H,N-C$\underline{H}$=C)

^{13}C NMR (100.61MHz,$CDCl_3$): δ14.37(-$CH_2\underline{C}H_3$), 19.52(-$\underline{C}H_3$), 30.01 (-C(4'')), 56.31-60.86(O-CH_3), 59.74 (O-$\underline{C}H_2CH_3$), 104.03(C(3'',5'')), 106.60(Ar-C(2,6)), 118.79 (Ar-C(2',6')), 126.05, 126.94, 129.27(Ar-C(3',4',5')), 137.48 (Ar-C(1)), 140.01(Ar-C(4)), 143.23 (C(2'',6'')), 151.45(C=N), 152.84 (Ar-C(3,5)),167.63(C=O).

EIMS (HR): $C_{31}H_{36}N_3O_7$ calculated $[M+H]^+$ 562.2553, observed $[M+H]^+$ 562.2549.

IR (NaCl/KBr): C=N absorbance 1600.44 cm^{-1}, C=O absorbance at 1690.49 cm^{-1}, C-O-ester absorbance at 1205.13 cm^{-1}.

6.4.10 Synthesis of 4-(1,3-Diphenyl-1H-pyrazol-4-yl)-2,6-dimethyl-1,4-dihydropyridine-3,5-dicarboxylic acid diethyl ester 170

This product was obtained from 1,3-diphenyl-1H-pyrazole-4-carbaldehyde (0.14 g, 0.3 mmol), ethyl acetoacetate (0.195 g, 1.5 mmol) and NH_4OH (33 % , 0.159 g, 1.5 mmol).

Yield: 7.9%, light yellow solid

MP: 196 ^oC

^{1}H NMR (400.13MHz,$CDCl_3$): δ 1.08 (t, 6H, J=7.04 Hz, CH_2-CH_3), 2.25 (s, 6H, -CH_3), 3.80 (m, 2H, CH_2-CH_3), 4.04 (m, 2H,CH_2-CH_3),

5.31 (s, 1H, -CH(4'')), 5.60 (s, 1H, N-H), 7.24-7.27 (m, 1H, Ar-H(4')),
7.34-7.38 (m, 1H, Ar-H(4)), 7.76 (s, 1H, N-CH=C),
7.41-7.45 (m, 4H, Ar-H (3,5,3',5')), 7.70 (d, 2H, J=8.04 Hz, Ar-C(2',6')),
7.86 (d, 2H, J=7.04 Hz, Ar-C(2,6)).

^{13}C NMR (100.61MHz,$CDCl_3$): δ13.87 (-$CH_2\underline{C}H_3$), 19.09 (-CH_3), 29.22 (-C (4'')), 59.26 (-$\underline{C}H_2CH_3$), 103.89 (-C(3'',5'')), 118.35 (Ar-C(2',6')), 126.62(Ar-C(4')), 127.00 (Ar-C(4)), 127.44 (N-$\underline{C}$H=C)), 128.15 (Ar-C (3,5)), 128.51 (Ar-C(2,6)), 128.77 (C-$\underline{C}$=C), 134.40 (Ar-C(1)),142.90 (-C(2'',6''), 150.79 (N=$\underline{C}$-), 167.11(C=O).

EIMS (HR): $C_{29}H_{32}N_3O_4$ calculated $[M+H]^+$ 472.2236, observed $[M+H]^+$ 472.2253.

IR (NaCl/KBr): C=O absorbance at 1668.49 cm^{-1}, C-O-ester absorbance at 1109.13 cm^{-1}.

6.4.11 Synthesis of 4-[3-(4-iodo-phenyl)-1-phenyl-*1H*-pyrazol-4-yl]-2,6-dimethyl-1,4-dihydro-pyridine-3,5-dicarboxylic acid diethyl ester 171

This product was obtained from 3-(4-iodo-phenyl)-1-phenyl-1H-pyrazole-4-carbaldehyde (0.112 g, 0.3 mmol), ethylacetoacetate (0.195 g, 1.5 mmol) and 33% NH_4OH (0.159 g, 1.5 mmol).

Yield: 17%, yellow solid

MP: 168-172 °C

^{1}H NMR (400.13MHz $CDCl_3$): δ 1.10 (t, 6H, J=7.24 Hz, CH_2-$C\underline{H}_3$),
2.27 (s, 6H, -$C\underline{H}_3$), 3.76-3.84 (m, 2H, $C\underline{H}_2$-CH_3), 4.01-4.09 (m, 2H, $C\underline{H}_2$-CH_3),
5.28 (s, 1H, -C$\underline{H}$(4'')), 5.76(s, N-H), 7.24-7.28 (m, 1H, Ar-H(4')),
7.41-.7.45 (m, 2H, Ar-H(3',5')), 7.67-7.72 (m, 4H, Ar-H(3,5,2',6')),
7.75 (s, 1H,N-C$\underline{H}$=C), 7.79(d, 2H,J=8.28 Hz, Ar-(2,6))

^{13}C NMR (100.61MHz. $CDCl_3$): δ 14.35 (-$CH_2\underline{C}H_3$), 19.57 (-CH_3),
29.59 (-$\underline{C}$H(4'')), 59.85(-$\underline{C}H_2CH_3$), 93.19(Ar-C(4)), 104.48 (-C(3'',5'')),
118.90(Ar-C(2',6')), 126.25, 127.49, 128.98, 129.30, 130.76(Ar-C(2,6,3',4',5')),
134.41(Ar-C(1)), 137.05(Ar-C(3,5)), 139.95(Ar-C(1')), 143.50(C(2'',6'')),
149.78(N=C-), 167.52(C=O).

EIMS (HR): $C_{28}H_{29}IN_3O_4$ calculated $[M+H]^+$ 598.1203, observed $[M+H]^+$ 598.1202.

IR (NaCl/KBr): C=N absorbance 1598.71 cm^{-1}, C=O absorbance at 1676.13 cm^{-1}, C-O-ester absorbance at 1213.39 cm^{-1}.

6.4.12 Synthesis of 4-[3-(3,4-dimethoxy-phenyl)-1-phenyl-*1H*-pyrazol-4-yl]-2,6-dimethyl-1,4-dihydro-pyridine-3,5-dicarboxylic acid diethyl ester 172

This product was obtained from 3-(3,4-dimethoxy-phenyl)-1-phenyl-1H-pyrazole-4-carbaldehyde (0.092 g, 0.3 mmol), ethylacetoacetate, (0.195 g, 1.5 mmol) and 33% NH_4OH(0.159 g, 1.5 mmol).

Yield: 48.67%, white solid

MP: 186 °C

^{1}H NMR 400.13MHz: δ 1.10 (t, 6H,J=7.04 Hz, CH_2-C$\underline{H}_3$), 2.24 (s, 6H, C-C$\underline{H}_3$), 3.94, 3.98(ds,6H,O-CH_3), 3.83-3.88 (m, 2H, C$\underline{H}_2$-CH_3), 4.01-4.09 (m, 2H, C$\underline{H}_2$-CH_3), 5.31 (s, 1H, CH(4'')), 5.70(s, N-H), 6.95(d,1H,J=8.8 Hz,Ar-H(5)), 7.22-7.26 (m, 1H, Ar-H(4')), 7.39-7.46(m,4H,Ar-H(2,6,3',5')), 7.69 (d, 2H,J=8.52 Hz, Ar-H(2',6')), 7.75(s,1H,N-C$\underline{H}$=C)

^{13}C NMR (100.61MHz,$CDCl_3$): δ 14.32(-$CH_2\underline{C}H_3$), 19.48(C-$\underline{C}H_3$), 29.85(-C(4'')), 56.06-56.10(O-CH_3), 59.74(O-$\underline{C}H_2$-CH_3), 104.31(-C(3'',5'')), 110.83(Ar-C(2)), 112.66(Ar-C(5)), 121.63, 125.94, 127.07, 127.70, 128.60, 129.23(Ar-C(6,2',3',4',5',6')), 140.05 (Ar-C (1')), 148.54,148.63(Ar-C(3,4)), 151.10(N=C), 167.67(C=O)

EIMS (HR): $C_{30}H_{34}N_3O_6$ calculated $[M+H]^+$ 532.2448, observed $[M+H]^+$ 532.2454.

IR (NaCl/KBr): C=N absorbance 1599.97 cm^{-1}, C=O absorbance at 1693,57cm^{-1}, C-O-ester absorbance at 1211.52 cm^{-1}.

6.4.13 Synthesis of diethyl 4-(3-(3,5-dibromo-4-hydroxyphenyl)-1-phenyl-*1H*-pyrazol-4-yl)-2,6-dimethyl-1,4-dihydropyridine-3,5-dicarboxylate 173

This product was obtained from 3-(3,5-dibromo-4-hydroxyphenyl)-1-phenyl-1H-pyrazole-4-carbaldehyde (0.127 g, 0.3 mmol), ethylacetoacetate(0.195 g,1.5 mmol) and 33% NH_4OH(0.159 g, 1.5 mmol).

Yield: 13.85%, white solid

MP: 168 °C

^{1}H NMR (400.13MHz, $CDCl_3$): δ1.00(t, 6H, J=7.04 Hz, CH_2-C$\underline{H}_3$), 2.27 (s, 6H, -C$\underline{H}_3$), 3.74-3.76 (m, 2H, C$\underline{H}_2$-CH_3), 3.92-3.97(m, 2H,C$\underline{H}_2$-CH_3), 4.68(s,OH), 5.09 (s, 1H, -CH(4'')), 7.29-7.31(m,1H,Ar-H(4')), 7.45-7.49(m,2H,Ar-H(3',5')), 7.79-7.84(m,2H,Ar-H(2',6')), 8.01-8.08(m,2H,Ar-H(2,6))

^{13}C NMR 100.61MHz $CDCl_3$: δ 14.60 (-$CH_2\underline{C}H_3$), 18.84 (-CH_3), 29.34 (-CH(4'')), 59.78(-$\underline{C}H_2CH_3$), 102.52(-C(3'',5'')), 112.07(Ar-C(3,5)), 118.70(Ar-C(2',6')), 126.63(N-$\underline{C}$H=C), 128.44, 129.26, 129.89(Ar-C(3',4',5')), 130.29(Ar-C(1)), 132.03, 132.56(Ar-C(2,6)), 139.68(Ar-C(1')), 145.90(C(2'',6'')), 147.14(Ar-C(1)), 148.59(N=$\underline{C}$-C), 150.69(Ar-C(4)), 167.34(C=O).

EIMS (HR): $C_{28}H_{27}N_3O_5NaBr_2$ calculated $[M+Na]^+$ 666.0215, observed $[M+Na]^+$ 666.0230

IR (NaCl/KBr): C=N absorbance 1599.75 cm^{-1}, C=O absorbance at 1649.81 cm^{-1}, C-O-ester absorbance at 1214.35 cm^{-1}.

6.4.14 Synthesis of 2,6-dimethyl-4-[3-(4-nitro-phenyl)-1-phenyl-1H-pyrazol-4-yl]-1,4-dihydro-pyridine-3,5-dicarboxylic acid diethyl ester 174

This product was obtained from 3-(4-nitro-phenyl)-1-phenyl-1H-pyrazole-4-carbaldehyde (0.088 g, 0.3 mmol), ethylacetoacetate (0.195 g, 1.5 mmol) and 33% NH_4OH(0.159 g, 1.5 mmol).

Yield: 25.5%, red solid

MP: 172°C

^{1}H NMR (400.13MHz $CDCl_3$): δ1.05 (t, 6H,J=7.04 Hz, CH_2-$C\underline{H}_3$), 2.32 (s, 6H, -$C\underline{H}_3$), 3.78-3.83 (m, 2H, $C\underline{H}_2$-CH_3), 3.98-4.04 (m, 2H, $C\underline{H}_2$-CH_3), 5.33 (s, 1H, -CH(4'')), 6.08(s, N-H), 7.27-7.31 (m, 1H, Ar-H(4'), 7.43-.7.47 (m, 2H,Ar-H(3',5')), 7.70 (d, 2H,J=7.8 Hz, Ar-H(2,6)), 7.82 (s, 1H,N-CH=), 8.28-8.34(m, 4H, Ar-(3,5,2',6')).

^{13}C NMR (100.61MHz, $CDCl_3$): δ14.34 (-$CH_2\underline{C}H_3$), 19.61 (-CH_3), 29.72 (-CH(4'')), 59.89(-$\underline{C}H_2CH_3$), 104.55 (-C(3'',5'')), 119.04,119.15(ArC(2',6')), 123.33, 124.06, 126.69, 128.15, 128.79, 129.39, 130.17(Ar-C(2,3,5,6,3',4',5')), 139.76(Ar-C(1)), 141.78(Ar-C(1')), 143.79(C(2'',6'')), 146.92(Ar-C(4)), 148.15(N=C), 167.44(C=O).

EIMS (HR): $C_{28}H_{28}N_4O_6Na$ calculated $[M+Na]^+$ 539.1907, observed $[M+Na]^+$ 539.1901.

IR (NaCl/KBr): C=N absorbance 1596.67 cm^{-1}, C=O absorbance at 1667.36 cm^{-1}, C-O-ester absorbance at 1210.53 cm^{-1}.

6.4.15 Synthesis of 4-[3-(4-methoxy-3-nitro-phenyl)-1-phenyl-*1H*-pyrazol-4-yl]-2,6-dimethyl-1,4-dihydro-pyridine-3,5-dicarboxylic acid diethyl ester 175

This product was obtained from 3-(4-methoxy-3-nitro-phenyl)-1-phenyl-1H-pyrazole-4-carbaldehyde (0.097 g, 0.3 mmol), ethylacetoacetate, (0.195 g, 1.5 mmol)

and 33% NH_4OH (0.159 g, 1.5 mmol).

Yield: 52.5%, dark yellow solid

MP: 152 °C

^{1}H NMR (400.13MHz, $CDCl_3$): δ 1.17(t, 6H,J=7.0 Hz, CH_2-$C\underline{H}_3$),
2.25 (s, 6H, -$C\underline{H}_3$), 3.85-3.89 (m, 2H, $C\underline{H}_2$-CH_3), 3.98-4.05 (m, 2H,$C\underline{H}_2$-CH_3),
4.03(s,3H,O-CH_3), 5.27 (s, 1H, -CH(4'')), 6.37(s, N-H),
7.17-7.24(m,2H,Ar-H(5,4')), 7.38-.7.41 (m, 2H, Ar-H(3',5')),
7.67 (d, 2H,J=8.04 Hz, Ar-H(2',6')), 7.81(s,1H,N-C$\underline{H}$=C),
8.25 (d, 2H,J=8.04 Hz, Ar-H(6)), 8.51(s, 1H, Ar-(2))

^{13}C NMR 100.61MHz $CDCl_3$: δ14.31(-$CH_2\underline{C}H_3$), 19.34 (-CH_3), 29.77 (-CH(4'')),
56.68(O-CH_3)), 59.79(-$\underline{C}H_2CH_3$), 104.11 (-C(3'',5'')), 113.12(Ar-C(5)),
118.81(Ar-C(2',6')), 125.61, 126.37, 127.85, 129.41(Ar-C(2,3',4',5')),
134.58(Ar-C(6)), 139.37,139.79(Ar-C(3,1')), 144.02(C(2'',6'')), 148.02(N=C-),
152.19 (Ar-C(4)), 167.57(C=O).

EIMS (HR): $C_{29}H_{30}N_4O_7Na$ calculated $[M+Na]^+$ 569.2012,
observed $[M+Na]^+$ 569.2032.

IR (NaCl/KBr): C=N absorbance 1623.04 cm^{-1}, C=O absorbance at 1687.76 cm^{-1},
C-O-ester absorbance at 1211.24 cm^{-1}.

6.4.16 Synthesis of 4-[3-(4-fluorphenyl)-1-phenyl-1H-pyrazol-4-yl]-2,6-dimethyl-1,4-dihydropyridine-3,5-dicarboxylic acid diethyl ester 176

This product was obtained from 3-(4-fluorophenyl)-1-phenyl-1H-pyrazole-4-carbaldehyde (0.147 g, 0.3 mmol), ethyl acetoacetate, (0.195 g, 1.5 mmol and 33% NH_4OH (0.159 g, 1.5 mmol).

Yield: 25.4%, brown solid

MP: 132-134 °C

^{1}H NMR (400.13MHz, $CDCl_3$): δ1.08 (t, 6H, J=7.52 Hz, CH_2-$C\underline{H}_3$),
2.24 (s, 6H, -$C\underline{H}_3$), 3.77-3.85 (m, 2H, $C\underline{H}_2$-CH_3), 3.99-4.07 (m, 2H, $C\underline{H}_2$-CH_3),
5.26 (s, 1H, -CH(4'')), 5.59 (s, 1H, N-H), 7.12 (d, 2H, J=8.52 Hz, Ar-H(3,5)),
7.22-7.25 (m, 1H, Ar-H(4')), 7.38-.7.42 (m, 2H, Ar-H(3',5')), 7.66 (d, 2H, J=8.56
Hz, Ar-H(2',6')), 7.73 (s, 1H, N-C$\underline{H}$=C), 7.86 (d, 2H, J=8.52 Hz, Ar-(2,6)).

^{13}C NMR 100.61MHz $CDCl_3$: δ14.27 (-$CH_2\underline{C}H_3$), 19.52 (-CH_3), 29.63 (-CH(4'')),
59.73(-$\underline{C}H_2CH_3$), 104.37 (-C(3'',5'')), 114.60, 114.81(Ar-C(3,5)),
118.77 (Ar-C(2',6')), 126.05 (Ar-C(4')), 127.18, 128.60, 129.21, 130.63,

130.90 (Ar-C(1,2,6,3',5')), 139.93 (ArC(1')), 143.29 (C(2'',6'')), 150.10 (N=C), 163.72 (Ar-C(4)), 167.47(C=O).

EIMS (HR): $C_{28}H_{29}FN_3O_4$ calculated $[M+H]^+$ 490.2142, observed $[M+H]^+$ 490.2152

IR (NaCl/KBr): C=O absorbance at 1693.92 cm^{-1}, C-O-ester absorbance at 1113.03 cm^{-1}.

6.4.17 Synthesis of diethyl diethyl 4-(3-(3-chloro-4-methoxyphenyl)-1-phenyl-*1H*-pyrazol-4-yl)-2,6-dimethyl-1,4-dihydropyridine-3,5-dicarboxylate 177

This product was obtained from 3-(3-chloro-4-methoxyphenyl)-1-phenyl-1H-pyrazole-4-carbaldehyde(0.094 g, 0.3 mmol), ethylacetoacetate(0.195 g, 1.5 mmol) and 33% NH_4OH(0.159 g, 1.5 mmol).

Yield: 33.95%, light yellow solid

MP: 172 °C

^{1}H NMR (400.13MHz, $CDCl_3$): δ 1.11(t, 6H, J=7.04 Hz, CH_2-C$\underline{H_3}$), 2.24 (s, 6H, -C$\underline{H_3}$), 3.83-3.91 (m, 2H, C$\underline{H_2}$-CH_3), 3.95(s,3H,O-CH_3), 4.03-4.11(m, 2H,C$\underline{H_2}$-CH_3), 5.28 (s, 1H, -CH(4'')), 5.88(s, N-H), 7.02(d,1H,J=8.56 Hz,Ar-H(5)), 7.23-7.26(m,1H,Ar-H(4')), 7.40-7.44 (m, 2H,Ar-H(3',5')), 7.68(d,2H,J=8.28 Hz,Ar-H(2',6')), 7.76(N-C$\underline{H}$=C), 7.79(d,1H,J=8.56 Hz,Ar-H(6)), 7.95(s,1H,Ar-H(2))

^{13}C NMR 100.61MHz $CDCl_3$: δ14.34 (-CH_2C$\underline{H_3}$), 19.45 (-CH_3), 29.77 (-CH(4'')), 56.30(O-CH_3)), 59.78(-C$\underline{H_2}$$CH_3$), 104.17 (-C(3'',5'')), 111.60(Ar-C(5)), 118.80(Ar-C(2',6')), 121.74(Ar-C(3)), 126.14, 127.40, 128.34, 129.28, 130.61(Ar-C(2,6,3',4',5')), 139.96(Ar-C(1')), 143.62(C(2'',6'')), 154.45(Ar-C(4)), 167.56(C=O).

EIMS (HR): $C_{29}H_{31}N_3O_5Cl$ calculated $[M+H]^+$ 536.1952, observed $[M+H]^+$ 536.1942

IR (NaCl/KBr): C=N absorbance 1599.52 cm^{-1}, C=O absorbance at 1652.92 cm^{-1}, C-O-ester absorbance at 1210.43 cm^{-1}.

6.4.18 Synthesis of 4-(3-Biphenyl-4-yl-1-phenyl-1H-pyrazol-4-yl)-2,6-dimethyl-1,4-dihydropyridine-3,5-dicarboxylic acid diethyl ester 178

This product was obtained from 3-biphenyl-4-yl-1-phenyl-1H-pyrazole-4-carbaldehyde (0.164 g, 0.3 mmol), ethyl acetoacetate, (0.195 g, 1.5 mmol and 33 % NH_4OH (0.159 g, 1.5 mmol).

Yield: 43.6%, yellow solid

MP: 144 °C

^{1}H NMR (400.13MHz. $CDCl_3$): δ 1.07 (t, 6H, J=7.04 Hz, CH_2-$C\underline{H}_3$), 2.26 (s, 6H, -$C\underline{H}_3$), 3.75-3.83 (m, 2H, $C\underline{H}_2$-CH_3), 4.00-4.08 (m, 2H, $C\underline{H}_2$-CH_3), 5.34 (s, 1H, C-H(4'')), 5.47 (s, 1H, N-H), 7.35-7.49 (m, 6H, Ar-H(2''',3''',4''',5''', 6''',4')), 7.64-7.71 (m, 6H, Ar-H(3, 5,2',3',5',6')), 7.76 (s, 1H, N-C$\underline{H}$=C), 7.96 (d, 2H, J=8.56 Hz, Ar-H(2,6)).

^{13}C NMR (100.61MHz. $CDCl_3$): δ14.24 (-$CH_2\underline{C}H_3$), 19.54 (-CH_3), 30.09 (-CH(4'')), 56.69(-$\underline{C}H_2CH_3$), 104.48 (-C(3'',5'')), 118.73(Ar-C(2',6')), 125.93, 126.56, 126.95, 127.10, 127.17, 128.76, 129.22 (Ar-C(2,3,5,6,3',4',5',2''',3''',4''',5''',6''')), 133.88 (Ar-C(1)), 140.01, 140.11 (Ar-C(4,1''')), 143.21(-C(2'',6'')), 150.62(N=C), 167.47(C=O).

EIMS (HR): $C_{34}H_{34}N_3O_4$ calculated $[M+H]^+$ 548.2549, observed $[M+H]^+$ 548.2537.

IR (NaCl/KBr): C=O absorbance at 1688.47 cm^{-1}, C-O-ester absorbance at 1114.23 cm^{-1}.

6.4.19 Synthesis of 2,6-Dimethyl-4-(3-naphthalen-2-yl-1-phenyl-1H-pyrazol-4-yl)-1,4-dihydr-pyridine-3,5-dicarboxylic acid diethyl ester 179

This product was obtained from 3-naphthalen-2-yl-1-phenyl-1H-pyrazole-4-carbaldehyde (0.156 g, 0.3 mmol), ethyl acetoacetate (0.195 g, 1.5 mmol and 33 % NH_4OH (0.159 g, 1.5 mmol).

Yield: 50.3%, yellow solid

MP: 165 °C

^{1}H NMR (400.13MHz. $CDCl_3$): δ1.01 (t, 6H, J=7.04 Hz, CH_2-$C\underline{H}_3$), 2.19 (s, 6H, -$C\underline{H}_3$), 3.71-3.80 (m, 2H, $C\underline{H}_2$-CH_3), 3.96-4.04 (m, 2H, $C\underline{H}_2$-CH_3), 5.36 (s, 1H, -H(4'')), 5.38 (s, 1H, N-H), 7.25-.7.28 (m, 1H, Ar-H(4')), 7.42-7.46 (m, 2H, Ar-H(3',5')), 7.48-7.52 (m, 2H, Ar-H(5,6)), 7.74(d, 2H, J=7.52 Hz, Ar-H(2',6')), 7.82 (s,1H, N-C$\underline{H}$=C), 7.87-8.00 (m, 4H, Ar-H(4,7,9,10), 8.33 (s, 1H, Ar-H(2)).

^{13}C NMR 100.61MHz. $CDCl_3$: δ13.79 (-$CH_2\underline{C}H_3$), 19.03 (-CH_3), 29.44 (-CH(4'')), 59.22 (-$\underline{C}H_2CH_3$), 103.72 (-C(3'',5'')), 118.39(Ar-C(2',6')), 125.33, 125.43, 125.59, 126.74, 126.93, 127.14, 127.36, 127.71, 128.48, 128.81 (Ar-C (2, 4, 5, 6, 7, 9, 10, 3', 4', 5')), 131.89, 132.36, 132.89 (Ar-C(1,3,4)), 139.64(Ar-C(1')), 142.94 (-C(2'',6'')), 150.80(N=$\underline{C}$-), 167.11(C=O).

EIMS (HR): $C_{26}H_{28}N_3O_4S$ calculated $[M+H]^+$ 478.1801,

observed $[M+H]^+$ 478.1798.

IR (NaCl/KBr): C=O absorbance at 1682.47 cm^{-1}, C-O-ester absorbance at 1116.46 cm^{-1}.

6.4.20 Synthesis of 2,6-dimethyl-4-(1-phenyl-3-thiophen-2-yl-*1H*-pyrazol-4-yl)-1,4-dihydro-pyridine-3,5-dicarboxylic acid diethyl ester 180

This product was obtained from 1-phenyl-3-thiophen-2-yl-1H-pyrazole-4-carbaldehyde (0.076 g, 0.3 mmol), ethylacetoacetate, (0.195 g, 1.5 mmol) and 33% NH_4OH (0.159 g, 1.5 mmol).

Yield: 16.3%, brown solid

MP: 178 °C

^{1}H NMR (400.13MHz. $CDCl_3$): δ 1.06(t, 6H, J=7.04 Hz,CH_2-C<u>H</u>$_3$), 2.34 (s, 6H, -C<u>H</u>$_3$), 3.86-3.94 (m, 2H,C<u>H</u>$_2$-CH_3), 4.02-4.10 (m, 2H,C<u>H</u>$_2$-CH_3), 5.34 (s, 1H, -CH(4'')), 5.62(s, N-H), 7.13-7.15 (m, 1H, C<u>H</u>=CH-S), 7.13-7.15(m,1H,Ar-H(4')), 7.41-7.45(m,2H,Ar-H(3',5'), 7.70(d,2H,J=7.52 Hz,Ar-H(2',6')), 7.77(s,1H,N-C<u>H</u>=C), 7.80(d,1H,J=4.52 Hz,S-C<u>H</u>=CH)

^{13}C NMR 100.61MHz. $CDCl_3$: δ14.25 (-CH_2<u>C</u>H_3), 19.65 (-CH_3), 29.76 (-CH(4'')), 59.85(-<u>C</u>H_2CH_3), 104.91 (-C(3'',5'')), 118.91 (Ar-C(2',6')), 124.90(N-<u>C</u>H=C), 126.19, 126.38, 127.10, 127.82, 129.24, 129.47(thiophene,C(3,4,5), Ar-C(3',4',5')), 135.96(N=C), 139.77(Ar-C(1')), 143.19 (-C(2'',6'')), 145.04(C=<u>C</u>-S), 167.52(C=O)

EIMS (HR): $C_{26}H_{28}N_3O_4S$ calculated $[M+H]^+$ 478.1801,

observed $[M+H]^+$ 478.1798.

IR (NaCl/KBr): C=N absorbance 1600.59 cm^{-1}, C=O absorbance at 1679.47 cm^{-1}, C-O-ester absorbance at 1204.26 cm^{-1}.

6.4.21 Synthesis of 2,6-Dimethyl-4-(1-phenyl-3-pyridin-4-yl-1H-pyrazol-4-yl)-1,4-dihydropyridine-3,5-dicarboxylic acid diethyl ester 181

This product was obtained from1-phenyl-3-pyridin-4-yl-1H-pyrazole-4-carbaldehyde (0.142 g, 0.3 mmol), ethyl acetoacetate (0.195 g, 1.5 mmol) and 33 % NH_4OH (0.159 g, 1.5 mmol).

Yield: 22.3%, brown solid

MP: 118-121 °C

^{1}H NMR (400.13MHz $CDCl_3$): δ1.04 (t, 6H, J=7.04 Hz, CH_2-C<u>H</u>$_3$),

2.31 (s, 6H, -C<u>H</u>$_3$), 3.74-3.82 (m, 2H, C<u>H</u>$_2$-CH$_3$), 3.97-4.05 (m, 2H, C<u>H</u>$_2$-CH$_3$), 5.34 (s, 1H, -H(4'')), 5.86 (s, N-H), 7.26-7.28 (m, 1H, Ar-H(4'), 7.41-7.45 (m, 2H, Ar-H(3',5')), 7.68 (d, 2H,J=7.52 Hz, Ar-H(2',6')), 7.78 (s, 1H, N-C<u>H</u>=C), 7.97(d, 2H, J=5.52 Hz, H-(2,6)), 8.68(d, 2H, J=5.0 Hz, Ar-H(3,5)).

^{13}C NMR (100.61MHz CDCl$_3$): δ13.86 (-CH$_2$<u>C</u>H$_3$), 19.20 (-CH$_3$), 29.54 (-CH(4'')), 59.82 (-<u>C</u>H$_2$CH$_3$), 104.63 (-C(3'',5'')), 119.00 (Ar-C(2',6')), 122.82 (N-<u>C</u>H=C), 126.13, 128.89, 129.52 (Ar-C(3',4',5')), 139.36 (Ar-C(1')), 143.51(-C(2'',6'')), 147.81(-C(1)), 149.52 (-C(3,5)), 167.35(C=O)

EIMS (HR): $C_{27}H_{29}N_4O_4$ calculated $[M+H]^+$ 473.2189; observed $[M+H]^+$ 473.2212.

IR (NaCl/KBr): C=O absorbance at 1679.32 cm^{-1}, C-O-ester absorbance at 1116.38 cm^{-1}.

6.4.22 Synthesis of dimethyl 4-(1,3-diphenyl-*1H*-pyrazol-4-yl)-2,6-dimethyl-1,4-dihydropyridine-3,5-dicarboxylate 183

This product was obtained from 3-(4-(benzyloxy)phenyl)-1-phenyl-1H-pyrazole-4-carbaldehyde(0.106 g, 0.3 mmol), methylacetoacetate(0.195 g,1.5 mmol)and 33% NH_4OH (0.159 g,1.5 mmol).

Yield: 23.6%, white solid

MP: 184 °C

^{1}H NMR (400.13MHz CDCl$_3$): δ2.24 (s, 6H, -CH$_3$), 3.36(s, 6H, OCH$_3$), 5.17(s, 2H, O-CH$_2$), 5.25(s, 1H, -CH(4'')), 5.88(s, N-H), 7.08 (d, 2H,J=9.04 Hz, Ar-H(3,5)), 7.21-7.25(m,1H,Ar-H(4''')), 7.31-7.35(m,1H,Ar-H(4')), 7.39-7.43(m,4H,Ar-H(3',5',3''',5''')), 7.48(d,2H,Ar-H(2''',6''')), 7.67(d,2H,J=8.04,Ar-H(3',5')), 7.70(s,1H,N-C<u>H</u>=C), 7.78(d,2H, J=9.04,Ar-C(2,6)).

^{13}C NMR (100.61MHz CDCl$_3$): δ18.79 (-CH$_3$), 29.05(-C (4'')), 50.26(O-<u>C</u>H$_3$), 69.43(O-CH$_2$), 103.64(-C(3'',5'')), 114.22(Ar-C(3,5)), 118.37(Ar-C(2',6')), 125.52, 126.66, 127.51, 128.14, 128.37, 128.77, 129.44(Ar-C(2,6,3',4',5',2''', 3''',4''',5''',6''')), 136.70(Ar-C(1''')), 139.60(Ar-C(1')), 143.33(-C(2'',6''), 150.36(N=<u>C</u>-C), 157.66(Ar-C(4)), 167.52(C=O).

EIMS (HR): $C_{33}H_{32}N_3O_5$ calculated $[M+H]^+$ 550.2342, observed $[M+H]^+$ 550.2328

IR (NaCl/KBr): C=N absorbance 1578.52 cm^{-1}, C=O absorbance at 1698.82 cm^{-1}, C-O-ester absorbance at 1215.38 cm^{-1}.

6.4.23 Synthesis of dimethyl 4-(3-(4-bromophenyl)-1-phenyl-*1H*-pyrazol-4-yl)-2,6-dimethyl-1,4-dihydropyridine-3,5-dicarboxylate 184

This product was obtained from 3-(4-bromophenyl)-1-phenyl-1H-pyrazole-4-carbaldehyde(0.098 g, 0.3 mmol), methylacetoacetate(0.195 g,1.5 mmol)and 33% NH_4OH (0.159 g,1.5 mmol).

Yield: 16.80%, yellow solid

MP: 202-206 ^{o}C

^{1}H NMR (400.13MHz $CDCl_3$): δ2.27 (s, 6H, -CH_3), 3.36(s, 6H, OCH_3), 5.24(s, 1H, -CH(4'')), 6.19(s,1H,NH), 7.22-7.26(m,1H,Ar-H(4')), 7.39-7.43(m,2H,Ar-H(3',5')), 7.60(d,2H,J=8.56 Hz,Ar-H(3,5)), 7.65(d,2H,J=8.52 Hz,Ar-H(2',6')), 7.70(s,1H,N-C<u>H</u>=C), 7.83(d,2H,J=8.56 Hz,Ar-H(2,6))

^{13}C NMR (100.61MHz $CDCl_3$): δ18.79 (-CH_3), 28.97(-C(4'')), 50.27(O-<u>C</u>H_3), 103.62(-C(3'',5'')), 118.50(Ar-C(2',6')), 121.05(Ar-C(4)), 125.86, 127.12, 128.83, 129.80, 130.74(Ar-C(2,3,5,6,3',4',5')), 133.43(Ar-C(1)), 139.44(Ar-C(1')), 143.58(-C(2'',6''), 149.15(N=<u>C</u>-C), 167.42(C=O).

EIMS (HR): $C_{26}H_{25}N_3O_4Br$ calculated $[M+H]^+$ 522.1028, observed $[M+H]^+$ 522.1024

IR (NaCl/KBr): C=N absorbance 1601.01 cm^{-1}, C=O absorbance at 1674.31 cm^{-1}, C-O-ester absorbance at 1216.28 cm^{-1}

6.4.24 Synthesis of dimethyl 4-(3-(4-aminophenyl)-1-phenyl-*1H*-pyrazol-4-yl)-2,6-dimethyl-1,4-dihydropyridine-3,5-dicarboxylate 185

This product was obtained from 3-(4-aminophenyl)-1-phenyl-1H-pyrazole-4-carbaldehyde(0.079 g, 0.3 mmol), methylacetoacetate(0.195 g,1.5 mmol)and 33% NH_4OH (0.159 g,1.5 mmol).

Yield: 3.40%, yellow solid

MP: 154-156 ^{o}C

^{1}H NMR (400.13MHz $CDCl_3$): δ 2.26 (s, 6H, -CH_3), 3.38(s,6H,OCH_3), 5.25(s, 1H, -CH(4'')), 6.13(s,NH_2), 7.20(d, 2H,J=8.04 Hz, Ar-H(3,5)), 7.25-7.29(m,2H,Ar-H(4')), 7.40-7.44(m,2H,Ar-H(3',5')), 7.67(d,2H,J=7.56 Hz,Ar-H(2',6')), 7.73(s,1H,N-C<u>H</u>=C), 7.79(d,2H,J=8.04 Hz,Ar-H(2,6))

^{13}C NMR (100.61MHz $CDCl_3$): δ18.86 (-CH_3), 29.04(-C(4'')), 50.32(O-<u>C</u>H_3),

103.74(-C(3'',5'')), 118.55(Ar-C(3,5)), 119.50(Ar-C(2',6')), 125.82, 126.89, 127.10, 128.70, 129.03(Ar-C(2,6,3',4',5')), 139.47(Ar-C(1')), 143.66(-C(2'',6''), 150.13(N=C-C), 161.92(Ar-C(4)), 167.46(C=O).

EIMS (HR): $C_{26}H_{26}N_4O_4$ calculated $[M+H]^+$ 459.1594, observed $[M+H]^+$

IR (NaCl/KBr): C=N absorbance 1599.44 cm^{-1}, C=O absorbance at 1685.20 cm^{-1}, C-O-ester absorbance at 1215.44 cm^{-1}

6.4.25 Synthesis of dimethyl 4-(1,3-diphenyl-*1H*-pyrazol-4-yl)-2,6-dimethyl-1,4-dihydropyridine-3,5-dicarboxylate 186

This product was obtained from 1,3-Diphenyl-1H-pyrazole-4-carbaldehyde(0.074 g, 0.3 mmol), methylacetoacetate(0.195 g, 1.5 mmol)and 33% NH_4OH (0.159 g, 1.5 mmol).

Yield: 4.63%, yellow solid

MP: 166 ^oC

^{1}H NMR (400.13MHz $CDCl_3$): δ2.30 (s, 6H, -CH_3), 3.38(s,6H,OCH_3), 5.30(s, 1H, -CH(4'')), 5.66(s, N-H), 7.24-7.29 (m, 2H, Ar-H(4,4')), 7.38-7.47(m,4H,Ar-H(3,5,3',5')), 7.70(d,2H,J=8.04 Hz,Ar-H(2',6')), 7.72(s,1H,N-C<u>H</u>=C), 7.88(d,2H, J=7.52 Hz,Ar-C(2,6)).

^{13}C NMR (100.61MHz $CDCl_3$): δ18.98 (-CH_3), 28.99(-C (4'')), 50.22(O-<u>C</u>H_3), 103.86(-C(3'',5'')), 118.45(Ar-C(2',6')), 123.53(CH=<u>C</u>-C), 125.60, 126.75, 126.96, 127.62, 127.62, 128.22, 128.41, 128.77(Ar-C(2,3,4,5,6,3',4',5')), 134.46(Ar-C(1)), 139.60(Ar-C(1')), 143.18(-C(2'',6''), 167.42(C=O).

EIMS (HR): $C_{26}H_{26}N_3O_4$ calculated $[M+H]^+$ 444.1923, observed $[M+H]^+$ 444.1916

IR (NaCl/KBr): C=N absorbance 1599.74 cm^{-1}, C=O absorbance at 1674.57 cm^{-1}, C-O-ester absorbance at 1216.36 cm^{-1}.

6.4.26 Synthesis of dimethyl 4-(3-(4-hydroxyphenyl)-1-phenyl-*1H*-pyrazol-4-yl)-2,6-dimethyl-1,4-dihydropyridine-3,5-dicarboxylate 187

This product was obtained from 3-(4-hydroxyphenyl)-1-phenyl-1H-pyrazole-4-carbaldehyde(0.079 g, 0.3 mmol), methylacetoacetate(0.195 g,1.5 mmol) and 33% NH_4OH (0.159 g,1.5 mmol).

Yield: 15.32%, white solid

MP: 270 ^oC

^{1}H NMR (400.13MHz $CDCl_3$): δ2.31 (s, 6H, -CH_3), 3.33(s,6H,OCH_3), 5.30(s, 1H, -CH(4'')), 6.97 (d, 2H,J=9.04 Hz, Ar-H(3,5)),

7.22-7.26(m,1H,Ar-H(4')), 7.41-7.45(m,2H,Ar-H(3',5')),

7.77(d,2H,J=3.92 Hz, 4.68 Hz, Ar-H(2',6')), 7.70(s,1H,N-C<u>H</u>=C),

7.79-7.83(m,2H,Ar-C(2,6)), 8.05(s,1H,N-C<u>H</u>=C)

^{13}C NMR(100.61MHz $CDCl_3$): δ17.34 (-CH_3), 49.23(O-<u>C</u>H_3), 102.87(-C(3'',5'')),

114.19(Ar-C(3,5)), 117.44(Ar-C(2',6')), 125.02, 126.52, 128.76,

129.29(Ar-C(2,6,3',4',5')), 139.75(Ar-C(1')), 144.27(-C(2'',6''), 150.03(N=<u>C</u>-C),

156.48(Ar-C(4)), 167.00(C=O).

EIMS (HR): $C_{26}H_{26}N_3O_5$ calculated $[M+H]^+$ 460.1872, observed $[M+H]^+$ 460.1871

IR (NaCl/KBr): C=N absorbance 1530.38 cm^{-1}, C=O absorbance at 1682.59 cm^{-1},

C-O-ester absorbance at 1216.59 cm^{-1}, O-H absorbance at 3338.65

6.4.27 Synthesis of dimethyl 4-(3-(4-methoxyphenyl)-1-phenyl-*1H*-pyrazol-4-yl)-2,6-dimethyl-1,4-dihydropyridine-3,5-dicarboxylate 188

This product was obtained from 3-(4-methoxyphenyl)-1-phenyl-1H-pyrazole-4-carbaldehyde(0.083 g, 0.3 mmol), methylacetoacetate(0.195 g,1.5 mmol) and 33% NH_4OH (0.159 g, 1.5 mmol).

Yield: 15.71%, white solid

MP: 98-100 °C

^{1}H NMR (400.13MHz $CDCl_3$): δ2.31 (s, 6H, -CH_3), 3.39(s,6H,OCH_3),

3.89(s, 3H, O-CH_3), 5.27(s, 1H, -CH(4'')), 5.64(s, N-H),

7.02 (d, 2H,J=9.04Hz, Ar-H(3,5)), 7.22-7.26(m,1H,Ar-H(4')),

7.40-7.44(m,2H,Ar-H(3',5')), 7.69(d,2H,J=7.56 Hz,Ar-H(2',6')),

7.70(s,1H,N-C<u>H</u>=C), 7.82(d, 2H,J=8.56 Hz,Ar-C(2,6)).

^{13}C NMR(100.61MHz $CDCl_3$): δ19.01 (-CH_3), 29.05(-C(4'')), 50.29(O-<u>C</u>H_3),

64.93(O-CH_3), 103.96(-C(3'',5'')), 113.01(Ar-C(3,5)), 118.34(Ar-C(2',6')),

127.12(Ar-C(1)), 125.46, 126.65, 128.12, 128.74, 129.38(Ar-C(2,6,3',4',5')),

143.05(-C(2'',6''), 150.29(N=<u>C</u>-C), 158.69(Ar-C(4)), 167.44(C=O).

EIMS (HR): $C_{27}H_{27}N_3O_5Na$ calculated $[M+Na]^+$ 496.1848,

observed $[M+Na]^+$ 496.1841

IR (NaCl/KBr): C=N absorbance 1578.60 cm^{-1}, C=O absorbance at 1696.00 cm^{-1},

C-O-ester absorbance at 1208.44 cm^{-1}.

6.4.28 Synthesis of (4-(3-(4-aminophenyl)-1-phenyl-*1H*-pyrazol-4-yl)-2,6-dimethyl-1,4-dihydropyridine-3,5-diyl)bis(phenylmethanone) 190

This product was obtained from 3-(4-aminophenyl)-1-phenyl-1H-pyrazole-4-carbaldehyde(0.079 g, 0.3 mmol), Benzoylacetone (0.267 g, 1.5 mmol) and 33% NH_4OH(0.159 g, 1.5 mmol).

Yield: 1.07%, yellow solid

MP: 130-140 ^oC

^{1}H NMR (400.13MHz, $CDCl_3$): δ 2.07(s, 6H,$C\underline{H}_3$), 5.35 (s, 1H, -CH(4'')), 5.87(s,NH), 6.65(d,2H,J=8.04 Hz,Ar-H(3,5)), 6.97-7.01(m,2H,Ar-H(4')), 7.18-7.67(m,16H,Ar-H)

^{13}C NMR 100.61MHz $CDCl_3$: δ 18.20(-CH_3), 31.12(-CH(4'')), 112.12(-C(3'',5'')), 117.55(Ar-C(3,5)), 118.48(Ar-C(2',6')), 126.41, 127.58, 127.78, 128.04, 128.30, 128.49, 128.67, 128.78, 129.23, 129.28, 130.99, 131.03, 133.27(Ar-C(2,6,3',4',5',2''',3''',4''',5''', 6''', 2'''', 3'''', 4'''', 5'''',6''''), 139.20,139.93(Ar-C(1',1''',1'''')), 140.14(Ar-C(4)), 149.97(N=$\underline{C}$-C), 197.18(C=O).

EIMS (HR): $C_{36}H_{31}N_4O_2$ calculated $[M+H]^+$ 551.2447, observed $[M+H]^+$ 551.2452

IR (NaCl/KBr): C=N absorbance 1597.89 cm^{-1}, C=O absorbance at 1677.63 cm^{-1}

6.4.29 Synthesis of (4-(3-(4-bromophenyl)-1-phenyl-*1H*-pyrazol-4-yl)-2,6-dimethyl-1,4-dihydropyridine-3,5-diyl)bis(phenylmethanone) 191

This product was obtained from 3-(4-bromophenyl)-1-phenyl-1H-pyrazole-4-carbaldehyde(0.098 g, 0.3 mmol), Benzoylacetone (0.267 g, 1.5 mmol) and 33% NH_4OH(0.159 g, 1.5 mmol).

Yield: 8.83%, brown solid

MP: 180 ^oC

^{1}H NMR (400.13MHz, $CDCl_3$): δ 2.06(s, 6H,$C\underline{H}_3$), 5.28 (s, 1H, -CH(4'')), 6.03 (s,NH), 6.76(d,2H,J=8.56 Hz,Ar-H(3,5)), 7.03-7.05(d,2H,J=8.52 Hz,Ar-H(2,6)), 7.24-7.28(m,2H,Ar-H(4''',4'''')), 7.32-7.36(m,4H,Ar-H(3''',5''',3'''',5'''')), 7.40-7.44(m,2H,Ar-H(3',5')), 7.47-7.48(m,5H,Ar-H(4',2''',6''',2'''',6'''')), 7.62-7.64(m,2H,Ar-H(2',6'))

^{13}C NMR 100.61MHz $CDCl_3$: δ18.25(-CH_3), 33.57(-CH(4'')), 112.43(-C(3'',5'')), 118.58(Ar-C(2',6')), 119.08($\underline{C}$=CH-N), 121.46(Ar-C(4)), 125.88, 126.28, 126.75, 127.64, 128.02, 128.65, 128.80, 129.09, 129.48, 129.97, 130.57, 131.08, 131.46, 131.67(Ar-C(2,3,5,6,3',4',5',2''',3''',4''',5''',6''',2'''',3'''',4'''',5'''',6'''')),

138.68(Ar-C(1)), 139.43, 139.48(Ar-C(1',1''',1'''')), 148.88(N=C-C), 197.28(C=O).

EIMS (HR): $C_{36}H_{28}N_3O_2NaBr$ calculated $[M+Na]^+$ 636.1263,

observed $[M+Na]^+$ 636.1274

IR (NaCl/KBr): C=N absorbance 1602.28 cm^{-1}, C=O absorbance at 1655.40 cm^{-1}.

6.4.30 Synthesis of (4-(1,3-diphenyl-*1H*-pyrazol-4-yl)-2,6-dimethyl-1,4-dihydropyridine-3,5-diyl)bis(phenylmethanone) 192

This product was obtained from 1,3-diphenyl-*1H*-pyrazole-4-carbaldehyde (0.074 g, 0.3 mmol), Benzoylacetone (0.267 g, 1.5 mmol) and 33% NH_4OH(0.159 g, 1.5 mmol).

Yield: 15.83%, yellow solid

MP: 110-116 °C

^{1}H NMR (400.13MHz, $CDCl_3$): δ 2.00(s, 6H,C$\underline{H}_3$), 5.34 (s, 1H, -CH(4'')), 6.09(s,NH), 6.98-7.01(m,4H,Ar-H(3,5,2',6')), 7.11-7.12(m,1H,Ar-H(4)), 7.22-7.26(m,1H,Ar-H(4')), 7.28-7.32(m,4H,Ar-H(3',5',4''',4''''), 7.38-7.43(m,4H,Ar-H(3''',5''',3'''',5'''')), 7.45-7.47(m,4H,Ar-H(2''',6''',2'''',6'''')), 7.54(s,1H,N-C$\underline{H}$=C), 7.65(d,2H,J=7.52 Hz,Ar-H(2,6))

^{13}C NMR 100.61MHz $CDCl_3$: δ18.33(-CH_3), 33.77(-CH(4'')), 112.31(-C(3'',5'')), 118.49(Ar-C(2',6')), 125.64, 125.98, 126.40, 127.07, 127.40, 127.70, 127.91, 128.08, 128.74, 131.00(Ar-C(2,3,4,5,6,3',4',5',2''',3''',4''',5''',6''',2'''',3'''',4'''',5'''', 6'''')), 132.72(Ar-C(1)), 139.04, 139.49(Ar-C(1',1''',1'''')), 150.51(N=C-C), 197.34(C=O).

EIMS (HR): $C_{36}H_{30}N_3O_2$ calculated $[M+H]^+$ 536.2338, observed $[M+H]^+$ 536.2341

IR (NaCl/KBr): C=N absorbance 1596.47 cm^{-1}, C=O absorbance at 1656.40 cm^{-1}

6.4.31 Synthesis of (4-(3-(4-(benzyloxy)phenyl)-1-phenyl-*1H*-pyrazol-4-yl)-2,6-dimethyl-1,4-dihydropyridine-3,5-diyl)bis(phenylmethanone) 193

This product was obtained from 3-(4-(benzyloxy)phenyl)-1-phenyl-1H-pyrazole-4-carbaldehyde (0.106 g, 0.3 mmol), Benzoylacetone (0.267 g,1.5 mmol) and 33% NH_4OH(0.159 g, 1.5 mmol).

Yield: 7.48%, yellow solid

MP: 110-116 °C

^{1}H NMR (400.13MHz, $CDCl_3$): δ 1.98(s, 6H,C$\underline{H}_3$), 5.03(s,2H,O-CH_2), 5.31(s, 1H, -CH(4'')), 5.90(s,NH), 6.61(d,2H,J=8.04 Hz,Ar-H(3,5)),

6.90(d,2H,J=8.0 Hz,Ar-H(2,6)),

7.23-7.53(m,18H,Ar-H(3', 4', 5', 2''', 3''', 4''', 5''', 6''', 2'''', 3'''', 4'''', 5'''', 6'''', 2''''', 3''''', 4''''',5''''',6''''')), 7.62(d,2H,J=7.52 Hz,Ar-H(2',6'))

^{13}C NMR 100.61MHz $CDCl_3$: δ18.26(-CH_3), 33.74(-CH(4'')), 69.30(O-CH_2), 112.35(-C(3'',5'')), 113.87(Ar-C(3,5)), 118.40(Ar-C(2',6')), 125.52, 125.87, 126.20, 127.08, 127.55, 127.73, 127.89, 128.18, 128.73, 129.29,

130.97(Ar-C(2,6,3',4',5',2''',3''',4''',5''', 6''', 2'''', 3'''', 4'''', 5'''', 6'''', 2''''', 3''''', 4''''', 5''''', 6''''')), 136.74(Ar-C(1''''')), 138.99, 139.40,

139.56(Ar-C(1',1''',1'''')), 150.25(N=C-C), 157.74(Ar-C(4)), 197.30(C=O).

EIMS (HR): $C_{43}H_{36}N_3O_3Na$ calculated $[M+H]^+$ 642.2757,

observed $[M+H]^+$ 642.2777.

IR (NaCl/KBr): C=N absorbance 1598.90 cm^{-1}

6.4.32 Synthesis of (4-(3-(4-methoxyphenyl)-1-phenyl-*1H*-pyrazol-4-yl)-2,6-dimethyl-1,4-dihydropyridine-3,5-diyl)bis(phenylmethanone) 194

This product was obtained from 3-(4-methoxyphenyl)-1-phenyl-1H-pyrazole-4-carbaldehyde(0.083 g, 0.3 mmol), Benzoylacetone (0.267 g, 1.5 mmol) and 33% NH_4OH(0.159 g, 1.5 mmol).

Yield: 11.47%, white solid

MP: 220 °C

^{1}H NMR (400.13MHz, $CDCl_3$): δ2.00(s, 6H,C$\underline{H}_3$), 5.34 (s, 1H, -CH(4'')), 5.76(s,NH), 6.98-7.02(m,4H,Ar-H(3,5,2,6)), 7.11-7.12(m,1H,Ar-H(4)), 7.23-7.27(m,1H,Ar-H(4')), 7.28-7.33(m,4H,Ar-H(3',5',4''',4''''), 7.39-7.45(m,4H,Ar-H(3''',5''',3'''',5'''')), 7.47-7.49(m,4H,Ar-H(2''',6''',2'''',6'''')), 7.55(N-C$\underline{H}$=C), 7.64(d,2H,J=7.52 Hz,Ar-H(2',6'))

^{13}C NMR (100.61MHz $CDCl_3$): δ 18.34(-CH_3), 33.77(-CH(4'')), 112.42(-C(3'',5'')), 118.47(Ar-C(2',6')), 125.61, 125.86, 126.33, 127.06, 127.39, 127.72, 127.92, 128.10, 128.73, 131.01(Ar-C(2, 3, 5, 6, 3', 4', 5', 2''', 3''', 4''', 5''', 6''', 2'''', 3'''', 4'''', 5'''', 6'''')), 132.76(Ar-C(1)), 139.00,139.17(Ar-C(1',1''',1'''')), 150.55(N=C-C), 197.25(C=O).

EIMS (HR): $C_{37}H_{31}N_3O_3Na$ calculated $[M+Na]^+$ 588.2263,

observed $[M+Na]^+$ 588.2261

IR (NaCl/KBr): C=N absorbance 1596.97 cm^{-1}, C=O absorbance at 1655.79 cm^{-1}

6.5 General procedure for synthesis of ester and amide derivatives

EDCI (0.28 mmol, 58.4 mg) and DMAP (0.02 mmol, 2.6 mg) were added to a round bottom flask as a catalyst. Nitrogen was introduced for 5 minutes to allow these components to combine in DCM. (0.2 mmol, 100 mg) of the 4-[3-(4-hydroxyphenyl)-1-phenyl-1H-pyrazol-4-yl]-2,6-dimethyl-1,4-dihydro-pyridine-3,5-dicarboxylic acid diethyl ester dissolved in 10 mL dried DCM was then added to the flask. Along with (0.2 mmol) non-steroidal anti-inflammatory's(NSAIDs) drug or acetic acid was also added into the reaction mixture in the flask and the mixture left at room temperature overnight. When the reaction was deemed to be complete, 50 mL of DCM poured into flask and the product were extracted, then washed with water and saturated $NaHCO_3$ 25 mL each. The organic layer was separated and dried with $NaSO_4$ before the solvent was removed by a rotary evaporator. The product was finally purified using column chromatography (Biotage SP1 instrument) to obtain yields of 13%-25%.

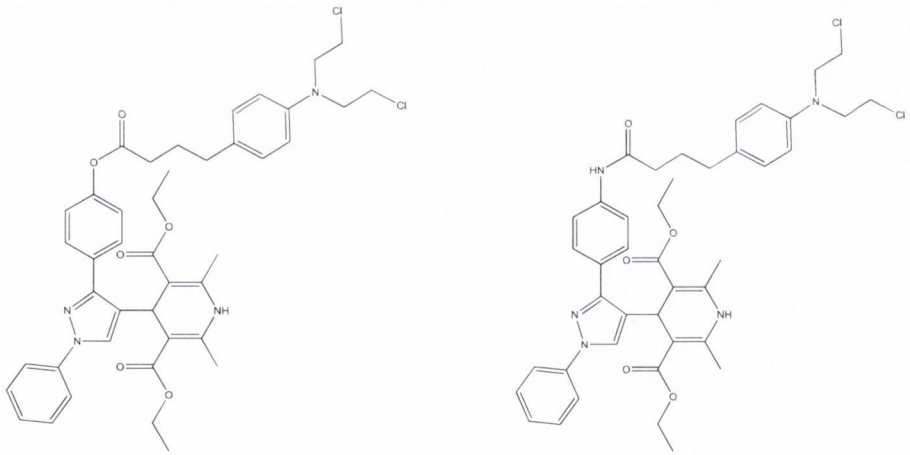

6.5.1 Synthesis of diethyl 4-(3-(4-(4-(4-(bis(2-chloroethyl)amino)phenyl) butanoyloxy)phenyl)-1-phenyl-*1H*-pyrazol-4-yl)-2,6-dimethyl-1,4-dihydropyridine-3,5-dicarboxylate 195

This product was obtained from 4-[3-(4-Hydroxy-phenyl)-1-phenyl-1H-pyrazol-4-yl]-2,6-dimethyl-1,4-dihydro-pyridine-3,5-dicarboxylic acid diethyl ester (100 mg, 0.2 mmol), dimethylaminopropyl-3-ethylcarboliimide hydrochloride (58.4 mg, 0.24 mmol), 4-dimethylaminopyridine (2.6 mg, 0.02 mmol) and chloroambucil (66.2 mg,0.2 mmol).

Yield: 95.95%, light yellow solid

MP: 152 ^{o}C

^{1}H NMR (400.13MHz, $CDCl_3$): δ1.14(t, 6H,J=7.04 Hz, CH_2-$C\underline{H}_3$), 2.06-2.10(m,2H,CH_2), 2.16(s, 6H, -$C\underline{H}_3$), 2.62-2.71(m,4H,CH_2), 3.63-3.67(m,4H,CH_2Cl), 3.71-3.75(m, 2H, $C\underline{H}_2$-CH_3), 3.75-3.78(m,4H,N-CH_2), 3.94-4.02(m, 2H, $C\underline{H}_2$-CH_3), 5.18(s, 1H, -CH(4'')), 6.67(d, 2H,J=8.76 Hz, Ar-H(3,5), 7.07(d,2H,J=8.8 Hz,Ar-H(3''',5''')), 7.14(d,2H,Ar-H(2''',6''')), 7.25-7.27(m,1H,Ar-H(4')), 7.41-7.45(m,2H,Ar-H(3',5')), 7.65(d,2H,J=8.8 Hz,Ar-H(2',6')), 7.69(d,2H,J=8.76 Hz,Ar-H(2,6)), 7.78(s,1H,N-C$\underline{H}$=C).

^{13}C NMR (100.61MHz, $CDCl_3$): δ13.56 (-$CH_2\underline{C}H_3$), 19.39(-CH_3), 26.74(-CH_2), 29.84(-CH(4'')), 33.67(-CH_2), 33.85(-CH_2), 40.51(-CH_2), 53.60(-CH_2), 59.10 (-$\underline{C}H_2CH_3$), 102.86(C(3'',5'')), 112.21(Ar-C(3''',5''')), 118.86(Ar-C(2',6')), 121.21(Ar-C(3,5), 128.36(Ar-C(1)), 126.08,126.50,129.28,129.78,130.21, 130.71(ArC(2,6,3',4',5',2''',6''')), 132.85(Ar-C(1''')), 140.41(Ar-C(1')), 144.33, 144.44(Ar-C(4,4''')), 150.30(N=C), 168.01(C=O), 173.34(C=O).

EIMS (HR): $C_{42}H_{46}N_4O_6NaCl_2$ calculated $[M+Na]^+$ 795.2692, observed $[M+Na]^+$ 795.2684.

IR (NaCl/KBr): C=N absorbance 1615.33 cm^{-1}, C-O-ester absorbance at 1209.78 cm^{-1}

6.5.2 Synthesis of diethyl 4-(3-(4-(4-(4-(bis(2-chloroethyl)amino)phenyl) butanamido)phenyl)-1-phenyl-*1H*-pyrazol-4-yl)-2,6-dimethyl-1,4-dihydropyridine-3,5-dicarboxylate 196

This product was obtained from diethyl 4-(3-(4-aminophenyl)-1-phenyl-1H-pyrazol-4-yl)-2,6-dimethyl-1,4-dihydropyridine-3,5-dicarboxylate (100 mg, 0.2 mmol), dimethylaminopropyl-3-ethylcarboliimide hydrochloride (58.4 mg, 0.24 mmol), 4-dimethylaminopyridine (2.6 mg, 0.02 mmol) and chloroambucil (66.2 mg,0.2 mmol).

Yield: 29.6%, yellow solid

MP: 186 °C

^{1}H NMR (400.13MHz, $CDCl_3$): δ 1.08(t, 6H, J=7.04 Hz, CH_2-$C\underline{H}_3$), 1.28(t,2H,J=7.52 Hz,CH_2), 2.06(t,2H,J=7.52 Hz,CH_2), 2.19(t,2H,J=7.52 Hz,CH_2), 2.27(s,6H,CH_3), 3.81-3.85(m,4H,CH_2Cl), 3.87-3.92(m,2H,$C\underline{H}_2$-CH_3), 4.01-4.08(m,4H, $C\underline{H}_2$-CH_3, N-CH_2), 4.11-4.16(m, 2H, N-CH_2), 5.27(s, 1H, -CH(4'')), 7.17(d, 2H,J=8.04 Hz, Ar-H(3''',5'''), 7.23-7.27(m,3H,Ar-H(4',2''',6''')), 7.40-7.44(m,2H,Ar-H(3',5')), 7.52(d,2H,J=8.56 Hz,Ar-H(2,6)),

7.68(d,2H,J=8.04 Hz,Ar-H(2',6')), 7.74(d,2H,J=8.56 Hz,Ar-H(3,5)),
7.78(s,1H,N-C<u>H</u>=C).

^{13}C NMR (100.61MHz, $CDCl_3$): δ 13.75,13.86 (-CH_2<u>C</u>H_3), 18.93,19.09(-CH_3), 20.64(-CH_2), 29.19, 29.46(-CH_2), 47.22(-CH_2), 59.30, 59.35(-CH_2Cl), 60.02(-<u>C</u>H_2CH_3), 103.15, 103.99(C(3'',5'')), 117.80(Ar-C(3''',5''')), 118.44(Ar-C(3,5)), 119.65(Ar-C(2',6')), 128.21(Ar-C(1)), 125.68, 125.76, 126.72, 129.38, 129.77, 131.13, 131.68(ArC(2,6,3',4',5',2''',6''')), 135.71(Ar-C(1''')), 139.54(Ar-C(1')), 143.47(Ar-C(4''')), 150.57(N=C), 159.08(C(2'',6'')), 167.27(C=O)

EIMS (HR): $C_{42}H_{47}N_5O_5NaCl_2$ calculated $[M+Na]^+$ 794.2852, observed $[M+Na]^+$ 794.2844.

IR (NaCl/KBr): C=N absorbance 1598.96 cm^{-1}, C=O absorbance at 1671.23 cm^{-1}, C-O-ester absorbance at 1211.73 cm^{-1}.

6.5.3 Synthesis of (Z)-diethyl 4-(3-(4-(2-(5-fluoro-2-methyl-1-(4-(methylsulfinyl) benzylidene)-1H-inden-3-yl)acetoxy)phenyl)-1-phenyl-*1H*-pyrazol-4-yl)-2,6-dimethyl-1,4-dihydropyridine-3,5-dicarboxylate 204

This product was obtained from diethyl 4-(3-(4-aminophenyl)-1-phenyl-1H-pyrazol-4-yl)-2,6-dimethyl-1,4-dihydropyridine-3,5-dicarboxylate (100 mg, 0.2 mmol), dimethylaminopropyl-3-ethylcarboliimide hydrochloride (58.4 mg, 0.24 mmol), 4-dimethylaminopyridine (2.6 mg, 0.02 mmol) and Sulindac (71.3 mg,0.2 mmol).

Yield: 32.55%, yellow solid

MP: 182 °C

^{1}H NMR (400.13MHz, $CDCl_3$): δ1.12(t,6H,J=7.32 Hz,CH_2-C<u>H</u>$_3$), 2.10(s,6H,CH_3), 2.29(s,3H,CH_3), 2.93(s,3H,CH_3), 3.84(s,2H,CH_2), 3.87-3.94(m,2H,C<u>H</u>$_2$-CH_3), 3.98-4.04(m,4H, C<u>H</u>$_2$-CH_3), 5.18(s, 1H, -CH(4'')), 6.22(s,1H,Ar-C<u>H</u>=C), 6.98(d,1H,J=8.8 Hz,Ar-H(3''')), 7.07(d,2H,J=8.32 Hz,Ar-H(3,5)), 7.18-7.24(m,3H,Ar-H(4',5''',6''')), 7.37-7.41(m,2H,Ar-H(3',5')), 7.65-7.73(m,8H,Ar-H(2,6,2',6',2'''',3'''',5'''',6'''')), 7.77(s,1H,N-C<u>H</u>=C).

^{13}C NMR (100.61MHz, $CDCl_3$): δ 10.26(-CH_3), 13.73,13.97(-CH_2<u>C</u>H_3), 18.79(-CH_3), 29.45(-CH(4'')), 36.07(-CH_2), 43.38(-CH_3), 59.15, 59.95(-<u>C</u>H_2CH_3), 102.29(C(3'',5'')), 105.40(Ar-C(3''')), 110.39, 110.62(Ar-C(5''',6''')), 118.38(Ar-C(2',6')), 120.45, 123.31, 125.69, 126.46, 128.16, 128.28, 129.08, 129.10, 130.34(Ar-C(2,3,5,6,3',4',5',1''',6''',2'''',3'''',5'''',6'''')), 132.28(C=C-CH_3),

138.34(Ar-C(1'''')), 139.31(Ar-C(1')), 141.03(C=CH), 144.97(Ar-C(4'''')), 144.05(C(2'',6'')), 146.05(Ar-C(2'''), 149.84(Ar-C(4)), 150.58(N=C), 162.11(Ar-C(4''')), 167.27(C=O), 169.35(C=O).

EIMS (HR): $C_{48}H_{45}N_3O_7FS$ calculated $[M+H]^+$ 826.2962, observed $[M+H]^+$ 826.2980.

IR (NaCl/KBr): C=N absorbance 1600.74 cm^{-1}, C=O absorbance at 1688.91 cm^{-1}, C-O-ester absorbance at 1209.15 cm^{-1}.

6.5.4 Synthesis of diethyl 4-(3-(4-(2-(1-(4-chlorobenzoyl)-4-methoxy-2-methyl-1H-indol-3-yl)acetoxy)phenyl)-1-phenyl-*1H*-pyrazol-4-yl)-2,6-dimethyl-1,4-dihydropyridine-3,5-dicarboxylate 205

This product was obtained from diethyl 4-(3-(4-aminophenyl)-1-phenyl-1H-pyrazol-4-yl)-2,6-dimethyl-1,4-dihydropyridine-3,5-dicarboxylate (100 mg, 0.2 mmol), dimethylaminopropyl-3-ethylcarboliimide hydrochloride (58.4 mg, 0.24 mmol), 4-dimethylaminopyridine (2.6 mg, 0.02 mmol) and indomethacin (71.6 mg,0.2 mmol).

Yield: 14.2%, yellow solid

MP: 168 °C

^{1}H NMR (400.13MHz, $CDCl_3$): δ1.20(t,6H,J=7.04 Hz,CH_2-C$\underline{H}_3$), 2.07(s,3H,CH_3), 2.51(s,3H,CH_3), 3.87(s,3H,OCH_3), 3.98(s,2H,COC$\underline{H}_2$), 3.97-4.02(m,2H,C$\underline{H}_2$-CH_3), 4.05-4.08(m,4H, C$\underline{H}_2$-CH_3), 5.17(s, 1H, -CH(4'')), 6.72-6.75(m,1H,Ar-H(4''')), 6.92(d,1H,J=9.04 Hz,Ar-H(6''')),7.04-7.08(m,3H,Ar-H(3,5,5''')), 6.98(d,1H,J=8.8 Hz,Ar-H(3''')), 7.07(d,2H,J=8.32 Hz,Ar-H(3,5)), 7.29-7.31(m,1H,Ar-H(4')), 7.44-7.48(m,2H,Ar-H(3',5')), 7.52(d,2H,J=8.56 Hz,Ar-H(3'''',5'''')), 7.58(d,2H,J=8.0 Hz,Ar-H(2',6')), 7.71-7.73(m,4H,Ar-H(2,6,2'''',6'''')), 7.82(s,1H,N-C$\underline{H}$=C).

^{13}C NMR (100.61MHz, $CDCl_3$): δ13.04, 13.99(-$CH_2\underline{C}H_3$), 19.01(-CH_3), 29.79(-CH(4'')), 30.11(-CH_2), 55.30(-OCH_3), 59.22(-$\underline{C}H_2CH_3$), 100.78(Ar-C(4''')), 101.84($\underline{C}$=C-CH_3), 111.31(Ar-C(6''')), 114.65(Ar-C(2''')), 118.69(Ar-C(2',6')), 120.50, 126.08, 126.55, 128.75, 128.95, 129.97, 130.42, 130.78(Ar-C(2,3,5,6,3',4',5',5''',2'''',3'''',5'''',6'''')), 138.87(Ar-C(1''')), 139.00(Ar-C(1')), 143.88(C(2'',6'')), 150.08(N=C), 155.69(Ar-C(3''')), 167.07(C=O), 170.32(C=O).

EIMS (HR): $C_{47}H_{44}N_4O_8Cl$ calculated $[M+H]^+$ 827.2848,

observed $[M+H]^+$ 827.2877.

IR (NaCl/KBr): C=N absorbance 1599.94 cm^{-1}, C=O absorbance at 1688.63 cm^{-1}, C-O-ester absorbance at 1213.52 cm^{-1}.

6.5.5 Synthesis of diethyl 4-(3-(4-(2-(4-isobutylphenyl)propanoyloxy)phenyl)-1-phenyl-*1H*-pyrazol-4-yl)-2,6-dimethyl-1,4-dihydropyridine-3,5-dicarboxylate 206

This product was obtained from 4-[3-(4-hydroxy-phenyl)-1-phenyl-1H-pyrazol-4-yl]-2,6-dimethyl-1,4-dihydro-pyridine-3,5-dicarboxylic acid diethyl ester (100 mg, 0.2 mmol), dimethylaminopropyl-3-ethylcarboliimide hydrochloride (58.4 mg, 0.24 mmol), 4-dimethylaminopyridine (2.6 mg, 0.02 mmol) and Ibuprofen (41.2 mg,0.2 mmol).

Yield: 45.95%, white solid

MP: 192 °C

^{1}H NMR (400.13MHz, $CDCl_3$): δ 0.94(d,6H,J=6.52 Hz,CH_3), 1.19(t,6H,J=7.0 Hz,CH_2-C$\underline{H}_3$), 1.65(d,3H,J=7.0 Hz,CHC$\underline{H}_3$), 1.88-1.92(m,1H,$CH_3C\underline{H}CH_3$), 2.10(s, 6H, -C$\underline{H}_3$), 2.51(d,2H,J=7.52 Hz,-CH_2), 3.97-4.06(m,5H,C$\underline{H}_2$-CH_3, C$\underline{H}CH_3$), 5.17(s, 1H, -CH(4'')), 5.89(s,NH), 6.97(d,2H,J=8.04 Hz,Ar-H(3''',5''')), 7.20(d,2H,J=8.0 Hz,Ar-H(3,5)), 7.22-7.26(m,1H,Ar-H(4')), 7.33(d,2H,J=8.04 Hz,Ar-H(2''',6''')), 7.40-7.44(m,2H,Ar-H(3',5')), 7.55(d,2H,J=8.52 Hz,Ar-H(2',6')), 7.69(d,2H,J=8.04 Hz,Ar-H(2,6)), 7.80(s,1H,N-C$\underline{H}$=C).

^{13}C NMR (100.61MHz, $CDCl_3$): δ14.00(-$CH_2\underline{C}H_3$), 18.14(-$CH\underline{C}H_3$), 18.87,18.92(-$\underline{C}H_3$), 21.96(-$\underline{C}H_3CH$), 29.83(-$CH_3\underline{C}HCH_3$), 29.76(-CH(4'')), 44.60(-CH_2), 44.81(-CH), 59.13(-$\underline{C}H_2CH_3$), 101.91(C(3'',5'')), 118.23(Ar-C(2',6')), 120.42(Ar-C(3,5)), 125.52(N-$\underline{C}$H=C), 127.73(Ar-C(1)), 126.70, 127.73, 128.84, 129.19, 130.61(Ar-C(2,6,3',4',5',2''',3''',5''',6''')), 132.39(Ar-C(1''')), 139.57(Ar-C(1')), 140.06(Ar-C(4''')), 144.06(-C(2'',6'')), 150.07(N=C), 151.44(Ar-C(4)), 167.24(C=O), 174.35(C=O).

EIMS (HR): $C_{41}H_{45}N_3O_6Na$ calculated $[M+Na]^+$ 698.3206, observed $[M+Na]^+$ 698.3211.

IR (NaCl/KBr): C=N absorbance 1600.92 cm^{-1}, C=O absorbance at 1694.01 cm^{-1}, C-O-ester absorbance at 1211.74 cm^{-1}.

6.5.6 Synthesis of diethyl 4-(3-(4-(2-(4-benzoylphenyl)propanoyloxy)phenyl)-1-phenyl-*1H*-pyrazol-4-yl)-2,6-dimethyl-1,4-dihydropyridine-3,5-dicarboxylate 207

This product was obtained from 4-[3-(4-hydroxy-phenyl)-1-phenyl-1H-pyrazol-4-yl]-2,6-dimethyl-1,4-dihydro-pyridine-3,5-dicarboxylic acid diethyl ester (100 mg, 0.2 mmol), dimethylaminopropyl-3-ethylcarboliimide hydrochloride (58.4 mg, 0.24 mmol), 4-dimethylaminopyridine (2.6 mg, 0.02 mmol) and Ketoprofen (50.8 mg,0.2 mmol).

Yield: 30.26%, white solid

MP: 178 ^{o}C

^{1}H NMR (400.13MHz, $CDCl_3$): δ1.19(t,6H,J=7.28 Hz,CH_2-C$\underline{H}_3$), 1.71(d,3H,J=7.04 Hz,-C$\underline{H}_3$CH), 2.10(s, 6H,-C$\underline{H}_3$), 3.99-4.14(m,5H,-C$\underline{H}_2$-CH_3,-C$\underline{H}CH_3$), 5.18(s, 1H, -CH(4'')), 5.77(s,NH), 6.99(d, 2H,J=8.52 Hz,Ar-H(3,5)), 7.23-7.27(m,1H,Ar-H(4')), 7.41-7.45(m,2H,Ar-H(3',5')), 7.50-7.54(m,2H,Ar-H(2''',6''')), 7.56-7.62(m,4H,Ar-H(2,6,3'''',5'''')), 7.64-7.70(m,3H,Ar-H(2',6',4'''')), 7.76-7.80(m,2H,Ar-H(3''',5''')), 7.85(d,2H,J=7.0 Hz,Ar-H(2'''',6'''')), 7.90(s,1H,N-C$\underline{H}$=C).

^{13}C NMR (100.61MHz, $CDCl_3$): δ 13.56(-CH$\underline{C}H_3$), 14.22,14.35(-$CH_2\underline{C}H_3$), 18.50, 18.64(-CH_3), 30.13(CH(4'')), 45.52(-CH), 59.63, 60.44(-$\underline{C}H_2CH_3$), 102.51, 102.56(C(3'',5'')), 118.74,119.11(Ar-C(2',6')), 120.76(Ar-C(3,5)), 126.03, 128.20, 128.41, 128.84, 128.92, 129.18, 129.23, 129.30, 129.39, 130.10, 131.10(Ar-C(2,6,3',4',5',2''',3''',5''',6''',2'''',3'''',5'''',6'''')), 132.70(Ar-C(4'''')), 137.39(Ar-C(4''')), 138.22(Ar-C(1'''')), 140.01, 140.27(Ar-C(1',1''')), 144.30, 144.33(-C(2'',6'')), 150.33(N=C), 151.76(Ar-C(4)), 167.68(C=O), 174.01(C=O), 196.51(C=O).

EIMS (HR): $C_{44}H_{41}N_3O_7Na$ calculated $[M+Na]^+$ 746.2842, observed $[M+Na]^+$ 746.2840.

IR (NaCl/KBr): C=N absorbance 1599.21 cm^{-1}, C=O absorbance at 1693.36 cm^{-1}, C-O-ester absorbance at 1211.49 cm^{-1}.

6.5.7 Synthesis of diethyl 4-(3-(4-(2-acetoxybenzoyloxy)phenyl)-1-phenyl-*1H*-pyrazol-4-yl)-2,6-dimethyl-1,4-dihydropyridine-3,5-dicarboxylate 208

This product was obtained from 4-[3-(4-Hydroxy-phenyl)-1-phenyl-1H-pyrazol-4-yl]-2,6-dimethyl-1,4-dihydro-pyridine-3,5-dicarboxylic acid diethyl ester (100 mg,

0.2 mmol), dimethylaminopropyl-3-ethylcarboliimide hydrochloride (58.4 mg, 0.24 mmol), 4-dimethylaminopyridine (2.6 mg, 0.02 mmol) and acetylsalicylic acid (36.0 mg,0.2 mmol).

Yield: 21.4%, white solid

MP: 186 ^{o}C

^{1}H NMR (400.13MHz, $CDCl_3$): δ1.23(t, 6H,J=7.04 Hz,CH_2-C<u>H</u>$_3$), 2.12(s, 6H, -C<u>H</u>$_3$), 2.33(s,3H, COC<u>H</u>$_3$), 3.99-4.06(m,2H,C<u>H</u>$_2$-CH_3), 4.07-4.14(m,2H,C<u>H</u>$_2$-CH_3), 5.20(s, 1H, -CH(4'')), 5.71(s,NH), 7.18(d, 2H,J=8.52 Hz,Ar-H(3,5)), 7.22-7.24(m,1H,Ar-H(4''')), 7.25-7.27(m,1H,Ar-H(4')), 7.43-7.47(m,3H,Ar-H(3',5',5''')), 7.62(d,2H,J=8.52 Hz,Ar-H(2,6)), 7.70-7.74(m,3H,Ar-H(2',6',3''')), 7.83(s,1H,N-C<u>H</u>=C), 8.28(dd,1H,J=1.84,9.52 Hz,Ar-H(6''))

^{13}C NMR (100.61MHz, $CDCl_3$): δ14.46(-CH_2<u>C</u>H$_3$), 19.43(-CH_3), 21.01(CO<u>C</u>H$_3$), 30.24(-CH(4'')), 59.63(-<u>C</u>H$_2$$CH_3$), 102.44(C(3'',5'')), 118.76(Ar-C(2',6')), 121.11(Ar-C(3,5)), 122.43(N-<u>C</u>H=C), 124.01(Ar-C(4')), 126.06, 126.32, 126.40, 128.09, 129.32, 131.43, 132.35(Ar-C(2,6,3',4',5',3''',5''')), 133.12(Ar-C(6''')), 134.91(Ar-C(4''')), 139.98(Ar-C(1')), 144.34(-C(2'',6'')), 150.26(N=C), 151.07, 151.92(Ar-C(4,2''')), 164.58(C=O), 167.65(C=O), 169.66(C=O).

EIMS (HR): $C_{37}H_{36}N_3O_8$ calculated $[M+H]^+$ 650.2502, observed $[M+H]^+$ 650.2513.

IR (NaCl/KBr): C=N absorbance 1604.40 cm^{-1}, C=O absorbance at 1689.10 cm^{-1}, C-O-ester absorbance at 1208.08 cm^{-1}.

6.5.8 Synthesis of diethyl 4-(3-(4-acetoxyphenyl)-1-phenyl-*1H*-pyrazol-4-yl)-2,6-dimethyl-1,4-dihydropyridine-3,5-dicarboxylate 209

This product was obtained from 4-[3-(4-hydroxy-phenyl)-1-phenyl-1H-pyrazol-4-yl]-2,6-dimethyl-1,4-dihydro-pyridine-3,5-dicarboxylic acid diethyl ester (100 mg, 0.2 mmol), dimethylaminopropyl-3-ethylcarboliimide hydrochloride (58.4 mg, 0.24 mmol), 4-dimethylaminopyridine (2.6 mg, 0.02 mmol) and acetic acid (12.0 mg,0.2 mmol).

Yield: 53.2%, white liquid

MP: Oil

^{1}H NMR (400.13MHz, $CDCl_3$): δ1.12(t, 6H,J=7.0 Hz,CH_2-C<u>H</u>$_3$), 2.07(s, 6H, -C<u>H</u>$_3$), 2.29(s,3H, COC<u>H</u>$_3$), 3.86-3.94(m,2H,C<u>H</u>$_2$-CH_3), 3.97-4.05(m,2H,C<u>H</u>$_2$-CH_3), 5.22(s, 1H, -CH(4'')), 6.36(s,NH), 7.05(d, 2H,J=8.0 Hz,Ar-H(3,5)),7.17-7.21(m,1H,

Ar-H(4')), 7.35-7.39(m,2H,Ar-H(3',5')),7.64(d,2H,J=8.52 Hz,Ar-H (2,6)), 7.72(d,2H,J=7.52 Hz,Ar-H(2',6')), 7.76(s,1H,N-C<u>H</u>=C).

^{13}C NMR (100.61MHz, $CDCl_3$): δ13.91(-CH_2<u>C</u>H_3), 18.64(-CH_3), 20.63(CO<u>C</u>H_3), 59.20(-<u>C</u>H_2CH_3), 102.13(C(3'',5'')), 118.30(Ar-C(2',6')), 120.60(Ar-C(3,5)), 125.60(N-<u>C</u>H=C), 126.30, 128.00, 128.81, 130.30(Ar-C(2,6,3',4',5')),139.45(Ar-C(1')), 144.26(-C(2'',6'')), 149.82(N=C), 150.91(Ar-C(4)), 166.34(C=O), 170.19(C=O).

EIMS (HR): $C_{30}H_{32}N_3O_6$ calculated $[M+H]^+$ 530.2291, observed $[M+H]^+$ 530.2302.

IR (NaCl/KBr): C=N absorbance 1615.33 cm^{-1}, C=O absorbance at 1690.66 cm^{-1}, C-O-ester absorbance at 1209.78 cm^{-1}.

6.5.9 Synthesis of (E)-diethyl 4-(3-(4-(3-(3-hydroxy-4-methoxyphenyl)-2-(3,4,5-trimethoxyphenyl)acryloyloxy)phenyl)-1-phenyl-1H-pyrazol-4-yl)-2,6-dimethyl-1,4-dihydropyridine-3,5-dicarboxylate 210

This product was obtained from 4-[3-(4-hydroxy-phenyl)-1-phenyl-1H-pyrazol-4-yl]-2,6-dimethyl-1,4-dihydro-pyridine-3,5-dicarboxylic acid diethyl ester (100 mg, 0.2 mmol), dimethylaminopropyl-3-ethylcarboliimide hydrochloride (58.4 mg, 0.24 mmol), 4-dimethylaminopyridine (2.6 mg, 0.02 mmol) and Combretastatin A-4 corboxylic acid (63.3 mg,0.2 mmol).

Yield: 16.2%, yellow solid

MP: 180 °C

^{1}H NMR (400.13MHz, $CDCl_3$): δ1.10(t, 6H, J=7.0 Hz, CH_2-C<u>H</u>$_3$), 2.20(s, 6H,-C<u>H</u>$_3$), 3.31(s, 3H, OCH_3), 3.80-3.88(m, 2H, C<u>H</u>$_2$-CH_3), 3.98-4.05(m, 2H, C<u>H</u>$_2$-CH_3), 4.90(s, 9H,OCH_3), 5.22(s, 1H, -OH), 6.87(d, 2H,J=8.76 Hz,Ar-H(3,5)), 7.25-7.29(m,1H,Ar-H(4')),7.42-7.46(m,2H,Ar-H(3',5')), 7.59(d,2H,J=8.76 Hz,Ar-H(2,6)), 7.65(d,2H,J=7.6 Hz,Ar-H(2',6')), 7.85(s,1H,N-C<u>H</u>=C).

^{13}C NMR (100.61MHz, $CDCl_3$): δ 11.05,11.33(-CH_2<u>C</u>H_3), 17.45(-CH_3), 27.65(-CH(4'')), 57.31(-<u>C</u>H_2CH_3), 100.45(C(3'',5'')), 112.36(Ar-C(5'''')), 116.74(Ar-C(2',6')), 123.38(Ar-C(1''')), 124.05(Ar-C(3,5)), 126.91(Ar-C(1'''')), 125.61,127.13,128.09(Ar-C(2,6,3',4',5')), 132.85(Ar-C(1''')), 137.75(Ar-C(4''')), 143.26(Ar-C(4)), 149.64(N=C), 155.17(Ar-C(3''',5''')), 166.34(C=O).

EIMS (HR): $C_{47}H_{48}N_3O_{11}$ calculated $[M+H]^+$ 830.3289,observed $[M+H]^+$ 830.3271.

IR (NaCl/KBr): C=N absorbance 1612.33 cm^{-1}, C=O absorbance at 1683.36 cm^{-1}, C-O-ester absorbance at 1210.32 cm^{-1}.

6.6 General procedure for synthesis of basic side chain derivatives

The appropriate phenol 4-[3-(4-hydroxy-phenyl)-1-phenyl-1H-pyrazol-4-yl]-2,6-dimethyl-1,4-dihydro-pyridine-3,5-dicarboxylic acid diethyl ester(10 mmol, 1 equiv.) was dissolved in 100 mL of dry acetone and placed in a round bottom flask. Anhydrous potassium carbonate (0.16 mol, 22 g, 16 equiv.) was added. They are stirred gently for 10 min under a nitrogen atmosphere and the corresponding basic side chain was then added (40 mmol,4 equiv.). The reaction was refluxed until complete on thin layer chromatography. On completion the solution was filtered and the solvent was removed by rotary evaporator. Residue was purified by column chromatography in silica gel.

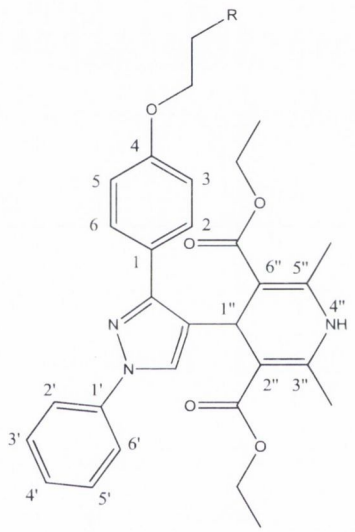

6.6.1 Synthesis of diethyl 2,6-dimethyl-4-(1-phenyl-3-(4-(2-(pyrrolidin-1-yl)ethoxy) phenyl)-*1H*-pyrazol-4-yl)-1,4-dihydropyridine-3,5-dicarboxylate 216

This product was obtained from 4-[3-(4-hydroxy-phenyl)-1-phenyl-1H-pyrazol-4-yl]-2,6-dimethyl-1,4-dihydro-pyridine-3,5-dicarboxylic acid diethyl ester (487.6 mg, 1 mmol), potassium carbonate (16 mmol, 2.2 g) and 1-(2-chloroethyl)pyrrolidine (4 mmol,680.3 mg).

Yield: 23.6%, white solid

MP: 178 ^{o}C

^{1}H NMR (400.13MHz, $CDCl_3$): δ1.14(t,6H,J=7.04 Hz,CH_2-$C\underline{H}_3$),1.76-1.82(m,4H,-CH_2), 2.26(s, 6H, -$C\underline{H}_3$), 2.56-2.62(m,4H,CH_2), 2.91(t,2H,J=5.04 Hz,CH_2-N), 3.75-3.80(m,2H,$C\underline{H}_2$-CH_3), 3.97-4.01(m,2H,$C\underline{H}_2$-CH_3), 4.15(t,2H,J=5.52 Hz,$C\underline{H}_2CH_2$-N), 5.17(s, 1H, -CH(4'')), 6.94(d,2H,J=9.04 Hz,Ar-H(3,5)), 7.19-7.23(m,1H,Ar-H(4')), 7.37-7.41(m,2H,Ar-H(3',5')),7.48(d,2H,J=9.04 Hz, Ar-H(2,6)),

7.65(d,2H,J=8.52 Hz,Ar-H(2',6')), 7.79(s,1H,N-C<u>H</u>=C).

^{13}C NMR (100.61MHz, $CDCl_3$): δ 13.88(-CH_2<u>C</u>H_3), 18.39(-CH_3), 23.01, 23.13(-CH_2) , 29.12(-CH(4'')), 54.28, 54.64(-CH_2), 57.74(-N-CH_2), 58.80, 58.93(-<u>C</u>H_2CH_3), 63.47(-<u>C</u>H_2CH_2-N), 102.02(C(3'',5'')), 113.29(Ar-C(3,5)), 118.22(Ar-C(2',6')), 125.37, 128.38, 128.80, 129.56, 130.42(Ar-C(2,6,3',4',5')), 139.66(Ar-C(1')), 145.22(C(2'',6'')), 156.08(Ar-C(4)), 167.31(C=O).

EIMS (HR): $C_{34}H_{41}N_4O_5$ calculated $[M+H]^+$ 585.3077, observed $[M+H]^+$ 585.3083.

IR (NaCl/KBr): C=N absorbance 1600.23 cm^{-1}, C=O absorbance at 1692.28 cm^{-1}, C-O-ester absorbance at 1211.34 cm^{-1}.

6.6.2 Synthesis of diethyl 2,6-dimethyl-4-(1-phenyl-3-(4-(2-(piperidin-1-yl)ethoxy)phenyl)-*1H*-pyrazol-4-yl)-1,4-dihydropyridine-3,5-dicarboxylate 217

This product was obtained from 4-[3-(4-Hydroxy-phenyl)-1-phenyl-1H-pyrazol-4-yl]-2,6-dimethyl-1,4-dihydro-pyridine-3,5-dicarboxylic acid diethyl ester (487.6 mg, 1 mmol), potassium carbonate (16 mmol, 2.2 g) and 1-(2-chloroethyl)piperidine (4 mmol,736.4 mg).

Yield: 9.28%, white solid

MP: 182 °C

^{1}H NMR (400.13MHz, $CDCl_3$): δ 1.08(t,6H,J=7.04 Hz,CH_2-C<u>H</u>$_3$), 1.22-1.26(m,2H,-CH_2), 1.62-1.64(m,4H,-CH_2), 2.18(s, 6H, -C<u>H</u>$_3$), 2.52-2.58(m,4H,CH_2), 2.81(t,2H,J=6.04 Hz,CH_2-N), 3.79-3.83(m,2H,C<u>H</u>$_2$-CH_3), 3.99-4.04(m,2H,C<u>H</u>$_2$-CH_3), 4.17(t,2H,J=5.52 Hz,C<u>H</u>$_2CH_2$-N), 5.24(s, 1H, -CH(4'')), 6.94(d,2H,J=8.52 Hz,Ar-H(3,5)), 7.18-7.22(m, 1H, Ar-H(4')), 7.36-7.40(m,2H,Ar-H(3',5')), 7.64(d,2H,J=8.52 Hz,Ar-H(2,6)), 7.71(s,1H,N-C<u>H</u>=C), 7.74(d,2H,J=8.52 Hz,Ar-H(2',6')).

^{13}C NMR (100.61MHz, $CDCl_3$): δ13.73,13.88(-CH_2<u>C</u>H_3), 18.76(-CH_3), 23.56(-CH_2), 25.22(-CH_2), 29.21(-CH(4'')), 54.59(-CH_2), 57.40(-N-CH_2), 59.18, 59.98(-<u>C</u>H_2CH_3), 65.33(-<u>C</u>H_2CH_2-N), 103.42(C(3'',5'')), 113.59(Ar-C(3,5)), 118.24(Ar-C(2',6')), 127.10(Ar-C(1)), 126.56, 128.24, 128.75, 129.69(Ar-C(2,6,3',4',5')), 139.58(Ar-C(1')), 143.45(C(2'',6'')), 150.61(N=C), 157.86(Ar-C(4)), 167.29(C=O).

EIMS (HR): $C_{35}H_{43}N_4O_5$ calculated $[M+H]^+$ 599.3233, observed $[M+H]^+$ 599.3207.

IR (NaCl/KBr): C=N absorbance 1600.34 cm^{-1}, C=O absorbance at 1693.74 cm^{-1}, C-O-ester absorbance at 1211.32 cm^{-1}.

6.6.3 Synthesis of diethyl 2,6-dimethyl-4-(3-(4-(2-morpholinoethoxy)phenyl)-1-phenyl-*1H*-pyrazol-4-yl)-1,4-dihydropyridine-3,5-dicarboxylate 218

This product was obtained from 4-[3-(4-hydroxy-phenyl)-1-phenyl-1H-pyrazol-4-yl]-2,6-dimethyl-1,4-dihydro-pyridine-3,5-dicarboxylic acid diethyl ester (487.6 mg, 1 mmol), potassium carbonate (16 mmol, 2.2 g) and 4-(2-chloroethyl)morpholine (4 mmol,744.3 mg).

Yield: 28.65%, white solid

MP: 170 ^{o}C

^{1}H NMR (400.13MHz, $CDCl_3$): δ1.06(t,6H,J=7.04 Hz,CH_2-$C\underline{H}_3$), 2.19(s, 6H, -$C\underline{H}_3$), 2.49(t,4H,J=4.0 Hz,-CH_2), 2.81(t,2H,J=5.52 Hz,CH_2-N), 3.75(t,4H,J=4.52 Hz,-CH_2), 3.78-3.81(m,2H,$C\underline{H}_2$-CH_3), 3.97-4.05(m,2H,$C\underline{H}_2$-CH_3), 4.15(t,2H,J=5.52 Hz,$C\underline{H}_2CH_2$-N), 5.26(s, 1H, -CH(4'')), 6.95(d, 2H,J=9.04 Hz, Ar-H(3,5)), 7.18-7.22(m, 1H, Ar-H(4')),7.36-7.40(m,2H,Ar-H(3',5')), 7.64(d,2H,J=9.04 Hz,Ar-H(2,6)), 7.71(s,1H,N-C$\underline{H}$=C), 7.80(d,2H,J=8.52 Hz,Ar-H(2',6')).

^{13}C NMR (100.61MHz, $CDCl_3$): δ 13.73,13.87(-$CH_2C\underline{H}_3$), 18.81(-CH_3), 29.14(-CH(4'')), 53.64(-CH_2), 57.17(-CH_2-N), 59.21(-$\underline{C}H_2CH_3$), 65.33(-$\underline{C}H_2CH_2$-N), 66.39(-CH_2), 103.70(C(3'',5'')), 113.66(Ar-C(3,5)), 118.27(Ar-C(2',6')), 125.46(N-$\underline{C}$H=C), 127.23(Ar-C(1)), 126.68(Ar-C(4')), 128.31, 128.76, 129.62(Ar-C(2,6,3',5')), 139.57(Ar-C(1')), 143.26(C(2'',6'')), 150.33(N=C), 157.82(Ar-C(4)), 167.25(C=O).

EIMS (HR): $C_{34}H_{41}N_4O_6$ calculated $[M+H]^+$ 601.3026, observed $[M+H]^+$ 601.3011.

IR (NaCl/KBr): C=N absorbance 1621.09 cm^{-1}

6.6.4 Synthesis of diethyl 4-(3-(4-(2-(diethylamino)ethoxy)phenyl)-1-phenyl-*1H*-pyrazol-4-yl)-2,6-dimethyl-1,4-dihydropyridine-3,5-dicarboxylate 219

This product was obtained from 4-[3-(4-hydroxy-phenyl)-1-phenyl-1H-pyrazol-4-yl]-2,6-dimethyl-1,4-dihydro-pyridine-3,5-dicarboxylic acid diethyl ester (487.6 mg, 1 mmol), potassium carbonate (16 mmol, 2.2 g) and 2-chloro-N,N-diethylethanamine (4 mmol,688.4 mg).

Yield: 30.8%, white solid

MP: 168 ^{o}C

^{1}H NMR (400.13MHz, $CDCl_3$): δ1.23-1.31(m,12H,CH_2-$C\underline{H}_3$), 2.41(s, 6H, -$C\underline{H}_3$), 2.92(q,4H,J=7.0,7.04 Hz,-$CH_3C\underline{H}_2$-N), 3.16(t,2H,J=5.04 Hz,CH_2), 3.96-4.04(m,2H, $C\underline{H}_2$-CH_3), 4.15-4.21(m,2H,$C\underline{H}_2$-CH_3), 4.34(t,2H,J=5.52 Hz,-$C\underline{H}_2CH_2$-N), 5.45(s,

1H, -CH(4'')),7.21(d,2H,J=9.04 Hz,Ar-H(3,5)), 7.38-7.42(m,1H,Ar-H(4')), 7.56-7.60 (m,2H,Ar-H(3',5')), 7.85(d,2H,J=9.04 Hz,Ar-H(2,6)), 7.99(d,2H,J=8.52 Hz,Ar-H(2',6')), 8.09(s,1H,N-C<u>H</u>=C)

^{13}C NMR (100.61MHz, $CDCl_3$): δ 8.77(-CH_2<u>C</u>H_3), 12.45(-CH_2<u>C</u>H_3), 16.44(-CH_3), 28.56(-CH(4'')), 50.08(-CH_2), 58.26(-CH_2<u>C</u>H_2-N), 59.08(-<u>C</u>H_2CH_3), 64.05(-CH_2), 101.67(C(3'',5'')), 112.66(Ar-C(3,5)), 117.49(Ar-C(2',6')), 126.23(Ar-C(1)), 126.52, 128.09, 128.25, 129.02(Ar-C(2,6,3',4',5')), 138.76(Ar-C(1')), 144.18(C(2'',6'')), 149.93(N=C), 157.40(Ar-C(4)), 167.14(C=O).

EIMS (HR): $C_{34}H_{43}N_4O_5$ calculated $[M+H]^+$ 587.3233, observed $[M+H]^+$ 587.3208.

IR (NaCl/KBr): C=N absorbance 1600.25 cm^{-1}, C=O absorbance at 1692.88 cm^{-1}, C-O-ester absorbance at 1211.34 cm^{-1}.

6.6.5 Synthesis of diethyl 4-(3-(4-(2-(dimethylamino)ethoxy)phenyl)-1-phenyl-1H-pyrazol-4-yl)-2,6-dimethyl-1,4-dihydropyridine-3,5-dicarboxylate 220

This product was obtained from 4-[3-(4-hydroxy-phenyl)-1-phenyl-1H-pyrazol-4-yl]-2,6-dimethyl-1,4-dihydro-pyridine-3,5-dicarboxylic acid diethyl ester (487.6 mg, 1 mmol), potassium carbonate (16 mmol, 2.2 g) and 2-chloro-N,N-dimethylethanamine (4 mmol,576.2 mg).

Yield: 16.2%, white solid

MP: 192 °C

^{1}H NMR (400.13MHz, $CDCl_3$): δ1.14(t,6H,J=7.04 Hz,CH_2-C<u>H</u>$_3$), 2.22(s, 6H, -C<u>H</u>$_3$), 2.55(s,6H,N-CH_3), 2.97(t,2H,J=5.52 Hz,N-CH_2), 3.86-3.94(m,2H,C<u>H</u>$_2$-CH_3), 4.01-4.09(m,2H,C<u>H</u>$_2$-CH_3), 4.28(t,2H,J=5.0 Hz,-C<u>H</u>$_2$$CH_2$-N), 5.25(s, 1H, -CH(4'')), 6.97(d,2H,J=8.52 Hz,Ar-H(3,5)), 7.22-7.26(m,1H,Ar-H(4')), 7.40-7.44(m,2H,Ar-H(3',5')),7.66-7.70(m,4H,Ar-H(2,6,2',6')),7.76(s,1H,N-C<u>H</u>=C).

^{13}C NMR (100.61MHz, $CDCl_3$): δ13.92(-CH_2<u>C</u>H_3), 18.94(-CH_3), 29.49(-CH(4'')), 45.25(-NCH_3), 57.67(-CH_2-N), 59.17(-<u>C</u>H_2CH_3), 64.92(-C<u>H</u>$_2$$CH_2$-N), 103.04(C(3'',5'')), 113.49(Ar-C(3,5)), 118.23(Ar-C(2',6')), 127.48(Ar-C(1)), 126.30, 128.77, 130.02(Ar-C(2,6,3',4',5')), 139.64(Ar-C(1')), 143.42(C(2'',6'')), 151.10(N=C), 157.56(Ar-C(4)), 167.26(C=O).

EIMS (HR): $C_{32}H_{39}N_4O_5$ calculated $[M+H]^+$ 559.2920, observed $[M+H]^+$ 559.2947.

IR (NaCl/KBr): C=N absorbance 1600.10 cm^{-1}, C=O absorbance at 1693.62 cm^{-1}, C-O-ester absorbance at 1211.51 cm^{-1}.

6.7 General procedure for synthesis of phenolic derivatives-I

A suspension of 4-[3-(4-hydroxy-phenyl)-1-phenyl-1H-pyrazol-4-yl]-2,6-dimethyl-1,4-dihydro-pyridine-3,5-dicarboxylic acid diethyl ester (0.49 g, 1 mmol), potassium carbonate (0.74 g, 5.3 mmol) and a catalytic amount of potassium iodide in acetone (20 mL) was stirred under Nitrogen for 15 min. Ethyl bromobutyrate (0.23 mL, 0.31 g, 1.58 mmol) or ethyl bromoacetate was added and the suspension refluxed for 8 h. The solution was cooled, filtered and the solvent removed under reduced pressure. The product was finally purified using column chromatography (Biotage SP1 instrument) to obtain yields of 13%-25%.

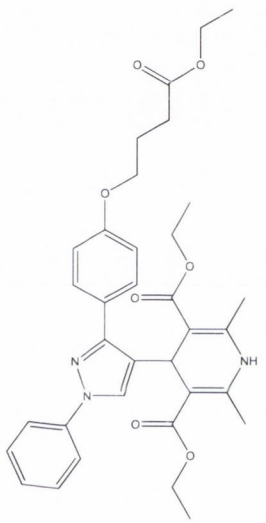

6.7.1 Synthesis of diethyl 4-(3-(4-(2-ethoxy-2-oxoethoxy)phenyl)-1-phenyl-1H-pyrazol-4-yl)-2,6-dimethyl-1,4-dihydropyridine-3,5-dicarboxylate 238

This product was obtained from diethyl 4-(3-(4-aminophenyl)-1-phenyl-1H-pyrazol-4-yl)-2,6-dimethyl-1,4-dihydropyridine-3,5-dicarboxylate **165**(0.49 g,1 mmol), potassium carbonate(0.74 g,5.3 mmol), and ethyl bromoacetate (263.9 mg,1.58 mmol)

Yield: 32.5%, yellow solid

MP: 196 ^{o}C

^{1}H NMR (400.13MHz, $CDCl_3$): δ 1.12(t, 6H,J=6.84 Hz, CH_2-C$\underline{H}_3$), 1.32(t,3H,J=6.88 Hz, CH_2-C$\underline{H}_3$), 2.14(s,6H,CH_3), 3.83-3.91(m, 2H, C$\underline{H}_2$-CH_3), 3.99-4.07(m,2H, C$\underline{H}_2$-CH_3), 4.24-4.29(m,2H, C$\underline{H}_2$-CH_3), 4.70(s,2H,-CH_2), 5.22(s, 1H, -C$\underline{H}$(4'')), 6.94(d, 2H,J=8.32 Hz,Ar-H(3,5), 7.19-7.22(m,1H,Ar-H(4')), 7.37-7.41(m,2H,Ar-H(3',5')), 7.65-7.68(m,4H,Ar-H(2,6,2',6')), 7.74(s,1H,N-C$\underline{H}$=C).

^{13}C NMR (100.61MHz, $CDCl_3$): δ 13.73(-CH_2C$\underline{H}_3$), 13.92(-CH_2C$\underline{H}_3$), 18.78(-CH_3), 29.40(-CH(4'')), 59.18 (-C$\underline{H}_2CH_3$), 61.01(-C$\underline{H}_2CH_3$), 64.56(-C$\underline{H}_2$-CO),

102.91(C(3'',5'')), 113.45(Ar-C(3,5)), 118.23(Ar-C(2',6')), 125.46(N-CH=C), 126.33(Ar-C(4')), 127.94(Ar-C(1)), 127.94, 128.09, 128.78, 130.09(ArC(2,6,3',5')), 139.58(Ar-C(1')), 143.56(C(2'',6'')), 150.92(N=C), 156.83(Ar-C(4)), 167.27(C=O), 168.82(C=O).

EIMS (HR): $C_{32}H_{36}N_3O_7$ calculated $[M+H]^+$ 574.2553, observed $[M+H]^+$ 574.2549.

IR (NaCl/KBr): C=N absorbance 1600.01 cm^{-1}, C=Oabsorbance at 1693.34 cm^{-1}, C-O-ester absorbance at 1210.20 cm^{-1}.

6.7.2 Synthesis of diethyl 4-(3-(4-(4-ethoxy-4-oxobutoxy)phenyl)-1-phenyl-*1H*-pyrazol-4-yl)-2,6-dimethyl-1,4-dihydropyridine-3,5-dicarboxylate 239

This product was obtained from 4-[3-(4-hydroxy-phenyl)-1-phenyl-1H-pyrazol-4-yl]-2,6-dimethyl-1,4-dihydro-pyridine-3,5-dicarboxylic acid diethyl ester **165** (0.49 g, 1 mmol), potassium carbonate (0.74 g, 5.3 mmol), and ethyl bromobutyrate (0.31 g, 1.58 mmol).

Yield: 18.7%, white solid

MP: 202 °C

^{1}H NMR (400.13MHz, $CDCl_3$): δ 1.08(t,6H,J=6.6 Hz,CH_2-CH_3), 1.26(t,6H,J=7.32 Hz, CH_2-CH_3),2.10-2.14(m,2H,-$CH_2CH_2CH_2$), 2.16(s, 6H, -CH_3), 2.52(t,2H,J=6.6 Hz,CH_2-CO), 3.78-3.83(m, 2H, CH_2-CH_3), 4.00-4.06(m, 2H, CH_2-CH_3, CH_2), 4.12-4.17(m,2H, CH_2-CH_3), 5.25(s, 1H, -CH(4'')), 6.93(d,2H,J=8.04 Hz,Ar-H(3,5), 7.17-7.21(m,1H,Ar-H(4')), 7.35-7.39(m,2H,Ar-H(3',5')), 7.64(d,2H,J=8.08 Hz,Ar-H(2,6)), 7.71(s,1H,N-CH=C), 7.76(d,2H,J=7.32 Hz,Ar-H(2',6')).

^{13}C NMR (100.61MHz, $CDCl_3$): δ 13.78(-CH_2CH_3), 13.88(-CH_2CH_3), 18.64(-CH_3), 24.11(-CH_2), 29.20(-CH(4'')), 30.49(-CH_2), 59.19(-CH_2CH_3), 60.08(-CH_2), 66.34(-CH_2), 103.35(C(3'',5'')), 113.56(Ar-C(3,5)), 118.26(Ar-C(2',6')), 127.01(Ar-C(1)), 126.62, 128.35, 128.77, 129.67(Ar-C(2,6,3',4',5')), 139.57(Ar-C(1')), 143.57(C(2'',6'')), 150.59(N=C), 157.86(Ar-C(4)), 167.33(C=O), 172.97(C=O).

EIMS (HR): $C_{34}H_{40}N_3O_7$ calculated $[M+H]^+$ 602.2866, observed $[M+H]^+$ 602.2859.

IR (NaCl/KBr): C=N absorbance 1611.44 cm^{-1}, C=O absorbance at 1670.23 cm^{-1}, C-O-ester absorbance at 1210.79 cm^{-1}.

6.8 General procedure for synthesis of phenolic derivatives -II

A solution of diethyl 4-(3-(4-(2-ethoxy-2-oxoethoxy)phenyl)-1-phenyl-1H-pyrazol-4-yl)-2,6-dimethyl-1,4-dihydropyridine-3,5-dicarboxylate was refluxed in 1M sodium hydroxide in water/methanol for 1 h. The solution was cooled, acidified and the aqueous layer extracted with DCM (2x30 mL). The combined organic layers were washed with brine, dried over sodium sulphate and the solvent removed under reduced pressure. The pure product was purified by Biotage SP1 instrument with eluent solvent system (ethylacetate/hexane) to obtain yields of 12%-30%.

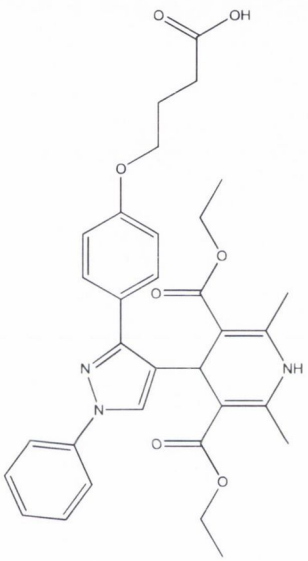

6.8.1 Synthesis of 2-(4-(4-(3,5-bis(ethoxycarbonyl)-2,6-dimethyl-1,4-dihydropyridin-4-yl)-1-phenyl-*1H*-pyrazol-3-yl)phenoxy)acetic acid 240

This product was obtained from diethyl 4-(3-(4-(2-ethoxy-2-oxoethoxy)phenyl)-1-phenyl-1H-pyrazol-4-yl)-2,6-dimethyl-1,4-dihydropyridine-3,5-dicarboxylate (0.272 g,0.5 mmol).

Yield: 22.76%, brown solid

MP: 188 °C

^{1}H NMR (400.13MHz, $CDCl_3$): δ 1.10(t, 6H,J=6.84 Hz, CH_2-C<u>H</u>$_3$), 2.13(s,6H,CH_3), 3.84-3.91(m, 2H, C<u>H</u>$_2$-CH_3), 4.01-4.09(m,2H, C<u>H</u>$_2$-CH_3), 4.71(s,2H,-CH_2), 5.21(s, 1H, -C<u>H</u>(4'')), 6.96(d, 2H,J=8.04 Hz,Ar-H(3,5), 7.18-7.21(m,1H,Ar-H(4')), 7.39-7.43(m,2H,Ar-H(3',5')), 7.63(d,2H,J=8.04 Hz,Ar-H(2,6)), 7.69(d,2H,J=8.32 Hz,Ar-H(2',6')), 7.74(s,1H,N-C<u>H</u>=C).

^{13}C NMR (100.61MHz, $CDCl_3$): δ 13.67(-CH_2<u>C</u>H_3), 18.64(-CH_3), 29.39(-CH(4'')), 59.23(-<u>C</u>H_2CH_3), 64.48(-<u>C</u>H_2-CO), 103.01(C(3'',5'')), 113.65(Ar-C(3,5)),

118.33(Ar-C(2',6')), 125.87(N-CH=C), 127.45(Ar-C(1)), 126.33, 128.31, 128.48, 129.89(ArC(2,6,3',5')), 139.66(Ar-C(1')), 143.38(C(2'',6'')), 150.67(N=C), 157.21(Ar-C(4)), 167.38(C=O), 168.98(C=O).

EIMS (HR): $C_{30}H_{31}N_3O_7Na$ calculated $[M+Na]^+$ 568.2060, observed $[M+Na]^+$ 568.2056.

IR (NaCl/KBr): C=N absorbance 1600.08 cm^{-1}, C=Oabsorbance at 1682.27 cm^{-1}, C-O-ester absorbance at 1214.21 cm^{-1}.

6.8.2 Synthesis of 4-(4-(4-(3,5-bis(ethoxycarbonyl)-2,6-dimethyl-1,4-dihydropyridin-4-yl)-1-phenyl-*1H*-pyrazol-3-yl)phenoxy)butanoic acid 241

This product was obtained from diethyl 4-(3-(4-(4-ethoxy-4-oxobutoxy)phenyl)-1-phenyl-1H-pyrazol-4-yl)-2,6-dimethyl-1,4-dihydropyridine-3,5-dicarboxylate (0.302 g,0.5 mmol).

Yield: 32.2%, white solid

MP: 194 °C

^{1}H NMR (400.13MHz, $CDCl_3$): δ 1.10(t,6H,J=6.84 Hz,CH_2-CH_3), 2.17(s, 6H, -CH_3), 2.13-2.22(m,2H,-$CH_2CH_2CH_2$), 2.56(t,2H,J=6.6 Hz,CH_2-CO), 3.84-3.86(m, 2H, CH_2-CH_3), 4.00-4.06(m, 4H, CH_2-CH_3, CH_2), 5.26(s, 1H, -CH(4'')), 6.94(d,2H,J=8.32 Hz,Ar-H(3,5), 7.19-7.23(m,1H,Ar-H(4')), 7.37-7.41(m,2H,Ar-H(3',5')), 7.65(d,2H,J=8.32 Hz,Ar-H(2,6)), 7.70(s,1H,N-CH=C), 7.74(d,2H,J=9.28 Hz,Ar-H(2',6')).

^{13}C NMR (100.61MHz, $CDCl_3$): δ 13.87, 14.73(-CH_2CH_3), 18.61, 18.78(-CH_3), 23.97(-CH_2), 29.23(-CH(4'')), 30.19(-CH_2), 59.34, 59.47(-CH_2CH_3), 66.25(-CH_2), 103.33, 103.43(C(3'',5'')), 113.59, 114.27(Ar-C(3,5)), 118.46, 118.52(Ar-C(2',6')), 126.92(Ar-C(1)), 125.62(N-CH=C), 126.82, 128.18, 128.37, 129.58, 129.75(Ar-C(2,6,3',4',5')), 139.50(Ar-C(1')), 143.79(C(2'',6'')), 150.70(N=C), 157.91(Ar-C(4)), 167.43, 167.75(C=O), 177.54(C=O).

EIMS (HR): $C_{32}H_{36}N_3O_7$ calculated $[M+H]^+$ 574.2553, observed $[M+H]^+$ 574.2535.

IR (NaCl/KBr): C=N absorbance 1613.11 cm^{-1}, C=O absorbance at 1695.30 cm^{-1}, C-O-ester absorbance at 1212.73 cm^{-1}.

6.9 General procedure for Suzuki Reaction

$Pd(PPh_3)_4$ (0.035 mmol) was added to a solution of the appropriate pyrazole 1,4-dihydropyridines (1.16 mmol), phenylboronic acid(1.74 mmol), and 2M Na_2CO_3 (5.80 mmol) in THF 20 mL and heated to reflux for 5-6 h. After cooling the mixture was portioned between water and ethyl acetate (40 mL each), filtered to remove the black, insoluble residues of the palladium-catalyst and finally the aqueous layer extracted with ethyl acetate (3x40 mL). The combined organic layers were washed with water and 27% brine (40 mL each), dried over $MgSO_4$ and the solvent removed in cacuo. The product was finally either purified using column chromatography (Biotage SP1 instrument) or recrystallized with methanol to obtain yields of 13%-46%.

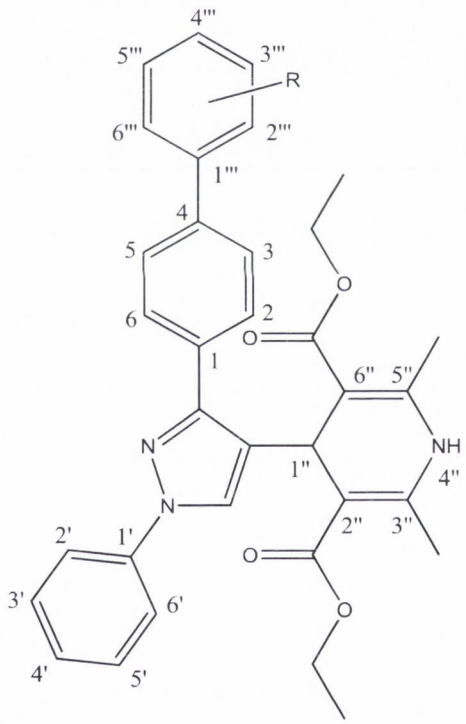

6.9.1 Synthesis of diethyl 4-(3-(4'-hydroxybiphenyl-4-yl)-1-phenyl-*1H*-pyrazol-4-yl)-2,6-dimethyl-1,4-dihydropyridine-3,5-dicarboxylate 221

This product was obtained from 4-[3-(4-bromo-phenyl)-1-phenyl-1H-pyrazol-4-yl]-2,6-dimethyl-1,4-dihydro-pyridine-3,5-dicarboxylic acid diethyl ester (550.5 mg, 1.0 mmol), 4-hydroxyphenylboronic acid (206.8 mg, 1.5 mmol) and $Pd(PPh_3)_4$ (40.4 mg, 0.035 mmol), 2M Na_2CO_3, 3 ml.

Yield: 67.67%, brown solid

MP: 182 ^{o}C

^{1}H NMR (400.13MHz $CDCl_3$): δ 1.12(t, 6H, J=7.28 Hz,CH_2-$C\underline{H}_3$),
2.21 (s, 6H, -CH_3), 3.85-3.89(m, 2H, $C\underline{H}_2$-CH_3), 4.06-4.10(m,2H,$C\underline{H}_2$-CH_3),
5.36 (s, 1H -CH(4'')), 6.05(s, O-H), 6.82 (d, 2H,J=8.56 Hz, Ar-H(3''',5''')),
7.23-7.27(m,1H,Ar-H(4')), 7.38-7.44(m,4H,Ar-H(3',5',2''',6''')),
7.52(d,2H,J=8.28 Hz,Ar-H(3,5)), 7.68(d,2H,J=7.52 Hz,Ar-C(2',6')),
7.80(s,1H,N-C$\underline{H}$=C), 7.85(d,2H, J=8.28 Hz,Ar-C(2,6)).

^{13}C NMR (100.61MHz $CDCl_3$): δ 14.32 (-$CH_2\underline{C}H_3$), 19.42 (-CH_3), 29.78 (-C (4'')),
60.06(-$\underline{C}H_2CH_3$), 103.92(-C(3'',5'')), 115.96, 116.14(Ar-C(3''',5''')),
119.20(Ar-C(2',6')), 126.06, 126.38, 127.60, 127.97, 128.74,
129.38(Ar-C(2,3,5,6,3',4',5',2''',6''')), 132.58, 132.64(Ar-C(1,1''')),
139.88(Ar-C(1')), 140.20(Ar-C(4)), 144.12(-C(2'',6''), 151.40(N=$\underline{C}$-),
156.13(Ar-C(4''')), 168.10(C=O).

EIMS (HR): $C_{34}H_{34}N_3O_5$ calculated $[M+H]^+$ 564.2498, observed $[M+H]^+$ 564.2487.

IR (NaCl/KBr): C=N absorbance 1598.96 cm^{-1}, C=O absorbance at 1679.06 cm^{-1},
C-O-ester absorbance at 1212.79 cm^{-1}, OH absorbance at 3337.54 cm^{-1}.

6.9.2 Synthesis of diethyl 4-(3-(3'-hydroxybiphenyl-4-yl)-1-phenyl-*1H*-pyrazol-4-yl)-2,6-dimethyl-1,4-dihydropyridine-3,5-dicarboxylate 222

This product was obtained from 4-[3-(4-bromo-phenyl)-1-phenyl-1H-pyrazol-4-yl]-2,6-dimethyl-1,4-dihydro-pyridine-3,5-dicarboxylic acid diethyl ester (550.5 mg, 1.0 mmol), 3-hydroxyphenylboronic acid (206.8 mg, 1.5 mmol) and $Pd(PPh_3)_4$ (40.4 mg, 0.035 mmol), 2M Na_2CO_3, 3 ml.

Yield: 6.62%, yellow solid

MP: 178 °C

^{1}H NMR (400.13MHz $CDCl_3$): δ 0.95(t, 6H, J=7.04 Hz,CH_2-$C\underline{H}_3$),
2.28 (s, 6H, -CH_3), 3.64-3.68(m, 2H, $C\underline{H}_2$-CH_3), 3.90-3.94(m,2H,$C\underline{H}_2$-CH_3),
5.26 (s, 1H -CH(4'')), 6.82 (d, 1H,J=8.0 Hz,Ar-H(4''')),
7.13-7.17(m,2H,Ar-H(4',6''')), 7.26-7.32(m,2H,Ar-H(2''',5''')),
7.46-7.50(m,2H,Ar-H(3',5')), 7.72(d,2H,J=8.28 Hz,Ar-H(3,5)),
7.85(d,2H,J=7.76 Hz,Ar-C(2',6')), 8.03(d,2H, J=8.28 Hz,Ar-C(2,6)),
8.07(s,1H,N-C$\underline{H}$=C)

^{13}C NMR (100.61MHz $CDCl_3$): δ 14.56 (-$CH_2\underline{C}H_3$), 18.75 (-CH_3), 29.38 (-C (4'')),
59.34(-$\underline{C}H_2CH_3$), 102.81(-C(3'',5'')), 113.82, 114.90(Ar-C(2''',4''')), 117.89,
118.54(Ar-C(2',6',6''')), 126.43, 126.65, 128.08, 129.12, 129.89, 130.44,

130.55(Ar-C(2,3,5,6,3',4',5',5''')), 134.10(Ar-C(1)), 139.88(Ar-C(1')), 142.04(Ar-C(4)), 145.68(Ar-C(1''')), 149.70(N=C-C), 158.34(Ar-C(3''')), 167.52(C=O).

EIMS (HR): $C_{34}H_{34}N_3O_5$ calculated $[M+H]^+$ 564.2498, observed $[M+H]^+$ 564.2493.

IR (NaCl/KBr): C=N absorbance 1595.82 cm^{-1}, C=O absorbance at 1677.41 cm^{-1}, C-O-ester absorbance at 1215.60 cm^{-1}, OH absorbance at 3343.90 cm^{-1}.

6.9.3 Synthesis of diethyl 2,6-dimethyl-4-(3-(4-(naphthalen-2-yl)phenyl)-1-phenyl-*1H*-pyrazol-4-yl)-1,4-dihydropyridine-3,5-dicarboxylate 223

This product was obtained from 4-[3-(4-bromo-phenyl)-1-phenyl-1H-pyrazol-4-yl]-2,6-dimethyl-1,4-dihydro-pyridine-3,5-dicarboxylic acid diethyl ester (550.5 mg, 1.0 mmol), naphthalen-2-ylboronic acid (258.0 mg, 1.5 mmol) and $Pd(PPh_3)_4$ (40.4 mg, 0.035 mmol), 2M Na_2CO_3, 3 ml.

Yield: 51.43%, brown solid

MP: 184 °C

^{1}H NMR (400.13MHz $CDCl_3$): δ 1.12(t, 6H, J=7.0 Hz,CH_2-CH_3), 2.28 (s, 6H, -CH_3), 3.83-3.87(m, 2H, CH_2-CH_3), 4.06-4.13(m,2H,CH_2-CH_3), 5.43 (s, 1H -CH(4'')), 6.01(s,N-H), 7.24-7.29 (m, 1H,Ar-H(4')), 7.42-7.46(m,2H,Ar-H(3',5')), 7.51-7.58(m,2H,Ar-H(5''',6''')), 7.74(d,2H,J=7.8 Hz,Ar-H(2',6')), 7.82(s,1H,Ar-H(2''')), 7.84-7.87(m,3H,Ar-H(3,5,10''')), 7.92(d,1H,J=7.52 Hz,Ar-H(9''')), 7.96-7.99(m,2H,Ar-C(4''',7''')), 8.10(d, 2H,J=8.28 Hz,Ar-C(2,6))

^{13}C NMR (100.61MHz $CDCl_3$): δ 14.23 (-$CH_2$$CH_3$), 19.45 (-$CH_3$), 29.70 (-C (4'')), 59.81(-CH_2CH_3), 104.47(-C(3'',5'')), 118.88(Ar-C(2',6')), 125.48, 125.54, 125.98, 126.11, 126.39, 126.94,127.38,127.70,128.24,128.54,129.21, 129.28, 129.39(Ar C(2,3,5,6,3',4',5',2''',4''',5''', 6''',7''',9''',10''')), 132.67,133.76(Ar-C(3''',8''')), 134.07(Ar-C(1''')), 138.42(Ar-C(1')), 140.10(Ar-C(4)), 143.70(-C(2'',6'')), 150.63(N=C-C), 167.71(C=O).

EIMS (HR): $C_{38}H_{36}N_3O_4$ calculated $[M+H]^+$ 598.2706, observed $[M+H]^+$ 598.2700.

IR (NaCl/KBr): C=N absorbance 1599.05 cm^{-1}, C=O absorbance at 1651.51 cm^{-1}, C-O-ester absorbance at 1210.13 cm^{-1}.

6.9.4 Synthesis of diethyl 4-(3-(4'-methoxybiphenyl-4-yl)-1-phenyl-*1H*-pyrazol-4-yl)-2,6-dimethyl-1,4-dihydropyridine-3,5-dicarboxylate 224

This product was obtained from 4-[3-(4-bromo-phenyl)-1-phenyl-1H-pyrazol-4-yl]-2,6-dimethyl-1,4-dihydro-pyridine-3,5-dicarboxylic acid diethyl ester (550.5 mg, 1.0 mmol), 4-methoxyphenylboronic acid (226.4 mg, 1.5 mmol) and $Pd(PPh_3)_4$ (40.4 mg, 0.035 mmol), 2M Na_2CO_3, 3 ml.

Yield: 21.64%, white solid

MP: 176 °C

^{1}H NMR (400.13MHz $CDCl_3$): δ 1.10(t, 6H, J=7.04 Hz,CH_2-C<u>H</u>$_3$), 2.28 (s, 6H, -CH_3), 3.80-3.86(m, 2H, C<u>H</u>$_2$-CH_3), 4.04-4.10(m,2H,C<u>H</u>$_2$-CH_3), 5.37 (s, 1H -CH(4'')), 5.57(s, N-H), 7.04(d, 2H,J=9.04 Hz, Ar-H(3''',5''')), 7.24-7.29(m,1H,Ar-H(4')), 7.42-7.46(m,2H,Ar-H(3',5')), 7.60-7.66(m,4H,Ar-C(2',6',2''',6''')), 7.72(d,2H,J=8.52 Hz,Ar-H(3,5)), 7.79(s,1H,N-C<u>H</u>=C), 7.96(d,2H, J=8.28 Hz,Ar-C(2,6)).

^{13}C NMR (100.61MHz $CDCl_3$): δ14.34 (-CH_2<u>C</u>H_3), 19.59 (-CH_3), 29.69 (-C (4'')), 55.42(O-CH_3), 59.78(-<u>C</u>H_2CH_3), 104.56(-C(3'',5'')), 114.30(Ar-C(3''',5''')), 118.82(Ar-C(2',6')), 126.00, 126.19, 127.18, 128.03, 128.86, 129.25, 129.29(Ar-C(2,3,5,6,3',4',5',2''',6''')), 133.33, 133.73(Ar-C(1,1''')), 139.80(Ar-C(1')), 140.11(Ar-C(4)), 143.35(-C(2'',6''), 150.83(N=<u>C</u>-), 159.18(Ar-C(4''')), 168.61(C=O).

EIMS (HR): $C_{35}H_{35}N_3O_5Na$ calculated $[M+Na]^+$ 600.2474, observed $[M+Na]^+$ 600.2489

IR (NaCl/KBr): C=N absorbance 1599.88 cm^{-1}, C=O absorbance at 1693.66 cm^{-1}, C-O-ester absorbance at 1211.60 cm^{-1}.

6.9.5 Synthesis of diethyl 4-(3-(4'-formylbiphenyl-4-yl)-1-phenyl-*1H*-pyrazol-4-yl)-2,6-dimethyl-1,4-dihydropyridine-3,5-dicarboxylate 225

This product was obtained from 4-[3-(4-bromo-phenyl)-1-phenyl-1H-pyrazol-4-yl]-2,6-dimethyl-1,4-dihydro-pyridine-3,5-dicarboxylic acid diethyl ester (550.5 mg, 1.0 mmol), 4-formylphenylboronic acid (224.9 mg, 1.5 mmol) and $Pd(PPh_3)_4$ (40.4 mg, 0.035 mmol), 2M Na_2CO_3, 3 ml.

Yield: 16.85%, white solid

MP: 180 °C

^{1}H NMR (400.13MHz $CDCl_3$): δ 1.08(t, 6H, J=7.52 Hz,CH_2-C<u>H</u>$_3$),

2.32 (s, 6H, -CH_3), 3.78-3.83(m, 2H, $C\underline{H_2}$-CH_3), 4.04-4.08(m,2H,$C\underline{H_2}$-CH_3),
5.38 (s, 1H -CH(4'')), 5.61(s, N-H), 7.43-7.47(m, 1H, Ar-H(4')),
7.67-7.76(m,6H,Ar-H(2',3',5',6',2''',6''')), 7.79(s,1H,N-C$\underline{H}$=C),
7.84(d,2H,J=8.04 Hz,Ar-H(3,5)), 8.01(d,2H,J=8.52 Hz,Ar-H(3''',5''')),
8.09(d,2H, J=8.04 Hz,Ar-C(2,6)), 10.10(s,1H,CH=O).

^{13}C NMR (100.61MHz $CDCl_3$): δ 14.32 (-$CH_2\underline{C}H_3$), 19.68 (-CH_3), 29.65 (-CH(4'')),
59.78(-$\underline{C}H_2CH_3$), 104.65(-C(3'',5'')), 119.01,119.23(Ar-C(2',6')), 126.25, 126.94,
127.52, 128.52, 128.63, 129.30,129.49,130.39,132.06,
132.16(Ar-C(2,3,5,6,3',4',5',2''',3''',5''',6''')), 135.13(Ar-C(1)),
138.64(Ar-C(4''')), 139.93(Ar-C(1')), 143.49(-C(2'',6''), 147.15(Ar-C(1''')),
150.04(N=$\underline{C}$-), 167.54(C=O), 191.96(CH=O),

EIMS (HR): $C_{35}H_{33}N_3O_5Na$ calculated $[M+Na]^+$ 598.2318,
observed $[M+Na]^+$ 598.2338

IR (NaCl/KBr): C=N absorbance 1601.02 cm^{-1}, C=O absorbance at 1693.73 cm^{-1},
C-O-ester absorbance at 1209.96 cm^{-1}.

6.9.6 Synthesis of diethyl 4-(3-(2'-fluoro-3'-formylbiphenyl-4-yl)-1-phenyl-*1H*-pyrazol-4-yl)-2,6-dimethyl-1,4-dihydropyridine-3,5-dicarboxylate 226

This product was obtained from 4-[3-(4-Bromo-phenyl)-1-phenyl-1H-pyrazol-4-yl]-2,6-dimethyl-1,4-dihydro-pyridine-3,5-dicarboxylic acid diethyl ester (550.5 mg, 1.0 mmol), 2-fluoro-3-formylphenylboronic acid (251.9 mg, 1.5 mmol) and $Pd(PPh_3)_4$ (40.4 mg, 0.035 m mol), 2M Na_2CO_3, 3 ml.

Yield: 30.9%, yellow solid

MP: 196 °C

^{1}H NMR (400.13MHz $CDCl_3$): δ 1.09(t, 6H, J=7.04 Hz,CH_2-$C\underline{H_3}$),
2.27 (s, 6H, -CH_3), 3.78-3.84(m, 2H, $C\underline{H_2}$-CH_3), 4.02-4.07(m,2H,$C\underline{H_2}$-CH_3),
5.28 (s, 1H, -CH(4'')), 5.89(s, N-H), 7.24-7.28(m, 1H, Ar-H(4')),
7.38-7.44(m,2H,Ar-H(3',5')), 7.58(d,2H,J=8.52 Hz,Ar-H(3,5)),
7.63-7.68(m,3H,Ar-H(2',6',4''')), 7.75(s,1H,N-C$\underline{H}$=C),
7.84(d,2H,J=8.0 Hz,Ar-H(2,6)), 8.06(d,1H,J=8.04 Hz,Ar-H(6''')),10.48(s,1H,CH=O).

^{13}C NMR (100.61MHz $CDCl_3$): δ 13.86 (-$CH_2\underline{C}H_3$), 19.10 (-CH_3), 29.14 (-CH(4'')),
59.35(-$\underline{C}H_2CH_3$), 103.95(-C(3'',5'')), 119.01, 119.23(Ar-C(2',6')),
121.14(Ar-C(3''')), 125.76, 126.93, 127.00, 128.22, 128.54, 128.69, 128.82, 130.06,
130.58(Ar-C(2,3,5,6,3',4',5',4''',5''',6''')), 131.54(Ar-C(1''')), 133.36(Ar-C(4)),

139.48(Ar-C(1')), 143.20(-C(2'',6''), 149.26(N=C-), 167.08(C=O)

EIMS (HR): $C_{35}H_{33}N_3O_5F$ calculated $[M+H]^+$ 594.2404, observed $[M+H]^+$ 594.2407

IR (NaCl/KBr): C=N absorbance 1599.87 cm^{-1}, C=O absorbance at 1694.09 cm^{-1}, C-O-ester absorbance at 1212.18 cm^{-1}.

6.9.7 Synthesis of diethyl 4-(3-(2'-fluoro-4'-formylbiphenyl-4-yl)-1-phenyl-*1H*-pyrazol-4-yl)-2,6-dimethyl-1,4-dihydropyridine-3,5-dicarboxylate 227

This product was obtained from 4-[3-(4-bromo-phenyl)-1-phenyl-1H-pyrazol-4-yl]-2,6-dimethyl-1,4-dihydro-pyridine-3,5-dicarboxylic acid diethyl ester (550.5 mg, 1.0 mmol), 2-fluoro-4-formylphenylboronic acid (251.9 mg, 1.5 mmol) and $Pd(PPh_3)_4$ (40.4 mg, 0.035 mmol), 2M Na_2CO_3, 3 ml.

Yield: 16.2%, yellow solid

MP: 184 °C

^{1}H NMR (400.13MHz $CDCl_3$): δ 1.10(t, 6H, J=7.04 Hz,CH_2-C$\underline{H}_3$), 2.29 (s, 6H, -CH_3), 3.80-3.85(m, 2H, C$\underline{H}_2$-CH_3), 4.03-4.09(m,2H,C$\underline{H}_2$-CH_3), 5.37 (s, 1H, -CH(4'')), 5.75(s, N-H), 7.25-7.29(m,1H,Ar-H(4')), 7.42-7.46(m,2H,Ar-H(3',5')), 7.67-7.73(m,6H,Ar-H(3,5,2',6',5''',6''')), 7.76(d,1H,J=5.52 Hz,Ar-H(3''')), 7.80(s,1H,N-C$\underline{H}$=C), 8.06(d,2H,J=8.28 Hz,Ar-H(2,6)), 10.05(s,1H,CH=O).

^{13}C NMR (100.61MHz $CDCl_3$): δ 14.32 (-$CH_2\underline{C}H_3$), 19.58 (-CH_3), 29.69 (-CH(4'')), 59.79(-$\underline{C}H_2CH_3$), 104.46(-C(3'',5'')), 116.21(Ar-C(3'''), 118.88(Ar-C(2',6')), 126.21, 127.40, 128.70, 129.16, 129.28, 130.55, 131.04, 131.39(Ar-C(2,3,5,6,3',4',5',5''',6''')), 133.50(Ar-C(1)), 135.39, 135.47, 135.52(Ar-C(4,1''',2''')), 137.03(Ar-C(4''')), 140.00(Ar-C(1')), 143.56(-C(2'',6''), 150.26(N=C-), 167.57(C=O), 190.70(CH=O).

EIMS (HR): $C_{35}H_{33}N_3O_5F$ calculated $[M+H]^+$ 594.2404, observed $[M+H]^+$ 594.2396

IR (NaCl/KBr): C=N absorbance 1600.64 cm^{-1}, C=O absorbance at 1693.79 cm^{-1}, C-O-ester absorbance at 1210.55 cm^{-1}.

6.9.8 Synthesis of diethyl 2,6-dimethyl-4-(3-(3'-nitrobiphenyl-4-yl)-1-phenyl-*1H*-pyrazol-4-yl)-1,4-dihydropyridine-3,5-dicarboxylate 228

This product was obtained from 4-[3-(4-bromo-phenyl)-1-phenyl-1H-pyrazol-4-yl]-2,6-dimethyl-1,4-dihydro-pyridine-3,5-dicarboxylic acid diethyl ester (550.5 mg, 1.0 mmol), 3-nitrophenylboronic acid (250.4 mg, 1.5 mmol) and $Pd(PPh_3)_4$ (40.4 mg, 0.035 mmol), 2M Na_2CO_3, 3 ml.

Yield: 32.4%, brown solid

MP: 194 °C

^{1}H NMR (400.13MHz $CDCl_3$): δ 1.09(t, 6H, J=7.04 Hz,CH_2-C<u>H</u>$_3$), 2.32 (s, 6H, -CH_3), 3.80-3.86(m, 2H, C<u>H</u>$_2$-CH_3), 4.03-4.09(m,2H,C<u>H</u>$_2$-CH_3), 5.38 (s, 1H, -CH(4'')), 5.67(s, N-H), 7.27-7.31(m,2H,Ar-H(4',6''')), 7.44-7.48(m,2H,Ar-H(3',5')), 7.64-7.69(m,1H,Ar-H(5''')), 7.72-7.76(m,4H,Ar-H(3,5,2',6')), 7.80(s,1H,N-C<u>H</u>=C), 7.99-8.01(m,1H,Ar-H(4''')), 8.13(d,2H,J=8.56 Hz,Ar-H(2,6)), 8.23-8.25(m,1H,Ar-H(2''')).

^{13}C NMR.(100.61MHz $CDCl_3$): δ 14.32 (-CH_2<u>C</u>H_3), 19.68 (-CH_3), 29.69 (-CH(4'')), 59.82(-<u>C</u>H_2CH_3), 104.68(-C(3'',5'')), 119.06(Ar-C(2',6')), 121.70, 122.02(Ar-C(2''',4''')), 126.36, 126.70, 127.72, 129.21, 129.31, 129.64, 129.82, 131.05(Ar-C(2,3,5,6,3',4',5',5''')), 132.90(Ar-C(1)), 135.04(Ar-C(6''')), 137.63(Ar-C(1''')), 139.81(Ar-C(1')), 142.76(Ar-C(4)), 143.41(-C(2'',6''), 148.84(Ar-C(3''')), 149.85(N=<u>C</u>-), 167.49(C=O)

EIMS (HR): $C_{34}H_{33}N_4O_6$ calculated $[M+H]^+$ 593.2400, observed $[M+H]^+$ 593.2396

IR (NaCl/KBr): C=N absorbance 1599.97 cm^{-1}, C=O absorbance at 1692.32 cm^{-1}, C-O-ester absorbance at 1211.85 cm^{-1}.

6.9.9 Synthesis of diethyl 2,6-dimethyl-4-(3-(2'-nitrobiphenyl-4-yl)-1-phenyl-*1H*-pyrazol-4-yl)-1,4-dihydropyridine-3,5-dicarboxylate 229

This product was obtained from 4-[3-(4-bromo-phenyl)-1-phenyl-1H-pyrazol-4-yl]-2,6-dimethyl-1,4-dihydro-pyridine-3,5-dicarboxylic acid diethyl ester (550.5 mg, 1.0 mmol), 3-nitrophenylboronic acid (250.4 mg, 1.5 mmol) and $Pd(PPh_3)_4$ (40.4 mg, 0.035 mmol), 2M Na_2CO_3, 3 ml.

Yield: 12.8%, white solid

MP: 164 °C

^{1}H NMR (400.13MHz $CDCl_3$): δ 1.10(t, 6H, J=7.28 Hz,CH_2-C<u>H</u>$_3$), 2.27 (s, 6H, -CH_3), 3.79-3.86(m, 2H, C<u>H</u>$_2$-CH_3), 4.01-4.08(m,2H,C<u>H</u>$_2$-CH_3), 5.29(s, 1H, -CH(4'')), 5.73(s, N-H), 7.26-7.29(m,1H,Ar-H(4')), 7.41-7.45(m,2H,Ar-H(3',5')), 7.58(d,2H,J=8.52 Hz,Ar-H(3,5)), 7.68(d,2H,J=7.52 Hz,Ar-H(2',6')), 7.76(s,1H,N-C<u>H</u>=C), 7.83(d,2H,J=8.52 Hz,Ar-H(2,6))

^{13}C NMR (100.61MHz $CDCl_3$): δ14.32 (-CH_2<u>C</u>H_3), 19.55(-CH_3), 29.65(-CH(4'')), 59.82(-<u>C</u>H_2CH_3), 104.48(-C(3'',5'')), 118.88(Ar-C(2',6')), 121.60(Ar-C(2''')),

126.22, 127.44, 128.94, 129.28, 130.56,

131.03(Ar-C(2,3,5,6,3',4',5',3''',4''',5''',6''')), 133.84(Ar-C(4)), 139.97(Ar-C(1')),

143.45(-C(2'',6''), 149.78(N=C-), 167.51(C=O)

EIMS (HR): $C_{34}H_{33}N_4O_6$ calculated $[M+H]^+$ 593.2400, observed $[M+H]^+$ 593.2402

IR (NaCl/KBr): C=N absorbance 1600.09 cm^{-1}, C=O absorbance at 1681.97 cm^{-1}, C-O-ester absorbance at 1212.61 cm^{-1}.

6.9.10 Synthesis of diethyl 2,6-dimethyl-4-(1-phenyl-3-(3',4',5'-trimethoxybiphenyl-4-yl)-*1H*-pyrazol-4-yl)-1,4-dihydropyridine-3,5-dicarboxylate 230

This product was obtained from 4-[3-(4-bromo-phenyl)-1-phenyl-1H-pyrazol-4-yl]-2,6-dimethyl-1,4-dihydro-pyridine-3,5-dicarboxylic acid diethyl ester (550.5 mg, 1.0 mmol), 3,4,5-trimethoxy phenylboronic acid (318.0 mg, 1.5 mmol) and $Pd(PPh_3)_4$ (40.4 mg, 0.035 mmol),2M Na_2CO_3 3ml.

Yield: 45.2%, white solid

MP: 172 °C

^{1}H NMR (400.13MHz $CDCl_3$): δ 1.08(t, 6H, J=7.04 Hz,CH_2-CH_3),

2.28 (s, 6H, -CH_3), 3.75-3.83(m, 2H, CH_2-CH_3), 3.93,3.97(ds,9H,O-CH_3),

4.01-4.09(m,2H,CH_2-CH_3), 5.37 (s, 1H, -CH(4'')), 6.07(s, N-H),

6.86(s,2H,Ar-H(2''',6''')), 7.23-7.27(m, 1H,Ar-H(4')), 7.40-7.44(m,2H,Ar-H(3',5')),

7.66(d,2H,J=8.0 Hz,Ar-C(2',6')), 7.70(d,2H,J=8.04 Hz,Ar-H(3,5)),

7.78(s,1H,N-CH=C), 8.04(d,2H,J=8.04 Hz,Ar-C(2,6)).

^{13}C NMR (100.61MHz $CDCl_3$): δ 13.89 (-CH_2CH_3), 18.98 (-CH_3), 29.12 (-CH(4'')),

55.78(O-CH_3), 59.29(-CH_2CH_3), 60.54(O-CH_3), 103.72, 104.56(-C(3'',5'')),

118.42(Ar-C(2',6')), 125.68, 126.11, 127.00, 128.74, 128.80(Ar-C(2,3,5,6,3',4',5')),

131.52(Ar-C(1)), 133.47(Ar-C(1''')), 137.08(O-CH3), 139.54(Ar-C(1')),

139.74(Ar-C(4)), 143.26(-C(2'',6''), 149.91(N=C-), 153.06(O-CH_3), 167.72(C=O).

EIMS (HR): $C_{37}H_{40}N_3O_7$ calculated $[M+H]^+$ 638.2866, observed $[M+H]^+$ 638.2858

IR (NaCl/KBr): C=N absorbance 1599.88 cm^{-1}, C=O absorbance at 1693.66 cm^{-1}, C-O-ester absorbance at 1211.60 cm^{-1}.

6.10 General procedure for synthesis of novel 1,4-dihydropyridines and related derivatives

Ethyl propiolate (20 mmol, 2 eqiv.), benzaldehyde (10 mmol, 1eqiv.) and aniline (10 mmol, 1eqiv.), in glacial acetic acid (0.5 mL) were heated at 80 °C for 30min. After cooling, the mixture was poured into water (20 mL), and stirred for 1 h. The solid product was filtered and washed with diethyl ether (3x30 mL) to give pure compound, which was recrystallized from cyclohexane or purified by column chromatography (Biotage SP1 instrument) to obtain yields of 1.5-70.99%.

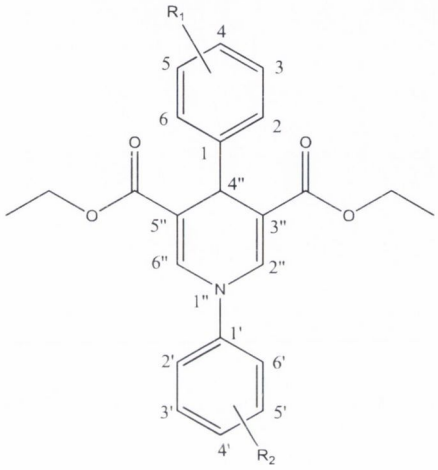

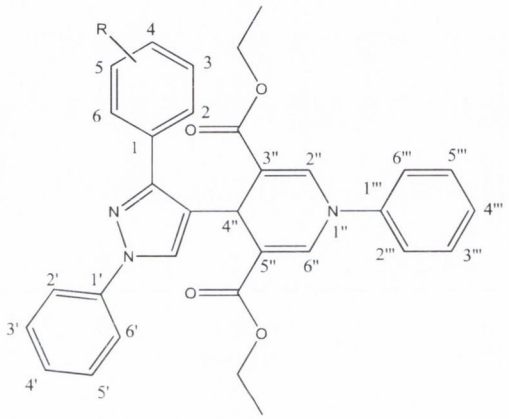

6.10.1 Synthesis of diethyl 1-benzyl-4-phenyl-1,4-dihydropyridine-3,5-dicarboxylate 242

This product was obtained from benzaldehyde(2.12 g, 2.0 mL, 20 mmol), ethyl propiolate (3.92 g, 4.1 mL,40 mmol) and benzylamine(2.14 g, 2.18 mL, 20 mmol).

Yield: 70.99%, yellow solid

MP: 136 °C

^{1}H NMR (400.13MHz $CDCl_3$): δ 1.19(t, 6H, J=7.04 Hz,CH_2-$C\underline{H}_3$), 4.06-4.10(m, 2H,$C\underline{H}_2$-CH_3), 4.61 (s, 2H, CH_2), 4.93(s, CH(4''), 7.16-7.18(m,1H,Ar-H), 7.24(m,2H,Ar-H), 7.29-7.32(m,7H,Ar-H,CH(2'',6'')), 7.38-7.46(m,3H,Ar-H)

^{13}C NMR (100.61MHz $CDCl_3$): δ 13.75 (-$CH_2\underline{C}H_3$), 36.93 (-CH(4'')), 57.85(N-CH_2), 59.64(-$\underline{C}H_2CH_3$), 108.64(-C(3'',5'')), 125.94, 126.78, 127.47, 127.85, 127.94, 128.71(Ar-C(2,3,4,5,6,2',3',4',5',6')), 135.74(Ar-C(1')), 137.19(Ar-C(1)), 146.10(CH(2'',6''), 166.53(C=O).

EIMS (HR): $C_{24}H_{26}NO_4$ calculated $[M+H]^+$ 392.1862, observed $[M+H]^+$ 392.1858.

IR (NaCl/KBr): C=O absorbance at 1693.89 cm^{-1}.

6.10.2 Synthesis of diethyl 4-(4-hydroxyphenyl)-1-(3,4,5-trimethoxyphenyl)-1,4-dihydropyridine-3,5-dicarboxylate 243

This product was obtained from 4-hydroxybenzaldehyde (2.44 g, 20 mmol), ethyl propiolate (3.92 g, 4.1 mL, 40 m mol) and 3,4,5-trimethoxyaniline (3.66 g, 20 mmol).

Yield: 28.33%, yellow solid

MP: 172 °C

^{1}H NMR (400.13MHz $CDCl_3$): δ 1.16(t, 6H, J=7.04 Hz,CH_2-$C\underline{H}_3$), 4.00(s,12H,O-CH_3), 4.21-4.25(m, 4H,$C\underline{H}_2$-CH_3), 6.74-6.76(m,4H,Ar-H), 7.36-7.42(m,4H,Ar-H,CH(3'',5'')

^{13}C NMR (100.61MHz $CDCl_3$): δ 13.40 (-$CH_2\underline{C}H_3$), 55.84, 60.89(O-CH_3), 61.11(-$\underline{C}H_2CH_3$), 102.85(Ar-C(2',6')), 115.12(-C(3'',5'')), 116.56, 129.55(Ar-C(2,3,5,6)), 131.58(Ar-C(4')), 140.46(-C(2'',6'')), 145.50, 146.10(Ar-C(1,1'), 156.69(Ar-C(4)), 157.34, 157.62(Ar-C(3',5')), 168.09(C=O).

EIMS (HR): $C_{26}H_{30}NO_8$ calculated $[M+H]^+$ 484.1971, observed $[M+H]^+$ 484.1966.

IR (NaCl/KBr): C=O absorbance at 1715.90 cm^{-1}.

6.10.3 Synthesis of diethyl 1-(4-methoxyphenyl)-4-(3,4,5-trimethoxyphenyl)-1,4-dihydropyridine-3,5-dicarboxylate 244

This product was obtained from 3,4,5-trimethoxybenzaldehyde (3.92 g, 20 mmol), ethyl propiolate (3.92 g, 4.1 ml,40 mmol) and 4-methoxyaniline (2.18 g, 20 mmol).

Yield: 24.75%, yellow solid

MP: 128 °C

^{1}H NMR (400.13MHz $CDCl_3$): δ 1.25(t, 6H, J=7.04 Hz,CH_2-$C\underline{H}_3$), 3.83,3.84, 3.86(ts,12H,O-CH3), 4.11-4.21(m, 4H,$C\underline{H}_2$-CH_3), 4.94(s,1H,CH(4'')), 6.63(s,2H,Ar-H(2,6)), 6.97-7.00(m,2H,Ar-H(2',6'),7.21-7.24(m,2H,Ar-H(3',5')), 7.58(s,2H,CH(3'',5''))

^{13}C NMR (100.61MHz $CDCl_3$): δ 13.87 (-$CH_2\underline{C}H_3$), 37.07(CH(4'')), 55.21, 55.54, 60.34(O-CH_3), 59.82(-$\underline{C}H_2CH_3$), 104.77(Ar-C(2,6)), 109.66(-C(3'',5'')), 114.60(Ar-C(3',5')), 122.40(Ar-C(2',6')), 135.85(-C(2'',6'')), 136.24(Ar-C(1)), 141.47(Ar-C(4)), 152.36(Ar-C(3,5)), 157.81(Ar-C(4')), 166.45(C=O).

EIMS (HR): $C_{27}H_{31}NO_8Na$ calculated $[M+Na]^+$ 520.1947,
observed $[M+Na]^+$ 520.1955.

IR (NaCl/KBr): C=O absorbance at 1682.23 cm^{-1}.

6.10.4 Synthesis of diethyl 4-(1,3-diphenyl-*1H*-pyrazol-4-yl)-1-phenyl-1,4-dihydropyridine-3,5-dicarboxylate 245

This product was obtained from 1,3-diphenyl-1H-pyrazole-4-carbaldehyde (4.96 g, 20 mmol), ethyl propiolate (3.92 g, 4.1 mL,40 mmol) and aniline (1.86 g, 20 mmol).

Yield: 1.5%, light yellow solid

MP: 162 °C

^{1}H NMR (400.13MHz $CDCl_3$): δ 1.27(t, 6H, J=7.0 Hz,CH_2-$C\underline{H}_3$), 3.72-3.77(m, 2H,$C\underline{H}_2$-CH_3), 4.18-4.22(m,2H, $C\underline{H}_2$-CH_3), 7.29(s,3H,Ar-H), 7.41-7.55(m,7H,Ar-H,N-C$\underline{H}$=C), 7.56(s,2H,-CH(2'',6'')), 7.82-7.87(m,6H,Ar-H),

^{13}C NMR (100.61MHz $CDCl_3$): δ 13.65(-$CH_2\underline{C}H_3$), 59.96(-$\underline{C}H_2CH_3$), 119.79(Ar-C(2''',6''')), 122.54(-C(3'',5'')), 128.00, 128.80, 129.00, 129.33, 129.71(Ar-C(2,3,4,5,6,3',4',5',3''',5''')), 130.97(-C(2'',6'')), 131.35(Ar-C(1)), 139.04(Ar-C(1''')), 154.85(N=C), 185.27(C=O).

EIMS (HR): $C_{32}H_{30}N_3O_4$ calculated $[M+H]^+$ 520.2236, observed $[M+H]^+$ 520.2230.

IR (NaCl/KBr): C=N absorbance at 1599.04, C=O absorbance at 1672.90 cm^{-1},

6.10.5 Synthesis of diethyl 4-(3-(4-hydroxyphenyl)-1-phenyl-*1H*-pyrazol-4-yl)-1-phenyl-1,4-dihydropyridine-3,5-dicarboxylate 246

This product was obtained from 3-(4-hydroxyphenyl)-1-phenyl-1H-pyrazole-4-carbaldehyde (5.28 g, 20 mmol), ethyl propiolate (3.92 g, 4.1 mL,40 m mol) and aniline (1.86g, 20 m mol).

Yield: 30.39%, yellow solid

MP: 168 °C

^{1}H NMR (400.13MHz $CDCl_3$): δ 1.48(t, 6H, J=7.0 Hz,CH_2-$C\underline{H}_3$), 3.58-3.65(m, 2H,$C\underline{H}_2$-CH_3), 4.15-4.26(m,2H, $C\underline{H}_2$-CH_3), 6.92-6.94(m,4H,Ar-H), 7.24-7.32(m,2H,Ar-H), 7.44(t,2H,J=7.56 Hz,Ar-H(3',5')), 7.58(t,3H,J=7.52 Hz,Ar-H(2,6),N-C$\underline{H}$=C), 7.77-7.80(m,2H,Ar-H), 7.91-7.94(m,2H,Ar-H)

^{13}C NMR (100.61MHz $CDCl_3$): δ 13.40(-$CH_2\underline{C}H_3$), 26.58(-$\underline{C}H_2CH_3$), 114.74, 114.96(Ar-C(2''',6''')), 119.38(Ar-C(3,5)), 122.53(-C(3'',5'')), 127.53, 129.19, 129.35, 130.10(Ar-C(2,6,3',4',5',3''',4''',5''')), 158.56(Ar-C(4)), 185.20(C=O).

EIMS (HR): $C_{32}H_{30}N_3O_5$ calculated $[M+H]^+$ 536.2185, observed $[M+H]^+$ 536.2196.

IR (NaCl/KBr): C=N absorbance at 1596.36, C=O absorbance at 1684.70 cm^{-1}

6.11 Synthesis of diethyl 1-benzyl-4-(4-hydroxyphenyl)-1,4-dihydropyridine-3,5-dicarboxylic acid 247

A mixture of 1,4-DHP (1 mmol) and 5N KOH(5 mmol) in Ethanol(10 mL) was stirred at 80 °C overnight. Afterward, the solvent was evaporated, the residue was eluted with water(30 mL) and the resulting solution acidified with 2N HCl. The obtained precipitate was filtered,washed with water(3x30 mL) and dried to afford pure compound, which was recrystaillized from ACN or methanol.

This product was obtained from diethyl 1-benzyl-4-phenyl-1,4-dihydropyridine-3,5-dicarboxylate, (0.78 g, 2mmol).

Yield: 83.2%, yellow solid

MP: 192 ^{o}C

^{1}H NMR (400.13MHz $CDCl_3$): δ4.60 (s, 2H, CH_2), 4.88(s, CH(4''), 7.14-7.17(m,1H,Ar-H), 7.20-7.24(m,2H,Ar-H), 7.26-7.30(m,7H,Ar-H,CH(3'',5'')), 7.36-7.43(m,2H,Ar-H)

^{13}C NMR (100.61MHz $CDCl_3$): δ 36.45 (-CH(4'')), 57.96(N-CH_2), 107.16, 109.73(-C(3'',5'')), 126.05, 126.81, 126.84, 127.54, 127.76, 128.03, 128.75, 128.78, 128.80,(Ar-C(2,3,4,5,6,2',3',4',5',6')),135.43(Ar-C(1')), 145.64(CH(2'',6''), 171.08(C=O).

EIMS (HR): $C_{20}H_{17}NO_4Na$ calculated $[M+Na]^+$ 358.1055,
observed $[M+Na]^+$ 358.1056.

IR (NaCl/KBr): C=O absorbance at 1686.40 cm^{-1}

6.12 General procedure for preparation of Grignard reaction series derivatives

Magnesium turning (0.6 g) was placed in an oven-dried 100 mL two-neck flask. Dry THF (10 mL) and a reflex condenser was fitted. Bromobenzene (4 g, 2.7 mL) from the stock bottle was collected and added 1 mL of bromobenzene down the condenser to the reaction flask. If there was no sign of reaction after a short time, gently warming the flask was tried. Once the reaction is under way, no further heating was necessary for some time as the reaction is exothermic. A further 10 mL of THF was added down the condenser, followed by the remainder of the bromobenzene when the reaction no longer boils without supplementary heating, it was refluxed in an oil bath for about 15 min. There should be little unreacted magnesium left in the flask. To the solution of phenylmagnesium bromide, a solution of aldehyde (1.8 g) in THF(10 mL) was added. The mixture was refluxed for 20 min. After cooling, the reaction mixture was poured into dilute sulphuric acid (10%, 25 mL) to hydrolyse. Using a mixture of ether and dilute acid to bring any solid remaining back into solution, ether layer was separated and wash with NaCl (2x20 mL). The solution was dry with $MgSO_4$ and recrystallized from ethanol.

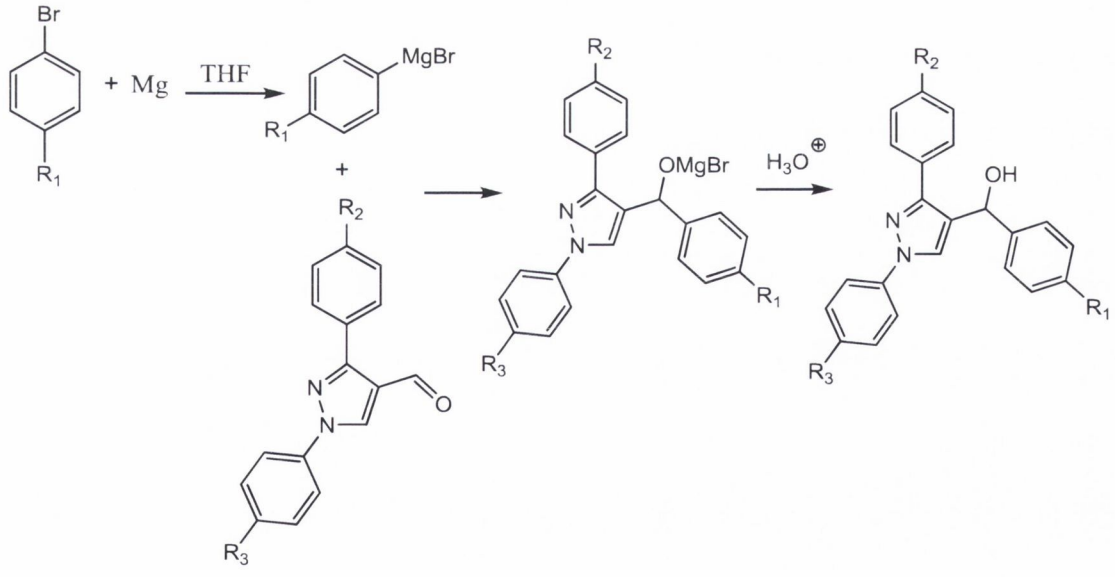

6.12.1 Synthesis of (3-(4-methoxyphenyl)-1-phenyl-*1H*-pyrazol-4-yl)(phenyl)methanol 267

This product was obtained from 3-(4-methoxyphenyl)-1-phenyl-1H-pyrazole-4-carbaldehyde(1.8 g, 6.5 mmol), Magnesium (0.6 g, 25 mmol) and bromobenzene (4.0

g, 25.6 mmol)

Yield: 28.35%, white solid

MP: 126 °C

^{1}H NMR 400.13MHz $CDCl_3$: δ3.88(s,3H,O-CH_3), 6.01(s,1H,CH), 6.99(d,2H,J=8.52 Hz, Ar-H(3,5)), 7.28-7.50(m,8H,Ar-H(3',4',5',2'',3'',4'',5'',6'')), 7.69(d,2H,J=8.52 Hz,Ar-H(2,6)), 7.67(s,1H,N-C<u>H</u>=C), 7.80(d,2H,J=8.52 Hz,Ar-H(2',6')

^{13}C NMR 100.61MHz $CDCl_3$: δ54.69(O-CH_3), 72.42(-CH), 113.23, 113.28(Ar-C(3,5), 118.42, 118.52(Ar-C(2',6')), 124.02(N-<u>C</u>H=C), 125.09(ArC(1)), 126.51, 127.00, 127.31, 127.92, 127.97, 128.11, 128.87, 128.90, 129.06, 129.17(Ar-C(2,6,3',4',5',2'',3'',4'',5'',6'')), 139.46(Ar-C(1')), 142.84(Ar-C(1'')), 151.43(N=<u>C</u>-C), 159.20(Ar-C(4))

EIMS (HR): $C_{23}H_{21}N_2O_2$ calculated $[M+H]^+$ 357.1603, observed $[M+H]^+$ 357.1589.

IR (NaCl/KBr): C=N absorbance 1601.00 cm^{-1}, OH absorbance at 3306.49 cm^{-1}.

6.12.2 Synthesis of (3-(4-(benzyloxy)phenyl)-1-phenyl-*1H*-pyrazol-4-yl)(4-methoxyphenyl)methanol 268

This product was obtained from 3-(4-(benzyloxy)phenyl)-1-phenyl-1H-pyrazole-4-carbaldehyde (2.30 g, 6.5 mmol), Magnesium (0.6 g, 25 mmol) and 1-bromo-4-methoxybenzene(4.79 g, 25.6 mmol)

Yield: 23.3%, white solid

MP: 162 °C

^{1}H NMR 400.13MHz $CDCl_3$: δ3.85(s,3H,O-CH_3), 5.16(s,2H,CH_2), 5.63(s,1H,-CH), 6.81-6.96(m,3H,Ar-H), 7.7.08-7.10(m,1H,Ar-H), 7.21-7.29(m,2H,Ar-H), 7.35-7.52(m,6H,Ar-H),7.63-7.78(m,3H,Ar-H).

^{13}C NMR 100.61MHz $CDCl_3$: δ54.86(O-CH_3), 69.37(CH_2), 71.72(-CH), 113.45, 113.48(Ar-C(3'',5''),114.37, 114.49(Ar-C(3,5)),118.42, 118.48(Ar-C(2',6')), 124.31(N-<u>C</u>H=C), 125.82(Ar-C(1)), 126.88, 127.05, 127.28, 127.56, 127.77, 128.13, 128.16, 128.52, 129.03, 129.18(Ar-C(2,6,3',4',5',2''',3''',4''',5''',6''')), 132.39(Ar-C(1''')), 133.03,133.19(Ar-C(2'',6''), 136.46(Ar-C(1'''), 139.45(Ar-C(1''), 151.16(N=<u>C</u>-C), 158.09(Ar-C(4)), 158.64(Ar-C(4''))

EIMS (HR): $C_{30}H_{27}N_2O_3$ calculated $[M+H]^+$ 463.2022, observed $[M+H]^+$ 463.2030.

IR (NaCl/KBr): C=N absorbance 1601.33 cm^{-1}, OH absorbance at 3360.26 cm^{-1}.

6.12.3 Synthesis of (3-(4-(benzyloxy)phenyl)-1-phenyl-*1H*-pyrazol-4-yl)(phenyl)methanol 269

This product was obtained from 3-(4-(benzyloxy)phenyl)-1-phenyl-1H-pyrazole-4-carbaldehyde (2.30 g, 6.5 mmol), Magnesium (0.6 g, 25 mmol) and bromobenzene(4.0 g, 25.6 mmol).

Yield: 42.65%, white solid

MP: 146 ^{o}C

^{1}H NMR 400.13MHz $CDCl_3$: δ2.21(s,OH), 5.15(s,2H,CH_2), 5.71(s,1H,-CH), 7.08(d,2H,J=9.0 Hz,Ar-H(3,5)), 7.27-7.50(m,19H,Ar-H(3',4',5',2'',3'',4'',5'',6'',2''',3''',4''',5''',6''')), 7.67(s,1H,N-C<u>H</u>=C), 7.69(d,2H,J=8.52 Hz,Ar-H(2,6)), 7.80(d,2H,J=8.52 Hz,Ar-H(2',6')).

^{13}C NMR 100.61MHz $CDCl_3$: δ69.44(CH_2), 72.50(-CH), 114.37, 114.49(Ar-C(3,5)),118.44, 118.51(Ar-C(2',6')), 124.08(N-<u>C</u>H=C), 125.38(Ar-C(1)), 125.93, 126.53, 127.02, 127.05, 127.29, 127.44, 127.52, 127.58, 127.94, 128.01, 128.10, 128.15, 128.89, 128.92, 129.08(Ar-C(2,6,3',4',5',2'',3'',4'',5'',6'',2''',3''',4''',5''', 6''')), 132.39(Ar-C(1''')), 133.03, 133.19(Ar-C(2'',6'')), 136.49(Ar-C(1''')), 139.44(Ar-C(1')), 141.11(Ar-C(1'')), 151.42(N=<u>C</u>-C), 158.14(Ar-C(4))

EIMS (HR): $C_{29}H_{25}N_2O_2$ calculated $[M+H]^+$ 433.1916, observed $[M+H]^+$ 433.1924.

IR (NaCl/KBr): C=N absorbance 1595.04 cm^{-1}, OH absorbance at 3366.32 cm^{-1}.

6.12.4 Synthesis of (4-(benzyloxy)phenyl)(3-(4-(benzyloxy)phenyl)-1-phenyl-*1H*-pyrazol-4-yl)methanol 270

This product was obtained from 3-(4-(benzyloxy)phenyl)-1-phenyl-1H-pyrazole-4-carbaldehyde(2.30 g, 6.5 mmol), Magnesium (0.6 g, 25 mmol) and 1-(benzyloxy)-4-bromobenzene(6.74 g, 25.6 mmol)

Yield: 21.23%, white solid

MP: 182 ^{o}C

^{1}H NMR 400.13MHz $CDCl_3$: δ2.09(s,OH), 4.66(s,2H,CH_2), 5.11(s,2H,CH_2), 7.07(d,4H,J=8.52 Hz,Ar-H(3,5)), 7.29(t,2H,J=7.52 Hz,Ar-H(4''',4'''')),7.36-7.50(m,16H,Ar-H(3', 4', 5', 2'', 6'', 2''', 3''', 4''', 5''', 6''', 2'''', 3'''', 4'''', 5'''', 6'''')), 7.70(d,2H,J=8.52 Hz,Ar-H(2,6)), 7.82(d,2H,J=8.56 Hz,Ar-H(2',6')), 7.88(s,1H,N-C<u>H</u>=C),

^{13}C NMR 100.61MHz $CDCl_3$: δ69.56(CH_2), 114.58(Ar-C(3,5,3'',5'')),

118.41(Ar-C(2',6')), 120.10(N-CH=C), 125.33(Ar-C(1)), 125.89, 127.12, 127.33, 128.20, 128.64, 129.00(Ar-C(2,6,3',4',5',2''',3''',4''',5''',6''',2'''',3'''',4'''',5'''', 6'''')),136.46(Ar-C(1''',1'''')),139.41(Ar-C(1')),150.85(N=C-C),158.36(Ar-C(4,4''))

EIMS (HR): $C_{29}H_{25}N_2O_2$ calculated $[M+H]^+$ 433.1916, observed $[M+H]^+$ 433.1924.

IR (NaCl/KBr): C=N absorbance 1597.83 cm^{-1}, OH absorbance at 3273.40 cm^{-1}

6.12.5 Synthesis of (4-(benzyloxy)phenyl)(3-(4-methoxyphenyl)-1-phenyl-*1H*-pyrazol-4-yl)Methanol 271

This product was obtained from 3-(4-methoxyphenyl)-1-phenyl-1H-pyrazole-4-carbaldehyde(1.8 g, 6.5 mmol), Magnesium (0.6 g, 25 mmol) and 1-(benzyloxy)-4-bromobenzene (6.74 g, 25.6 mmol)

Yield: 49.55%, yellow solid

MP: 168 °C

^{1}H NMR 400.13MHz $CDCl_3$: δ3.79(s,3H,O-CH_3), 5.60(s,2H,CH_2), 6.01(s,1H,CH), 6.88(d,2H,J=8.56 Hz, Ar-H(3'',5'')), 6.91(d,2H,J=8.52 Hz,Ar-H(3,5)), 7.22(d,,2H,J=8.56 Hz,Ar-H(2'',6'')),7.29-7.47(m,10H,Ar-H(2,6,3',4',5',2''',3''',4''', 5''',6''')), 7.68(s,1H,N-CH=C), 7.70(d,2H,J=8.52 Hz,Ar-H(2',6')

^{13}C NMR 100.61MHz $CDCl_3$: δ 54.75(O-CH_3), 69.62(CH_2), 72.03(-CH), 113.22, 113.54(Ar-C(3'',5''), 114.16, 114.22(Ar-C(3,5)), 118.39, 118.48(Ar-C(2',6')), 125.13(N-CH=C), 125.21(Ar-C(1)), 126.81, 127.07, 127.10, 127.98, 128.11, 128.15, 128.44, 128.85, 128.90, 129.02, 129.12, 129.16(Ar-C(2,6,3',4',5',2'',6'',2''',3''', 4''',5''',6''')), 133.48(Ar-C(1'')), 136.51(Ar-C(1''')), 139.47(Ar-C(1')), 151.23(N=C-C), 158.93(Ar-C(4'')), 159.16(Ar-C(4))

EIMS (HR): $C_{30}H_{27}N_2O_3$ calculated $[M+H]^+$ 463.2022, observed $[M+H]^+$ 463.2022.

IR (NaCl/KBr): C=N absorbance 1611.13 cm^{-1}, OH absorbance at 3337.13 cm^{-1}.

6.12.6 Synthesis of (4-methoxyphenyl)(3-(4-methoxyphenyl)-1-phenyl-*1H*-pyrazol-4-yl)methanol 272

This product was obtained from 3-(4-methoxyphenyl)-1-phenyl-1H-pyrazole-4-carbaldehyde(1.8 g, 6.5 mmol), Magnesium (0.6 g, 25 mmol) and 1-bromo-4-methoxybenzene (4.79 g, 25.6 mmol)

Yield: 51.06%, white solid

MP: 182 °C

^{1}H NMR 400.13MHz $CDCl_3$: δ3.83(s,3H,O-CH_3), 3.86(s,3H,O-CH_3), 5.94(s,1H,CH), 6.01(s,1H,CH), 6.91(d,2H,J=8.56 Hz, Ar-H(3'',5'')),

6.97(d,2H,J=8.52 Hz,Ar-H(3,5)), 7.23(d,2H,J=8.52 Hz,Ar-H(2,6)), 7.37(d,2H,J=8.56 Hz,Ar-H(2'',6'')), 7.42-7.46(m,3H,Ar-H(3',4',5')), 7.69(s,1H,N-CH=C), 7.76(d,2H,J=8.56 Hz,Ar-H(2',6').

^{13}C NMR 100.61MHz $CDCl_3$: δ54.69(O-CH_3), 54.86(O-CH_3), 72.05(-CH), 113.22, 113.25(Ar-C(3'',5''), 113.34, 113.41(Ar-C(3,5)), 118.40, 118.44(Ar-C(2',6')), 124.32(N-CH=C), 125.20(Ar-C(1)), 126.85, 127.28, 127.36, 128.46, 128.91, 129.01, 129.12(Ar-C(2,6,3',4',5',2'',6'')), 133.21(Ar-C(1''), 139.47(Ar-C(1')), 151.25(N=C-C), 158.93(Ar-C(4'')), 159.13(Ar-C(4))

EIMS (HR): $C_{24}H_{23}N_2O_3$ calculated $[M+H]^+$ 387.1709, observed $[M+H]^+$ 387.1702.

IR (NaCl/KBr): C=N absorbance 1599.88 cm^{-1}, OH absorbance at 3400.08 cm^{-1}.

6.12.7 Synthesis of (3-(4-methoxyphenyl)-1-phenyl-*1H*-pyrazol-4-yl)(4-(tetrahydro-2H-pyran-2-yloxy)phenyl)methanol 273

This product was obtained from 3-(4-methoxyphenyl)-1-phenyl-1H-pyrazole-4-carbaldehyde(1.8 g, 6.5 mmol), Magnesium (0.6 g, 25 mmol) and p-Tetrahydropyranyloxy bromobenzene(6.58 g, 25.6 mmol)

Yield: 17.23%, orange solid

MP: 186 °C

^{1}H NMR 400.13MHz $CDCl_3$: δ1.69, 1.88, 2.07(m,6H,-CH_2-), 3.69(s,3H,O-CH_3), 3.72-3.80(m,2H,-CH_2-), 5.66(s,1H,O-CH-), 6.82(dd,2H,J=8.52 Hz, Ar-H(3'',5'')), 7.04(d,2H,J=8.56 Hz,Ar-H(3,5)), 7.26(d,2H,J=8.52 Hz,Ar-H(2'',6'')), 7.34(d,2H,J=8.56 Hz,Ar-H(2,6)), 7.39-7.46(m,3H,Ar-H(3',4',5')), 7.66(s,1H,N-CH=C), 7.70(d,2H,J=8.56 Hz,Ar-H(2',6').

^{13}C NMR 100.61MHz $CDCl_3$: δ18.46, 24.77, 29.97(CH_2), 54.82(O-CH_3), 61.74(CH_2), 72.10(-CH), 113.29, 113.49(Ar-C(3'',5''), 115.80, 115.88(Ar-C(3,5)), 118.42, 118.45(Ar-C(2',6')), 124.46(N-CH=C), 125.21(Ar-C(1)), 126.98, 128.37, 128.44, 129.19, 129.25, 134.09, 134.22(Ar-C(2,6,3',4',5',2'',6'')), 133.44(Ar-C(1''), 139.47(Ar-C(1')), 151.39(N=C-C), 158.97(Ar-C(4'')), 159.09(Ar-C(4))

EIMS (HR): $C_{28}H_{29}N_2O_4$ calculated $[M+H]^+$ 457.2127, observed $[M+H]^+$ 457.2125.

IR (NaCl/KBr): C=N absorbance 1600.45 cm^{-1}, OH absorbance at 3420.18 cm^{-1}.

6.13 General procedure for oxidation of alcohol form derivatives

Pyridinium chlorochromate (PCC) (10 mmol, 2.114 g) was suspended in 15 mL of anhydrous DCM. The corresponding alcohol (Grignard product) (15 mmol, 1.5 eqiv.) was dissolved in 20 mL of DCM and then added at the suspension. The solution became briefly homogenous before depositing the black insoluble reduced reagent, and was stirred for 2 h. The reaction mixture was then diluted with 5 volumes of anhydrous ether. The solvent was decanted and the black residue was further washed with ether until the entire product was recovered. The solvent was then removed *in vacuo*.

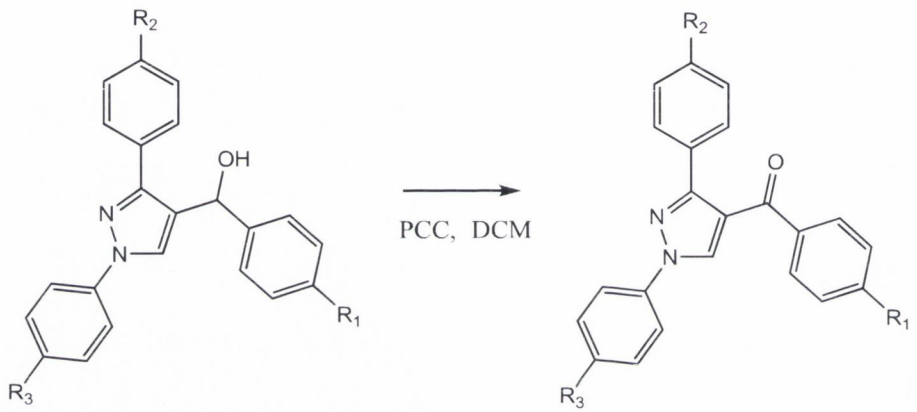

6.13.1 Synthesis of (3-(4-(benzyloxy)phenyl)-1-phenyl-*1H*-pyrazol-4yl)(phenyl) methanone 274

This product was obtained from (3-(4-(benzyloxy)phenyl)-1-phenyl-1H-pyrazol-4-yl)(phenyl)methanol (1.5 mmol, 649.0 mg), and Pyridinium chlorochromate(PCC) (1.0 mmol, 211.4 mg)

Yield: 34.2%, white solid

MP: 176 ^{o}C

^{1}H NMR 400.13MHz $CDCl_3$: δ 5.12(s,2H,-CH_2), 6.99(d,2H,J=6.52 Hz,Ar-H(3,5)), 7.29-7.52(m,12H,Ar-H(2,6,2',3',4',5',6',2''',3''',4''',5''',6''')), 7.74-7.88(m,5H,Ar-H(2'',3'',4'',5'',6'')), 8.28(s,1H,N-C<u>H</u>=C).

^{13}C NMR 100.61MHz $CDCl_3$: δ69.50(CH_2), 114.11(Ar-C(3,5)), 119.08(Ar-C(2',6'),120.41(N-CH=<u>C</u>), 124.38(Ar-C(1)), 127.04, 127.53, 127.94, 128.15, 129.02, 129.16, 129.80(Ar-H(2,6,3',4',5',2'',3'',5'',6'',2''',3''',4''', 5''',6''')), 132.00(Ar-C(4'')), 132.13(Ar-C(1'')), 136.44(Ar-C(1''')), 138.79(Ar-C(1')), 189.65(C=O)

EIMS (HR): $C_{29}H_{22}N_2O_2Na$ calculated $[M+Na]^+$ 453.1579,

observed $[M+Na]^+$ 453.1573.

IR (NaCl/KBr): C=N absorbance 1599.76 cm^{-1}, C=O absorbance at 1693.27 cm^{-1}

6.13.2 Synthesis of (3-(4-methoxyphenyl)-1-phenyl-*1H*-pyrazol-4-yl)(phenyl)methanone 275

This product was obtained from (3-(4-methoxyphenyl)-1-phenyl-1H-pyrazol-4-yl)(phenyl)methanol (1.5 mmol, 534.6 mg), and Pyridinium chlorochromate (PCC) (1.0 mmol, 211.4 mg)

Yield: 18.8%, light yellow solid

MP: 174 °C

^{1}H NMR 400.13MHz $CDCl_3$: δ 3.84(s,3H,-OCH_3), 6.92(d,2H,J=8.76 Hz,Ar-H(3,5)), 7.35-7.39(m,1H,Ar-H(4')), 7.43-7.47(m,2H,Ar-H(3',5')), 7.49-7.53(m,2H,Ar-H(3'',5'')), 7.54-7.58(m,1H,Ar-H(4'')), 7.77(d,2H,J=8.76 Hz,Ar-H(2,6)), 7.79-7.81(m,2H,Ar-H(2',6')), 7.87-7.89(m,2H,Ar-H(2'',6'')).

^{13}C NMR 100.61MHz $CDCl_3$: δ55.30(O-CH_3), 113.65(Ar-C(3,5)), 119.51(Ar-C(2',6'), 120.87(N-CH=C),124.67(Ar-C(1)), 127.42, 128.42, 129.48, 129.62, 130.28(Ar-H(2,6,3',4',5',2'',3'',5'',6'')), 132.45(Ar-C(4'')), 132.58(Ar-C(1'')), 139.11(Ar-C(1')), 153.77(N=C-C), 160.03(Ar-C(4)), 190.05(C=O)

EIMS (HR): $C_{23}H_{19}N_2O_2$ calculated $[M+H]^+$ 355.1447, observed $[M+H]^+$ 355.1451.

IR (NaCl/KBr): C=N absorbance 1597.26 cm^{-1}, C=O absorbance at 1695.34 cm^{-1}

6.13.3 Synthesis of (3-(4-(benzyloxy)phenyl)-1-phenyl-*1H*-pyrazol-4-yl)(4-methoxyphenyl)methanone 276

This product was obtained from (3-(4-(benzyloxy)phenyl)-1-phenyl-1H-pyrazol-4-yl)(4-methoxyphenyl)methanol (1.5 mmol, 693.8 mg), and Pyridinium chlorochromate (PCC) (1.0 mmol, 211.4 mg)

Yield: 26.3%, white solid

MP: 170 °C

^{1}H NMR 400.13MHz $CDCl_3$: δ 3.88(s,3H,-OCH_3), 5.10(s,2H,-CH_2), 6.93(d,2H,J=8.76 Hz,Ar-H(3,5)), 6.99(d,2H,J=8.56 Hz,Ar-H(3'',5'')), 7.29-7.47(m,7H,Ar-H(2,6,3',5',3''',4''',5''')), 7.50-7.54(m,1H,Ar-H(4')), 7.75(d,2H,J=9.0 Hz,Ar-H(2''',6''')), 7.81(d,2H,J=8.0 Hz,Ar-H(2',6')), 7.90(d,2H,J=8.56 Hz,Ar-H(2'',6'')), 8.26(s,1H,N-CH=C)

^{13}C NMR 100.61MHz $CDCl_3$: δ55.07(O-CH_3), 69.50(CH_2), 113.18(Ar-C(3,5)),

114.16(Ar-C(3'',5'')), 118.97(Ar-C(2',6'), 120.61(N-CH=C), 124.54(Ar-C(1)), 126.84, 127.06, 127.54, 128.16, 129.15, 129.66(Ar-H(2,6,3',4',5',2''',3''',4''', 5''',6''')), 131.11, 131.21(Ar-C(2'',6'')), 136.45(Ar-C(1''')), 138.89(Ar-C(1')), 152.86(N=C-C), 158.65(Ar-C(4)), 162.89(Ar-C(4'')), 188.50(C=O)

EIMS (HR): $C_{30}H_{24}N_2O_3Na$ calculated $[M+Na]^+$ 483.1685, observed $[M+Na]^+$ 483.1671.

IR (NaCl/KBr): C=N absorbance 1598.12 cm^{-1}, C=O absorbance at 1696.23 cm^{-1}.

6.13.4 Synthesis of (3-(4-methoxyphenyl)-1-phenyl-*1H*-pyrazol-4-yl)(4-(tetrahydro-2H-pyran-2-yloxy)phenyl)methanone 277

This product was obtained from (3-(4-methoxyphenyl)-1-phenyl-1H-pyrazol-4-yl)(4-(tetrahydro-2H-pyran-2-yloxy)phenyl)methanol(1.5 mmol, 684.8 mg), and Pyridinium chlorochromate (PCC) (1.0 mmol, 211.4 mg).

Yield: 54.12%, white solid

MP: 162 ^oC

^{1}H NMR 400.13MHz $CDCl_3$: δ 1.46,1.57(m,2H,CH_2),1.66,1.72(m,2H,CH_2), 1.91,2.03(m,2H,CH_2), 3,64,3.67(m,2H,CH_2), 3.84(s,3H,O-CH_3), 6.91(d,2H,J=8.52 Hz,Ar-H(3'',5'')), 7.08(d,2H,J=8.56 Hz,Ar-H(3,5)), 7.36-7.39(m,1H,Ar-H(4')), 7.50-7.54(m,2H,Ar-H(3',5')), 7.73(d,2H,J=8.56,Ar-H(2,6)), 7.80(d,2H,J=7.52 Hz,Ar-H(2',6')), 7.88(d,2H,J=8.52 Hz,Ar-H(2'',6''), 8.26(s,1H,N-CH=C)

^{13}C NMR 100.61MHz $CDCl_3$: δ55.07(O-CH_3), 69.50(CH_2), 113.18(Ar-C(3,5)), 114.16(Ar-C(3'',5'')), 118.97(Ar-C(2',6'),120.61(N-CH=C),124.54(Ar-C(1)), 126.84,127.06, 127.54, 128.16,129.15, 129.66(Ar-H(2,6,3',4',5',2''',3''',4''', 5''',6''')), 131.11,131.21(Ar-C(2'',6'')), 136.45(Ar-C(1''')), 138.89(Ar-C(1')), 152.86(N=C-C), 158.65(Ar-C(4)), 162.89(Ar-C(4'')), 188.50(C=O)

IR (NaCl/KBr): C=N absorbance 1599.76 cm^{-1}, C=O absorbance at 1693.27 cm^{-1}.

6.14 General procedure for preparation of p-Tetrahydropyranyloxy bromobenzene

To a solution of bromophenol (57.8 mmol, 10 g) in 3,4-dihydro-2H-pyran(15 mL, 13.83 g, 164.4 mmol) were added 2 drops of 2N HCl. After stirring at room temperature for 3 h, the solution was diluted with diethyl ether (100 mL) washed with 2N NaOH, water and brine (75 mL each) and dried over $MgSO_4$. After evaporation of the solvent, the remaining oil was recrystallized from methanol at 4 °C.

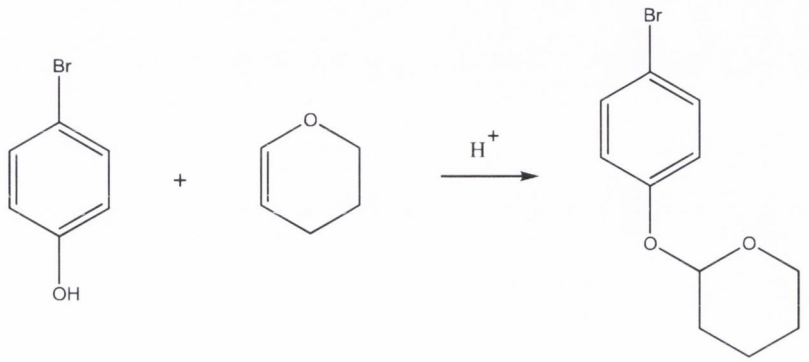

6.14.1 Synthesis of 2-(4-bromophenoxy)tetrahydro-*2H*-pyran 266

This product was obtained from bromophenol (57.8 mmol, 10 g) and 3,4-dihydro-2H-pyran(15 mL, 13.83 g, 164.4 mmol).

Yield: 55.74%, white solid

MP: 102 °C

^{1}H NMR 400.13MHz $CDCl_3$: δ 1.61-1.72(m,4H,-CH_2), 1.86-1.89(m,2H,-CH_2), 1.99-2.03(m,2H,-CH_2), 3.60-3.64(m,2H,-CH_2), 5.39(s,1H,O-CH-), 6.96(d,2H,J=9.04 Hz, Ar-H(2,6)), 7.39(d,2H,J=9.04 Hz,Ar-H(2,6)).

^{13}C NMR 100.61MHz $CDCl_3$: δ 18.18(CH_2),24.67(CH_2),29.79(CH_2), 61.56(CH_2), 96.01(O-CH-), 113.38(Ar-C(4)), 117.83(Ar-C(2,6)),131.75,131.97(Ar-C(3,5)), 156.69(Ar-C(1)).

EIMS (HR): $C_{11}H_{14}N_2Br$ calculated $[M+H]^+$ 257.0177, observed $[M+H]^+$ 257.0182.

IR (NaCl/KBr): C-O absorbance 1078.45 cm^{-1}

6.15 General procedure for preparation of Hydrolyzing Tetrahydropyranyl ether

A Solution of tetrahydropyranyl ether (1.0 mmol) and tetrabromomethane CBr_4 (0.05 mmol) in anhydrous methanol (5 mL/ROTHP 1 mmol) is refluxed at 65 °C for 0.5-3 h. The solution was cooled to room temperature and poured into an aqueous $NaHCO_3$ solution (5%, 10 mL) and then extracted with diethyl ether (3x10 mL). The organic layer was washed with brine (10 mL), dried over $MgSO_4$, filtered and the solvent was removed under reduced pressure. The curde product was purified by column chromatography over silica gel on the SP1 system.

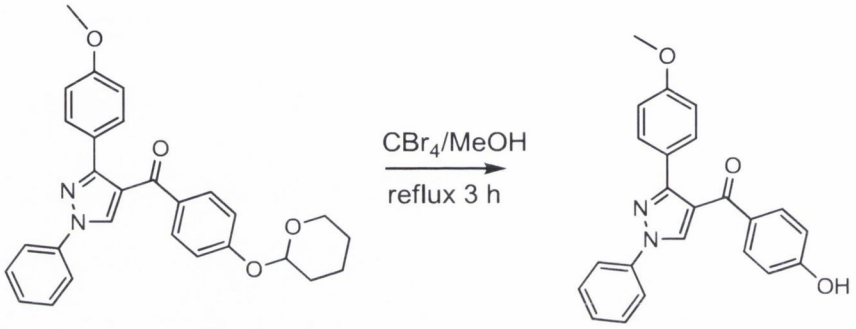

6.15.1 Synthesis of (4-hydroxyphenyl)(3-(4-methoxyphenyl)-1-phenyl-*1H*-pyrazol-4-yl)methanone 281

This product was obtained from (3-(4-methoxyphenyl)-1-phenyl-1H-pyrazol-4-yl)(4-(tetrahydro-2H-pyran-2-yloxy)phenyl)methanone (1.0 mmol, 553.7 mg), and CBr_4 (0.05 mmol, 16.6 mg).

Yield: 85.97%, orange yellow solid

MP: 160 °C

^{1}H NMR 400.13MHz $CDCl_3$: δ3.82(s,3H,-OCH_3), 6.83(d,2H,J=9.04 Hz,Ar-H(3,5)), 6.90(d,2H,J=7.04 Hz,Ar-H(3'',5'')), 7.27-7.29(m,2H,Ar-H(3',5')), 7.35-7.39(m,1H,Ar-H(4')), 7.49-7.53(m,2H,Ar-H(2',6')),7.69(d,2H,J=9.04 Hz,Ar-H(2,6)), 7.80(d,2H,J=7.0 Hz,Ar-H(2'',6'')), 8.26(s,1H,N-C<u>H</u>=C).

^{13}C NMR 100.61MHz $CDCl_3$: δ 54.83(O-CH_3), 113.22(Ar-C(3,5)), 114.79(Ar-C(3'',5'')), 119.04(Ar-C(2',6'), 120.54(N-CH=<u>C</u>),124.20(Ar-C(1)), 126.89, 129.15, 129.64, 130.94(Ar-H(2,6,3',4',5')), 131.28, 131.79(Ar-C(2'',6'')), 138.86(Ar-C(1')), 159.43, 159.74(Ar-C(4,4'')), 209.23(C=O)

EIMS (HR): $C_{23}H_{17}N_2O_3$ calculated $[M+H]^+$ 369.1239, observed $[M+H]^+$ 369.1255.

IR (NaCl/KBr): C=N absorbance 1599.25 cm^{-1}, O-H absorbance 3417.90 cm^{-1}

6.16 General procedure for preparation of product with basic side chain ether

The phenolic starting material (1 mmol, 1.0 eqiv.) was dissolved in 30 mL dry acetone and placed in a two-neck round bottomed flask. Anhydrous potassium carbonate (16 mmol, 16.0 eqiv) was added in, then the reaction mixture was stirred gently for 10 min under N_2 and the corresponding basic side chain halide was added (4 mmol, 4.0 eqiv.). Subsquently, the reaction mixture was refluxed until the reaction was complete on TLC. The reaction mixture was filtered and solvent was removed under reduce pressure.

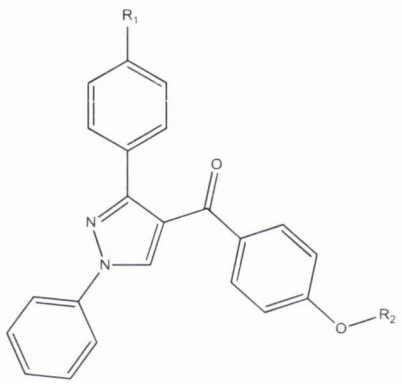

6.16.1 Synthesis of (3-(4-methoxyphenyl)-1-phenyl-*1H*-pyrazol-4-yl)(4-(2-(pyrrolidin-1-yl)ethoxy)phenyl)methanone 282

This product was obtained from (4-hydroxyphenyl)(3-(4-methoxyphenyl)-1-phenyl-1H-pyrazol-4-yl)methanone (1.0 mmol, 370.4 mg), and 1-(2-chloroethyl)pyrrolidine (4.0 mmol, 534.4 mg).

Yield: 12.43%, white solid

MP: 178 °C

^{1}H NMR 400.13MHz $CDCl_3$: δ 1.59-1.68(m,4H,-CH_2), 2.43-2.56(m,4H,-CH_2), 2.92(t,2H,J=5.04 Hz,-O-$CH_2C\underline{H}_2$), 3.74(s,3H,-OCH_3), 4.12(t,2H,J=5.52 Hz,$OC\underline{H}_2CH_2$), 6.81(d,2H,J=8.8 Hz,Ar-H(3'',5'')), 7.01(d,2H,J=8.52 Hz,Ar-H(3,5)), 7.26-7.29(m,1H,Ar-H(4')), 7.38-7.42(m,2H,Ar-H(3',5')), 7.63(d,2H,J=8.52 Hz,Ar-H(2,6)), 7.71-7.81(m,4H,Ar-H(2',6',2'',6'')), 8.20(s,1H,N-C$\underline{H}$=C).

^{13}C NMR 100.61MHz $CDCl_3$: δ21.11(-CH_2), 54.82(O-CH_3), 57.90-($OCH_2\underline{C}H_2$), 58.25(-CH_2), 66.51(-$O\underline{C}H_2CH_2$), 113.74, 113.87(Ar-C(3,5)), 115.41(Ar-C(3'',5'')), 118.88(Ar-C(2',6'), 120.39(N-CH=$\underline{C}$), 124.22(Ar-C(1)), 126.82, 129.10,

129.57,129.61(Ar-H(2,6,3',4',5')), 131.32(N-CH=C), 131.60, 131.66(Ar-C(2'',6'')), 138.64(Ar-C(1')), 152.79(N=C-C), 159.38(Ar-C(4)), 162.03(Ar-C(4'')), 188.19(C=O).

EIMS (HR): $C_{29}H_{30}N_3O_3$ calculated $[M+H]^+$ 468.2287, observed $[M+H]^+$ 468.2273.

IR (NaCl/KBr): C=N absorbance 1599.25 cm^{-1}, C=O absorbance 1712.32 cm^{-1}.

6.16.2 Synthesis of (3-(4-methoxyphenyl)-1-phenyl-*1H*-pyrazol-4-yl)(4-(2-(piperidin-1-yl)ethoxy)phenyl)methanone 283

This product was obtained from (4-hydroxyphenyl)(3-(4-methoxyphenyl)-1-phenyl-1H-pyrazol-4-yl)methanone (1.0 mmol, 370.4 mg), and 1-(2-chloroethyl)piperidine (4.0 mmol, 590.4 mg).

Yield: 23.2%, white solid

MP: 184 °C

^{1}H NMR 400.13MHz $CDCl_3$: δ 1.38-2.29(m,6H,-CH_2), 2.60-2.98(m,4H,-CH_2), 3.32(t,2H,J=6.04 Hz,-CH_2), 3.83(s,3H,-OCH_3), 4.08(t,2H,J=6.56 Hz,-CH_2), 6.89(d,2H,J=8.56 Hz,Ar-H(3'',5'')), 6.93(d,2H,J=8.52 Hz,Ar-H(3,5)), 7.35-7.39(m,1H,Ar-H(4')), 7.49-7.53(m,2H,Ar-H(3',5')), 7.70(d,2H,J=8.52 Hz,Ar-H(2,6)), 7.78-7.82(m,4H,Ar-H(2',6',2'',6'')), 8.27(s,1H,N-CH=C).

^{13}C NMR 100.61MHz $CDCl_3$: δ 21.44(CH_2), 22.20(CH_2), 36.15(CH_2), 53.53(CH_2), 54.84(O-CH_3), 57.83(CH_2), 113.20(Ar-C(3,5)), 114.90(Ar-C(3'',5'')), 119.01(Ar-C(2',6'), 120.58(N-CH=C), 124.27(Ar-C(1)), 126.83, 129.13, 129.62, 130.65(Ar-H(2,6,3',4',5')), 131.22, 131.72(Ar-C(2'',6'')), 138.88(Ar-C(1')), 159.40, 160.32(Ar-C(4,4'')).

EIMS (HR): $C_{30}H_{32}N_3O_3$ calculated $[M+H]^+$ 482.2444, observed $[M+H]^+$ 482.2459.

IR (NaCl/KBr): C=N absorbance 1600.43 cm^{-1}, C=O absorbance 1700.90 cm^{-1}.

6.16.3 Synthesis of (3-(4-methoxyphenyl)-1-phenyl-*1H*-pyrazol-4-yl)(4-(2-morpholinoethoxy) phenyl)methanone 284

This product was obtained from (4-hydroxyphenyl)(3-(4-methoxyphenyl)-1-phenyl-1H-pyrazol-4-yl)methanone (1.0 mmol, 370.4 mg), and 4-(2-chloroethyl)morpholine (4.0 mmol, 598.4 mg).

Yield: 32.1%, white solid

MP: 190 °C

^{1}H NMR 400.13MHz $CDCl_3$: δ2.62(t,4H,J=4.0 Hz,CH_2), 2.85(t,2H,J=5.52 Hz,CH_2),

3.77(t,4H,J=4.0 Hz,CH_2), 3.83(s,3H,-OCH_3), 4.19(t,2H,J=5.52 Hz,CH_2),
6.89(d,2H,J=8.52 Hz,Ar-H(3'',5'')), 6.91(d,2H,J=9.04 Hz,Ar-H(3,5)),
7.35-7.39(m,1H,Ar-H(4')), 7.49-7.53(m,2H,Ar-H(3',5')),
7.70(d,2H,J=9.04 Hz,Ar-H(2,6)), 7.80(d,2H,J=7.52 Hz,Ar-H(2',6')),
7.86(d,2H,J=8.52 Hz,Ar-H(2'',6'')), 8.25(s,1H,N-C<u>H</u>=C).

^{13}C NMR 100.61MHz $CDCl_3$: δ 53.61(CH_2), 54.83(O-CH_3), 56.96(CH_2),
57.99(CH_2), 65.48(CH_2), 66.36(CH_2), 113.20, 113.70(Ar-C(3,5)),
114.83(Ar-C(3'',5'')), 119.00(Ar-C(2',6'), 120.57(N-CH=<u>C</u>), 124.24(Ar-C(1)),
126.86, 129.14, 129.62(Ar-H(2,6,3',4',5')), 131.21(N-<u>C</u>H=C), 131.49,
131.75(Ar-C(2'',6'')), 138.87(Ar-C(1')), 152.90(N=<u>C</u>-C), 159.42,
161.93(Ar-C(4,4'')), 188.55(C=O).

EIMS (HR): $C_{29}H_{30}N_3O_4$ calculated $[M+H]^+$ 484.2236, observed $[M+H]^+$ 484.2227.

IR (NaCl/KBr): C=N absorbance 1600.68 cm^{-1}, C=O absorbance 1711.36 cm^{-1}.

6.16.4 Synthesis of (4-(2-(diethylamino)ethoxy)phenyl)(3-(4-methoxyphenyl)-1-phenyl-*1H*-pyrazol-4-yl)methanone 285

This product was obtained from (4-hydroxyphenyl)(3-(4-methoxyphenyl)-1-phenyl-1H-pyrazol-4-yl)methanone (1.0 mmol, 370.4 mg), and 2-chloro-diethylethanamine (4.0 mmol, 540.3 mg).

Yield: 9.24%, white solid

MP: 168 °C

^{1}H NMR 400.13MHz $CDCl_3$: δ1.36(t,6H,J=4.0 Hz,CH_2), 2.72(t,2H,J=5.52 Hz,CH_2),
3.31(t,4H,J=4.0 Hz,CH_2), 3.83(s,3H,-OCH_3), 4.13(t,2H,J=5.52 Hz,CH_2),
6.89(d,2H,J=9.04 Hz,Ar-H(3'',5'')), 6.92(d,2H,J=8.52 Hz,Ar-H(3,5)),
7.35-7.39(m,1H,Ar-H(4')), 7.49-7.53(m,2H,Ar-H(3',5')),
7.72(d,2H,J=8.52 Hz,Ar-H(2,6)), 7.79(d,2H,J=7.52 Hz,Ar-H(2',6')),
7.87(d,2H,J=9.04 Hz,Ar-H(2'',6'')), 8.25(s,1H,N-C<u>H</u>=C).

^{13}C NMR 100.61MHz $CDCl_3$: δ 15.43(CH_3), 51.34(CH_2), 54.82(O-CH_3),
57.46(CH_2), 66.18(CH_2), 113.29(Ar-C(3,5)), 114.11(Ar-C(3'',5'')),
118.99(Ar-C(2',6'), 120.58(N-CH=<u>C</u>), 124.23(Ar-C(1)), 126.76, 129.03, 129.26,
129.65(Ar-H(2,6,3',4',5')), 131.10(N-<u>C</u>H=C), 131.26, 131.54(Ar-C(2'',6'')),
138.76(Ar-C(1')), 152.87(N=<u>C</u>-C), 159.41,161.91(Ar-C(4,4'')), 188.52(C=O).

EIMS (HR): $C_{29}H_{32}N_3O_3$ calculated $[M+H]^+$ 470.2444, observed $[M+H]^+$ 470.2447.

IR (NaCl/KBr): C=N absorbance 1601.23 cm^{-1}, C=O absorbance 1711.56 cm^{-1}.

6.16.5 Synthesis of (4-(2-(dimethylamino)ethoxy)phenyl)(3-(4-methoxyphenyl)-1-phenyl-*1H*-pyrazol-4-yl)methanone 286

This product was obtained from (4-hydroxyphenyl)(3-(4-methoxyphenyl)-1-phenyl-1H-pyrazol-4-yl)methanone (1.0 mmol, 370.4 mg), and 2-chloro-dimethylethanamine (4.0 mmol, 430.3 mg).

Yield: 13.4%, white solid

MP: 192 °C

^{1}H NMR 400.13MHz $CDCl_3$: δ2.36(s,6H,CH_3), 2.76(t,2H,J=5.52 Hz,CH_2), 3.83(s,3H,-OCH_3), 4.13(t,2H,J=5.52 Hz,CH_2), 6.89(d,2H,J=9.04 Hz,Ar-H(3'',5'')), 6.92(d,2H,J=8.52 Hz,Ar-H(3,5)), 7.35-7.38(m,1H,Ar-H(4')), 7.49-7.53(m,2H,Ar-H(3',5')), 7.70(d,2H,J=8.52 Hz,Ar-H(2,6)), 7.80(d,2H,J=7.52 Hz,Ar-H(2',6')), 7.86(d,2H,J=9.04 Hz,Ar-H(2'',6'')), 8.26(s,1H,N-C<u>H</u>=C).

^{13}C NMR 100.61MHz $CDCl_3$: δ 45.49(CH_3), 54.82(O-CH_3), 57.66(CH_2), 65.78(CH_2), 113.19(Ar-C(3,5)), 113.71(Ar-C(3'',5'')), 118.98(Ar-C(2',6'), 120.60(N-CH=<u>C</u>),124.26(Ar-C(1)), 126.82, 129.13, 129.61, 129.70(Ar-H(2,6,3',4',5')), 131.08(N-<u>C</u>H=C), 131.16, 131.44(Ar-C(2'',6'')), 138.89(Ar-C(1')), 152.87(N=<u>C</u>-C), 159.41, 162.16(Ar-C(4,4'')), 188.53(C=O).

EIMS (HR): $C_{27}H_{28}N_3O_3$ calculated $[M+H]^+$ 442.2131, observed $[M+H]^+$ 442.2141.

IR (NaCl/KBr): C=N absorbance 1600.19 cm^{-1}, C=O absorbance 1712.46 cm^{-1}.

6.17 General procedure for reductive amination

To a stirred solution of pyrazole carbaldehyde (11.45 mmol) in dry methanol (50 mL) was added piperazine (80 mmol) and sodium cyanoborohydride (15.92 mmol) and the reaction was stirred at 20 °C for 72 h. The pH of the reaction was occasionally adjusted to pH5-6 by the addition of 4M methanolic HCl, as determined by damp universal pH paper. Excess hydride was decomposed by the addition of 10% aqueous HCl (150 mL) and resulting aqueous phase washed with DCM (3x50 mL). The aqueous phase was basified with 15% aqueous NaOH solution and extracted with DCM (3x50 mL). The organic phases were combined, dried over anhydrous Na_2SO_4 and the solvent was removed *in vacuo* leaving the product as an oil.

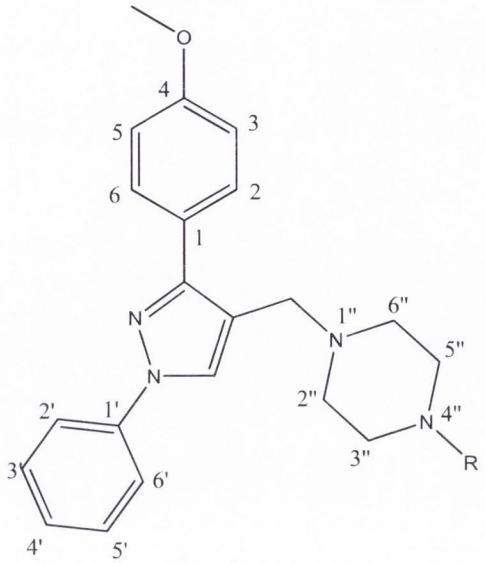

6.17.1 Synthesis of 1-((3-(4-methoxyphenyl)-1-phenyl-*1H*-pyrazol-4-yl)methyl)-4-methylpiperazine 250

This product was obtained from 3-(4-methoxyphenyl)-1-phenyl-1H-pyrazole-4-carbaldehyde(3.186 g, 11.45 mmol), sodium cyanoborohydride(1.00 g, 15.92 mmol) and 1-methyl piperazine (8.01 g, 80 mmol)

Yield: 23.2%, white solid

MP: 156 ^{o}C

^{1}H NMR (400.13MHz $CDCl_3$): δ2.34(s,3H,CH_3), 2.52(bs,8H,CH_2), 3.53(s,2H,CH_2), 3.87(s,3H,O-CH_3), 6.99(d, 2H,J=8.52 Hz,Ar-H(3,5)), 7.27(m, 1H, Ar-H(4')), 7.45(m,2H,Ar-H(3',5')), 7.76(d,2H,J=7.52 Hz,Ar-C(2',6')), 7.90(d,2H, J=8.52 Hz,Ar-C(2,6)), 8.00(N-C<u>H</u>=C).

^{13}C NMR (100.61MHz $CDCl_3$): δ 45.36(CH_3), 52.02 (-CH_2), 54.63(-CH_2-), 54.84 (O-CH_3), 57.62(-CH_2-), 113.37(Ar-C(3,5)), 118.25(Ar-C(2',6')), 125.58(N-<u>C</u>H=C), 125.63(Ar-C(1)), 127.77, 128.93, 129.17(Ar-C(2,6,3',4',5')), 139.56(Ar-C(1')), 151.94(N=C), 158.96(Ar-C(4)).

EIMS (HR): $C_{22}H_{27}N_4O$ calculated $[M+H]^+$ 363.2185, observed $[M+H]^+$ 363.2186.

IR (NaCl/KBr): C=N absorbance 1600.00 cm^{-1}.

6.17.2 Synthesis of 1-benzyl-4-((3-(4-methoxyphenyl)-1-phenyl-*1H*-pyrazol-4-yl)methyl)piperazine 251

This product was obtained from 3-(4-methoxyphenyl)-1-phenyl-1H-pyrazole-4-carbaldehyde(280.6 mg, 1 mmol), sodium cyanoborohydride (99.6 mg, 1.5 mmol) and 1-Benzyl piperazine(1.23 g,7 mmol).

Yield: 43.2%, white solid

MP: 138 °C

^{1}H NMR (400.13MHz $CDCl_3$): δ2.89(bs,8H,CH_2), 3.73(s,2H,CH_2), 3.86(s,3H,O-CH_3), 4.02(s,2H,CH_2), 6.99(d, 2H,J=8.52 Hz,Ar-H(3,5)), 7.27-7.34(m, 6H, Ar-H(4',2'',3'',4'',5'',6'')), 7.43-7.47(m,2H,Ar-H(3',5')), 7.58(d,2H,J=8.52 Hz,Ar-H(2,6)),7.77(d,2H,J=8.04 Hz,Ar-H(2',6'))

^{13}C NMR.(100.61MHz $CDCl_3$): δ 49.98 (-CH_2-), 50.36(-CH_2), 54.92(O-CH_3), 61.15(-CH_2), 113.87(Ar-C(3,5)), 118.63(Ar-C(2',6')), 124.35(N-CH=C),126.35, 128.02, 128.31, 129.02, 129.20, 129.49(Ar-C(2,6,3',4',5',2'',3'',4'',5'',6'')), 139.04(Ar-C(1')), 152.48(N=C), 159.38(Ar-C(4)).

EIMS (HR): $C_{28}H_{31}N_4O$ calculated $[M+H]^+$ 439.2498, observed $[M+H]^+$ 439.2505.

IR (NaCl/KBr): C=N absorbance 1598.89 cm^{-1}.

6.17.3 Synthesis of 1-(benzo[d][1,3]dioxol-5-ylmethyl)-4-((3-(4-methoxyphenyl)-1-phenyl-*1H*-pyrazol-4-yl)methyl)piperazine 252

This product was obtained from 3-(4-methoxyphenyl)-1-phenyl-1H-pyrazole-4-carbaldehyde(421.4 mg, 1.5 mmol), sodium cyanoborohydride(137 mg, 2 mmol) and 1-piperonyl piperazine (2.209 g, 10 mmol).

Yield: 11.5%, yellow solid

MP: 124 °C

^{1}H NMR (400.13MHz $CDCl_3$): δ2.53-2.66(m,8H,CH_2), 3.46(s,2H,CH_2), 3.56(s,2H,CH_3), 3.88(s,3H,O-CH_3), 5.97(s,2H,O-CH_2-O), 6.76(m, 2H, Ar-H(5'',6'')), 6.88(s,1H,Ar-H(2'')), 7.00(dd,2H,J=9.04 Hz,Ar-H(3,5)), 7.27-7.31(m,1H,Ar-H(4')), 7.45-7.49(m,2H,Ar-H(3',5')), 7.76(d,2H,J=7.52 Hz,Ar-H(2',6')), 7.86(dd,2H,J=9.04 Hz,Ar-H(2,6)), 7.95(s,1H,N-CH=C).

^{13}C NMR (100.61MHz $CDCl_3$): δ 52.34,52.65,52.91(-CH_2-), 55.32(O-CH_3), 62.72(-CH_2), 100.91(O-CH_2-O), 107.88(Ar-C(5'')), 109.65(Ar-C(2'')), 113.85(Ar-C(3,5)), 118.76(Ar-C(2',6')), 122.43(Ar-C(6'')), 126.01, 126.12, 128.26, 129.39, 129.69(Ar-C(2,6,3',4',5')), 140.02(Ar-C(1')), 146.64, 147.62(Ar-C(3'',4'')), 152.49(N=C), 159.43(Ar-C(4)).

EIMS (HR): $C_{29}H_{31}N_4O_3$ calculated $[M+H]^+$ 483.2396, observed $[M+H]^+$ 483.2397.

IR (NaCl/KBr): C=N absorbance 1600.43 cm^{-1}.

6.17.4 Synthesis of 1-allyl-4-((3-(4-methoxyphenyl)-1-phenyl-*1H*-pyrazol-4-yl)methyl)piperazine 253

This product was obtained from 3-(4-methoxyphenyl)-1-phenyl-1H-pyrazole-4-carbaldehyde(429.7 mg, 1.5 mmol), sodium cyanoborohydride (133.4 mg, 2 mmol) and 1-allylpiperazine (757.2 mg, 0.83 mL, 6 mmol).

Yield: 36.2%, yellow Oil

MP: Oil

^{1}H NMR (400.13MHz $CDCl_3$): δ 2.53(m,8H,CH_2), 3.02(m,2H,CH_2), 3.42(s,2H,CH_2), 3.85(s,3H,O-CH_3), 4.69(s,1H,CH=C$\underline{H}_2$), 5.16(t,1H,J=1.76 Hz,CH=CH_2), 5.84-5.90(m,1H,C$\underline{H}$=CH_2), 6.98(d, 2H,J=8.76 Hz,Ar-H(3,5)), 7.25-7.29(m,1H,Ar-H(4')), 7.42-7.46(m,2H,Ar-H(3',5')), 7.70(d,2H,J=8.28 Hz,Ar-H(2',6')), 7.74(dd,2H,J=9.04 Hz,Ar-H(2,6)), 7.93(s,1H,N-C$\underline{H}$=C).

^{13}C NMR (100.61MHz $CDCl_3$): δ 52.27, 52.48, 52.99(-CH_2-), 55.29(O-CH_3), 55.66(-CH_2), 61.69(-CH_2), 113.84, 114.04(Ar-C(3,5)), 117.13($\underline{C}H_2$=CH), 118.80, 118.84(Ar-C(2',6')), 125.61, 126.18, 126.27, 129.07, 129.41(Ar-C(2,6,3',4',5')), 134.49($\underline{C}$H=CH_2), 139.96(Ar-C(1')), 152.52(N=C), 159.43(Ar-C(4)).

EIMS (HR): $C_{24}H_{29}N_4O$ calculated $[M+H]^+$ 389.2341, observed $[M+H]^+$ 389.2346.

IR (NaCl/KBr): C=N absorbance 1600.09 cm^{-1}.

6.17.5 Synthesis of 1-((3-(4-methoxyphenyl)-1-phenyl-*1H*-pyrazol-4-yl)methyl)-4-phenylpiperazine 254

This product was obtained from 3-(4-methoxyphenyl)-1-phenyl-1H-pyrazole-4-carbaldehyde(427.9 mg, 1.5 mmol),sodium cyanoborohydride (129.4 mg, 2 mmol) and 1-phenylpiperazine (1.62 g, 1.5 mL, 10 mmol).

Yield: 38.7%, white solid

MP: 148 °C

^{1}H NMR (400.13MHz $CDCl_3$): δ2.71-2.74(m,4H,CH_2), 3.25-3.38(m,4H,CH_2), 3.61(s,2H,CH_2), 3.89(s,3H,O-CH_3), 6.88-6.92(m,1H,Ar-H(4'')), 6.97(d,2H,J=8.04 Hz,Ar-H(2'',6'')), 7.03(d,2H,J=8.52 Hz,Ar-H(3,5)), 7.29-7.33(m,3H,Ar-H(4',3'',5'')), 7.48-7.52(m,2H,Ar-H(3',5')), 7.80(d,2H,J=7.52 Hz,Ar-H(2',6')), 7.95(d,2H,J=8.52 Hz,Ar-H(2,6)), 7.98(s,1H,N-C$\underline{H}$=C).

^{13}C NMR.(100.61MHz $CDCl_3$): δ 48.80(-CH_2-), 52.09(CH_2), 52.40(-CH_2-), 54.88(-CH_2), 113.42(Ar-C(3,5)), 115.65(Ar-C(2'',6'')), 116.78(CH=C), 118.29(Ar-C(2',6')), 125.60, 125.69, 127.80, 128.69, 128.99, 129.24(Ar-C(2,6,3',4',5',3'',4'',5'')), 139.60(Ar-C(1')), 150.90(Ar-C(1'')), 152.03(N=C), 159.02(Ar-C(4)).

EIMS (HR): $C_{27}H_{29}N_4O$ calculated $[M+H]^+$ 425.2341, observed $[M+H]^+$ 425.2329.

IR (NaCl/KBr): C=N absorbance 1599.14 cm^{-1}.

6.17.6 Synthesis of 1-((3-(4-methoxyphenyl)-1-phenyl-*1H*-pyrazol-4-yl)methyl)piperazine 255

This product was obtained from 3-(4-methoxyphenyl)-1-phenyl-1H-pyrazole-4-carbaldehyde(569.8 mg, 2 mmol), sodium cyanoborohydride (107.3 mg, 1.5 mmol) and piperazine (620.3 mg,7 mmol).

Yield: 13.6%, yellow solid

MP: 126 °C

^{1}H NMR (400.13MHz $CDCl_3$): δ1.80(s,1H,NH), 3.88(s,3H,O-CH_3), 4.78(s,2H,-CH_2), 7.01(d, 2H,J=8.56 Hz,Ar-H(3,5)), 7.29-7.33(m,1H,Ar-H(4')), 7.48(m,2H,Ar-H(3',5')), 7.76(d,2H,J=8.04 Hz,Ar-H(2',6')), 7.83(d,2H,J=8.56 Hz,Ar-H(2,6)), 8.01(s,1H,N-CH=C).

^{13}C NMR (100.61MHz $CDCl_3$): δ 54.88(-CH_2), 55.63(O-CH_3), 113.64(Ar-C(3,5)), 118.45(Ar-C(2',6')), 119.93(CH=C), 125.09, 125.89, 127.24, 128.60, 128.99(Ar-C(2,6,3',4',5')), 139.49(Ar-C(1')), 150.97(N=C), 159.18(Ar-C(4)).

EIMS (HR): $C_{21}H_{25}N_4O$ calculated $[M+H]^+$ 349.2028, observed $[M+H]^+$ 349.2029.

IR (NaCl/KBr): C=N absorbance 1599.78 cm^{-1}.

6.17.7 Synthesis of 1-((3-(4-methoxyphenyl)-1-phenyl-*1H*-pyrazol-4-yl)methyl)piperidine 256

This product was obtained from 3-(4-methoxyphenyl)-1-phenyl-1H-pyrazole-4-carbaldehyde(553.7 mg, 2 mmol), sodium cyanoborohydride (188.5 mg, 3 mmol) and piperidine (1.27 g, 15 mmol).

Yield: 12.4%, white solid

MP: 162 °C

^{1}H NMR (400.13MHz $CDCl_3$): δ1.59-1.65(m,6H,-CH_2-) 2.47(m,4H,-CH_2-), 3.49(s,2H,CH_2), 3.88(s,3H,O-CH_3), 7.00(d, 2H,J=8.52 Hz,Ar-H(3,5)), 7.26-7.30(m,1H,Ar-H(4')), 7.45-7.49(m,2H,Ar-H(3',5')),

7.70(d,2H,J=8.56 Hz,Ar-H(2',6')), 7.89(d,2H,J=8.52 Hz,Ar-H(2,6)),
7.98(s,1H,N-C<u>H</u>=C).

^{13}C NMR (100.61MHz $CDCl_3$): δ24.02, 25.57(-CH_2-), 52.82(-CH_2), 54.85(O-CH_3), 55.57(-CH_2-), 113.32, 113.63(Ar-C(3,5)), 117.49(CH=<u>C</u>), 118.25, 118.43(Ar-C(2',6')), 120.01(N-<u>C</u>H=C), 125.51, 125.86, 127.60, 128.60, 128.98(Ar-C(2,6,3',4',5')), 139.66(Ar-C(1')), 151.94(N=C), 159.16(Ar-C(4)).

EIMS (HR): $C_{22}H_{26}N_3O$ calculated $[M+H]^+$ 348.2076, observed $[M+H]^+$ 348.2068.

IR (NaCl/KBr): C=N absorbance 1599.65 cm^{-1}.

6.17.8 Synthesis of 3-(4-methoxyphenyl)-1-phenyl-4-(pyrrolidin-1-ylmethyl)-*1H*-pyrazole 257

This product was obtained from 3-(4-methoxyphenyl)-1-phenyl-1H-pyrazole-4-carbaldehyde (551.5 mg, 2 mmol),sodium cyanoborohydride(191.3 mg, 3 mmol)and pyrrolidine(1.07 g,15m mol)

Yield: 8.72%, yellow solid

MP: 124 °C

^{1}H NMR (400.13MHz $CDCl_3$): δ 2.53(m,8H,CH_2), 3.02(m,2H,CH_2), 3.42(s,2H,CH_2), 3.85(s,3H,O-CH_3), 4.69(s,1H,CH=C<u>H</u>$_2$), 5.16(t,1H,J=1.76 Hz,CH=CH_2), 5.84-5.90(m,1H,C<u>H</u>=CH_2), 6.98(d, 2H,J=8.76 Hz,Ar-H(3,5)), 7.25-7.29(m,1H,Ar-H(4')), 7.42-7.46(m,2H,Ar-H(3',5')), 7.70(d,2H,J=8.28 Hz,Ar-H(2',6')), 7.74(dd,2H,J=9.04 Hz,Ar-H(2,6)), 7.93(s,1H,N-C<u>H</u>=C).

^{13}C NMR (100.61MHz $CDCl_3$): δ 52.27, 52.48, 52.99(-CH_2-), 55.29(O-CH_3), 55.66(-CH_2), 61.69(-CH_2), 113.84, 114.04(Ar-C(3,5)), 117.13(<u>C</u>H_2=CH), 118.80, 118.84(Ar-C(2',6')), 125.61, 126.18, 126.27, 129.07, 129.41(Ar-C(2,6,3',4',5')), 152.52(N=C)

EIMS (HR): $C_{24}H_{29}N_4O$ calculated $[M+H]^+$ 389.2341, observed $[M+H]^+$ 389.2346.

IR (NaCl/KBr): C=N absorbance 1600.09 cm^{-1}.

6.18 General procedure for sodium borohydride reduction of carbaldehyde

In a 100 mL two-neck round bottomed flask, (278.31 mg, 1 mmol) of pyrazole carbaldehyde was dissolved in 5 mL of 95% ethanol and the solution was cooled to produce a fine suspension. Then 50 mg of sodium borohydride (large excess) was added. The mixture was warmed up, and after a few minutes, 5 mL of water was added, heated to the boiling point, filter and dilute with more water (10 mL). Set the solution aside to crystallize.

6.18.1 Synthesis of (3-(4-methoxyphenyl)-1-phenyl-*1H*-pyrazol-4-yl)methanol 258

This product was obtained from 3-(4-methoxyphenyl)-1-phenyl-1H-pyrazole-4-carbaldehyde(277.6 mg, 1 mmol), sodium Borohydride (50 mg, 1mmol)

Yield: 69.8%, white solid

MP: 164-168 ^{o}C

^{1}H NMR (400.13MHz $CDCl_3$): δ 1.89(s,OH), 3.88(s,3H,O-CH_3), 4.76(s,2H,CH_2), 7.01(d, 2H,J=9.04 Hz,Ar-H(3,5)), 7.29-7.32(m,1H,Ar-H(4')), 7.45-7.49(m,2H,Ar-H(3',5')), 7.74(d,2H,J=8.04 Hz,Ar-H(2',6')), 7.82(dd,2H,J=9.04 Hz,Ar-H(2,6)), 7.98(s,1H,N-C<u>H</u>=C).

^{13}C NMR (100.61MHz $CDCl_3$): δ 54.88(-CH_2), 55.58(O-CH_3), 113.64(Ar-C(3,5)), 118.46(Ar-C(2',6')), 119.97(CH=<u>C</u>), 125.05(Ar-C(1)), 125.91, 127.28, 128.61, 128.99(Ar-C(2,6,3',4',5')), 139.45(Ar-C(1')), 150.94(N=C), 159.18(Ar-C(4)).

EIMS (HR): Nd

IR (NaCl/KBr): C=N absorbance 1599.83 cm^{-1}.

6.19 XRD Studies

A saturated solution of the test compound **162** was prepared in ethanol. This solution was transferred to a 5mL test tube and an equal quantity of ethanol was added leading to a 50% saturated solution. The tube was then stoppered and a needle used to punch a small hole in the stopper to allow for the slow evaporation of the solvent. The tubes were placed in the dark at room temperature until they had evaporated to dryness (approximately 6 months). The crystals thus obtained were checked under the microscope for defects before being mounted for XRD analysis.

The crystal structure of compounds was determined by X-ray diffraction on a Bruker SMART APEX (2001) diffractometer using MoKa radiation from a fine focus sealed source and a graphite monochromator. The structure solution was found using SHELXS-97 and the structure refinement was carried out using SHELXL-97.

The crystal structure data is presented in Appendix 1.

6.20 Biochemical Testing

Cell Medium

Complete growth medium for the MCF-7 cell line was prepared as follows: 10% foetal calf serum, 1% L-glutamine, 1% non-essential amino acids, 1% penicillin streptomycin and 87% MEME.

Cell Growth

Cells from the MCF-7 cell line were obtained as pellets in a mixture of 10% DMSO and 90% cell medium, frozen in liquid nitrogen. The pellet was warmed to room temperature in a water bath at 37°C, then immediately added to a centrifuge vial containing complete growth medium (final volume of 10mL). The vial was spun at 1250 rpm for 5 minutes. Supernatant liquid was poured off and pellet resuspended in complete growth medium (9mL), then transferred to a 25 cm^2 tissue culture flask fitted with a filter screw cap. The plate was incubated at 37°C in a humid atmosphere with 5% CO_2. Once cells reached 80% confluencey (3-5 days) they were transferred to a larger 75 cm^2 flask with complete growth medium (14mL).

Plate Seeding

Upon reaching 80% confluence, the cell medium was poured off and the biofilm remaining in the flask was rinsed with medium (10mL), and this rinse was discarded. Trypsin (2-3mL depending on confluency of cells) was added and the flask returned to the incubator for 3 minutes. Upon removal from the incubator, the biofilm was seen to have dissolved. Complete growth medium (10mL) was added to the flask and this suspension was then centrifuged at 1250 rpm for 5 minutes. The supernatant liquid was poured off and the remaining pellet was resuspended in complete growth medium (1mL, 2mL, 3mL depending on size of pellet).

The density of cells present in the suspension prepared above was determined by counting a 12μL sample with a haemocytometer under a microscope. A serial dilution was carried out to produce a suspension with a density of $2.5x10^4$cells/mL. Sterile 96 well plates were seeded with this suspension (200μL per well) with the wells around the outside of the plate remaining empty. Plates were then incubated for 24 hours prior to dosing.

Dosing

A 10mM solution of the compound to be tested was prepared in 60% DMSO/40% ethanol. The combination of DMSO and ethanol was used because of the cytotoxic effects of DMSO. From this stock solution, a serial dilution was carried out producing solutions of 5mM, 1mM, 0.5mM, 0.1mM, 10μM, 1μM, and 100nM. The plate was dosed as illustrated in **Figure 5.1**. Two compounds were tested per plate – one in the top three rows and one in the bottom three rows. Each well was dosed with 2μL of test compound which represented a 1 in 100 dilution factor. The columns marked "C" and "B" were for the control and blank used in the assays. The column marked "V" was the vehicle i.e. dosed with 2μL of the solvent used to dissolve the test compound. The plates were then incubated for a further 72 hours before the assays were carried out.

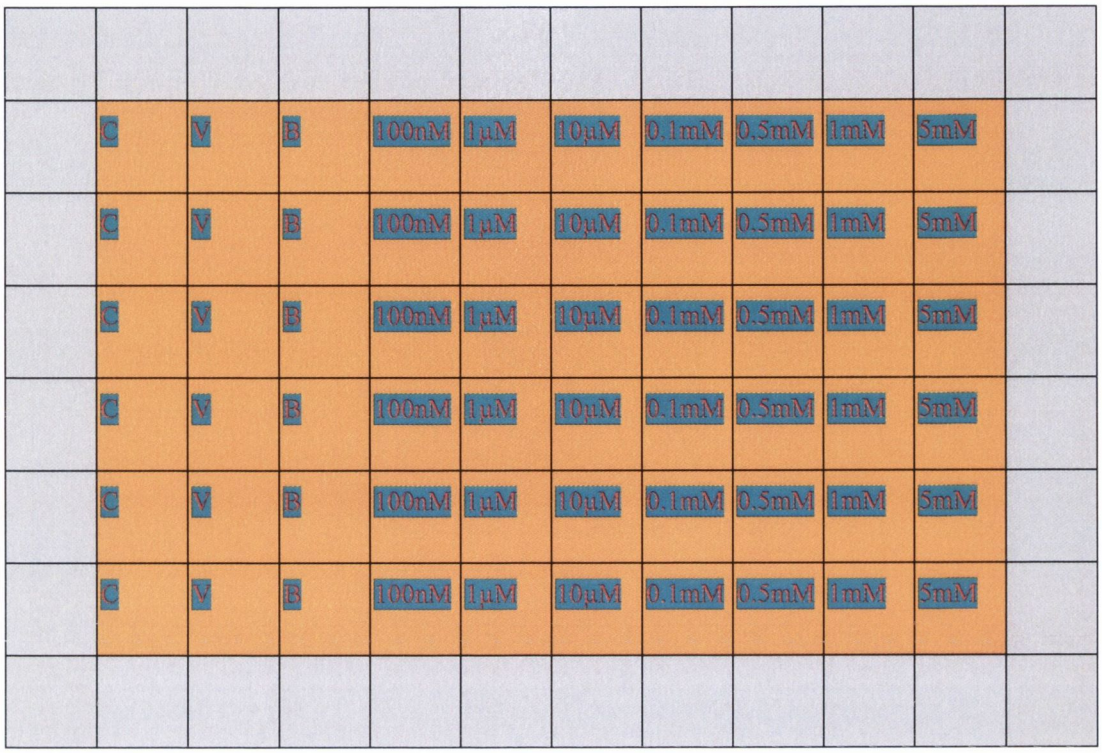

Figure 6.1 Dosing regime for 96-well plates seeded with MCF-7 cells

Assays

The cytotoxity and antiproliferative effects of each compound were determined by the LDH and MTT assay respectively. Cell lysis solution (30μL) was added to each control well in the plates. This served as the 100% cell death control, with the blank well serving as the 0% cell death controls. From each well 30μL of the medium was withdrawn and transferred to a non-sterile 96 well plate along with 30μL of LDH solution. These plates were wrapped in tinfoil and left at room temperature for 20 minutes. Stop solution (30μL per well) was added to each plate after 20 minutes, the plate placed in a plate reader and read at 490nm.

The remaining medium in the sterile plates was poured off and the plate washed twice with phosphate buffered saline before being dried. MTT solution (50μL per well) was added to each plate. The plates were wrapped immediately in tinfoil and placed in the incubator for a further 2 hours. After incubation, DMSO (200μL per well) was added to each plate and any purple crystals fully dissolved up before the plate was placed in a plate reader and read at 595nm.

Data manipulation

The crude data obtained from the plate reader was analysed using GraphPad Prism 4.0 software.

6.21 Stability Studies

System

Stability studies were carried out using a Waters HPLC system fitted with a Spherisorb column (2-5μm particle size, 4.5x250mm) supplied by Alltech Associates Incorporated. A mobile phase of 60/40 acetonitrile/water with 0.1% (v/v) TFA added to prevent peak tailing was used throughout. The mobile phase was only prepared from HPLC grade solvents and degassed by sonication prior to use. Flow rate was maintained at 1mL per minute with a pressure of approximately 1300 psi on a Waters 1525 binary pump equipped with an in line degasser. Where samples were run over a protracted period of time, the mobile phase was recycled back to the reservoir without any detriment to separation. Elution was detected at 280nm with a Waters 2487 dual wavelength detector. Multiple injections were carried out using a Waters 717 autosampler. All samples were filtered via a syringe filter (Pall, 0.45μM) prior to injection. The system was flushed with 2-propanol before shutting down for protracted periods of time.

Buffers

Phosphate buffers at the desired pH (4.0, 7.4, 9.0) were prepared in accordance with the BP monograph (A139). The only deviation was a reduction by a factor of four in the volume of buffer prepared at any one time. Buffers were freshly prepared just prior to use. pH meter used for pH determinations was calibrated once per day prior to use as per the manufacturers specifications.

Stock Solutions

Stock solutions were prepared by dissolving approx. 11mg of compound in 25mL acetonitrile by sonication for 20 min before filtering through a syringe filter resulting in an appromiately 1.1mM solution. Minimum purity of stock solution was 98% by peak area in all cases. Stock solution was able to be stored at -20°C without affecting purity as determined by HPLC.

System Performance

A linear calibration curve was obtained by preparing serial dilutions of the stock solution and injecting in triplicate. A data point in the middle of this calibration was selected and injected six times as a measure of reproducibility.

Blood Plasma

Whole blood (50mL) was withdrawn from a healthy 25 year old male with 5mL 2% sodium citrate. Plasma was obtained by centrifuging at 5000 rpm for 10 min and drawing off the supernatant layer of plasma to obtain approx. 20mL of plasma from each 50mL of whole blood. The plasma was aliquoted (1mL) into 1.5mL epfendorfs and stored at -20°C until needed. Assays using plasma were carried out within 6 weeks of obtaining the plasma. All waste that came into contact with the plasma was disposed of in accordance with School of Pharmacy, TCD, guidelines for biohazard waste.

pH Stability Studies

The appropriate phosphate buffer was prepared as described above and warmed to 37°C in a water bath for at least 30 min prior to use. The stock solution was removed from the fridge and allowed to warm to room temperature. T_0 was determined by taking the stock solution (50μL) and mixing by vortex with acetonitrile (900μL). Three separate injections (10μL) of this solution were made and the average peak area taken as T_0. The test solution was prepared by mixing the stock solution (500μL) in the prewarmed buffer (9000μL) by vortex. This dilution results in a final concentration of 58μM of the analyte in the buffer. The moment of contact of the stock solution with the buffer was recorded. The test solution was maintained at 37°C by immersion in a water bath. Samples were withdrawn from the test solution at predetermined intervals as follows. The test solution was thoroughly mixed by vortexing before 1.2mL of sample was withdrawn by syringe, filtered, and injected (10μL) onto the system.

Blood Plasma Studies

pH 7.4 phosphate buffer was prepared as described above and warmed to 37°C in a water bath for at least 30 min prior to use. The blood plasma was removed from the freezer and quickly warmed to 37°C in the water bath. The plasma (2.5mL) was added to prewarmed buffer (10mL) and mixed together by vortex and placed back in

the water bath to insure the mixture had equilibrated to 37°C. To this mixture, stock solution (1.4mL) was added and mixed well by vortex resulting in a final concentration of 112μM. The moment of contact of the stock solution with the buffer was recorded. The test solution was maintained at 37°C by immersion in a water bath. Samples were withdrawn from the test solution at predetermined intervals as follows. The test solution was thoroughly mixed by vortexing before 1000 μL of sample was withdrawn and added to 1000μL of 2% (w/v) $ZnSo_4$, and the resulting mixture was centrifuged at 4000 rpm for 5 min, before the supernatant was filtered and injected (10μL) onto the system. T_0 was determined by adding the stock solution (700 μL) to acetonitrile (6.25mL) and mixing well by vortex before filtering and injecting onto the system. Three separate injections (10μL) of this solution were made and the average peak area was taken as T_0. For disposed of biohazard waste need to be in accordance with School of Pharmacy, TCD guidelines.

Appendix

Appendix I

NCI60 cell line screen results for the testing of compounds

Compound code	NCI code	Structure
161	S750277	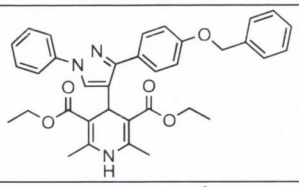
176	S750281	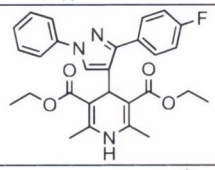
179	S750282	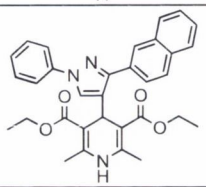
221	S757150	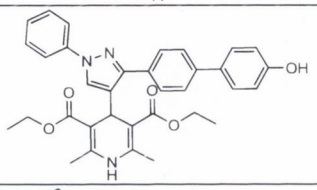
222	S757151	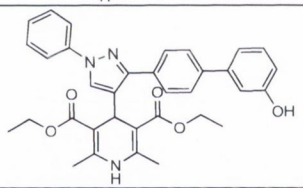
229	S757152	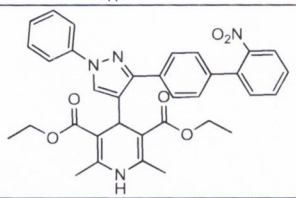
227	S757158	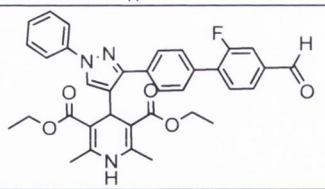
240	S757164	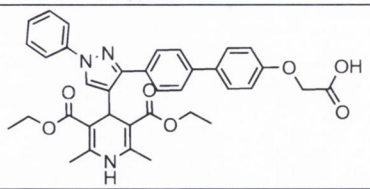

Table A1 Selected compounds for five dose screening test in NCI 60 cell line

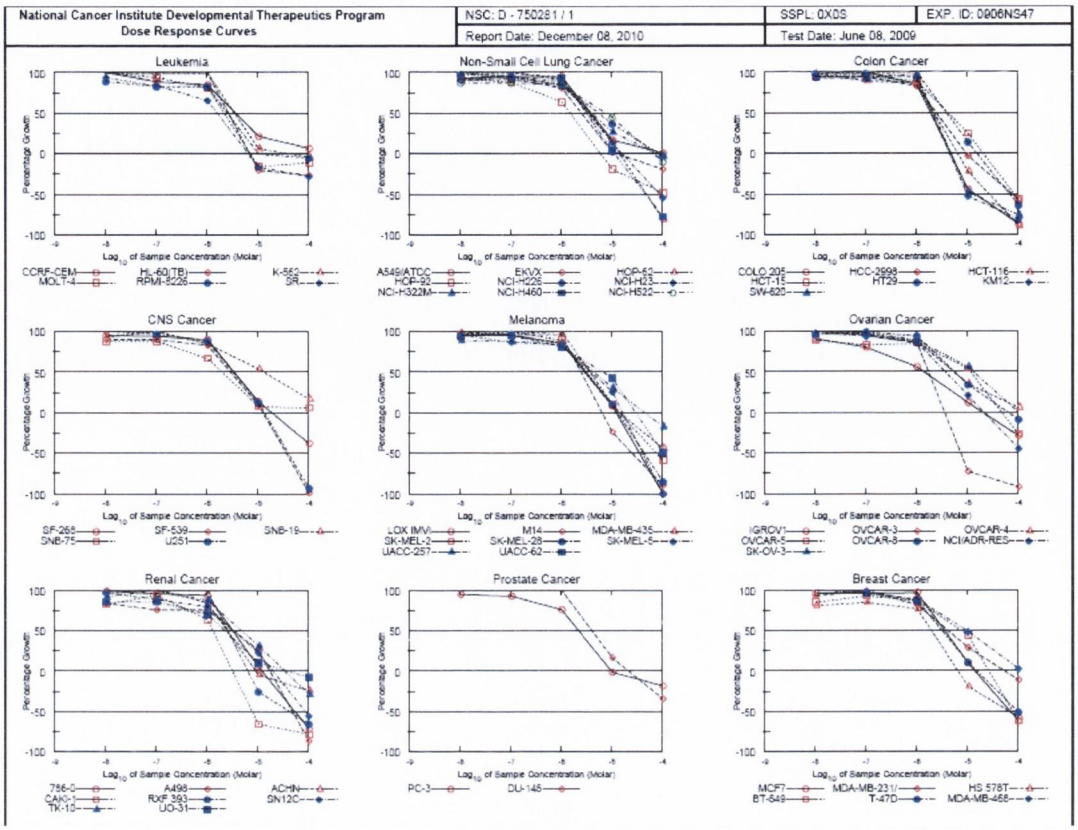
National Cancer Institute Developmental Therapeutics Program
Dose Response Curves
NSC: D - 750281 / 1
Report Date: December 08, 2010
SSPL: 0X0S
Test Date: June 08, 2009
EXP. ID: 0906NS47
Leukemia
CCRF-CEM
HL-60(TB)
K-562
MOLT-4
RPMI-8226
SR
Non-Small Cell Lung Cancer
A549/ATCC
EKVX
HOP-62
HOP-92
NCI-H226
NCI-H23
NCI-H322M
NCI-H460
NCI-H522
Colon Cancer
COLO 205
HCC-2998
HCT-116
HCT-15
HT29
KM12
SW-620
CNS Cancer
SF-268
SF-539
SNB-19
SNB-75
U251
Melanoma
LOX IMVI
M14
MDA-MB-435
SK-MEL-2
SK-MEL-28
SK-MEL-5
UACC-257
UACC-62
Ovarian Cancer
IGROV1
OVCAR-3
OVCAR-4
OVCAR-5
OVCAR-8
NCI/ADR-RES
SK-OV-3
Renal Cancer
786-0
A498
ACHN
CAKI-1
RXF 393
SN12C
TK-10
UO-31
Prostate Cancer
PC-3
DU-145
Breast Cancer
MCF7
MDA-MB-231/ATCC
HS 578T
BT-549
T-47D
MDA-MB-468
Percentage Growth
Log10 of Sample Concentration (Molar)

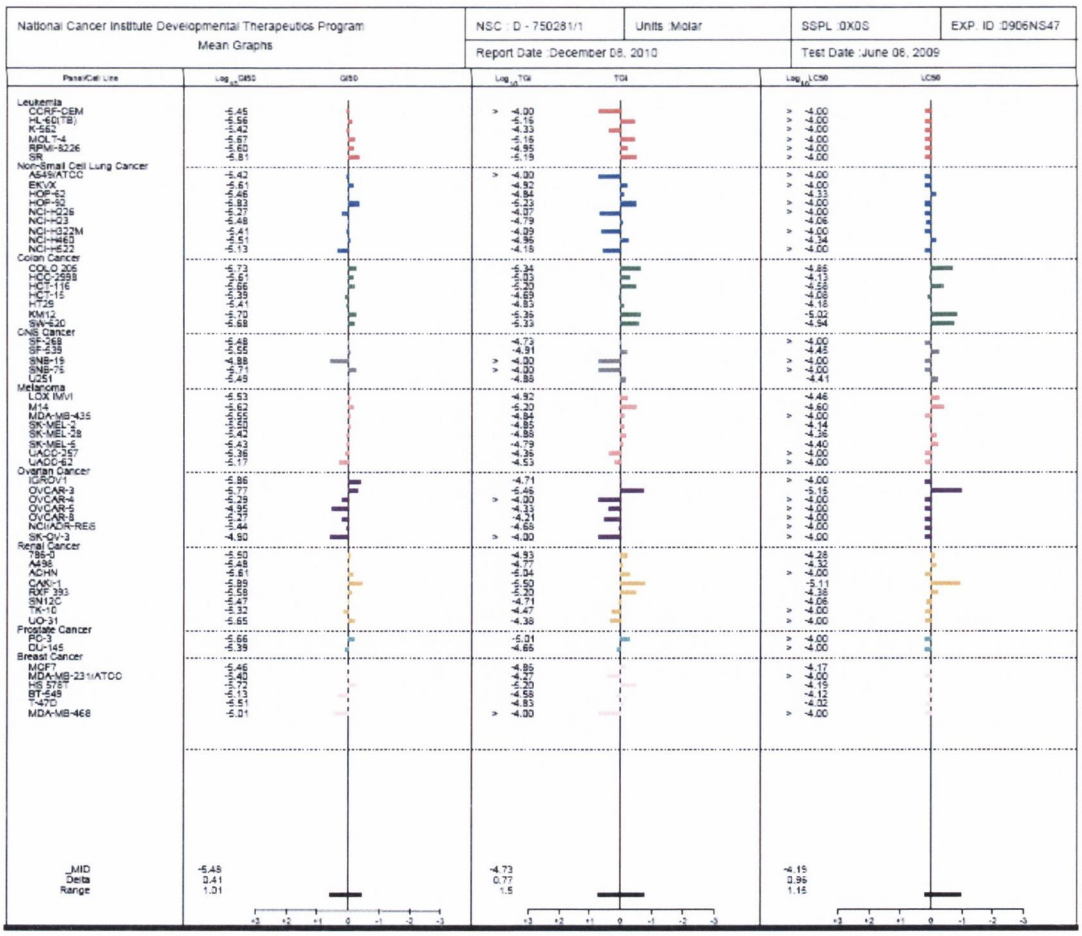
National Cancer Institute Developmental Therapeutics Program
Mean Graphs
NSC : D - 750281/1
Units :Molar
SSPL :0X0S
EXP. ID :0906NS47
Report Date :December 08, 2010
Test Date :June 08, 2009
Panel/Cell Line
Log10GI50
GI50
Log10TGI
TGI
Log10LC50
LC50
Leukemia
CCRF-CEM -5.45 > -4.00 > -4.00
HL-60(TB) -5.56 -5.15 > -4.00
K-562 -5.42 -4.33 > -4.00
MOLT-4 -5.67 -5.15 > -4.00
RPMI-8226 -5.63 -4.95 > -4.00
SR -5.81 -5.19 > -4.00
Non-Small Cell Lung Cancer
A549/ATCC -5.42 > -4.00 > -4.00
EKVX -5.61 -4.92 > -4.00
HOP-62 -5.66 -4.84 > -4.00
HOP-92 -5.83 -5.23 > -4.00
NCI-H226 -5.37 -4.97 > -4.00
NCI-H23 -5.48 -4.79 -4.06
NCI-H322M -5.41 -4.89 > -4.00
NCI-H460 -5.51 -4.96 -4.34
NCI-H522 -5.13 -4.19 > -4.00
Colon Cancer
COLO 205 -5.73 -5.34 -5.66
HCC-2998 -5.67 -5.20 -5.13
HCT-116 -5.66 -5.20 -5.66
HCT-15 -5.39 -4.89 -5.08
HT29 -5.41 -4.85 -5.16
KM12 -5.70 -5.39 -5.32
SW-620 -5.68 -5.33 -5.94
CNS Cancer
SF-268 -5.48 -4.73 > -4.00
SF-539 -5.55 -4.91 -4.45
SNB-19 -4.88 > -4.00 > -4.00
SNB-75 -5.71 > -4.00 > -4.00
U251 -5.49 -4.88 -4.41
Melanoma
LOX IMVI -5.53 -4.92 -4.46
M14 -5.62 -5.20 -4.80
MDA-MB-435 -5.55 -4.84 > -4.00
SK-MEL-2 -5.05 -4.85 -4.14
SK-MEL-28 -5.42 -4.88 -4.36
SK-MEL-5 -5.43 -4.79 -4.40
UACC-257 -5.36 -4.39 > -4.00
UACC-62 -5.17 -4.53 > -4.00
Ovarian Cancer
IGROV1 -5.86 -4.71 > -4.00
OVCAR-3 -5.77 -5.46 -5.15
OVCAR-4 -5.29 > -4.00 > -4.00
OVCAR-5 -5.95 -4.83 > -4.00
OVCAR-8 -5.77 -4.21 > -4.00
NCI/ADR-RES -5.44 -4.55 > -4.00
SK-OV-3 -4.90 > -4.00 > -4.00
Renal Cancer
786-0 -5.53 -4.93 -4.38
A498 -5.48 -4.77 -4.33
ACHN -5.61 -5.04 > -4.00
CAKI-1 -5.89 -5.50 -5.11
RXF 393 -5.68 -5.20 -5.36
SN12C -5.47 -4.71 -4.06
TK-10 -5.32 -4.47 > -4.00
UO-31 -5.65 -4.38 > -4.00
Prostate Cancer
PC-3 -5.66 -5.31 > -4.00
DU-145 -5.39 -4.65 > -4.00
Breast Cancer
MCF7 -5.46 -4.85 -4.17
MDA-MB-231/ATCC -5.48 -4.59 > -4.00
HS 578T -5.72 -5.20 -4.15
BT-549 -5.13 -4.56 -4.12
T-47D -5.51 -4.83 -4.32
MDA-MB-468 -6.01 > -4.00 > -4.00
_MID -5.48 -4.73 -4.15
Delta 0.41 0.77 0.96
Range 1.01 1.5 1.15

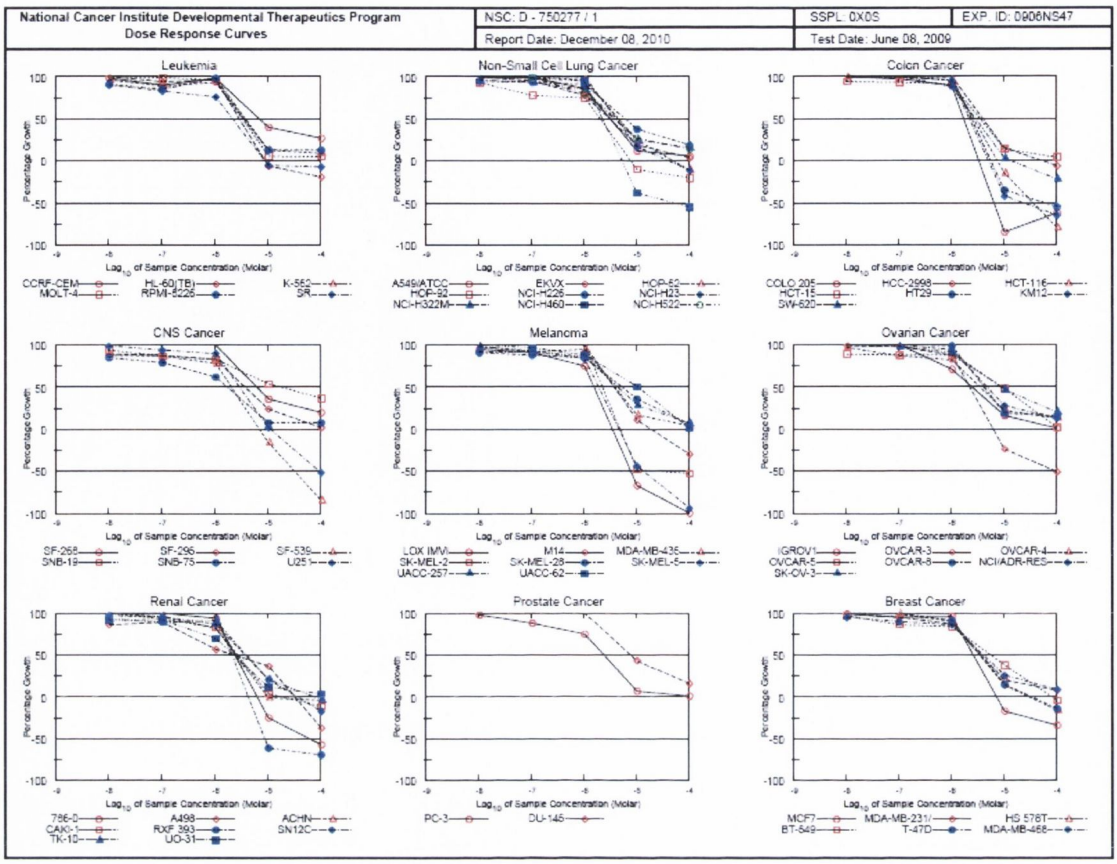
National Cancer Institute Developmental Therapeutics Program
Dose Response Curves
NSC: D - 750277 / 1
Report Date: December 08, 2010
SSPL: 0X0S
EXP. ID: 0906NS47
Test Date: June 08, 2009
Leukemia
CCRF-CEM
HL-60(TB)
K-562
MOLT-4
RPMI-8226
SR
Non-Small Cell Lung Cancer
A549/ATCC
EKVX
HOP-62
HOP-92
NCI-H226
NCI-H23
NCI-H322M
NCI-H460
NCI-H522
Colon Cancer
COLO 205
HCC-2998
HCT-116
HCT-15
HT29
KM12
SW-620
CNS Cancer
SF-268
SF-295
SF-539
SNB-19
SNB-75
U251
Melanoma
LOX IMVI
M14
MDA-MB-435
SK-MEL-2
SK-MEL-28
SK-MEL-5
UACC-257
UACC-62
Ovarian Cancer
IGROV1
OVCAR-3
OVCAR-4
OVCAR-5
OVCAR-8
NCI/ADR-RES
SK-OV-3
Renal Cancer
786-0
A498
ACHN
CAKI-1
RXF 393
SN12C
TK-10
UO-31
Prostate Cancer
PC-3
DU-145
Breast Cancer
MCF7
MDA-MB-231/ATCC
HS 578T
BT-549
T-47D
MDA-MB-468
Percentage Growth
Log10 of Sample Concentration (Molar)

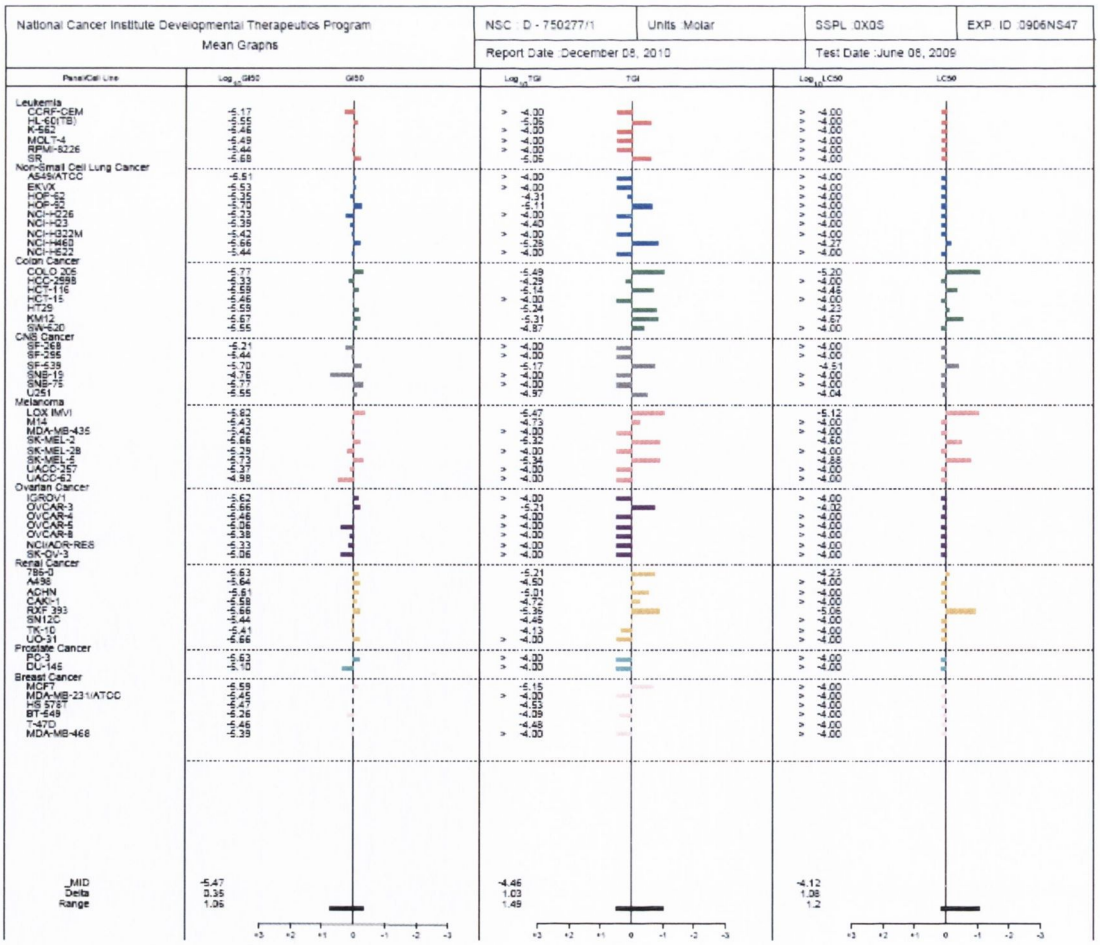
National Cancer Institute Developmental Therapeutics Program
Mean Graphs
NSC : D - 750277/1
Units :Molar
SSPL :0X0S
EXP. ID :0906NS47
Report Date :December 08, 2010
Test Date :June 08, 2009
Panel/Cell Line
Log10 GI50
GI50
Log10 TGI
TGI
Log10 LC50
LC50
Leukemia
CCRF-CEM
HL-60(TB)
K-562
MOLT-4
RPMI-8226
SR
Non-Small Cell Lung Cancer
A549/ATCC
EKVX
HOP-62
HOP-92
NCI-H226
NCI-H23
NCI-H322M
NCI-H460
NCI-H522
Colon Cancer
COLO 205
HCC-2998
HCT-116
HCT-15
HT29
KM12
SW-620
CNS Cancer
SF-268
SF-295
SF-539
SNB-19
SNB-75
U251
Melanoma
LOX IMVI
M14
MDA-MB-435
SK-MEL-2
SK-MEL-28
SK-MEL-5
UACC-257
UACC-62
Ovarian Cancer
IGROV1
OVCAR-3
OVCAR-4
OVCAR-5
OVCAR-8
NCI/ADR-RES
SK-OV-3
Renal Cancer
786-0
A498
ACHN
CAKI-1
RXF 393
SN12C
TK-10
UO-31
Prostate Cancer
PC-3
DU-145
Breast Cancer
MCF7
MDA-MB-231/ATCC
HS 578T
BT-549
T-47D
MDA-MB-468
MID
Delta
Range

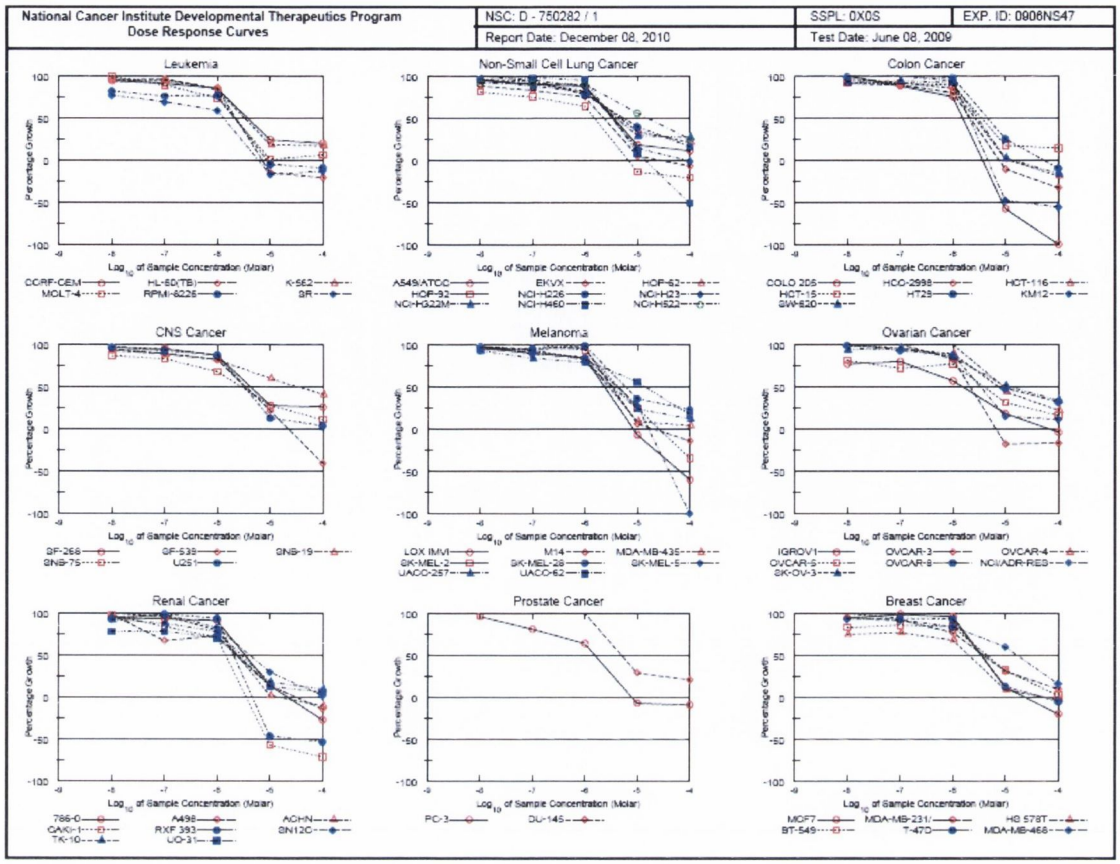
National Cancer Institute Developmental Therapeutics Program
Dose Response Curves
NSC: D - 750282 / 1
Report Date: December 08, 2010
SSPL: 0X0S
Test Date: June 08, 2009
EXP. ID: 0906NS47
Leukemia
Non-Small Cell Lung Cancer
Colon Cancer
CNS Cancer
Melanoma
Ovarian Cancer
Renal Cancer
Prostate Cancer
Breast Cancer
Percentage Growth
Log10 of Sample Concentration (Molar)
CCRF-CEM
HL-60(TB)
K-562
MOLT-4
RPMI-8226
SR
A549/ATCC
EKVX
HOP-62
HOP-92
NCI-H226
NCI-H23
NCI-H322M
NCI-H460
NCI-H522
COLO 205
HCC-2998
HCT-116
HCT-15
HT29
KM12
SW-620
SF-268
SF-539
SNB-19
SNB-75
U251
LOX IMVI
M14
MDA-MB-435
SK-MEL-2
SK-MEL-28
SK-MEL-5
UACC-257
UACC-62
IGROV1
OVCAR-3
OVCAR-4
OVCAR-5
OVCAR-8
NCI/ADR-RES
SK-OV-3
786-0
A498
ACHN
CAKI-1
RXF 393
SN12C
TK-10
UO-31
PC-3
DU-145
MCF7
MDA-MB-231/ATCC
HS 578T
BT-549
T-47D
MDA-MB-468

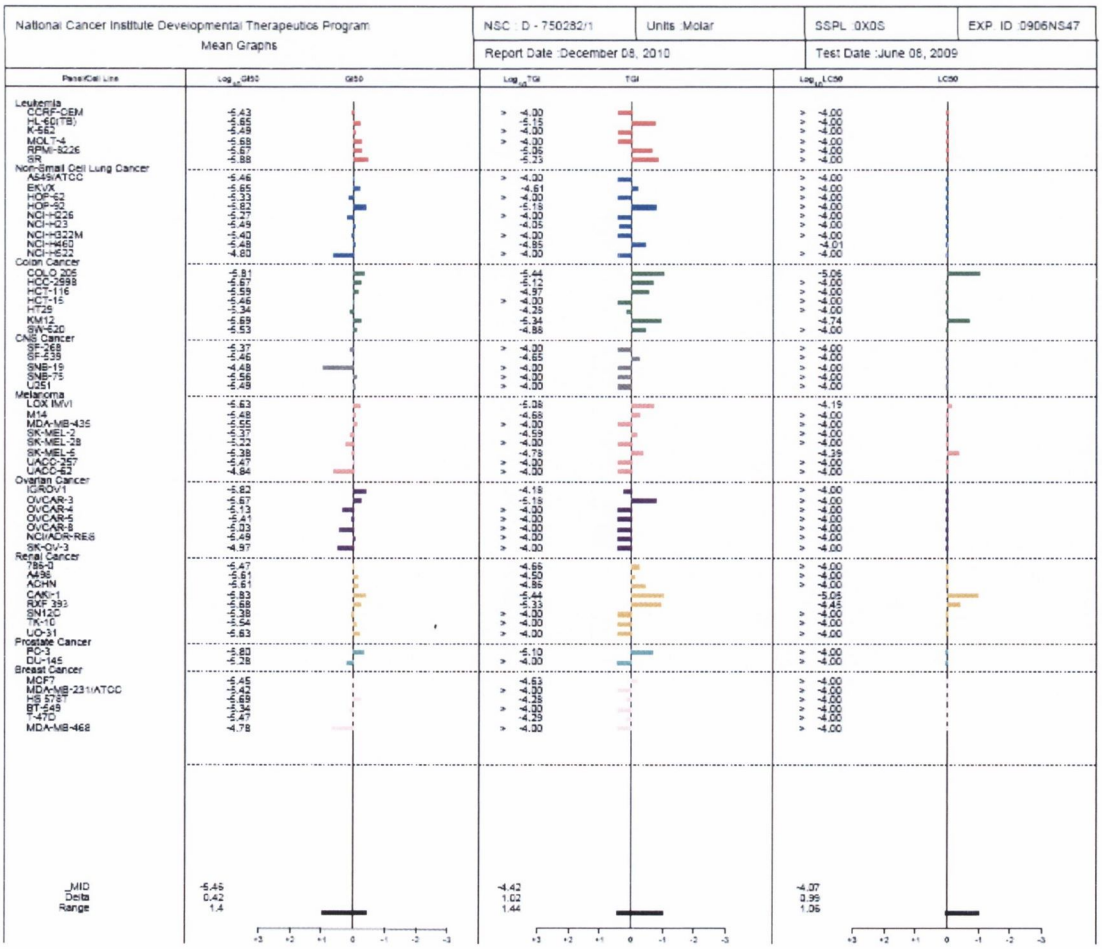
National Cancer Institute Developmental Therapeutics Program
Mean Graphs
NSC : D - 750282/1
Units :Molar
SSPL :0X0S
EXP. ID :0906NS47
Report Date :December 08, 2010
Test Date :June 08, 2009
Panel/Cell Line
Log10GI50
GI50
Log10TGI
TGI
Log10LC50
LC50
Leukemia
CCRF-CEM -5.43 > -4.00 > -4.00
HL-60(TB) -5.65 -5.15 > -4.00
K-562 -5.49 > -4.00 > -4.00
MOLT-4 -5.68 > -4.00 > -4.00
RPMI-8226 -5.67 -5.06 > -4.00
SR -5.88 -5.23 > -4.00
Non-Small Cell Lung Cancer
A549/ATCC -5.46 > -4.00 > -4.00
EKVX -5.65 -4.61 > -4.00
HOP-62 -5.33 > -4.00 > -4.00
HOP-92 -5.82 -5.15 > -4.00
NCI-H226 -5.27 > -4.00 > -4.00
NCI-H23 -5.49 -4.05 > -4.00
NCI-H322M -5.40 > -4.00 > -4.00
NCI-H460 -5.48 -4.85 > -4.01
NCI-H522 -4.80 > -4.00 > -4.00
Colon Cancer
COLO 205 -5.81 -5.44 -5.06
HCC-2998 -5.67 -5.12 > -4.00
HCT-116 -5.59 -4.97 > -4.00
HCT-15 -5.46 > -4.00 > -4.00
HT29 -5.34 -4.25 > -4.00
KM12 -5.69 -5.34 -4.74
SW-620 -5.53 -4.88 > -4.00
CNS Cancer
SF-268 -5.37 > -4.00 > -4.00
SF-539 -5.46 -4.65 > -4.00
SNB-19 -4.48 > -4.00 > -4.00
SNB-75 -5.56 > -4.00 > -4.00
U251 -5.49 > -4.00 > -4.00
Melanoma
LOX IMVI -5.63 -5.08 -4.19
M14 -5.48 -4.68 > -4.00
MDA-MB-435 -5.55 > -4.00 > -4.00
SK-MEL-2 -5.37 -4.59 > -4.00
SK-MEL-28 -5.32 > -4.00 > -4.00
SK-MEL-5 -5.38 -4.78 -4.39
UACC-257 -5.47 > -4.00 > -4.00
UACC-62 -4.84 > -4.00 > -4.00
Ovarian Cancer
IGROV1 -5.82 -4.18 > -4.00
OVCAR-3 -5.67 -5.19 > -4.00
OVCAR-4 -5.13 > -4.00 > -4.00
OVCAR-5 -5.41 > -4.00 > -4.00
OVCAR-8 -5.33 > -4.00 > -4.00
NCI/ADR-RES -5.49 > -4.00 > -4.00
SK-OV-3 -4.97 > -4.00 > -4.00
Renal Cancer
786-0 -5.47 -4.65 > -4.00
A498 -5.61 -4.50 > -4.00
ACHN -5.61 -4.86 > -4.00
CAKI-1 -5.83 -5.44 -5.05
RXF 393 -5.68 -5.33 -4.45
SN12C -5.38 > -4.00 > -4.00
TK-10 -5.54 > -4.00 > -4.00
UO-31 -5.63 > -4.00 > -4.00
Prostate Cancer
PC-3 -5.80 -5.10 > -4.00
DU-145 -5.28 > -4.00 > -4.00
Breast Cancer
MCF7 -5.45 -4.63 > -4.00
MDA-MB-231/ATCC -5.42 > -4.00 > -4.00
HS 578T -5.68 -4.35 > -4.00
BT-549 -5.34 > -4.00 > -4.00
T-47D -5.47 -4.29 > -4.00
MDA-MB-468 -4.78 > -4.00 > -4.00
_MID -5.46 -4.42 -4.07
Delta 0.42 1.02 0.99
Range 1.4 1.44 1.06

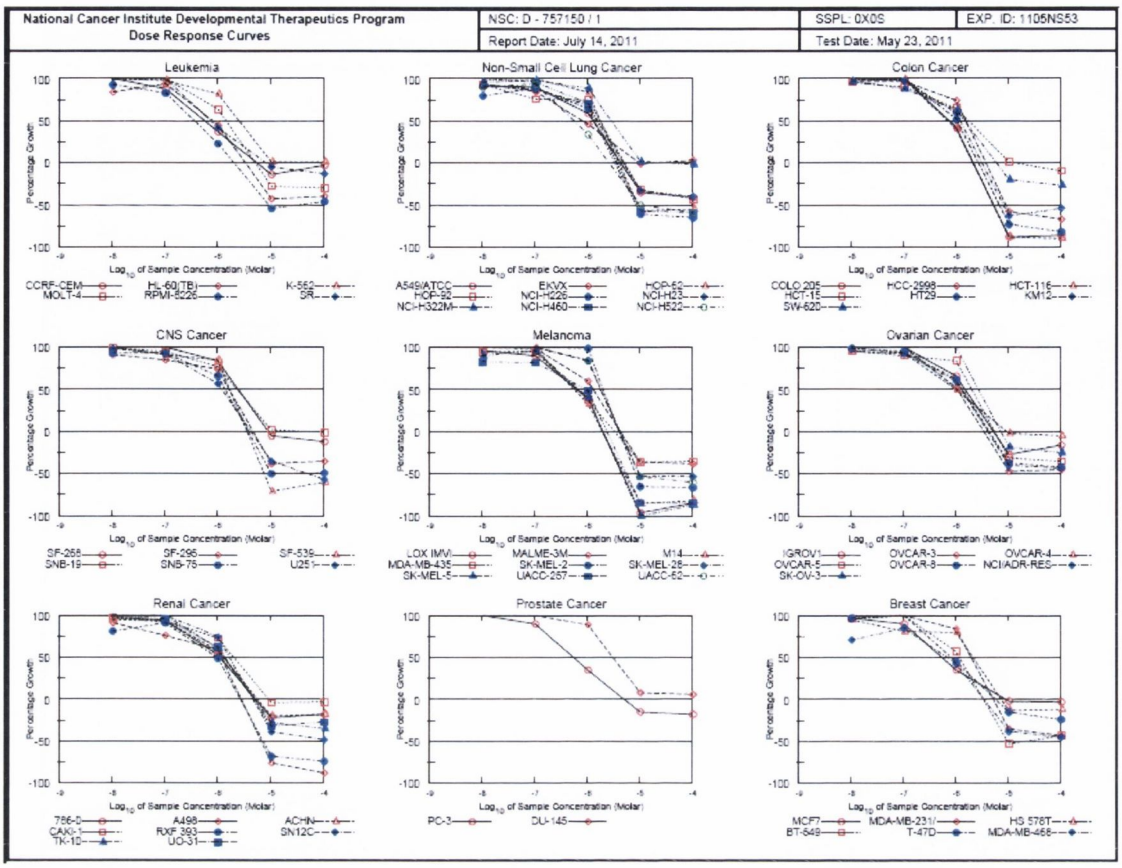
National Cancer Institute Developmental Therapeutics Program
Dose Response Curves
NSC: D - 757150 / 1
Report Date: July 14, 2011
SSPL: 0X0S
Test Date: May 23, 2011
EXP. ID: 1105NS53
Leukemia
CCRF-CEM
HL-60(TB)
K-562
MOLT-4
RPMI-8226
SR
Non-Small Cell Lung Cancer
A549/ATCC
EKVX
HOP-62
HOP-92
NCI-H226
NCI-H23
NCI-H322M
NCI-H460
NCI-H522
Colon Cancer
COLO 205
HCC-2998
HCT-116
HCT-15
HT29
KM12
SW-620
CNS Cancer
SF-268
SF-295
SF-539
SNB-19
SNB-75
U251
Melanoma
LOX IMVI
MALME-3M
M14
MDA-MB-435
SK-MEL-2
SK-MEL-28
SK-MEL-5
UACC-257
UACC-62
Ovarian Cancer
IGROV1
OVCAR-3
OVCAR-4
OVCAR-5
OVCAR-8
NCI/ADR-RES
SK-OV-3
Renal Cancer
786-0
A498
ACHN
CAKI-1
RXF 393
SN12C
TK-10
UO-31
Prostate Cancer
PC-3
DU-145
Breast Cancer
MCF7
MDA-MB-231/ATCC
HS 578T
BT-549
T-47D
MDA-MB-468
Percentage Growth
Log10 of Sample Concentration (Molar)

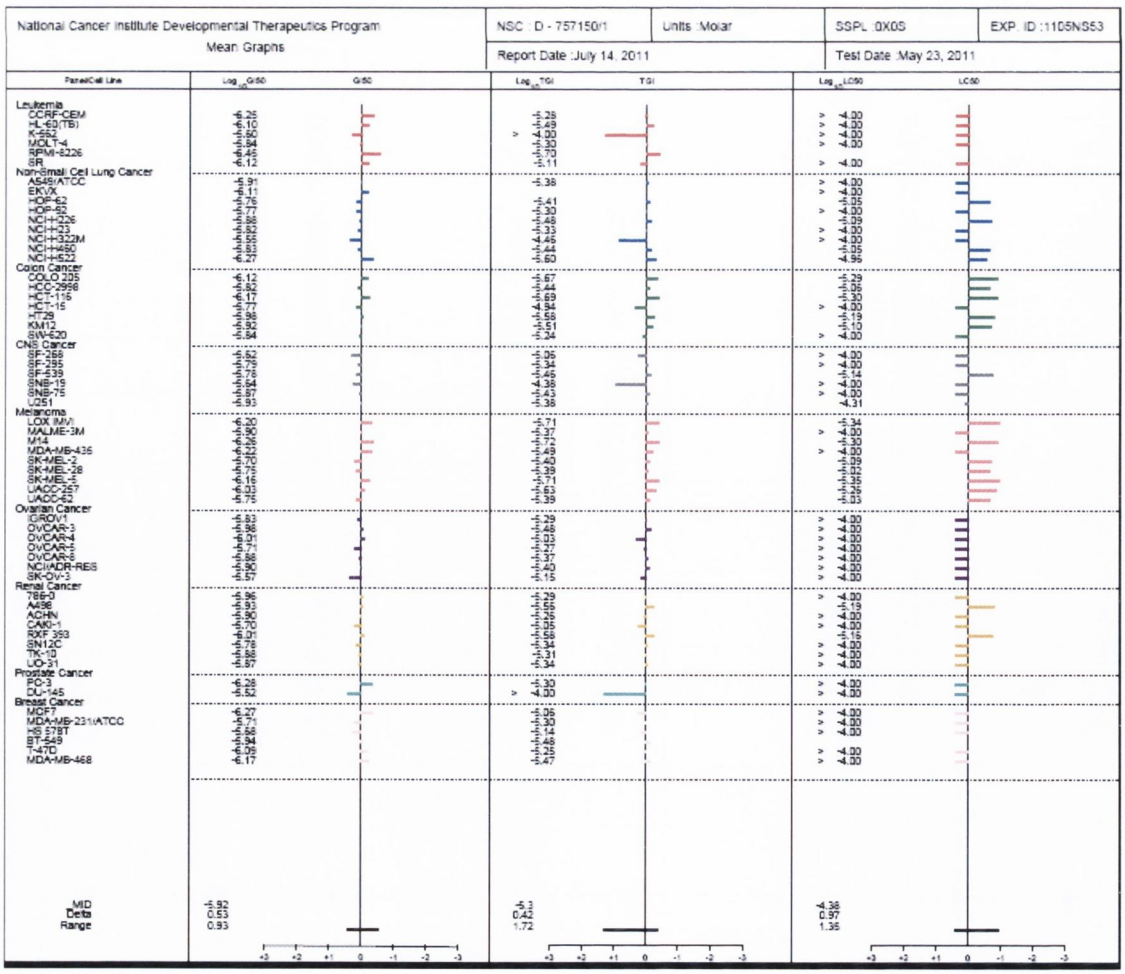
National Cancer Institute Developmental Therapeutics Program
Mean Graphs
NSC : D - 757150/1
Units :Molar
SSPL :0X0S
EXP. ID :1105NS53
Report Date :July 14, 2011
Test Date :May 23, 2011
Panel/Cell Line
Log10 GI50
GI50
Log10 TGI
TGI
Log10 LC50
LC50
Leukemia
CCRF-CEM
HL-60(TB)
K-562
MOLT-4
RPMI-8226
SR
Non-Small Cell Lung Cancer
A549/ATCC
EKVX
HOP-62
HOP-92
NCI-H226
NCI-H23
NCI-H322M
NCI-H460
NCI-H522
Colon Cancer
COLO 205
HCC-2998
HCT-116
HCT-15
HT29
KM12
SW-620
CNS Cancer
SF-268
SF-295
SF-539
SNB-19
SNB-75
U251
Melanoma
LOX IMVI
MALME-3M
M14
MDA-MB-435
SK-MEL-2
SK-MEL-28
SK-MEL-5
UACC-257
UACC-62
Ovarian Cancer
IGROV1
OVCAR-3
OVCAR-4
OVCAR-5
OVCAR-8
NCI/ADR-RES
SK-OV-3
Renal Cancer
786-0
A498
ACHN
CAKI-1
RXF 393
SN12C
TK-10
UO-31
Prostate Cancer
PC-3
DU-145
Breast Cancer
MCF7
MDA-MB-231/ATCC
HS 578T
BT-549
T-47D
MDA-MB-468
MID
Delta
Range
-5.92
0.53
0.93
-5.3
0.42
1.72
-4.38
0.97
1.35

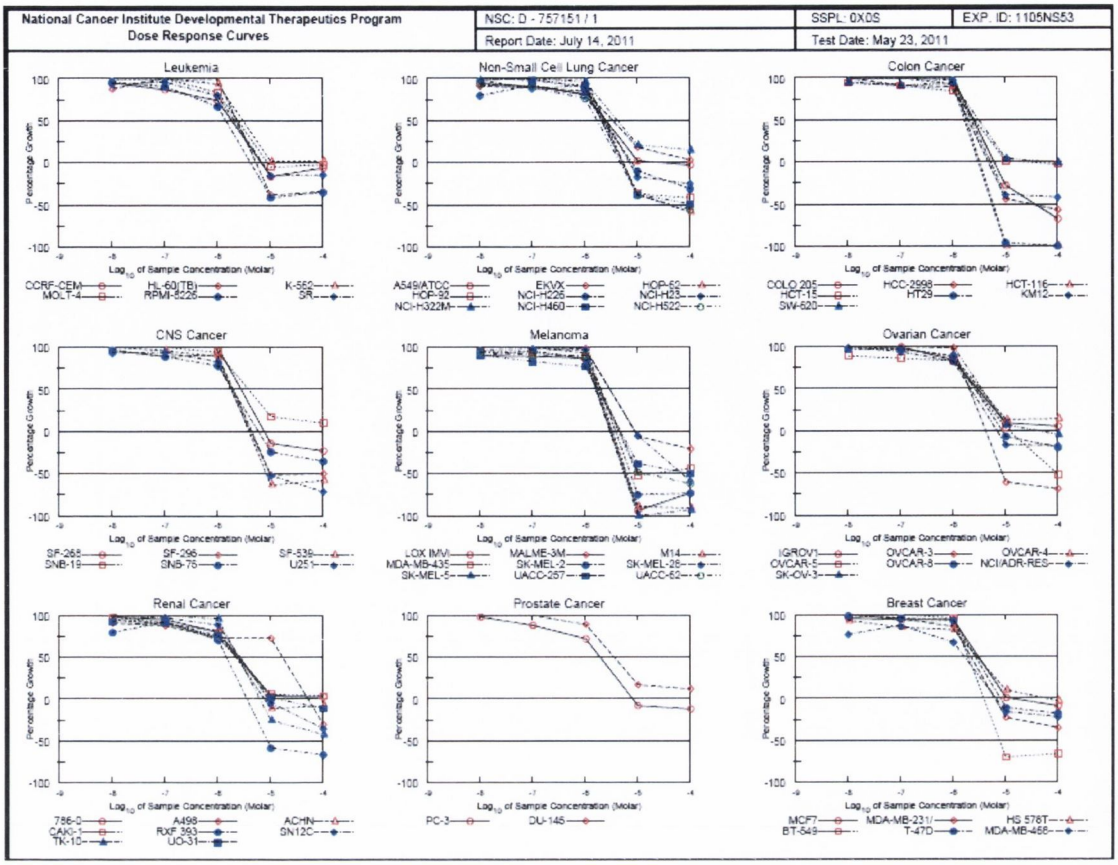
National Cancer Institute Developmental Therapeutics Program
Dose Response Curves
NSC: D - 757151 / 1
Report Date: July 14, 2011
SSPL: 0X0S
Test Date: May 23, 2011
EXP. ID: 1105NS53
Leukemia
CCRF-CEM
HL-60(TB)
K-562
MOLT-4
RPMI-8226
SR
Non-Small Cell Lung Cancer
A549/ATCC
EKVX
HOP-62
HOP-92
NCI-H226
NCI-H23
NCI-H322M
NCI-H460
NCI-H522
Colon Cancer
COLO 205
HCC-2998
HCT-116
HCT-15
HT29
KM12
SW-620
CNS Cancer
SF-268
SF-295
SF-539
SNB-19
SNB-75
U251
Melanoma
LOX IMVI
MALME-3M
M14
MDA-MB-435
SK-MEL-2
SK-MEL-28
SK-MEL-5
UACC-257
UACC-62
Ovarian Cancer
IGROV1
OVCAR-3
OVCAR-4
OVCAR-5
OVCAR-8
NCI/ADR-RES
SK-OV-3
Renal Cancer
786-0
A498
ACHN
CAKI-1
RXF 393
SN12C
TK-10
UO-31
Prostate Cancer
PC-3
DU-145
Breast Cancer
MCF7
MDA-MB-231/ATCC
HS 578T
BT-549
T-47D
MDA-MB-468
Percentage Growth
Log10 of Sample Concentration (Molar)

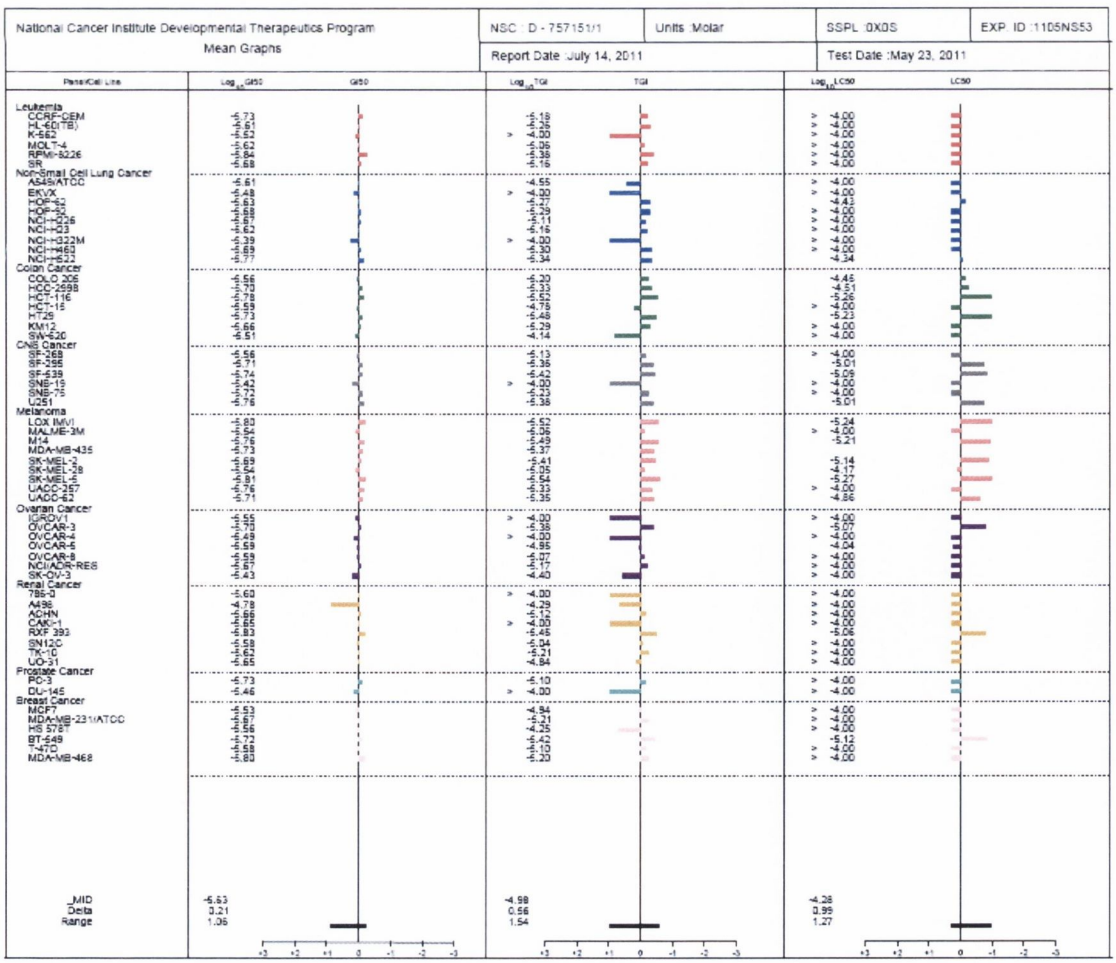
National Cancer Institute Developmental Therapeutics Program
Mean Graphs
NSC : D - 757151/1
Units :Molar
SSPL :0X0S
EXP. ID :1105NS53
Report Date :July 14, 2011
Test Date :May 23, 2011
Panel/Cell Line
Log10GI50
GI50
Log10TGI
TGI
Log10LC50
LC50
Leukemia
CCRF-CEM
HL-60(TB)
K-562
MOLT-4
RPMI-8226
SR
Non-Small Cell Lung Cancer
A549/ATCC
EKVX
HOP-62
HOP-92
NCI-H226
NCI-H23
NCI-H322M
NCI-H460
NCI-H522
Colon Cancer
COLO 205
HCC-2998
HCT-116
HCT-15
HT29
KM12
SW-620
CNS Cancer
SF-268
SF-295
SF-539
SNB-19
SNB-75
U251
Melanoma
LOX IMVI
MALME-3M
M14
MDA-MB-435
SK-MEL-2
SK-MEL-28
SK-MEL-5
UACC-257
UACC-62
Ovarian Cancer
IGROV1
OVCAR-3
OVCAR-4
OVCAR-5
OVCAR-8
NCI/ADR-RES
SK-OV-3
Renal Cancer
786-0
A498
ACHN
CAKI-1
RXF 393
SN12C
TK-10
UO-31
Prostate Cancer
PC-3
DU-145
Breast Cancer
MCF7
MDA-MB-231/ATCC
HS 578T
BT-549
T-47D
MDA-MB-468
MID
Delta
Range
-5.53
3.21
1.06
-4.98
0.56
1.54
-4.28
0.99
1.27

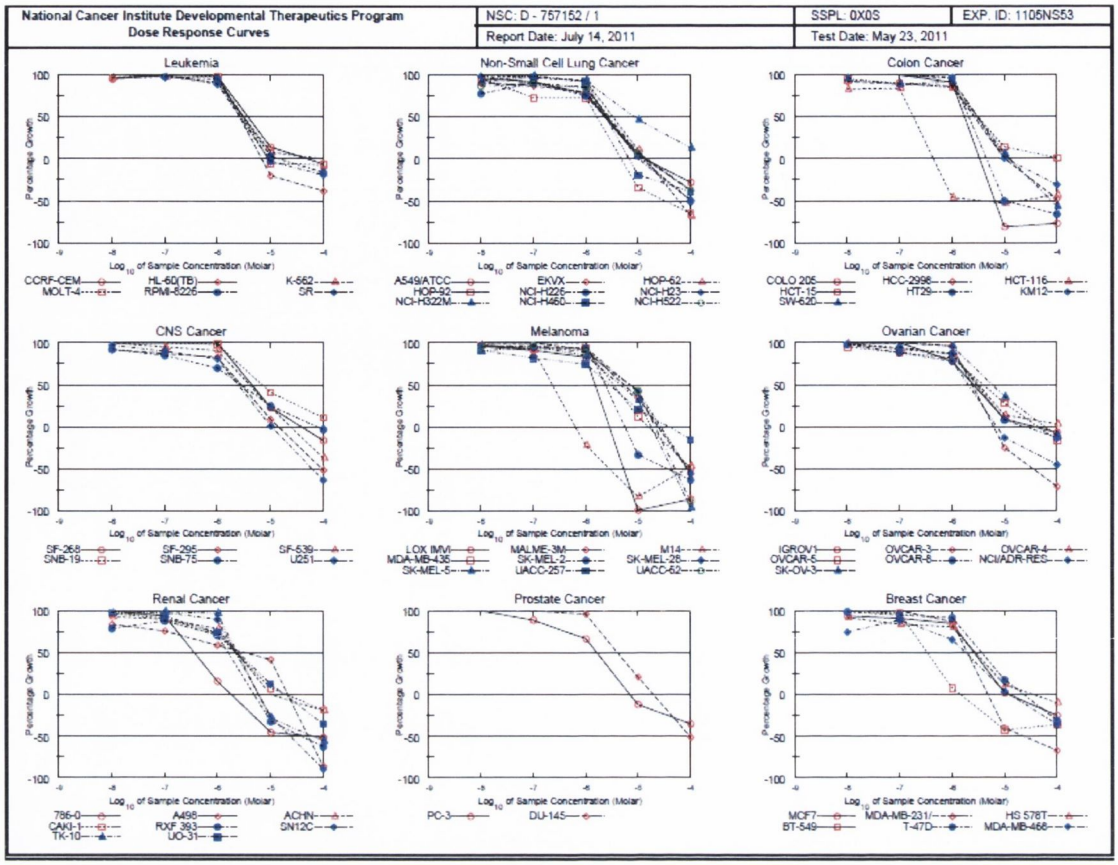
National Cancer Institute Developmental Therapeutics Program
Dose Response Curves
NSC: D - 757152 / 1
Report Date: July 14, 2011
SSPL: 0X0S
Test Date: May 23, 2011
EXP. ID: 1105NS53
Leukemia
CCRF-CEM
HL-60(TB)
K-562
MOLT-4
RPMI-8226
SR
Non-Small Cell Lung Cancer
A549/ATCC
EKVX
HOP-62
HOP-92
NCI-H226
NCI-H23
NCI-H322M
NCI-H460
NCI-H522
Colon Cancer
COLO 205
HCC-2998
HCT-116
HCT-15
HT29
KM12
SW-620
CNS Cancer
SF-268
SF-295
SF-539
SNB-19
SNB-75
U251
Melanoma
LOX IMVI
MALME-3M
M14
MDA-MB-435
SK-MEL-2
SK-MEL-28
SK-MEL-5
UACC-257
UACC-62
Ovarian Cancer
IGROV1
OVCAR-3
OVCAR-4
OVCAR-5
OVCAR-8
NCI/ADR-RES
SK-OV-3
Renal Cancer
786-0
A498
ACHN
CAKI-1
RXF 393
SN12C
TK-10
UO-31
Prostate Cancer
PC-3
DU-145
Breast Cancer
MCF7
MDA-MB-231/ATCC
HS 578T
BT-549
T-47D
MDA-MB-468
Percentage Growth
Log10 of Sample Concentration (Molar)

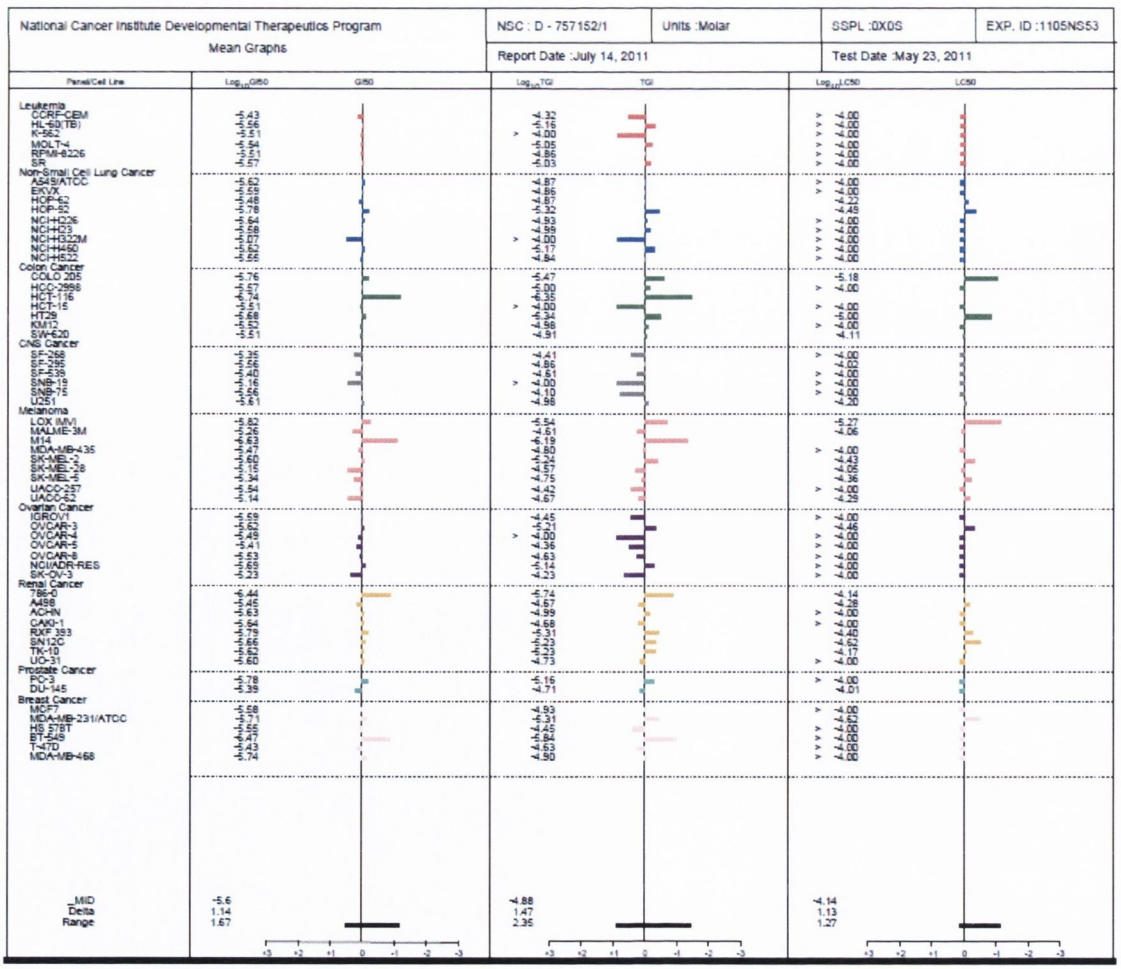
National Cancer Institute Developmental Therapeutics Program
Mean Graphs
NSC : D - 757152/1
Units :Molar
SSPL :0X0S
EXP. ID :1105NS53
Report Date :July 14, 2011
Test Date :May 23, 2011
Panel/Cell Line
Log10GI50
GI50
Log10TGI
TGI
Log10LC50
LC50
MID
Delta
Range

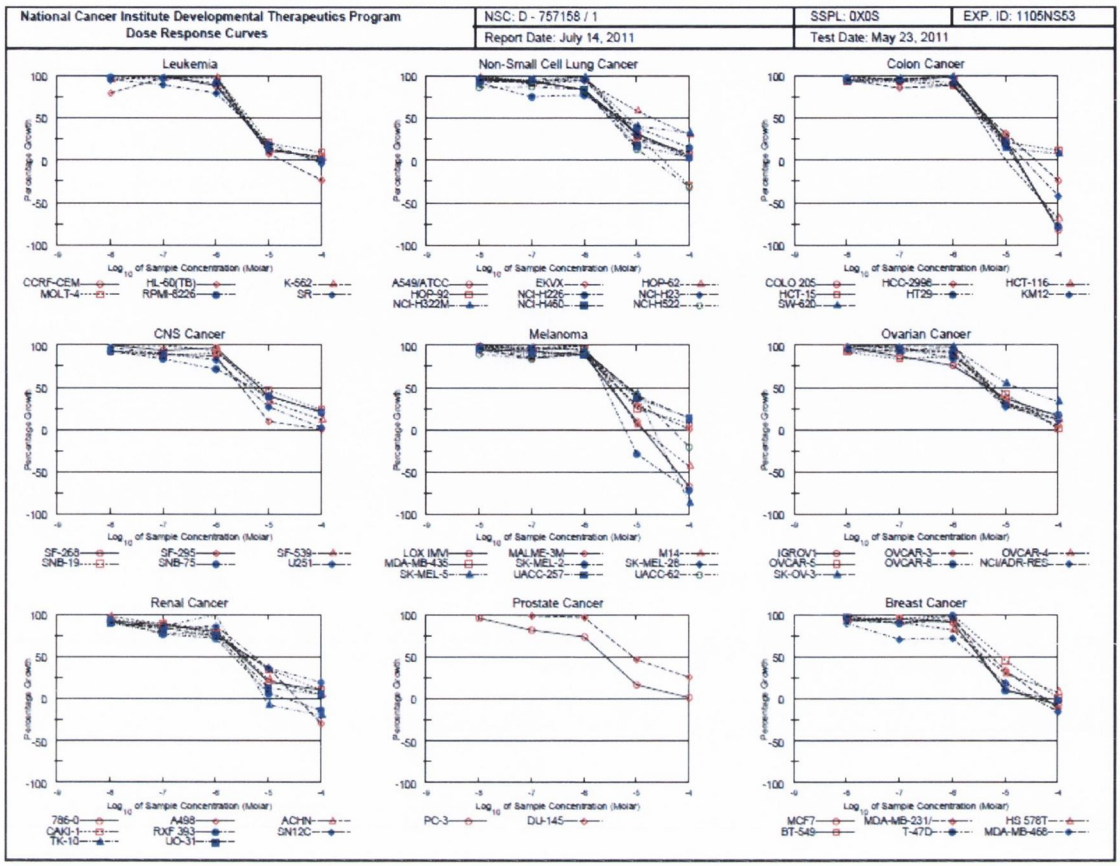
National Cancer Institute Developmental Therapeutics Program
Dose Response Curves
NSC: D - 757158 / 1
Report Date: July 14, 2011
SSPL: 0X0S
Test Date: May 23, 2011
EXP. ID: 1105NS53
Leukemia
CCRF-CEM
HL-60(TB)
K-562
MOLT-4
RPMI-8226
SR
Non-Small Cell Lung Cancer
A549/ATCC
EKVX
HOP-62
HOP-92
NCI-H226
NCI-H23
NCI-H322M
NCI-H460
NCI-H522
Colon Cancer
COLO 205
HCC-2998
HCT-116
HCT-15
HT29
KM12
SW-620
CNS Cancer
SF-268
SF-295
SF-539
SNB-19
SNB-75
U251
Melanoma
LOX IMVI
MALME-3M
M14
MDA-MB-435
SK-MEL-2
SK-MEL-28
SK-MEL-5
UACC-257
UACC-62
Ovarian Cancer
IGROV1
OVCAR-3
OVCAR-4
OVCAR-5
OVCAR-8
NCI/ADR-RES
SK-OV-3
Renal Cancer
786-0
A498
ACHN
CAKI-1
RXF 393
SN12C
TK-10
UO-31
Prostate Cancer
PC-3
DU-145
Breast Cancer
MCF7
MDA-MB-231/ATCC
HS 578T
BT-549
T-47D
MDA-MB-468
Percentage Growth
Log10 of Sample Concentration (Molar)

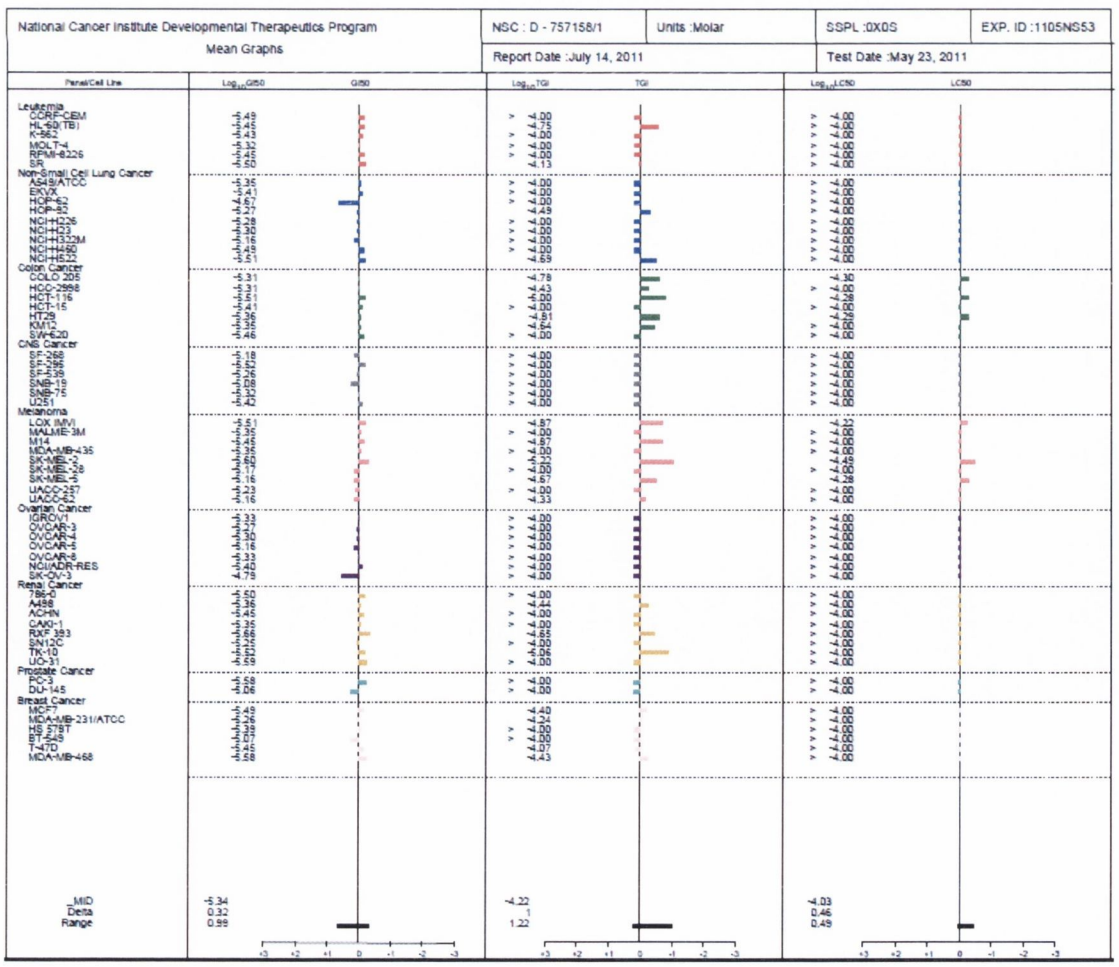
National Cancer Institute Developmental Therapeutics Program
Mean Graphs
NSC : D - 757158/1
Units :Molar
SSPL :0X0S
EXP. ID :1105NS53
Report Date :July 14, 2011
Test Date :May 23, 2011
Panel/Cell Line
GI50
TGI
LC50
MID
Delta
Range

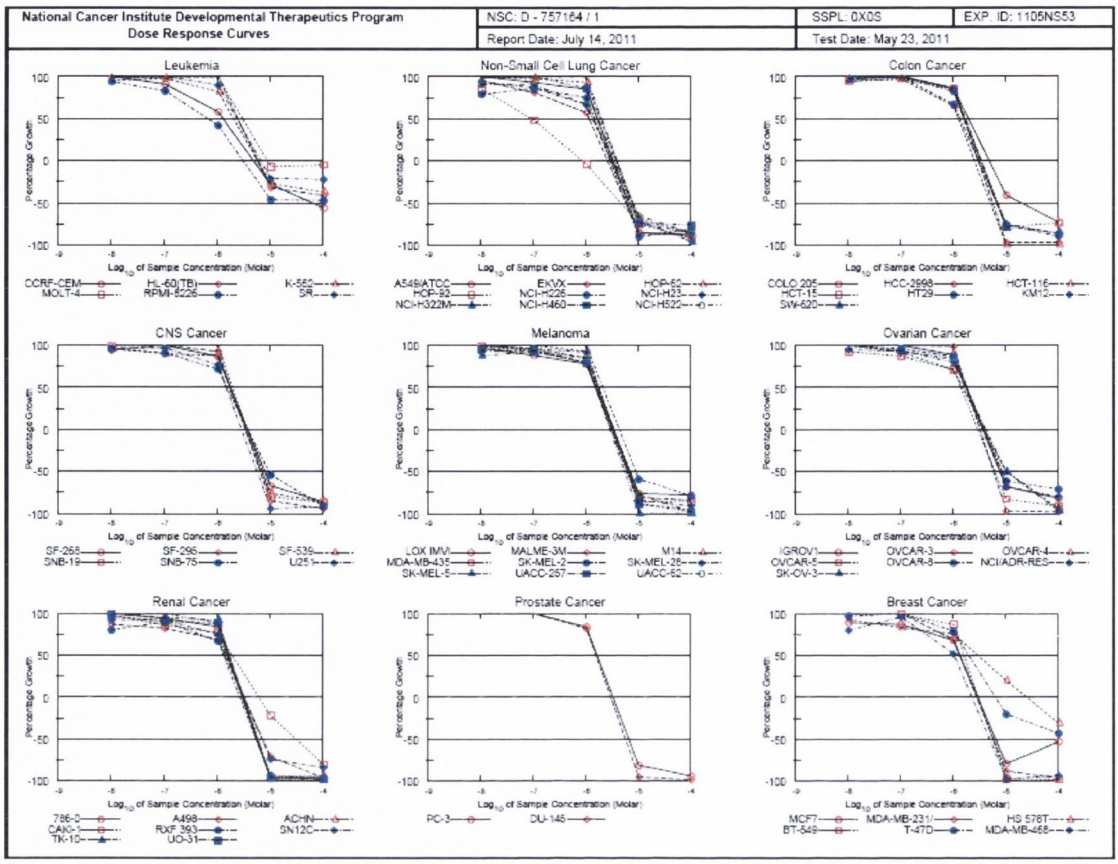
National Cancer Institute Developmental Therapeutics Program
Dose Response Curves
NSC: D - 757164 / 1
Report Date: July 14, 2011
SSPL: 0X0S
EXP. ID: 1105NS53
Test Date: May 23, 2011
Leukemia
CCRF-CEM
HL-60(TB)
K-562
MOLT-4
RPMI-8226
SR
Non-Small Cell Lung Cancer
A549/ATCC
EKVX
HOP-62
HOP-92
NCI-H226
NCI-H23
NCI-H322M
NCI-H460
NCI-H522
Colon Cancer
COLO 205
HCC-2998
HCT-116
HCT-15
HT29
KM12
SW-620
CNS Cancer
SF-268
SF-295
SF-539
SNB-19
SNB-75
U251
Melanoma
LOX IMVI
MALME-3M
M14
MDA-MB-435
SK-MEL-2
SK-MEL-28
SK-MEL-5
UACC-257
UACC-62
Ovarian Cancer
IGROV1
OVCAR-3
OVCAR-4
OVCAR-5
OVCAR-8
NCI/ADR-RES
SK-OV-3
Renal Cancer
786-0
A498
ACHN
CAKI-1
RXF 393
SN12C
TK-10
UO-31
Prostate Cancer
PC-3
DU-145
Breast Cancer
MCF7
MDA-MB-231/ATCC
HS 578T
BT-549
T-47D
MDA-MB-468
Percentage Growth
Log10 of Sample Concentration (Molar)

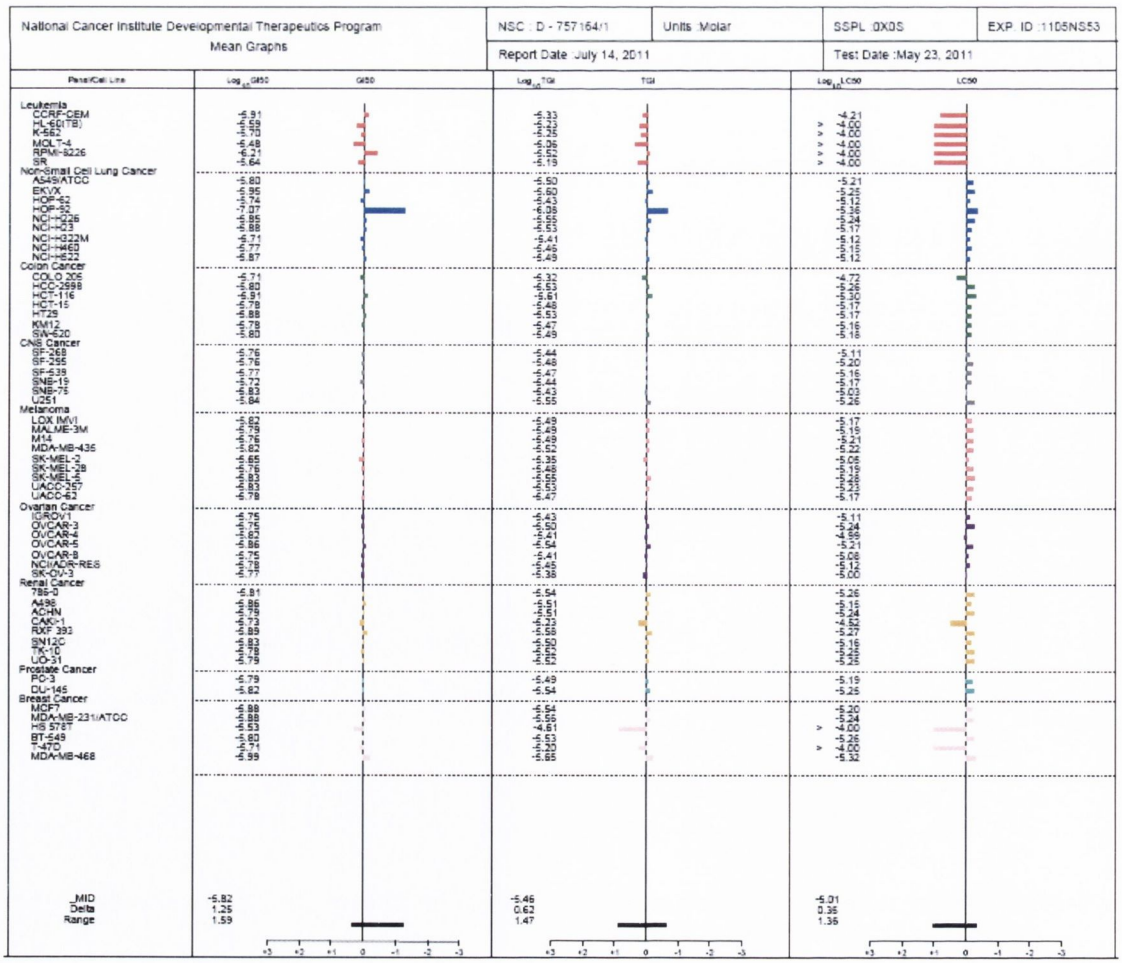
National Cancer Institute Developmental Therapeutics Program
Mean Graphs
NSC : D - 757164/1
Units :Molar
SSPL :0X0S
EXP. ID :1105NS53
Report Date :July 14, 2011
Test Date :May 23, 2011
Panel/Cell Line
Log10 GI50
GI50
Log10 TGI
TGI
Log10 LC50
LC50
Leukemia
CCRF-CEM -5.91 -4.21
HL-60(TB) -5.59 > -4.00
K-562 -5.70 > -4.00
MOLT-4 -6.48 > -4.00
RPMI-8226 -6.21 > -4.00
SR -5.64 > -4.00
Non-Small Cell Lung Cancer
A549/ATCC -5.80 -5.21
EKVX -5.95 -5.25
HOP-62 -5.74 -5.12
HOP-92 -7.07 -5.36
NCI-H226 -5.85 -5.24
NCI-H23 -5.88 -5.17
NCI-H322M -5.71 -5.12
NCI-H460 -5.77 -5.15
NCI-H522 -5.87 -5.12
Colon Cancer
COLO 205 -5.71 -4.72
HCC-2998 -5.80 -5.26
HCT-116 -5.91 -5.30
HCT-15 -5.78 -5.17
HT29 -5.88 -5.17
KM12 -5.78 -5.18
SW-620 -5.83 -5.18
CNS Cancer
SF-268 -5.76 -5.11
SF-295 -5.78 -5.20
SF-539 -5.77 -5.16
SNB-19 -5.72 -5.17
SNB-75 -5.83 -5.03
U251 -5.84 -5.26
Melanoma
LOX IMVI -5.82 -5.17
MALME-3M -5.79 -5.19
M14 -5.76 -5.21
MDA-MB-435 -5.82 -5.22
SK-MEL-2 -5.65 -5.06
SK-MEL-28 -5.76 -5.19
SK-MEL-5 -5.83 -5.24
UACC-257 -5.83 -5.23
UACC-62 -5.78 -5.17
Ovarian Cancer
IGROV1 -5.75 -5.11
OVCAR-3 -5.75 -5.24
OVCAR-4 -5.82 -4.58
OVCAR-5 -5.86 -5.21
OVCAR-8 -5.75 -5.06
NCI/ADR-RES -5.78 -5.12
SK-OV-3 -5.77 -5.00
Renal Cancer
786-0 -5.81 -5.26
A498 -5.86 -5.15
ACHN -5.79 -5.24
CAKI-1 -5.73 -4.50
RXF 393 -5.89 -5.27
SN12C -5.83 -5.16
TK-10 -5.78 -5.25
UO-31 -5.79 -5.25
Prostate Cancer
PC-3 -5.79 -5.19
DU-145 -5.82 -5.25
Breast Cancer
MCF7 -5.88 -5.20
MDA-MB-231/ATCC -5.88 -5.24
HS 578T -5.53 > -4.00
BT-549 -5.80 > -5.26
T-47D -5.71 > -4.00
MDA-MB-468 -5.99 -5.32
MID -5.82 -5.46 -5.31
Delta 1.25 0.62 0.36
Range 1.59 1.47 1.36

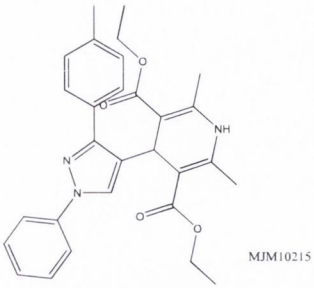

MJM10215

Chemical Formula: $C_{29}H_{31}N_3O_4$
Exact Mass: 485.2315
Molecular Weight: 485.5741
m/z: 485.2315 (100.0%), 486.2348 (31.4%), 487.2382 (4.7%), 486.2285 (1.1%)
Elemental Analysis: C, 71.73; H, 6.43; N, 8.65; O, 13.18

Developmental Therapeutics Program

One Dose Mean Graph

NSC: D-750280 / 1	Conc: 1.00E-5 Molar	Test Date: May 04, 2009
Experiment ID: 0905OS13		Report Date: Dec 08, 2010

Panel/Cell Line	Growth Percent
Leukemia	
CCRF-CEM	78.42
HL-60(TB)	86.75
K-562	78.35
MOLT-4	55.23
RPMI-8226	50.88
SR	55.33
Non-Small Cell Lung Cancer	
A549/ATCC	62.94
EKVX	40.07
HOP-62	86.03
NCI-H226	88.93
NCI-H23	71.21
NCI-H322M	76.35
NCI-H460	52.16
NCI-H522	68.78
Colon Cancer	
COLO 205	69.35
HCC-2998	63.81
HCT-116	42.26
HCT-15	74.67
HT29	55.24
KM12	59.35
SW-620	84.89
CNS Cancer	
SF-268	65.48
SF-295	74.43
SF-539	61.87
SNB-19	80.36
SNB-75	66.84
U251	71.26
Melanoma	
LOX IMVI	66.72
MALME-3M	87.14
M14	75.25
MDA-MB-435	81.49
SK-MEL-2	98.33
SK-MEL-28	100.48
SK-MEL-5	74.64
UACC-257	82.64
UACC-62	93.84
Ovarian Cancer	
IGROV1	70.42
OVCAR-3	70.28
OVCAR-4	75.58
OVCAR-5	68.24
OVCAR-8	74.37
NCI/ADR-RES	62.93
SK-OV-3	83.94
Renal Cancer	
786-0	65.50
ACHN	70.71
CAKI-1	36.67
RXF 393	59.91
SN12C	72.87
TK-10	110.46
UO-31	48.11
Prostate Cancer	
PC-3	29.20
DU-145	92.69
Breast Cancer	
MCF7	50.31
MDA-MB-231/ATCC	57.83
HS 578T	46.69
BT-549	85.79
T-47D	32.42
MDA-MB-468	74.58
Mean	69.33
Delta	40.13
Range	81.26

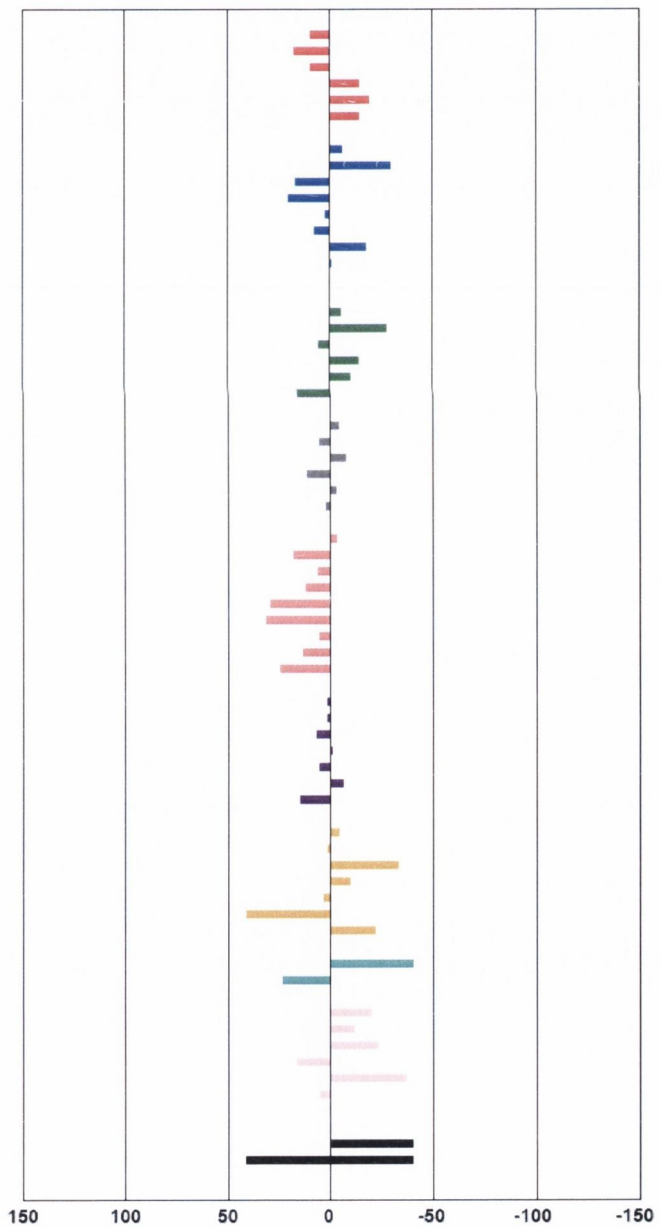

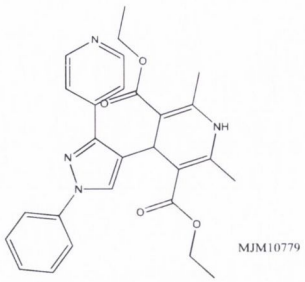

Chemical Formula: $C_{27}H_{28}N_4O_4$
Exact Mass: 472.2111
Molecular Weight: 472.5356
m/z: 472.2111 (100.0%), 473.2144 (29.2%), 474.2178 (4.1%), 473.2081 (1.5%)
Elemental Analysis: C, 68.63; H, 5.97; N, 11.86; O, 13.54

Developmental Therapeutics Program

One Dose Mean Graph

NSC: D-750279 / 1	Conc: 1.00E-5 Molar	Test Date: May 04, 2009
Experiment ID: 0905OS13		Report Date: Dec 08, 2010

Panel/Cell Line	Growth Percent
Leukemia	
CCRF-CEM	77.86
HL-60(TB)	78.19
K-562	111.70
MOLT-4	70.80
RPMI-8226	72.78
SR	80.74
Non-Small Cell Lung Cancer	
A549/ATCC	82.93
EKVX	62.92
HOP-62	80.71
NCI-H226	101.18
NCI-H23	83.78
NCI-H322M	98.14
NCI-H460	88.82
NCI-H522	76.07
Colon Cancer	
COLO 205	92.08
HCC-2998	91.22
HCT-116	74.88
HCT-15	96.19
HT29	78.02
KM12	89.02
SW-620	95.78
CNS Cancer	
SF-268	79.14
SF-295	80.04
SF-539	80.32
SNB-19	84.59
SNB-75	69.17
U251	98.17
Melanoma	
LOX IMVI	93.08
MALME-3M	75.68
M14	99.45
MDA-MB-435	94.07
SK-MEL-2	93.63
SK-MEL-28	112.56
SK-MEL-5	86.83
UACC-257	94.18
UACC-62	78.50
Ovarian Cancer	
IGROV1	62.87
OVCAR-3	79.02
OVCAR-4	73.61
OVCAR-5	85.66
OVCAR-8	86.12
NCI/ADR-RES	79.74
SK-OV-3	90.59
Renal Cancer	
786-0	86.26
ACHN	87.80
CAKI-1	64.56
RXF 393	91.34
SN12C	90.50
TK-10	105.39
UO-31	73.47
Prostate Cancer	
PC-3	52.49
DU-145	97.39
Breast Cancer	
MCF7	90.86
MDA-MB-231/ATCC	77.63
HS 578T	69.01
BT-549	87.18
T-47D	79.20
MDA-MB-468	60.91
Mean	84.05
Delta	31.56
Range	60.07

Mean Growth Percent - Growth Percent

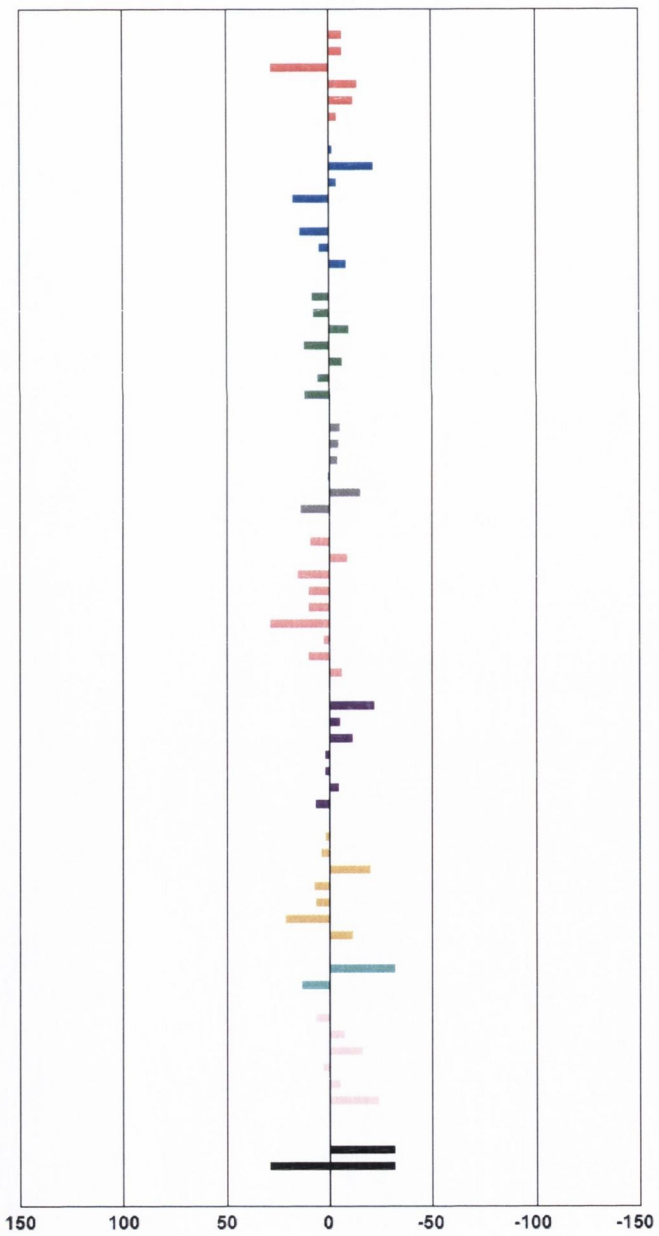

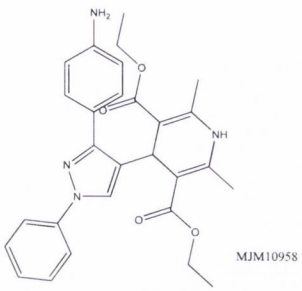

MJM10958

Chemical Formula: $C_{28}H_{30}N_4O_4$
Exact Mass: 486.2267
Molecular Weight: 486.5622
m/z: 486.2267 (100.0%), 487.2301 (30.3%), 488.2334 (4.4%), 487.2237 (1.5%)
Elemental Analysis: C, 69.12; H, 6.21; N, 11.51; O, 13.15

Developmental Therapeutics Program	NSC: D-750278 / 1	Conc: 1.00E-5 Molar	Test Date: May 04, 2009
One Dose Mean Graph	Experiment ID: 0905OS13		Report Date: Dec 08, 2010

Panel/Cell Line	Growth Percent
Leukemia	
CCRF-CEM	94.02
HL-60(TB)	66.71
K-562	92.69
MOLT-4	60.71
RPMI-8226	58.82
SR	111.72
Non-Small Cell Lung Cancer	
A549/ATCC	95.67
EKVX	76.22
HOP-62	86.47
HOP-92	38.44
NCI-H226	94.84
NCI-H23	86.02
NCI-H322M	108.72
NCI-H460	89.00
NCI-H522	81.36
Colon Cancer	
COLO 205	58.97
HCC-2998	81.12
HCT-116	77.60
HCT-15	95.92
HT29	88.03
KM12	98.86
SW-620	111.04
CNS Cancer	
SF-268	89.39
SF-295	96.00
SF-539	81.24
SNB-19	72.76
SNB-75	65.36
U251	86.66
Melanoma	
LOX IMVI	84.31
MALME-3M	72.38
M14	94.16
MDA-MB-435	100.37
SK-MEL-2	99.60
SK-MEL-28	105.86
SK-MEL-5	69.96
UACC-257	95.17
UACC-62	81.19
Ovarian Cancer	
IGROV1	74.99
OVCAR-3	88.26
OVCAR-4	72.87
OVCAR-5	87.57
OVCAR-8	84.49
NCI/ADR-RES	76.30
SK-OV-3	83.24
Renal Cancer	
786-0	78.87
ACHN	85.12
CAKI-1	80.53
RXF 393	98.48
SN12C	89.98
TK-10	121.25
UO-31	70.49
Prostate Cancer	
PC-3	55.75
DU-145	94.61
Breast Cancer	
MCF7	65.46
MDA-MB-231/ATCC	66.76
HS 578T	83.37
BT-549	77.11
T-47D	57.02
MDA-MB-468	71.42
Mean	83.24
Delta	44.80
Range	82.81

Mean Growth Percent - Growth Percent

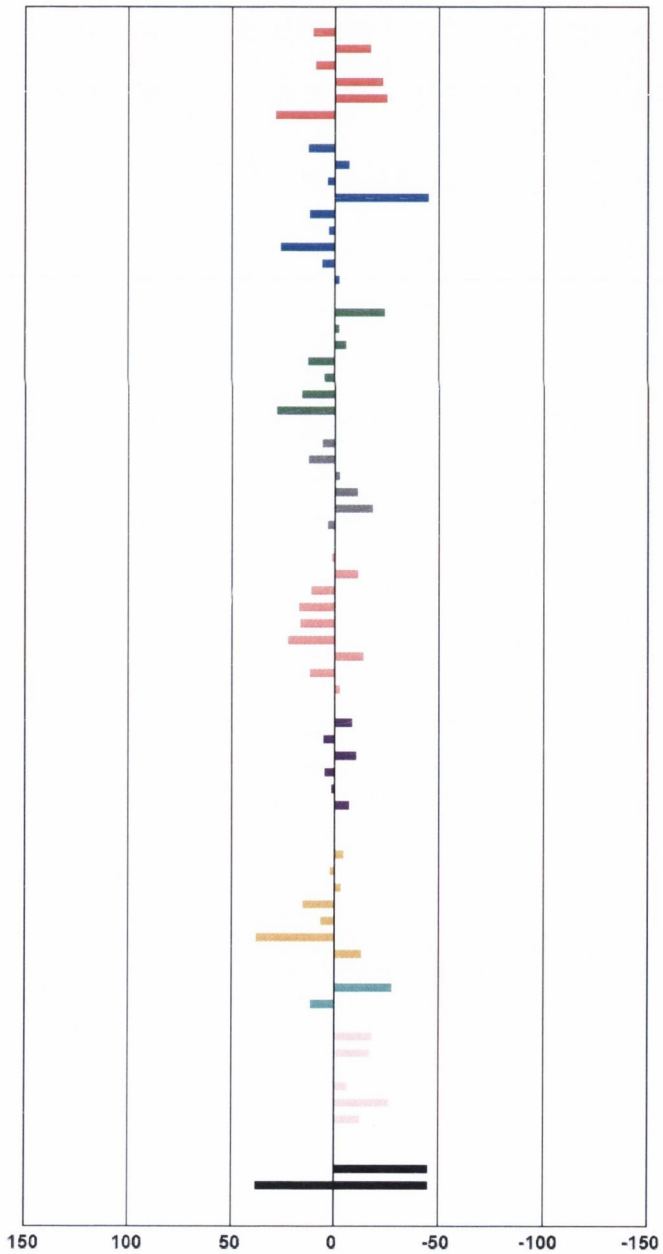

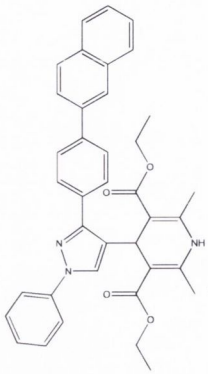

diethyl 2,6-dimethyl-4-(3-(4-(naphthalen-2-yl)phenyl)-1-phenyl-1*H*-pyrazol-4-yl)-1,4-dihydropyridine-3,5-dicarboxylate

Chemical Formula: $C_{38}H_{33}N_3O_4$
Molecular Weight: 597.7022
Elemental Analysis: C, 76.36; H, 5.90; N, 7.03; O, 10.71

Developmental Therapeutics Program	NSC: D-757153 / 1	Conc: 1.00E-5 Molar	Test Date: Apr 11, 2011
One Dose Mean Graph	Experiment ID: 1104OS33		Report Date: May 10, 2011

Panel/Cell Line	Growth Percent
Leukemia	
CCRF-CEM	46.72
HL-60(TB)	96.47
K-562	47.00
MOLT-4	50.59
RPMI-8226	64.82
Non-Small Cell Lung Cancer	
A549/ATCC	78.70
EKVX	61.62
HOP-62	97.95
HOP-92	50.01
NCI-H226	106.47
NCI-H23	87.99
NCI-H322M	80.79
NCI-H460	41.07
NCI-H522	66.76
Colon Cancer	
COLO 205	97.76
HCC-2998	75.58
HCT-116	67.48
HCT-15	92.40
HT29	67.31
KM12	52.33
SW-620	86.14
CNS Cancer	
SF-268	72.50
SF-295	93.61
SF-539	98.90
SNB-19	109.96
SNB-75	62.82
U251	76.30
Melanoma	
LOX IMVI	51.38
MALME-3M	136.61
M14	91.86
MDA-MB-435	91.93
SK-MEL-28	109.72
SK-MEL-5	104.33
UACC-257	94.68
UACC-62	109.26
Ovarian Cancer	
IGROV1	76.58
OVCAR-3	92.25
OVCAR-4	104.88
OVCAR-5	89.58
OVCAR-8	87.57
NCI/ADR-RES	74.54
SK-OV-3	95.07
Renal Cancer	
786-0	79.66
A498	95.57
ACHN	87.34
CAKI-1	72.38
RXF 393	98.63
SN12C	91.96
TK-10	80.21
UO-31	52.83
Prostate Cancer	
PC-3	32.84
DU-145	91.77
Breast Cancer	
MCF7	80.33
MDA-MB-231/ATCC	88.05
HS 578T	77.33
BT-549	94.73
T-47D	78.06
MDA-MB-468	93.81
Mean	81.65
Delta	48.81
Range	103.77

Mean Growth Percent - Growth Percent

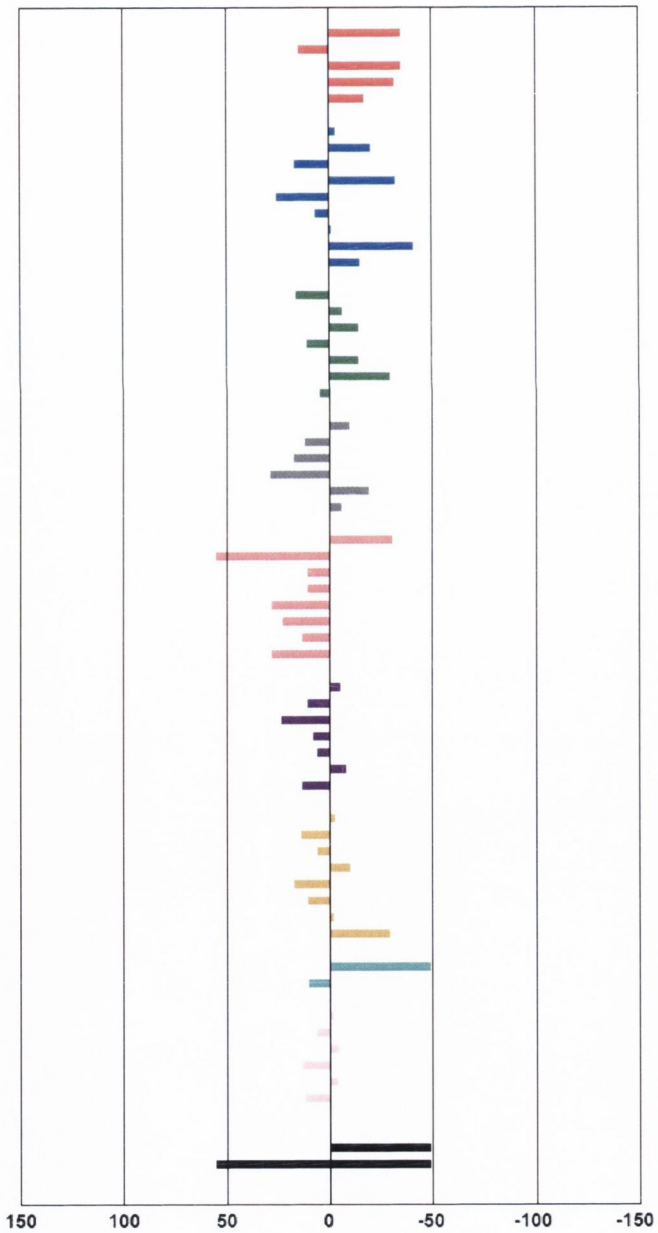

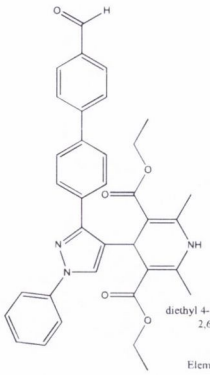

diethyl 4-(3-(4'-formylbiphenyl-4-yl)-1-phenyl-1*H*-pyrazol-4-yl)-2,6-dimethyl-1,4-dihydropyridine-3,5-dicarboxylate
Chemical Formula: $C_{33}H_{33}N_3O_5$
Molecular Weight: 575.6536
Elemental Analysis: C, 73.03; H, 5.78; N, 7.30; O, 13.90

Developmental Therapeutics Program	NSC: D-757154 / 1	Conc: 1.00E-5 Molar	Test Date: Apr 11, 2011
One Dose Mean Graph	Experiment ID: 1104OS33		Report Date: May 10, 2011

Panel/Cell Line	Growth Percent
Leukemia	
CCRF-CEM	24.47
HL-60(TB)	73.34
K-562	30.13
MOLT-4	46.74
RPMI-8226	36.79
Non-Small Cell Lung Cancer	
A549/ATCC	83.48
EKVX	64.83
HOP-62	92.64
HOP-92	63.55
NCI-H226	89.97
NCI-H23	75.79
NCI-H322M	88.53
NCI-H460	60.73
NCI-H522	53.11
Colon Cancer	
COLO 205	96.28
HCC-2998	79.82
HCT-116	54.41
HCT-15	77.31
HT29	83.04
KM12	58.96
SW-620	79.54
CNS Cancer	
SF-268	75.59
SF-295	71.46
SF-539	72.44
SNB-19	81.91
SNB-75	36.10
U251	62.00
Melanoma	
LOX IMVI	62.72
MALME-3M	77.72
M14	63.40
MDA-MB-435	28.11
SK-MEL-28	88.06
SK-MEL-5	87.88
UACC-257	71.46
UACC-62	88.55
Ovarian Cancer	
IGROV1	70.62
OVCAR-3	77.18
OVCAR-4	71.68
OVCAR-5	109.83
OVCAR-8	76.98
NCI/ADR-RES	56.55
SK-OV-3	95.26
Renal Cancer	
786-0	68.43
A498	88.19
ACHN	81.20
CAKI-1	74.24
RXF 393	64.87
SN12C	86.54
TK-10	65.64
UO-31	35.23
Prostate Cancer	
PC-3	34.88
DU-145	88.14
Breast Cancer	
MCF7	62.81
MDA-MB-231/ATCC	94.08
HS 578T	74.35
BT-549	88.53
T-47D	67.48
MDA-MB-468	85.60
Mean	70.68
Delta	46.21
Range	85.36

Mean Growth Percent - Growth Percent

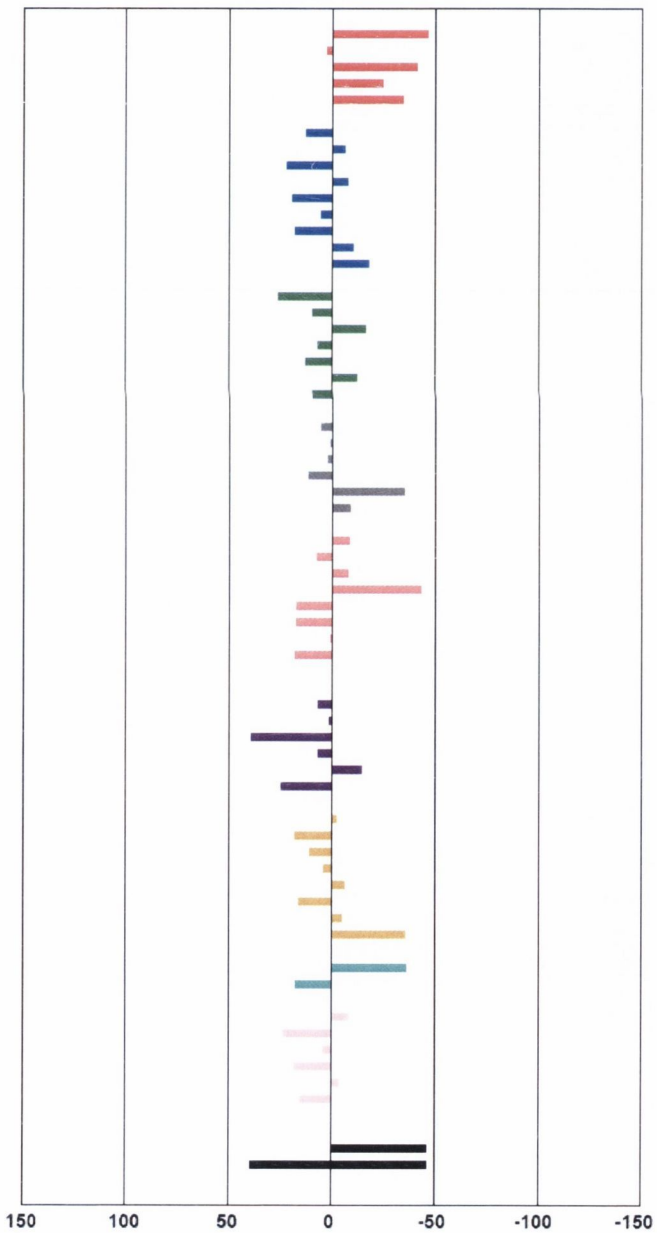

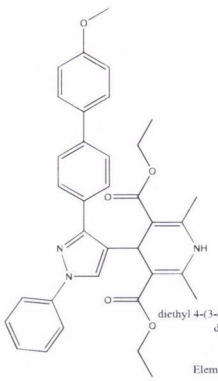

diethyl 4-(3-(4'-methoxybiphenyl-4-yl)-1-phenyl-1*H*-pyrazol-4-yl)-2,6-dimethyl-1,4-dihydropyridine-3,5-dicarboxylate
Chemical Formula: $C_{33}H_{33}N_3O_5$
Molecular Weight: 577.6695
Elemental Analysis: C, 72.77; H, 6.11; N, 7.27; O, 13.85

Developmental Therapeutics Program	NSC: D-757155 / 1	Conc: 1.00E-5 Molar	Test Date: Apr 11, 2011
One Dose Mean Graph	Experiment ID: 1104OS33		Report Date: May 10, 2011

Panel/Cell Line	Growth Percent
Leukemia	
CCRF-CEM	62.00
HL-60(TB)	103.20
K-562	69.08
MOLT-4	64.11
RPMI-8226	64.11
Non-Small Cell Lung Cancer	
A549/ATCC	61.40
EKVX	51.24
HOP-62	90.12
HOP-92	89.03
NCI-H226	103.01
NCI-H23	82.08
NCI-H322M	76.41
NCI-H460	70.51
NCI-H522	51.46
Colon Cancer	
COLO 205	94.99
HCC-2998	65.88
HCT-116	51.99
HCT-15	70.11
HT29	58.54
KM12	63.97
SW-620	91.71
CNS Cancer	
SF-268	76.01
SF-295	90.39
SF-539	88.30
SNB-19	88.54
SNB-75	21.28
U251	71.44
Melanoma	
LOX IMVI	52.43
MALME-3M	104.11
M14	74.59
MDA-MB-435	83.13
SK-MEL-28	98.81
SK-MEL-5	91.98
UACC-257	80.37
UACC-62	91.69
Ovarian Cancer	
IGROV1	51.58
OVCAR-3	92.72
OVCAR-4	78.26
OVCAR-5	82.81
OVCAR-8	77.62
NCI/ADR-RES	69.89
SK-OV-3	99.94
Renal Cancer	
786-0	68.99
A498	96.64
ACHN	73.97
CAKI-1	67.06
RXF 393	78.59
SN12C	68.20
TK-10	76.09
UO-31	36.77
Prostate Cancer	
PC-3	47.95
DU-145	99.81
Breast Cancer	
MCF7	65.01
MDA-MB-231/ATCC	57.06
HS 578T	76.18
BT-549	86.69
T-47D	53.82
MDA-MB-468	69.11
Mean	74.53
Delta	53.25
Range	82.83

Mean Growth Percent - Growth Percent

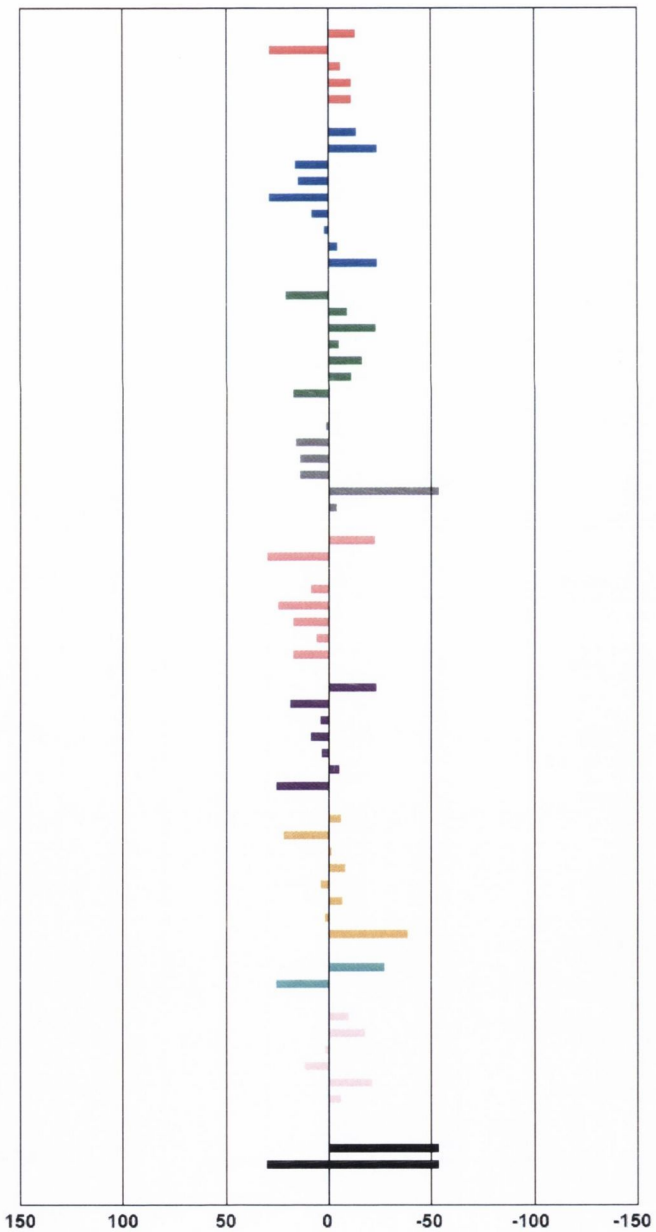

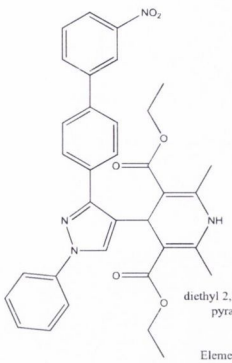

diethyl 2,6-dimethyl-4-(3-(3'-nitrobiphenyl-4-yl)-1-phenyl-1*H*-pyrazol-4-yl)-1,4-dihydropyridine-3,5-dicarboxylate
Chemical Formula: $C_{34}H_{32}N_4O_6$
Molecular Weight: 592.6411
Elemental Analysis: C, 68.91; H, 5.44; N, 9.45; O, 16.20

Developmental Therapeutics Program	NSC: D-757156 / 1	Conc: 1.00E-5 Molar	Test Date: Apr 11, 2011
One Dose Mean Graph	Experiment ID: 1104OS33		Report Date: May 10, 2011

Panel/Cell Line	Growth Percent
Leukemia	
CCRF-CEM	65.55
HL-60(TB)	101.52
K-562	56.64
MOLT-4	44.21
RPMI-8226	58.03
Non-Small Cell Lung Cancer	
A549/ATCC	60.85
EKVX	50.99
HOP-62	89.52
HOP-92	57.27
NCI-H226	85.68
NCI-H23	77.51
NCI-H322M	66.14
NCI-H460	78.75
NCI-H522	56.62
Colon Cancer	
COLO 205	85.19
HCC-2998	77.45
HCT-116	64.93
HCT-15	84.01
HT29	74.52
KM12	73.26
SW-620	94.47
CNS Cancer	
SF-268	82.16
SF-295	94.57
SF-539	83.03
SNB-19	94.17
SNB-75	24.90
U251	69.14
Melanoma	
LOX IMVI	62.18
MALME-3M	78.32
M14	90.27
MDA-MB-435	84.56
SK-MEL-2	59.57
SK-MEL-28	100.37
SK-MEL-5	87.26
UACC-257	80.06
UACC-62	92.49
Ovarian Cancer	
IGROV1	51.87
OVCAR-3	85.24
OVCAR-4	76.60
OVCAR-5	89.23
OVCAR-8	79.39
NCI/ADR-RES	75.01
SK-OV-3	90.65
Renal Cancer	
786-0	68.95
A498	73.52
ACHN	74.59
CAKI-1	53.47
RXF 393	62.60
SN12C	79.47
TK-10	62.63
UO-31	28.70
Prostate Cancer	
PC-3	45.34
DU-145	91.72
Breast Cancer	
MCF7	77.17
MDA-MB-231/ATCC	76.13
HS 578T	70.54
BT-549	80.21
T-47D	63.66
MDA-MB-468	61.10
Mean	72.95
Delta	48.05
Range	76.62

Mean Growth Percent - Growth Percent

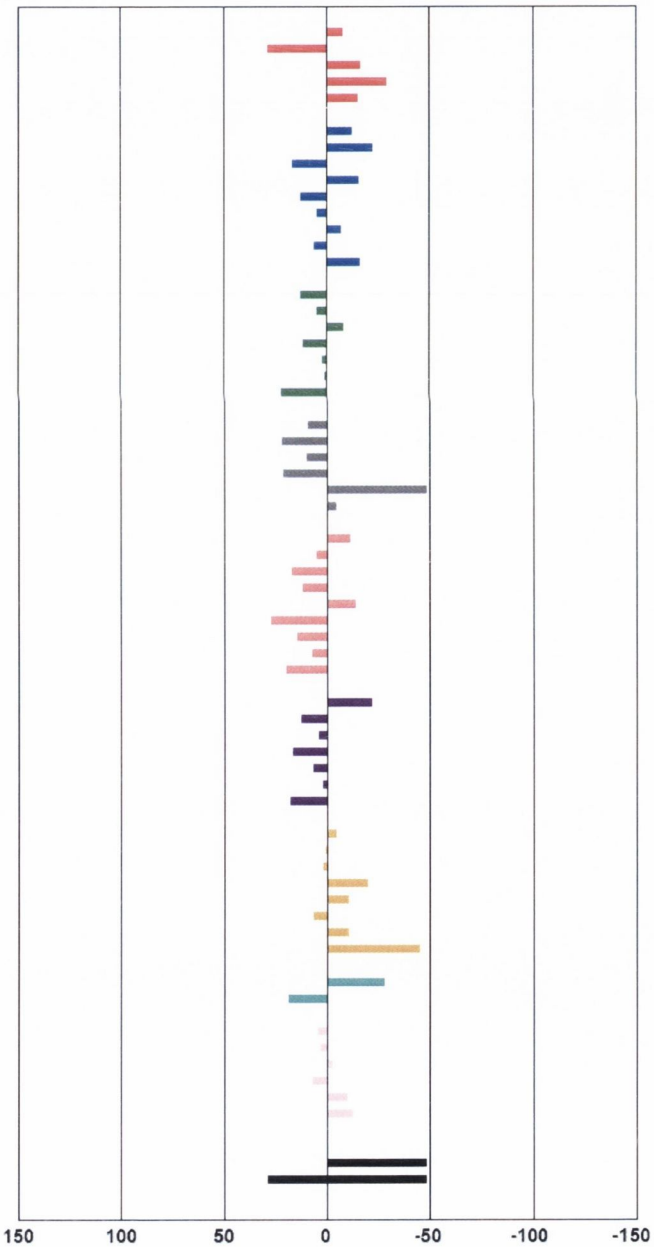

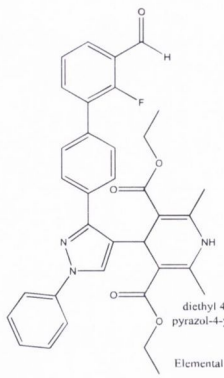

diethyl 4-(3-(2'-fluoro-3'-formylbiphenyl-4-yl)-1-phenyl-1*H*-pyrazol-4-yl)-2,6-dimethyl-1,4-dihydropyridine-3,5-dicarboxylate
Chemical Formula: $C_{35}H_{33}FN_2O_5$
Molecular Weight: 593.6441
Elemental Analysis: C, 70.81; H, 5.43; F, 3.20; N, 7.08; O, 13.48

Developmental Therapeutics Program	NSC: D-757157 / 1	Conc: 1.00E-5 Molar	Test Date: Apr 11, 2011
One Dose Mean Graph	Experiment ID: 1104OS33		Report Date: May 10, 2011

Panel/Cell Line	Growth Percent
Leukemia	
CCRF-CEM	40.07
HL-60(TB)	27.97
K-562	12.42
MOLT-4	4.43
RPMI-8226	47.71
Non-Small Cell Lung Cancer	
A549/ATCC	65.21
EKVX	47.96
HOP-62	89.09
HOP-92	30.74
NCI-H226	85.37
NCI-H23	84.36
NCI-H322M	68.84
NCI-H460	38.58
NCI-H522	84.82
Colon Cancer	
COLO 205	98.17
HCC-2998	86.96
HCT-116	41.43
HCT-15	89.38
HT29	80.92
KM12	40.57
SW-620	52.76
CNS Cancer	
SF-268	49.66
SF-295	84.08
SF-539	73.74
SNB-19	85.25
SNB-75	50.98
U251	63.65
Melanoma	
LOX IMVI	47.88
MALME-3M	94.94
M14	78.04
MDA-MB-435	64.11
SK-MEL-2	73.10
SK-MEL-28	108.69
SK-MEL-5	87.30
UACC-257	75.42
UACC-62	92.73
Ovarian Cancer	
IGROV1	52.12
OVCAR-3	47.76
OVCAR-4	84.50
OVCAR-5	94.71
OVCAR-8	74.61
NCI/ADR-RES	65.90
SK-OV-3	91.33
Renal Cancer	
786-0	65.60
A498	65.71
ACHN	80.97
CAKI-1	49.55
RXF 393	70.67
SN12C	83.31
TK-10	73.66
UO-31	17.59
Prostate Cancer	
PC-3	24.09
DU-145	68.93
Breast Cancer	
MCF7	78.88
MDA-MB-231/ATCC	74.85
HS 578T	53.41
BT-549	84.28
T-47D	57.74
MDA-MB-468	74.30
Mean	65.79
Delta	61.36
Range	104.26

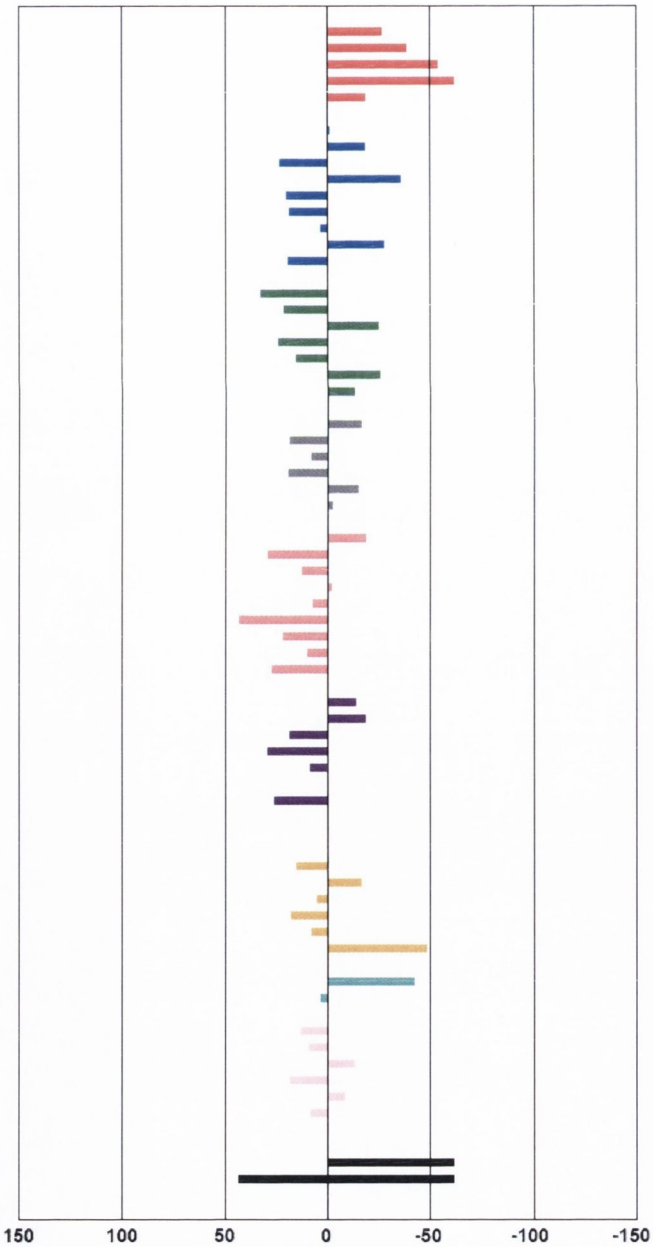

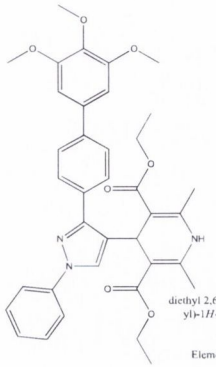

diethyl 2,6-dimethyl-4-(1-phenyl-3-(3',4',5'-trimethoxybiphenyl-4-yl)-1*H*-pyrazol-4-yl)-1,4-dihydropyridine-3,5-dicarboxylate
Chemical Formula: $C_{35}H_{38}N_2O_7$
Molecular Weight: 637.7215
Elemental Analysis: C, 69.68; H, 6.16; N, 6.59; O, 17.56

Developmental Therapeutics Program	NSC: D-757159 / 1	Conc: 1.00E-5 Molar	Test Date: Apr 11, 2011
One Dose Mean Graph	Experiment ID: 1104OS33		Report Date: May 10, 2011

Panel/Cell Line	Growth Percent
Leukemia	
CCRF-CEM	58.32
HL-60(TB)	92.67
K-562	64.91
MOLT-4	42.17
RPMI-8226	45.39
Non-Small Cell Lung Cancer	
A549/ATCC	54.69
EKVX	40.22
HOP-62	87.68
NCI-H226	80.56
NCI-H23	74.71
NCI-H322M	75.56
NCI-H460	60.03
NCI-H522	59.95
Colon Cancer	
COLO 205	81.29
HCC-2998	73.66
HCT-116	41.23
HCT-15	75.10
HT29	60.93
KM12	71.39
SW-620	87.06
CNS Cancer	
SF-268	79.04
SF-295	70.55
SF-539	68.01
SNB-19	86.73
SNB-75	18.66
U251	66.17
Melanoma	
LOX IMVI	60.05
MALME-3M	85.28
M14	86.99
MDA-MB-435	68.85
SK-MEL-2	76.12
SK-MEL-28	93.19
SK-MEL-5	67.87
UACC-257	63.01
UACC-62	87.11
Ovarian Cancer	
IGROV1	62.02
OVCAR-3	72.84
OVCAR-4	65.79
OVCAR-5	91.12
OVCAR-8	76.87
NCI/ADR-RES	69.56
SK-OV-3	84.97
Renal Cancer	
786-0	66.26
A498	64.72
ACHN	64.40
CAKI-1	46.97
RXF 393	60.65
SN12C	75.94
TK-10	79.54
UO-31	16.73
Prostate Cancer	
PC-3	34.48
DU-145	90.79
Breast Cancer	
MCF7	89.47
MDA-MB-231/ATCC	87.78
HS 578T	63.59
BT-549	71.69
T-47D	61.28
MDA-MB-468	66.99
Mean	68.44
Delta	51.71
Range	76.46

Mean Growth Percent - Growth Percent

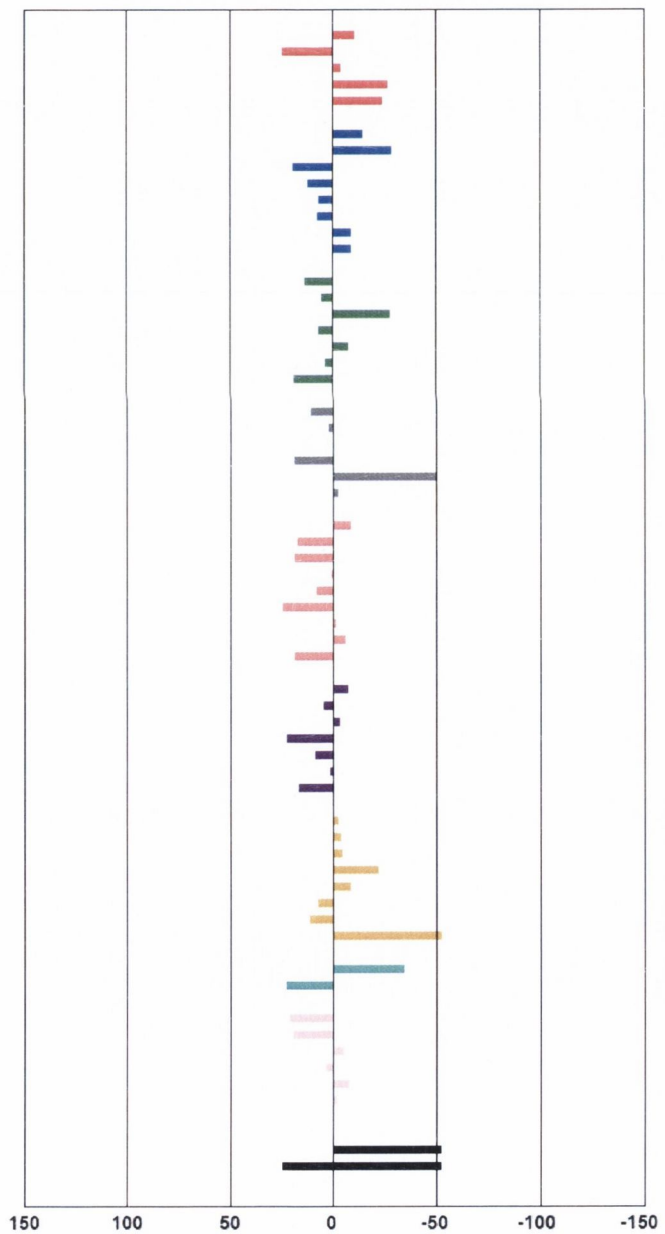

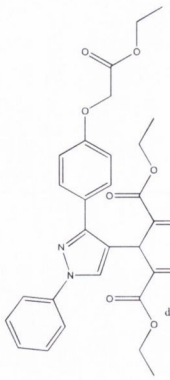

diethyl 4-(3-(4-(2-ethoxy-2-oxoethoxy)phenyl)-1-phenyl-1*H*-pyrazol-4-yl)-2,6-dimethyl-1,4-dihydropyridine-3,5-dicarboxylate
Chemical Formula: $C_{32}H_{35}N_3O_7$
Molecular Weight: 573.6362
Elemental Analysis: C, 67.00; H, 6.15; N, 7.33; O, 19.52

Developmental Therapeutics Program	NSC: D-757160 / 1	Conc: 1.00E-5 Molar	Test Date: Apr 11, 2011
One Dose Mean Graph	Experiment ID: 1104OS33		Report Date: May 10, 2011

Panel/Cell Line	Growth Percent
Leukemia	
CCRF-CEM	90.15
HL-60(TB)	80.68
K-562	56.38
MOLT-4	57.13
RPMI-8226	88.95
Non-Small Cell Lung Cancer	
A549/ATCC	95.91
EKVX	100.16
HOP-62	85.72
HOP-92	73.82
NCI-H226	95.20
NCI-H23	97.96
NCI-H322M	103.35
NCI-H460	91.19
NCI-H522	82.93
Colon Cancer	
COLO 205	105.80
HCC-2998	92.19
HCT-116	84.49
HCT-15	97.52
HT29	96.29
KM12	113.83
SW-620	93.41
CNS Cancer	
SF-268	103.27
SF-295	93.78
SF-539	91.74
SNB-19	96.00
SNB-75	85.40
U251	98.82
Melanoma	
LOX IMVI	94.30
MALME-3M	100.04
M14	96.19
MDA-MB-435	85.26
SK-MEL-2	112.91
SK-MEL-28	100.23
SK-MEL-5	94.52
UACC-257	93.86
UACC-62	95.36
Ovarian Cancer	
IGROV1	89.47
OVCAR-3	109.52
OVCAR-4	96.54
OVCAR-5	107.53
OVCAR-8	83.58
NCI/ADR-RES	103.14
SK-OV-3	90.68
Renal Cancer	
786-0	99.12
A498	92.97
ACHN	96.52
CAKI-1	103.16
RXF 393	103.01
SN12C	93.31
TK-10	111.06
UO-31	78.50
Prostate Cancer	
PC-3	79.71
DU-145	107.55
Breast Cancer	
MCF7	84.83
MDA-MB-231/ATCC	107.36
HS 578T	85.38
BT-549	92.82
T-47D	86.69
MDA-MB-468	89.62
Mean	93.51
Delta	37.13
Range	57.45

Mean Growth Percent - Growth Percent

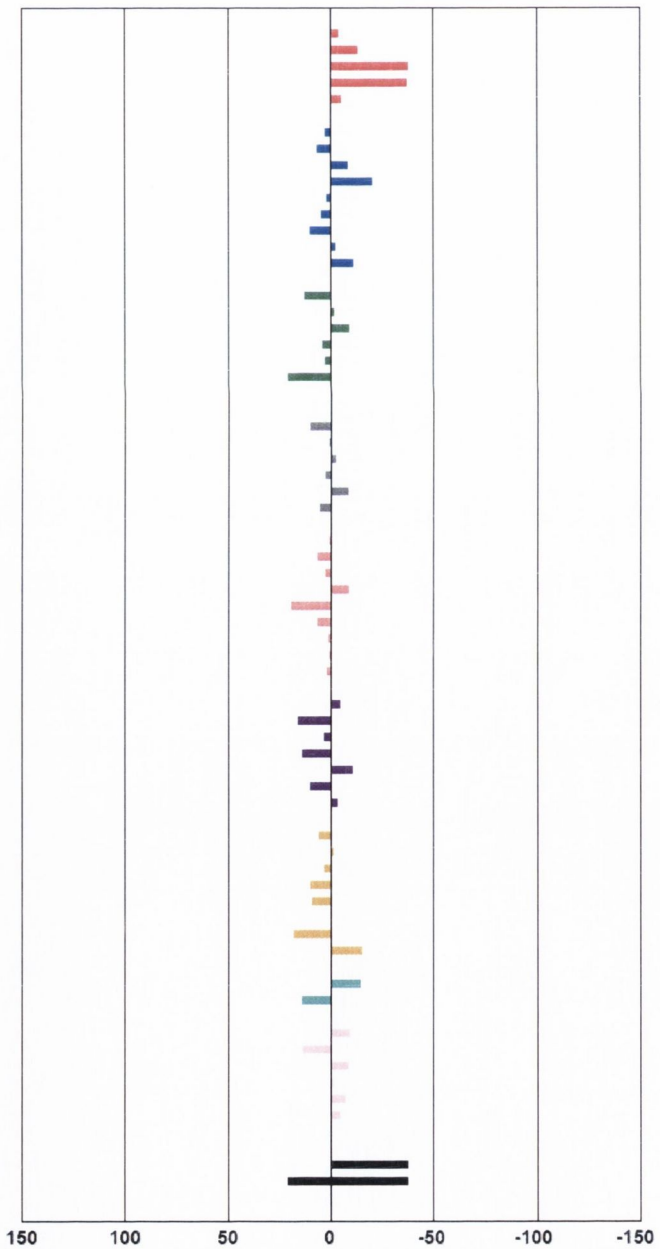

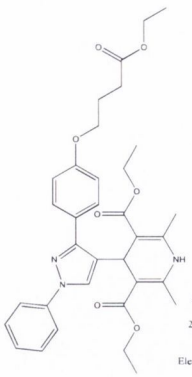

diethyl 4-(3-(4-(4-ethoxy-4-oxobutoxy)phenyl)-1-phenyl-1*H*-pyrazol-4-yl)-2,6-dimethyl-1,4-dihydropyridine-3,5-dicarboxylate
Chemical Formula: $C_{34}H_{38}N_2O_7$
Molecular Weight: 601.6894
Elemental Analysis: C, 67.87; H, 6.53; N, 6.98; O, 18.61

Developmental Therapeutics Program	NSC: D-757161 / 1	Conc: 1.00E-5 Molar	Test Date: Apr 11, 2011
One Dose Mean Graph	Experiment ID: 1104OS33		Report Date: May 10, 2011

Panel/Cell Line	Growth Percent
Leukemia	
CCRF-CEM	66.78
HL-60(TB)	98.21
K-562	75.31
MOLT-4	49.61
RPMI-8226	72.16
Non-Small Cell Lung Cancer	
A549/ATCC	81.41
EKVX	86.26
HOP-62	85.59
HOP-92	66.86
NCI-H226	81.18
NCI-H23	97.94
NCI-H322M	102.87
NCI-H460	87.07
NCI-H522	78.24
Colon Cancer	
COLO 205	88.93
HCC-2998	92.70
HCT-116	94.80
HCT-15	99.44
HT29	94.79
KM12	99.01
SW-620	92.83
CNS Cancer	
SF-268	94.61
SF-295	88.97
SF-539	103.69
SNB-19	91.01
SNB-75	71.92
U251	74.72
Melanoma	
LOX IMVI	86.80
MALME-3M	114.92
M14	101.71
MDA-MB-435	98.29
SK-MEL-28	110.91
SK-MEL-5	93.07
UACC-257	87.38
UACC-62	99.14
Ovarian Cancer	
IGROV1	92.68
OVCAR-3	92.87
OVCAR-4	92.63
OVCAR-5	105.25
OVCAR-8	92.71
NCI/ADR-RES	92.69
SK-OV-3	92.34
Renal Cancer	
786-0	91.05
A498	70.78
ACHN	98.16
CAKI-1	80.18
RXF 393	104.40
SN12C	99.60
TK-10	80.85
UO-31	69.32
Prostate Cancer	
PC-3	61.12
DU-145	103.96
Breast Cancer	
MCF7	88.23
MDA-MB-231/ATCC	94.17
HS 578T	103.71
BT-549	94.90
T-47D	81.84
MDA-MB-468	85.44
Mean	89.28
Delta	39.67
Range	65.31

Mean Growth Percent - Growth Percent

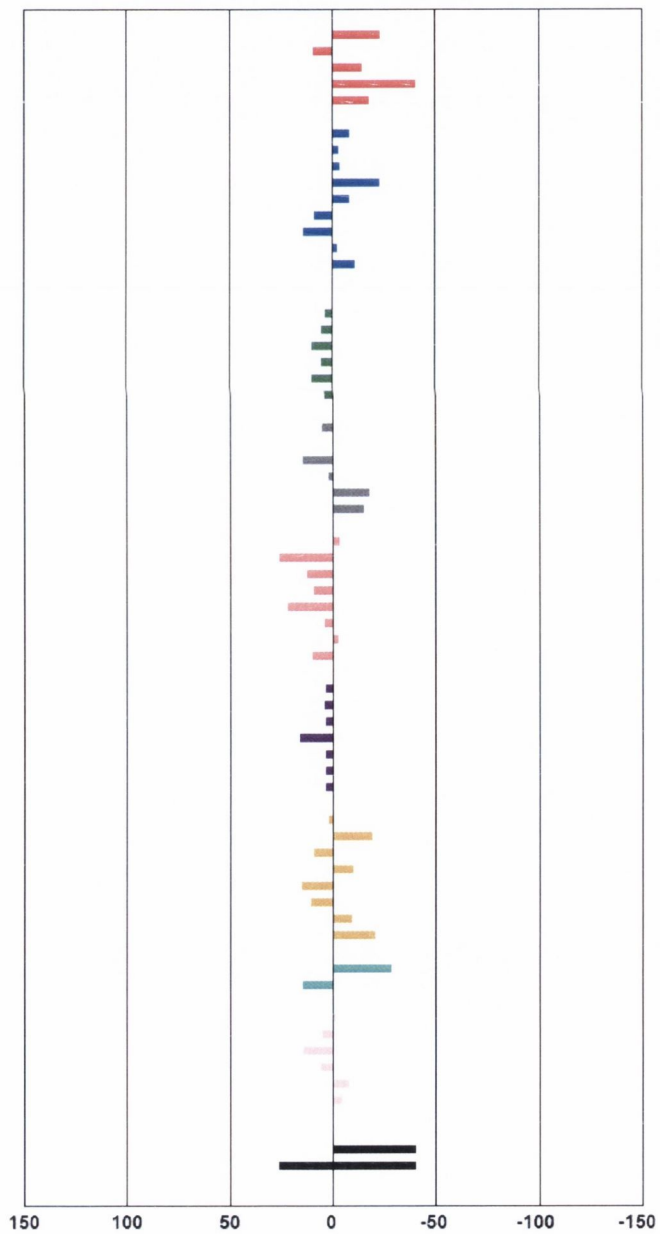

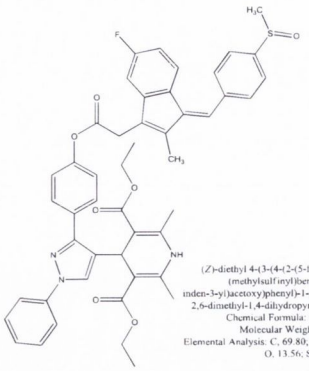

(Z)-diethyl 4-(3-(4-((2-(5-fluoro-2-methyl-1-(4-(methylsulfinyl)benzylidene)-1*H*-inden-3-yl)acetoxy)phenyl)-1-phenyl-1*H*-pyrazol-4-yl)-2,6-dimethyl-1,4-dihydropyridine-3,5-dicarboxylate
Chemical Formula: $C_{44}H_{44}FN_3O_7S$
Molecular Weight: 825.9423
Elemental Analysis: C, 69.80; H, 5.37; F, 2.30; N, 5.09; O, 13.56; S, 3.88

Developmental Therapeutics Program	NSC: D-757162 / 1	Conc: 1.00E-5 Molar	Test Date: Apr 11, 2011
One Dose Mean Graph	Experiment ID: 1104OS33		Report Date: May 10, 2011

Panel/Cell Line	Growth Percent
Leukemia	
CCRF-CEM	85.29
HL-60(TB)	105.17
K-562	85.27
MOLT-4	80.95
RPMI-8226	74.62
Non-Small Cell Lung Cancer	
A549/ATCC	82.50
EKVX	74.59
HOP-62	93.13
HOP-92	82.31
NCI-H226	76.39
NCI-H23	96.33
NCI-H322M	104.44
NCI-H460	93.18
NCI-H522	75.72
Colon Cancer	
COLO 205	97.64
HCC-2998	99.94
HCT-116	91.63
HCT-15	98.62
HT29	92.53
KM12	97.75
SW-620	97.34
CNS Cancer	
SF-268	101.07
SF-295	86.27
SF-539	84.14
SNB-19	105.57
SNB-75	83.49
U251	84.27
Melanoma	
LOX IMVI	93.66
MALME-3M	84.99
M14	99.72
MDA-MB-435	98.96
SK-MEL-28	99.75
SK-MEL-5	94.67
UACC-257	86.11
UACC-62	97.57
Ovarian Cancer	
IGROV1	95.88
OVCAR-3	104.26
OVCAR-4	93.15
OVCAR-5	115.08
OVCAR-8	92.95
NCI/ADR-RES	91.10
SK-OV-3	90.59
Renal Cancer	
786-0	91.52
A498	88.14
ACHN	96.60
CAKI-1	83.76
RXF 393	97.30
SN12C	98.20
TK-10	93.25
UO-31	70.46
Prostate Cancer	
PC-3	69.12
DU-145	105.95
Breast Cancer	
MCF7	85.45
MDA-MB-231/ATCC	92.82
HS 578T	99.59
BT-549	105.50
T-47D	81.41
MDA-MB-468	81.86
Mean	91.54
Delta	22.42
Range	45.96

Mean Growth Percent - Growth Percent

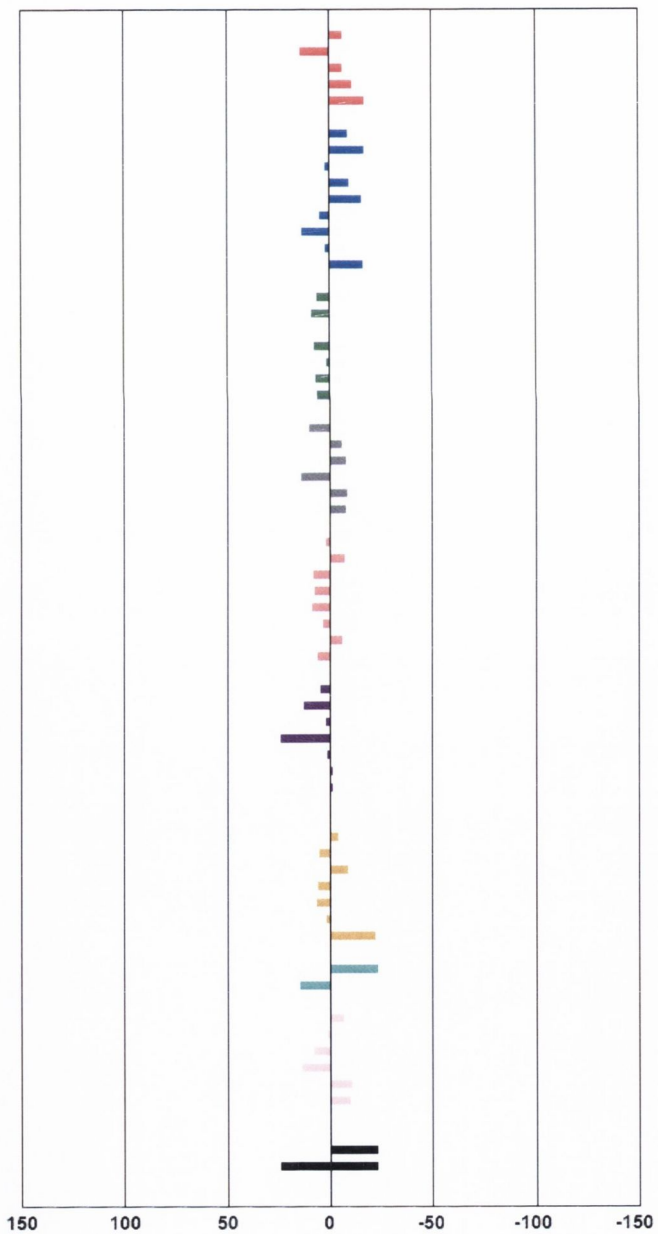

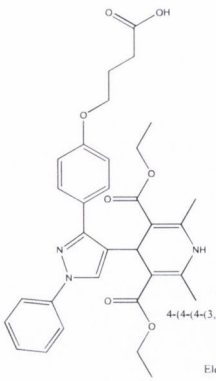

4-(4-(4-(3,5-bis(ethoxycarbonyl)-2,6-dimethyl-1,4-dihydropyridin-4-yl)-1-phenyl-1*H*-pyrazol-3-yl)phenoxy)butanoic acid
Chemical Formula: $C_{32}H_{36}N_2O_7$
Molecular Weight: 573.6362
Elemental Analysis: C, 67.00; H, 6.15; N, 7.33; O, 19.52

Developmental Therapeutics Program	NSC: D-757163 / 1	Conc: 1.00E-5 Molar	Test Date: Apr 11, 2011
One Dose Mean Graph	Experiment ID: 1104OS33		Report Date: May 10, 2011

Panel/Cell Line	Growth Percent
Leukemia	
CCRF-CEM	89.07
HL-60(TB)	112.49
K-562	100.88
MOLT-4	94.38
RPMI-8226	86.12
Non-Small Cell Lung Cancer	
A549/ATCC	84.58
EKVX	96.73
HOP-62	95.27
HOP-92	82.46
NCI-H226	89.22
NCI-H23	98.85
NCI-H322M	107.24
NCI-H460	108.15
NCI-H522	74.37
Colon Cancer	
COLO 205	112.97
HCC-2998	100.40
HCT-116	93.45
HCT-15	99.54
HT29	104.79
KM12	103.86
SW-620	99.20
CNS Cancer	
SF-268	108.56
SF-295	90.44
SF-539	101.51
SNB-19	97.30
SNB-75	87.11
U251	91.16
Melanoma	
LOX IMVI	101.29
MALME-3M	93.64
M14	98.53
MDA-MB-435	101.59
SK-MEL-28	103.88
SK-MEL-5	99.44
UACC-257	86.58
UACC-62	96.70
Ovarian Cancer	
IGROV1	99.90
OVCAR-3	109.02
OVCAR-4	96.61
OVCAR-5	108.26
OVCAR-8	95.79
NCI/ADR-RES	102.78
SK-OV-3	95.44
Renal Cancer	
786-0	99.85
A498	82.57
ACHN	102.89
CAKI-1	94.09
RXF 393	104.71
SN12C	96.39
TK-10	103.40
UO-31	75.50
Prostate Cancer	
PC-3	92.28
DU-145	110.45
Breast Cancer	
MCF7	85.62
MDA-MB-231/ATCC	118.96
HS 578T	96.17
BT-549	99.85
T-47D	82.91
MDA-MB-468	99.18
Mean	97.32
Delta	22.95
Range	44.59

Mean Growth Percent - Growth Percent

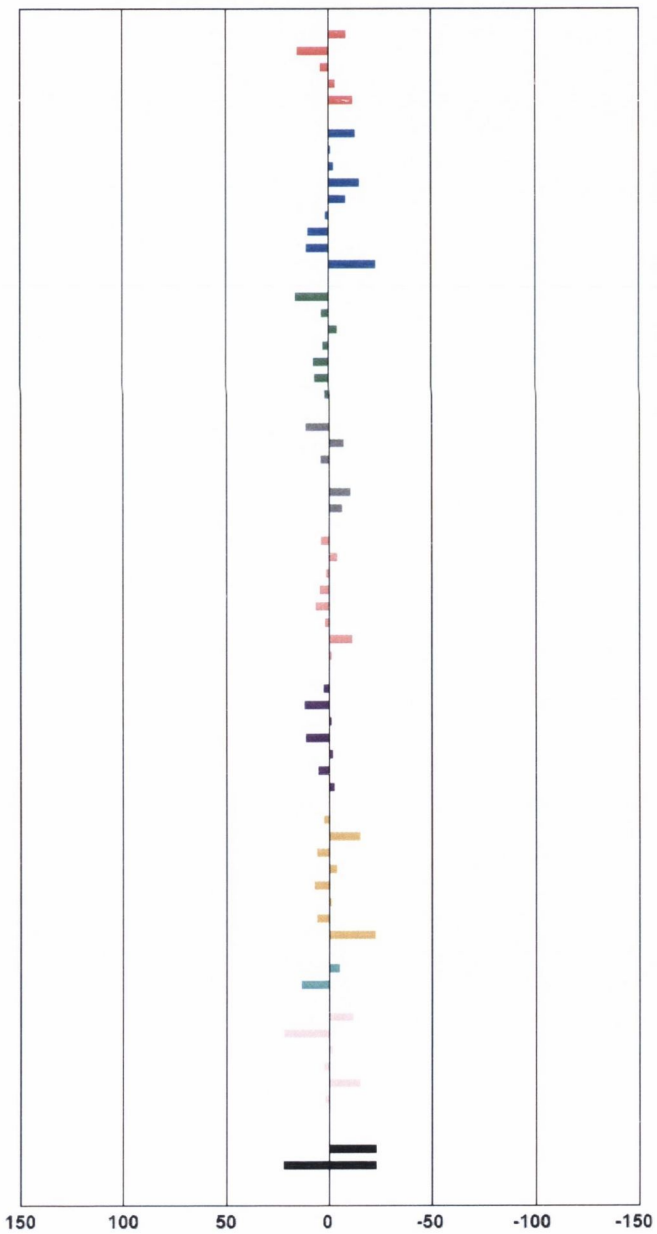

Appendix II

Compare anylysis

Table A2 Standard COMPARE Analysis of dihydropyridine 161[a]

Rank	Compound	*r*
	Based on GI_{50} mean graph	
1	Tamoxifen	0.485
2	Nitrogen mustard	0.476
3	Rhizoxin	0.446
4	Aclacinomycin	0.370
5	Rifamycin	0.367
	Based on TGI mean graph	
1	Asaley	0.463
2	Tamoxifen	0.453
3	Actinomycin D	0.390
4	CCNU	0.383
5	Caracemide	0.364
	Based on LC_{50} mean graph	
1	A-TGDR	0.608
2	B-TGDR	0.511
3	Breqinar	0.479
4	Rhixon	0.457
5	Vinblastine sulphate	0.424

[a] The target set was the standard agent database and the target set endpoints were selected to be equal to the seed end points. Standard COMPARE analysis was performed. Correlation values (*r*) are Pearson correlation coefficients.

Table A3 Standard COMPARE Analysis of dihydropyridine 179[a]

Rank	Compound	*r*
	Based on GI_{50} mean graph	
1	Rhizoxin	0.497
2	Tamoxifen	0.459
3	Spirogermanium	0.397
4	Hycanthone	0.385
5	Batrycyclin	0.375
	Based on TGI mean graph	
1	Tamoxifen	0.529
2	5-Fluorouracil	0.458
3	Asaley	0.444
4	CHIP	0.440
5	Aphodicolin glycinate	0.426
	Based on LC_{50} mean graph	
1	Chromomycin	0.758
2	Deoxythioguanosine	0.709
3	Thioguanine	0.691
4	Bactobolin	0.689
5	L-Asparaginase	0.644

[a] The target set was the standard agent database and the target set endpoints were selected to be equal to the seed end points. Standard COMPARE analysis was performed. Correlation values (*r*) are Pearson correlation coefficients.

Table A4 Standard COMPARE Analysis of dihydropyridine 176[a]

Rank	Compound	*r*
	Based on GI_{50} mean graph	
1	Tamoxifen	0.504
2	Nitrogen mustard	0.390
3	Caracemide	0.351
4	Rhizoxin	0.315
5	Acivicin	0.314
	Based on TGI mean graph	
1	Tamoxifen	0.480
2	5-Fluorouracil	0.464
3	Nitrogen mustard	0.458
4	Thioguanine	0.447
5	Actinomycin	0.427
	Based on LC_{50} mean graph	
1	B-TGDR	0.586
2	Thioguanine	0.577
3	L-Asparaginase	0.575
4	Paclitaxel	0.566
5	Morpholino-ADR	0.548

[a] The target set was the standard agent database and the target set endpoints were selected to be equal to the seed end points. Standard COMPARE analysis was performed. Correlation values (*r*) are Pearson correlation coefficients.

Table A5 Standard COMPARE Analysis of dihydropyridine 218[a]

Rank	Compound	*r*	Cell lines
	Based on GI_{50} mean graph		
1	Maytansine	0.542	41
2	Rifamycin SV	0.484	57
3	Anguidine (hiConc:10^{-4}M)	0.482	59
4	Anguidine (hiConc:10^{-7}M)	0.474	56
5	Tamoxifen	0.467	60
	Based on TGI mean graph		
1	Dichloroallyl lawsone	0.529	46
2	Actinomycin D (hiConc:$10^{-6.6}$M)	0.473	59
3	Bactobolin	0.458	52
4	Actinomycin D (hiConc:$10^{-5.6}$M)	0.455	51
5	Actinomycin D (hiConc:10^{-4}M)	0.451	56
	Based on LC_{50} mean graph		
1	Amonafide	0.691	56
2	Bactobolin (hiConc:10^{-4}M)	0.691	53
3	Anguidine	0.683	57
4	Homoharringtonine	0.657	56
5	Bactoblin (hiConc:$10^{-3.6}$M)	0.639	56

[a] The target set was the standard agent database and the target set endpoints were selected to be equal to the seed end points. Standard COMPARE analysis was performed. Correlation values (*r*) are Pearson correlation coefficients. Auguidine, actinomycin D and bactobolin outline at different concentrations as they have been tested by the NCI at multiple concentration ranges.

Table A6 Standard COMPARE Analysis of dihydropyridine 219[a]

Rank	Compound	*r*	Cell lines
	Based on GI_{50} mean graph		
1	Maytansine	0.486	41
2	Thioguanine	0.454	54
3	Asaley	0.424	49
4	Trimethyltrimethylolmelamine	0.421	56
5	Tamoxifen	0.403	57
	Based on TGI mean graph		
1	Actinomycin D (hiConc:$10^{-6.6}$M)	0.497	60
2	Vincristine sulfate	0.49	59
3	Actinomycin D (hiConc:10^{-4}M)	0.483	57
4	Bactobolin	0.481	53
5	Actinomycin D (hiConc:$10^{-5.6}$M)	0.464	52
	Based on LC_{50} mean graph		
1	Thalicarpine	0.591	57
2	5-azacytidine	0.547	56
3	CHIP	0.54	58
4	Methyl-CCNU	0.538	57
5	Pancratiastatin	0.537	56

[a] The target set was the standard agent database and the target set endpoints were selected to be equal to the seed end points. Standard COMPARE analysis was performed. Correlation values (*r*) are Pearson correlation coefficients. Actinomycin D outlines at different concentrations as it has been tested by the NCI at multiple concentration ranges.

Table A7 Standard COMPARE Analysis of dihydropyridine 226[a]

Rank	Compound	*r*	Cell lines
	Based on GI_{50} mean graph		
1	Hycanthone (hiConc:10^{-3}M)	0.487	54
2	Emofolin sodium	0.445	57
3	8Cl-cyc-AMP	0.421	58
4	D-tetrandrine	0.409	58
5	Hycanthone (hiConc:10^{-2}M)	0.389	45
	Based on TGI mean graph		
1	Hepsulfam	0.487	57
2	Dichloroallyl lawsone	0.462	47
3	Maytansine	0.459	47
4	Rifamycin SV	0.443	57
5	Amonafide	0.411	58
	Based on LC_{50} mean graph		
1	Mitramycin	0.655	46
2	L-asparaginase	0.636	56
3	B-TGDR	0.618	56
4	Bactobolin	0.617	52
5	Rifamycin SV	0.576	55

[a] The target set was the standard agent database and the target set endpoints were selected to be equal to the seed end points. Standard COMPARE analysis was performed. Correlation values (*r*) are Pearson correlation coefficients. Hycanthone outline at different concentrations as it has been tested by the NCI at multiple concentration ranges.

Table A8 Standard COMPARE Analysis of dihydropyridine 224[a]

Rank	Compound	*r*	Cell lines
	Based on GI_{50} mean graph		
1	Tamoxifen	0.556	60
2	Rhizoxin	0.539	47
3	Rifamyxin SV	0.408	57
4	Caracemide	0.395	58
5	Maytansine	0.387	41
	Based on TGI mean graph		
1	Thioguanine	0.509	60
2	Mitramycin	0.458	47
3	Rifamycin SV	0.456	57
4	B-TGDR	0.455	58
5	Macbecin II	0.417	57
	Based on LC_{50} mean graph		
1	Dihydro-5-azacytidine	0.709	58
2	Didemnin B	0.697	55
3	B-TGDR	0.67	58
4	Cyanomorpholino-ADR	0.666	47
5	Oxanthrazole	0.664	55

[a] The target set was the standard agent database and the target set endpoints were selected to be equal to the seed end points. Standard COMPARE analysis was performed. Correlation values (*r*) are Pearson correlation coefficients.

Table A9 Standard COMPARE Analysis of dihydropyridine 237[a]

Rank	Compound	*r*	Cell lines
	Based on GI_{50} mean graph		
1	Flavoneacetic acid	0.765	57
2	Piperazine alkylator	0.514	56
3	Pentamethylmelamine	0.488	58
4	L-buthionine sulfoximine	0.47	57
5	Spirohydantoin mustard	0.419	47
	Based on TGI mean graph		
1	Pentamethylmelamine	0.574	58
2	Spirohydantoin mustard	0.523	47
3	Flavoneacetic acid	0.479	57
4	Tetrocarcin A sodium salt	0.42	57
5	Nitrogen mustard	0.399	58
	Based on LC_{50} mean graph		
1	"O,P'-DDD"	0.841	58
2	Emofolin sodium	0.783	57
3	Hycanthone	0.691	53
4	Tamoxifen	0.69	60
5	Rapamycin	0.681	60

[a] The target set was the standard agent database and the target set endpoints were selected to be equal to the seed end points. Standard COMPARE analysis was performed. Correlation values (*r*) are Pearson correlation coefficients.

Appendix III

Determination of crystal structures by XRD

Crystal Data for 162: $C_{112}H_{112}Br_4N_{12}O_{16}$, M_W 2201.78 (4 molecules). Monoclinic, space group P2(1)/c; a = 9.923(6), b = 18.930(9), c = 14.542(6)A°, β = 112.14(3)°; U = 2530(2)(Å)^3; Z = 1; D_c = 1.445 Mg m^{-3}; m = 1.166 mm^{-1}; Range for data collection = 1.12–25.00; Reflections collected 28,265 , unique reflections 4452 [R_{int} = 0.0332]; data/restraints/parameters 4452/0/329; Goodness-of-fit on F_2 1.067; R indices (all data) = R_1 = 0.0332, wR_2 = 0.0726; Final R indices [I >2s(I)] = R_1 = 0.0304, wR_2 = 0.0726. CCDC deposition No. 787943.

Crystal Data for nifedipine: $C_{68}H_{72}N_8O_{24}$, (4 molecules). M_W1384.34, Monoclinic, Space group P2(1)/c; a = 10.621(3), b = 10.419(3), c=14.794(4)A°, β = 94.768(3)°; U = 1631.4(8)(Å)^3; Z = 1; Dc = 1.410Mg m^{-3}; m = 0.11 mm^{-1}; Range for data collection = 1.12–25.00; Reflections collected 12798 , unique reflections 2789[R_{int} = 0.0571]; Data/restraints/parameters 2789/0/230; Goodness-of-fit on F_2 1.065; R indices (all data) = R1 = 0.0491, wR_2 = 0.1245; Final R indices [I >2s(I)] = R_1 = 0.0457, wR_2 = 0.1240. CCDC deposition No. 787942.

Bibliography

1. Anand P, Kunnumakkara AB. Cancer is a preventable disease that requires major lifestyle changes. Pharm Res. 2008 Sept; 25(9):2097-116
2. Pubmed Healthe [Internet]. Available from: http://www.ncbi.nlm.nih.gov/pubmedhealth/PMH0002267
3. [Internet]. Available from: http://www.cancer.ie/research/why.php.
4. The National Cancer Registry Ireland [Internet]. Available from: http://www.ncri.ie/ncri/index.shtml.
5. Cross SE, Jin YS, Rao J, Gimzewski JK. Nanomechanical analysis of cells from cancer patients. Nat Nanotechnol 2007 Dec;2(12):780-3.
6. Anand P, Sundaram C, Jhurani S, Kunnumakkara AB, Aggarwal BB. Curcumin and cancer: An "old-age" disease with an "age-old" solution. Cancer Lett 2008 Aug 18;267(1):133-64.
7. [Internet]. Available from: http://www.ncbi.nlm.nih.gov/pmc/articles/PMC2515569/pdf/11095_2008_Article_9661.pdf.
8. Sasco AJ, Secretan MB, Straif K. Tobacco smoking and cancer: A brief review of recent epidmiological evidence. Lung Cancer 2004;45 suppl 2:3-9.
9. Seitz HK, Poschl G, Simanowski UA. Alcohol and cancer. Recent Dev Alcohol 1998;14:67-95.
10. Berrington de Gonzalez A, Mahesh M, Kim KP, Bhargavan M, Lewis R, Mettler F, Land C. Projected cancer risks from computed tomographic scans performed in the united states in 2007. Arch Intern Med 2009 Dec 14;169(22):2071-7.
11. Brenner DJ, Hall EJ. Compouted tomography-an increasing source of radiation exposure. N Engl J Med 2007;357(22):2277-84.
12. Pagano JS, Blaser M, Buendia MA, Damania B, Khalili K, Raab-Traub N, Roizman B. Infectious agents and cancer: Criteria for a causal relation. Semin Cancer Biol 2004 Dec;14(6):453-71.
13. Roukos DH. Genome-wide association studies: How predictable is a person's cancer risk? Expert Rev Anticancer Ther 2009 Apr;9(4):389-92.
14. Whitehead MI, King RJ, McQueen J, Campbell S. Endometrial histology and biochemistry in climacteric women during oestrogen and oestrogen/progestogen therapy. J R Soc Med 1979 May;72(5):322-7.
15. [Internet]: National cancer institute. Available from: http://www.cancer.gov/.
16. Hanahan D, Weinberg RA. The hallmarks of cancer. Cell 2000 Jan 7;100(1):57-70.
17. Anderson, Phil. "Cell cycles: interphase, Mitosis, Cytokinesis." [Internet]. http://schoolworkhelper.net/. November 2, 2010.
18. Smith JA, Martin L. Do cells cycle? Proc Natl Acad Sci U S A 1973 Apr;70(4):1263-7.
19. Wu RS, Bonner WM. Separation of basal histone synthesis from S-phase histone synthesis in dividing cells. Cell 1981 Dec;27(2 Pt 1):321-30.
20. Nelson DM, Hall C, Ye X, Adams PD. Coupling of DNA synthesis and histone synthesis in S phase independent of cyclin/cdk2 activity. Cell 2002;22:7459-72.
21. Lilly MA, Duronio RJ. New insights into cell cycle control from the drosophila endocycle. Oncogene 2005 Apr 18;24(17):2765-75.
22. Negrini S, Gorgoulis VG, Halazonetis TD. Genomic instability--an evolving hallmark of cancer. Nat Rev Mol Cell Biol 2010 Mar;11(3):220-8.
23. Pietras K, Ostman A. Hallmarks of cancer: Interactions with the tumor stroma. Exp Cell Res 2010 May 1;316(8):1324-31.

25. Fact sheet No. 297: Cancer [Internet]: World Health Organization; c2006. Available from: www.who.int.
26. Sanchez-Zamorano LM, Flores-Luna L, Angeles-Llerenas A, Romieu I, Lazcano-Ponce E, Miranda-Hernandez H, Mainero-Ratchelous F, Torres-Mejia GG. Healthy lifestyle on the risk of breast cancer. Cancer Epidemiol Biomarkers Prev 2011 Feb 18.
27. Sotirou C, Pusztai L. Molecular origin of cancer: Gene-expression signatures in breast cancer. N Engl J Med 2009.
28. Dahlman-Wright K, Cavailles V, Fuqua SA, Jordan VC, Katzenellenbogen JA, Korach KS, Maggi A, Muramatsu M, Parker MG, Gustafsson JA. International union of pharmacology. LXIV. estrogen receptors. Pharmacol Rev 2006 Dec;58(4):773-81.
29. Levin ER. Integration of the extranuclear and nuclear actions of estrogen. Mol Endocrinol 2005 Aug;19(8):1951-9.
30. Li X, Huang J, Yi P, Bambara RA, Hilf R, Muyan M. Single-chain estrogen receptors (ERs) reveal that the ERalpha/beta heterodimer emulates functions of the ERalpha dimer in genomic estrogen signaling pathways. Mol Cell Biol 2004 Sep;24(17):7681-94.
31. Bourguet W,Germain P, Gronemeyer H . Nuclear receptor ligand-binding domains: three-dimensional structures, molecular interactions and pharmacological implications. Trends Pharmacol Sci 2000; 21:381-88
32. Vanden Heuvel JP. Nuclear hormone receptor: A brief overview. Nuclear Recepor Resource.
33. Collins JM, Grieshaber CK, Chabner BA. Pharmacologically guided phase I clinical trials based upon preclinical drug development. J Natl Cancer Inst 1990 Aug 15;82(16):1321-6.
34. Wiebe VJ, Benz CC, Shemano I, Cadman TB, DeGregorio MW. Pharmacokinetics of toremifene and its metabolites in patients with advanced breast cancer. Cancer Chemother Pharmacol 1990;25(4):247-51.
35. De Vita VT,Jr, Hubbard SM, Longo DL. Treatment of hodgkin's disease. J Natl Cancer Inst Monogr 1990;(10)(10):19-28.
36. Hait WN, Byrne TN, Piepmeier J, Durivage HJ, Choudhury S, Davis CA, Gates JA. The effect of calmodulin inhibitors with bleomycin on the treatment of patients with high grade gliomas. Cancer Res 1990 Oct 15;50(20):6636-40.
37. Jones SE, Durie BGM, Salmon SE. Combination chemotherapy with adriamycin and cyclophosphamide for advanced breast cancer. Cancer 1975;36:90-97.
38. Luikart SD, Witman GB, Portlock CS. Adriamycin (doxorubicin), vinblastine, and mitomycin C combination chemotherapy in refractory breast carcinoma. Cancer 1984 Oct 1;54(7):1252-5.
39. Smalley RV, Lefante J, Bartolucci A, Carpenter J, Vogel C, Krauss S. A comparison of cyclophosphamide, adriamycin, and 5-fluorouracil (CAF) and cyclophosphamide, methotrexate, 5-fluorouracil, vincristine, and prednisone (CMFVP) in patients with advanced breast cancer. Breast Cancer Res Treat 1983;3(2):209-20.
40. Rosner D, Nemoto T, Lane WW. A randomized study of intensive versus moderate chemotherapy programs in metastatic breast cancer. Cancer 1987 Mar 1;59(5):874-83.
41. Bonadonna G, Brusamoline E, Valagussa P, et al. Combination chemoperapy as an adjuvant treatment in operable breast cancer. New Engl J Med 1976;294:405-10.

41. Bonadonna G, Brusamoline E, Valagussa P, et al. Combination chemoperapy as an adjuvant treatment in operable breast cancer. New Engl J Med 1976;294:405-10.
42. Marschke RF,Jr, Ingle JN, Schaid DJ, Krook JE, Mailliard JA, Cullinan SA, Pfeifle DM, Votava HJ, Ebbert LP, Windschitl HE. Randomized clinical trial of CFP versus CMFP in women with metastatic breast cancer. Cancer 1989 May 15;63(10):1931-7.
43. Copper RG, Holland JF, Glidwell O. Adjuvant chemotherapy of breast cancer. Cancer 1979;44:793-8.
44. Hortobagyi GN, Gutterman JU, Blumenschein GR, Tashima CK, Burgess MA, Einhorn L, Buzdar AU, Richman SP, Hersh EM. Combination chemoimmunotherapy of metastatic breast cancer with 5-fluorouracil, adriamycin, cyclophosphamide, and BCG. Cancer 1979 Nov;44(5):1955-62.
45. Navarro M, Bellmunt J, Balana C, Colomer R, Jolis L, del Campo JM. Mitomycin-C and vinblastine in advanced breast cancer. Oncology 1989;46(3):137-42.
46. Hirshaut Y, Kesselheim H. Prolonged remissions of metastatic breast cancer achieved with a six-drug regimen of relatively low toxicity. Cancer 1983 Jun 1;51(11):1998-2004.
47. Hart RD, Perloff M, Holland JF. One-day VAth (vinblastine, adriamycin,thiotepa and halotestin) therapy for advanced breast cancer refractory to prior chemotherapy. Cancer 1981;48:1522-7.
48. Takimoto CH, Calvo E, editors. Principles of oncologic pharmacotherapy. ; 2008. .
49. Schwartz EL. Antivascular actions of microtubule-binding drugs. Clin Cancer Res 2009 Apr 15;15(8):2594-601.
50. Beal K, Abrey LE, Gutin PH. Antiangiogenic agents in the treatment of recurrent or newly diagnosed glioblastoma: Analysis of single-agent and combined modality approaches. Radiat Oncol 2011 Jan 7;6:2.
51. Dawson RJ, Locher KP. Structure of the multidrug ABC transporter Sav1866 from staphylococcus aureus in complex with AMP-PNP. FEBS Lett 2007 Mar 6;581(5):935-8.
52. Oldham ML, Davidson AL, Chen J. Structural insights into ABC transporter mechanism. Curr Opin Struct Biol 2008 Dec;18(6):726-33.
53. Chang G. Multidrug resistance ABC transporters. FEBS Lett 2003 Nov 27;555(1):102-5.
54. Esteva FJ, Valero V, Pusztai L, Boehnke-Michaud L, Buzdar AU, Hortobagyi GN. Chemotherapy of metastatic breast cancer: What to expect in 2001 and beyond. Oncologist 2001;6(2):133-46.
55. Jordan VC. Tamoxifen: A personal retrospective. Lancet Oncol 2000 Sep;1(1):43-9.
56. Clemons M, Danson S, Howell A. Tamoxifen ("nolvadex"): A review. Cancer Treat Rev 2002;28:165-80.
57. Bago-Horvath Z, Rudas M, Dubsky P, Jakesz R, Singer CF, Kemmerling R, Greil R, Jelen A, Bohm G, Jasarevic Z, et al. Adjuvant sequencing of tamoxifen and anastrozole is superior to tamoxifen alone in postmenopausal women with low proliferating breast cancer. Clin Cancer Res 2011 Dec 6.
58. Price N, Sartor O, Hutson T, Mariani S. Role of 5a-reductase inhibitors and selective estrogen receptor modulators as potential chemopreventive agents for prostate cancer. Clin Prostate Cancer 2005 Mar;3(4):211-4.

60. Fisher B, Costantino JP, wickerham DL. Tamoxifen for prevention of breast cancer:Report of the national surigical adjuvant breast and bowel project p-1 study. J Natl Cancer Inst 1998;90:1371-88.
61. Know AJ, Meegan MJ, Sobolev V, Frost D, Zisterer DM, Williams DC, Lloyd DG. Target specific virtual screening:Optimisation of an estrogen receptor screening platform. J Med Chem 2007;50:5301-10.
62. Lloyd DG, Smith HM, O'Sullivan T, Knox AS, Zisterer DM, Meegan MJ. Antiestrogenically active 2-benzyl-1,1-diarylbut-2-enes: Synthesis, structure-activity relationships and molecular modeling study for flexible estrogen receptor antagonists. Med Chem 2006 Mar;2(2):147-68.
63. Knox AJ, Meegan MJ, Lloyd DG. Estrogen receptors: Molecular interactions, virtual screening and future prospects. Curr Top Med Chem 2006;6(3):217-43.
64. U.S. Food and Drug administration (2007-09-14). FDA approves new uses for evista. .
65. Knox AJ, Meegan MJ, Lloyd DG. Estrogen receptors: Molecular interactions, virtual screening and future prospects. Curr Top Med Chem 2006;6(3):217-43.
66. Robertson JF. Estrogen receptor downregulators: New antihormonal therapy for advanced breast cancer. Clin Ther 2002;24 Suppl A:A17-30.
67. Kansra S, Yamagata S, Sneade L, Foster L, Ben-Jonathan N. Differential effects of estrogen receptor antagonists on pituitary lactotroph proliferation and prolactin release. Mol Cell Endocrinol 2005 Jul 15;239(1-2):27-36.
68. Juretic A, Saric N, Bisof V, Basic-Koretic M. Fulvestrant: A new agent in endocrine treatment for breast cancer]. Lijec Vjesn 2006 Jan-Feb;128(1-2):31-6.
69. Mokbel K. The evolving role of aromatase inhibitors in breast cancer. Int J Clin Oncol 2002 Oct;7(5):279-83.
70. Simpson ER. Sources of estrogen and their importance. J Steroid Biochem Mol Biol 2003 Sep;86(3-5):225-30.
71. Esteva FJ, Hortobagyi GN. Gaining ground on breast cancer. Sci Am 2008 Jun;298(6):58-65.
72. Pohlmann PR, Mayer IA, Mernaugh R. Resistance to trastuzumab in breast cancer. Clin Cancer Res 2009 Dec 15;15(24):7479-91.
73. Bailey RC. Grand challenge commentary: Informative diagnostics for personalized medicine. Nat Chem Biol 2010 Dec;6(12):857-9.
74. Hudis CA. Trastuzumab--mechanism of action and use in clinical practice. N Engl J Med 2007 Jul 5;357(1):39-51.
75. Francia G, Cruz-Munoz W, Man S, Xu P, Kerbel RS. Mouse models of advanced spontaneous metastasis for experimental therapeutics. Nat Rev Cancer 2011 Feb;11(2):135-41.
76. Jani JP, Finn RS, Campbell M, Coleman KG, Connell RD, Currier N, Emerson EO, Floyd E, Harriman S, Kath JC, et al. Discovery and pharmacologic characterization of CP-724,714, a selective ErbB2 tyrosine kinase inhibitor. Cancer Res 2007 Oct 15;67(20):9887-93.
77. Weiner LM, Surana R, Wang S. Monoclonal antibodies: Versatile platforms for cancer immunotherapy. Nat Rev Immunol 2010 May;10(5):317-27.
78. de Bono JS, Bellmunt J, Attard G, Droz JP, Miller K, Flechon A, Sternberg C, Parker C, Zugmaier G, Hersberger-Gimenez V, et al. Open-label phase II study evaluating the efficacy and safety of two doses of pertuzumab in castrate chemotherapy-naive patients with hormone-refractory prostate cancer. J Clin Oncol 2007 Jan 20;25(3):257-62.

chemotherapy-naive patients with hormone-refractory prostate cancer. J Clin Oncol 2007 Jan 20;25(3):257-62.
79. Constantinou A, Chen C, Deonarain MP. Modulating the pharmacokinetics of therapeutic antibodies. Biotechnol Lett 2010 May;32(5):609-22.
80. Barros FF, Powe DG, Ellis IO, Green AR. Understanding the HER family in breast cancer: Interaction with ligands, dimerization and treatments. Histopathology 2010 Apr;56(5):560-72.
81. Olayioye MA, Neve RM, Lane HA, Hynes NE. The ErbB signaling network: Receptor heterodimerization in development and cancer. EMBO J 2000 Jul 3;19(13):3159-67.
82. Vogel CL, Cobleigh MA, Tripathy D, Gutheil JC, Harris LN, Fehrenbacher L, Slamon DJ, Murphy M, Novotny WF, Burchmore M, et al. Efficacy and safety of trastuzumab as a single agent in first-line treatment of HER2-overexpressing metastatic breast cancer. J Clin Oncol 2002 Feb 1;20(3):719-26.
83. Sridhar SS, Seymour L, Shepherd FA. Inhibitors of epidermal-growth-factor receptors: A review of clinical research with a focus on non-small-cell lung cancer. Lancet Oncol 2003 Jul;4(7):397-406.
84. Nagasawa J, Mizokami A, Koshida K, Yoshida S, Naito K, Namiki M. Novel HER2 selective tyrosine kinase inhibitor, TAK-165, inhibits bladder, kidney and androgen-independent prostate cancer in vitro and in vivo. Int J Urol 2006 May;13(5):587-92.
85. Sordella R, Bell DW, Haber DA, Settleman J. Gefitinib-sensitizing EGFR mutations in lung cancer active anti-apoptotic pathway. Science 2004;305(5687):1163-7.
86. Takimoto CH, Calve E, editors. Cancer management:A mutlidisciplinary approach. ; 2008. .
87. Okamoto I. Epidermal growth factor receptor in relation to tumor development: EGFR-targeted anticancer therapy. FEBS J 2010 Jan;277(2):309-15.
88. Speake G, Holloway B, Costello G. Recent developments related to the EGFR as a target for cancer chemotherapy. Curr Opin Pharmacol 2005 Aug;5(4):343-9.
89. Moreira C, Kaklamani V. Lapatinib and breast cancer: Current indications and outlook for the future. Expert Rev Anticancer Ther 2010 Aug;10(8):1171-82.
90. Giampaglia M, Chiuri VE, Tinelli A, De Laurentiis M, Silvestris N, Lorusso V. Lapatinib in breast cancer: Clinical experiences and future perspectives. Cancer Treat Rev 2010 Nov;36 Suppl 3:S72-9.
91. Wood ER, Truesdale AT, McDonald OB, Yuan D, Hassell A, Dickerson SH, Ellis B, Pennisi C, Horne E, Lackey K, et al. A unique structure for epidermal growth factor receptor bound to GW572016 (lapatinib): Relationships among protein conformation, inhibitor off-rate, and receptor activity in tumor cells. Cancer Res 2004 Sep 15;64(18):6652-9.
92. Allen LF, Eiseman IA, Fry DW, Lenehan PF. CI-1033, an irreversible pan-erbB receptor inhibitor and its potential application for the treatment of breast cancer. Semin Oncol 2003 Oct;30(5 Suppl 16):65-78.
93. Slichenmyer WJ, Elliott WL, Fry DW. CI-1033, a pan-erbB tyrosine kinase inhibitor. Semin Oncol 2001 Oct;28(5 Suppl 16):80-5.
94. Calvo E, Tolcher AW, Hammond LA, Patnaik A, de Bono JS, Eiseman IA, Olson SC, Lenehan PF, McCreery H, Lorusso P, et al. Administration of CI-1033, an irreversible pan-erbB tyrosine kinase inhibitor, is feasible on a 7-day on, 7-day off schedule: A phase I pharmacokinetic and food effect study. Clin Cancer Res 2004 Nov 1;10(21):7112-20.

96. Los M, Roodhart JM, Voest EE. Target practice: Lessons from phase III trials with bevacizumab and vatalanib in the treatment of advanced colorectal cancer. Oncologist 2007 Apr;12(4):443-50.
97. FDA (2010-12-16). FDA begins process to remove breast cancer indication from avastin label. .
98. Miller KD, Trigo JM, Wheeler C, Barge A, Rowbottom J, Sledge G, Baselga J. A multicenter phase II trial of ZD6474, a vascular endothelial growth factor receptor-2 and epidermal growth factor receptor tyrosine kinase inhibitor, in patients with previously treated metastatic breast cancer. Clin Cancer Res 2005 May 1;11(9):3369-76.
99. Sarkar S, Mazumdar A, Dash R, Sarkar D, Fisher PB, Mandal M. ZD6474, a dual tyrosine kinase inhibitor of EGFR and VEGFR-2, inhibits MAPK/ERK and AKT/PI3-K and induces apoptosis in breast cancer cells. Cancer Biol Ther 2010 Apr;9(8):592-603.
100. End DW, Smets G, Todd AV, Applegate TL, Fuery CJ, Angibaud P, Venet M, Sanz G, Poignet H, Skrzat S, et al. Characterization of the antitumor effects of the selective farnesyl protein transferase inhibitor R115777 in vivo and in vitro. Cancer Res 2001 Jan 1;61(1):131-7.
101. Warnberg F, White D, Anderson E, Knox F, Clarke RB, Morris J, Bundred NJ. Effect of a farnesyl transferase inhibitor (R115777) on ductal carcinoma in situ of the breast in a human xenograft model and on breast and ovarian cancer cell growth in vitro and in vivo. Breast Cancer Res 2006;8(2):R21.
102. de Bono JS, Tolcher AW, Rowinsky EK. Farnesyltransferase inhibitors and their potential in the treatment of breast carcinoma. Semin Oncol 2003 Oct;30(5 Suppl 16):79-92.
103. Reuter CW, Morgan MA, Bergmann L. Targeting the ras signaling pathway: A rational, mechanism-based treatment for hematologic malignancies? Blood 2000 Sep 1;96(5):1655-69.
104. Sharma S, Kemeny N, Kelsen DP, Ilson D, O'Reilly E, Zaknoen S, Baum C, Statkevich P, Hollywood E, Zhu Y, et al. A phase II trial of farnesyl protein transferase inhibitor SCH 66336, given by twice-daily oral administration, in patients with metastatic colorectal cancer refractory to 5-fluorouracil and irinotecan. Ann Oncol 2002 Jul;13(7):1067-71.
105. Morgan DO, editor. *Principles of control.* london: New science press. 1st ed. London: New Science Press.
106. Liu X, Lam F, Shi S, Fischer PM, Wang S. In vitro antitumor mechanism of a novel cyclin-dependent kinase inhibitor CDKI-83. Invest New Drugs 2011 Feb 18.
107. Senderowicz AM. Flavopiridol: The first cyclin-dependent kinase inhibitor in human clinical trials. Invest New Drugs 1999;17(3):313-20.
108. Wang LM, Ren DM. Flavopiridol, the first cyclin-dependent kinase inhibitor: Recent advances in combination chemotherapy. Mini Rev Med Chem 2010 Oct;10(11):1058-70.
109. Ali S, El-Rayes BF, Aranha O, Sarkar FH, Philip PA. Sequence dependent potentiation of gemcitabine by flavopiridol in human breast cancer cells. Breast Cancer Res Treat 2005 Mar;90(1):25-31.
110. Mizuno K, Noda K, Ueda Y. UCN-01, an anti-tumour drug, is a selective inhibitor of the conventional PKC subfamily. FEBS Letters 1995;359(2-3):259-61.

110. Mizuno K, Noda K, Ueda Y. UCN-01, an anti-tumour drug, is a selective inhibitor of the conventional PKC subfamily. FEBS Letters 1995;359(2-3):259-61.
111. Facchinetti MM, De Siervi A, Toskos D, Senderowicz AM. UCN-01-induced cell cycle arrest requires the transcriptional induction of p21(waf1/cip1) by activation of mitogen-activated protein/extracellular signal-regulated kinase kinase/extracellular signal-regulated kinase pathway. Cancer Res 2004 May 15;64(10):3629-37.
112. Nahta R, Hortobagyi GN, Esteva FJ. Signal transduction inhibitors in the treatment of breast cancer. Curr Med Chem Anticancer Agents 2003 May;3(3):201-16.
113. Hay N, Sonenberg N. Upstream and downstream of mTOR. Genes Dev 2004 Aug 15;18(16):1926-45.
114. Beevers CS, Li F, Liu L, Huang S. Curcumin inhibits the mammalian target of rapamycin-mediated signaling pathways in cancer cells. Int J Cancer 2006 Aug 15;119(4):757-64.
115. Dancey JE. Therapeutic targets: MTOR and related pathways. Cancer Biol Ther 2006 Sep;5(9):1065-73.
116. Brown EJ, Albers MW, Shin TB, Ichikawa K, Keith CT, Lane WS, Schreiber SL. A mammalian protein targeted by G1-arresting rapamycin-receptor complex. Nature 1994 Jun 30;369(6483):756-8.
117. Wan X, Shen N, Mendoza A, Khanna C, Helman LJ. CCI-779 inhibits rhabdomyosarcoma xenograft growth by an antiangiogenic mechanism linked to the targeting of mTOR/Hif-1alpha/VEGF signaling. Neoplasia 2006 May;8(5):394-401.
118. Chan S, Scheulen ME, Johnston S, Mross K, Cardoso F, Dittrich C, Eiermann W, Hess D, Morant R, Semiglazov V, et al. Phase II study of temsirolimus (CCI-779), a novel inhibitor of mTOR, in heavily pretreated patients with locally advanced or metastatic breast cancer. J Clin Oncol 2005 Aug 10;23(23):5314-22.
119. de Bono JS, Tolcher AW, Rowinsky EK. The future of cytotoxic therapy: Selective cytotoxicity based on biology is the key. Breast Cancer Res 2003;5(3):154-9.
120. Novartis reports positive results from phase II tuberous slerosis study. 2010.
121. Mackay HJ, Twelves CJ. Targeting the protein kinase C family: Are we there yet? Nat Rev Cancer 2007 Jul;7(7):554-62.
122. Heim M, Scharifi M, Zisowsky J, Jaehde U, Voliotis D, Seeber S, Strumberg D. The raf kinase inhibitor BAY 43-9006 reduces cellular uptake of platinum compounds and cytotoxicity in human colorectal carcinoma cell lines. Anticancer Drugs 2005 Feb;16(2):129-36.
123. Mattingly RR, et al. The MEK inhibitor PD184352/CI-1040 selectively induces apoptosis in malignant schwannoma cells lines. J Pharmacol Exp Ther 2006;316:456-65.
124. Gills JJ, Dennis PA. Perifosine: Update on a novel akt inhibitor. Curr Oncol Rep 2009 Mar;11(2):102-10.
125. Waza M, Adachi H, Katsuno M, Minamiyama M, Sang C, Tanaka F, Inukai A, Doyu M, Sobue G. 17-AAG, an Hsp90 inhibitor, ameliorates polyglutamine-mediated motor neuron degeneration. Nat Med 2005 Oct;11(10):1088-95.
126. Steward WP. Marimastat (BB2516): Current status of development. Cancer Chemother Pharmacol 1999;43 Suppl:S56-60.

128. Butler LM, Zhou X, Xu WS, Scher HI, Rifkind RA, Marks PA, Richon VM. The histone deacetylase inhibitor SAHA arrests cancer cell growth, up-regulates thioredoxin-binding protein-2, and down-regulates thioredoxin. Proc Natl Acad Sci U S A 2002 Sep 3;99(18):11700-5.
129. Carr M. Dr Miriam Carr's PhD thesis.2006 .
130. Penning TD, Talley JJ, Bertenshaw SR, Carter JS, Collins PW, Docter S, Graneto MJ, Lee LF, Malecha JW, Miyashiro JM, et al. Synthesis and biological evaluation of the 1,5-diarylpyrazole class of cyclooxygenase-2 inhibitors: Identification of 4-[5-(4-methylphenyl)-3-(trifluoromethyl)-1H-pyrazol-1-yl]benze nesulfonamide (SC-58635, celecoxib). J Med Chem 1997 Apr 25;40(9):1347-65.
131. Eicher T, Hauptmann S, editors. The chemistry of heterocycles:Structure, reactions,synthesis,and applications. Wiley-VCH; 2003. .
132. Pechmann HV. Pyrazol aus acetylen und diazomethan. Berichte Der Deutschen Chemischen Gesellschaft 1898;31(3):2950-1.
133. Hazebroucq G. The vilsmeier and haack reaction]. Ann Pharm Fr 1966 Dec;24(12):793-806.
134. Heller ST, Natarajan SR. 1,3-diketones from acid chlorides and ketones: A rapid and general one-pot synthesis of pyrazoles. Org Lett 2006 Jun 22;8(13):2675-8.
135. Peruncheralathan S, Khan TA, Ila H, Junjappa H. Regioselective synthesis of 1-aryl-3,4-substituted/annulated-5-(methylthio)pyrazoles and 1-aryl-3-(methylthio)-4,5-substituted/annulated pyrazoles. J Org Chem 2005 Nov 25;70(24):10030-5.
136. Mohamed Ahmed MS, Kobayashi K, Mori A. One-pot construction of pyrazoles and isoxazoles with palladium-catalyzed four-component coupling. Org Lett 2005 Sep 29;7(20):4487-9.
137. Gerstenberger BS, Rauckhorst MR, Starr JT. One-pot synthesis of N-arylpyrazoles from arylhalides. Org Lett 2009 May 21;11(10):2097-100.
138. Deng X, Mani NS. Base-mediated reaction of hydrazones and nitroolefins with a reversed regioselectivity: A novel synthesis of 1,3,4-trisubstituted pyrazoles. Org Lett 2008 Mar 20;10(6):1307-10.
139. Deng X, Mani NS. Reaction of N-monosubstituted hydrazones with nitroolefins: A novel regioselective pyrazole synthesis. Org Lett 2006 Aug 3;8(16):3505-8.
140. Butler MS. The role of natural product chemistry in drug discovery. J Nat Prod 2004 Dec;67(12):2141-53.
141. Martin R, Rodriguez Rivero M, Buchwald SL. Domino cu-catalyzed C--N coupling/hydroamidation: A highly efficient synthesis of nitrogen heterocycles. Angew Chem Int Ed Engl 2006 Oct 27;45(42):7079-82.
142. Nargund LV, Hariprasad V, Reedy GR. Synthesis and anti-inflammatory activity of fluorinated phenyl styryl ketones and N-phenyl-5-substituted aryl-3-p-(fluorophenyl) pyrazolins and pyrazoles. J Pharm Sci 1992 Sep;81(9):892-4.
143. Bauer VJ, Dalalian HP, Fanshawe WJ, Safir SR. 4-[3(5)-pyrazolyl]pyridinium salts. A new class of hypoglycemic agents. J Med Chem 1968 Sep;11(5):981-4.
144. Menozzi G, Schenone P, Mosti L, Mattioli F. Synthesis of 5-substituted 1-aryl-1H-pyrazole-4-acetonitriles, 4-methyl-1-phenyl-1H-pyrazole-3-carbonitriles and pharmacologically active 1-aryl-1H-pyrazole-4-acetic acids. J Heterocycl Chem 1993;30(4):997-1002.
145. Ashton WT, Hutchins SM, Greenlee WJ, Doss GA, Chang RS, Lotti VJ, Faust KA, Chen TB, Zingaro GJ, Kivlighn SD. Nonpeptide angiotensin II antagonists

pharmacologically active 1-aryl-1H-pyrazole-4-acetic acids. J Heterocycl Chem 1993;30(4):997-1002.
145. Ashton WT, Hutchins SM, Greenlee WJ, Doss GA, Chang RS, Lotti VJ, Faust KA, Chen TB, Zingaro GJ, Kivlighn SD. Nonpeptide angiotensin II antagonists derived from 1H-pyrazole-5-carboxylates and 4-aryl-1H-imidazole-5-carboxylates. J Med Chem 1993 Nov 12;36(23):3595-605.
146. Waldo JP, Mehta S, Larock RC. Room temperature ICl-induced dehydration/iodination of 1-acyl-5-hydroxy-4,5-dihydro-1H-pyrazoles. a selective route to substituted 1-acyl-4-iodo-1H-pyrazoles. J Org Chem 2008 Sep 5;73(17):6666-70.
147. Rosa FA, Martins MAPea. Straightforward and regiospecific synthesis of pyrazole-5-carboxylates from unsymmetrical enaminodiketones. Synlett 2008:1673-8.
148. Hari Y, Tsuchida S, Sone R, Aoyama T. An efficient synthesis of 2-diazo-2-(trimethylsilyl)ethanols and their application to pyrazole synthesis. Synthesis 2007:3371-5.
149. Hari Y, Tuychida S, Sone R, Aoyama T. An efficient synthesis of 2-diazo-2-(trimethylsilyl)ethanols and their application to pyrazole synthesis. Synthesis 2007:3371-5.
150. Nakamichi N, Kawashita Y, Hayashi M. Activated carbon-promoted oxidative aromatization of hantzsch 1,4-dihydropyridines and 1,3,5-trisubstituted pyrazolines using molecular oxygen. Synthesis 2004:1015-20.
151. Malhotra S, Shafiq N, Pandhi P. COX-2 inhibitors: A CLASS act or just VIGORously promoted. MedGenMed 2004 Mar 23;6(1):6.
152. Silverstein FE, Faich G, Goldstein JL, Simon LS, Pincus T, Whelton A, Makuch R, Eisen G, Agrawal NM, Stenson WF, et al. Gastrointestinal toxicity with celecoxib vs nonsteroidal anti-inflammatory drugs for osteoarthritis and rheumatoid arthritis: The CLASS study: A randomized controlled trial. celecoxib long-term arthritis safety study. JAMA 2000 Sep 13;284(10):1247-55.
153. Neurocrine Biosciences I. Neurocrine receives approvable letter for indiplon capsules with additional safety and efficacy data required by FDA. 2007.
154. Lippa A, Czobor P, Stark J, Beer B, Kostakis E, Gravielle M, Bandyopadhyay S, Russek SJ, Gibbs TT, Farb DH, et al. Selective anxiolysis produced by ocinaplon, a GABA(A) receptor modulator. Proc Natl Acad Sci U S A 2005 May 17;102(20):7380-5.
155. Dundar Y, Dodd S, Strobl J, Boland A, Dickson R, Walley T. Comparative efficacy of newer hypnotic drugs for the short-term management of insomnia: A systematic review and meta-analysis. Hum Psychopharmacol 2004 Jul;19(5):305-22.
156. Lan R, Liu Q, Fan P, Lin S, Fernando SR, McCallion D, Pertwee R, Makriyannis A. Structure-activity relationships of pyrazole derivatives as cannabinoid receptor antagonists. J Med Chem 1999 Feb 25;42(4):769-76.
157. Hall TL. Fomepizole in the treatment of ethylene glycol poisoning. CJEM 2002 May;4(3):199-204.
158. International programme on chemical saftey (IPCS): Methanol PIM 335. .
159. U.S. Environmental protection Agency. Tebufenpyrad pesticide fact sheet. .
160. Green GA. Understanding NSAIDs: From aspirin to COX-2. Clin Cornerstone 2001;3(5):50-60.

derivatives possessing antiproliferative activity. Bioorg Med Chem Lett 2002 Nov 4;12(21):3191-3.
163. Bechem M, Goldmann S, Gross R, Hallermann S, Hebisch S, Hutter J, Rounding HP, Schramm M, Stoltefuss J, Straub A. A new type of ca-channel modulation by a novel class of 1,4-dihydropyridines. Life Sci 1997;60(2):107-18.
164. Briede J, Daija D, Bisenieks E, Makarova N, Uldrikis J, Poikans J, Duburs G. Effects of some 1,4-dihydropyridine ca antagonists on the blast transformation of rat spleen lymphocytes. Cell Biochem Funct 1999 Jun;17(2):97-105.
165. Ferry DR, Russell MA, Cullen MH. P-glycoprotein possesses a 1,4-dihydropyridine-selective drug acceptor site which is allosterically coupled to a vinca-alkaloid-selective binding site. Biochem Biophys Res Commun 1992 Oct 15;188(1):440-5.
166. Richter M, Molnar J, Hilgeroth A. Biological evaluation of bishydroxymethyl-substituted cage dimeric 1,4-dihydropyridines as a novel class of p-glycoprotein modulating agents in cancer cells. J Med Chem 2006 May 4;49(9):2838-40.
167. Coburger C, Wollmann J, Krug M, Baumert C, Seifert M, Molnar J, Lage H, Hilgeroth A. Novel structure-activity relationships and selectivity profiling of cage dimeric 1,4-dihydropyridines as multidrug resistance (MDR) modulators. Bioorg Med Chem 2010 Jul 15;18(14):4983-90.
168. Zhou XF, Yang X, Wang Q, Coburn RA, Morris ME. Effects of dihydropyridines and pyridines on multidrug resistance mediated by breast cancer resistance protein: In vitro and in vivo studies. Drug Metab Dispos 2005 Aug;33(8):1220-8.
169. Nguyen JT, Velazquez CA, Knaus EE. Hantzsch 1,4-dihydropyridines containing a diazen-1-ium-1,2-diolate nitric oxide donor moiety to study calcium channel antagonist structure-activity relationships and nitric oxide release. Bioorg Med Chem 2005 Mar 1;13(5):1725-38.
170. Asada Y, Kuroishi C, Ukita Y, Sumii R, Endo S, Matsunaga T, Hara A, Kunishima N. Dimeric crystal structure of rabbit L-gulonate 3-dehydrogenase/lambda-crystallin: Insights into the catalytic mechanism. J Mol Biol 2010 Sep 3;401(5):906-20.
171. Asada Y, Kuroishi C, Ukita Y, Sumii R, Endo S, Matsunaga T, Hara A, Kunishima N. Dimeric crystal structure of rabbit L-gulonate 3-dehydrogenase/lambda-crystallin: Insights into the catalytic mechanism. J Mol Biol 2010 Sep 3;401(5):906-20.
172. Triggle DJ. The 1,4-dihydropyridine nucleus: A pharmacophoric template part 1. actions at ion channels. Mini Rev Med Chem 2003 May;3(3):215-23.
173. Luksa J, Josic D, Kremser M, Kopitar Z, Milutinovic S. Pharmacokinetic behaviour of R-(+)- and S-(-)-amlodipine after single enantiomer administration. J Chromatogr B Biomed Sci Appl 1997 Dec 5;703(1-2):185-93.
174. Chan CS, Guzman JN, Ilijic E, Mercer JN, Rick C, Tkatch T, Meredith GE, Surmeier DJ. 'Rejuvenation' protects neurons in mouse models of parkinson's disease. Nature 2007 Jun 28;447(7148):1081-6.
175. Huang RI, Patel P, Walinsky P, Fischman DL, Ogilby JD, Awar M, Frankil C, Savage MP. Efficacy of intracoronary nicardipine in the treatment of no-reflow during percutaneous coronary intervention. Catheter Cardiovasc Interv 2006 Nov;68(5):671-6.

175. Huang RI, Patel P, Walinsky P, Fischman DL, Ogilby JD, Awar M, Frankil C, Savage MP. Efficacy of intracoronary nicardipine in the treatment of no-reflow during percutaneous coronary intervention. Catheter Cardiovasc Interv 2006 Nov;68(5):671-6.
176. Belfort MA, Anthony J, Saade GR, Allen JC. a comparison of maganesium sulfate and nimodipine for the prevention of eclampsia. N Engl J Med 2003;348(4):304-11.
177. Estacio RO, Jeffers BW, Hiatt WR, Biggerstaff SL, Gifford N, Schrier RW. The effect of nisoldipine as compared with enalapril on cardiovascular outcomes in patients with non-insulin-dependent diabetes and hypertension. N Engl J Med 1998 Mar 5;338(10):645-52.
178. Kiani J, Imam SZ. Medicinal importance of grapefruit juice and its interaction with various drugs. Nutr J 2007 Oct 30;6:33.
179. Berridge MJ, Bootman MD, Lipp P. Calcium--a life and death signal. Nature 1998 Oct 15;395(6703):645-8.
180. Roderick HL, Cook SJ. Ca2+ signalling checkpoints in cancer: Remodelling Ca2+ for cancer cell proliferation and survival. Nat Rev Cancer 2008 May;8(5):361-75.
181. Lee WJ, Monteith GR, Roberts-thomson SJ. Calcium transport and signalling in the mammary gland: Target for breast cancer. Biochimica Et Biophysica Acta 2006(1765):225-35.
182. Triggle DJ. Calcium channel antagonists: Clinical uses--past, present and future. Biochem Pharmacol 2007 Jun 30;74(1):1-9.
183. Safak C, Simsek R. Fused 1,4-dihydropyridines as potential calcium modulatory compounds. Mini Rev Med Chem 2006 Jul;6(7):747-55.
184. Harris VK, Kagan BL, Ray R, Coticchia CM, Liaudet-Coopman ED, Wellstein A, Tate Riegel A. Serum induction of the fibroblast growth factor-binding protein (FGF-BP) is mediated through ERK and p38 MAP kinase activation and C/EBP-regulated transcription. Oncogene 2001 Mar 29;20(14):1730-8.
185. Lai YM, Fukuda N, Su JZ, Suzuki R, Ikeda Y, Takagi H, Tahira Y, Kanmatsuse K. Novel mechanisms of the antiproliferative effects of amlodipine in vascular smooth muscle cells from spontaneously hypertensive rats. Hypertens Res 2002 Jan;25(1):109-15.
186. Ziesche R, Petkov V, Lambers C, Erne P, Block LH. The calcium channel blocker amlodipine exerts its anti-proliferative action via p21(Waf1/Cip1) gene activation. FASEB J 2004 Oct;18(13):1516-23.
187. Ohba T, Watanabe H, Murakami M, Radovanovic M, Iino K, Ishida M, Tosa S, Ono K, Ito H. Amlodipine inhibits cell proliferation via PKD1-related pathway. Biochem Biophys Res Commun 2008 May 2;369(2):376-81.
188. Bang LM, Chapman TM, Goa KL. Lercanidipine : A review of its efficacy in the management of hypertension. Drugs 2003;63(22):2449-72.
189. Herbette LG, Mason PE, Gaviraghi G, Tulenko TN, Mason RP. The molecular basis for lacidipine's unique pharmacokinetics: Optimal hydrophobicity results in membrane interactions that may facilitate the treatment of atherosclerosis. J Cardiovasc Pharmacol 1994;23 Suppl 5:S16-25.
190. Aouam K, Berdeaux A. Dihydropyridines from the first to the fourth generation: Better effects and safety]. Therapie 2003 Jul-Aug;58(4):333-9.
191. Crosta L, Candiloro V, Meli M, Tolomeo M, Rausa L, Dusonchet L. Lacidipine and josamycin: Two new multidrug resistance modulators. Anticancer Res 1994 Nov-Dec;14(6B):2685-9.

193. Tanabe H, Tasaka S, Ohmori H, Gomi N, Sasaki Y, Machida T, Iino M, Kiue A, Naito S, Kuwano M. Newly synthesized dihydropyridine derivatives as modulators of P-glycoprotein-mediated multidrug resistance. Bioorg Med Chem 1998 Nov;6(11):2219-27.
194. Kawase M, Shah A, Gaveriya H, Motohashi N, Sakagami H, Varga A, Molnar J. 3,5-dibenzoyl-1,4-dihydropyridines: Synthesis and MDR reversal in tumor cells. Bioorg Med Chem 2002 Apr;10(4):1051-5.
195. Yoshida J, Ishibashi T, Nishio M. G1 cell cycle arrest by amlodipine, a dihydropyridine Ca2+ channel blocker, in human epidermoid carcinoma A431 cells. Biochem Pharmacol 2007 Apr 1;73(7):943-53.
196. Ryabokon NI, Goncharova RI, Duburs G, Rzeszowska-Wolny J. A 1,4-dihydropyridine derivative reduces DNA damage and stimulates DNA repair in human cells in vitro. Mutat Res 2005 Nov 10;587(1-2):52-8.
197. Zhu XQ, Zhao BJ, Cheng JP. Mechanisms of the oxidations of NAD(P)H model hantzsch 1,4-dihydropyridines by nitric oxide and its donor N-methyl-N-nitrosotoluene-p-sulfonamide. J Org Chem 2000 Dec 1;65(24):8158-63.
198. Li M, Zuo Z, Wen L, Wang S. Microwave-assisted combinatorial synthesis of hexa-substituted 1,4-dihydropyridines scaffolds using one-pot two-step multicomponent reaction followed by a S-alkylation. J Comb Chem 2008 May-Jun;10(3):436-41.
199. Tanabe H, Tasaka S, Ohmori H, Gomi N, Sasaki Y, Machida T, Iino M, Kiue A, Naito S, Kuwano M. Newly synthesized dihydropyridine derivatives as modulators of P-glycoprotein-mediated multidrug resistance. Bioorg Med Chem 1998 Nov;6(11):2219-27.
200. Voigt B, Coburger C, Monar J, Hilgeroth A. Structure-activity relationships of novel N-acyloxy-1,4-dihydropyridines as P-glycoprotein inhibitors. Bioorg Med Chem 2007 Aug 1;15(15):5110-3.
201. Nogae I, Kohno K, Kikuchi J, Kuwano M, Akiyama S, Kiue A, Suzuki K, Yoshida Y, Cornwell MM, Pastan I. Analysis of structural features of dihydropyridine analogs needed to reverse multidrug resistance and to inhibit photoaffinity labeling of P-glycoprotein. Biochem Pharmacol 1989 Feb 1;38(3):519-27.
202. Abadi AH, Eissa AA, Hassan GS. Synthesis of novel 1,3,4-trisubstituted pyrazole derivatives and their evaluation as antitumor and antiangiogenic agents. Chem Pharm Bull (Tokyo) 2003 Jul;51(7):838-44.
203. Knox AJ, Meegan MJ, Sobolev V, Frost D, Zisterer DM, Williams DC, Lloyd DG. Target specific virtual screening: Optimization of an estrogen receptor screening platform. J Med Chem 2007 Nov 1;50(22):5301-10.
204. Lanyi JK. Mechanism of base-catalyzed schiff base deprotonation in halorhodopsin. Biochemistry 1986 Oct 21;25(21):6706-11.
205. Marson CM. Reaction of carbonyl compounds with(monohalo) methyleniminium salts(vilsmeier reagents). Tetrahedron 1992;48(18):3659-726.
206. Smith M, Smith MB, March J, editors. March's advanced organic chemistry:Reaction,mechanisms,and structure. ; 1979. .
207. Alunni S, Linda P, Marino G, Santini S, Savelli G. The mechanism of the vilsmeier-haack reaction.part II.A kinetic study of the formylation of thiophen derivatives with demethylformamide and phosporous oxychloride or carbonyl chloride in 1,2-dichloroethane. Journal of the Chemical Society,Perkin Transactions 2 1972(14):2070-3.

derivatives with demethylformamide and phosporous oxychloride or carbonyl chloride in 1,2-dichloroethane. Journal of the Chemical Society,Perkin Transactions 2 1972(14):2070-3.
208. Hazebroucq G. The vilsmeier and haack reaction. Ann Pharm Fr 1966 Dec;24(12):793-806.
209. Loader CE, Barnett GH, Anderson HJ. Can J Chem 1982(60):383.
210. Pellet M, Huet F. Tetrahedron 1988(44):4463.
211. Arnold Z, Zemlicka J. Proc Chem Soc (London) 1958:227.
212. Arnold Z, Zemlicka J. Coll Czech Commun 1959(24):2378-85.
213. Jutz C, Heinicke R. Chem Ber 1969(102):623.
214. Raju B, Krishna Rao GS. Ind J Chem 1987(26B):175.
215. Ramage R, Atrash B, Hopton D, Parrott MJ. J.Chem.Soc.,Perkin Trans.1 1985:1617.
216. Kumar A, Maurya RA. Efficient synthesis of hantzsch esters and polyhydroquinoline derivatives in aqueous micelles. Synlett 2008:883-5.
217. Sharma GVM, Reddy KL, Lakshmi PS, Krishna PR. 'In situ'; generated 'HCl'; - an efficient catalyst for solvent-free hantzsch reaction at room temperature: Synthesis of new dihydropyridine glycoconjugates. Synthesis 2006:55-8.
218. Debache A, Boulcina R, Belfaitah A, Rhouati S, Carboni B. One-pot synthesis of 1,4-dihydropyridines via a phenylboronic acid catalyzed hantzsch three-component reaction. Synlett 2008:509-12.
219. De Paolis O, Baffoe J, Landge SM, Török B. Multicomponent domino cyclization-oxidative aromatization on a bifunctional Pd/C/K-10 catalyst: An environmentally benign approach toward the synthesis of pyridines. Synthesis 2008:3423-8.
220. Wang LM, Sheng J, Zhang L, Han JW, Fan ZY, Tian H, Qian CT. Facile yb$(OTf)_3$ promoted one-pot synthesis of polyhydroquinoline derivatives through hantzsch reaction. Tetrahedron 2005(61):1539-43.
221. Katritzky AR, Ostercamp DL, Yousaf TI. The mechanism of the hantzsch pyridine synthesis: A study by ^{15}N and ^{13}C NMR spectroscopy. Tetrahedron 1986(20):5729-38.
222. Filipan-Litvic M, Litvic M, Cepanec I, Vinkovic V. Hantzsch synthesis of 2,6-dimethyl-3,5-dimethoxycarbonyl-4-(o-methoxyphenyl)-1,4-dihydropyridine ; a novel cyclisation leading to an unusual formation of 1-amino-2-methoxy-carbonyl-3,5-bis(o-methoxyphenyl)-4-oxa-cyclohexan-1-ene. Molecules 2007 Nov 26;12(11):2546-58.
223. Maiti S, Menéndez JC. A mild protocol for the efficient synthesis of 5,6-unsubstituted 1,4-dihydropyridines. Synlett 2009:2249-52.
224. Bartoli G, Babiuch k, Bosco M, Carlone A, Galzerano P, Melchiorre P, Sambri L. Magnesium perchlorate as efficient lewis acid: A simple and convenient route to 1,4-dihydropyridines. Synlett 2007:2897-901.
225. Wang LM, Sheng J, Zhang L, Fan ZY, Tian H, Qian CT. Facile yb(OTf)3 promoted one-pot synthesis of polyhydroquinoline derivatives through hantzsch reaction. Tetrahedron 2005(61):1539-43.
226. Sabitha G, Reddy GSKK, Reddy CS, Yadav JS. A novel TMSI-mediated synthesis of hantzsch 1,4-dihydropyridines at ambient temperature. Tetrahedron Letters 2003(44):4129-31.
227. Kawase M, Shah A, Gaveriya H, Motohashi N, Sakagami H, Varga A, Molnar J. 3,5-dibenzoyl-1,4-dihydropyridines: Synthesis and MDR reversal in tumor cells. Bioorg Med Chem 2002 Apr;10(4):1051-5.

229. England R. Microwave synthesis: A new wave of synthetic organic chemistry. Chemical Synthesis 2003.
230. Klinowski J, Paz FA, Silva P, Rocha J. Microwave-assisted synthesis of metal-organic frameworks. Dalton Trans 2011 Jan 14;40(2):321-30.
231. Patil SA, Patil R, Miller DD. Microwave-assisted synthesis of medicinally relevant indoles. Curr Med Chem 2011;18(4):615-37.
232. Eynde J, Mayence A. Synthesis and armatization of hantzsch 1,4-dihydropyridines under microwave irradiation.an overview. Molecules 2003(8):381-91.
233. Alajarin R, Vaquero J, Garcia Navio J, varez-Builla J. Synthesis of 1,4-dihydropyridines under microwave irradiation. Synlett 1992:297-8.
234. Liao YY, Sun DM, Zhong CP, Lai XS. Evaluation of the immediate effect of acupuncture on cervical spondylosis of vertebral artery type based on orthogonal design. Zhongguo Zhen Jiu 2011 Jun;31(6):499-502.
235. Ishida T, Kiba T, Takeda M, Matsuyama K, Teramukai S, Ishiwata R, Masuda N, Takatsuka Y, Noguchi S, Ishioka C, et al. Phase II study of capecitabine and trastuzumab combination chemotherapy in patients with HER2 overexpressing metastatic breast cancers resistant to both anthracyclines and taxanes. Cancer Chemother Pharmacol 2009 Jul;64(2):361-9.
236. Yadav MR, Nimekar DM, Ananthakrishnan A, Brahmkshatriya PS, Shirude ST, Giridhar R, Parmar A, Balaraman R. Synthesis of new chemical entities from paracetamol and NSAIDs with improved pharmacodynamic profile. Bioorg Med Chem 2006 Dec 15;14(24):8701-6.
237. Verma A, Das N, Dhanawat M, Shrivastava SK. Conjugation of some NSAIDs with 5-phenyl-2aminothiazole for reduced ulcerogenicity. Thai J Pharm Sci 2010(34):49-57.
238. Martin R, Buchwald SL. Palladium-catalyzed suzuki-miyaura cross-coupling reactions employing dialkylbiaryl phosphine ligands. Acc Chem Res 2008 Nov 18;41(11):1461-73.
239. Matos K, Soderquist JA. Alkylboranes in the suzuki-miyaura coupling: Stereochemical and mechanistic studies. J Org Chem 1998 Feb 6;63(3):461-70.
240. Ding SY, Gao J, Wang Q, Zhang Y, Song WG, Su CY, Wang W. Construction of covalent organic framework for catalysis: Pd/COF-LZU1 in suzuki-miyaura coupling reaction. J Am Chem Soc 2011 Dec 14;133(49):19816-22.
241. Yu Y, Hu T, Chen X, Xu K, Zhang J, Huang J. Pd nanoparticles on a porous ionic copolymer: A highly active and recyclable catalyst for suzuki-miyaura reaction under air in water. Chem Commun (Camb) 2011 Mar 28;47(12):3592-4.
242. Dreher SD, Lim SE, Sandrock DL, Molander GA. Suzuki-miyaura cross-coupling reactions of primary alkyltrifluoroborates with aryl chlorides. J Org Chem 2009 May 15;74(10):3626-31.
243. Kirchhoff JH, Netherton MR, Hills ID, Fu GC. Boronic acids: New coupling partners in room-temperature suzuki reactions of alkyl bromides. crystallographic characterization of an oxidative-addition adduct generated under remarkably mild conditions. J Am Chem Soc 2002 Nov 20;124(46):13662-3.
244. Baxter JM, Steinhuebel D, Palucki M, Davies IW. Stereoselective enol tosylation: Preparation of trisubstituted alpha,beta-unsaturated esters. Org Lett 2005 Jan 20;7(2):215-8.
245. Maiti S, Sridharan V, Menendez JC. Synthesis of a library of 5,6-unsubstituted 1,4-dihydropyridines based on a one-pot 4CR/elimination process and their

245. Maiti S, Sridharan V, Menendez JC. Synthesis of a library of 5,6-unsubstituted 1,4-dihydropyridines based on a one-pot 4CR/elimination process and their application to the generation of structurally diverse fused nitrogen heterocycles. J Comb Chem 2010 Sep 13;12(5):713-22.
246. Ioele G, De Luca M, Oliverio F, Ragno G. Prediction of photosensitivity of 1,4-dihydropyridine antihypertensives by quantitative structure-property relationship. Talanta 2009 Oct 15;79(5):1418-24.
247. Zhang W, Yang X, Chen W, Xu X, Li L, Zhai H, Li Z. Design, multicomponent synthesis, and bioactivities of novel neonicotinoid analogues with 1,4-dihydropyridine scaffold. J Agric Food Chem 2010 Mar 10;58(5):2741-5.
248. Maxwell MM, Tomkinson EM, Nobles J, Wizeman JW, Amore AM, Quinti L, Chopra V, Hersch SM, Kazantsev AG. The sirtuin 2 microtubule deacetylase is an abundant neuronal protein that accumulates in the aging CNS. Hum Mol Genet 2011 Oct 15;20(20):3986-96.
249. Stauffer SR, Huang YR, Aron ZD, Coletta CJ, Sun J, Katzenellenbogen BS, Katzenellenbogen JA. Triarylpyrazoles with basic side chains: Development of pyrazole-based estrogen receptor antagonists. Bioorg Med Chem 2001 Jan;9(1):151-61.
250. Lee JH, Wen Y, Polan ML, Chen B. The effect of raloxifene, a SERM, on extracellular matrix protein expression of pelvic fibroblasts. Int Urogynecol J 2011 Sep 21.
251. Lee OY, Law KL, Yang D. Secondary amine formation from reductive amination of carbonyl compounds promoted by lewis acid using the InCl3/Et3SiH system. Org Lett 2009 Aug 6;11(15):3302-5.
252. Abdel-Magid AF, Carson KG, Harris BD, Maryanoff CA, Shah RD. Reductive amination of aldehydes and ketones with sodium triacetoxyborohydride. studies on direct and indirect reductive amination procedures(1). J Org Chem 1996 May 31;61(11):3849-62.
253. Zhang M, Yang H, Zhang Y, Zhu C, Li W, Cheng Y, Hu H. Direct reductive amination of aromatic aldehydes catalyzed by gold(I) complex under transfer hydrogenation conditions. Chem Commun (Camb) 2011 Jun 21;47(23):6605-7.
254. Lee OY, Law KL, Ho CY, Yang D. Highly chemoselective reductive amination of carbonyl compounds promoted by InCl3/Et3SiH/MeOH system. J Org Chem 2008 Nov 21;73(22):8829-37.
255. Basso LA, Engel PC, Walmsley AR. The mechanism of substrate and coenzyme binding to clostridial glutamate dehydrogenase during reductive amination. Eur J Biochem 1995 Dec 1;234(2):603-15.
256. Bodineau N, Mattalia JM, Thimokhin VV, Handoo K, Negrel JC, Chanon M. Formation of grignard reagents from aryl halides: Effective radical probes hint at a nonparticipation of dianions in the mechanism. Org Lett 2000 Jul 27;2(15):2303-6.
257. Maruyama K, Katagiri T. Mechanism of the grignard reaction. J Phys Org Chem 1989;2(3):205.
258. Yamazaki S, Yamabe S. A computational study on addition of grignard reagents to carbonyl compounds. J Org Chem 2002 Dec 27;67(26):9346-53.
259. Smith MB, March J, editors. Wiley Interscience; 2001. .
260. Corey EJ, Suggs W. Tetrahedron Lett 1975;16 (31): 2647–2650(31):2647-50.
261. De Ruggieri P, Fazio M, Montoro G, Sighinolfi O. Steroidal heterocyclic compounds: [16,15-c]-pyrazole derivatives of estradiol and of estrone. Farmaco Sci 1975 Jul;30(7):547-60.

262. Ruzicka J, Weisbecker C, Attygalle AB. Collision-induced dissociation mass spectra of positive ions derived from tetrahydropyranyl (THP) ethers of primary alcohols. J Mass Spectrom 2010 Nov 30.
263. Wang R, Jiang H. 1,6-hexanediamine methanesulfonate: A mild and efficient catalyst for the tetrahydropyranylation of alcohols under solvent-free conditions. Prep Biochem Biotechnol 2010 Jul;40(3):171-6.
264. Xue WL, Warshawsky D. Synthesis and characterization of monohydroxylated derivatives of 7H-dibenzo[c,g]carbazole. Chem Res Toxicol 1992 Jan-Feb;5(1):130-3.
265. Shah ABJ, Molnár J, Kawase M, Motohashi N, editors. Advanced dihydropyridines as novel multidrug resistance modifiers and reversing agents. in flavonoids and anthocyanins in plants, and latest bioactive heterocycles. ; 2008. .
266. Voigt B, Coburger C, Monar J, Hilgeroth A. Structure-activity relationships of novel N-acyloxy-1,4-dihydropyridines as P-glycoprotein inhibitors. Bioorg Med Chem 2007 Aug 1;15(15):5110-3.
267. Tasaki Y, Nakagawa M, Ogata J, Kiue A, Tanimura H, Kuwano M, Nomura Y. Reversal by a dihydropyridine derivative of non-P-glycoprotein-mediated multidrug resistance in etoposide-resistant human prostatic cancer cell line. J Urol 1995 Sep;154(3):1210-6.
268. Hrycyna CA, Ramachandra M, Ambudkar SV, Ko YH, Pedersen PL, Pastan I, Gottesman MM. Mechanism of action of human P-glycoprotein ATPase activity. photochemical cleavage during a catalytic transition state using orthovanadate reveals cross-talk between the two ATP sites. J Biol Chem 1998 Jul 3;273(27):16631-4.
269. Dantzig AH, de Alwis DP, Burgess M. Considerations in the design and development of transport inhibitors as adjuncts to drug therapy. Adv Drug Deliv Rev 2003 Jan 21;55(1):133-50.
270. Varma MV, Ashokraj Y, Dey CS, Panchagnula R. P-glycoprotein inhibitors and their screening: A perspective from bioavailability enhancement. Pharmacol Res 2003 Oct;48(4):347-59.
271. Zhou XF, Zhang L, Tseng E, Scott-Ramsay E, Schentag JJ, Coburn RA, Morris ME. New 4-aryl-1,4-dihydropyridines and 4-arylpyridines as P-glycoprotein inhibitors. Drug Metab Dispos 2005 Mar;33(3):321-8.
272. Swarnalatha G, Sirisha N, Madhusudhana Chetty C. 1,4-dihydropyridines: A multifunctional molecule- A review. International Journal of Chem Tech Research 2011;3:75-89.
273. Kawase M, Shah A, Gaveriya H, Motohashi N, Sakagami H, Varga A, Molnar J. 3,5-dibenzoyl-1,4-dihydropyridines: Synthesis and MDR reversal in tumor cells. Bioorg Med Chem 2002 Apr;10(4):1051-5.
274. Morshed SR, Hashimoto K, Murotani Y, Kawase M, Shah A, Satoh K, Kikuchi H, Nishikawa H, Maki J, Sakagami H. Tumor-specific cytotoxicity of 3,5-dibenzoyl-1,4-dihydropyridines. Anticancer Res 2005 May-Jun;25(3B):2033-8.
275. Cindric M, Cipak A, Serly J, Plotniece A, Jaganjac M, Mrakovcic L, Lovakovic T, Dedic A, Soldo I, Duburs G, et al. Reversal of multidrug resistance in murine lymphoma cells by amphiphilic dihydropyridine antioxidant derivative. Anticancer Res 2010 Oct;30(10):4063-9.
276. Soule HD, Vazguez J, Long A, Albert S, Brennan M. A human cell line from a pleural effusion derived from a breast carcinoma. J Natl Cancer Inst 1973 Nov;51(5):1409-16.

277. Gallagher R, Collins S, Trujillo J, McCredie K, Ahearn M, Tsai S, Metzgar R, Aulakh G, Ting R, Ruscetti F, et al. Characterization of the continuous, differentiating myeloid cell line (HL-60) from a patient with acute promyelocytic leukemia. Blood 1979 Sep;54(3):713-33.
278. Stegmaier K, Ross KN, Colavito SA, O'Malley S, Stockwell BR, Golub TR. Gene expression-based high-throughput screening(GE-HTS) and application to leukemia differentiation. Nat Genet 2004 Mar;36(3):257-63.
279. Mosmann T. Rapid colorimetric assay for cellular growth and survival: Application to proliferation and cytotoxicity assays. J Immunol Methods 1983 Dec 16;65(1-2):55-63.
280. Hong J, Kandasamy K, Marimuthu M, Choi CS, Kim S. Electrical cell-substrate impedance sensing as a non-invasive tool for cancer cell study. Analyst 2011 Jan 21;136(2):237-45.
281. Bagnaninchi PO, Drummond N. Real-time label-free monitoring of adipose-derived stem cell differentiation with electric cell-substrate impedance sensing. Proc Natl Acad Sci U S A 2011 Apr 19;108(16):6462-7.
282. Park HE, Kim D, Koh HS, Cho S, Sung JS, Kim JY. Real-time monitoring of neural differentiation of human mesenchymal stem cells by electric cell-substrate impedance sensing. J Biomed Biotechnol 2011;2011:485173.
283. Li YJ, Chen J, Li Y, Li P. Identification and quantification of free radical scavengers in the flower buds of lonicera species by online HPLC-DPPH assay coupled with electrospray ionization quadrupole time-of-flight tandem mass spectrometry. Biomed Chromatogr 2011 Aug 31.
284. Bielawska A, Bielawski K, Muszynska A. Synthesis and biological evaluation of new cyclic amidine analogs of chlorambucil. Farmaco 2004 Feb;59(2):111-7.
285. Klopman G, Zhu H. Recent methodologies for the estimation of n-octanol/water partition coefficients and their use in the prediction of membrane transport properties of drugs. Mini Rev Med Chem 2005 Feb;5(2):127-33.
286. Edwards MP, Price DA. Role of physicochemical properties and ligand lipophilicity efficiency in addressing drug safety risks. Annual Reports in Medicinal Chemistry 2010(45):381-91.
287. Bazargan L, Fouladdel S, Shafiee A, Amini M, Ghaffari SM, Azizi E. Evaluation of anticancer effects of newly synthesized dihydropyridine derivatives in comparison to verapamil and doxorubicin on T47D parental and resistant cell lines in vitro. Cell Biol Toxicol 2008 Apr;24(2):165-74.
288. Kobayashi Y, Yamashiro T, Nagatake H, Yamamoto T, Watanabe N, Tanaka H, Shigenobu K, Tsuruo T. Expression and function of multidrug resistance P-glycoprotein in a cultured natural killer cell-rich population revealed by MRK16 monoclonal antibody and AHC-52. Biochem Pharmacol 1994 Oct 18;48(8):1641-6.
289. Tasaka S, Ohmori H, Gomi N, Iino M, Machida T, Kiue A, Naito S, Kuwano M. Synthesis and structure--activity analysis of novel dihydropyridine derivatives to overcome multidrug resistance. Bioorg Med Chem Lett 2001 Jan 22;11(2):275-7.
290. Tanabe H, Tasaka S, Ohmori H, Gomi N, Sasaki Y, Machida T, Iino M, Kiue A, Naito S, Kuwano M. Newly synthesized dihydropyridine derivatives as modulators of P-glycoprotein-mediated multidrug resistance. Bioorg Med Chem 1998 Nov;6(11):2219-27.

291. Lage H. ABC-transporters: Implications on drug resistance from microorganisms to human cancers. Int J Antimicrob Agents 2003 Sep;22(3):188-99.
292. Lee WJ, Monteith GR, Roberts-Thomson SJ. Calcium transport and signaling in the mammary gland: Targets for breast cancer. Biochim Biophys Acta 2006 Apr;1765(2):235-55.
293. Lee WJ, Robinson JA, Holman NA, McCall MN, Roberts-Thomson SJ, Monteith GR. Antisense-mediated inhibition of the plasma membrane calcium-ATPase suppresses proliferation of MCF-7 cells. J Biol Chem 2005 Jul 22;280(29):27076-84.
294. Taylor JM, Simpson RU. Inhibition of cancer cell growth by calcium channel antagonists in the athymic mouse. Cancer Res 1992 May 1;52(9):2413-8.
295. Holbeck SL, Collins JM, Doroshow JH. Analysis of food and drug administration-approved anticancer agents in the NCI60 panel of human tumor cell lines. Mol Cancer Ther 2010 May;9(5):1451-60.
296. Shoemaker RH. The NCI60 human tumour cell line anticancer drug screen. Nat Rev Cancer 2006 Oct;6(10):813-23.
297. DTP national cancer institute (NCI)/Division of cancer treatment and diagnosis (DCTD)/Developmental therapeutics program. .
298. Paull KD, Shoemaker RH, Hodes L, Monks A, Scudiero DA, Rubinstein L, Plowman J, Boyd MR. Display and analysis of patterns of differential activity of drugs against human tumor cell lines: Development of mean graph and COMPARE algorithm. J Natl Cancer Inst 1989 Jul 19;81(14):1088-92.
299. DTP Human Tumour Cell Line Screen Standard Agent Database [Internet]. Available from: http://dtp.nci.nih.gov/docs/cancer/searches/standard_agent.html.
300. Paull KD, Lin CM, Malspeis L, Hamel E. Identification of novel antimitotic agents acting at the tubulin level by computer-assisted evaluation of differential cytotoxicity data. Cancer Res 1992 Jul 15;52(14):3892-900.
301. Wei YJ, Wang M, Yuan MR, Jia XB, Zhang RT, Tan W. Study on dynamic changes and stability of effective components of arnerbia euchroma. Zhong Yao Cai 2011 Apr;34(4):611-5.
302. Jin HE, Kang IH, Shim CK. Fluorescence detection of zabofloxacin, a novel fluoroquinolone antibiotic, in plasma, bile, and urine by HPLC: The first oral and intravenous applications in a pharmacokinetic study in rats. J Pharm Pharm Sci 2011;14(3):291-305.
303. Meyer H, Wehinger E, Bossert F, Scherling D. Nimodipine: Synthesis and metabolic pathway. Arzneimittelforschung 1983;33(1):106-12.
304. Pavez P, Encinas MV. Photophysics and photochemical studies of 1,4-dihydropyridine derivatives. Photochem Photobiol 2007 May-Jun;83(3):722-9.
305. Tucker FA, Minty PS, MacGregor GA. Study of nifedipine photodecomposition in plasma and whole blood using capillary gas-liquid chromatography. J Chromatogr 1985 Jul 12;342(1):193-8.
306. Shamsipur M, Hemmateenejad B, Akhond M, Javidnia K, Miri R. A study of the photo-degradation kinetics of nifedipine by multivariate curve resolution analysis. J Pharm Biomed Anal 2003 Apr 1;31(5):1013-9.
307. Bassem Yasien. PhD thesis. ; 2011.
308. Sanchez-moreno C, Larrauri JA, Saura-Calixto F. A procedure to measure the antiradical efficiency of polyphenols. Journal of the Science of Food and Agriculture 1998;76(2):270-6.

309. Diaz-Araya G, Godoy L, Naranjo L, Squella JA, Letelier ME, Nunez-Vergara LJ. Antioxidant effects of 1,4-dihydropyridine and nitroso aryl derivatives on the Fe+3/ascorbate-stimulated lipid peroxidation in rat brain slices. Gen Pharmacol 1998 Sep;31(3):385-91.
310. Qin Z, Kastrati I, Chandrasena RE, Liu H, Yao P, Petukhov PA, Bolton JL, Thatcher GR. Benzothiophene selective estrogen receptor modulators with modulated oxidative activity and receptor affinity. J Med Chem 2007 May 31;50(11):2682-92.
311. Praveen, C., Kumar, K., Hemanth,'M.D., Perumal, P.T., Tetrahedron, Vol. 64, Issue 10, 2369-2374, 2008
312. Huff, A.M., Hall, H.L., Smith, M.J, O'Grady, S.A., Waters, F.C., Fengl, R.W., Welsh, J.A., Beam, C.F.,Journal of Heterocyclic Chemistry,Vol.22: 501-504, 1985.
313. Afshin Zarghi., Azar Tahghighi., Zohreh Soleimani., Bahram Daraie., Orkideh Gorban Dadrass., Hedayati., MehdiScientia Pharmaceutica, Vol 76,Issue 3: 361-37, 2008.
314. Finar, I.L., Godfrey, K.E., 1954. Journal of the Chemical Society: 2293-2298
315. Krishna, J.,C., Renuka, J.,Saroj, G., Journal of the Indian Chemical Society, Vol.62, Issue 5: 388-390, 1985.
316. Downs,J.R., Pastine, S.J., Townsend, J.D., Journal of Heterocyclic Chemistry, Vol 38, Issue 3, 695-701, 2001.
317. Calavaire,A.,Pallud, R., Comptes Rendus Hebdomadaire des. Seances de I'Academie des Sciences, Vol 250: 1960-3194, 1960.
318. Homes, T.P. Filomena Mattner., Paul A. Keller., Andrew Katsifis., Bioorganic & Medicinal Chemistry, Vol 14,Issue 11, 3938-3946, 2006.
319. Bekhit,A.A., Fahmy H.T.Y., Rostom S.A.F., European Journal of Medicinal Chemistry, Vol. 38: 27-30, 2003.
320. Meierhoefer, MA., Dunn, S.P., Hajiaghamohseni, L.M., Walters, M.J., Embree, M.C., Grant, S.P., Downs, J.R., Townsend, J.D., Metz, C.R.,Beam, C.F., Pennington, W.T., Vanderveer, D.G., Camper, N.D., Journal of Heterocyclic Chemistry, Vol. 47, Issue 6, 1095-1099, 2005
321. Rainer, G., et.al., Arzneimittel Forschnng. Vol. 31, Issue 4, 649-655, 1981.
322. Chornous,V.O.,Bratenko, M.K., Vovk, M.V., Synthetic Communications Vol. 34, Issue 1,79-83, 2004.
323. Gaonkar,S.L., Rai, K.M.L., Tetrahedron Letters, Vol. 46, Issue: 35, 5969-5970, 2005.
324. Downs, J,R., et.al, Journal of Heterocyclic Chemistry, Vol 38, Issue 3, 691-694, 2001.
325. Vovk, M.V., Bol'but, A.V., Dorokhov ,V.I., Synthetic Communications Vol. 32, Issue 24, 3749-3753, 2002.
326. Bratenko,M.K., Chernyuk, I.N., Vovk, M.V., Zhurral Organicheskoi Khimii Vol. 33, Issue 2, 81-83, 1997.
327. Chornous, V.O., Bratenko, M.K., Vovk, M.V., Synthetic Communications, Vol. 34, Issue 1, 79-84. 2004.